การศึกษาทางพฤกษเคมีของไก่เตี้ยและประ

นางสาว ดวงเพ็ญ ปัทมดิลก

วิทยานิพนธ์นี้เป็นส่วนหนึ่งของการศึกษาตามหลักสูตรปริญญาวิทยาศาสตรดุษฎีบัณฑิต
สาขาวิชาเภสัชเวท
คณะเภสัชศาสตร์ จุฬาลงกรณ์มหาวิทยาลัย
ปีการศึกษา 2550

PHYTOCHEMICAL STUDY OF *CANAVALIA ROSEA* AND *ELATERIOSPERMUM TAPOS*

Miss Duangpen Pattamadilok

A Dissertation Submitted in Partial Fulfillment of the Requirements
for the Degree of Doctor of Philosophy Program in Pharmacognosy
Faculty of Pharmaceutical Sciences
Chulalongkorn University
Academic Year 2007

Thesis Title	PHYTOCHEMICAL STUDY OF *CANAVALIA ROSEA* AND *ELATERIOSPERMUM TAPOS*
By	Miss Duangpen Pattamadilok
Field of study	Pharmacognosy
Thesis Advisor	Associate Professor Rutt Suttisri, Ph.D.

Accepted by the Faculty of Pharmaceutical Sciences, Chulalongkorn University in Partial Fulfillment of the Requirements for the Doctoral Degree

Pornpen Premyothin ..... Dean of the Faculty of Pharmaceutical Sciences

(Associate Professor Pornpen Premyothin, Ph.D.)

THESIS COMMITTEE

K. Likhit ..... Chairman

(Associate Professor Kittisak Likhitwitayawuid, Ph.D.)

Rutt Suttisri ..... Thesis Advisor

(Associate Professor Rutt Suttisri, Ph.D.)

Thitima Pengsuparp ..... Member

(Associate Professor Thitima Pengsuparp, Ph.D.)

Witchuda Thanakitcharoenpath ..... Member

(Witchuda Thanakitcharoenpath, Ph.D.)

Uthai Sotanaphun ..... External Member

(Associate Professor Uthai Sotanaphun, Ph.D.)

ควงเพ็ญ ปัทมดิลก : การศึกษาทางพฤกษเคมีของไก่เตี้ยและประ (PHYTOCHEMICAL STUDY OF *CANAVALIA ROSEA* AND *ELATERIOSPERMUM TAPOS*)
อ. ที่ปรึกษา : รศ.ดร.รุทธ์ อุทธิศรี, 338 หน้า.

การศึกษาทางพฤกษเคมีของส่วนเหนือดินของไก่เตี้ย (วงศ์ Papilionaceae) สามารถแยกสารได้ 6 ชนิด เป็นสารใหม่ในกลุ่ม guanidine alkaloid 1 ชนิด คือ canarosine, สารกลุ่ม flavonoid glycoside 1 ชนิด คือ rutin, สาร epi-inositol 6-*O*-methyl ether, β-sitosterol glucoside และสารผสมระหว่าง β-sitosterol และ stigmasterol ในอัตราส่วน 2:1 สาร canarosine ที่ความเข้มข้น 100 ไมโครกรัม/มิลลิลิตร สามารถยับยั้งการจับตัวรับโดปามีน-1 ได้ถึง 95% และมีค่า IC_{50} 39.4 ไมโครโมลาร์ อัลคาลอยด์นี้จึงมีฤทธิ์ต้านเชื้อ *Plasmodium falciparum* สายพันธุ์ K1 โดยมีค่า IC_{50} 4.48 ไมโครกรัม/มิลลิลิตร และมีฤทธิ์ปานกลางในการต้านเชื้อ Herpes simplex virus type 1

การศึกษาองค์ประกอบทางเคมีของประ (วงศ์ Euphorbiaceae) สามารถแยกสารได้ทั้งสิ้น 25 ชนิดจากลำต้น ดอกและใบของพืชชนิดนี้ จากลำต้นประสามารถแยกสารได้ 14 ชนิด เป็นสารกลุ่ม triterpenoid 4 ชนิด คือ lupeol, lupeol acetate, acetyl aleuritolic acid และ germanicol palmitate, เป็นสารใหม่ในกลุ่ม cleistanthane diterpenoid 1 ชนิด คือ 2,3-*seco* sonderianol, สารกลุ่ม pimarane diterpenoid 2 ชนิด คือ yucalexin P-17 และ yucalexin P-15, สารกลุ่ม beyerane diterpenoid 1 ชนิด คือ yucalexin B-22, สารกลุ่ม biflavonoid 1 ชนิด คือ amentoflavone, พร้อมทั้ง scopoletin, syringaldehyde, oleic acid และสารผสมของ β-sitosterol กับ stigmasterol ในอัตราส่วน 1:1 จากดอกประ สามารถแยกสารได้ 8 ชนิด ได้แก่ lupeol, lupeol acetate, สารกลุ่ม flavonoid 1 ชนิด คือ quercetin, สารกลุ่ม biflavonoid 2 ชนิด คือ amentoflavone และ putraflavone, ellagic acid 3,3′-dimethyl ether และสารผสมของ β-sitosterol กับ stigmasterol ในอัตราส่วน 1:1 จากใบประสามารถแยกสารได้ 13 ชนิด เป็นสารใหม่ในกลุ่ม taraxerane triterpenoid 2 ชนิด คือ 2,3-*seco*-taraxer-14-ene-2,3,28-trioic acid 2,3 dimethyl ester และ 2,3-*seco*-taraxer-14-ene-2,3,28-trioic acid 3-methyl ester, สารกลุ่ม triterpenoid ที่เคยมีรายงานมาก่อน 2 ชนิด คือ hopenol-B และ aleuritolic acid, สารกลุ่ม biflavonoid 4 ชนิด คือ amentoflavone, sequoiaflavone, putraflavone และ ginkgetin, สารกลุ่ม flavonoid 1 ชนิด คือ kaempferol, ellagic acid 3,3′-dimethyl ether, β-sitosterol glucoside และ สารผสมของ β-sitosterol กับ stigmasterol

ในส่วนของสารที่สกัดได้จากประ พบว่าสาร 2,3-seco-taraxer-14-ene-2,3,28-trioic acid 2,3-dimethyl ester มีความเป็นพิษระดับปานกลางต่อ BC cell line ด้วยค่า IC_{50} 7.08 ไมโครกรัม/มิลลิลิตร เป็นพิษสูงต่อ NCI-H187 cell line ด้วยค่า IC_{50} 4.65 ไมโครกรัม/มิลลิลิตร และ มีฤทธิ์ต้านเชื้อ *Mycobacterium tuberculosis* โดยมีค่า MIC 3.13 ไมโครกรัม/มิลลิลิตร สาร lupeol มีความเป็นพิษระดับอ่อนต่อ NCI-H187 cell line ด้วยค่า IC_{50} 18.4 ไมโครกรัม/มิลลิลิตร สาร ginkgetin มีความเป็นพิษระดับอ่อนต่อ KB และ BC cell line ด้วยค่า IC_{50} 18.5 และ 10.3 ไมโครกรัม/มิลลิลิตร ตามลำดับ อย่างไรก็ดี สาร lupeol, ginkgetin และ putraflavone มีความเป็นพิษต่อ Vero cell ด้วยค่า IC_{50} 13.4, 34.8 และ 35.4 ไมโครกรัม/มิลลิลิตร ตามลำดับ ทั้งสาร 2,3-seco-taraxer-14-ene-2,3,28-trioic acid 3-methyl ester และ lupeol ต่างก็มีฤทธิ์ต้าน *M. tuberculosis* ด้วยค่า MIC 50 ไมโครกรัม/มิลลิลิตร ในกลุ่ม biflavonoid พบว่าสาร ginkgetin, putraflavone, amentoflavone และ sequoiaflavone มีฤทธิ์ต้าน *M. tuberculosis* ด้วยค่า MIC 25, 50, 100 และ 200 ไมโครกรัม/มิลลิลิตร ตามลำดับ ส่วนสาร yucalexin P-17 มีฤทธิ์ต้านเชื้อ Herpes simplex virus type 1 ด้วยค่า IC_{50} 3.60 ไมโครกรัม/มิลลิลิตร

สาขาวิชา เภสัชเวท
ปีการศึกษา 2550

ลายมือชื่อนิสิต.....
ลายมือชื่ออาจารย์ที่ปรึกษา.....รุทธ์ อุทธิศรี.....

4676956233 : MAJOR PHARMACOGNOSY

KEY WORD: *CANAVALIA ROSEA* / *ELATERIOSPERMUM TAPOS* / TRITERPENOIDS / DITERPENOIDS / ALKALOIDS

DUANGPEN PATTAMADILOK : PHYTOCHEMICAL STUDY OF *CANAVALIA ROSEA* AND *ELATERIOSPERMUM TAPOS*. THESIS ADVISOR : ASSOC. PROF. RUTT SUTTISRI, Ph.D. , 338 pp.

Phytochemical investigation of the chemical constituents of *Canavalia rosea* (Papilionaceae) aerial parts led to the isolation of six compounds including a new guanidine alkaloid, canarosine, a flavonoid glycoside, rutin, epi-inositol 6-*O*-methyl ether, β-sitosterol glucoside, and a 2:1 mixture of β-sitosterol and stigmasterol. Canarosine, at 100 μg/ml, caused 95% inhibition dopamine-1 receptor binding with the IC_{50} value of 39.4 μM. The alkaloid was also active against *Plasmodium falciparum* K1 strain with IC_{50} value of 4.48 μg/ml, was moderately active against Herpes simplex virus type 1.

Study of chemical constituents of *Elateriospermum tapos* (Euphorbiaceae) led to the isolation of a total of twenty-five compounds from the stem, flowers and leaves of this plant. From the stem, fourteen compounds including four triterpenoids, lupeol, lupeol acetate, acetyl aleuritolic acid and germanicol palmitate, a new cleistanthane diterpenoid, 2,3-*seco*-sonderianol, two pimarane diterpenoids, yucalexin P-17 and yucalexin P-15, a beyerane diterpenoid, yucalexin B-22, a biflavonoid, amentoflavone, along with scopoletin, syringaldehyde, oleic acid and a β-sitosterol/stigmasterol (1:1) mixture were isolated. Isolation of its flowers yielded eight compounds including lupeol, lupeol acetate, a flavonoid, quercetin, two biflavonoids, amentoflavone and putraflavone, ellagic acid 3,3′-dimethyl ether and a β-sitosterol/stigmasterol (1:1) mixture. Thirteen compounds were isolated from the leaves of this plant, including two new taraxerane triterpenoids, 2,3-*seco*-taraxer-14-ene-2,3,28-trioic acid 2,3-dimethyl ester and 2,3-*seco*-taraxer-14-ene-2,3,28-trioic acid 3-methyl ester, two known triterpenoids, hopenol-B and aleuritolic acid, four biflavonoids, amentoflavone, sequoiaflavone, putraflavone and ginkgetin, a flavonoid, kaempferol, ellagic acid 3,3′-dimethyl ether, β-sitosterol glucoside and a β-sitosterol/stigmasterol mixture.

Among the compounds isolated from *E. tapos*, 2,3-*seco*-taraxer-14-ene-2,3,28-trioic acid 2,3-dimethyl ester exhibited moderate cytotoxicity against BC cell line with IC_{50} 7.08 μg/ml, strong cytotoxicity against NCI-H187 cell line with IC_{50} value of 4.65 μg/ml, and anti-*Mycobacterium tuberculosis* with MIC value of 3.13 μg/ml. Lupeol was weakly cytotoxic against NCI-H187 cell line with IC_{50} 18.4 μg/ml. Ginkgetin showed weak cytotoxic activity against KB and BC cell lines, with IC_{50} values of 18.5 and 10.3 μg/ml, respectively. However, lupeol, ginkgetin and putraflavone were cytotoxic against Vero cells with IC_{50} values of 13.4, 34.8 and 35.4 μg/ml, respectively. Both 2,3-*seco*-taraxer-14-ene 2,3,28-trioic acid 3-methyl ester and lupeol were active against *M. tuberculosis* with the same MIC value of 50 μg/ml. Among the biflavonoids, ginkgetin, putraflavone, amentoflavone and sequoiaflavone showed antituberculosis activity with MIC values of 25, 50, 100 and 200 μg/ml, respectively. Yucalexin P-17 displayed anti-Herpes simplex virus type 1 activity with IC_{50} value of 3.60 μg/ml.

Field of study: Pharmacognosy Student's signature D. Pattamadilok

Academic year: 2007 Advisor's signature Rutt Suttisri

ACKNOWLEDGEMENTS

I would like to express my deepest gratitude to my thesis advisor, Associate Professor Dr. Rutt Suttisri of the Department of Pharmaceutical Botany, Faculty of Pharmaceutical Sciences, Chulalongkorn University, for his valuable advice, guidance, patience, and constant encouragement throughout my research study.

I would like to thank all members of my thesis committee for their critical perusal and for serving on my examination committee.

I am grateful to Associate Professor Dr. Thitima Pengsuparp of the Department of Biochemistry, Faculty of Pharmaceutical Sciences, Chulalongkorn University for the evaluation of dopamine-1 receptor inhibitory activity.

I am very thankful to Dr. Prapai Wongsinkongman of the Medicinal Plant Research Institute, Department of Medical Science, Ministry of Public Health for providing EI mass spectral data and helpful assistance in spectroscopic experiments.

I would also like to acknowledge financial support by a grant from Chulalongkorn University through a 90th Anniversary grant (Ratchadaphiseksomphot Endowment Fund).

On the personal side, I would like to thank previous/present graduate students and all staff members of the Department of Pharmaceutical Botany, Faculty of Pharmaceutical Sciences, Chulalongkorn University for their friendship, kind support and encouragement throughout the period of my study.

My appreciations are also extended to Mrs. Tidarat Boonruad and all staff members of the Medicinal Plant Research Institute, Department of Medical Science, Ministry of Public Health and Mrs.Yenchit Techadamrongsin of the Department for Development of Thai Traditional and Alternative Medicine, Ministry of Public Health for her kind support and encouragement throughout my study.

Finally, I would like to express my special and deepest appreciation to my family for their love, understanding and encouragement.

CONTENTS

CHAPTER **Page**

CHAPTER **Page**

CHAPTER **Page**

CHAPTER **Page**

CHAPTER **Page**

CHAPTER **Page**

LIST OF TABLES

Table **Page**

LIST OF FIGURES

Figure **Page**

Figure **Page**

Figure **Page**

Figure **Page**

Figure **Page**

Figure **Page**

Figure **Page**

Figure **Page**

LIST OF SCHEMES

LIST OF ABBREVIATIONS AND SYMBOLS

$[\alpha]^{25}_{D}$	=	Specific rotation at 25 °C and sodium D line (589 nm)
acetone-d_6	=	Deuterated acetone
α	=	Alpha
β	=	Beta
br	=	Broad (for NMR spectra)
br s	=	Broad singlet (for NMR spectra)
BSA	=	Bovine serum albumin
BuOH	=	Butanol
c	=	Concentration
°C	=	Degree celcius
calcd	=	Calculated
CD_3OD	=	Deuterated methanol
$CDCl_3$	=	Deuterated chloroform
CFU	=	Colony forming unit
$CHCl_3$	=	Chloroform
CH_2Cl_2	=	Dichloromethane
cm	=	Centimeter
cm^{-1}	=	reciprocal centimeter (unit of wave number)
^{13}C NMR	=	Carbon-13 Nuclear Magnetic Resonance
2D NMR	=	Two dimensional Nuclear Magnetic Resonance
DEPT	=	Distortionless Enhancement by Polarization Transfer
DMSO-d_6	=	Deuterated dimethyl sulfoxide
d	=	doublet (for NMR spectra)
dd	=	doublet of doublets (for NMR spectra)
ddd	=	doublet of doublets of doublets (for NMR spectra)
dt	=	doublet of triplets (for NMR spectra)
EI MS	=	Electron Impact Mass Spectrometry
ESI TOF MS	=	Electrospray Ionization Time of Flight Mass Spectrometry
EtOAc	=	Ethyl acetate
EtOH	=	Ethanol
FT-IR	=	Fourier Transform Infrared Spectrum

g	=	Gram
h	=	Hour
^{1}H NMR	=	Proton Nuclear Magnetic Resonance
^{1}H-^{1}H COSY	=	Homonuclear (Proton-Proton) Correlation Spectroscopy
HMBC	=	^{1}H-detected Heteronuclear Multiple Bond Coherence
HMQC	=	^{1}H-detected Heteronuclear Multiple Quantum Coherence
HR ESI MS	=	High Resolution Electrospray Ionization Mass Spectrometry
HSQC	=	Heteronuclear Single Quantum Correlation
Hz	=	Hertz
IC_{50}	=	Median Inhibitory Concentration
J	=	Coupling constant
KBr	=	Potassium bromide
Kg	=	Kilogram
L	=	Liter
m	=	Meter
m	=	Multiplet (for NMR spectra)
$[M+H]^{+}$	=	Protonated molecular ion
mm	=	Millimeter
ml	=	Milliliter
mp	=	Melting point
MS	=	Mass Spectrometry
mult.	=	Multiplicity
MW	=	Molecular weight
m/z	=	Mass to charge ratio
nm	=	nanometer
NMR	=	Nuclear Magnetic Resonance
NOESY	=	Nuclear Overhauser Enhancement Spectroscopy
OD	=	Optical density
PBS	=	Phosphate Buffer Saline
ppm	=	Part-per-million
q	=	Quartet (for NMR spectra)
rpm	=	Round per minute
s	=	Singlet (for NMR spectra)
sp.	=	Species

t	=	Triplet (for NMR spectra)
td	=	Triplet of doublets (for NMR spectra)
TLC	=	Thin layer chromatography
δ	=	Chemical shift
UV	=	Ultraviolet
μg	=	Microgram
μl	=	Microliter
ν_{max}	=	Wave number at maximal absorption
ε	=	Molar absorptivity

CHAPTER I

INTRODUCTION

The Leguminales is an order of trees, shrubs or herbs which occur worldwide. The leaves of these plants are simple to bipinnate, with or without stipules. Their flowers are either actinomorphic or zygomorphic, with free or some partially united petals. Their stamens are few to numerous, free or variously connate (mostly diadelphous). The fruit is often a legume or indehiscent, sometimes winged, with seeds that are without endosperm. This order can be separated into three families: Caesalpiniaceae, Mimosaceae and Papilionaceae.

The family Papilionaceae comprises about 400 genera and at least 10,000 species (Porter, 1967). In Thailand, at least 76 genera and 267 species of this plant family have been documented (ส่วนพฤกษศาสตร์ป่าไม้ สำนักวิชาการป่าไม้ กรมป่าไม้, 2544). These genera and approximate number of species (in parenthesis) in each genus are as follows:

Abrus (2)	*Aeschynomene* (3)	*Afgekia* (3)
Aganope (2)	*Alysicarpus* (1)	*Antheroporum* (1)
Apios (1)	*Arachis* (1)	*Butea* (2)
Cajanus (4)	*Callerya* (4)	*Campylotropis* (2)
Canavalia (4)	*Centrosema* (1)	*Christia* (3)
Cicer (1)	*Clitoria* (4)	*Codariocalyx* (2)
Crotalaria (24)	*Cyamopsis* (1)	*Dalbergia* (23)
Dendrolobium (6)	*Derris* (12)	*Desmodium* (10)
Dicerma (1)	*Dolichos* (2)	*Droogmansia* (1)
Dumasia (1)	*Dunbaria* (1)	*Dysolobium* (2)
Eriosema (1)	*Erythrina* (5)	*Euchresta* (1)
Flemingia (8)	*Galactia* (1)	*Gliricidia* (1)
Glycine (1)	*Glycyrrhiza* (2)	*Hegnera* (1)
Indigofera (16)	*Lablab* (1)	*Lathyrus* (1)
Lens (1)	*Macroptilium* (1)	*Mecopus* (1)
Melilotus (1)	*Millettia* (16)	*Mucuna* (10)

Ormocarpum (1)	*Ormosia* (4)	*Ostryocarpus* (1)	
Pachyrhizus (1)	*Paracalyx* (1)	*Parochetus* (1)	
Phaseolus (2)	*Phylacium* (1)	*Phyllodium* (5)	
Pisum (1)	*Psophocarpus* (1)	*Pterocarpus* (3)	
Pueraria (6)	*Pycnospora* (1)	*Rhynchosia* (3)	
Sesbania (5)	*Shuteria* (1)	*Sinodolichos* (1)	
Smithia (2)	*Sophora* (3)	*Spatholobus* (4)	
Strongylodon (1)	*Stylosanthes* (2)	*Tadehagi* (1)	
Tephrosia (4)	*Uraria* (8)	*Vicia* (1)	*Vigna* (8)

Papilionaceae is an important plant family because the seeds and pods of many of its herbaceous species are valuable commodities. They are rich in protein and mineral; the most important being peas (*Pisum sativum* L.), broad bean (*Vicia faba* L.), ground nuts (*Arachis hypogaea* L.), soy beans (*Glycine max* Merr.), lentil (*Lens culinaris* Medix) and clover (*Trifolium pretense* L. and *T. repens* L.). Other useful species are, for examples, licorice (*Glycyrrhiza glabra* L.), tragacanth (*Astragalus gummifer* Lab.) and tolu balsam (*Myroxylon balsamum* Harm.) are employed in pharmaceutical formulations, indigo (*Indigofera tinctoria* L.), which provides blue dye, and *Derris* and *Lonchocarpus* spp., which contain the insecticidal rotenone.

Canavalia rosea (Sw.) DC. (syn. *C. maritima* Thouars) (ถั่วคล้า, ไก่เตี้ย) is a ground plant of the family Papilionaceae commonly found in coastal sand. It is 6 to 12 inches in height, but can occasionally be found climbing a small tree. It has evergreen, trifoliate leaves. Leaf-rachis is (inclusive of 2-15 cm petiole) 3 ½ -19 cm long. Leaflets are obovate or broadly oval, rounded, truncate or emarginated, often with triangular apical point, 3-15 cm by 2-2 ½ cm. Small racemes inflorescences occur among these bright green leaves throughout the year. The flower has 6-26 cm peduncle; 5-12 cm rachis of raceme, rarely up to 18 cm long; 3-12 floriferous tubercles; 4-6 mm pedicel; 8-11 mm calyx- tube; 4-5 mm upper lip. Corolla is pink to purple; standard with a white median streak, emarginated; 2 to 2 ¾ cm-long-limbs. These flowers then turn into robust, woody pods. The pods is linear, straight or faintly curved, 6-15 cm by 1 ¾ -3 cm, 2-10 seeds (Backer and Van Den Brink, 1968). On the Gulf Coast of Mexico, this plant is smoked as marijuana substitute, producing effect similar to marijuana, but its psychoactive substance have not been isolated. L-betonicine has been isolated from this plant, however, there is no evidence that this

compound is hallucinogen. Other species of this genus, *C. gladiata* is used medicinally. In China, the pods and seeds have tonic, stomachic and bechic properties and strengthen the kidneys. Ashes of the pods and seeds are in a preparation to treat lumbago, and in an ointment for swelling. In Indo-China, pods and young seeds are edible, but ripe seeds soften only imperfectly even after prolonged cooking. In Indonesia, the seeds, after soaking, are roasted and eaten as delicacies, also sold in the market as medicine. They contain phytosterols, cystine, canavaline, arginine, choline, trigonelline, kitogene, and urease. Canavaline is a non-toxic antibiotic useful in treating certain pneumococci (Perry and Metzger, 1980).

Three other *Canavalia* species found in Thailand are *C. cathartica* Thouars (ถั่วกระเป๋า), *C. ensiformis* (L.) DC. (ถั่วแขก) and *C. gladiata* (Jacq.) DC. (ถั่วพร้า).

Elateriospermum tapos Blume is another plant investigated in this study. It belongs to the family Euphorbiaceae, which is a large, worldwide plant family occasionally with milky juice. The majority of euphorbiaceous species is found in tropical and subtropical regions. The leaves of these plants are alternate or opposite, simple or seldom trifoliate or sometimes reduced to scales, mostly stipulated. The flowers are regular, unisexual, and may occur either on the same plant (monoecious), as in *Euphorbia*, or on different plants (dioecious), as in *Mercurialis*. Their sepals are valvate or imbricate or in very specialized inflorescences sometimes much reduced or absent. The flowers usually have five perianth segments, but in some genera (e.g. *Jatropha*, *Aleurites* and *Caperonia*) petals are also present and in others the perianth is lacking altogether. There are one to very numerous stamens, free or connate, with mostly 2-locular (sometimes 3 or 4-locular) anther. Ovary is superior and usually 3-locular. The fruits are usually a schizocarp, sometimes a drupe (Heywood, 1978; Hutchinson, 1959).

The family Euphorbiaceae comprises about 300 genera and 5000 species (Chayamarit and Van Welzen, 2005). In Thailand, about 73 genera and 377 species of this plant family can be found (ส่วนพฤกษศาสตร์ป่าไม้ สำนักวิชาการป่าไม้กรมป่าไม้, 2544). These genera and their approximate number of species (in parenthesis) are as follows.

Acalypha (10)	*Actephila* (3)	*Agrostistachys* (2)
Alchornea (3)	*Aleurites* (1)	*Antidesma* (15)

Aporosa (21)	*Baccaurea* (11)	*Balakata* (1)
Baliospermum (5)	*Bischofia* (1)	*Blachia* (2)
Blumeodendron (1)	*Breynia* (7)	*Bridelia* (10)
Chaetocarpus (1)	*Chondrostylis* (1)	*Chorisandrachne* (1)
Chrozophora (1)	*Cladogynos* (1)	*Claoxylon* (4)
Cleidion (1)	*Cleistanthus* (14)	*Cnesmone* (3)
Codiaeum (1)	*Colobocarpos* (1)	*Croton* (27)
Dalechampia (1)	*Drypetes* (16)	*Elateriospermum* (1)
Endospermum (3)	*Epiprinus* (2)	*Erismanthus* (2)
Euphorbia (29)	*Excoecaria* (5)	*Flueggea* (1)
Galearia (1)	*Glochidion* (25)	*Hevea* (1)
Homalanthus (1)	*Homonoia* (1)	*Hura* (1)
Hymenocardia (1)	*Jatropha* (5)	*Koilodepas* (1)
Macaranga (17)	*Mallotus* (17)	*Manihot* (2)
Margaritaria (1)	*Megistostigma* (1)	*Microdesmis* (1)
Microstachys (1)	*Ostodes* (1)	*Paracroton* (1)
Pedilanthus (2)	*Phyllanthus* (33)	*Ptychopyxis* (1)
Ricinus (1)	*Sampantaea* (1)	*Sapium* (1)
Sauropus (25)	*Severinia* (1)	*Shirakiopsis* (1)
Spathiostemon (1)	*Strophioblachia* (1)	*Sumbaviopsis* (1)
Suregada (1)	*Thyrsanthera* (1)	*Trewia* (1)
Triadica (1)	*Trigonostemon* (13)	*Vernicia* (2) *Wetria* (1)

This family furnishes several plant species of significant economic importance, such as para rubber (*Hevea brasiliensis* Mull. Arg.), tapioca (*Manihot esculenta* Crantz) and physic nut (*Jatropha curcas* L.). Castor oil is obtained from the seeds of *Ricinus communis* L. and a very powerful purgative comes from the seeds of *Croton tiglium* L. Kamala is a red dye obtained from the regmata of *Mallotus philippensis* Mull.Arg. Plaunotol, an antiulcer drug, can be extracted from the leaves of a Thai plant, *Croton stellatopilosus* Ohba.

Elateriospermum tapos Blume, known in Thai as “Pra” or “Kra”, is a tree 27-50 m in height. In Indonesia, its sticky white latex is used as dressing for wounds and, in Sarawak, it is applied on the foot as a treatment for cracked sole. Its leaf blade is elliptic to obovate, 5-24 by 2-7.5 cm, with 1-8 cm long petiole. Its triangular stipule is 2-3 mm long. The young leaves are red in color. The inflorescence is up to 19 cm

long, hairy, with cymules 0.5-6 cm long. The flowers are white to pale yellow, fragrant with unpleasant smell. Its flowering indicates the start of the rice season. The staminate flowers are 2.4-3.5 mm in diameter; their pedicels are 2-7 mm long. The sepals are ovate, with rounded apex, hairy outside. The disc is 0.8-1.3 mm long. The stamens are yellow, with filaments of 0.3-2 mm in length. The anthers are about 0.8-1.2 by 0.2-0.4 mm. The pistillate flowers are 3.2-5.3 mm in diameter, and the pedicels are 1.3-4.2 mm long, hairy. The sepals are ovate, 4.5-8 by 3.2-5.5 mm, with disc of 1-1.3 mm high. The ovary is 2.5-4 by 2-2.6 mm, densely hairy. The style and stigma are 0.3-0.5 mm long. Its oblong-ellipsoid fruit is longitudinally 3-grooved, 3.2-5.3 by 2.2-4.5 cm, glabrous. Its color changes from green via red to dark brown. The seeds are 3.2-3.6 by 1.4-2.2 cm, brownish-grey to dark brown. These seeds contain hydrocyanic acid and, thus, are poisonous. However, they can be eaten after being cooked or roasted, although when excess consumption can cause dizziness (Chayamarit and Van Welzen, 2005).

Preliminary bioactivity screening has revealed that the 95% ethanol extract of the aerial parts of *C. rosea* exhibited inhibitory activity of dopamine-1 receptor for 50% and cytotoxicity against human small cell lung cancer (NCI-H187) cell line with IC_{50} values of 6.30 μg/ml. In addition, the hexane extract of *E. tapos* leaves exhibited cytotoxicity against human small cell lung cancer (NCI-H187), breast cancer (BC) and oral human epidermoid carcinoma (KB) cell lines at IC_{50} values of 8.53, 7.69 and 3.29 μg/ml, respectively, as well as antimycobacterial activity at MIC value of 12.5 μg/ml. Therefore, these plants were selected for further investigation of their bioactive chemical constituents. Therefore, the purposes of this research are as follows:

1. Isolation and purification of compounds from aerial parts of *Canavalia rosea* and *Elateriospermum tapos*
2. Determination of chemical structures of the isolated compounds
3. Evaluation of biological activities of the isolated compounds

Figure 1. *Canavaria rosea* (Sw) DC. (http://www.google.com/canavalia)

- **A.** Leaves
- **B.** Inflorescence
- **C.** Flower
- **D.** Pod

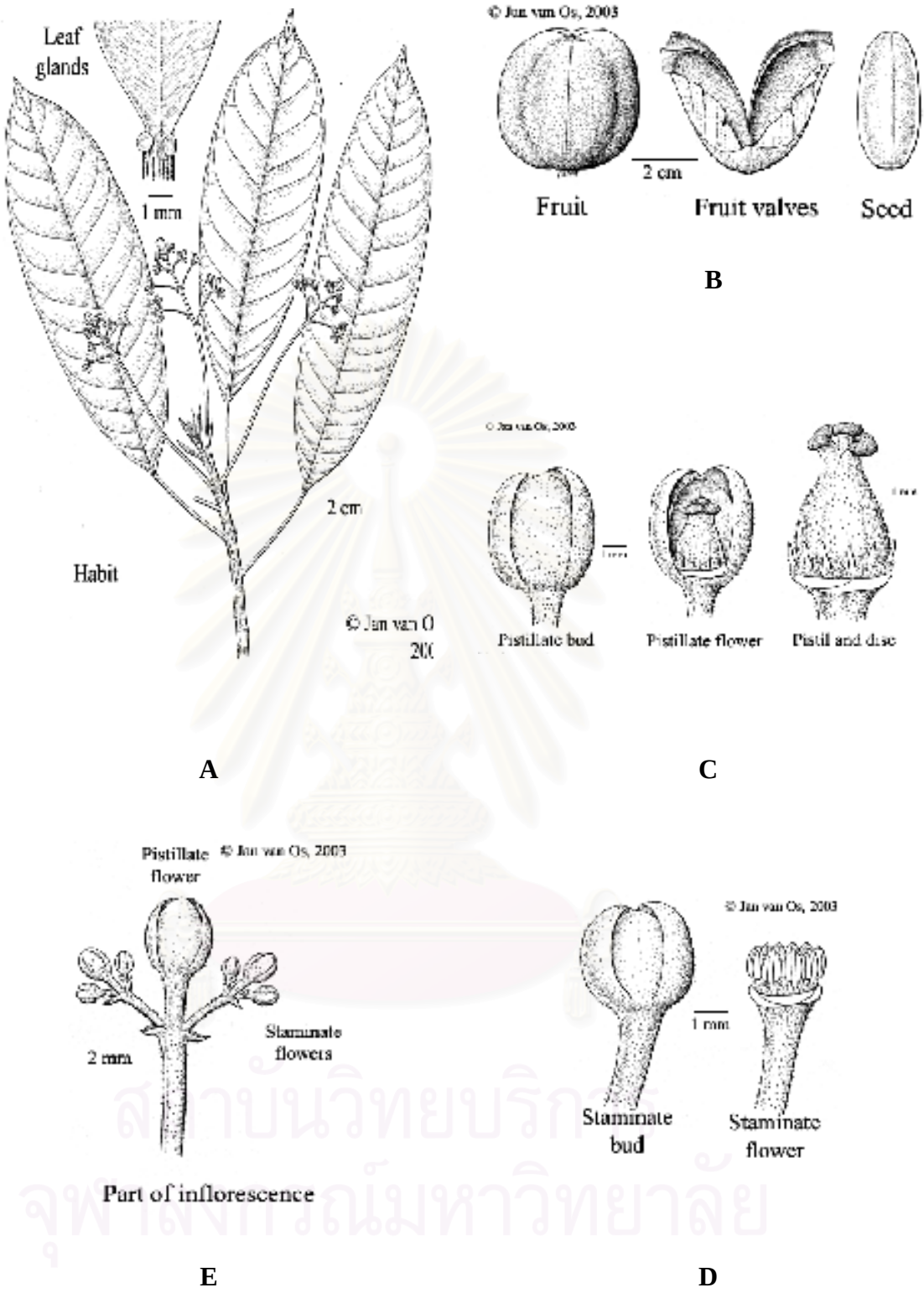

Figure 2. *Elateriospermum tapos* Blume (http://www.google.com/elateriospermum)

A. Whole plant **B.** Fruit and Seed **C.** Pistillate flower

D. Staminate flower **E.** Part of inflorescence

CHAPTER II

HISTORICAL

Canavaria rosea (Sw.) DC. belongs to the family Leguminosae. Plants in this family contain several characteristic chemical constituents such as guanidine alkaloids, tetrahydroisoquinoline alkaloids, pterocarpans, aurones and isoflavanoids.

Another plant in this study, *Elateriospermum tapos*, belongs to the family Euphorbiaceae. Studies of the chemical constituents of euphorbiaceous plants revealed the presence of various types of compounds, some of which are bioactive secondary metabolites displaying bioactivities including antiulcer, anticancer, antimalarial, antibacterial, antifungal and anti-inflammatory activities.

In this chapter, reviews of guanidine-type alkaloids in higher plants, pimarane and beyerane diterpenoids in euphorbiaceous plants and cleistanthane diterpenoids in the plant kingdom, taraxerane triterpenoids and biflavones in the plants, as well as previously reported chemical constituents of *E. tapos*, are presented.

Guanidine alkaloids

Guanidine alkaloids are from various natural sources such as terrestrial, marine and freshwater microorganisms, marine invertebrates, marine sponges and higher plants. A number of plant families including Amaranthaceae, Compositae, Ranunculaceae, Euphorbiaceae, Leguminosae, Labiatae, Caryophyllaceae and Graminae were shown to contain guanidine alkaloids. These compounds were demonstrated to possess various biological activities. For example, argifin is a guanidine derivative isolated from the fungi *Gliocladium* sp. (Berlinck, 2002). Two guanidine alkaloids from a marine sponge, *Theonella* aff. *mirabilis*, were enzyme inhibitors: tokaramide A was a cathepsin B inhibitor, whereas miraziridine was a cysteine protease inhibitor (Berlinck, 2002). Neamphamide A, an inhibitor of HIV-1 cytopathic effect, was isolated from the sponge *Neamphius huxleyi* (Berlinck and Kossuga, 2005). Cyclotheonamides E4 and E5 are tryptase inhibitors isolated from a sponge of the genus *Ircinia* (Berlinck and Kossuga, 2005). Segetalin H possesses an estrogen-like activity isolated from plant of the family Caryophyllaceae, *Vaccaria segetalis* (Berlinck, 1999).

Distribution of guanidine alkaloids in the higher plants is shown in **Table 1**, and their structures are shown in **Figure 3**.

Table 1. Distribution of guanidine alkaloids in higher plants

Compounds	Sources	Family	Part	References
Alchorneine **(1.1)**	*Alchornea floribunda*	Euphorbiaceae	Root bark, leaves	Khuong-Huu *et al*., 1972
Alchornidine **(1.2)**	*A. javanensis*		Leaves	Hart *et al*., 1970
Alchornine **(1.3)**			Leaves, bark	
Caracasanamide G1 **(1.4)**	*Verbesina caracasana*	Compositae	Leaves	Fabricant *et al*., 2005
Caracasanamide G2 **(1.5)**				
Caracasanamide G3 **(1.6)**				
Caracasanamide G5 **(1.7)**				
Caracasanamide G6 **(1.8)**				
Caracasanamide G7 (Galegine) **(1.9)**	*Galega officinalis*	Leguminosae	Whole plant	Benn *et al*., 1996
	V. caracasana	Compositae	Leaves	Fabricant *et al*., 2005
	Verbena encelioides	Verbenaceae		
Cassiadinine **(1.10)**	*Cassia siamea*	Leguminosae	Flowers	Biswas and Mallik, 1986
Celogentin A **(1.11)**	*Celosia argentea*	Amaranthaceae	Seeds	Kobayashi *et al*., 2001
Celogentin B **(1.12)**				
Celogentin C **(1.13)**				
Celogentin D **(1.14)**				Suzuki *et al*., 2003
Celogentin E **(1.15)**				
Celogentin F **(1.16)**				
Celogentin G **(1.17)**				
Celogentin H **(1.18)**				
Celogentin J **(1.19)**				
Cimipronidine **(1.20)**	*Cimicifuga racemosa*	Ranunculaceae	Roots	Fabricant *et al*., 2005
4-Coumaroyl agmatine **(1.21)**	*Albizzia julibrissin*	Leguminosae	Leaves	

Table 1. Distribution of guanidine alkaloids in higher plants (continued)

Compounds	Sources	Family	Part	References
4-Coumaroyl agmatine **(1.21)**	*Hordeum bulbosum*	Gramineae	Seedling	Smith and Best, 1978
	H. distichon			
	H. jubatum			
	H. murinum			
	H. spontaneum			
5a,9a-Dihydro-5a-hydroxy millaurine **(1.22)**	*Millettia laurentii*	Leguminosae	Seeds	Ngamga, Free and Fomum, 1994
Fontaineine **(1.23)**	*Fontainea pancheri*	Euphorbiaceae	Leaves	Lontsi *et al.*, 1998
4-Hydroxy galegine **(1.24)**	*Galega officinalis*	Leguminosae	Whole plant	Benn *et al*., 1996
4-Hydroxy smirnovine **(1.25)**	*G. orientalis*			
Isoalchorneine **(1.26)**	*Alchornea floribunda*	Euphorbiaceae	Root bark, leaves	Khuong-Huu *et al*., 1972
	A. hirtella			
N1,*N2*-Diisopen-tenyl guanidine (Pterogynine) **(1.27)**	*A. cordifolia*			Mavar-Manga *et al*., 2008
Leonurine **(1.28)**	*Leonurus artemisia*	Labiatae	Whole plant	Yeung *et al*., 1977
	L. sibiricus			
Martinellic acid **(1.29)**	*Martinella iquitosensis*	Bignoniaceae	Roots	Witherup *et al*., 1995
Martinelline **(1.30)**				
Millaurine A **(1.31)**	*Millettia laurentii*	Euphorbiaceae	Seeds	Ngamga *et al*., 2007
Millettonine **(1.32)**			Stem bark	Kamnaing *et al*., 1994
Moroidin **(1.33)**	*Laportea moroides*	Labiatae	Whole plant	Kobayachi *et al*., 2001
Segetalin H **(1.34)**	*Vaccaria segetalis*	Caryophyllaceae	Seeds	Fabricant *et al*., 2005
Spherophysine **(1.35)**	*Galega orientalis*	Leguminosae	Whole plant	Benn *et al*., 1996
	Sphaerophysa salsula		Leaves	Southon and Buckingham, 1989
Smirnovine **(1.36)**	*Galega orientalis*		Whole plant	Benn *et al*., 1996
	Smirnowia turkestana		Roots	Southon and Buckingham, 1989

Table 1. Distribution of guanidine alkaloids in higher plants (continued)

Compounds	Sources	Family	Part	References
Smirnovinine **(1.37)**	*Smirnowia turkestana*	Leguminosae	Roots	Southon and Buckingham, 1989
Stizolamine **(1.38)**	*Stizolobium hassjoo*		Seeds	Yoshida, 1976
N1,N2,N3-Triisopentenyl guanidine **(1.39)**	*Alchornea cordifolia*	Euphorbiaceae	Leaves, root bark	Mavar-Manga *et al*., 2008
	A. glandulosa		Leaves	Calvo *et al*., 2007

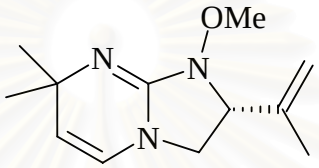

Alchorneine **(1.1)**

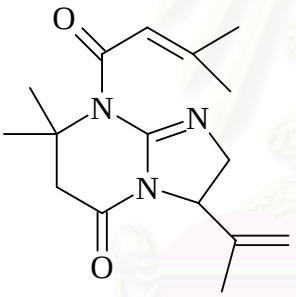

Alchornidine **(1.2)**

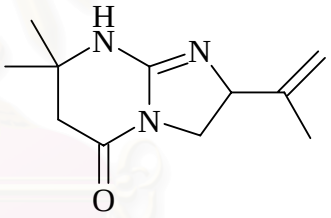

Alchornine **(1.3)**

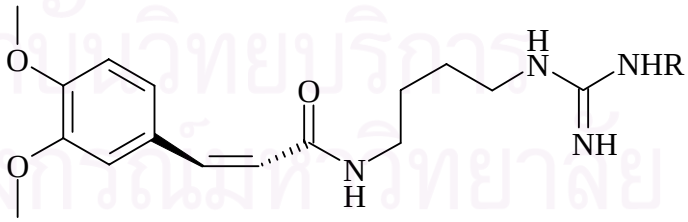

Caracasanamide G1 **(1.4)** R = prenyl
Caracasanamide G5 **(1.7)** R = H

Figure 3. Chemical structures of guanidine alkaloids from higher plants

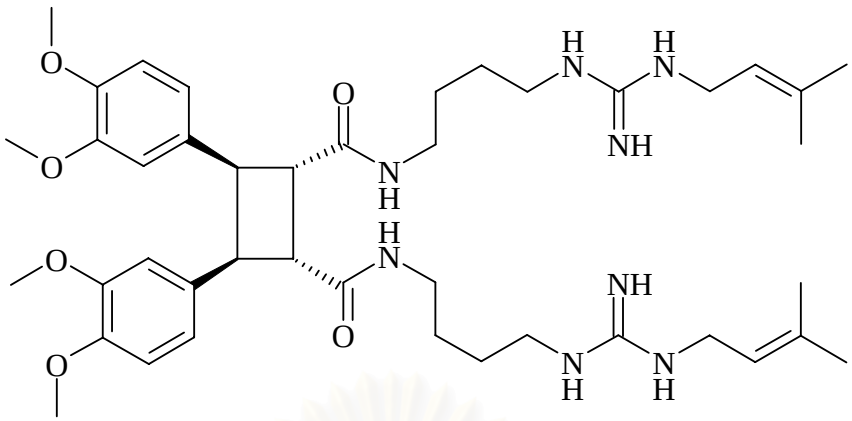

Caracasanamide G2 **(1.5)**

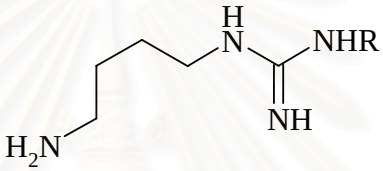

Caracasanamide G3 **(1.6)** R = prenyl
Caracasanamide G6 **(1.8)** R = H

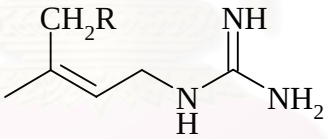

Caracasanamide G7 (Galegine) **(1.7)** R = H
4-Hydroxygalegine **(1.24)** R = OH

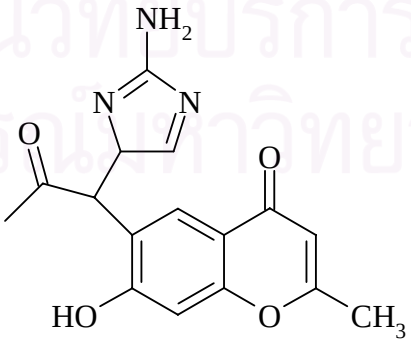

Cassiadinine **(1.10)**

Figure 3. Chemical structures of guanidine alkaloids from higher plants (continued)

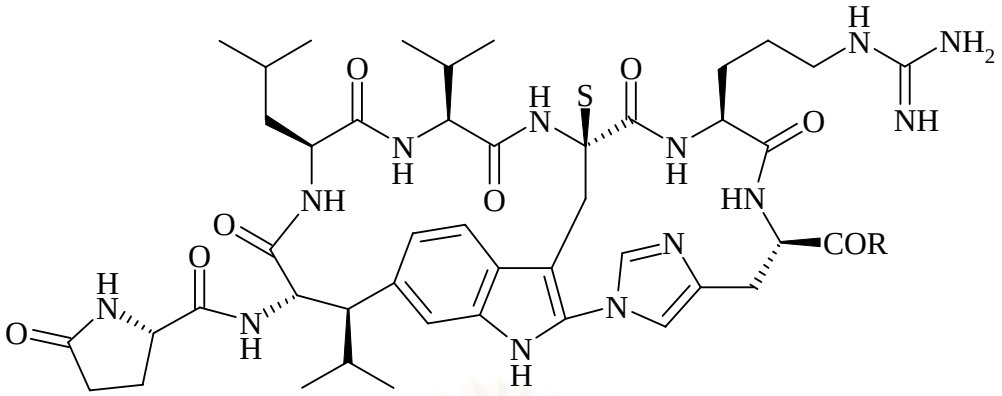

Celogentin A **(1.11)** R = H
Celogentin B **(1.12)** R = Histidine

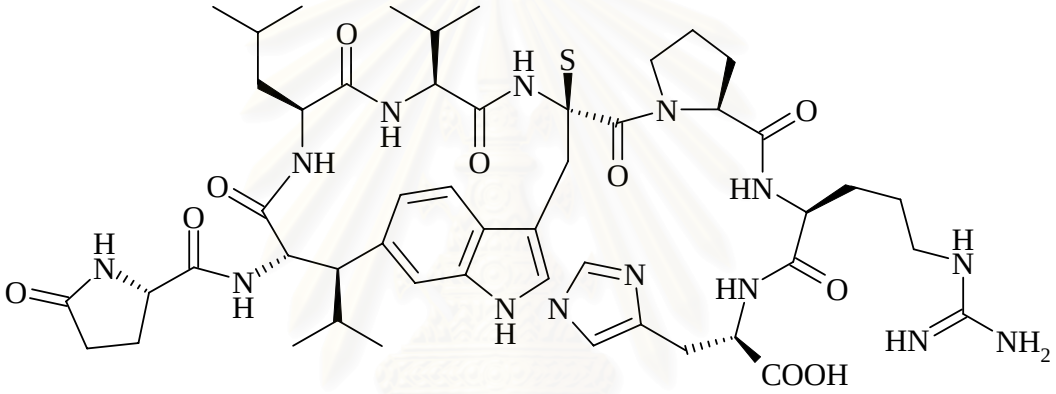

Celogentin C **(1.13)**

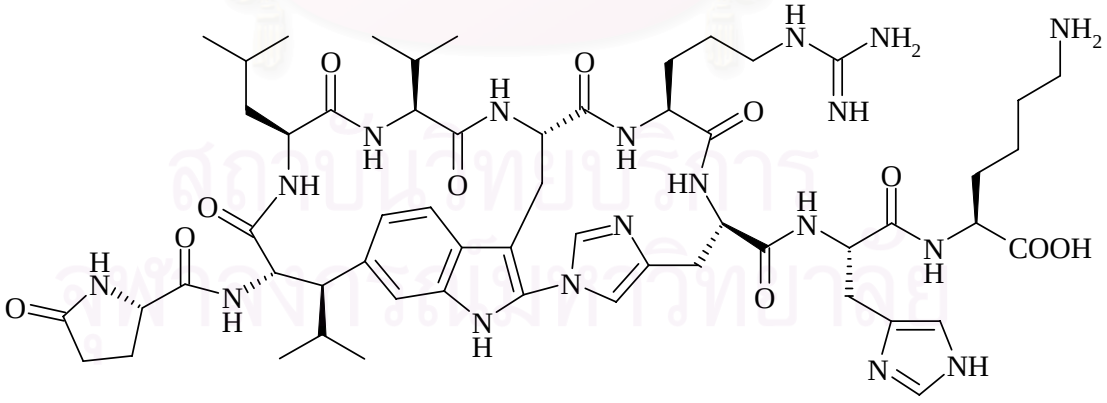

Celogintin D **(1.14)**

Figure 3. Chemical structures of guanidine alkaloids from higher plants (continued)

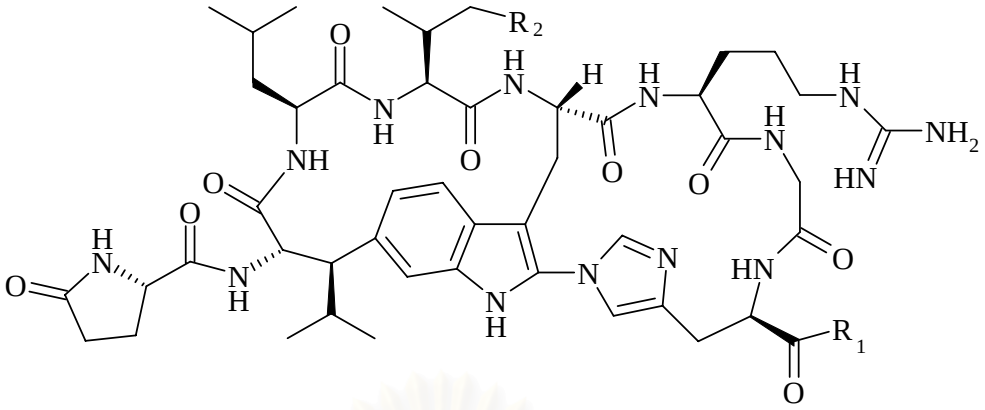

		R_1	R_2
Celogentin E	**(1.51)**	L-Asp	H
Celogentin F	**(1.16)**	L-Arg	H
Celogentin G	**(1.17)**	OH	Me
Celogentin H	**(1.18)**	L-Asp	Me
Celogentin J	**(1.19)**	L-Arg	Me

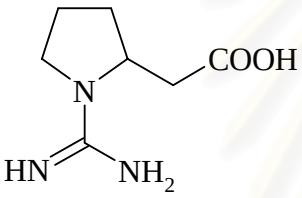

Cimipronidine **(1.20)**

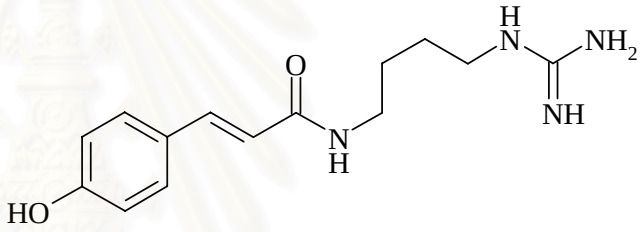

4-Coumaroylagmatine **(1.21)**

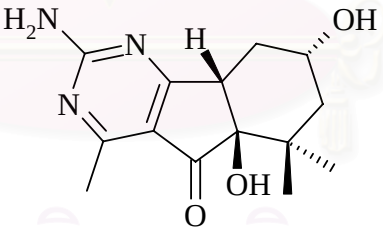

5a,9a-Dihydro-5a-hydroxymillaurine **(1.22)**

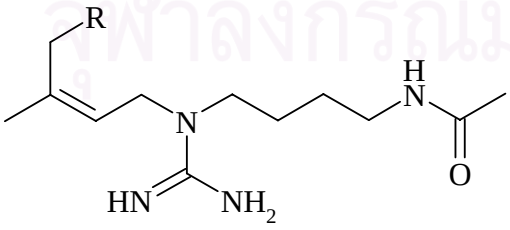

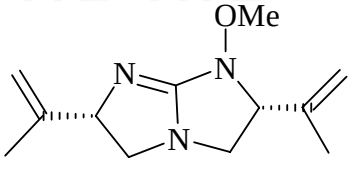

4-Hydroxy smirnovine **(1.25)** R = OH
Spherophysine **(1.33)** R = H

Isoalchorneline **(1.26)**

Figure 3. Chemical structures of guanidine alkaloids from higher plants (continued)

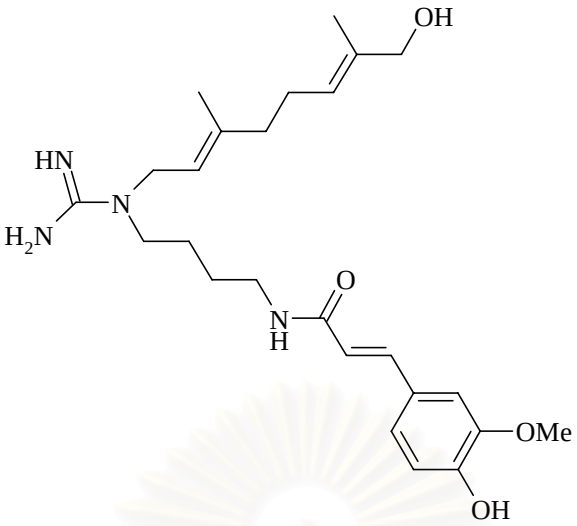

Fontaineine **(1.23)**

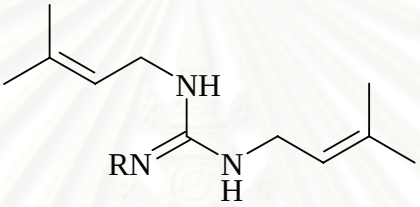

N1,*N2*-Diisopentenyl guanidine **(1.26)** R = H
N1,*N2*,*N3*-Triisopentenyl guanidine **(1.39)** R = isopentenyl

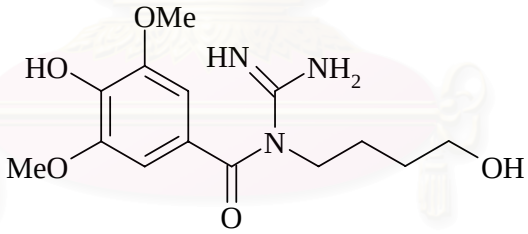

Leonurine **(1.28)**

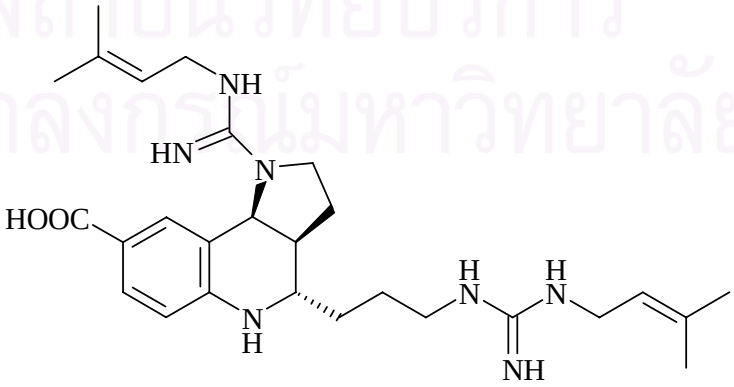

Martinellic acid **(1.29)**

Figure 3. Chemical structures of guanidine alkaloids from higher plants (continued)

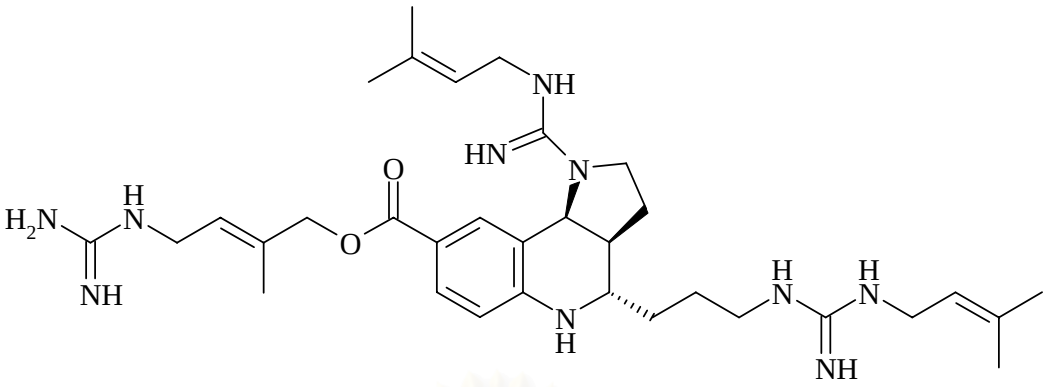

Martinelline **(1.30)**

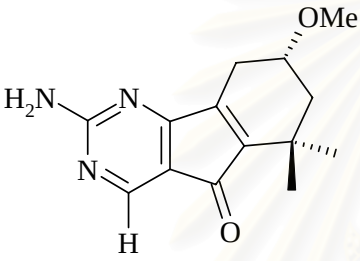

Millaurine A **(1.31)**

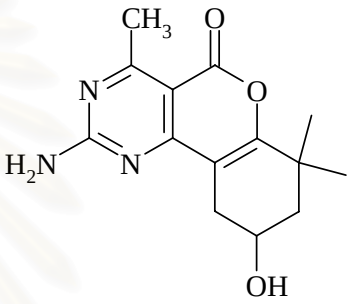

Millettonine **(1.32)**

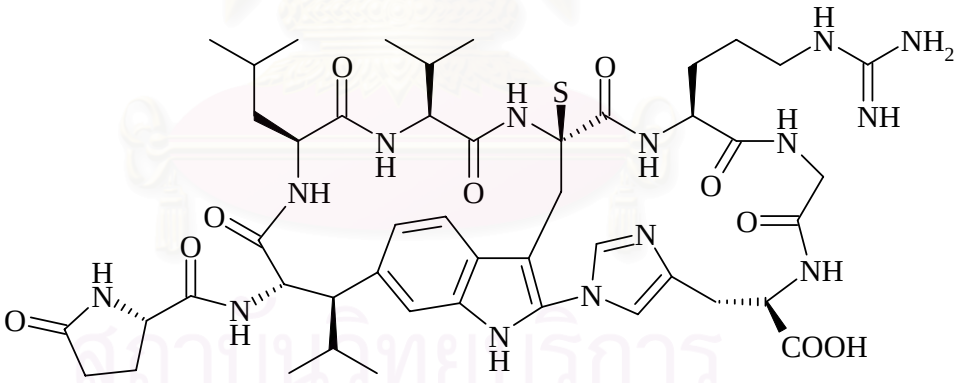

Moroidin **(1.33)**

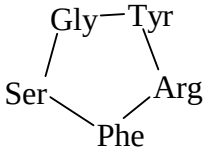

Segatalin H **(1.34)**

Figure 3. Chemical structures of guanidine alkaloids from higher plants (continued)

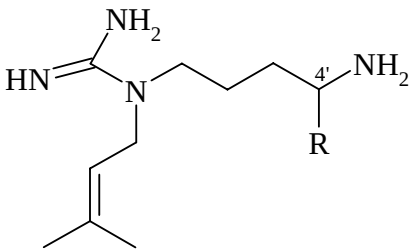

	R
Smirnovine **(1.36)**	Ac
Smirnovinine **(1.37)**	Carboxyacetyl

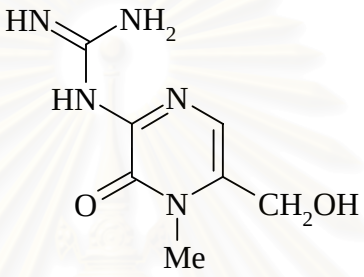

Stizolamine **(1.38)**

Figure 3. Chemical structures of guanidine alkaloids from higher plants (coninued)

Pimarane diterpenes of the family Euphorbiaceae

Pimarane diterpenes have been found in a number of plant families such as Labiatae (e.g. esquirolin B from the aerial parts of *Hyptis dilatata* and orthosiphons D and E from the aerial parts of *Orthosiphon stamineus*) (Takeda *et al*., 1993; Urones *et al*., 1998), Icacinaceae (e.g. icacine and icaceine from the leaves and roots of *Icacina guesfeidtii* and icacenone from the roots of *I. mannii* (On′okoko and Vanhaelen, 1980; On′okoko *et al*., 1985), Velloziaceae (e.g. compactone from the roots, stem and leaf sheath of *Vellozia piresiana* (Pinto, Peixoto and Fiorani, 1984), Polemoniaceae (e.g. akhdardiol from *Polemonium viscosum*) (Stierle, Stierle and Larsen, 1988), Scrophulariaceae (e.g. lapidate from the aerial parts of *Calceolaria lepida*) (Chamy *et al*., 1990) and Euphorbiaceae.

There have been few reports on the activities of these diterpenoids. Two pimarane diterpenes, pimaric acid and levopimaric acid, isolated from the roots of *Viguiera arenaria* (Compositae), were shown to exhibit inhibitory activity on the aggregation of rabbit platelets induced by platelet-activating factor (PAF), adenosine

diphosphate (ADP) and a calcium ionophore, while another pimarane diterpene, pimaradienoic acid, displayed inhibitory effect on vascular contractility by blocking extracellular calcium ion influx (Ambrosio *et al*., 2006).

Distribution of pimarane diterpenes in euphorbiaceous plants is summarized in **Table 2**, and their structures are shown in **Figure 4**.

Table 2. Distribution of pimarane diterpenes in euphorbiaceous plants

Compound	Source	Plant part	References
Ent-12α,16-dihydroxy-13[*R*]-pimar-8(14)-ene-3,15-dione **(2.1)**	*Euphorbia fidjiana*	Heartwood	Lal *et al*., 1990
Ent-12β-hydroxy methyl-3-oxo-16-nor pimar-8(14)-ene-15,21-carbolactone **(2.2)**			
Ent-16-hydroxy-13[*R*]-pimar-8(14)-ene-3,15-dione **(2.3)**			
Ent-pimara-8(14),15-dien-3β-ol **(2.4)**	*E. characias*	Leaves and stem	Appendino *et al*., 2000
3β-Hydroxy-19-*O*-acetyl-pimara-8(9),15-dien-7-one **(2.5)**	*Croton joufra*	Leaves	Sutthivaiyakit *et al*., 2001
Macarangonol **(2.6)**	*Macaranga tanarius*	Stem	Hui *et al*., 1971
Petalostigmone A **(2.7)**	*Petalostigma pubescens*	Heartwood	Grace *et al*., 2006
Petalostigmone B **(2.8)**			
Oblongifoliol **(2.9)**	*Croton oblongifolius*	Stem bark	Rao *et al*., 1968
3β,15ζ,16-Triacetoxy pimara-8(14)-ene **(2.10)**	*Euphorbia characias*	Leaves and stem	Appendino *et al*., 2000
3β,15ζ,16-Triacetoxy pimara-8(14)-en-2-one **(2.11)**			
Yucalexin P-4 **(2.12)**	*Manihot esculenta*	Roots	Sakai and Nakagawa, 1988
Yucalexin P-8 **(2.13)**			
Yucalexin P-10 **(2.14)**			
Yucalexin P-12 **(2.15)**			
Yucalexin P-13 **(2.16)**			
Yucalexin P-15 **(2.17)**			
Yucalexin P-17 **(2.18)**			
Yucalexin P-21 **(2.19)**			

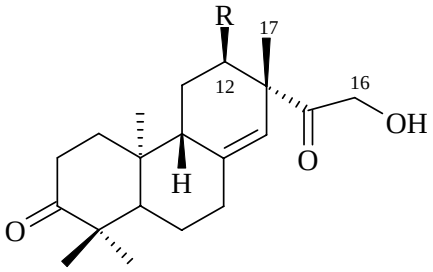

	R
Ent-12α,16-dihydroxy-13[*R*]-pimar-8(14)-ene-3,15-dione **(2.1)**	OH
Ent-16-hydroxy-13[*R*]-pimar-8(14)-ene-3,15-dione **(2.3)**	H

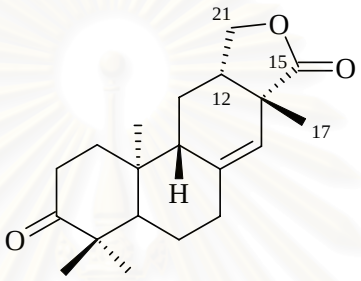

Ent-12β-hydroxymethyl-3-oxo-16-norpimar-8(14)-ene-15,21-carbolactone **(2.2)**

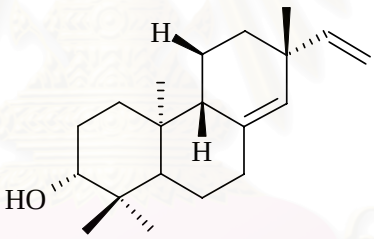

Ent-pimara-8(14),15-dien-3β-ol **(2.4)**

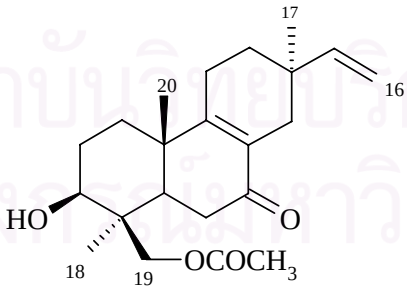

3β-Hydroxy-19-*O*-acetyl-pimara-8(9),15-dien-7-one **(2.5)**

Figure 4. Chemical structures of pimarane diterpenes in euphorbiaceous plants

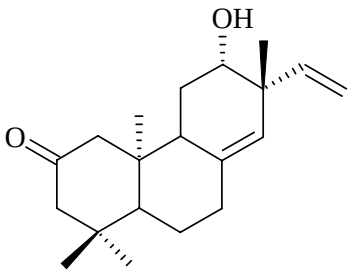

Macarangonol **(2.6)**

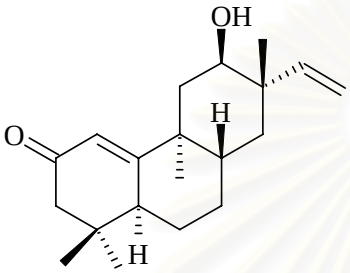

Petalostigmone A **(2.7)**

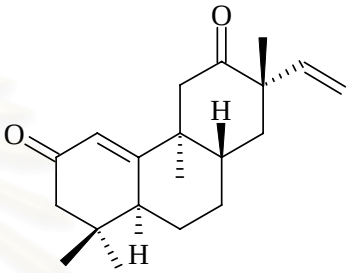

Petalostigmone B **(2.8)**

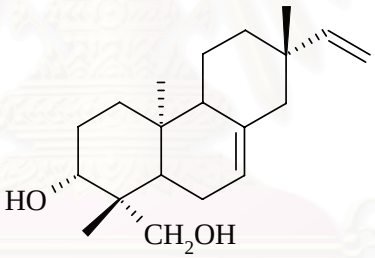

Oblongifoliol **(2.9)**

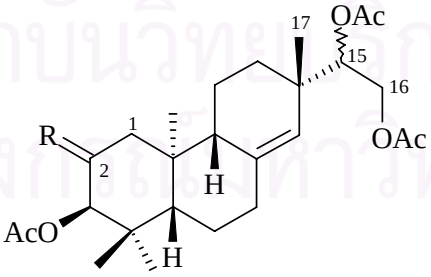

	R
3β,15ζ,16-Triacetoxypimara-8(14)-ene **(2.10)**	H, H
3β,15ζ,16-Triacetoxypimara-8(14)-en-2-one **(2.11)**	=O

Figure 4. Chemical structures of pimarane diterpenes in euphorbiaceous plants (continued)

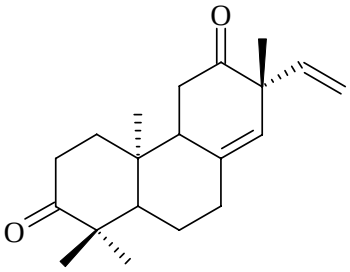

Yucalexin P-4 **(2.12)**

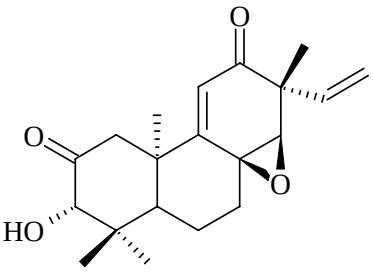

Yucalexin P-8 **(2.13)**

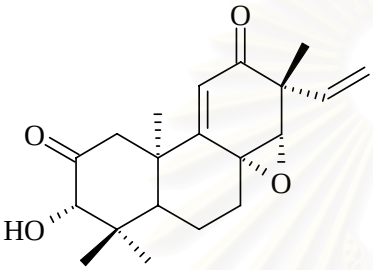

Yucalexin P-10 **(2.14)**

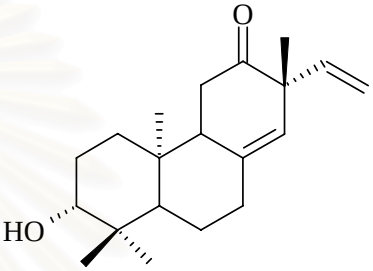

Yucalexin P-12 **(2.15)**

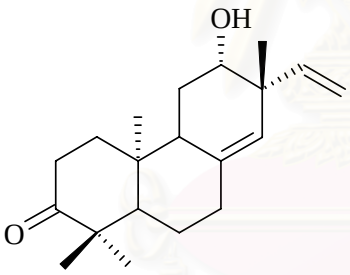

Yucalexin P-13 **(2.16)**

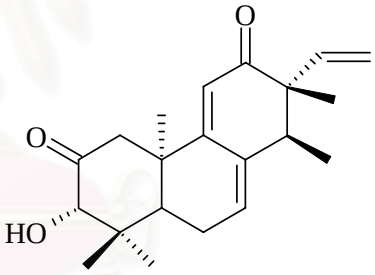

Yucalexin P-15 **(2.17)**

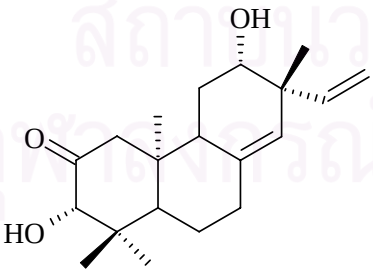

Yucalexin P-17 **(2.18)**

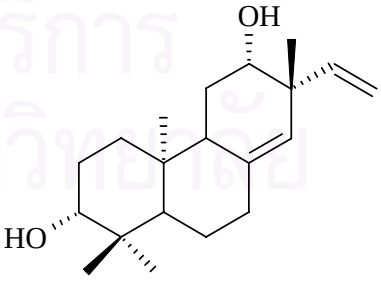

Yucalexin P-21 **(2.19)**

Figure 4. Chemical structures of pimarane diterpenes in euphorbiaceous plants (continued)

Beyerane diterpenes of the family Euphorbiaceae

Beyerane diterpenes were reported to be constituents of a number of plant families, including Euphorbiaceae, Compositae (e.g. nidoanomalin from the aerial parts of *Nidorella anomala* and beyerenic acid from the aerial parts of *Stevia aristata*) (Bohlmann and Wegner, 1982; Zdero, Bohlmann and Schmeda-Hirschmann, 1987), Labiatae (e.g. beyerenic acid from *Perymenium klattianum*; benuol, tobarrol and conchitriol from the aerial parts of *Sideritis reverchonii*; pusillatetrol from the aerial parts of *Sideritis valverdei*) (De Quesada, Rodri′quez and Valverde, 1974; Mar′quez *et al*., 1975; Bohlmann, Jakupovic and Schuster, 1985), Umbelliferae (e.g. elasclepial and elasclepic acid from the roots of *Elaeoselinum asclepium*) (Grande, Mancheno, and Sanchez, 1991), Erythroxylaceae (e.g. erythroxylol A and its malonate derivative from the timber of *Erythroxylum monogynum*) (Martin′, Rovirosa and Castillo, 1983), and Solanaceae (e.g. *ent*-19-hydroxy-17-acetoxybeyer-15-ene from the aerial parts of *Petunia patagonica*) (Guerreiero, De Fernandez and Giordano, 1984).

Distribution of beyerane diterpenes in plants of the family Euphorbiaceae is presented in **Table 3**, and their structures are shown in **Figure 5**. Several of these compounds are seco-ring A diterpenes, either between positions 2,3 or 3,4.

Table 3. Distribution of beyerane diterpenes in plants of the family Euphorbiaceae

Compound	Source	Plant part	References
Agallochin H **(3.1)**	*Excoecaria agallocha*	Wood	Konishi *et al*., 2003
Ent-6α,17-dihydroxy-3,4-*seco*-15-beyeren-3-oic acid **(3.2)**	*Beyeria calycina*	Whole plant	Ghisalberti, Jefferies and Sefton, 1978
Ent-15-epoxy-beyerane-3α-ol **(3.3)**	*E. agallocha*	Wood	Konishi *et al*., 2003
(4*S*)-*Ent*-18-hydroxy-3,4-*seco*-beyer-15-ene-3,17-dioate **(3.4)**	*B. calycina*	Whole plant	Ghisalberti *et al.*, 1978
(4*S*)-*Ent*-18-hydroxy-3,4-*seco*-beyer-15-ene-3,17-dioic acid **(3.5)**			
Ent-12-oxo-2,3-*seco*-beyer-15-ene-2,3-dioic acid **(3.6)**	*E. agallocha*	Wood	Konishi *et al*., 2003
Yucalexin B-5 **(3.7)**	*Manihot esculenta*	Roots	Sakai and Nakagawa, 1988
Yucalexin B-7 **(3.8)**			
Yucalexin B-9 **(3.9)**			
Yucalexin B-11 **(3.10)**			

Table 3. Distribution of beyerane diterpenes in plants of the family Euphorbiaceae (continued)

Compound	Source	Plant part	References
Yucalexin B-14 **(3.11)**	*Manihot esculenta*	Roots	Sakai and Nakagawa, 1988
Yucalexin B-16 **(3.12)**			
Yucalexin B-18 **(3.13)**			
Yucalexin B-20 **(3.14)**			
Yucalexin B-22 **(3.15)**			

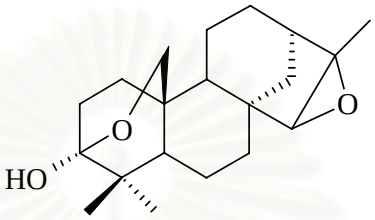

Agallochin H **(3.1)**

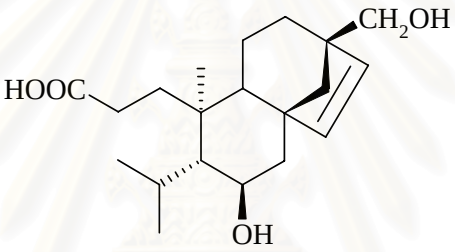

Ent-6α,17-dihydroxy-3,4-*seco*-15-beyeren-3-oic acid **(3.2)**

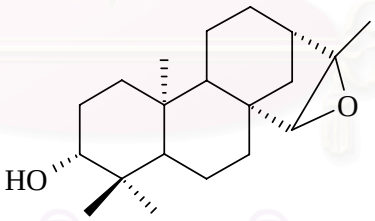

Ent-15-epoxy-beyerane-3α-ol **(3.3)**

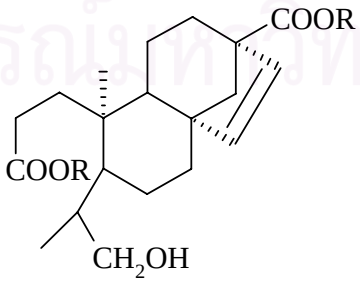

(4*S*)-*Ent*-18-hydroxy-3,4-*seco*-beyer-15-ene-3,17-dioate **(3.4)** R = Me
(4*S*)-*Ent*-18-hydroxy-3,4-*seco*-beyer-15-ene-3,17-dioic acid **(3.5)** R = H

Figure 5. Chemical structures of beyerane diterpenes in euphorbiaceous plants

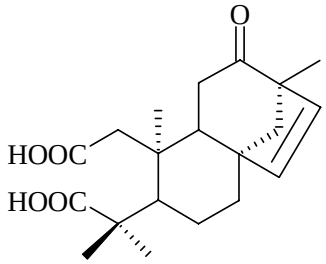

Ent-12-oxo-2,3-*seco*-beyer-15-ene-2,3-dioic acid **(3.6)**

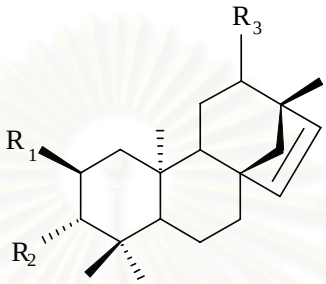

	R_1	**R_2**	**R_3**
Yucalexin B-5 **(3.7)**	=O	=O	=O
Yucalexin B-9 **(3.9)**	=O	β-OH	=O
Yucalexin B-18 **(3.13)**	=O	β-OH	β-OH
Yucalexin B-20 **(3.14)**	=O	β-OH	α-OH
Yucalexin B-22 **(3.15)**	α-OH	β-OH	=O

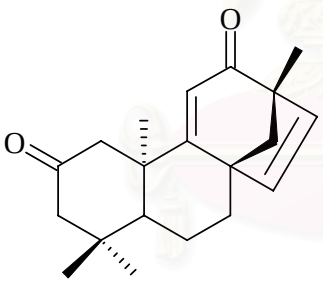

Yucalexin B-7 **(3.8)**

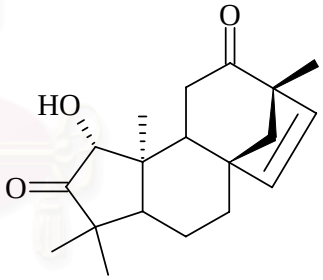

Yucalexin B-11 **(3.10)**

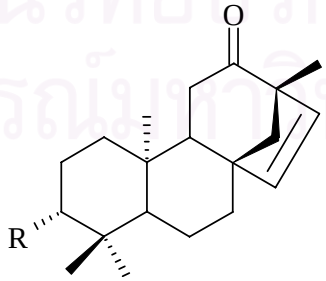

	R
Yucalexin B-14 **(3.11)**	OH
Yucalexin B-16 **(3.12)**	=O

Figure 5. Chemical structures of beyerane diterpenes in euphorbiaceous plants (continued)

Cleistanthane diterpenes in plant kingdom

Distribution of cleistanthane diterpenes in the plants is shown in **Table 4**, and their structures are presented in **Figure 6**.

Table 4. Distribution of cleistanthane diterpenes in plants

Compound	Source	Family	Plant part	References
20-Carboxalde-hyde-8,11,13-cleistanthatrien-7-one **(4.1)**	*Vellozia declinans*	Velloziaceae	Roots, stem, leaf sheath	Pinto, De A. Epifanio and Pizzolatii, 1992
6,8,11,13-Cleis-tanthatetraene **(4.2)**				
1,8,11,13-Cleis-tanthatetraen-3,7-dione **(4.3)**	*V. piresiana*			Pinto, Peixoto and Fiorani, 1984
8,11,13-Cleistan-thatriene **(4.4)**	*V. declinans*			Pinto, De A. Epifanio and Pizzolatii, 1992
8,11,13-Cleistan-thatrien-17-al (Veadeiral) **(4.5)**	*V. flavans*			Pinto *et al*., 1995
(4*R*,5*S*,10*S*)-Cleistantha-8,11, 13-trien-19-al **(4.6)**				Pinto *et al*., 1987
8,11,13-Cleistan-thatrien-17,19-dioic acid dimethyl ester **(4.7)**				Pinto *et al*., 1995
8,11,13-Cleistan-thatrien-3,7-dione **(4.8)**	*V. piresiana*			Pinto *et al*., 1984
8,11,13-Cleistan-thatrien-17-oic acid (Veadeiroic acid) **(4.9)**	*V. flavans*			Pinto *et al*., 1995
(4*R*,5*S*,10*S*)-Cleistantha-8,11,13-trien-19-oic acid **(4.10)**	*V. flavicans*			Pinto *et al*., 1987
8,11,13-Cleistanthatrien-17-oic acid methyl ester **(4.11)**	*V. flavans*			Pinto *et al*., 1995

Table 4. Distribution of cleistanthane diterpenes in plants (continued)

Compound	Source	Family	Plant part	References
8,11,13-Cleistanthatrien-17-ol (Veadeirol) **(4.12)**	*V. flavans*	Velloziaceae	Roots, stem, leaf sheath	Pinto *et al*., 1995
8,11,13-Cleistanthatrien-19-oic acid methyl ester **(4.13)**				
(4*R*,5*S*,10*S*)-Cleistantha-8,11,13-trien-19-ol **(4.14)**	*V. flavicans*			Pinto *et al*., 1987
8,11,13-Cleistanthatrien-7-one **(4.15)**	*V. declinans*			Pinto *et al*., 1992
	V. compacta			Riehl and Pinto, 2000
8,11,13-Cleistanthatrien-7-one-17-oic acid **(4.16)**	*V. flavans*			Pinto *et al*., 1995
8,11,13-Cleistanthatrien-7-one-19-oic acid **(4.17)**				
8,11,13-Cleistanthatrien-7-one-17-oic acid methyl ester **(4.18)**				
8,11,13-Cleistanthatrien-7-one-19-oic acid methyl ester **(4.19)**				
Cleistantha-8,11,13-triene-7-one-19,20β-olide **(4.20)**	*V. compacta*			Riehl and Pinto, 2000
Cleistanthol **(4.21)**	*Phyllanthus oxyphyllus*	Euphorbiaceae	Roots	Sutthivaiyakit *et al*., 2003
(5*S*,7*S*,10*R*)-7α,16,7β,20-Diepoxycleistantha-1,8,11,13-tetraen-3-one **(4.22)**	*V. declinans*	Velloziaceae	Roots, stem, leaf sheath	Pinto *et al*., 1992
	V. compacta			Riehl and Pinto, 2000

Table 4. Distribution of cleistanthane diterpenes in plants (continued)

Compound	Source	Family	Plant part	References
(5*S*,7*S*,10*R*)-7α,16,7β,20-Diepoxycleistantha-8,11,13-trien-3-one **(4.23)**	*V. declinans*	Velloziaceae	Roots, stem, leaf sheath	Pinto *et al.*, 1992
7,16-Epoxy-20-nor-1,5,7,9,11,13-cleistantha hexaen-3-one **(4.24)**				
7,16-Epoxy-20-nor-5,7,9,11,13-cleistantha pentaene **(4.25)**				
7,16-Epoxy-20-nor-5,7,9,11,13-cleistanthapentaen-3-one **(4.26)**				
(5*S*,7*S*,10*S*)-7β-Hydroxy-8,11,13-cleistantha-triene **(4.27)**				
20-Hydroxy-8,11,13-Cleistan-thatrien-7-one **(4.28)**				
(3*S*,5*S*,7*S*,10*R*)-3β-Hydroxy-7α,16,7β,20-diepoxycleistantha-8,11,13-trien **(4.29)**				
3,4-*Seco*-sonderianol **(4.30)**	*Croton sonderianus*	Euphorbiaceae	Heartwood	Craveiro and Silveira, 1982
Sonderianol **(4.31)**	*Petalostigma pubescens*			Grace *et al.*, 2006
Spruceanol **(4.32)**	*Phyllanthus oxyphyllus*		Roots	Sutthivaiyakit *et al.*, 2003

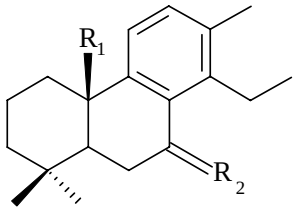

	R_1	R_2
20-Carboxaldehyde-8,11,13-cleistanthatrien-7-one **(4.1)**	CHO	O
8,11,13-Cleistanthatriene **(4.4)**	CH_3	H, H
(5*S*,10*S*)-8,11,13-Cleistanthatrien-7-one **(4.15)**	CH_3	O
(5*S*,7*S*,10*S*)-7β-Hydoxy-8,11,13-cleistanthatriene **(4.27)**	CH_3	β-OH, H
20-Hydroxy-8,11,13-cleistanthatrien-7-one **(4.23)**	CH_2OH	O

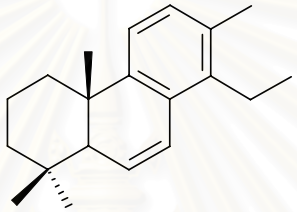

6,8,11,13-Cleistanthatetraene **(4.2)**

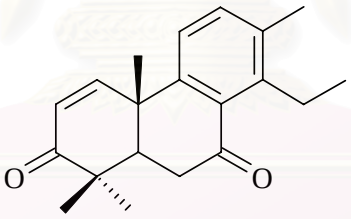

1,8,11,13-Cleistanthatetraen-3,7-dione **(4.3)**

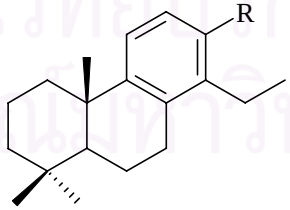

	R
8,11,13-Cleistanthatrien-17-al **(4.5)**	CHO
8,11,13-Cleistanthatrien-17-oic acid **(4.9)**	COOH
8,11,13-Cleistanthatrien-17-oic acid methyl ester **(4.11)**	COOMe
8,11,13-Cleistanthatrien-17-ol **(4.12)**	CH_2OH

Figure 6. Chemical structures of cleistanthane diterpenes in plants

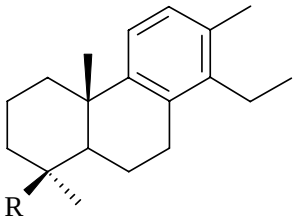

	R
(4*R*,5*S*,10*S*)-Cleistantha-8,11,13-trien-19-al **(4.6)**	CHO
(4*R*,5*S*,10*S*)-Cleistantha-8,11,13-trien-19-oic acid **(4.10)**	COOH
(4*R*,5*S*,10*S*)-Cleistantha-8,11,13-trien-19-ol **(4.15)**	CH_2OH
8,11,13-Cleistanthatrien-19-oic acid methyl ester **(4.13)**	COOMe

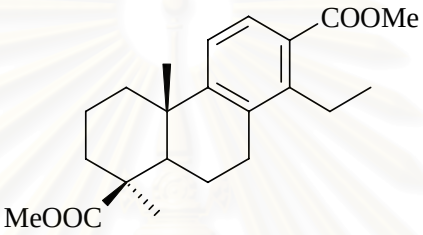

8,11,13-Cleistanthatrien-17,19-dioic acid dimethyl ester **(4.7)**

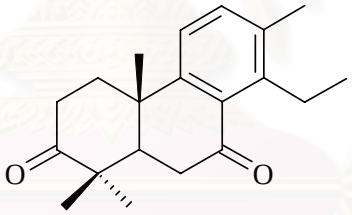

8,11,13-Cleistanthatrien-3,7-dione **(4.8)**

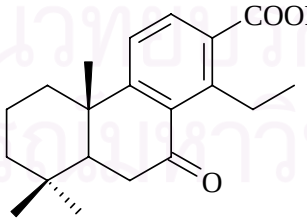

	R
8,11,13-Cleistanthatrien-7-one-17-oic acid **(4.16)**	H
8,11,13-Cleistanthatrien-7-one-17-oic acid methyl ester **(4.18)**	CH_3

Figure 6. Chemical structures of cleistanthane diterpenes in plants (continued)

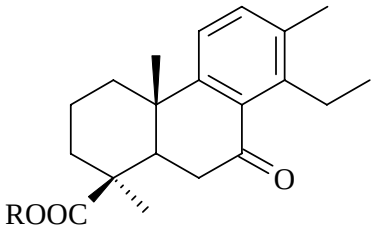

	R
8,11,13-Cleistanthatrien-7-one-19-oic acid **(4.17)**	H
8,11,13-Cleistanthatrien-7-one-19-oic acid methyl ester **(4.19)**	CH_3

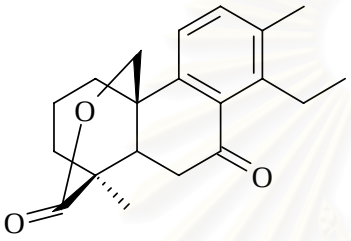

Cleistantha-8,11,13-trien-7-one-19,20β-olide **(4.20)**

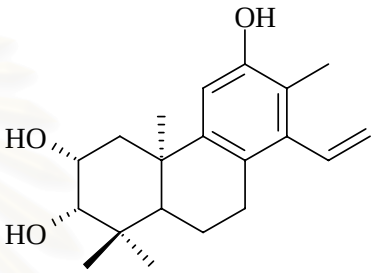

Cleistanthol **(4.21)**

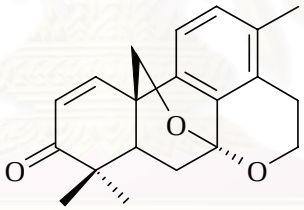

(5*S*,7*S*,10*R*)-7α,16,7β,20-Diepoxycleistantha-1,8,11,13-tetraen-3-one **(4.22)**

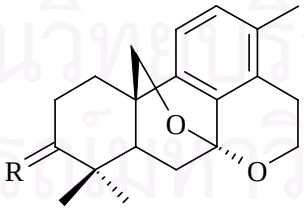

	R
(5*S*,7*S*,10*R*)-7α,16,7β,20-Diepoxycleistantha-8,11,13-trien-3-one **(4.23)**	O
(3*S*,5*S*,7*S*,10*R*)-3β-Hydroxy-7α,16,7β,20-diepoxycleistantha-8,11,13-triene **(4.29)**	β-OH, H

Figure 6. Chemical structures of cleistanthane diterpenes in plants (continued)

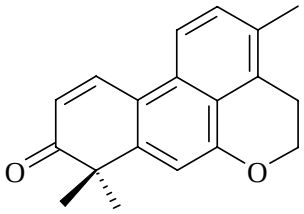

7,16-Epoxy-20-nor-1,5,7,9,11,13-cleistanthahexaen-3-one **(4.24)**

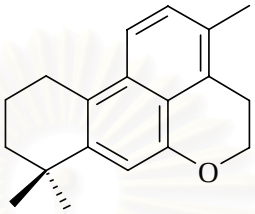

7,16-Epoxy-20-nor-5,7,9,11,13-cleistanthapentaene **(4.25)**

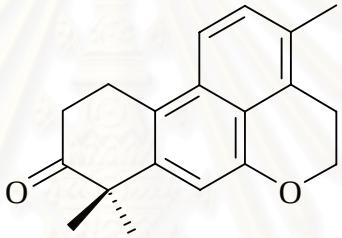

7,16-Epoxy-20-nor-5,7,9,11,13-cleistanthapentaen-3-one **(4.26)**

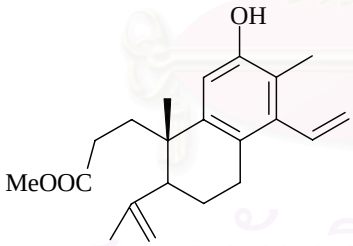

3,4-*Seco*-sonderianol **(4.30)**

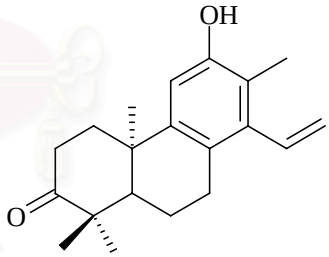

Sonderianol **(4.31)**

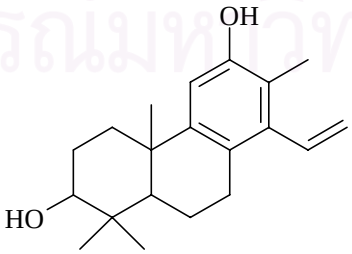

Spruceanol **(4.32)**

Figure 6. Chemical structures of cleistanthane diterpenes in plants (continued)

Taraxerane triterpenes in the plant kingdom

Triterpenoids are isopentenoids composed of thirty carbon atoms and may possess acyclic, mono-, di-, tri-, tetra- or pentacyclic carbon skeletons. Pentacyclic triterpenoids are dominant constituents of this class and have been widely investigated. Some of these terpenoids displayed potential as candidates for drug development. For example, the lupane-type triterpene betulinic acid exhibited significant antimalarial activity both *in vitro* and *in vivo* (Steele *et al*., 1999). The compound is also selectively cytotoxic against melanoma, neuroectodermal and malignant brain tumor cell lines (Zuco *et al*., 2002). Other types of triterpenoids have also been reported as cytotoxic, for example, the cycloartane-type triterpenes, cycloart-23-ene-3β,25-diol and cycloart-25-ene-3β,24-diol, isolated from *Euphorbia pulcherrima*, were cytotoxic against Ehrlich ascites tumor cells (Smith *et al*., 1996).

Taraxerane-type triterpenoids were found in various plant families, and some of them have been reported as being cytotoxic. An example is *seco*-3,4-taraxerone which displayed *in vitro* cytotoxic activity against Hep-G2 and A-431 human cancer cell lines and were potent inhibitors of topoisomerase II (Setzer *et al*., 2000). Another taraxerane triterpene, aleuritolic acid, demonstrated DNA ligase inhibitory activity (Tan *et al*., 1996). The distribution of this type of triterpenoids in higher plants is presented in **Table 5**, and their structures are shown in **Figure 7**.

Table 5. Distribution of taraxerane triterpenes in higher plants

Compound	Source	Family	Plant part	References
3β-acetoxy-11α, 12α-epoxy-14-taraxerene **(5.1)**	*Ficus microcarpa*	Moraceae	Aerial roots	Chiang *et al*., 2005
3β-acetoxy-11α, 12α-epoxy-16-oxo-14-taraxerene **(5.2)**				
Acetyl aleuritolic acid **(5.3)**	*Alchornea cordifolia*	Euphorbiaceae	Leaves, root bark	Mavar-Manga *et al*., 2008
	Cnidoscolus vitifolius		Stem	Brum *et al*., 1998.
	Croton cajucara		Bark	Maciel *et al*., 1998.

Table 5. Distribution of taraxerane triterpenes in higher plants (continued)

Compound	Source	Family	Plant part	References
Acetyl aleuritolic acid **(5.3)**	*C. crassifolius*	Euphorbiaceae	Roots	Boonyarathana-kornkit *et al*., 1988
	C. lacciferus			Bandara, Wimalasiri and Macleod, 1988
	C. megalocarpus		Bark	Addae-Mansah *et al*., 1992
	C. oblongifolius			Bandopadhyay *et al*., 1972
	Jatropha isabelli		Rhizome	Pertino *et al*., 2007
	Mallotus philippinensis		Bark	Bandopadhyay *et al*., 1972.
	Maprounea africana		Roots	Chaudhuri *et al*., 1995
	Phytolacca americana	Phytolaccaceae	Seeds	Woo and Wagner, 1977
	P. esculenta			Won and Sam, 1985.
	Sapium baccatum	Euphorbiaceae	Stem, trunk bark	Ray, Misra and Khastgir, 1975
	S. pachystachys, S. rigidifolium		n.i.	Siems *et al*., 1993
3-Acetyl myricardiol **(5.4)**	*P. esculenta*	Phytolaccaceae	Seeds	Won and Sam, 1985
29-Acetyl-14-Taraxeren-3-one **(5.5)**	*Lithocarpus cornea*	Fagaceae	Stem	Hui and Li, 1976b
Aleuritolic acid **(5.6)**	*Aleurites montana*	Euphorbiaceae	n.i.	Misra and Khastgir, 1970
	Euphorbia guyoniana		Roots	Haba *et al*., 2007
	Maprounea africana			Chaudhuri *et al*., 1995
	Sapium baccatum		Bark	Pradhan, Amer Nath and Shoolery, 1984
	S. sebiferum			Pradhan *et al*., 1984
Baccatin **(5.7)**	*S. baccatum*		n.i.	Saha *et al*., 1977

n.i. = not indicated

Table 5. Distribution of taraxerane triterpenes in higher plants (continued)

Compound	Source	Family	Plant part	References
3β-*E*-Caffeoyl taraxerol **(5.8)**	*Rhizophora mucronata*	Rhizophoraceae	Fruits	Laphookhieo, Karalai and Ponglimanont, 2004
3β-*Z*-Caffeoyl taraxerol **(5.9)**				
Careaborin **(5.10)**	*Bridelia micrantha*	Euphorbiaceae	Wood	Pegel and Rogers, 1968
	Careya arborea	Lecythidaceae	Leaves	Talapatra, Basak and Talapatra, 1981
Cis-Careaborin **(5.11)**	*R. apicalata*	Rhizophoraceae		Kokpol and Chavasiri, 1990
1β,2α-Dihydroxyaleuritolic acid 2,3-bis-*p*-hydroxy benzoate **(5.12)**	*Maprounea africana*	Euphorbiaceae	Roots	Chaudhuri *et al*., 1995
Epiacetyl aleuritolic acid **(5.13)**	*Phytolacca acinosa*	Phytolaccaceae	Berries	Razdan *et al*., 1982
Epialeuritolic acid **(5.14)**				
3-Epitaraxerol (Isotaraxerol) **(5.15)**	*Euphorbia royleana*	Euphorbiaceae	Latex	Bani *et al*., 2005
	Excoecaria agallocha		Leaves	Hui and Sung, 1968
	Macaranga tanarius		Stem	Markstadter *et al*., 2000
	M. triloba		Leaves	Jang *et al*., 2004
	Skimmia wallichii	Rutaceae	Stem, trunk bark	Ray *et al*., 1975
Epitaraxeryl acetate **(5.16)**	*Melaleuca leucadendron*	Myrtaceae	Leaves, stem	Hui and Li, 1976a
Euphorginol **(5.17)**	*Euphorbia tirucalli*	Euphorbiaceae	Stem bark	Rasool, Khan and Malik, 1989
Herranone **(5.18)**	*Herrania cuatrecasana*	Sterculiaceae	Wood	Wiedemann *et al*., 1999
Herrantrione **(5.19)**				
1β-Hydroxy aleuritolic acid 3-*p*-hydroxy benzoate **(5.20)**	*Maprounea africana*	Euphorbiaceae	Roots	Beutler *et al*., 1995; Chaudhuri *et al*., 1995
2α-Hydroxy aleuritolic acid 2-*p*-hydroxy benzoate **(5.21)**	*M. africana, M. membranacea*			Beutler *et al*., 1995

Table 5. Distribution of taraxerane triterpenes in higher plants (continued)

Compound	Source	Family	Plant part	References
2α-Hydroxy aleuritolic acid 3-*p*-hydroxy benzoate **(5.22)**	*M. africana*	Euphorbiaceae	Roots	Beutler *et al*., 1995
2α-Hydroxy aleuritolic acid 2,3-bis-*p*-hydro-xybenzoate **(5.23)**				Chaudhuri *et al*., 1995
3α-Hydroxy aleuritolic acid 2β-*p*-hydroxy benzoate **(5.24)**				
3-(4-Hydroxy-benzoyl) aleuritolic acid **(5.25)**	*M. membranacea*		Bark	Beutler *et al*., 1995
7β-Hydroxy-maprounic acid 3-*p*-hydroxy-benzoate **(5.26)**	*M. africana*		Roots	Chaudhuri *et al*., 1995
14-Hydroxy 3-taraxeranone **(5.27)**	*Lithocarpus cornea*	Fagaceae	Stem	Hui and Li, 1976b
29-Hydroxy-14-Taraxeren-3-one **(5.28)**				
Marsformoxide B **(5.30)**	*Marsdenia formosana*	Asclepiadaceae	Dried herb	Ito and Lai, 1978
Miricolone **(5.31)**	*Myrica rubra*	Myricaceae	Stem bark	Sakurai, Yaguchi and Inoue, 1987
Myricardiol **(5.32)**	*Lithocarpus cornea*	Fagaceae	Stem	Hui and Li, 1976b
	Maytenus umbellata	Celastraceae	Roots	González *et al*., 1986
	Myrica rubra	Myricaceae	Stem bark	Sakurai *et al*., 1987
	Tamarix aphylla	Tamaricaceae	Bark	Merfort *et al*., 1992
Myricetrione **(5.33)**	*Myrica rubra*	Myricaceae		Tao *et al*., 2002
11α,12α-Oxido-taraxerol **(5.34)**	*Euphorbia chamaesyce*	Euphorbiaceae	Seeds	Tanaka *et al*., 1994

Table 5. Distribution of taraxerane triterpenes in higher plants (continued)

Compound	Source	Family	Plant part	References
11α,12α-Oxido-taraxerol **(5.34)**	*E. supina*	Euphorbiaceae	Whole herb	Tanaka and Matsunaga, 1988
Phytolaccanol **(5.35)**	*Phytolacca acinosa*	Phytolaccaceae	Berries	Razdan *et al*., 1982
Sawamilletin **(5.36)**	*Bosistoa sapindiformis*	Rutaceae	Leaves	Croft, Ritchie and Taylor, 1975
	Saccharum officinarum	Graminae	Stem wax	Bryce *et al*., 1967
Sebiferenic acid **(5.37)**	*Sapium sebiferum*	Euphorbiaceae	Bark	Pradhan *et al*., 1984
3,4-*Seco*-taraxerone **(5.38)**	*Alchornea latifolia*		Leaves	Setzer *et al*., 2000
1,14-Taraxera-dien-3-one **(5.39)**	*Quercus bambusaefolia, Q. myrsinaefolia*	Fagaceae		Hui and Li, 1977b
3,14-Taraxe-ranediol **(5.40)**	*Lithocarpus cornea*		Stem	Hui and Li, 1976b
14-Taraxeren-7-ol **(5.41)**	*Polypodium amamianum, P. niponicum*	Polypodiaceae	Rhizome	Ageta and Arai, 1983
14-Taraxeren-23-ol **(5.42)**	*Vernonia cinerea*	Compositae	Roots	Misra *et al*., 1984
14-Taraxerene **(5.43)**	*Ficus microcarpa*	Moraceae	Aerial roots	Chiang *et al*., 2005
14-Taraxerene-3,24-diacetate **(5.44)**	*Parsonia laevigata*	Apocynaceae	Leaves	Ogihara *et al*., 1987
14-Taraxerene-3,29-diacetate **(5.45)**	*Lithocarpus cornea*	Fagaceae	Stem	Hui and Li, 1976b
14-Taraxerene-3,16-diol **(5.46)**	*Quercus bambusaefolia*		Leaves	Hui and Li, 1977b
14-Taraxerene-3,24-diol **(5.47)**	*Parsonia laevigata*	Apocynaceae		Ogihara *et al*., 1987
14-Taraxerene-3,29-diol **(5.48)**	*Lithocarpus cornea*	Fagaceae	Stem	Hui and Li, 1976b
14-Taraxerene-3,30-diol **(5.49)**	*Phytolacca acinosa*	Phytolaccaceae	Berries	Razdan *et al*., 1982
14-Taraxerene-3,16-dione **(5.50)**	*Quercus bambusaefolia*	Fagaceae	Leaves	Hui and Li, 1977b

Table 5. Distribution of taraxerane triterpenes in higher plants (continued)

Compound	Source	Family	Plant part	References
14-Taraxeren-16-one **(5.51)**	*Polypodium spp.*	Polypodiaceae	Rhizome	Ageta and Arai, 1983
14-Taraxeren-24-oic acid (Taraxeric acid) **(5.52)**	*Daphne papyracea*	Thymilliaceae	Aerial parts	Katti and Tandon, 1979
Taraxerol **(5.53)**	*Aesculus hippocastanum*	Hippocastana-ceae	Seeds	Stankovic, Bastic and Jovanovic, 1985
	Alchornea latifolia	Euphorbiaceae	Leaves	Setzer *et al*., 2000
	Bridelia micrantha		Wood	Pegel and Rogers, 1968
	Callophyllum cordato-oblongum	Guttiferae	Twigs	Dharmaratne *et al*., 1998
	C. moonii		Root bark	Dharmaratne and Wijesinghe, 1997
	Canarium zeylanicum	Burseraceae	Bark, timber	Bandaranayake, 1980
	Codonopsis pilosula	Campanulaceae	Roots	Wang *et al*., 1995
	Croton caudatus	Euphorbiaceae	Stem bark	Banerji, Nandi and Kundu, 1988
	Daphne papyracea	Thymelaeaceae	Aerial parts	Katti and Tandon, 1979
	Diospyros hirsuta, D. moonii D. quaesita, D. spinescens, D. thwaitesii, D. walkeri, Diospyros sp.	Ebenaceae	Bark, timber	Herath *et al*., 1978
	Embelia schimperi	Myrsinaceae	Leaves	Manguro, Okwiri and Lemmen, 2006
	Euphorbia antiquorum	Euphorbiaceae	Stem	Zhi-Da *et al*., 1989
	E. pilulifera		Leaves, stem	Atallah and Nicholas, 1972
	Gochnatia polymorpha	Compositae	Aerial parts	Sacilotto, Vichnewski and Herz, 1997
	Hoya lacunosa	Asclepiadaceae	Leaves	Baas, 1983

Table 5. Distribution of taraxerane triterpenes in higher plants (continued)

Compound	Source	Family	Plant part	References
Taraxerol **(5.53)**	*Lithocarpus polystachya*	Fagaceae	Stem	Hui and Li, 1977a
	Macaranga tanarius	Euphorbiaceae		Markstadter *et al*., 2000
	M. triloba		Leaves	Jang *et al*., 2004
	Mimusops hexandra	Sapotaceae	Bark	Misra and Mitra, 1966
	M. hexandra		Leaves, roots	Misra and Mitra, 1968
	Myrica rubra	Myricaceae	Bark	Tao *et al*., 2002
	Opuntia dillenii	Cactaceae	Stem	Jiang *et al*., 2006
	Quercus robur	Fagaceae	Leaves	Prasad, Müller and Gülz, 1990
	Rhizophora apiculata	Rhizophoraceae		Kokpol and Chavasiri, 1990
	Sapium discolor	Euphorbiaceae	Leaves, stem	Hui and Sung, 1968
	Skimmia wallichii	Rutaceae	Stem, trunk bark	Ray *et al*., 1975
	Strobilanthes callosus	Acanthaceae	Aerial parts	Singh, Sahu and Sharma, 2002
	Uvaria hookeri	Annonaceae	Root bark	Padmaja, Thankamany and Hisham, 1993
	U. narum			Hisham *et al*., 1991
	Vaccinium membraneceum, V. parvifolium	Ericaceae	Under-ground part	Sheth *et al*., 1968
Taraxerone **(5.54)**	*Agauria salicifolia*		Bark	Gregoire and Nyembo, 1977
	Alchornea latifolia	Euphorbiaceae	Leaves	Setzer *et al*., 2000
	Bridelia micrantha		Wood	Pegel and Rogers, 1968
	Calophyllum moonii	Guttiferae	Root bark	Dharmaratne and Wijesinghe, 1997
	Canarina canariensis	Campanulaceae	Leaf wax	Gaydou, Faure and Wollen-weber, 1996
	Croton caudatus	Euphorbiaceae	Stem bark	Banerji *et al*., 1988

Table 5. Distribution of taraxerane triterpenes in higher plants (continued)

Compound	Source	Family	Plant part	References
Taraxerone **(5.54)**	*Cymbidium gigantum*	Orchidaceae	Whole plant	Juneja, Sharma and Tandon, 1985
	Daphne papyracea	Thymelaeaceae	Aerial parts	Katti and Tandon, 1979
	Diospyros hirsuta, D. moonii, D. quaesita, D. spinescens, D. thwaitesii, D. walkeri, Diospyros sp.	Ebenaceae	Bark, timber	Herath *et al*., 1978
	Embelia schimperi	Myrsinaceae	Leaves	Manguro *et al*., 2006
	Euphorbia antiquorum	Euphorbiaceae	Stem	Anjaneyulu and Ravi, 1989
	E. pilulifera		Leaves, stem	Atallah and Nicholas, 1972
	E. stygiana		Leaves	Lima, Medeiros and Davin, 2003
	Lithocarpus spp.	Fagaceae	Leaves, stem	Hui *et al*., 1975
	Macaranga tanarius	Euphorbiaceae	Stem	Markstadter *et al*., 2000
	Myrica rubra	Myricaceae	Stem bark	Sakurai *et al*., 1987
	Neolitsea villosa	Lauraceae	Roots	Li and Duh, 1993
	Pertusaria ophthalmiza	Pertusariaceae	Whole plant	Huneck, Tonsberg and Bohlmann, 1986
	Polygonum nepalense	Polygonaceae		Rathore, Sharma and Tandon, 1986
	Skimmia wallichii	Rutaceae	Stem, trunk bark	Ray *et al*., 1975
	Vaccinium membranaceum	Ericaceae	Under-ground part	Sheth *et al*., 1968
	V. parvifolium			
Taraxerone **(5.54)**	*Vellozia piresiana*	Velloziaceae	Roots, stem, leaf sheath	Pinto, Peixoto and Fiorni, 1984

Table 5. Distribution of taraxerane triterpenes in higher plants (continued)

Compound	Source	Family	Plant part	References
Taraxeryl acetate **(5.55)**	*Cissus quadrangularis*	Vitaceae	Aerial parts	Gupta and Verma, 1991
	Codonopsis pilosula	Campanulaceae	Roots	Wang *et al*., 1995
	Croton caudatus	Euphorbiaceae	Stem bark	Banerji *et al.*, 1988
	Daphne papyracea	Thymelaeaceae	Aerial parts	Katti and Tandon, 1979
	Euphorbia maculata	Euphorbiaceae	Whole herb	Matsunaga, Tanaka and Akagi, 1988
	E. stygiana		Leaves	Lima *et al*., 2003
	Mimusops hexandra	Sapotaceae	Bark	Misra and Mitra, 1966

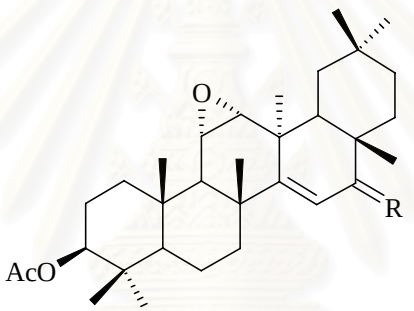

	R
3β-acetoxy-11α,12α-epoxy-14-taraxerene **(5.1)**	H, H
3β-acetoxy-11α,12α-epoxy-16-oxo-14-taraxerene **(5.2)**	O

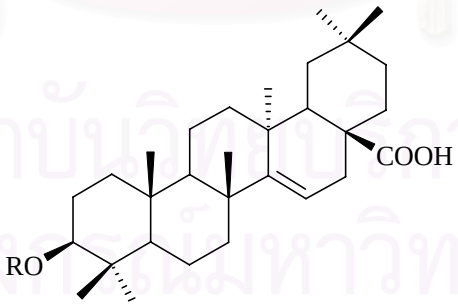

	R
Acetyl aleuritolic acid **(5.3)**	Ac
Aleuritolic acid **(5.6)**	H
Epiacetyl aleuritolic acid (3α-form) **(5.13)**	Ac
Epialeuritolic acid (3α-form) **(5.14)**	H
3-(4-Hydroxybenzoyl) aleuritolic acid **(5.25)**	3-(4-Hydroxybenzoyl)

Figure 7. Chemical structures of taraxerane triterpenes in plants

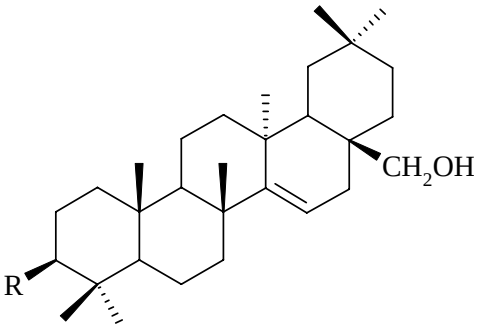

	R
3-Acetyl myricadiol **(5.4)**	OAc
Miricolone **(5.31)**	=O
Myricadiol **(5.32)**	OH

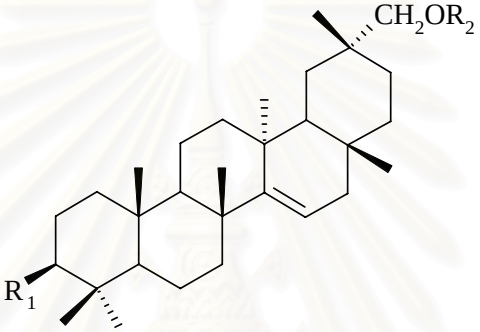

	R_1	**R_2**
29-Acetyl-14-taraxerene-3-one **(5.5)**	=O	Ac
29-Hydroxy-14-taraxeren-3-one **(5.28)**	=O	H
14-Taraxerene-3,29-diacetate **(5.45)**	OAc	Ac
14-Taraxerene-3,29-diol **(5.48)**	OH	H

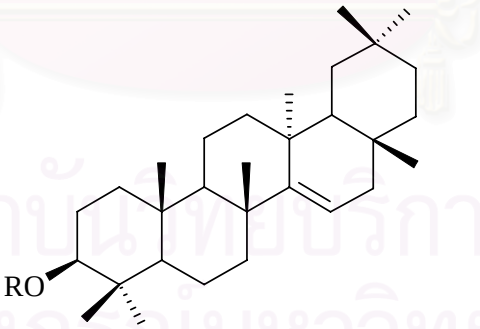

	R
3β-*E*-Caffeoyltaraxerol **(5.8)**	Caffeoyl (*E*-)
3β-*Z*-Caffeoyltaraxerol **(5.9)**	Caffeoyl (*Z*-)
Careaborin **(5.10)**	4-Hydroxycinnamoyl (*E*-)
cis-Careaborin **(5.11)**	4-Hydroxycinnamoyl (*Z*-)
Sawamilletin **(5.36)**	Me
Taraxerol **(5.53)**	H
Taraxeryl acetate **(5.55)**	Ac

Figure 7. Chemical structures of taraxerane triterpenes in plants (continued)

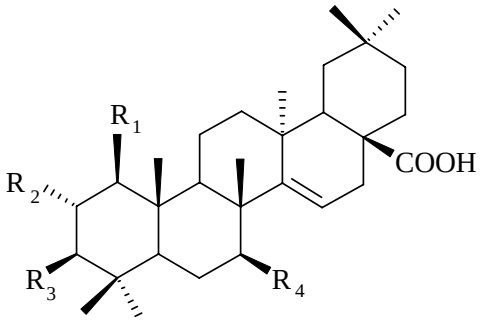

A = *O*-*p*-hydroxybenzoyl

	R_1	**R_2**	**R_3**	**R_4**
1β,2α-Dihydroxyaleuritolic acid 2,3-bis-*p*-hydroxybenzoate **(5.12)**	OH	A	A	H
1β-Hydroxyaleuritolic acid 3-*p*-hydroxy benzoate **(5.20)**	OH	H	A	H
2α-Hydroxyaleuritolic acid 2-*p*-hydroxy benzoate **(5.21)**	H	A	OH	H
2α-Hydroxyaleuritolic acid 3-*p*-hydroxy benzoate **(5.22)**	H	OH	A	H
2α-Hydroxyaleuritolic acid 2,3-bis-*p*-hydroxybenzoate **(5.23)**	H	A	A	H
3α-Hydroxyaleuritolic acid 2β-*p*-hydroxy benzoate **(5.24)**	H	A	α-OH	H
17β-Hydroxyaleuritolic acid 3-*p*-hydroxy benzoate **(5.26)**	H	H	A	OH

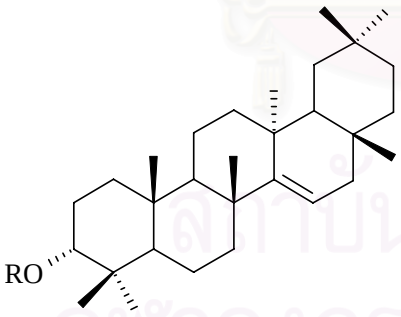

	R
3-Epitaraxerol **(5.15)**	H
Epitaraxeryl acetate **(5.16)**	Ac

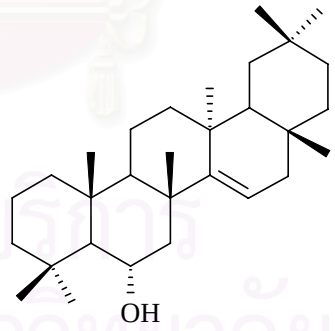

Euphorginol **(5.17)**

Figure 7. Chemical structures of taraxerane triterpenes in plants (continued)

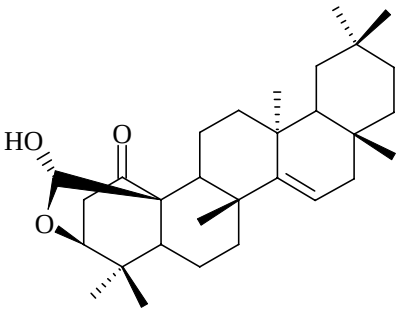

Herranone **(5.18)**

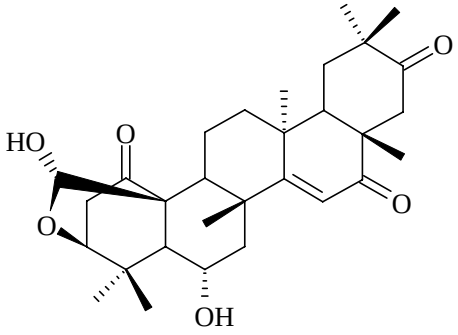

Herrantrione **(5.19)**

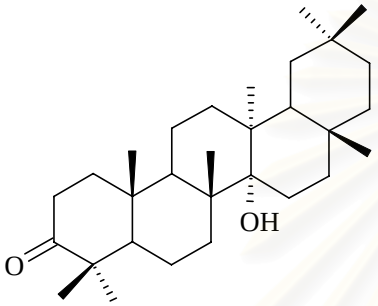

14-Hydroxy-3-taraxeranone **(5.27)**

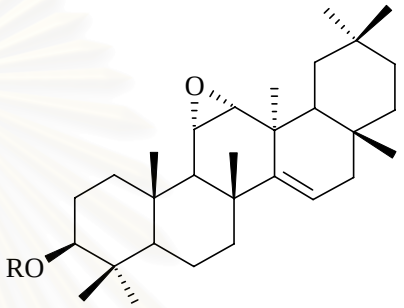

	R
Marsformoxide B **(5.30)**	Ac
11α,12α-Oxidotaraxerol **(5.34)**	H

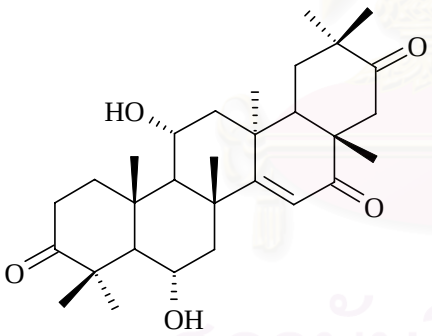

Myricetrione **(5.33)**

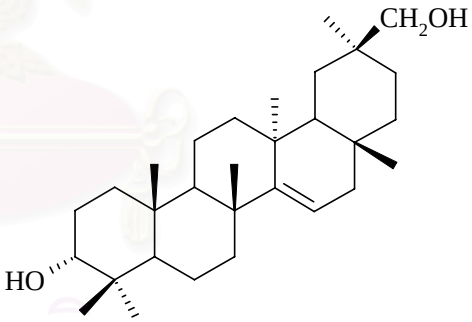

Phytolaccanol **(5.35)**

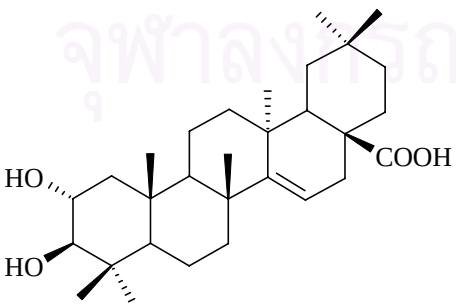

Sebiferenic acid **(5.37)**

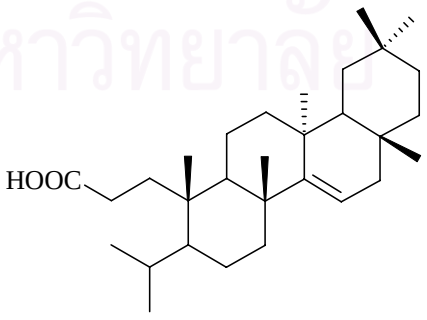

3,4-*Seco*-taraxerone **(5.38)**

Figure 7. Chemical structures of taraxerane triterpenes in plants (continued)

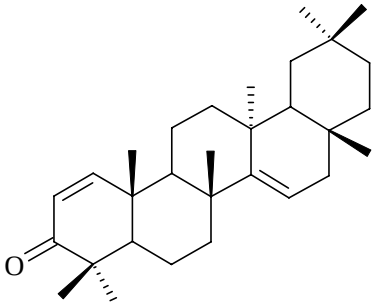

1,14-Taraxeradien-3-one **(5.39)**

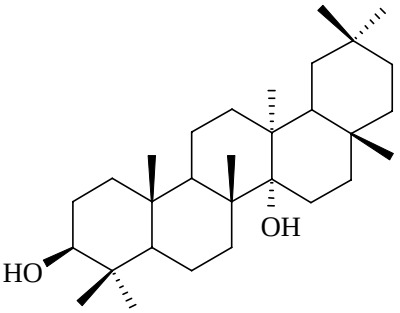

3,14-Taraxeranediol **(5.40)**

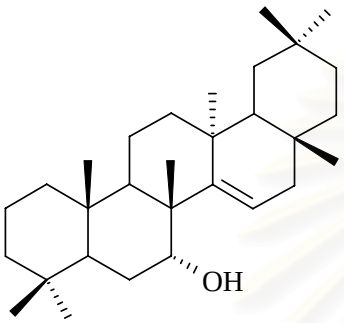

14-Taraxeren-7-ol **(5.41)**

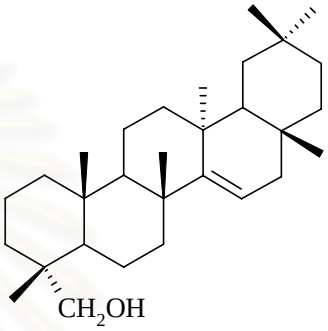

14-Taraxeren-23-ol **(5.42)**

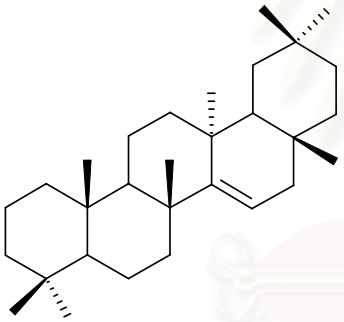

14-Taraxerene **(5.43)**

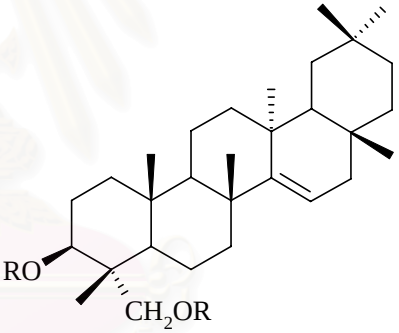

14-Taraxerene-3,24-diacetate **(5.44)** R = Ac
14-Taraxerene-3,24-diol **(5.47)** R = H

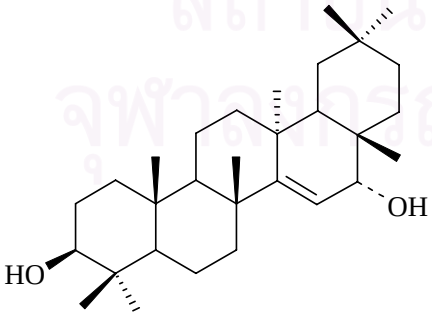

14-Taraxerene-3,16-diol **(5.46)**

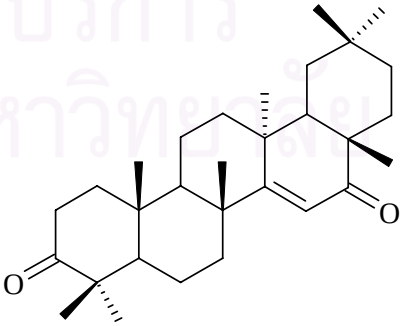

14-Taraxerene-3,16-dione **(5.50)**

Figure 7. Chemical structures of taraxerane triterpenes in plants (continued)

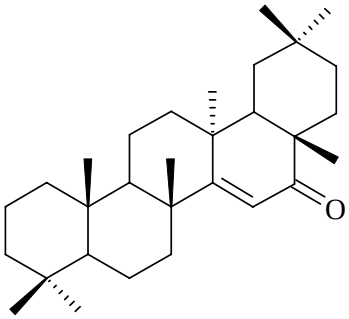

14-Taraxeren-16-one **(5.51)**

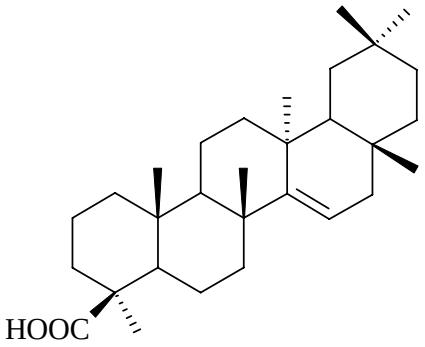

Taraxeric acid **(5.52)**

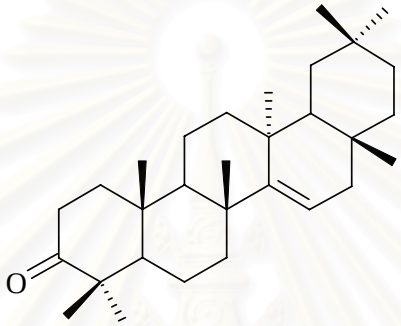

Taraxerone **(5.54)**

Figure 7. Chemical structures of taraxerane triterpenes in plants (continued)

Biflavonoids

Biflavonoids are flavonoid dimers that include flavone-flavone, flavanone-flavone, flavanone-flavanone, isoflavone-flavone, flavone-chalcone, flavanone-aurone subunit connected with a C-C or C-O-C bond. More than 100 biflavonoids have been identified from plants since the isolation of ginkgetin in 1929. A variety of biological activities for biflavonoids have been published, including anti-inflammatory, antimicrobial, antioxidant, anti-HIV-1, anti-HBV, and others. A review of biflavonoids focusing on flavone-flavone subunit connected with C-C linkage is presented herein. Distribution of these biflavones in the plant kingdom is shown in **Table 6**, and their structures are shown in **Figure 8**.

Table 6. Distribution of C-C biflavones in plants

Compound	Source	Family	Plant part	References
Abiesin **(6.1)**	*Abies webbiana*	Pinaceae	Leaves	Chatterjee *et al*., 1984
Agathisflavone **(6.2)**	*Amphipterygium amplifolium*	Julianiaceae		Wannan and Quinn, 1988
	Garcinia multiflora	Guttiferae	Seed kernels	Lin *et al*., 2001
	Orthopterygium amplifolium	Julianiaceae	Leaves	Wannan and Quinn, 1988
	O. huaucui			
	Ouratea sulcata	Ochnaceae		Pegnyemb *et al*., 2005
	Rhus dentata	Anacardiaceae		Svenningsen *et al*., 2006
	R. pentheri			Svenningsen *et al*., 2006
	R. pyroides			
	R. succedanea		Seed kernels	Lin *et al*., 2001
Amentoflavone **(6.3)**	*Actinostrobus acuminatus*	Cupressaceae	Leafy twigs	Gadex and Quinn, 1983
	A. pyramidalis			
	Amphipterygium amplifolium	Julianiaceae	Leaves	Wannan and Quinn, 1988
	Araucaria angustifolia	Araucariaceae	Needles	Yamaguchi *et al*., 2005
	Athrotaxis cupressoides, A. laxifolia, A. selaginoides	Taxodiaceae	Leaves	Gadex and Quinn, 1989
	Austrocedrus chilensis	Cupressaceae	Leafy twigs	Gadex and Quinn, 1983
	Biota orientalis			Gadek and Quinn, 1985
	Brysonima crassa	Malpighiaceae	Leaves	Sannomiya *et al*., 2005
	Callitris canescens, C. columellaris, C. endlicheri, C. macleayana	Cupressaceae	Leafy twigs	Gadex and Quinn, 1982
	C. macleayana, C. neocaledonica, C. oblonga			Gadex and Quinn, 1983
	C. pressii, C. rhomboidea			Gadex and Quinn, 1982
	C. sulcata			Gadex and Quinn, 1983

Table 6. Distribution of C-C biflavones in plants (continued)

Compound	Source	Family	Plant part	References
Amentoflavone **(6.3)**	*Calocedrus decurrens*	Cupressaceae	Leafy twigs	Gadek and Quinn, 1985
	Calophyllum calaba	Guttiferae	Leaves	Gunatilaka *et al*., 1984
	Chamaecyparis formosansis, C. lawsoniana, C. nootkatensis, C. thyroides	Cupressaceae	Leafy twigs	Gadek and Quinn, 1985
	Cryptomeria japonica	Taxodiaceae	Leaves	Gadex and Quinn, 1989
	Cunninghamia lanceolata			
	Cupressus lusitanica	Cupressaceae	Leafy twigs	Gadek and Quinn, 1985
	C. sempervirens			
	Cycas beddomei	Cycadaceae	Leaves	Rani *et al*., 1998
	C. revoluta			Geiger and De Groot Pflei-derer, 1971
	C. rumphii			Uddin *et al*., 2004
	Diselma archerii	Cupressaceae	Leafy twigs	Gadex and Quinn, 1983
	Fitzroya cupressoides			
	Fokienia hodginsii			Gadek and Quinn, 1985
	Garcinia multiflora	Guttiferae	Seed kernels	Lin *et al*., 2001
	Glyptostrobus lineata	Taxodiaceae	Leaves	Gadex and Quinn, 1989
	Isophysis tasmanica	Iridaceae		William, Harborne and Tomas-Bar-beran, 1987
	Juniperus bermudiana, J. communis, J. drupacea, J. excelsa, J. oxycedrus, J. procera, J. virginiana	Cupressaceae	Leafy twigs	Gadek and Quinn, 1985
	Libocedrus plumose			Gadek and Quinn, 1983

Table 6. Distribution of C-C biflavones in plants (continued)

Compound	Source	Family	Plant part	References
Amentoflavone **(6.3)**	*L. yateensis*	Cupressaceae	Leafy twigs	Gadek and Quinn, 1983
	Metasequoia glyptostroboides	Taxodiaceae	Leaves	Beckmann, Geiger and De Groot Pfleiderer, 1971
	Neocallitropis pancheri	Cupressaceae		Gadek and Quinn, 1983
	Orthopterygium amplifolium	Julianiaceae		Wannan and Quinn, 1988
	O. huaucui			
	Ouratea hexasperma	Ochnaceae	n.i.	Felicio *et al*., 2004
	O. multiflora		Leaves	Felicio *et al*., 2001
	O. parviflora			Felicio *et al*., 2004
	O. semiserrata		n.i.	
	O. sulcata		Leaves	Pegnyemb *et al*., 2005
	Papuacedrus papuana	Cupressaceae	Leafy twigs	Gadex and Quinn, 1983.
	Papuacedrus torricellensis			
	Pilgerodendron uniferum			
	Podocarpus elongate, P. gracitior, P. latifolius, P. nagi, P. nerifolius, P. taxifolia	Podocarpaceae	Leaves	Roy *et al*., 1987
	Rhus pyroides	Anacardiaceae		Svenningsen *et al*., 2006
	R. succedanea		Seed kernels	Lin *et al*., 2001
	Sciadopitys verticillata	Taxodiaceae	Leaves	Gadex and Quinn, 1989
	Selaginella tamariscina	Selaginellaceae		Kang *et al*., 2005
	S. willdenowii			Silva *et al*., 1995

n.i. = not indicated

Table 6. Distribution of C-C biflavones in plants (continued)

Compound	Source	Family	Plant part	References
Amentoflavone **(6.3)**	*Sequoia sempervirens*	Taxodiaceae	Leaves	Gadex and Quinn, 1989
	Sequoiadendron giganteum			
	Taiwania cryptomeriodes			
	Taxodium ascendens			
	T. distichum			
	Tetraclinus articulata	Cupressaceae	Leafy twigs	Gadex and Quinn, 1983
	Thuja koraiensis, T. occidentalis, T. plicata, T. standishii, Thujopsis dolobrata			Gadek and Quinn, 1985
	V. pichinchense			Weniger *et al*., 2006
	V. prunifolium		Cortex	Lobstein *et al*., 1999
	Widdringtonia cupressoides, W. dracomantana, W. juniperoides, W. whytei	Cupressaceae	Leafy twigs	Gadex and Quinn, 1983
	Xerophyta plicata	Velloziaceae	Leaves	William *et al.*, 1987
3′,3‴-biapigenin **(6.4)**	*Homalothecium lutescens*	Brachythecia-ceae	Gameto-phytes	Seeger *et al*., 1993
Bilobetin **(6.5)**	*Callitris neocaledonica*	Cupressaceae	Leafy twigs	Gadex and Quinn, 1983
	Cephalotaxus koreana	Cephalotaxa-ceae		Lee *et al*., 2006
	Chamaecyparis thyroides	Cupressaceae		Gadek and Quinn, 1985
	Cryptomeria japonica	Taxodiaceae	Leaves	Gadex and Quinn, 1989
	Diselma archerii	Cupressaceae	Leafy twigs	Gadex and Quinn, 1983
	Dysoxylum lenticellare	Meliaceae	Leaves	He *et al*., 1996

Table 6. Distribution of C-C biflavones in plants (continued)

Compound	Source	Family	Plant part	References
Bilobetin **(6.5)**	*Gingko biloba*	Ginkgoaceae		Kang *et al*., 2005
	Podocarpus latifolius, P. taxifolia	Podocarpaceae	Leaves	Roy *et al*., 1987
	Sciadopitys verticillata	Taxodiaceae		Gadex and Quinn, 1989
	Selaginella willdenowii	Selaginellaceae		Silva *et al*., 1995
	Sequoiadendron giganteum, Taxodium ascendens, T. distichum	Taxodiaceae		Gadex and Quinn, 1989
	Tetraclinus articulata	Cupressaceae	Leafy twigs	Gadex and Quinn, 1983
	Thujopsis dolobrata			Gadek and Quinn, 1985
	Widdringtonia cupressoides, W. dracomantana, W. juniperroides, W. whytei			Gadex and Quinn, 1983
5′,6′′-Biluteolin **(6.6)**	*Dicranoloma robustum, D. robustum*	Dicranaceae	Whole plant	Markham, Anderson and Viotto, 1988
5′,8′′-Biluteolin **(6.7)**				
Cupressufla-vone **(6.8)**	*Biota orientalis, Calocedrus decurrens, Chamaecyparis nootkatensis*	Cupressaceae	Leafy twigs	Gadek and Quinn, 1985
	Fitzroya cupressoides			Gadex and Quinn, 1983
	Juniperus bermudiana, J. communis, J. drupacea, J. excelsa, J. oxycedrus, J. virginiana			Gadek and Quinn, 1985
	Tetraclinus articulata			Gadex and Quinn, 1983
	Thuja occidentalis			Gadek and Quinn, 1985

Table 6. Distribution of C-C biflavones in plants (continued)

Compound	Source	Family	Plant part	References
3′′′-Desoxy dicranolomin **(6.9)**	*Plagiomnium undulatum*	Mniaceae	Gameto phytes	Rampendahl *et al*., 1996
Dicranolomin **(6.10)**	*Dicranoloma robustum*	Dicranaceae	Whole plant	Markham *et al*., 1988
	Plagiomnium undulatum	Mniaceae	Gameto phytes	Rampendahl *et al*., 1996
5′,3′′′-Dihydroxy amentoflavone **(6.11)**	*Campylopus clavatus*	Dicranaceae	Whole plant	Geiger and Markham, 1992
	C. holomitrium			
5′,3′′′-Dihydroxy robustaflavone **(6.12)**	*C ampylopus clavatus*			
	C. holomitrium			
	Plagiomnium undulatum	Mniaceae	Gameto phytes	Rampendahl *et al*., 1996
7,7′′-Dimethyl agathisflavone **(6.13)**	*Agathis atropurpurea, A. australis, A. ovata, A. robusta*	Araucariaceae	Leaves	Ofman *et al*., 1995
7,7′′-Di-*O*-methyl amentoflavone **(6.14)**	*Taiwania cryptomerioides*	Taxodiaceae		Gadex and Quinn, 1989
4′,7′′-Di-*O*-methyl amentoflavone **(6.15)**	*Cephalotaxus koreana*	Cephalotaxa-ceae	Leafy twigs	Lee *et al*., 2006
	Selaginella willdenowii	Selaginellaceae	Leaves	Silva *et al*., 1995
7′′, 4′′′-Di-*O*-methyl amentoflavone **(6.16)**	*Callitris neocaledonica, C. oblonga, C. sulcata, Diselma archerii*	Cupressaceae	Leafy twigs	Gadex and Quinn, 1983
	Metasequoia glyptostroboides	Taxodiaceae	Leaves	Beckmann *et al*., 1971
	Neocallitris pancheri, Papuacedrus papuana, Widdrintonia cupressoides, W. whytei	Cupressaceae	Leafy twigs	Gadex and Quinn, 1983

Table 6. Distribution of C-C biflavones in plants (continued)

Compound	Source	Family	Plant part	References
7,7′′-Dimethyl cupressflavone **(6.17)**	*Agathis atropurpurea, A. australis, A. ovata, A. robusta*	Araucariaceae	Leaves	Ofman *et al*., 1995
	Diselma archerii, Fitzroya cupressoides, Widdringtonia cupressoides, W. dracomantana, W. juniperoides, W. whytei	Cupressaceae	Leafy twigs	Gadex and Quinn, 1983
4′,7′′-Dimethyl robustaflavone **(6.18)**	*Dysoxylum lenticellare*	Meliaceae	Leaves	He *et al*., 1996
Ginkgetin **(6.19)**	*Araucaria angustifolia*	Araucariaceae	Needles	Yamaguchi *et al*., 2005
	Cephalotaxus koreana	Cephalotaxa-ceae	Leafy twigs	Lee *et al*., 2006
	Chamaecyparis formosansis, C. lawsoniana, C. nootkatensis, C. thyroides	Cupressaceae	Leafy twigs	Gadex and Quinn, 1985
	Ginkgo biloba	Ginkgoaceae	Leaves	Kang *et al*., 2005; Weniger *et al*., 2006
	Cryptomeria japonica	Taxodiaceae		Gadex and Quinn, 1989
	Cunninghamia lanceolata			
	Fokienia hodginsii	Cupressaceae	Leafy twigs	Gadex and Quinn, 1985
	Glyptostrobus lineata	Taxodiaceae	Leaves	Gadex and Quinn, 1989
	Juniperus bermudiana, J. virginiana	Cupressaceae	Leafy twigs	Gadex and Quinn, 1985
	Sciadopitys verticillata, Sequoia sempervirens	Taxodiaceae	Leaves	Gadex and Quinn, 1989

Table 6. Distribution of C-C biflavones in plants (continued)

Compound	Source	Family	Plant part	References
Ginkgetin **(6.19)**	*Taiwania cryptomerioides, Taxodium ascendens*	Taxodiaceae	Leaves	Gadex and Quinn, 1989
	Taxus yunnanensis	Taxaceae	Bark, twigs, leaves	Shinozaki *et al*., 2002
	Thuja koraiensis, T. occidentalis, T. standishii, Thujopsis dolobrata			Gadex and Quinn, 1985
Hexamethyl amentoflavone **(6.20)**	*Actinostrobus acuminatus, A. pyramidalis, Austrocedrus chilensis, Callitris macleayana, C. neocaledonica, C. oblonga, C. sulcata, Diselma archerii, Fitzroya cupressoides, Libocedrus plumose, L. yateensis, Neocallitropsis pancheri, Papuacedrus papuana, P. torricellensis, Pilgerodendron uniferum, Tetraclinus articulate, Widdringtonia cupressoides, W. dracomantana, W. juniperoides, W. whytei*	Cupressaceae	Leafy twigs	Gadex and Quinn, 1983

Table 6. Distribution of C-C biflavones in plants (continued)

Compound	Source	Family	Plant part	References
Hexamethyl cupressuflavone **(6.21)**	*Diselma archerii, Fitzroya cupressoides, Tetraclinus articulate, Widdringtonia cupressoides, W. dracomantana, W. juniperoides, W. whytei*	Cupressaceae	Leafy twigs	Gadex and Quinn, 1983
Hexamethyl robustaflavone **(6.22)**	*Diselma archerii*			
Heveaflavone **(6.23)**	*Podocarpus taxifolia*	Podocarpaceae	Leaves	Roy *et al*., 1987
Isoginkgetin **(6.24)**	*Araucaria angustifolia*	Araucariaceae	Callus culture	Fonseca *et al*., 2000
	Chamaecyparis formosansis, C. nootkatensis	Cupressaceae	Leafy twigs	Gadek and Quinn, 1985
	Cunninghamia lanceolata	Taxodiaceae	Leaves	Gadex and Quinn, 1989
	Dysoxylum lenticellare	Meliaceae		He *et al*., 1996
	Fokienia hodginsii	Cupressaceae	Leafy twigs	Gadek and Quinn, 1985
	Ginkgo biloba	Ginkgoaceae	Leaves	Kang *et al*., 2005; Weniger *et al*., 2006
	Glyptostrobus lineate, Metasequoia glyptostro-boides	Taxodiaceae		Gadex and Quinn, 1989
	Podocarpus gracitior, P. latifolius, P. nagi, P. nerifolius	Podocarpaceae		Roy *et al*., 1987
	Sciadopitys verticillata, Sequoia sempervirens,	Taxodiaceae		Gadex and Quinn, 1989

Table 6. Distribution of C-C biflavones in plants (continued)

Compound	Source	Family	Plant part	References
Isoginkgetin **(6.24)**	*Sequoiadendron giganteum*, *Taxodium distichum*	Taxodiaceae	Leaves	Gadex and Quinn, 1989
Kayaflavone **(6.25)**	*Podocarpus gracitior*, *P. latifolius*	Podocarpaceae		Roy *et al*., 1987
7-*O*-Methyl agathisflavone **(6.26)**	*Agathis atropurpurea*, *A. australis*, *A. ovata*, *A. robusta*	Araucariaceae		Ofman *et al*., 1995
7-*O*-Methyl cupressflavone **(6.27)**	*Agathis atropurpurea*, *A. australis*, *A. ovata*, *A. robusta*			
7″-*O*-methyl robustaflavone **(6.28)**	*Diselma archerii*, *Neocallitropsis pancheri*	Cupressaceae	Leafy twigs	Gadex and Quinn, 1983
	Selaginella willdenowii	Selaginellaceae	Leaves	Silva *et al*., 1995
	Widdringtonia dracomantana, *W. juniperoides*, *W. whytei*	Cupressaceae	Leafy twigs	Gadex and Quinn, 1983
Philonotisflavone **(6.29)**	*Mnium hornum*	Mniaceae	Gamatophytes	Brinkmeier, Geiger and Zinsmeister, 1999
Philonotisflavone-4‴-methyl ether **(6.30)**				
Podocarpusflavone A **(6.31)**	*Actinostrobus acuminatus*, *A. pyramidalis*	Cupressaceae	Leafy twigs	Gadex and Quinn, 1983
	Athrotaxis cupressoides	Taxodiaceae	Leaves	Gadex and Quinn, 1989
	Austrocedrus chilensis	Cupressaceae	Leafy twigs	Gadex and Quinn, 1983

Table 6. Distribution of C-C biflavones in plants (continued)

Compound	Source	Family	Plant part	References
Podocarpusflavone A **(6.31)**	*Biota orientalis*	Cupressaceae	Leafy twigs	Gadek and Quinn, 1985
	Callitris canescens, C. columellaris, C. endlicheri, C. macleayana			Gadex and Quinn, 1982
	C. macleayana, C. neocaledonica, C. oblonga			Gadex and Quinn, 1983
	C. pressii, C. rhomboidea			Gadex and Quinn, 1982
	C. sulcata			Gadex and Quinn, 1983
	Calocedrus decurrens, Chamaecyparis formosansis, C. lawsoniana, C. nootkatensis			Gadek and Quinn, 1985
	Cunninghamia lanceolata	Taxodiaceae	Leaves	Gadex and Quinn, 1989
	Cupressus lusitanica, C. sempervirens	Cupressaceae	Leafy twigs	Gadek and Quinn, 1985
	Fitzroya cupressoides			Gadex and Quinn, 1983
	Fokienia hodginsii			Gadek and Quinn, 1985
	Glyptostrobus lineata	Taxodiaceae	Leaves	Gadex and Quinn, 1989
	Isophysis tasmanica	Iridaceae		William *et al*., 1987
	Juniperus procera, J. virginiana	Cupressaceae	Leafy twigs	Gadek and Quinn, 1985
	Libocedrus plumose, L. yateensis			Gadex and Quinn, 1983
	Metasequoia glyptostro-boides	Taxodiaceae	Leaves	Gadex and Quinn, 1989
	Neocallitropsis pancheri	Cupressaceae	Leafy twigs	Gadex and Quinn, 1983

Table 6. Distribution of C-C biflavones in plants (continued)

Compound	Source	Family	Plant part	References
Podocarpusflavone A **(6.31)**	*Papuacedrus papuana, P. torricellensis, Pilgerodendron uniforum*	Cupressaceae	Leafy twigs	Gadex and Quinn, 1983
	Podocalyx loranthoides	Euphorbiaceae	Aerial parts	Suárez *et al*., 2003
	Podocarpus elongate, P. gracitior, P. macrophylla, P. nagi, P. nerifolius, P. taxifolia, P. uranii	Podocarpaceae	Leaves	Roy *et al*., 1987
	Sequoiadendron giganteum	Cupressaceae		Gadex and Quinn, 1989
	Taxodium distichum, T. mucronarum	Taxodiaceae		
	Tetraclinus articulata	Cupressaceae	Leafy twigs	Gadex and Quinn, 1983
	Thuja koraiensis, T. occidentalis, T. plicata, Thujopsis dolobrata			Gadek and Quinn, 1985
	Trattinnickia glaziovii	Burseraceae	Leaves	Siani and Ribeiro, 1995
	Widdringtonia cupressoides, W. juniperoides	Cupressaceae	Leafy twigs	Gadex and Quinn, 1983
Putraflavone **(6.32)**	*Athrotaxis cupressoides, A. laxifolia, A. selaginoides, Cryptomeria japonica, Cunninghamia lanceolata, Metasequoia glyptostro-boides*	Taxodiaceae	Leaves	Gadex and Quinn, 1989

Table 6. Distribution of C-C biflavones in plants (continued)

Compound	Source	Family	Plant part	References
Putraflavone **(6.32)**	*Podocalyx loranthoides*	Euphorbiaceae	Aerial parts	Suárez *et al*., 2003
	Podocarpus macrophylla, P. nerifolius, P. taxifolia	Podocarpaceae	Leaves	Roy *et al*., 1987
	Putranjiva roxburghii	Euphorbiaceae	Trunk bark, leaves	Garg and Mitra, 1971
	Taiwania cryptomeriodes, Taxodium distichum	Taxodiaceae	Leaves	Gadex and Quinn, 1989
Ridiculuflavone A **(6.33)**	*Aristolochia ridicula*	Aristolochia-ceae		Machado and Lopes, 2005
Ridiculuflavone B **(6.34)**				
Robustaflavone **(6.35)**	*Fokienia hodginsii*	Cupressaceae	Leafy twigs	Gadek and Quinn, 1985
	Garcinia multiflora	Guttiferae	Seed kernels	Lin *et al*., 2001
	Rhus succedanea	Anacardiaceae		
	Selaginella willdenowii	Selaginellaceae	Leaves	Silva *et al*., 1995
	Thujopsis dolobrata	Cupressaceae	Leafy twigs	Gadek and Quinn, 1985
Sciadopitysin **(6.36)**	*Araucaria angustifolia*	Araucariaceae	Callus culture	Fonseca *et al*., 2000
	Athrotaxis cupressoides	Taxodiaceae	Leaves	Gadex and Quinn, 1989
	Cephalotaxus koreana	Cephalotaxa-ceae	Leafy twigs	Lee *et al*., 2006
	Gingko biloba	Ginkgoaceae	Leaves	Kang *et al*., 2005
	Metasequoia glyptostro-boides	Taxodiaceae		Beckmann *et al*., 1971; Gadex and Quinn, 1989
	Podocarpus elongata, P. macrophylla, P. taxifolia, P. uranii	Podocarpaceae		Roy *et al*., 1987

Table 6. Distribution of C-C biflavones in plants (continued)

Compound	Source	Family	Plant part	References
Sciadopitysin **(6.36)**	*Sciadopitys verticillata, Taxodium ascendens, T. distichum, T. mucronarum*	Taxodiaceae	Leaves	Gadex and Quinn, 1989
	Taxus yunnanensis	Taxaceae	Bark, twigs, leaves	Shinozaki *et al*., 2002
Sequoiaflavone **(6.37)**	*Athrotaxis cupressoides, A. laxifolia, A. selaginoides, Cryptomeria japonica, Cunninghamia lanceolata, M. glyptostro-boides*	Taxodiaceae	Leaves	Gadex and Quinn, 1989
	Podocarpus taxifolia	Podocarpaceae		Roy *et al*., 1987
	Sequoiadendron giganteum, Sequoia sempervirens, Taiwania cryptomeri-oides, Taxodium ascendens, T. distichum	Taxodiaceae		Gadex and Quinn, 1989
Sotetsuflavone **(6.38)**	*Cycas revoluta*	Cycadaceae		Geiger *et al.*, 1971
	M. glyptostro-boides	Taxodiaceae		Beckmann *et al.*, 1971.
Stephaflavone A **(6.39)**	*Stephania tetrandra*	Menisperma-ceae	Aerial parts	Si *et al*., 2001
Stephaflavone B **(6.40)**				
4‴, 5, 5″, 7″-Tetrahydroxy–3‴, 4′, 7-trimethoxy-3,6″-biflavone **(6.41)**	*Aristolochia ridicula*	Aristolochia-ceae	Stem	Carneiro *et al*., 2000

Table 6. Distribution of C-C biflavones in plants (continued)

Compound	Source	Family	Plant part	References
4′′′, 5′′, 7, 7′′-Tetrahydroxy-3′′′, 4′, 5-trimethoxy-3, 6′′-biflavone **(6.42)**	*Aristolochia ridicula*	Aristolochia-ceae	Stem	Carneiro *et al*., 2000
4′,4′′′,7,7′′-Tetra-*O*-methyl agathisflavone **(6.43)**	*Agathis australis, A. ovata*	Araucariaceae	Leaves	Ofman *et al*., 1995
7,4′,7′′,4′′′-Tetra-*O*-methyl amentoflavone **(6.44)**	*Araucaria angustifolia*		Needles	Yamaguchi *et al*., 2005
	Cephalotaxus koreana	Cephalotaxa-ceae	Leafy twigs	Lee *et al*., 2006
	Podocarpus taxifolia	Podocarpaceae	Leaves	Roy *et al*., 1987
4′,4′′′,7,7′′-Tetra-*O*-methyl cupressflavone **(6.45)**	*Agathis australis, A. ovata*	Araucariaceae		Ofman *et al*., 1995
4',7,7"-Tri-*O*-methyl agathisflavone **(6.46)**	*Agathis atropurpurea, A. australis, A. ovata*			
7, 4′, 7′′-Tri-*O*-methyl amentoflavone **(6.47)**	*Araucaria angustifolia*		Callus culture	Fonseca *et al*., 2000
7′′,4′,4′′′-Tri-*O*-methyl amentoflavone **(6.48)**	*Cryptomeria japonica, Cunninghamia lanceolata*	Taxodiaceae	Leaves	Gadex and Quinn, 1989
4′,7,7′′-Tri-*O*-methyl cupressflavone **(6.49)**	*Agathis atropurpurea A. australis, A. ovata*	Araucariaceae		Ofman *et al*., 1995

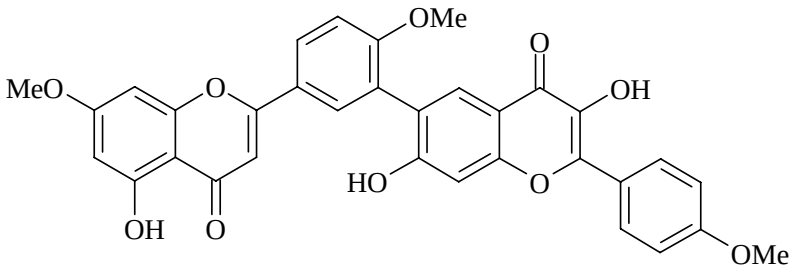

Abiesin **(6.1)**

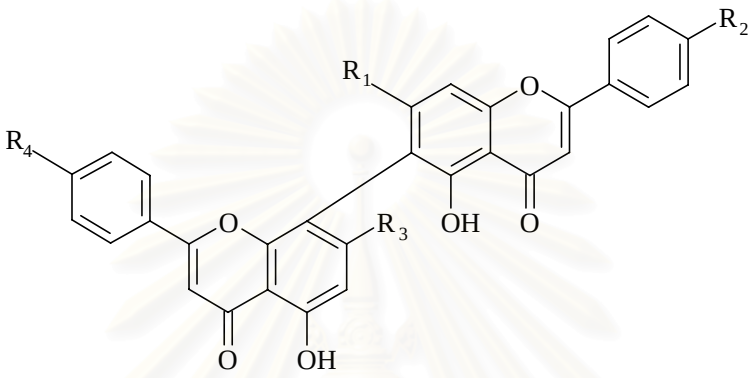

	R_1	R_2	R_3	R_4
Agathisflavone **(6.2)**	OH	OH	OH	OH
7,7′′-Di-*O*-methyl agathisflavone **(6.13)**	OCH_3	OH	OCH_3	OH
7-*O*-Methyl agathisflavone **(6.26)**	OCH_3	OH	OH	OH
4′,4′′′,7,7′′-Tetra-*O*-methyl agathisflavone **(6.43)**	OCH_3	OCH_3	OCH_3	OCH_3
4′,7,7′′-Tri-*O*-methyl agathisflavone **(6.46)**	OCH_3	OCH_3	OCH_3	OH

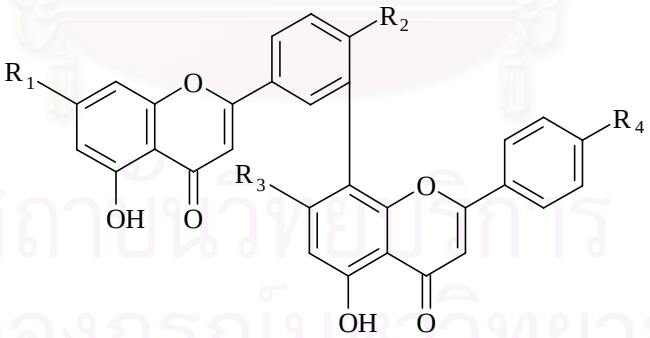

	R_1	R_2	R_3	R_4
Amentoflavone **(6.3)**	OH	OH	OH	OH
Bilobetin **(6.5)**	OH	OCH_3	OH	OH
7,7′′-Di-*O*-methyl amentoflavone **(6.14)**	OCH_3	OH	OCH_3	OH
4′,7′′-Di-*O*-methyl amentoflavone **(6.15)**	OH	OCH_3	OCH_3	OH

Figure 8. Chemical structures of C-C biflavones in plants (continued)

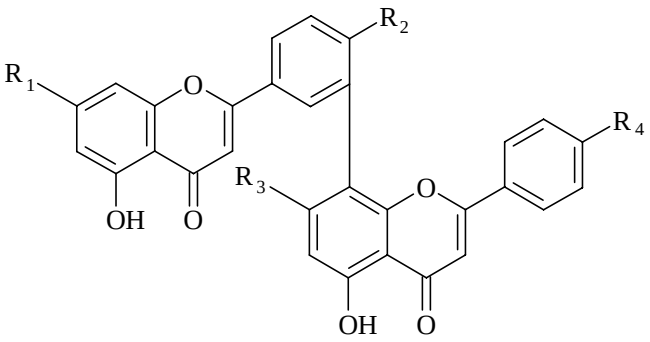

	R_1	**R_2**	**R_3**	**R_4**
7″,4‴-Di-*O*-methyl amentoflavone **(6.16)**	OH	OH	OCH_3	OCH_3
Ginkgetin **(6.19)**	OCH_3	OCH_3	OH	OH
Heveaflavone **(6.23)**	OCH_3	OH	OCH_3	OCH_3
Isoginkgetin **(6.24)**	OH	OCH_3	OH	OCH_3
Kayaflavone **(6.25)**	OH	OCH_3	OCH_3	OCH_3
Podocarpusflavone A **(6.31)**	OH	OH	OH	OCH_3
Putraflavone **(6.32)**	OCH_3	OH	OH	OCH_3
Sciadopitysin **(6.36)**	OCH_3	OCH_3	OH	OCH_3
Sequoiaflavone **(6.37)**	OCH_3	OH	OH	OH
Sotetsuflavone **(6.38)**	OH	OH	OCH_3	OH
7,4′,7″,4‴-Tetra-*O*-methyl amentoflavone **(6.44)**	OCH_3	OCH_3	OCH_3	OCH_3
7,4′,7″-Tri-*O*-methyl amentoflavone **(6.47)**	OCH_3	OCH_3	OCH_3	OH
7″,4′,4‴-Tri-*O*-methyl amentoflavone **(6.48)**	OH	OCH_3	OCH_3	OCH_3

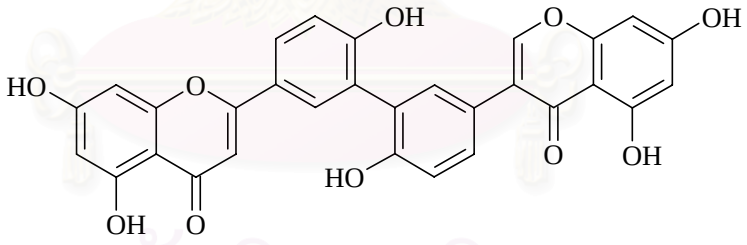

3′,3″-Biapigenin **(6.4)**

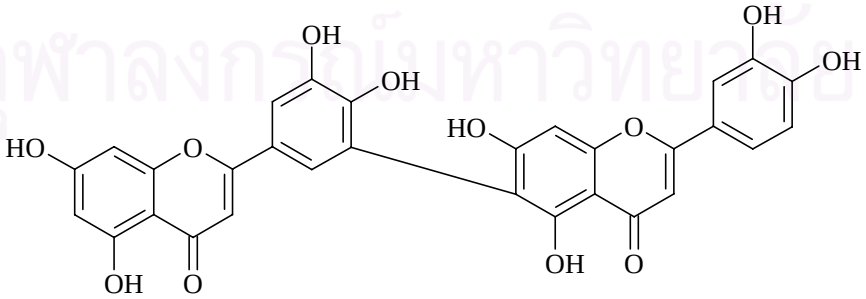

5′, 6″-Biluteolin **(6.6)**

Figure 8. Chemical structures of C-C biflavones in plants (continued)

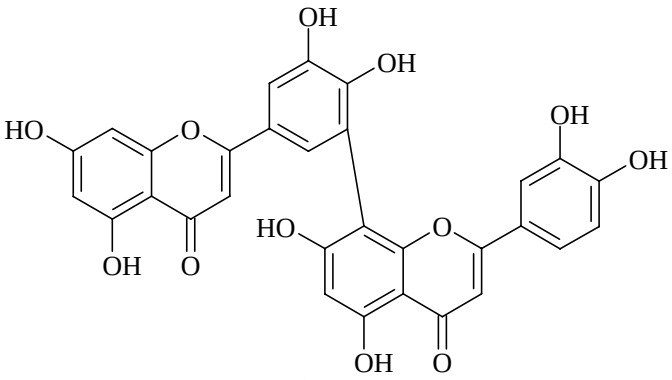

5′, 8′′-Biluteolin **(6.7)**

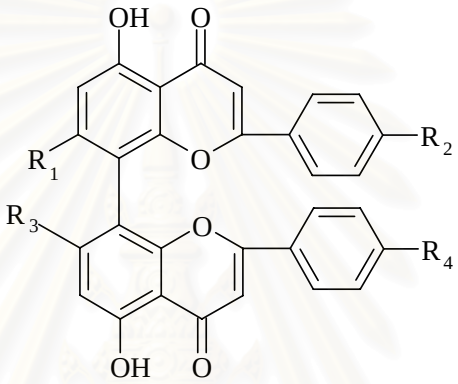

	R_1	R_2	R_3	R_4
Cupressflavone **(6.8)**	OH	OH	OH	OH
7,7′′-Di-*O*-methyl cupressflavone **(6.17)**	OCH_3	OH	OCH_3	OH
7-*O*-Methyl cupressflavone **(6.27)**	OCH_3	OH	OH	OH
4′,4′′′,7,7′′-Tetra-*O*-methyl cupressflavone **(6.45)**	OCH_3	OCH_3	OCH_3	OCH_3
4′,7,7′′-Tri-*O*-methyl cupressflavone **(6.49)**	OCH_3	OCH_3	OCH_3	OH

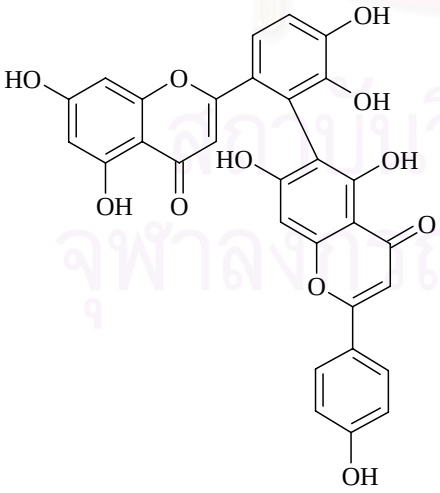

3′′′-Desoxydicranolomin **(6.9)**

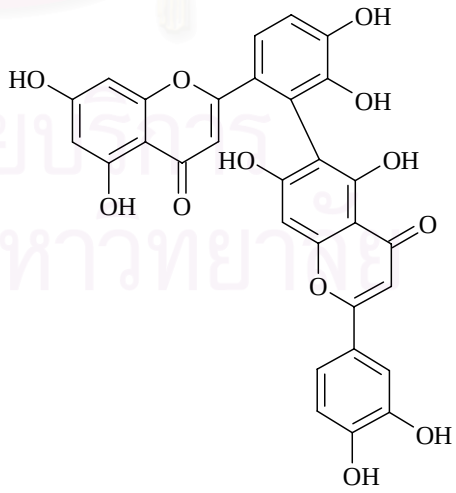

Dicranolomin **(6.10)**

Figure 8. Chemical structures of C-C biflavones in plants (continued)

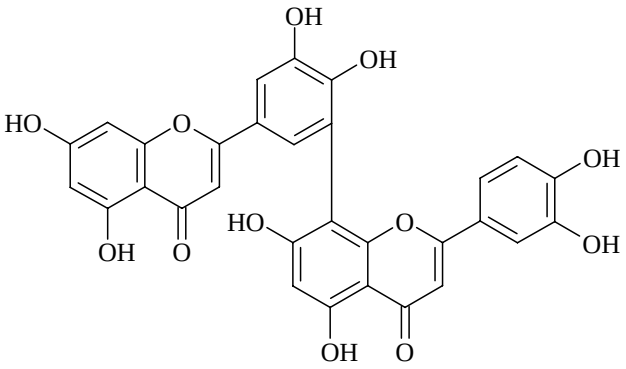

5′, 3‴-Dihydroxy amentoflavone **(6.11)**

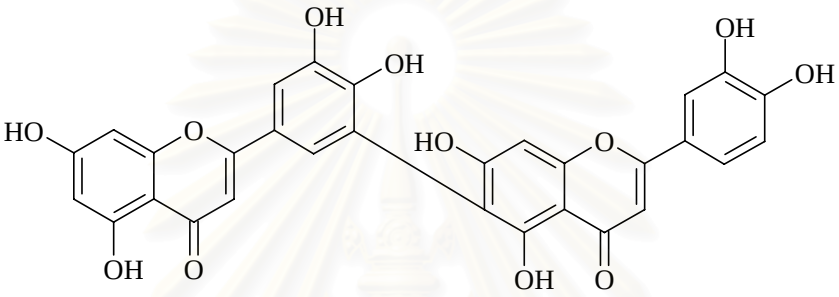

5′, 3‴-Dihydroxy robustaflavone **(6.12)**

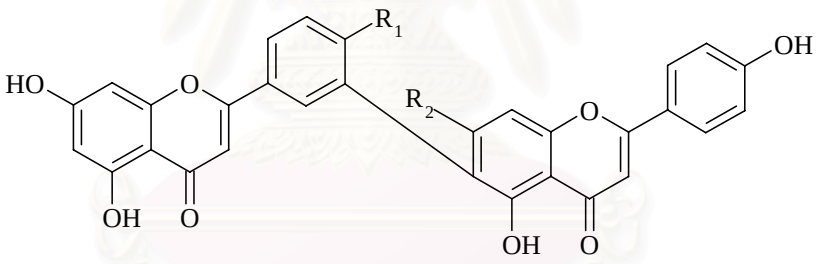

	R_1	R_2
4′,7″-Di-*O*-methyl robustaflavone **(6.18)**	OCH_3	OCH_3
7″-*O*-Methyl robustaflavone **(6.28)**	OH	OCH_3
Robustaflavone **(6.35)**	OH	OH

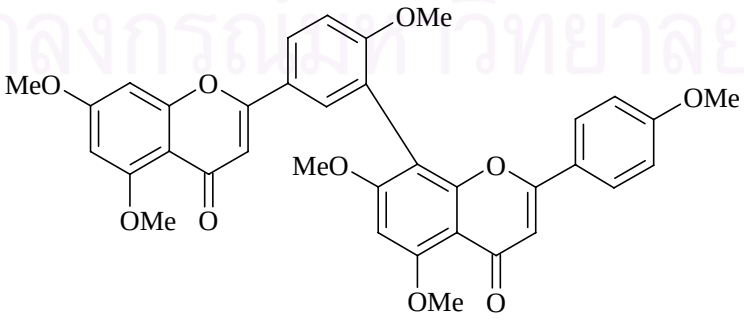

Hexamethyl amentoflavone **(6.20)**

Figure 8. Chemical structures of C-C biflavones in plants (continued)

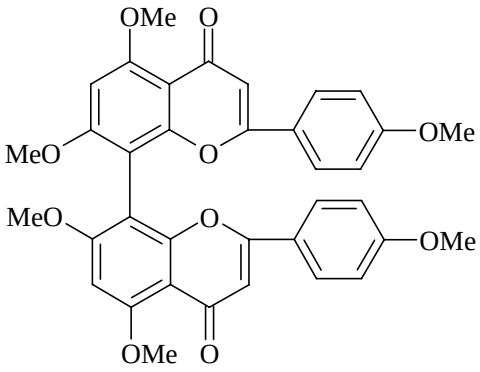

Hexamethyl cupressflavone **(6.21)**

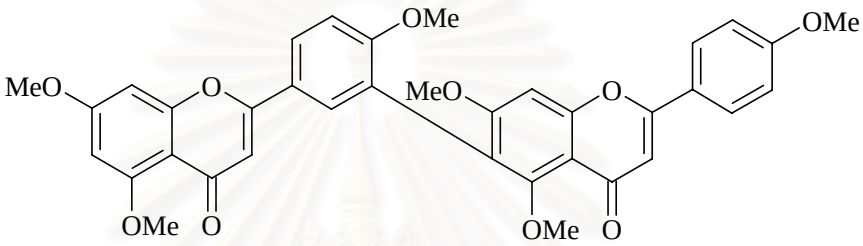

Hexamethyl robustaflavone **(6.22)**

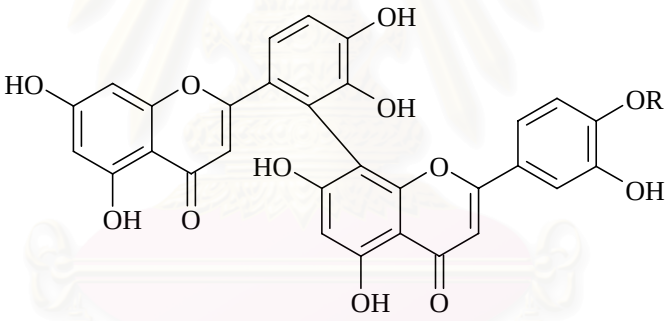

Philonotisflavone **(6.29)** R = H
Philonotisflavone-4′′′-methyl ether **(6.30)** R = CH_3

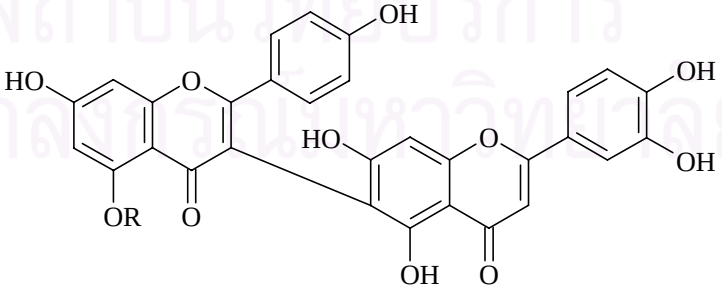

Ridiculuflavone A **(6.33)** R = H
Ridiculuflavone B **(6.34)** R = CH_3

Figure 8. Chemical structures of C-C biflavones in plants (continued)

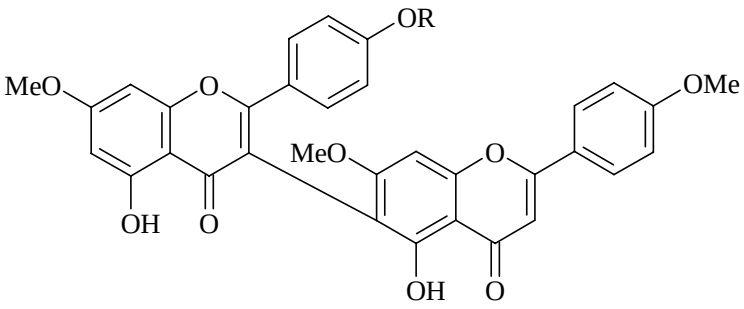

	R
Stephaflavone A **(6.39)**	CH_3
Stephaflavone B **(6.40)**	H

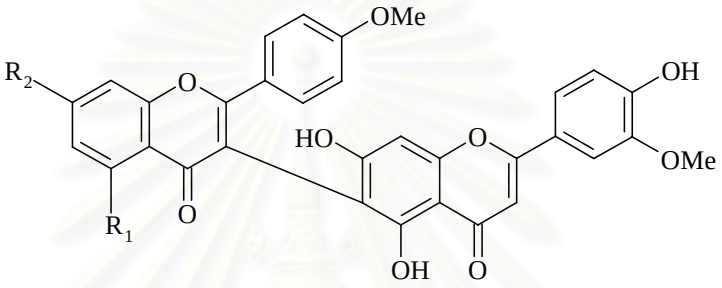

	R_1	**R_2**
4‴,5,5″,7″-Tetrahydroxy-3‴,4″,7-trimethoxy-3,6″-biflavone **(6.41)**	OH	OMe
4‴,5″,7,7″-Tetrahydroxy-3‴,4″,5-trimethoxy-3,6″-biflavone **(6.42)**	OMe	OH

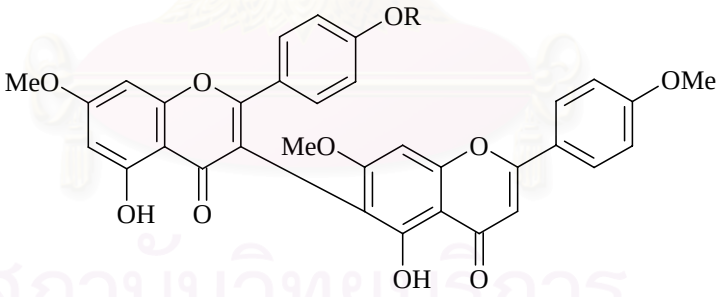

	R
Stephaflavone A **(6.39)**	CH_3
Stephaflavone B **(6.40)**	H

Figure 8. Chemical structures of C-C biflavones in plants (continued)

Chemical constituents of *Elateriospermum tapos* Blume

There have been two previous reports on the chemical constituents of *Elateriospermum tapos* (Chow and Quon, 1970; Ling *et al*., 2006). Two cyanogenic glycosides were found in the leaves of this plant, along with some flavonoids,

triterpenoids and tannins. A number of glycosides were also found in its wood. These chemical constituents of *E. tapos* are shown in **Table 7**, and their structures are displayed in **Figure 9**.

Table 7. Previously reported chemical constituents of *E. tapos*

Compound	Category	Plant part	References
AC trimer **(7.1)**	Condensed tannin	Leaves	Ling *et al*., 2006
Amentoflavone **(7.2)**	Biflavone		
β-Amyrin acetate **(7.3)**	Triterpene		Chow and Quon, 1970
β-Amyrin palmitate **(7.4)**			
2-((6-*O*-(β-D-Apiofuranosyl)-β-D-glucopyranosyl)oxy) butane **(7.5)**	Glycoside	Wood	Ling *et al*., 2006
2-((6-*O*-(β-D-Apiofuranosyl)-β-D-glucopyranosyl)oxy) propane **(7.6)**			
Catechin **(7.7)**	Flavan-3-ol	Leaves	
3,5-Dimethoxy-4-hydroxybenzyl alcohol 4-*O*-β-D-gluco pyranoside **(7.8)**	Aromatic glycoside	Wood	
Epiafzelechin-(4β→8)-catechin **(7.9)**	Condensed tannin	Leaves	
Gallocatechin **(7.10)**	Flavan-3-ol		
Germanicol acetate **(7.11)**	Triterpene		Chow and Quon, 1970
Germanicol palmitate **(7.12)**			
Guaiacyl glycerol **(7.13)**	Phenyl propane		Ling *et al*., 2006
Linamarin **(7.14)**	Cyanogenic glycoside		
Leonuriside A **(7.15)**	Aromatic glycoside		
Linolenyl stearyl 3-*O*-(α-D-galactopyranosyl-(1′′→6′)-*O*-β-D-galactopyranosyl)-*sn*-glycerol **(7.16)**	Glycerol derivative		
Lotaustralin **(7.17)**	Cyanogenic glycoside		
Lupeol acetate **(7.18)**	Triterpene		Chow and Quon, 1970
Procyanidin B-1 **(7.19)**	Condensed tannin		Ling *et al*., 2006
Procyanidin B-3 **(7.20)**			
Roseoside **(7.21)**	Megastigmane glycoside		
ψ-Taraxasterol acetate **(7.22)**	Triterpene		Chow and Quon, 1970

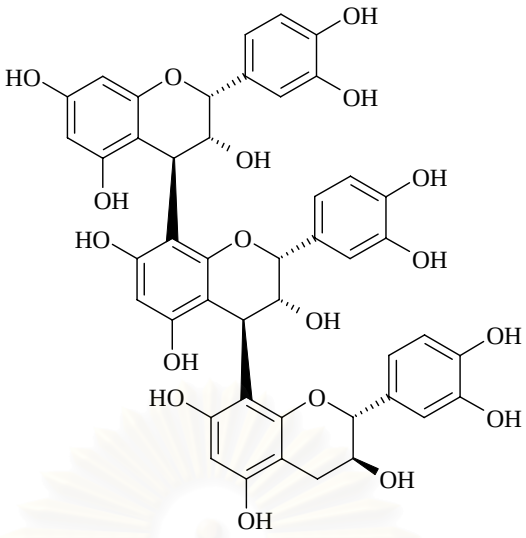

AC trimer **(7.1)**

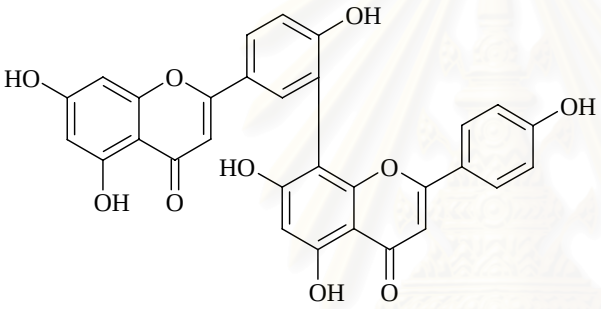

Amentoflavone **(7.2)**

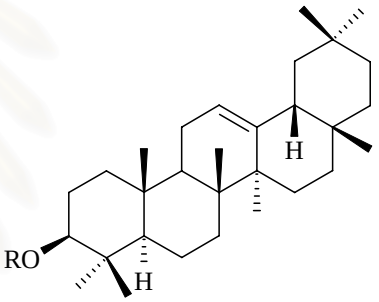

β-amyrin acetate **(7.3)** R = OAc
β-amyrin palmitate **(7.4)**
R = *O*-hexadecanoyl

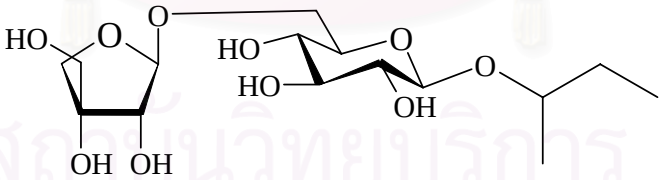

2-((6-*O*-(β-D-Apiofuranosyl)-β-D-glucopyranosyl)oxy) butane **(7.5)**

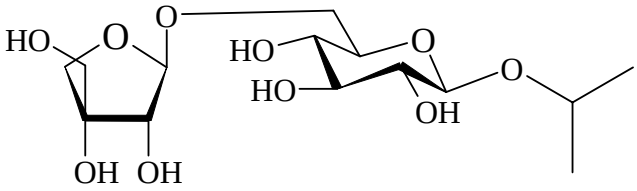

2-((6-*O*-(β-D-Apiofuranosyl)-β-D-glucopyranosyl)oxy) propane **(7.6)**

Figure 9. Previously reported chemical constituents of *E. tapo*s

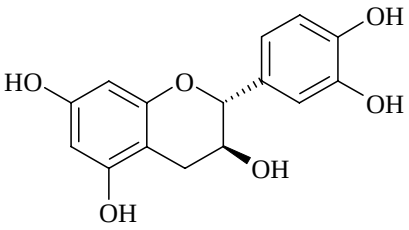

Catechin **(7.7)**

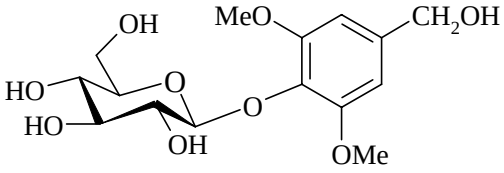

3,5-Dimethoxy-4-hydroxybenzyl alcohol 4-*O*-β-D-glucopyranoside **(7.8)**

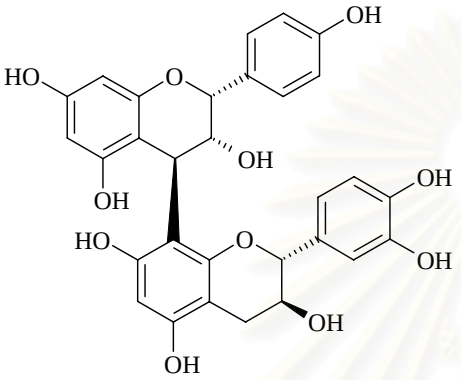

Epiafzelechin-(4β→8)-catechin **(7.9)**

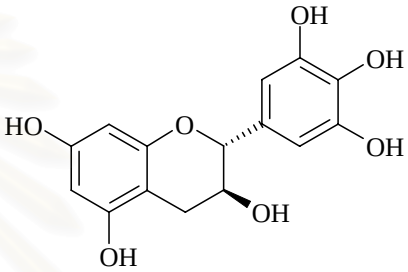

Gallocatechin **(7.10)**

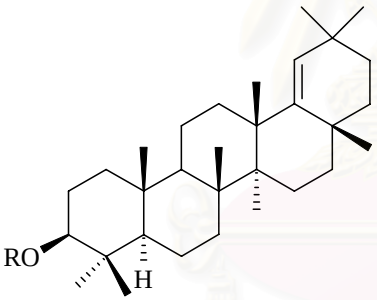

Germanicol acetate **(7.11)** R = OAc
Germanicol palmitate **(7.12)** R = *O*-hexadecanoyl

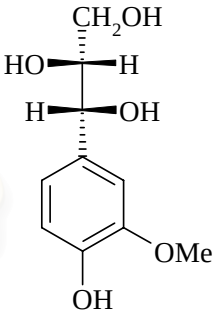

Guaiacyl glycerol **(7.13)**

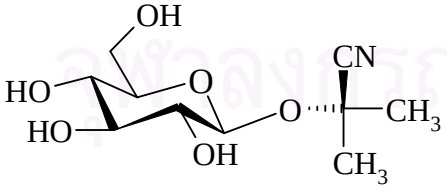

Linamarin **(7.14)**

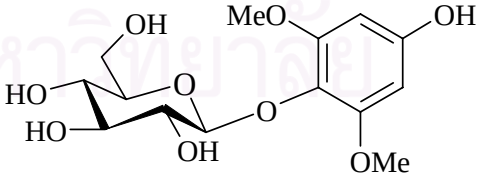

Leonuriside A **(7.15)**

Figure 9. Previously reported chemical constituents of *E. tapos* (continued)

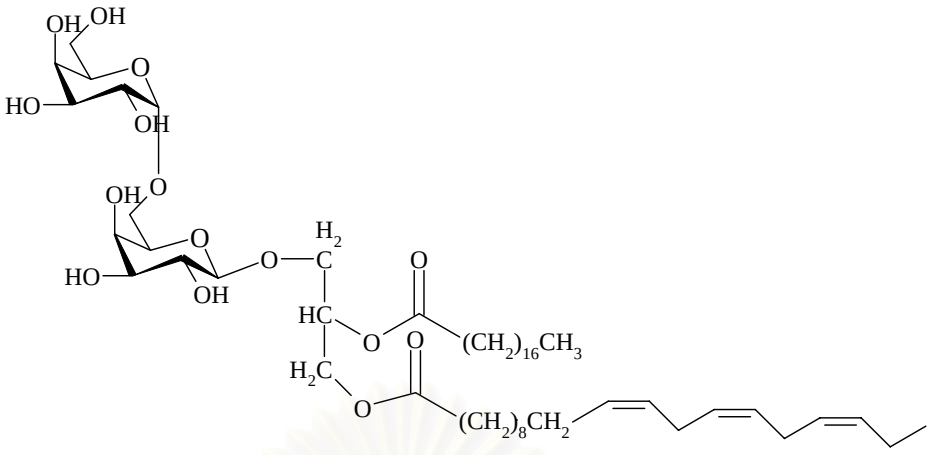

Linolenyl stearyl 3-*O*-(α-D-galactopyranosyl-(1′′→6′)-*O*-β-D-galactopyranosyl)-*sn*-glycerol **(7.16)**

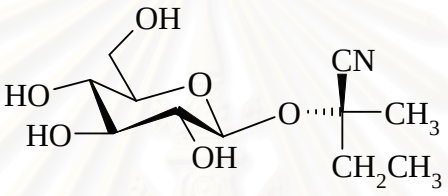

Lotaustralin **(7.17)**

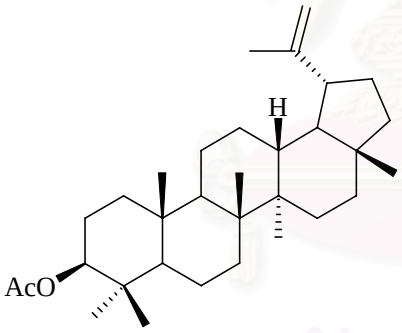

Lupeol acetate **(7.18)**

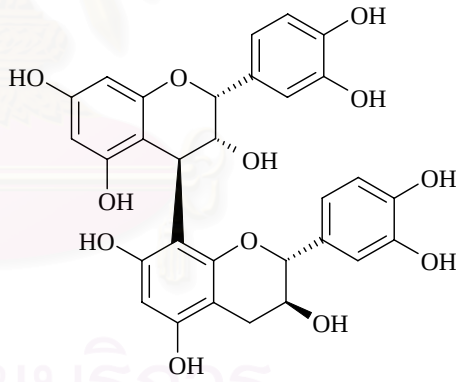

Procyanidin B-1 **(7.19)**

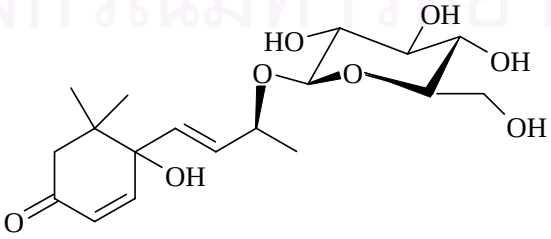

Roseoside **(7.21)**

Figure 9. Previously reported chemical constituents of *E. tapo*s (continued)

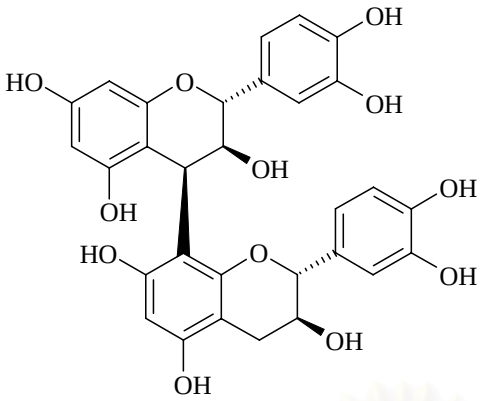

Procyanidin B-3 **(7.20)**

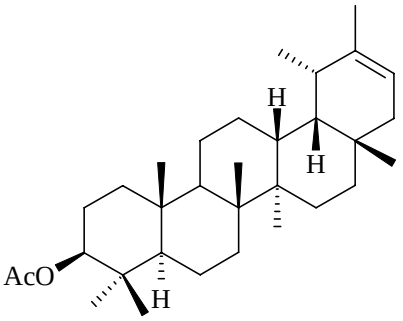

ψ-Taraxasterol acetate **(7.22)**

Figure 9. Previously reported chemical constituents of *E. tapos* (continued)

CHAPTER III

EXPERIMENTAL

1. Sources of Plant Materials

The aerial parts of *Canavalia rosea* (Sw.) DC. were collected from Rayong, in June, 2003. The leaves, stem and flowers of *Elateriospermum tapos* Blume were collected from Khao Luang, Nakhon Si Thammarat, in March, 2004. Voucher herbarium specimens of both plants have been deposited at the herbarium of the Department of Pharmaceutical Botany, Faculty of Pharmaceutical Sciences, Chulalongkorn University, Bangkok, Thailand.

2. General Techniques

2.1 Solvents

Throughout this work, all organic solvents were commercial grade and were redistilled prior to use.

2.2 Analytical Thin-Layer Chromatography (TLC)

Technique	:	One dimension, ascending
Adsorbent	:	Silica gel 60 F_{254} (E. Merck) precoated plate
Layer thickness	:	0.2 mm
Distance	:	5.0 cm
Temperature	:	Laboratory temperature (25-30°C)
Detection	:	1. Ultraviolet light (254 and 365 nm)
		2. Anisaldehyde-H_2SO_4 and heat at 105°C for 10 min

2.3 Column Chromatography

2.3.1 Conventional Column Chromatography

Adsorbent	:	Silica gel 60 (No. 7734) particle size 0.063-0.200 nm (E. Merck)
Packing method	:	Dry Packing
Sample loading	:	The sample was dissolved in a small amount of the organic solvent, mixed with a small quantity of adsorbent, triturated, dried and then placed gently on top of the column.

Detection : Fractions were examined by TLC technique in the same manner as described in section 2.2

2.3.2 Vacuum Liquid Chromatography

Adsorbent : Silica gel 60 (No. 9385) particle size 0.040-0.063 nm (E. Merck)

Packing method : Wet Packing

The adsorbent was mixed with the eluent into a slurry, then poured into a column and allowed to settle.

Sample loading : The sample was dissolved in a small amount of the eluent, and then applied gently on top of the column.

Detection : Fractions were examined by TLC technique in the same manner as described in section 2.2

2.3.3 Gel Filtration Chromatography

Gel Filter : Sephadex LH 20 (Pharmacia Biotech AB)

Packing method : Gel filter was suspended in the eluent and left standing to swell for 24 hours prior to use. It was then poured into the column and allow to set tightly.

Sample loading : The sample was dissolved in a small amount of the eluent, and then applied gently on top of the column.

Detection : Fractions were examined by TLC technique in the same manner as described in section 2.2

2.4 Spectroscopy

2.4.1 Ultraviolet (UV) Spectra

UV spectra were obtained on a Shimadzu UV-160A spectrophotometer (Pharmaceutical Research Instrument Center, Faculty of Pharmaceutical Sciences, Chulalongkorn University).

2.4.2 Infrared (IR) Spectra

IR spectra (KBr disc and film) were recorded on a Perkin Elmer FT-IR 1760X spectrometer (Scientific and Technological Research Equipment Center, Chulalongkorn University).

2.4.3 Mass Spectra

Electrospray Ionization Time of Flight (ESI-TOF) mass spectra and high resolution Electrospray Ionization Time of Flight (HRESI-TOF) mass spectra were measured on a Micromass LCT mass spectrometer (BIOTEC Central Research

Unit, National Center for Genetic Engineering and Biotechnology). Electron impact (EI) mass spectra were recorded on a Agilent 7890A mass spectrometer (Medicinal Plant Research Institute, Department of Medical Sciences, Ministry of Public Health).

2.4.4 Proton and Carbon-13 Nuclear Magnetic Resonance (^{1}H and ^{13}C NMR) Spectra

^{1}H (300 MHz) and ^{13}C (75 MHz) NMR spectra were measured on a Bruker DPX-300 FT-NMR spectrometer (Pharmaceutical Research Instrument Center, Faculty of Pharmaceutical Sciences, Chulalongkorn University).

^{1}H (500 MHz) and ^{13}C (125 MHz) NMR spectra were measured on a JEOL JMN-A 500 spectrometer, Varian ^{unity}INOVA spectrometer (Scientific and Technological Research Equipment Center, Chulalongkorn University), and a Bruker-AV 500 MHz spectrometer (BIOTEC Central Research Unit, National Center for Genetic Engineering and Biotechnology).

The solvents for NMR spectra were deuterated chloroform ($CDCl_3$), deuterated methanol (CD_3OD), deuterated acetone (acetone-d_6) and deuterated dimethylsulfoxide (DMSO-d_6). The chemical shifts were reported in ppm scale using the chemical shift of the solvent as the reference signal.

2.5 Physical Properties

2.5.1 Melting Points

Melting points were obtained on a Fisher-John melting point apparatus (Department of Pharmaceutical Botany, Faculty of Pharmaceutical Sciences, Chulalongkorn University).

2.5.2 Optical Rotations

Optical rotations were measured on a Perkin-Elmer 341 polarimeter using a sodium lamp operating at 589 nm (Pharmaceutical Research Instrument Center, Faculty of Pharmaceutical Sciences, Chulalongkorn University).

3. Extraction and Isolation

3.1 Extraction and Isolation of Compounds from *Canavalia rosea*

3.1.1 Extraction of *C. rosea* Aerial Parts

The dried aerial parts (940 g) were ground, then macerated with 95% ethanol (3 × 4L). The filtrate was pooled and evaporated under reduced pressure at temperature not exceeding 40°C to afford the ethanol extract (132.76 g, 14.12 % of

dried plant weight). The ethanol extract was redissolved with 70% ethanol and partitioned with CH_2Cl_2.

Evaporation of the CH_2Cl_2 layer gave CH_2Cl_2 extract (31.65 g, 3.37 % of dried plant weight). The extract was dissolved with 70% ethanol, then partitioned with hexane to give, after evaporation under reduced pressure, hexane extract (23.11 g, 2.46 % of dried plant weight) and CH_2Cl_2 extract (6.40 g, 0.68 % of dried plant weight), respectively.

The aqueous layer was concentrated under reduced pressure, and further partitioned with BuOH to afford BuOH extract (20.10 g, 2.14 % of dried plant weight) and aqueous extract (80.85 g, 8.60 % of dried plant weight).

3.1.2 Isolation of Compounds from the Hexane Extract of *C. rosea*

The hexane extract (23.11 g) was dissolved in a small amount of hexane, triturated with kieselguhr and dried at room temperature. It was then applied on top of a silica gel column (380 g, 10 × 10 cm) eluted stepwise with a gradient mixture of hexane-EtOAc (1:0 to 0:1), then EtOAc-MeOH (1:0 to 0:1). Two hundred 100-ml fractions were collected and the eluates examined by TLC (solvent system: hexane-EtOAc = 4:1). Fractions with similar chromatographic pattern were combined to yield 8 pooled fractions (A1-A8, **Table 8**)

Table 8. Combined fractions from the hexane extract of *C. rosea*

Fraction code	Weight (g)
A1	0.11
A2	0.14
A3	1.12
A4	1.34
A5	11.81
A6	1.88
A7	1.71
A8	1.54

3.1.2.1 Isolation of Component CAR-1 (Mixture of β-Sitosterol and Stigmasterol)

Fraction A4 (1.34 g) was chromatographed on a silica gel column (100 g, 2.5 × 20 cm), using a gradient mixture of hexane-EtOAc (9:1 to 0:1) as eluent. Ninety-four 20-ml fractions were obtained, examined by TLC (solvent system: hexane-EtOAc = 4:1), then pooled into 7 fractions (A41-A47). Fraction A41, showing a major purple spot at R_f = 0.28, gave component CAR-1 as colorless needles (41.0 mg, 0.0044% yield).

3.1.2.2 Isolation of Compound CAR-2 (β-Sitosterol glucoside)

Solution of fraction A6 (1.88 g) in hexane-EtOAc (3:2), after being left to stand at room temperature overnight, yielded compound CAR-2 as a pale brown precipitate (90.0 mg, 0.0096% yield).

3.1.2.3 Isolation of Compound CAR-6 (Canarosine)

Compound CAR-6 (7.1 mg, 0.0008% yield) crystallized from fraction A8 as pale yellow needle.

3.1.3 Isolation of Compounds from the CH_2Cl_2 Extract of *C. rosea*

The extract (5.2 g) was chromatographed on a silica gel column (200 g, 10 × 8 cm), eluted with a gradient mixture of CH_2Cl_2-MeOH (1:0 to 0:1), to give 113 collected fractions (50 ml each). These fractions were examined by TLC (solvent system: CH_2Cl_2-MeOH = 43:2), then the ones with similar TLC pattern were combined into 4 major fractions (B1-B4, **Table 9**)

Table 9. Combined fractions from the CH_2Cl_2 extract of *C. rosea*

Fraction code	Weight (g)
B1	0.05
B2	0.43
B3	0.60
B4	3.11

3.1.3.1 Isolation of Compound CAR-4 (*Epi*-inositol-6-*O*-methyl ether)

Fraction B4 (3.11 g) was recrystallized from a mixture of CH_2Cl_2-MeOH (2:1) to give compound CAR-4 as colorless needles (16.2 mg, 0.0021% yield).

3.1.4 Isolation of Compounds from the BuOH Extract of *C. rosea*

3.1.4.1 Isolation of Compound CAR-3 (Rutin)

Compound CAR-3 precipitated as yellow powder (2.13 g, 0.2263% yield) from the BuOH extract of *C. rosea*.

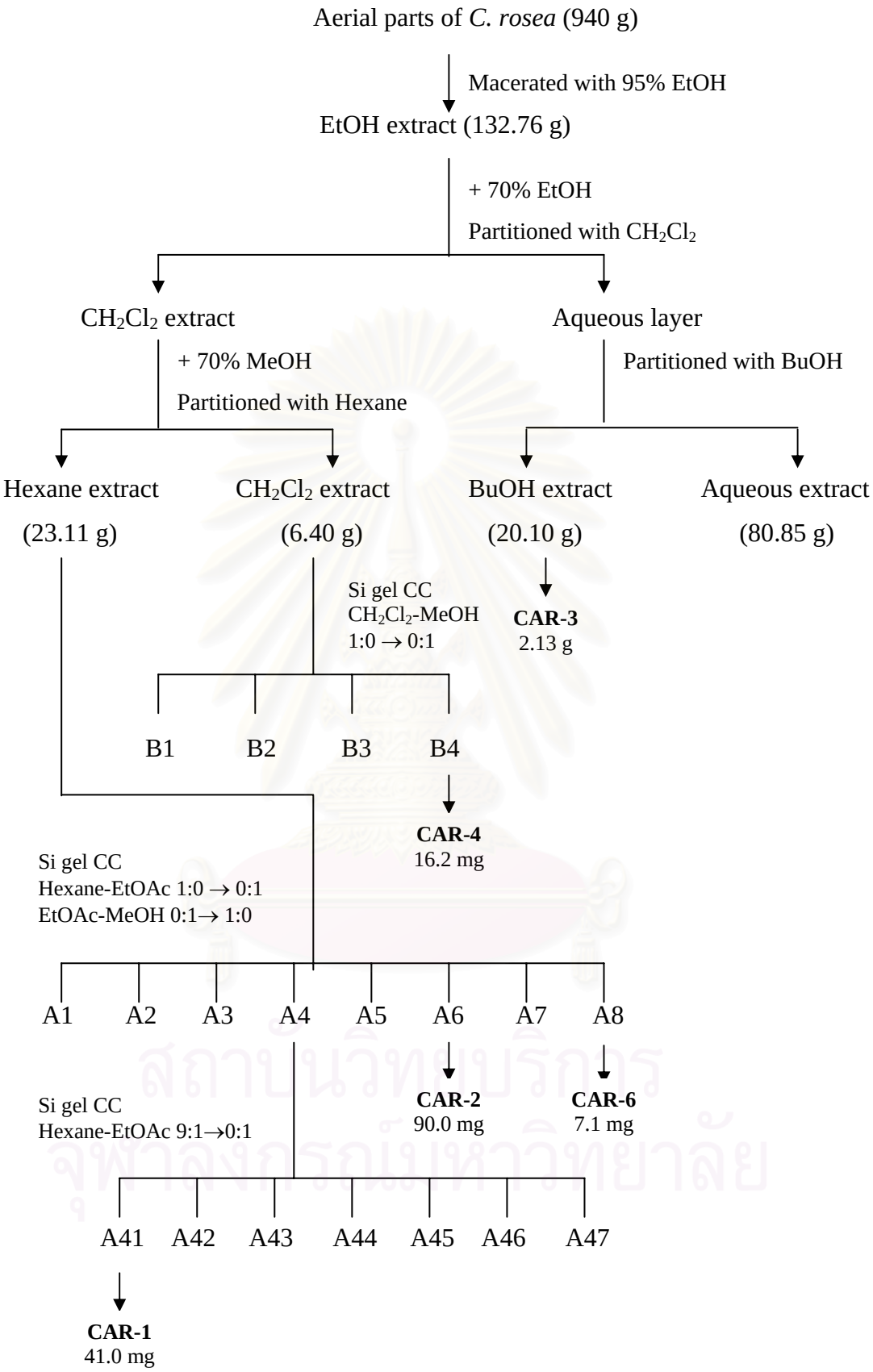

Scheme 1. Extraction and isolation of *C. rosea* aerial parts

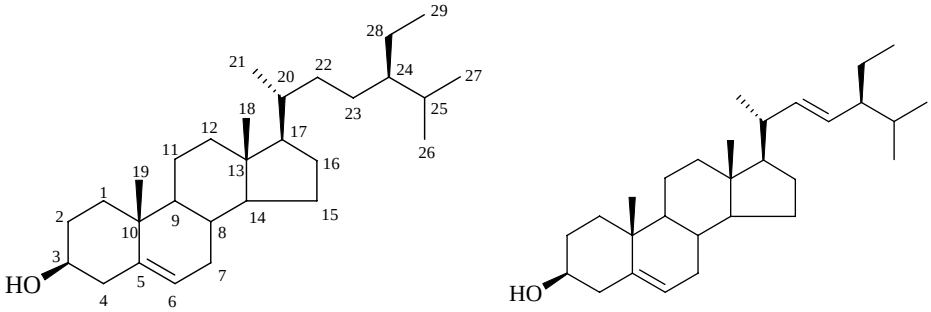

CAR-1

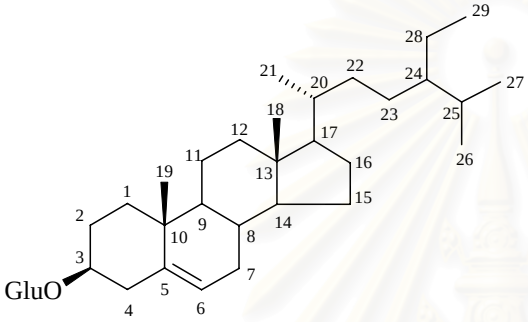

CAR-2

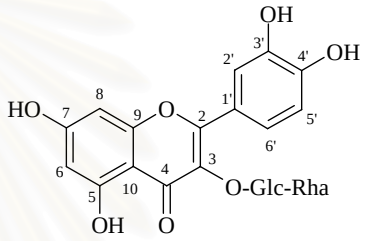

CAR-3

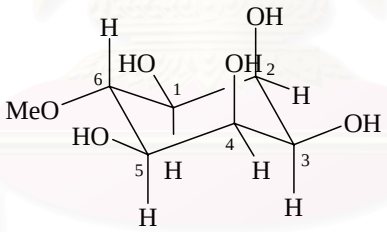

CAR-4

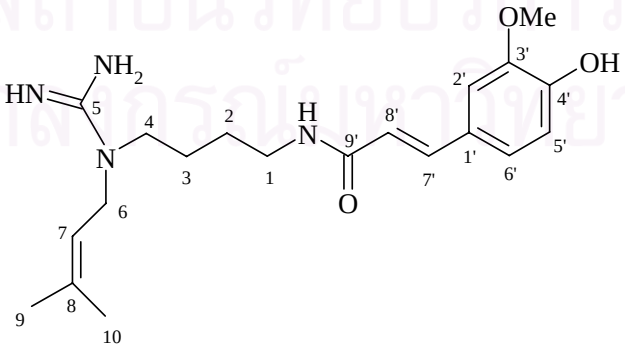

CAR-6

Figure 10. Structures of compounds isolated from *C. rosea* aerial parts

3.2 Extraction and Isolation of Compounds from *Elateriospermum tapos*

3.2.1. Extraction of *E. tapos* Stem

The dried stem (3.8 kg) were ground, then macerated with hexane (3 × 5L), CH_2Cl_2 (3 × 5L) and MeOH (3 × 5L), respectively. Each pooled filtrate was evaporated under reduced pressure at temperature not exceeding 40°C to afford hexane extract (19.57 g, 0.52% of dried weight), CH_2Cl_2 extract (19.04 g, 0.50% of dried weight) and MeOH extract (80.00 g, 2.11% of dried weight), respectively.

3.2.2 Isolation of Compounds from the Hexane Extract of *E. tapos* Stem

The hexane extract (19.57 g) was chromatographed on a silica gel column (400 g, 9.5 × 10 cm). Elution was performed using a gradient mixture of hexane-acetone (1:0 to 17:3) to give 53 fractions (100 ml each). Fractions were combined according to their TLC pattern (solvent system: hexane-acetone = 5:1) to yield 6 pooled fractions (A1-A6, **Table 10**)

Table 10. Combined fractions from the hexane extract of *E. tapos* stem

Fraction code	Weight (g)
A1	0.58
A2	0.32
A3	0.08
A4	8.37
A5	3.00
A6	5.84

3.2.2.1 Isolation of Compound ET-S1 (Lupeol acetate)

Fraction A4 (8.37 g) was separated on a silica gel column (75 g, 2.5 × 20 cm), eluting with a gradient mixture of hexane-acetone (1:0 to 17:3), to give 95 fractions (10 ml each). After TLC monitoring (solvent system: hexane-acetone 5:1), these were pooled into 6 fractions (fractions A41-A46). Fraction A43 (1.23 g) was further separated on another silica gel column (30 g, 2.5 × 10 cm), eluting with a gradient mixture of 2-5% acetone in hexane. Forty-seven fractions (10 ml each) were collected. Fractions showing a purple spot (R_f = 0.88, solvent system: hexane-acetone

= 5:1) on TLC upon spraying with anisaldehyde-H_2SO_4 were combined to afford compound ET-S1 as colorless needles (407.8 mg, 0.0107% yield).

3.2.2.2 Isolation of Compound ET-S5 (Germanicol palmitate)

Fraction A42 (0.59 g) was chromatographed on a silica gel column (15 g, 2 × 13 cm), eluting with a gradient mixture of 0.5-2% acetone in hexane. Fractions showing a purple spot at R_f value of 0.94 on TLC (solvent system: hexane-acetone = 5:1) were combined to yield compound ET-S5 as white powder (238.0 mg, 0.0063% yield).

3.2.2.3 Isolation of Compound ET-S3 (Lupeol)

Fraction A44 (0.38 g) was subjected to silica gel column (20 g, 2 × 15 cm), using a gradient mixture of 2-15% acetone in hexane as eluent, to give 70 fractions (10 ml each). These fractions were monitored by TLC (solvent system: hexane-acetone = 5:1), then fractions showing a purple spot (R_f = 0.38) were combined and subjected to repeated silica gel column chromatography (20 g, 2 × 15 cm). Elution was performed using a gradient mixture of hexane-acetone (1:0 to 19:1) to afford compound ET-S3 (17.0 mg, 0.0004% yield).

3.2.2.4 Isolation of Compound ET-S2 (Acetyl aleuritolic acid)

Fraction A45 (0.87 g) was crystallized from a mixture of CH_2Cl_2-MeOH (2:1) to give compound ET-S2 (37.2 mg, 0.001% yield).

3.2.2.5 Isolation of Component ET-S4 (Mixture of β-Sitosterol and Stigmasterol)

Fraction A6 (5.84 g) was subjected to silica gel column chromatography (150 g, 2.5 × 20 cm), eluting with a gradient mixture of hexane-acetone (1:0 to 0:1), to give 80 fractions (50 ml each). Fractions with similar TLC pattern (solvent system: hexane-acetone = 5:1) were combined into 6 fractions (A61-A66). Component ET-S4 (42.0 mg, 0.0011% yield) was obtained from fraction A63.

3.2.3 Isolation of Compounds from the CH_2Cl_2 Extract of *E. tapos* Stem

The CH_2Cl_2 extract (19.04 g) was chromatographed on a silica gel column (400 g, 9.5 × 10 cm), eluting with a gradient mixture of hexane-acetone (1:0 to 2:3), to afford 160 fractions (100 ml each). TLC monitoring (solvent system: hexane-acetone = 2:1) led to combination of these fractions into 8 major ones (fractions B1-B8, **Table 11**).

Table 11. Combined fractions from the CH_2Cl_2 extract of *E. tapos* stem

Fraction code	Weight (g)
B1	0.35
B2	0.32
B3	2.88
B4	0.81
B5	1.48
B6	1.10
B7	0.94
B8	0.98

3.2.3.1 Isolation of Compound ET-S6 (Yucalexin B-22)

Fraction B6 (1.10 g) was separated on a silica gel column (30 g, 2 × 8 cm), using a gradient mixture of 25-30% acetone in hexane, to obtain 66 fractions (20 ml each). Fractions showing similar TLC pattern (solvent system: hexane-acetone = 2:1) were combined into 5 fractions (B61-B65).

Fraction B63 (0.52 g) was chromatographed on a silica gel column (30 g, 2 × 8 cm) eluting with a gradient mixture of 20-30% acetone in hexane. Forty eight fractions (20 ml each) were collected and combined according to their TLC pattern (solvent system: hexane-acetone 2:1) into 6 pooled fractions (B631-B636). Compound ET-S6 (7.9 mg, 0.0002% yield) was obtained from fraction B632.

3.2.3.2 Isolation of Compounds ET-S12 and ET-S15 (Yucalexin P-15 and Syringaldehyde)

Fraction B634 (0.36 g) was chromatographed on a Sephadex LH-20 column, washed down with CH_2Cl_2-MeOH (1:1) to afford compound ET-S12 (17.6 mg, 0.0005% yield). The remaining fraction was separated on another Sephadex LH-20 column, using CH_2Cl_2-MeOH (2:1) as eluent, to give compound ET-S15 (10.1 mg, 0.0003% yield).

3.2.3.3 Isolation of Compound ET-S7 (Yucalexin P-17)

Fraction B5 (1.48 g) was chromatographed on a silica gel column (40 g, 2 × 15 cm) eluting with a gradient mixture of hexane-acetone (1:0 to 4:1) to give 64 fractions (10 ml each). Fractions showing a purple spot on TLC (R_f = 0.4, solvent

system: hexane-acetone = 2:1) were combined to give compound ET-S7 (60.6 mg, 0.0016% yield).

3.2.3.4 Isolation of Compound ET-S8 (Scopoletin)

Fraction B7 (0.94 g) was purified on a silica gel column (80 g, 2.5 × 20 cm), eluting with a gradient mixture of hexane-acetone (7:3 to 0:1), to give 51 collected fractions (10 ml each). Fractions showing a fluorescent blue spot under UV at 365 nm were combined to afford compound ET-S8 (70.1 mg, 0.0018% yield). The same compound (115.2 mg, 0.0030% yield) was also obtained from fraction B65.

3.2.3.5 Isolation of Compound ET-S11 (2,3-*Seco*-sonderianol)

Fraction B8 (0.98 g) was separated on a silica gel column (100 g, 2.5 × 25 cm) eluting with a gradient mixture of hexane and acetone (3:2 to 0:1). Sixty fractions were collected (50 ml/fraction) and combined according to their TLC pattern (solvent system: hexane-acetone = 2:1) into 8 fractions (B81-B88). Fraction B82 was further purified on a Sephadex LH-20 column, eluting with a mixture of CH_2Cl_2-MeOH (1:1), to yield compound ET-S11 (7.0 mg, 0.0002% yield).

3.2.3.6 Isolation of Compound ET-S14 (Oleic acid)

Fraction B3 (2.88 g) was chromatographed on a silica gel column (40 g, 2.5 × 6 cm), eluted with a gradient mixture of hexane-acetone (1:0 to 19:1), to obtain 44 fractions which were examined by TLC (solvent system: hexane-acetone = 2:1), then combined into 6 fractions (B31-B36). Fraction B32 (0.41 g) was subjected to a silica gel column (30 g, 2.5 × 11 cm), eluting with 2% acetone in hexane, to afford compound ET-S14 (5.3 mg, 0.0001% yield).

3.2.3.7 Isolation of Component ET-S10 (Mixture of β-Sitosterol and Stigmasterol)

Fraction B33 (0.46 g), subjected to silica gel column chromatography, eluting with a gradient mixture of hexane-acetone (1:0 to 93:7), to give 70 fractions (10 ml each). Fractions showing a purple spot on TLC (R_f = 0.67, solvent system: hexane-acetone = 2:1) were combined to yield component ET-S10 (24 mg, 0.0006% yield).

3.2.4 Isolation of Compounds from the MeOH Extract of *E. tapos* Stem

The MeOH extract (40.0 g) was subjected to vacuum liquid column chromatography on a silica gel column (400g, 13 × 6 cm), eluting stepwise with a gradient mixture of CH_2Cl_2-MeOH (1:0 to 0:1). Each collected fraction was 400 ml.

Forty-four fractions were collected and combined according to their TLC pattern into 4 fractions (C1-C4, **Table 12**).

Table 12. Combined fractions from the MeOH extract of *E. tapos* stem

Fraction code	Weight (g)
C1	3.37
C2	1.96
C3	26.80
C4	4.47

3.2.4.1 Isolation of Compound ET-S16 (Scopoletin)

Fraction C1 (3.37 g) was subjected to silica gel column chromatography (140 g, 5 × 8 cm), eluting with a gradient mixture of CH_2Cl_2-MeOH (1:0 to 0:1), to yield 138 fractions (15 ml each). TLC monitoring (solvent system: EtOAc-MeOH = 5:3) led to the combination of these fractions into 7 pooled fractions (C11-C17). Fraction C12 (0.12 g) was separated by gel filtration chromatography on a Sephadex LH-20 column, using CH_2Cl_2-MeOH (1:1) as eluent. Fractions showing a fluorescent blue spot on TLC (R_f = 0.72, solvent system: EtOAc-MeOH = 5:3) were combined to afford compound ET-S16 (2.4 mg, 0.0001% yield).

3.2.4.2 Isolation of Compound ET-S17 (Amentoflavone)

Fraction C13 (0.51 g) was chromatographed on a Sephadex LH-20 column, eluting with CH_2Cl_2-MeOH (1:1), to give 20 fractions (5 ml each). Fractions showing a yellow spot on TLC (R_f = 0.95, solvent system: CH_2Cl_2-MeOH = 2:1) were combined and further purified on two successive Sephadex LH-20 columns, eluting with CH_2Cl_2-MeOH (1:1) and CH_2Cl_2-MeOH (2:1), respectively, to afford compound ET-S17 (1.7 mg, 0.0002% yield).

3.2.5 Extraction of *E. tapos* Flowers

The dried flowers of *E. tapos* (260.0 g) were ground and macerated with hexane (3 × 2L), CH_2Cl_2 (3 × 2L) and MeOH (3 × 2L), respectively, to afford, after evaporation under reduced pressure at temperature not exceeding 40°C, the hexane extract (10.4 g, 4.00% of dried weight), CH_2Cl_2 extract (3.68 g, 1.42% of dried weight) and MeOH extract (11.14 g, 4.28% dried weight), respectively.

3.2.6 Isolation of Compounds from the Hexane Extract of *E. tapos* Flowers

The hexane extract (8.83 g) was chromatographed on a silica gel column (150 g, 2.5 × 15 cm), eluting with a gradient mixture of hexane-acetone (1:0 to 0:1), to give 111 fractions (30 ml each). These fractions were combined according to their TLC pattern (solvent system: hexane-acetone = 5:1) into 4 major fractions (D1-D4, **Table 13**)

Table 13. Combined fractions from the hexane extract of *E. tapos* flowers

Fraction code	Weight (g)
D1	1.25
D2	2.09
D3	3.58
D4	0.57

3.2.6.1 Isolation of Compound ET-F3 (Lupeol 3-acetate)

Fraction D2 (2.09 g) was separated on a silica gel column (100 g, 2.5 × 10 cm), eluting with a gradient mixture of hexane-acetone (1:0 to 23:2), into 58 fractions (10 ml each). These fractions were monitored by TLC (solvent system: hexane-acetone = 5:1), then combined into 3 fractions (D21-D23). Fraction D22 (0.16 g) was subjected to another silica gel column (30 g, 1.5 × 10 cm), eluting with a gradient mixture of hexane-acetone (1:0 to 49:1), to give 110 collected fractions (5 ml each). Fractions showing a purple spot on TLC (R_f = 0.88, solvent system: hexane-acetone = 5:1) were combined to afford compound ET-F3 as colorless needles (121.5 mg, 0.0467% yield).

3.2.6.2 Isolation of Compound ET-F4 (Lupeol)

Fraction D23 (1.41 g) was subjected to silica gel column chromatography (20 g, 2 × 15 cm), eluting with a gradient mixture of 2-10% acetone in hexane, to give 90 fractions (5 ml each). These fractions were monitored by TLC (solvent system: hexane-acetone = 5:1), then combined into 5 fractions (D231-D235). Fraction D233, which showed a purple spot (R_f = 0.38) on TLC, yielded compound ET-F4 (8.0 mg, 0.0031 % yield).

3.2.6.3 Isolation of Component ET-F5 (Mixture of β-Sitosterol and Stigmasterol)

Component ET-F5 (36.7 mg, 0.0141% yield) crystallized as colorless needles from fraction D234.

3.2.7 Isolation of Compounds from the CH_2Cl_2 Extract of *E. tapos* Flowers

The CH_2Cl_2 extract (3.68 g) was chromatographed on a silica gel column (60 g, 1.5 × 10 cm), eluting with a gradient mixture of hexane-acetone (19:1 to 3:1), to yield 252 fractions (10 ml each). Fractions with similar TLC pattern (solvent system: hexane-acetone = 2:1) were combined into 5 fractions (E1-E5, **Table 14**).

Table 14. Combined fractions from the CH_2Cl_2 extract of *E. tapos* flowers

Fraction code	Weight (g)
E1	0.03
E2	1.66
E3	0.12
E4	0.42
E5	0.27

3.2.7.1 Isolation of Compound ET-F6 (Putraflavone)

Compound ET-F6 (3.3 mg, 0.0013 % yield) precipitated as yellow amorphous powder from fraction E3.

3.2.7.2 Isolation of Compound ET-F7 (Ellagic acid 3,3′-dimethyl ether)

Fraction E4 (0.42 g) was subjected to a Sephadex LH-20 column, eluting with CH_2Cl_2-MeOH (3:1), to give 26 fractions (5 ml each). Fractions displaying a quenching spot on TLC (R_f = 0.17, solvent system: hexane-acetone = 2:1) under UV light at 254 nm were combined to give compound ET-F7 (2.0 mg, 0.0008 % yield).

3.2.8 Isolation of Compounds from the MeOH Extract of *E. tapos* Flowers

The MeOH extract (11.41 g) was subjected to silica gel column chromatography (300g, 13 × 5 cm), eluting with a gradient mixture of CH_2Cl_2-MeOH (1:0 to 0:1). Each collected fraction was 50 ml and the eluates were examined by

TLC (solvent system: CH_2Cl_2-MeOH 9:1). One hundred and sixty fractions were collected and combined into 6 major fractions (F1-F6, **Table 15**)

Table 15. Combined fractions from the MeOH extract of *E. tapos* flowers

Fraction code	Weight (g)
F1	0.37
F2	0.22
F3	1.77
F4	1.06
F5	1.34
F6	1.11

3.2.8.1 Isolation of Compound ET-FM2 (Amentoflavone)

Fraction F2 (0.22 g) was subjected to gel filtration chromatography on a Sephadex LH-20 column eluting with CH_2Cl_2-MeOH (2:1). Twenty-five fractions (5 ml each) were collected and examined by TLC (solvent system: CH_2Cl_2-MeOH = 2:1), then combined into 5 fractions (F21-F25). Fraction F22 (0.02 g), which showed a yellow spot on TLC (R_f = 0.95), were repeatedly chromatographed on Sephadex LH-20 columns eluting with CH_2Cl_2-MeOH (2:1) as eluent, to give compound ET-FM2 (5.5 mg, 0.0021 % yield).

3.2.8.2 Isolation of Compound ET-FM3 (Quercetin)

Compound ET-FM3 precipitated from fraction F24 as yellow amorphous powder (3.3 mg, 0.0013 %yield).

3.2.9 Extraction of *E. tapos* Leaves

Dried *E. tapos* leaves (1.3 kg) were ground and macerated with 95% EtOH (3 × 8L) to give EtOH extract, which was dissolved in 40% EtOH, then partitioned with hexane and CH_2Cl_2 to give hexane extract (31.8 g, 2.45% of dried weight), CH_2Cl_2 extract (9.5 g, 0.73% of dried weight) and aqueous alcoholic extract, respectively.

3.2.10 Isolation of the Hexane Extract of *E. tapos* Leaves

The hexane extract (31.8 g) was chromatographed on a silica gel column (400 g, 9.5 × 10 cm), eluting with a gradient mixture of hexane-acetone (1:0 to 0:1), to give 184 fractions (50 ml each). These fractions were combined according to their TLC

pattern (solvent systems: hexane-acetone = 5:1-2:1) into 9 pooled fractions (G1-G9, **Table 16**).

Table 16. Combined fractions from the hexane extract of *E. tapos* leaves

Fraction code	Weight (g)
G1	0.64
G2	9.00
G3	1.77
G4	4.07
G5	1.08
G6	1.20
G7	1.36
G8	1.33
G9	2.32

3.2.10.1 Isolation of Compound ET-L1 (β-Sitosterol glucoside)

Fraction G9, which displayed a single orange spot on TLC (R_f = 0.17, solvent system: hexane-acetone = 2:1), afforded compound ET-L1 as pale brown powder (46.8 mg, 0.0036% yield).

3.2.10.2 Isolation of Compound ET-L2 (Hopenol-B)

Fraction G2 (9.00 g) was separated on a silica gel column (150 g, 2.5 × 20 cm), eluting with a gradient mixture of hexane-acetone (1:0 to 17:3), to give 48 fractions (20 ml/fraction). Fractions which exhibited a purple spot on TLC (R_f = 0.54, solvent system: hexane-acetone = 6:1) were combined to yield compound ET-L2 (93.1 mg, 0.0072% yield).

3.2.10.3 Isolation of Compound ET-L3 (2,3-*Seco*-taraxer-14-ene-2,3,28-trioic acid 2,3-dimethyl ester)

Fraction G4 (4.07 g) was chromatographed on a silica gel column (100 g, 2.5 × 15 cm), eluting with a gradient mixture of hexane-acetone (1:0 to 0:1), to obtain 75 fractions (20 ml each). TLC monitoring of these fractions (solvent system: hexane-acetone = 5:1) helped combine them into 6 fractions (G41-G46). Compound ET-L3 (11.3 mg, 0.0009% yield) precipitated from fraction G44.

3.2.10.4 Isolation of Component ET-L4 (Mixture of β-sitosterol and stigmasterol)

Component ET-L4, which appeared as a purple spot on TLC (R_f = 0.29, solvent system: hexane-acetone = 5:1), crystallized as colorless needles (8.6 mg, 0.0007% yield) from fraction G42.

3.2.10.5 Isolation of Compound ET-L12 (Aleuritolic acid)

Fraction G46 (1.13 g) was gel filtration chromatographed on a Sephadex LH-20 column (1 × 40 cm) eluting with CH_2Cl_2-MeOH (2:1). Seventy-five fractions (5 ml each) were collected and examined by TLC (solvent system: hexane-acetone = 4:1). Fractions showing a purple spot at the R_f value of 0.24 were combined to yield compound ET-L12 (12.4 mg, 0.0010% yield).

3.2.10.6 Isolation of Compound ET-L5 (2,3-*Seco*-taraxer-14-ene-2,3,28-trioic acid 3-methyl ester)

Fraction G6 (1.20 g) was subjected to silica gel column chromatography (60 g, 3 × 15 cm), eluting with a gradient mixture of hexane-acetone (9:1 to 0:1), to give 61 fractions (10 ml each). Fractions were combined according to their TLC pattern (solvent system: hexane-acetone = 2:1) into 9 pooled ones (G61-G69). Compound ET-L5 (17.3 mg, 0.0013% yield) precipitated from fraction G69. The same compound (45.1 mg, 0.0035% yield) was also obtained when fraction G7 (1.36 g) was chromatographed on a silica gel column (30.0 g, 2.5 × 10 cm), using a gradient mixture of hexane-acetone (17:3 to 0:1) as eluent.

3.2.11 Isolation of the CH_2Cl_2 Extract of *E. tapos* Leaves

The extract (9.5 g) was chromatographed on a silica gel column (200 g, 5 × 15 cm), eluting with a gradient mixture of hexane-acetone (1:0 to 0:1), to give 180 fractions (30 ml each) which were combined according to similarity of their TLC pattern (solvent system: hexane-acetone = 5:1 to 1:1) into 12 fractions (H1-H12, **Table 17**)

3.2.11.1 Isolation of Compound ET-LC1 (Putraflavone)

Compound ET-LC1 precipitated as yellow powder (93.1 mg, 0.0072% yield) from fraction H7.

Table 17. Combined fractions from the CH_2Cl_2 extract of *E. tapos* leaves

Fraction code	Weight (g)
H1	0.44
H2	0.16
H3	0.21
H4	0.31
H5	0.33
H6	0.23
H7	1.53
H8	0.42
H9	0.46
H10	0.57
H11	1.02
H12	1.36

3.2.11.2 Isolation of Compound ET-LC2 (2,3-*Seco*-taraxer-14-ene-2,3,28-trioic acid 3-methyl ester)

Both fractions H1 (0.44 g) and H2 (0.16 g) were gel filtration chromatographed on Sephadex LH-20 columns, eluting with CH_2Cl_2-MeOH (2:1), to yield compound ET-LC2 (11.4 mg, 0.0009% yield and 11.9 mg, 0.0009% yield, respectively).

3.2.11.3 Isolation of Compound ET-LC4 (Kaempferol)

Fraction H6 (0.23 g) was separated on a Sephadex LH-20 column, eluting with CH_2Cl_2-MeOH (2:1), into 17 fractions (5 ml each). Fractions with similar TLC pattern (solvent system: hexane-acetone 2:1) were combined into 5 pooled fractions (H61-H65). Fraction H64, which displayed a quenching spot under UV light (R_f = 0.19, solvent system: hexane-acetone = 2:1), was purified on a Sephadex LH-20 column eluting with CH_2Cl_2-MeOH (2:1) to afford compound ET-LC4 (2.0 mg, 0.0002% yield).

3.2.11.4 Isolation of Compound ET-LC5 (Amentoflavone)

Fraction H9 (0.46 g) was chromatographed on a Sephadex LH-20 column eluting with CH_2Cl_2-MeOH (2:1) to give 22 fractions (5 ml each). Fractions

displaying a yellow spot on TLC (R_f = 0.2, solvent system: hexane-acetone = 1:1) were combined to yield compound ET-LC5 (15.7 mg, 0.0012% yield).

3.2.11.5 Isolation of Compound ET-LC7 (Sequoiaflavone)

Fraction H8 (0.42 g) was separated on a Sephadex LH-20 column using CH_2Cl_2-MeOH (2:1) as eluent into 43 fractions, which were examined by TLC (solvent system: hexane-acetone = 1:1). Fractions showing a yellow spot (R_f = 0.3) on TLC were combined to yield compound ET-LC7 (10.2 mg, 0.0002% yield).

3.2.11.6 Isolation of Compound ET-LC13 (Ginkgetin)

Fraction H11 (1.02 g) was further purified on a Sephadex LH-20 column using CH_2Cl_2-MeOH (2:1) as eluent. Thirty fractions (5 ml each) were collected and examined by TLC (solvent system: hexane-acetone = 2:3). Fractions which displayed a yellow spot (R_f = 0.8) on TLC were combined to yield compound ET-LC13 (5.6 mg, 0.0004% yield).

3.2.11.7 Isolation of Compounds ET-LC17 (Ellagic acid 3,3′-dimethyl ether)

Fraction H62 was purified by gel filtration chromatography on a Sephadex LH-20 column, eluting with CH_2Cl_2-MeOH (2:1), to give 15 fractions (5 ml each). These fractions were monitored by TLC (solvent system: hexane-acetone = 2:1), then combined to yield 3 main fractions (H621-H623). Fraction H622 was subjected to another Sephadex LH-20 column, using the same mobile phase. Fractions showing a quenching spot on TLC (R_f = 0.17, solvent system: hexane-acetone = 2:1) under UV light were combined to give compound ET-LC17 (1.0 mg, 0.0001% yield).

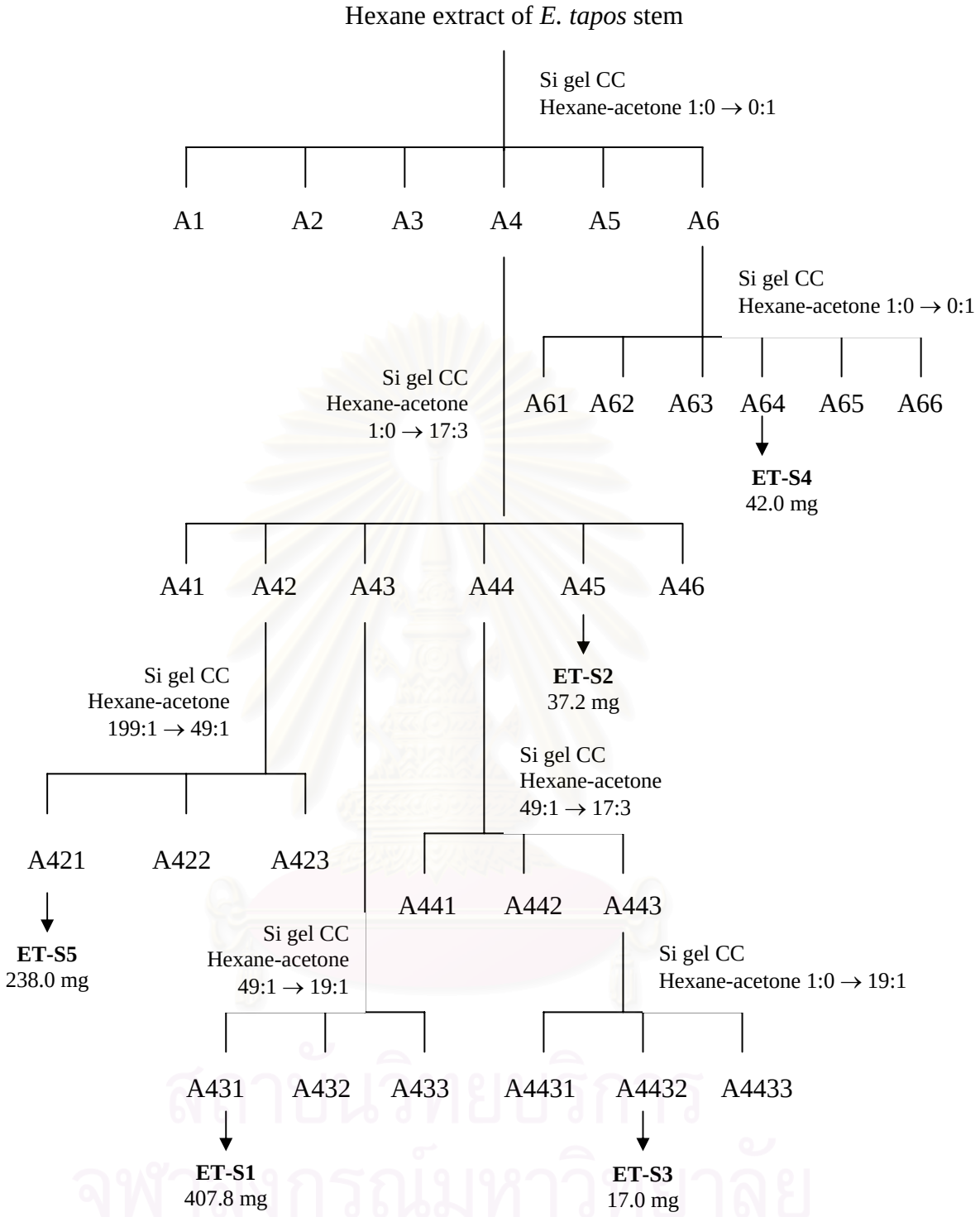

Scheme 2. Isolation of compounds from the hexane extract of *E. tapos* stem

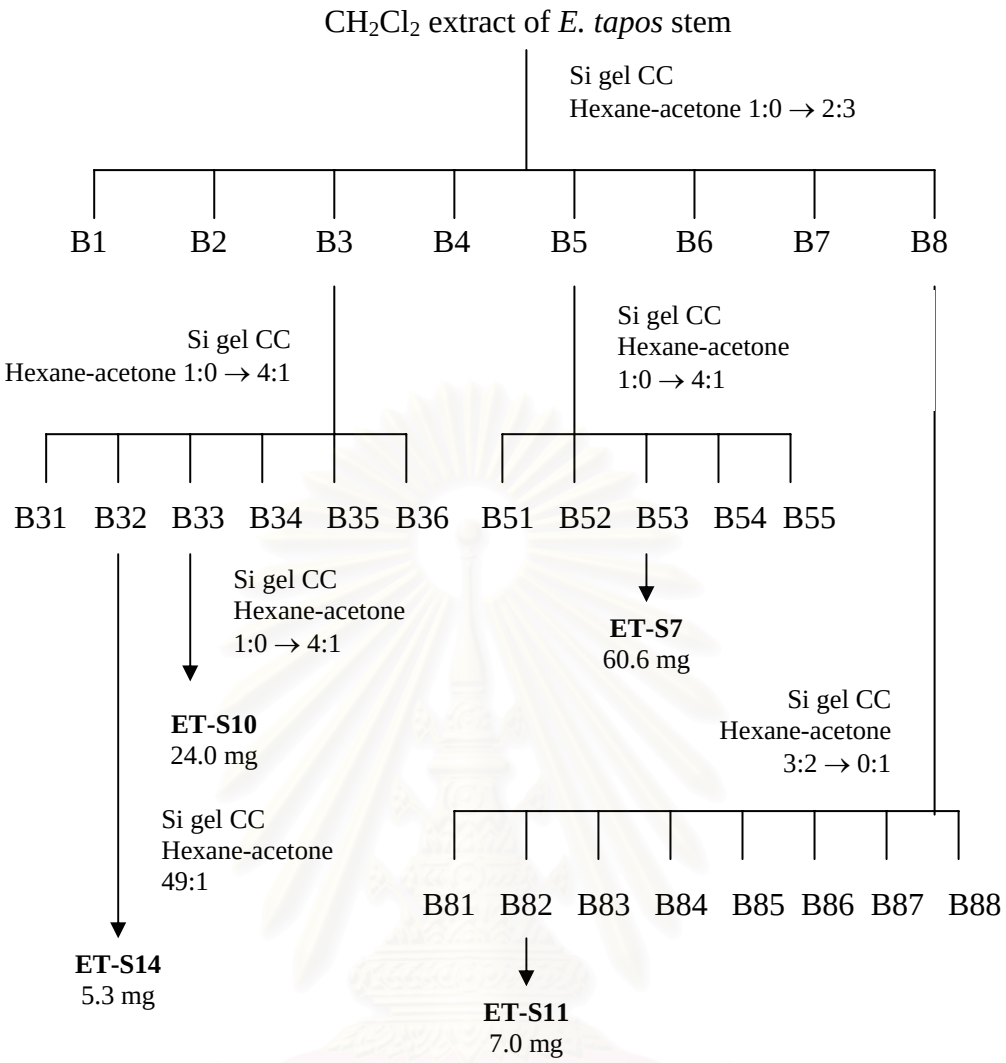

Scheme 3. Isolation of compounds from the CH_2Cl_2 extract of *E. tapos* stem

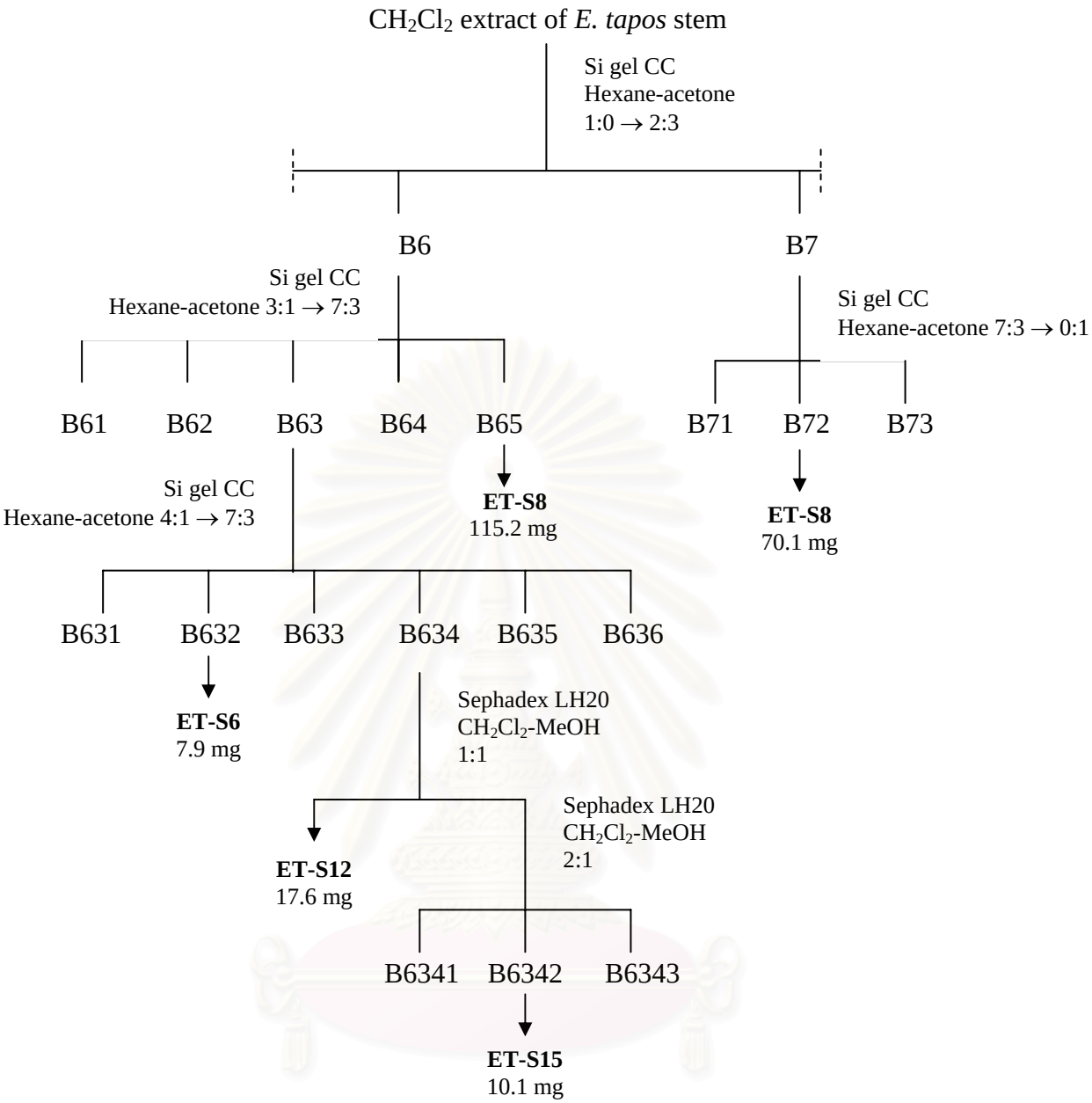

Scheme 3. Isolation of compounds from the CH_2Cl_2 extract of *E. tapos* stem (continued)

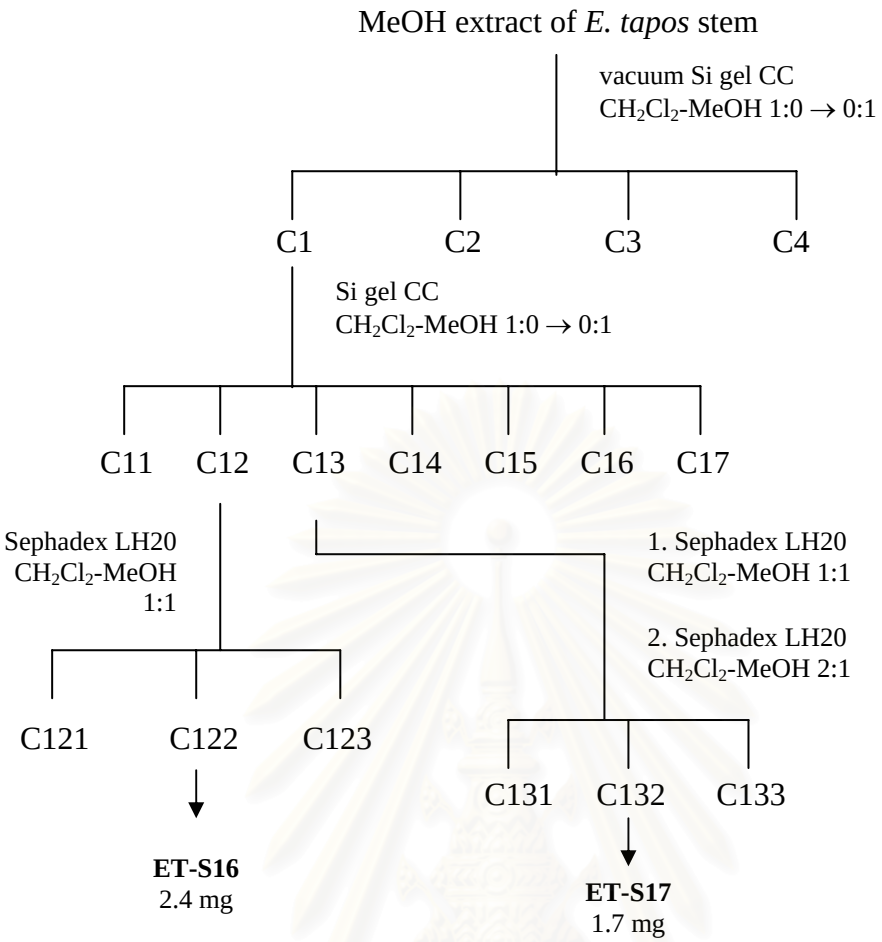

Scheme 4. Isolation of compounds from the MeOH extract of *E. tapos* stem

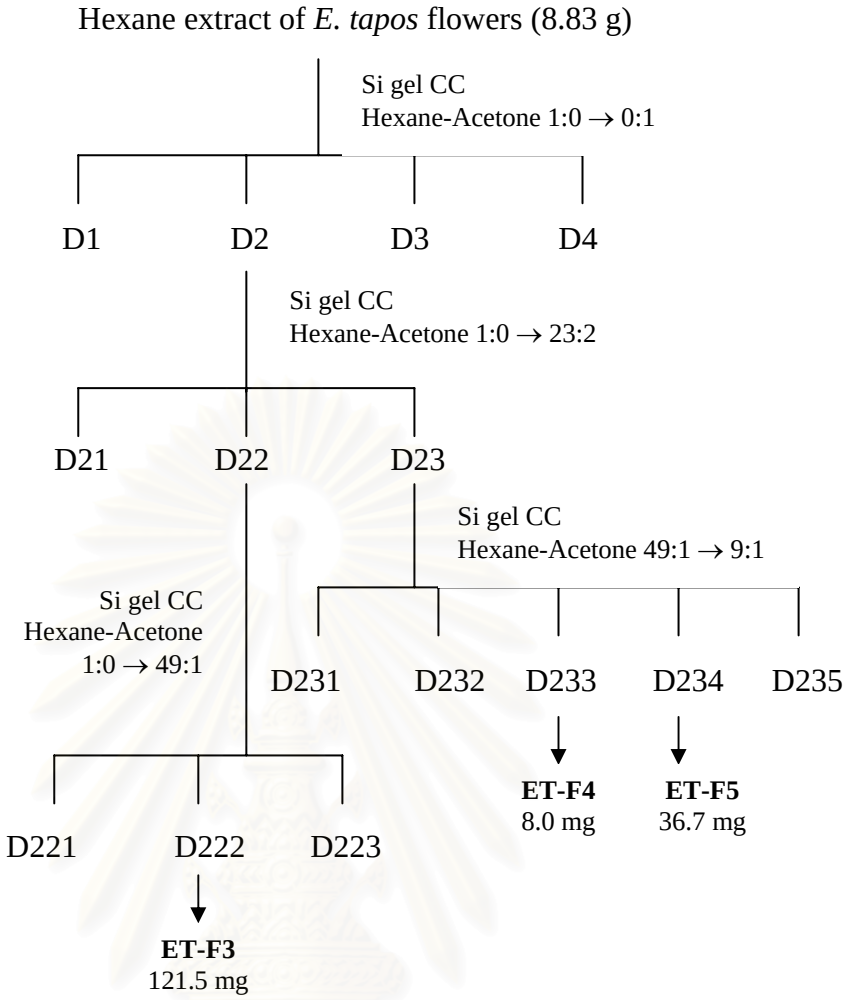

Scheme 5. Isolation of compounds from the hexane extract of *E. tapos* flowers

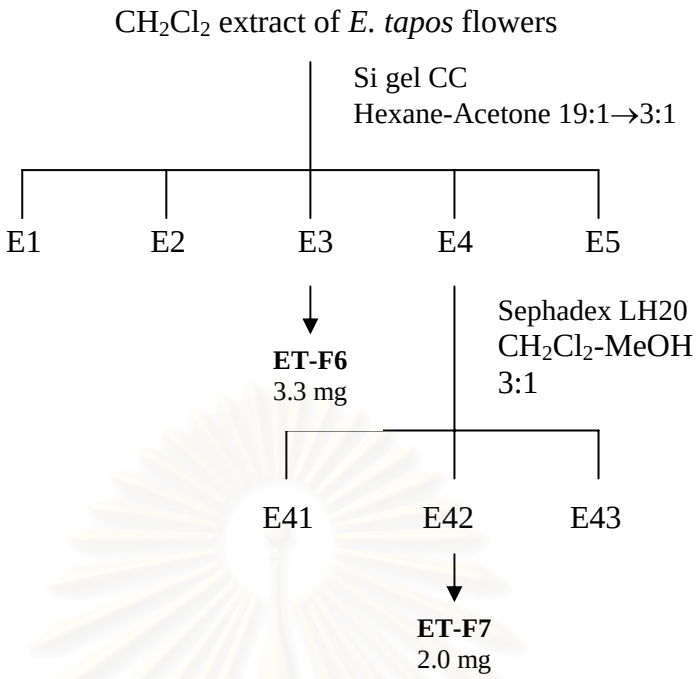

Scheme 6. Isolation of compounds from the CH_2Cl_2 extract of *E. tapos* flowers

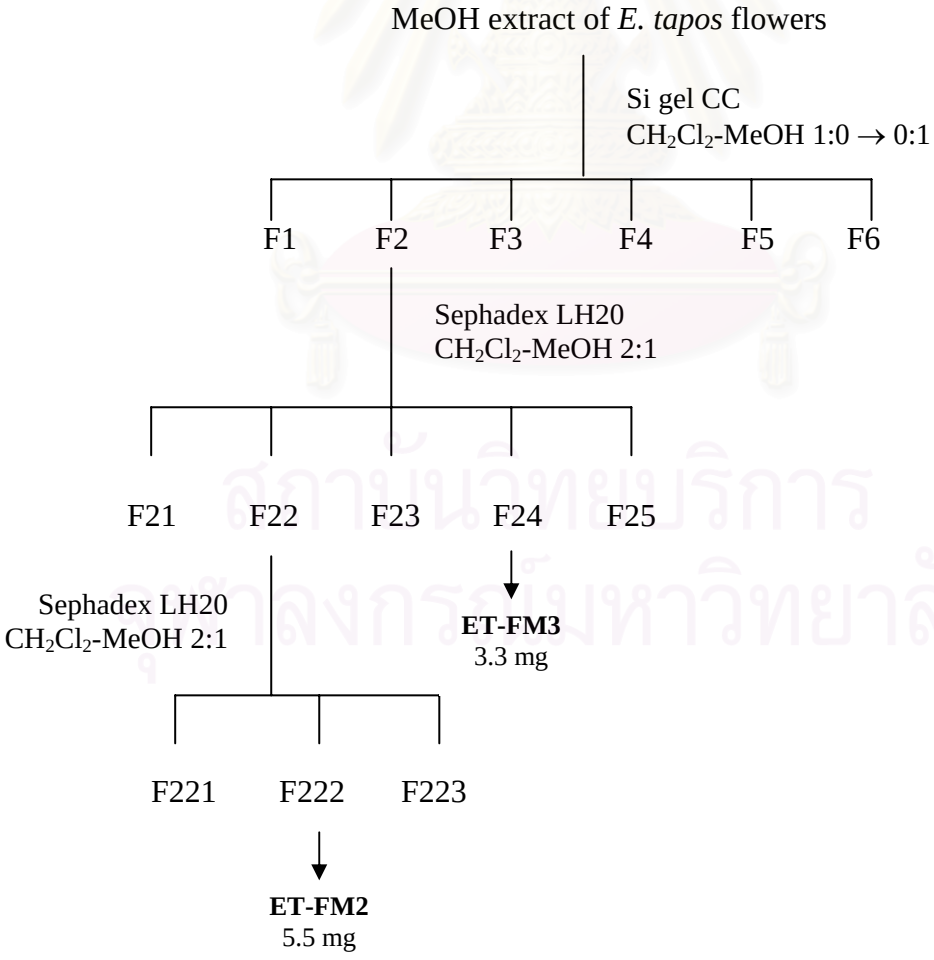

Scheme 7. Isolation of compounds from the MeOH extract of *E. tapos* flowers

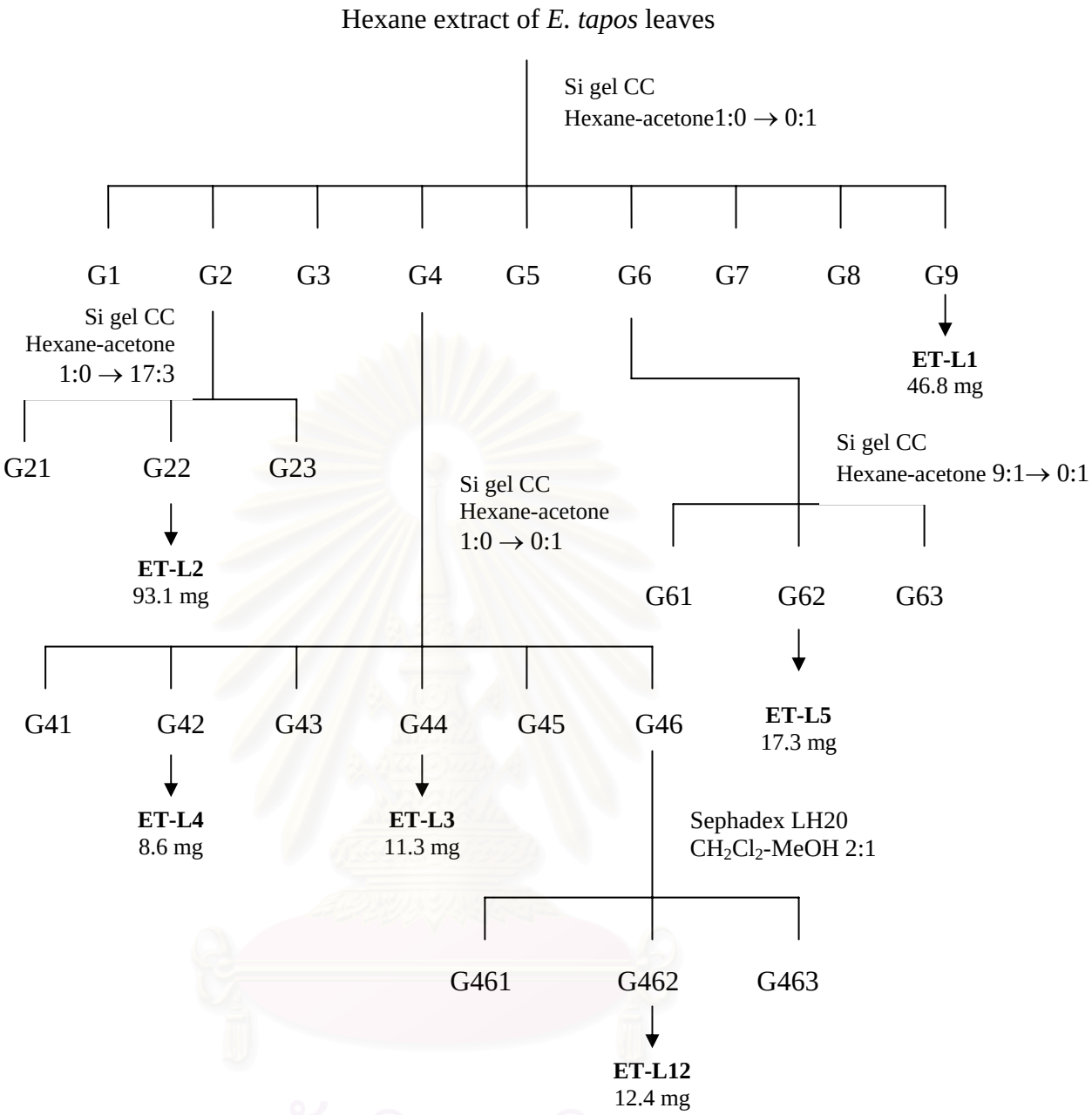

Scheme 8. Isolation of compounds from the hexane extract of *E. tapos* leaves

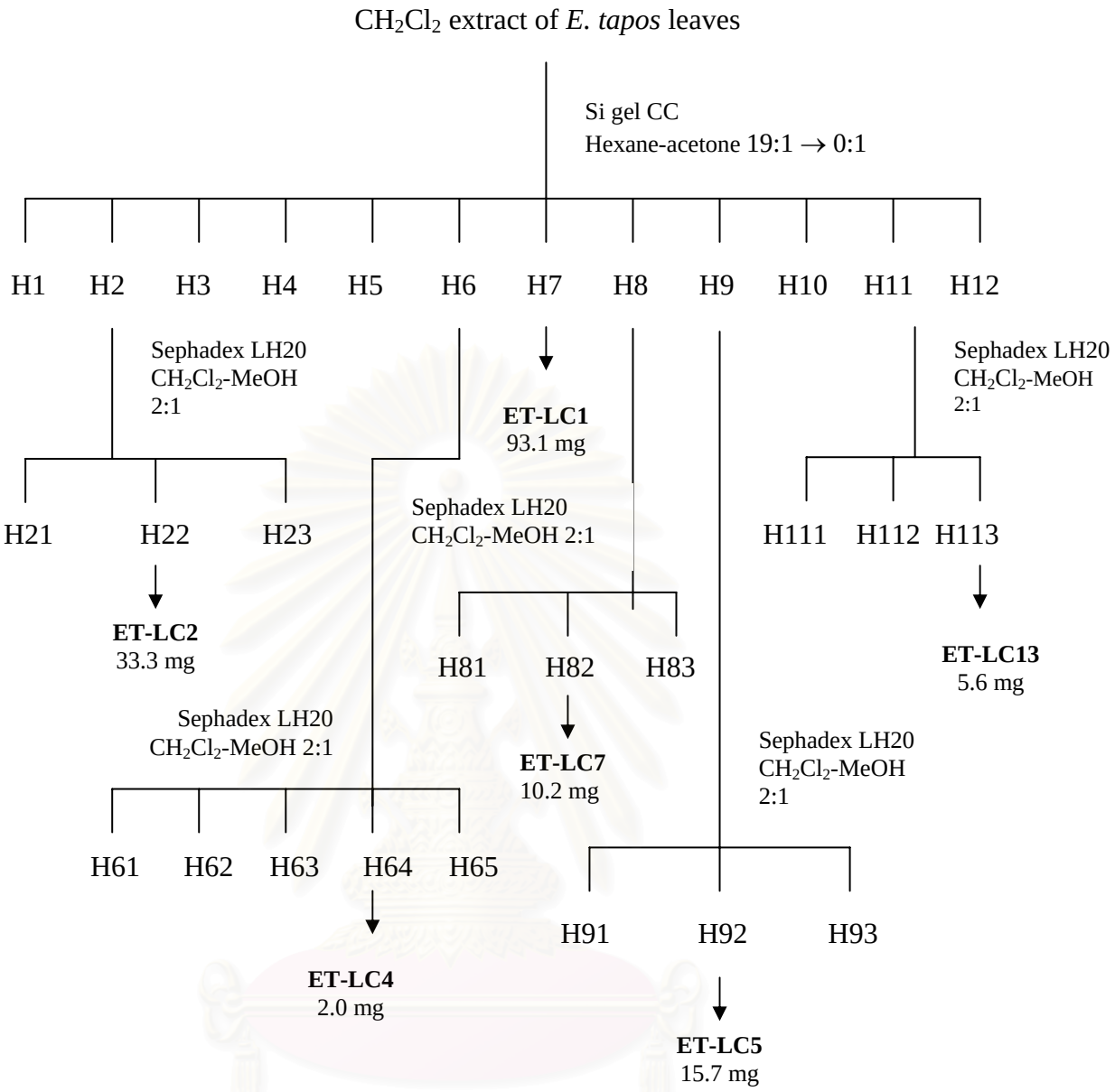

Scheme 9. Isolation of compounds from the CH_2Cl_2 extract of *E. tapos* leaves

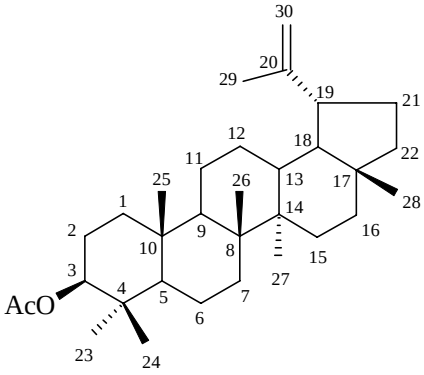

ET-S1 (ET-F3)

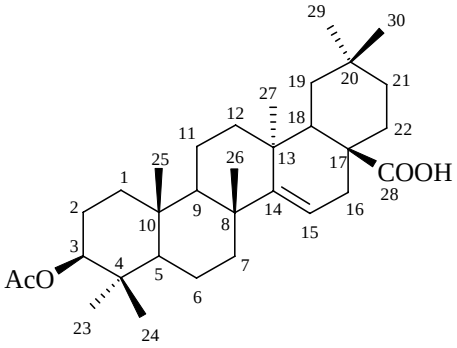

ET-S2

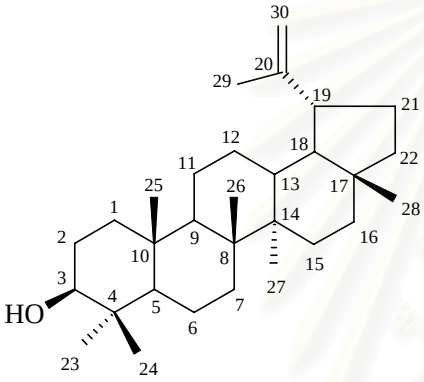

ET-S3 (ET-F4)

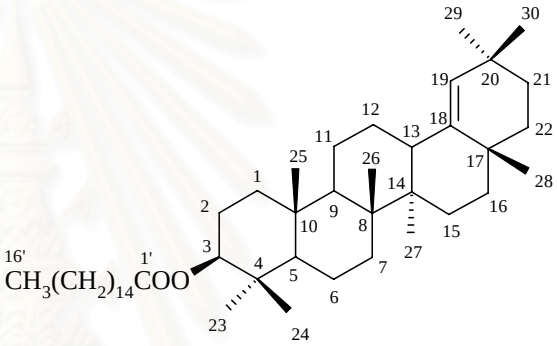

ET-S5

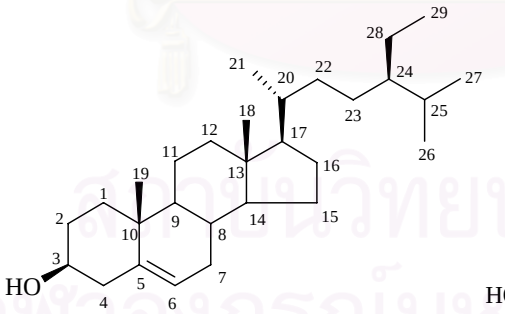

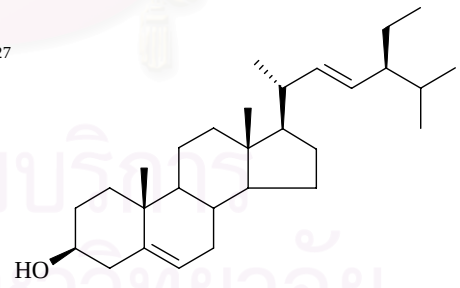

ET-S4 (CAR-1, ET-S10, ET-F5, ET-L4)

Figure 11. Structures of compounds isolated from *E. tapos*

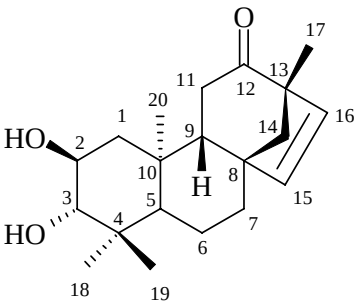

ET-S6

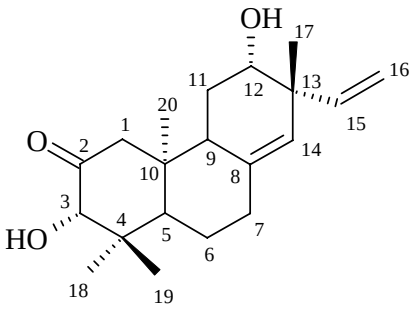

ET-S7

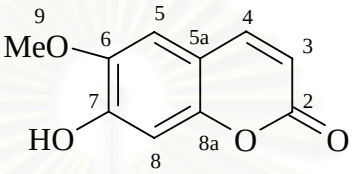

ET-S8 (ET-S16)

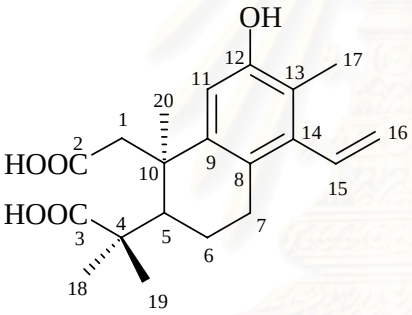

ET-S11

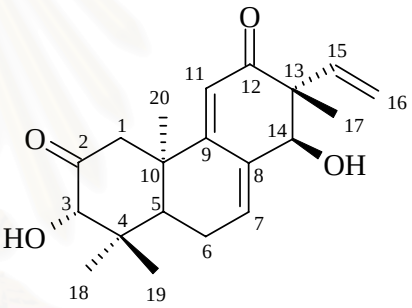

ET-S12

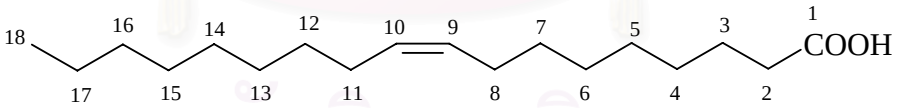

ET-S14

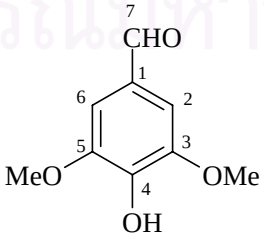

ET-S15

Figure 11. Structures of compounds isolated from *E. tapos* (continued)

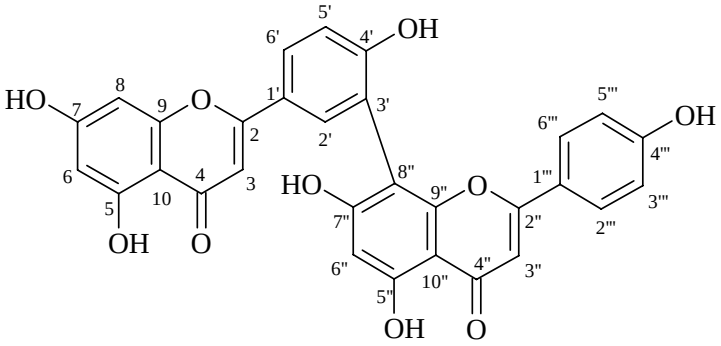

ET-S17 (ET-FM2, ET-LC5)

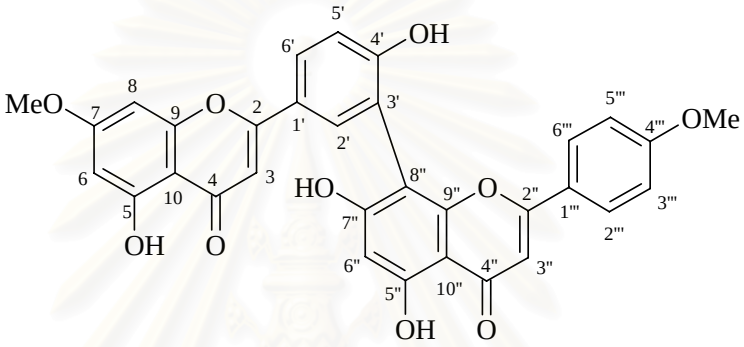

ET-F6 (ET-LC1)

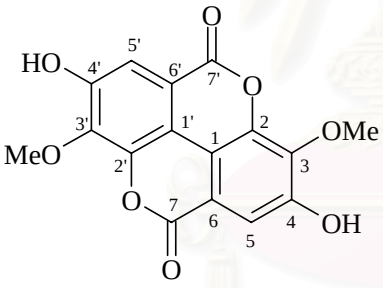

ET-F7 (ET-FM5, ET-LC17)

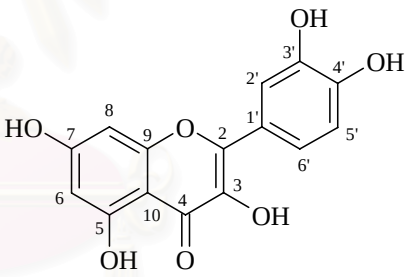

ET-FM3

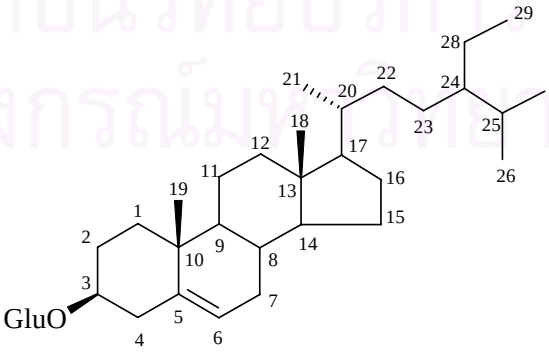

ET-L1 (CAR-2)

Figure 11. Structures of compounds isolated from *E. tapos* (continued)

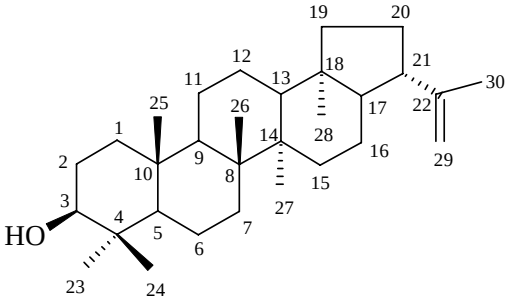

ET-L2

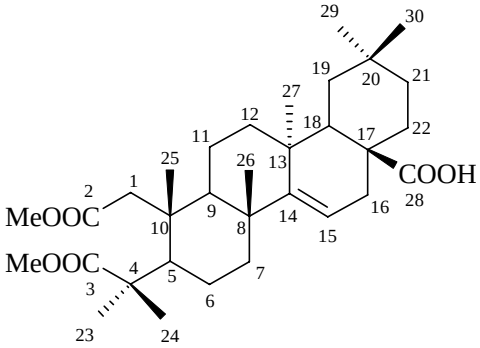

ET-L3

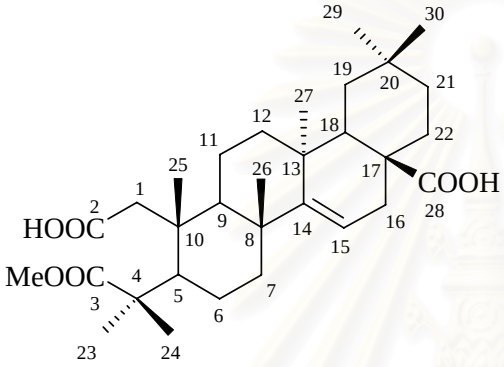

ET-L5 (ET-LC2)

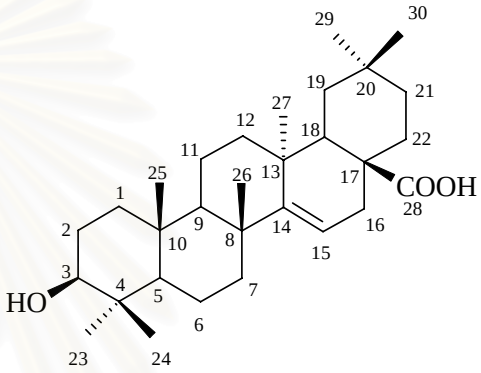

ET-L12

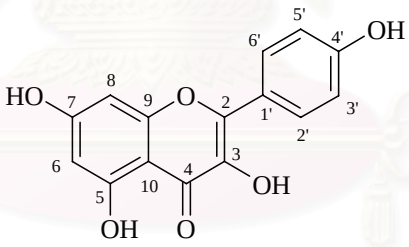

ET-LC4

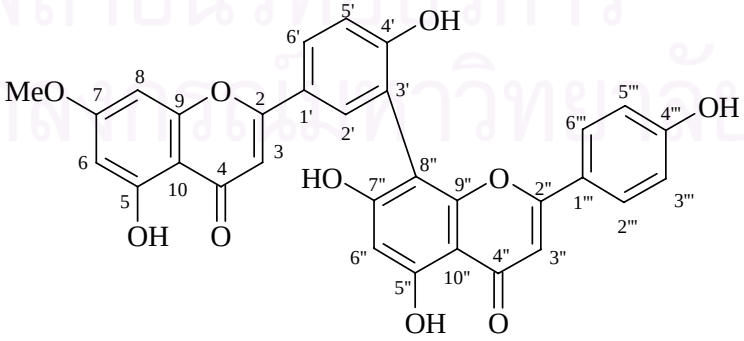

ET-LC7

Figure 11. Structures of compounds isolated from *E. tapos* (continued)

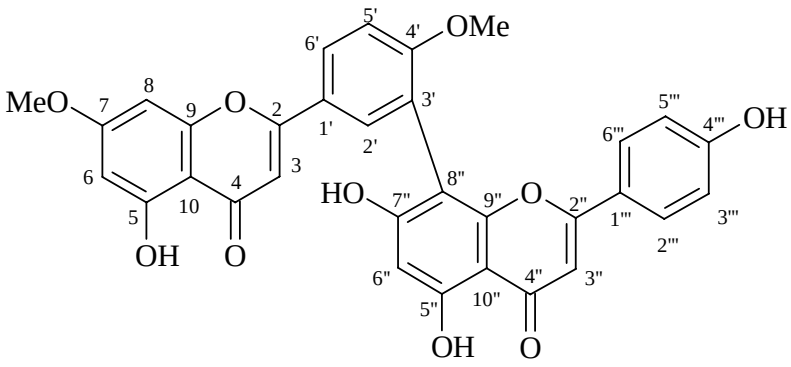

ET-LC13

Figure 11. Structures of compounds isolated from *E. tapos* (continued)

4. Physical and Spectral Data of Isolated Compounds

4.1 Component CAR-1 (or ET-S4, ET-S10, ET-F5 and ET-L4) (Mixture of β-Sitosterol and Stigmasterol)

Component CAR-1 was obtained as colorless needles.

mp : 135-137 °C

IR : ν_{max} (KBr): 3428, 2961, 2937, 1465, 1382,1368, 1062, 1054 cm^{-1}; see **Figure 12**

^{1}H NMR : δ ppm, 300 MHz, in $CDCl_3$; see **Figure 13**, **Table 18**

^{13}C NMR : δ ppm, 75 MHz, in $CDCl_3$; see **Figure 14**, **Table 18**

4.2 Compound CAR-2 (or ET-L1) (β-Sitosterol Glucoside)

Compound CAR-2 was obtained as white needle crystals.

mp : 180-184 °C

^{1}H NMR : δ ppm, 300 MHz, in DMSO-d_6; see **Figure 15**, **Table 19**

^{13}C NMR : δ ppm, 75 MHz, in DMSO-d_6; see **Figure 16**, **Table 19**

4.3 Compound CAR-3 (Rutin)

Compound CAR-3 was obtained as yellow amorphous powder.

ESI-MS : *m/z* 609 $[M-H]^+$; see **Figure 19**

mp : 191-214 °C

UV : λ_{max} nm (log ε), in MeOH: 210 (4.52), 258 (4.37), 356 (4.30); see **Figure 17**

IR : ν_{max} (KBr): 3427, 1655, 1600, 1504, 1457, 1363, 1296, 1203, 1064, 1015, 971, 808 cm^{-1} see **Figure 18**

^{1}H NMR : δ ppm, 300 MHz, in DMSO-d_6; see **Figure 20**, **Table 20**

^{13}C NMR : δ ppm, 75 MHz, in DMSO-d_6; see **Figure 21**, **Table 20**

4.4 Compound CAR-4 (*Epi*-inositol 6-*O*-methyl ether)

Compound CAR-4 was obtained as colorless needles.

ESI-MS : *m/z* 217 $[M+Na]^+$; see **Figure 27**

mp : 185-189 °C

IR : ν_{max} (KBr): 3336, 2940, 2929, 1631, 1502, 1438, 1324, 1140, 1103, 1050, 1015, 657 cm^{-1}; see **Figure 26**

^{1}H NMR : δ ppm, 300 MHz, in DMSO-d_6; see **Figure 28**, **Table 21**

^{13}C NMR : δ ppm, 75 MHz, in DMSO-d_6; see **Figure 29, Table 21**

4.5 Compound CAR-6 (Canarosine)

Compound CAR-6 was obtained as pale yellow needles.

HR ESI-MS : *m/z* 375.2469 $[M+H]^+$; see **Figure 35**

mp : 235-237 °C

IR : ν_{max} (KBr): 3429, 1657, 1613, 1575, 1409, 651 cm^{-1}; see **Figure 34**

^{1}H NMR : δ ppm, 500 MHz, in CD_3OD; see **Figures 36a-36d**, **Table 22**

^{13}C NMR : δ ppm, 75 MHz, in CD_3OD; see **Figure 37**, **Table 22**

4.6 Compound ET-S1 (or ET-F3) (Lupeol 3-acetate)

Compound ET-S1 was obtained as colorless needles.

EI-MS : *m/z* 468 $[M]^+$; see **Figure 43**

mp : 187-190 °C

IR : ν_{max} (KBr): 2946, 2872, 1734, 1455, 1379, 1369, 1245, 1027, 979 cm^{-1}; see **Figure 42**

^{1}H NMR : δ ppm, 300 MHz, in $CDCl_3$; see **Figure 44**, **Table 23**

^{13}C NMR : δ ppm, 75 MHz, in $CDCl_3$; see **Figures 45a-45b**, **Table 23**

4.7 Compound ET-S2 (Acetyl aleuritolic acid)

Compound ET-S2 was obtained as colorless needles.

ESI-MS : *m/z* 521 $[M+Na]^+$; see **Figure 48**

mp : 272-276 °C

IR : ν_{max} (KBr): 3434, 2939, 2865, 1734, 1688, 1246, 1028 cm^{-1}; see **Figure 47**

^{1}H NMR : δ ppm, 300 MHz, in $CDCl_3$; see **Figure 49**, **Table 24**

^{13}C NMR : δ ppm, 75 MHz, in $CDCl_3$; see **Figure 50**, **Table 24**

4.8 Compound ET-S3 (or ET-F4) (Lupeol)

Compound ET-S3 was obtained as colorless needles.

EI-MS : *m/z* 426 $[M]^+$; see **Figure 53**

mp : 130-133 °C

IR : ν_{max} (KBr): 3323, 2917, 2871, 2849, 1463, 1379 cm^{-1}; see **Figure 52**

^1H NMR : δ ppm, 300 MHz, in $CDCl_3$; see **Figure 54**, **Table 25**

^{13}C NMR : δ ppm, 75 MHz, in $CDCl_3$; see **Figure 55**, **Table 25**

4.9 Compound ET-S5 (Germanicol palmitate)

Compound ET-S5 was obtained as white powder.

EI-MS : *m/z* 664 $[M]^+$; see **Figure 58**

mp : 95-99 °C

IR : ν_{max} (KBr): 2955, 2921, 2851, 1725, 1467, 1378, 1257, 1247, 1177, 984, 720 cm^{-1}; see **Figure 57**

^1H NMR : δ ppm, 300 MHz, in $CDCl_3$; see **Figure 59**, **Table 26**

^{13}C NMR : δ ppm, 75 MHz, in $CDCl_3$; see **Figure 60**, **Table 26**

4.10 Compound ET-S6 (Yucalexin B-22)

Compound ET-S6 was obtained as colorless needles.

ESI-MS : *m/z* 341.22 $[M+Na]^+$; see **Figure 62**

$[\alpha]^{25}_D$: -213.85 (*c* 0.015, $CHCl_3$)

IR : ν_{max} (KBr): 3397, 2965, 2928, 2857, 1706, 1450, 1089, 1055, 758 cm^{-1}; see **Figure 61**

^1H NMR : δ ppm, 300 MHz, in $CDCl_3$; see **Figure 63**, **Table 27**

^{13}C NMR : δ ppm, 75 MHz, in $CDCl_3$; see **Figure 64**, **Table 27**

4.11 Compound ET-S7 (Yucalexin P-17)

Compound ET-S7 was obtained as colorless needles.

ESI-MS : *m/z* 319 $[M+H]^+$; see **Figure 70**

mp : 230-233 °C

$[\alpha]^{25}_D$: +95.97 (c 0.085, $CHCl_3$)

IR : ν_{max} (KBr): 3459, 2969, 2953, 1701, 1450, 1282, 1119, 1072, 1056, 927, 708, 657 cm^{-1}; see **Figure 69**

^1H NMR : δ ppm, 300 MHz, in $CDCl_3$; see **Figure 71**, **Table 28**

^{13}C NMR : δ ppm, 75 MHz, in $CDCl_3$; see **Figure 72**, **Table 28**

4.12 Compound ET-S8 (or ET-S16) (Scopoletin)

Compound ET-S8 was obtained as yellow needles.

ESI-MS : *m/z* 215 $[M+Na]^+$; see **Figure 79**

mp : 198-201 °C

UV : λ_{max} nm (log ε), in MeOH: 208 (4.33), 229 (4.24), 254 (3.80), 348 (4.17); see **Figure 77**

IR : ν_{max} (KBr): 3338, 1704, 1608, 1566, 1510, 1290, 1263, 1140, 1018, 922, 862, 592 cm^{-1}; see **Figure 78**

^{1}H NMR : δ ppm, 500 MHz, in $CDCl_3$; see **Figure 80**, **Table 29**

^{13}C NMR : δ ppm, 75 MHz, in $CDCl_3$; see **Figure 81**, **Table 29**

4.13 Compound ET-S11 (2,3-*Seco*-sonderianol)

Compound ET-S11 was obtained as colorless needles.

HR-ESI-MS : *m/z* 369.1682 $[M+Na]^+$; see **Figure 87**

mp : 230-233 °C

$[\alpha]^{25}_D$: +9.35 (*c* 0.048, MeOH)

UV : λ_{max} nm (log ε), in MeOH: 215 (4.17), 292 (3.31); see **Figure 85**

IR : ν_{max} (KBr): 3431, 2984, 1698, 1269, 927 cm^{-1}; see **Figure 86**

^{1}H NMR : δ ppm, 300 MHz, in DMSO-d_6; see **Figure 88**, **Table 30**

^{13}C NMR : δ ppm, 75 MHz, in DMSO-d_6; see **Figure 89**, **Table 30**

4.14 Compound ET-S12 (Yucalexin P-15)

Compound ET-S12 was obtained as yellow oil.

ESI-MS : *m/z* 331 $[M+H]^+$; see **Figure 96**

$[\alpha]^{25}_D$: +14.89 (*c* 0.048, $CHCl_3$)

UV : λ_{max} nm (log ε), in $CHCl_3$: 319 (2.64); see **Figure 94**

IR : ν_{max} (KBr): 3446, 2974, 2935, 2874, 1718, 1667, 1653, 1394, 1112, 755 cm^{-1}; see **Figure 95**

^{1}H NMR : δ ppm, 300 MHz, in $CDCl_3$; see **Figure 97**, **Table 31**

^{13}C NMR : δ ppm, 75 MHz, in $CDCl_3$; see **Figure 98**, **Table 31**

4.15 Compound ET-S14 (Oleic Acid)

Compound ET-S14 was obtained as white plates.

EI-MS : *m/z* 282 $[M]^+$; see **Figure 104**

IR : ν_{max} (KBr): 2918, 2850,1705, 1464, 1296, 941 cm^{-1}; see **Figure 103**

^{1}H NMR : δ ppm, 300 MHz, in $CDCl_3$; see **Figure 105**, **Table 32**

^{13}C NMR : δ ppm, 75 MHz, in $CDCl_3$; see **Figure 106**, **Table 32**

4.16 Compound ET-S15 (Syringaldehyde)

Compound ET-S15 was obtained as colorless needles.

ESI-MS : *m/z* 205 $[M+Na]^+$; see **Figure 108**

mp : 110-112 °C

IR : ν_{max} (KBr): 3346, 1675, 1607, 1587, 1512, 1464, 1329, 1213, 1143, 1113, 729, 626 cm^{-1}; see **Figure 107**

^{1}H NMR : δ ppm, 300 MHz, in $CDCl_3$; see **Figure 109**, **Table 33**

^{13}C NMR : δ ppm, 75 MHz, in $CDCl_3$; see **Figure 110**, **Table 33**

4.17 Compound ET-S17 (or ET-FM2 and ET-LC5) (Amentoflavone)

Compound ET-S17 was obtained as yellow powder.

ESI-MS : *m/z* 537 $[M-H]^+$; see **Figure 117**

mp : 260-265 °C

UV : λ_{max} nm (log ε), in MeOH: 215 (4.82), 271 (4.67), 334 (4.62); see **Figure 115**

IR : ν_{max} (KBr): 3434, 2924, 2854, 1645, 1603, 1352, 1283, 1244, 1162, 835 cm^{-1}; see **Figure 116**

^{1}H NMR : δ ppm, 300 MHz, in acetone-d_6; see **Figure 118**, **Table 34**

^{13}C NMR : δ ppm, 75 MHz, in acetone-d_6; see **Figure 119**, **Table 34**

4.18 Compound ET-F6 (or ET-LC1) (Putraflavone)

Compound ET-F6 was obtained as pale yellow amorphous powder.

ESI-MS : *m/z* 567 $[M+H]^+$; see **Figure 125**

mp : 218-220 °C

UV : λ_{max} nm (log ε), in MeOH: 215 (4.52), 270 (4.45), 332 (4.43); see **Figure 123**

IR : ν_{max} (KBr): 3407, 1663, 1655, 1606, 1338, 1190, 833 cm^{-1}; see **Figure 124**

^{1}H NMR : δ ppm, 300 MHz, in DMSO-d_6; see **Figure 126**, **Table 35**

^{13}C NMR : δ ppm, 75 MHz, in DMSO-d_6; see **Figure 127**, **Table 35**

4.19 Compound ET-F7 (or ET-FM5 and ET-LC17) (Ellagic acid 3, 3′-dimethyl ether)

Compound ET-F7 was obtained as pale yellow needles.

EI-MS : *m/z* 330 $[M]^+$; see **Figure 132**

mp : > 300 °C

^{1}H NMR : δ ppm, 300 MHz, in DMSO-d_6; see **Figure 133**, **Table 36**

^{13}C NMR : δ ppm, 75 MHz, in DMSO-d_6; see **Figure 134**, **Table 36**

4.20 Compound ET-FM3 (Quercetin)

Compound ET-FM3 was obtained as yellow powder.

ESI-MS : *m/z* 301 $[M-H]^+$; see **Figure 140**

mp : 245-250 °C

UV : λ_{max} nm (log ε), in MeOH: 210 (4.59), 256 (4.47), 367 (4.43); see **Figure 138**

IR : ν_{max} (KBr): 3420, 2924, 2853, 1656, 1612, 1522, 1263, 1169, 1015, 825 cm^{-1}; see **Figure 139**

^{1}H NMR : δ ppm, 300 MHz, in DMSO-d_6; see **Figure 141**, **Table 37**

^{13}C NMR : δ ppm, 75 MHz, in DMSO-d_6; see **Figure 142**, **Table 37**

4.21 Compound ET-L2 (Hopenol B)

Compound ET-L2 was obtained as colorless needles.

EI-MS : *m/z* 426 $[M]^+$; see **Figure 147**

mp : 226-228 °C

$[\alpha]^{25}_D$: + 114.25 (*c* 0.048, MeOH)

IR : ν_{max} (KBr): 3389, 2945, 2865, 1700, 1643, 1446, 1046, 993, 890 cm^{-1}; see **Figure 146**

^{1}H NMR : δ ppm, 500 MHz, in acetone-d_6; see **Figure 148**, **Table 38**

^{13}C NMR : δ ppm, 125 MHz, in acetone-d_6; see **Figures 149a-149b**, **Table 38**

4.22 Compound ET-L3 (2,3-*Seco*-taraxer-14-ene-2,3,28-trioic acid 2,3-dimethyl ester)

Compound ET-L3 was obtained as colorless needles.

HR-ESI-MS : *m/z* 553.3509 $[M+Na]^+$; see **Figure 155**

mp : 232-233 °C

$[\alpha]^{25}_D$: +13.63 (*c* 0.046, MeOH)

IR : ν_{max} (KBr): 3434, 2949, 2865, 1729, 1692, 1456, 1250, 1145 cm^{-1}; see **Figure 154**

^{1}H NMR : δ ppm, 500 MHz, in acetone-d_6; see **Figures 156a-156d**, **Table 39**

^{13}C NMR : δ ppm, 125 MHz, in acetone-d_6; see **Figures 157a-157b**, **Table 39**

4.23 Compound ET-L5 (or ET-LC2) (2,3-*Seco*-taraxer-14-ene-2,3,28-trioic acid 2,3-dimethyl ester)

Compound ET-L5 was obtained as colorless needles.

HR-ESI-MS : *m/z* 539.3344 $[M+Na]^+$; see **Figure 162**

mp : >300 °C

$[\alpha]^{25}_D$: +81.55 (*c* 0.106, MeOH)

IR : ν_{max} (KBr): 3430, 2949, 2864, 1728, 1690, 1250, 1143 cm^{-1}; see **Figure 161**

^{1}H NMR : δ ppm, 500 MHz, in DMSO-d_6; see **Figures 163a-163e**, **Table 40**

^{13}C NMR : δ ppm, 125 MHz, in DMSO-d_6; see **Figure 164**, **Table 40**

4.24 Compound ET-L12 (Aleuritolic acid)

Compound ELT-L12 was obtained as colorless needles.

ESI-MS : *m/z* 455 $[M-H]^+$; see **Figure 169**

mp : 258-260 °C

IR : ν_{max} (KBr): 3434, 2939, 2867, 1690, 1467, 1296, 1250, 1212, 1031, 996 cm^{-1}; see **Figure 168**

^{1}H NMR : δ ppm, 300 MHz, in DMSO-d_6; see **Figure 170**, **Table 41**

^{13}C NMR : δ ppm, 75 MHz, in DMSO-d_6; see **Figure 171**, **Table 41**

4.25 Compound ET-LC4 (Kaempferol)

Compound ET-LC4 was obtained as yellow powder.

ESI-MS : *m/z* 287.16 $[M+H]^+$; see **Figure 175**

mp : 276-278 °C

UV : λ_{max} nm (log ε), in MeOH: 210 (3.49), 265 (3.44), 366 (3.50); see **Figure 173**

IR : ν_{max} (KBr): 3423, 1659, 1615, 1508, 1383, 1176, 818, 796 cm^{-1}; see **Figure 174**

^{1}H NMR : δ ppm, 300 MHz, in $CD_3OD+CDCl_3$; see **Figure 176**, **Table 42**

^{13}C NMR : δ ppm, 75 MHz, in $CD_3OD+CDCl_3$; see **Figure 177**, **Table 42**

4.26 Compound ET-LC7 (Sequoiaflavone)

Compound ET-LC7 was obtained as pale yellow powder.

ESI-MS : m/z 551 $[M-H]^+$; see **Figure 183**

mp : >300 °C

UV : λ_{max} nm (log ε), in MeOH: 215 (4.71), 270 (4.61), 336 (4.60); see **Figure 181**

IR : ν_{max} (KBr): 3367, 2925, 1659, 1597, 1502, 1336, 1161, 837 cm^{-1}; see **Figure 182**

^{1}H NMR : δ ppm, 500 MHz, in DMSO-d_6; see **Figures 184a-184b**, **Table 43**

^{13}C NMR : δ ppm, 125 MHz, in DMSO-d_6; see **Figures 185a-185c**, **Table 43**

4.27 Compound ET-LC13 (Ginkgetin)

Compound ET-LC13 was obtained as yellow powder.

ESI-MS : *m/z* 565 $[M-H]^+$; see **Figure 192**

mp : 234-239 °C

UV : λ_{max} nm (log ε), in MeOH: 216 (4.54), 270 (4.46), 333 (4.43); see **Figure 190**

IR : ν_{max} (KBr): 3435, 1655, 1606, 1506, 1424, 1337, 1253, 1190, 1160 833 cm^{-1}; see **Figure 191**

^{1}H NMR : δ ppm, 500 MHz, in DMSO-d_6; see **Figure 193**, **Table 44**

^{13}C NMR : δ ppm, 125 MHz, in DMSO-d_6; see **Figures 194a-194c**, **Table 44**

5. Evaluation of Biological Activities

5.1 Determination of Inhibitory Activity on Dopamine-1 Receptor

Inhibitory activity on dopamine-1 receptor was determined using the radioligand binding receptor assay (Tatsumi *et al.*, 1999; Page *et al.*, 2000)**.**

The striata of rat brain were dissected out on ice and homogenized in ice-cold 50 mM Tris-HCl (pH 7.4). The homogenate was centrifuged at 800×g for 10 min at 4°C, and the supernatant obtained was centrifuged for 15 min at 18,000×g. The membranes were washed, resuspended in ice-cold 50 mM Tris-HCl (pH 7.4) and centrifuged for 15 min at 18,000×g twice. They were then resuspended in ice-cold buffer containing 50 mM Tris-HCl (pH 7.4), 1 mM EDTA, 5 mM $MgCl_2$, and 150 mM NaCl. The protein content was determined by Bradford method (Bradford, 1976) using bovine serum albumin (BSA) as standard.

The binding experiment was performed at 25°C in plastic tube containing 750 μg of membrane protein in binding buffer containing 50 mM Tris-HCl (pH 7.4), 1 mM EDTA, 5 mM $MgCl_2$, 150 mM NaCl, 1 mM dithiotreitol, 0.1% sodium metabisulfite and 0.1% BSA. The binding was initiated by addition of 100 μl of 5 nM [^{3}H] SCH23390 (a dopamine-1 receptor antagonist) in the presence and absence of test solution in DMSO. Non-specific binding was measured in the presence of 50 μl of 10^{-4} M (+)-butaclamol. Incubation was performed for 30 min and terminated by addition of 3 ml of ice-cold washing buffer [50 mM Tris-HCl (pH 7.4), 1 mM EDTA, 5 mM $MgCl_2$, 150 mM NaCl]. The suspension was immediatedly filtered under vacuum through Whatman GF/B filters previously soaked for 1 hour in 0.3% polyethyleneimine. The filters were washed rapidly twice with 3 ml of ice-cold washing buffer and placed in scintillation vials containing 5 ml of scintillation cocktail (Ultima Gold®, Perkin Elmer). Radioactivity was determined by liquid scintillation spectrometry. Total binding was determined in DMSO solvent control experiment. SCH23390 was used as the reference compound. % Inhibition was obtained as follows:

Specific binding = total binding – non-specific binding

% inhibition = $100 - [(\text{specific binding})_{test} / (\text{specific binding})_{control}] \times 100$

5.2 Determination of Antimycobacterial Activity

Antimycobacterial activity was assessed against *Mycobacterium tuberculosis* $H_{37}Ra$ using the Microplate Alamar Blue Assay (MABA) (Collins and Franzblau, 1997). The mycobacteria were grown in 100 ml of 7H9GC broth containing 0.005% Tween 80. Cultures were incubated in 500-ml plastic flask on a rotary shaker at 200 rpm and 37 °C until they reached an optical density of 0.4-0.5 at 550 nm. Bacteria were washed and suspended in 20 ml of phosphate-buffered saline solution and passed through a filter. The filtrates were aliquoted and stored at -80 °C.

The susceptibility testing was performed in 96-well microplates. Samples were initially diluted with either dimethylsulfoxide or distilled deionized water, followed by Middlebrook 7H9 media containing 0.2% v/v glycerol and 1.0 gm/L 7H9GC broth. Subsequent two-fold dilutions were performed in 0.1 ml of 7H9GC broth in microplates. Frozen inocula were diluted 1:100 in 7H9GC broth and addition of 0.1 ml of this solution to the well resulted in final bacterial titers of about 5×10^4 CFU/ml. Wells containing sample only were used to determine whether the tested-

samples themselves can reduce the dye or not. Additional control wells consisted of bacteria only (B) and medium only (M). Plates were incubated at 37 °C. Starting at day 6 of incubation, 20 µl of Alamar Blue solution and 12.5 µl of 20% Tween 80 were added to one B well and one M well, and plates were re-incubated at 37 °C. The B wells were observed for a color change from blue to pink, at which time reagents were added to all remaining wells. Plates were then incubated at 37 °C, and results were recorded at 24 hour post-reagent addition. Visual MIC values were defined as the lowest concentration of sample that prevented a color change. Standard drugs, *i.e.* rifampicin, isoniazid and kanamycin sulfate, were used as the reference compounds.

5.3 Determination of Antimalarial Activity

Plasmodium falciparum (K1, multi-drug resistant strain) was cultivated *in vitro* using the method of Trager and Jensen (1976) in RPMI 1640 medium containing 20 mM HEPES (N-2-hydroxyethylpiperazine-N′-2-ethanesulfonic acid), 32 mM $NaHCO_3$ and 10% heat-inactivated human serum with 3% erythrocytes and incubated at 37 °C in an incubator with 3% CO_2. Cultures were diluted with fresh medium and erythrocytes every day according to cell growth. Quantitative assessment of antimalarial activity *in vitro* was determined by microculture radioisotope techniques based upon the method of Desjardins *et al.* (1979). Briefly, a mixture of 200 µl of 1.5% erythrocytes with 1% parasitemia at the early ring stage was pre-exposed to 25 µl of the medium containing a test sample dissolved in 1% DMSO (0.1% final concentration) for 24 hours, employing the incubation condition described above. Subsequently, 25 µl of [^{3}H]-hypoxanthine (Amersham, USA) in culture medium (0.5 µCi) were added to each well and plates were incubated for an additional 24 hours. Levels of incorporated labeled hypoxanthine indicating parasite growth were determined using the TopCount microplate scintillation counter (Packard, USA). The IC_{50} value represents the concentration which indicates 50% reduction of parasite growth. The standard sample was dihydroartemisinin (DHA).

5.4 Determination of Cytotoxic Activity

5.4.1 Human Small Cell Lung Carcinoma (NCI-H187)

Cytotoxicity to NCI-H187 cells (human small cell lung carcinoma, ATCC CRL-5804) was determined by MTT assay (Plumb *et al*., 1989). Briefly, cells were diluted to 10^5 cells/ml. Test compounds were diluted in distilled water and added to microplates in a total volume of 200 µl. Plates were incubated at 37 °C, 5%

CO_2 for 3 days. Then, 50 μl of 2 mg/ml MTT solution (3-[4,5-dimethylthiazol-2-yl]-2,5-diphenyltetrazolium bromide or thiazolyl blue) were added to each well of the plate. Plates were wrapped with aluminium foil and incubated for 4 hours. MTT was then removed from the wells and the formazan crystals were dissolved in 200 μl of DMSO and 25 μl of Sorensen's glycine buffer. Absorbance was read in microplate reader at the wavelength of 510 nm. The reference substance was ellipticine. The activity was expressed as 50% inhibitory concentration (IC_{50}), which is the concentration that inhibits cell growth by 50% compared with untreated cells.

5.4.2 Human Epidermoid Carcinoma (KB) and Breast Cancer (BC)

Cytotoxicity to KB (human epidermoid carcinoma of cavity, ATCC CCL-17) and BC (breast cancer) cell lines was determined by a colorimetric assay that measured cell growth from cellular protein content (Skehan *et al*., 1990). Ellipticine and doxorubicin were used as positive control. DMSO was used as negative control. Briefly, cells at a logarithmic growth phase were harvested and diluted to 10^5 cells/ml with fresh medium and gently mixed. Extracts or test compounds were diluted in distilled water and put into microplates in a total volume of 200 μl. Plates were incubated at 37 °C, 5% CO_2 for 72 hours. After incubation period, cells were fixed by 50% trichloroacetic acid. The plates were incubated at 4 °C for 30 min, washed with tap water and air-dried at room temperature. The plates were then stained with 0.05% sulforhodamine B (SRB) for 30 min. After staining period, SRB was removed with 1% acetic acid. Plates were air-dried before bound dye was solubilized with 10 mM Tris-base for 5 min on shaker. Absorbance was read in microplate reader at the wavelength of 510 nm. The compound was considered strongly active if its IC_{50} value was less than 5 μg/ml, moderately active if its IC_{50} value was between 5-10 μg/ml, weakly active when IC_{50} value was between 10-20 μg/ml, and inactive if IC_{50} value was more than 20 μg/ml.

5.4.3 Vero Cells

Compounds were tested for their cytotoxicity against Vero cells (African green monkey kidney fibroblast) in 96-well tissue culture plates. Vero cell suspension (190 μl) containing 1×10^5 cells/ml and 10 μl of tested compound solution were added to each well in triplicate. Ellipticine and 10% DMSO were used as positive and negative control, respectively. The cells were incubated at 37 °C for 72 hours in 5% CO_2. After incubation, the cytotoxicity was determined as in 5.4.2. If %

cell viability was greater than or equal to 50%, reported as IC_{50} > 50 μg/ml and if % cell viability was less than 50%, reported an IC_{50} value which determined from two-fold serial dilution.

5.5 Determination of Anti-Herpes Simplex Activity

Anti-herpes simplex virus type 1 (HSV-1) activity of pure compounds was tested against HSV-1 strain ATCC VR260, using colorimetric microplate assay as in 5.4.2. The growth of host cells (vero cell line ATCC CCL-81) infected with virus and treated with the extract was compared with control cells, which were infected with virus only. Acyclovir and DMSO were used as positive and negative control, respectively. The extracts were tested at non-cytotoxic concentrations (inhibition of cell growth < 50%). Extract which produced more than 50% inhibition was considered active, while those which gave 35-50% and 25-35% inhibition were considered moderately active and weakly active, respectively.

The active extracts (more than 50% inhibition of the virus) were further tested to determine their IC_{50} values.

CHAPTER IV
RESULTS AND DISCUSSION

Maceration of the aerial parts of *Canavalia rosea* (Sw) DC. with EtOH gave an EtOH extract, which was partitioned with CH_2Cl_2 to give CH_2Cl_2 and aqueous alcoholic fractions. The CH_2Cl_2 fraction was further partitioned with hexane to yield hexane and CH_2Cl_2 extracts. The aqueous alcoholic fraction was partitioned with BuOH to give a BuOH extract. Four compounds, CAR-1, CAR-2 and CAR-6, were isolated from the hexane extract; whereas, compound CAR-4 was obtained from the CH_2Cl_2 extract, and compound CAR-3 was isolated from the BuOH extract.

The stems and flowers of *Elateriospermum tapos* Blume were separately macerated with hexane, CH_2Cl_2 and MeOH to give each solvent extract, respectively. In addition, the leaves of *E. tapos* was macerated with EtOH, then partitioned with hexane and CH_2Cl_2 to yield hexane, CH_2Cl_2 and aqueous EtOH extracts, respectively. Fourteen compounds (ET-S1 - ET-S8, ET-S11, ET-S12, ET-S14, ET-S15 and ET-S17) were isolated from the stem extracts. The flower extracts were extensively chromatographed to yield eight compounds (ET-F3 – ET-F7, ET-FM2 and ET-FM3). Finally, the leaf extracts furnished thirteen compounds (ET-L1 – ET-L5, ET-L12, ET-LC1, ET-LC4, ET-LC5, ET-LC7, ET-LC13 and ET-LC17).

The structures of all isolated compounds were elucidated and identified through interpretation of their UV, IR, MS and NMR spectral data, and were confirmed by comparison with literature values.

1. Structure Determination of Compounds Isolated from *Canavalia rosea*

1.1 Identification of Component CAR-1 (β-Sitosterol/Stigmasterol Mixture)

Component CAR-1 was obtained as colorless needles, giving a green color in the Liebermann-Burchard test indicative of a steroidal skeleton. The ^{13}C NMR spectrum (**Figure 14**) of CAR-1 displayed 46 signals, some of which were doubled. The proton signals at δ 5.12 (*dd*, *J* = 15.2, 8.4 Hz) and 5.03 (*dd*, *J* = 15.2, 8.4 Hz) (**Figure 13**) could be assigned to H-22 and H-23, respectively, of stigmasterol. The olefinic proton signal at δ 5.34 belongs to H-6 of both β-sitosterol and stigmasterol. The integration ratio of H-6, H-22 and H-23 was approximately 3:1:1. Therefore, CAR-1 was identified as a 2:1 mixture of β-sitosterol and stigmasterol by comparison

of its ^{1}H and ^{13}C NMR data with reported values (Wright *et al*., 1978; Khalil and Idler, 1980; Iribarren and Pomilio, 1985; Heupel *et al*., 1986).

Comparison of its ^{13}C NMR data with reported values for β-sitosterol and stigmasterol (Wright *et al*., 1978) was shown in **Table 18.**

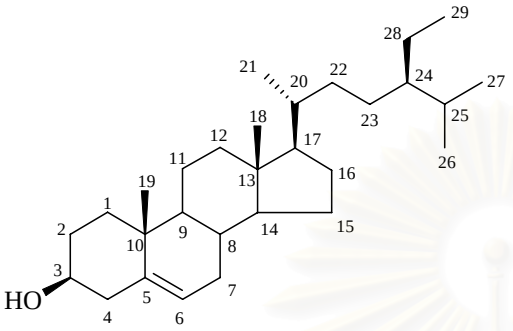

β-Sitosterol

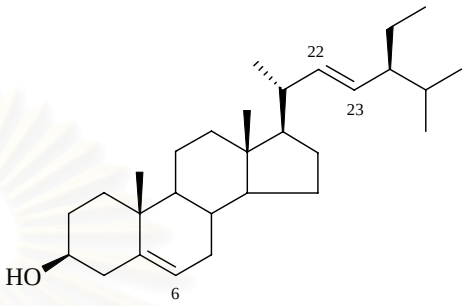

Stigmasterol

Table 18. ^{13}C NMR (75 MHz) spectral data of β-sitosterol, stigmasterol and component CAR-1 (in $CDCl_3$)

Position	δ (ppm)		
	β-Sitosterol [a]	Stigmasterol [a]	CAR-1
1	37.3	37.3	37.4, 37.4*
2	31.6	31.7	31.8, 31.8*
3	71.7	71.8	71.8, 71.8*
4	42.5	42.4	42.4, 42.4*
5	140.8	140.8	140.6, 140.6*
6	121.6	121.7	121.6, 121.6*
7	31.9	31.9	32.0, 32.0*
8	31.9	31.9	32.0, 32.0*
9	50.2	50.2	50.2, 50.2*
10	36.5	36.6	36.6, 36.6*
11	21.1	21.1	21.2, 21.2*
12	39.8	39.7	39.9, 39.8*
13	42.3	42.4	42.4, 42.4*
14	56.8	56.9	56.8, 56.9*
15	24.3	24.4	24.4, 24.4*

Table 18. ^{13}C NMR (75 MHz) spectral data of β-sitosterol, stigmasterol and component CAR-1 (in $CDCl_3$) (continued)

Position	δ (ppm)		
	β-Sitosterol [a]	Stigmasterol [a]	CAR-1
16	28.3	29.0	28.4, 29.0*
17	56.1	56.1	56.0, 56.1*
18	11.9	12.1	12.0, 12.1*
19	19.4	19.4	19.5, 19.5*
20	36.2	40.5	36.2, 40.6*
21	18.8	21.1	18.9, 21.2*
22	34.0	138.4	34.1, 138.2*
23	26.1	129.3	26.2, 129.1*
24	45.9	51.3	45.9, 51.3*
25	29.2	31.9	29.3, 32.0*
26	19.8	21.3	20.0, 21.4*
27	19.0	19.0	19.2, 19.2*
28	23.1	25.4	23.2, 25.5*
29	12.3	12.3	12.0, 12.1*

[a] Wright *et al.*, 1978
* Stigmasterol

1.2 Identification of Compound CAR-2 (β-Sitosterol glucoside)

Compound CAR-2 was obtained as white needle crystals which gave purple coloration upon spraying with anisaldehyde-H_2SO_4. Liebermann-Burchard test of this compound gave green color, suggesting the presence of a steroid skeleton.

In the ^1H NMR spectrum (**Figure 15**), a broad singlet at δ 5.31 could be assigned to the vinylic H-6 of the steroid nucleus. Two methyl singlets, three methyl doublets and a methyl triplet appeared between δ 0.60-1.00. A group of resonances appearing at around δ 2.70-3.20 were those belonging to a sugar moiety, while the doublet at δ 4.21 (J = 7.8 Hz) was assignable to its β-anomeric proton. The sugar component of this compound was concluded to be β-D-glucopyranose.

The ^{13}C NMR spectrum (**Figure** 16) exhibited 35 carbon signals. The two most downfield signals at δ 140.3 and 121.1 could be assigned to the olefinic C-5 and

C-6, respectively. The signal at δ 76.7 represented the oxygenated C-3 of the steroid skeleton. The signal at δ 100.7 corresponding to the anomeric C-1′ and five signals in the range of δ 62.9-78.7 confirmed that compound CAR-2 should be a monoglycoside of β-sitosterol. Comparison of its ^{13}C NMR data with those values previously reported for β-sitosterol glucoside (Kojima *et al*., 1990; Mizushina *et al*., 2006) revealed them to be fully in agreement (**Table 19**).

β-Sitosterol glucoside has been identified as a constituent of various plants from several different families, including *Spilanthes acmella* (family Compositae) (Krishnaswamy and Prasanna, 1975), *Aframomum escapum* (family Zingiberaceae) (Ayimele, Tane and Connolly, 2004) and *Thymelea hirsute* (family Thymelaeaceae) (Rizk and Rimpler, 1972). The compound, isolated from *Tribulus terrestris* (family Zygophyllaceae), exhibited anthelmintic activity *in vitro* against the nematode *Caenorhabditis elegans* (Deepak *et al*., 2002) and also stimulated human peripheral blood lymphocyte proliferation (Bouic *et al*., 1996). It was also found in the brown-skin of onions (*Allium cepa*) and shown to selectively inhibit the activity of mammalian DNA polymerase λ (pol λ) *in vitro* (Mizushina *et al*., 2006).

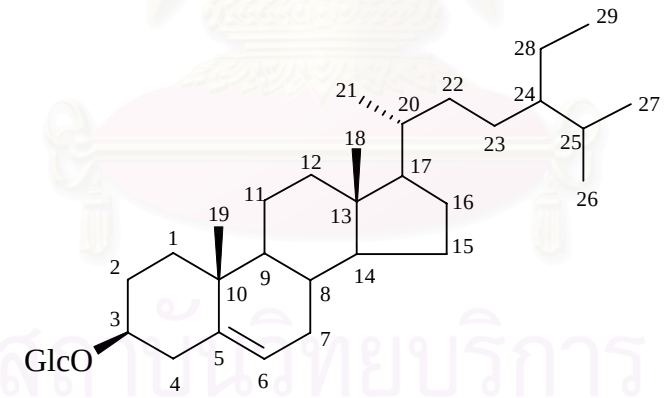

β-Sitosterol glucoside

Table 19. ^{13}C NMR (75 MHz) spectral data of β-sitosterol-3-*O*-β-D-glucopyranoside and compound CAR-2 (in DMSO-d_6)

position	β-sitosterol-3-*O*-β-D-glucopyranoside [a, b]	ET-L1
1	37.5	36.9
2	30.3	29.4
3	78.2	76.7
4	39.4	38.4
5	141.0	140.3
6	122.0	121.1
7	32.2	31.5
8	32.1	31.5
9	50.4	49.7
10	38.0	36.3
11	21.3	20.7
12	40.0	39.0
13	42.5	41.9
14	56.9	56.2
15	24.6	24.0
16	28.6	27.9
17	56.3	55.5
18	12.0	11.8
19	19.3	19.2
20	36.4	35.6
21	19.1	18.8
22	34.3	33.5
23	26.4	25.6
24	46.1	45.2
25	29.5	28.8
26	19.5	19.8
27	20.0	19.1
28	23.4	22.8

Table 19. ^{13}C NMR (75 MHz) spectral data of β-sitosterol-3-*O*-β-D-glucopyranoside and compound CAR-2 (in DMSO-d_6) (continued)

position	β-sitosterol-3-*O*-β-D-glucopyranoside [a, b]	ET-L1
29	12.2	11.9
1′	102.6	100.7
2′	75.4	73.5
3′	78.7	76.9
4′	71.8	70.1
5′	78.6	76.8
6′	62.9	61.2

[a] 400 MHz NMR, in pyridine-d_5
[b] Mizushina *et al*., 2006

1.3 Identification of Compound CAR-3 (Rutin)

Compound CAR-3 was obtained as yellow powder. Its molecular formula was determined as $C_{27}H_{30}O_{16}$, according to $[M-H]^+$ ion peak in the ESIMS at *m/z* 609 (**Figure 19**). Its IR spectrum (**Figure 18**) exhibited absorption bands of hydroxyl function at 3427 cm^{-1} and conjugated carbonyl at 1600 cm^{-1}.

Five aromatic proton signals of two aromatic rings could be observed in its ^{1}H NMR spectrum (**Figure 20**). Two broad singlets at δ 6.18 and 6.37 were assigned to the *meta*-coupling H-6 and H-8, respectively, of ring A of a flavonol aglycone. Another aromatic proton system includes a signal at δ 6.83 (1H, *d*, *J* = 8.4 Hz, H-5′), which *ortho*-coupled to a signal at δ 7.53 (1H, *d*, *J* = 8.4 Hz, H-6′), and a broad singlet at δ 7.51. These three resonances represents the 1,3,4-trisubstituted ring B of the flavonoid. A doublet appearing at δ 0.97 (3H, *d*, *J* = 5.1 Hz) and a broad singlet at δ 4.37 were assigned to the methyl group and the α-anomeric proton, respectively, of a rhamnose unit; whereas, a doublet at δ 5.32 (1H, *J* = 7.2 Hz) could be assigned to the β-anomeric proton of a glucose moiety. Other sugar protons resonated in the region of δ 2.80-3.80.

The ^{13}C NMR spectrum (**Figure 21**), in combination with DEPT experiments (**Figure 22**), displayed 27 carbon signals including 15 signals of the flavonol

aglycone and 12 signals of two sugar units. The quercetin aglycone was represented by one carbonyl signal at δ 177.0 (C-4), five methine carbon signals at δ 93.4 (C-8), 98.5 (C-6), 115.0 (C-2′), 116.0 (C-5′) and 121.3 (C-6′), and nine quaternary carbon signals at δ 103.7 (C-10), 120.9 (C-1′), 133.0 (C-3), 144.4 (C-3′), 148.1 (C-4′), 156.1 (C-2), 156.3 (C-9), 160.9 (C-5) and 163.8 (C-7). Two anomeric carbons resonated at δ 100.5 (Rha-1) and 101.0 (Glc-1). Comparison of these spectral data with previously published literature identified compound CAR-3 to be the flavonol glycoside rutin (or quercetin 3-rutinoside) (De Britto *et al*., 1995).

Rutin has been used medicinally in the treatment of several ailments. For example, it is an antioxidant with potential use for strengthening the immune system. One study showed rutin to be effective in reducing oxidative damage to red blood cells (Grinberg, Rachmilewitz and Newmark, 1994). It may also possess anti-inflammatory and vasoactive properties (Casa *et al*., 2000). The flavonoid glycoside displayed beneficial protective effects against reflux oesophagitis by inhibiting gastric acid secretion, oxidative stress, inflammatory cytokine production (i.e. interleukin-1-β (IL-1-β), and intracellular calcium mobilization in polymorphonucleocytes (PMNs) in rats (Shin *et al*., 2002). Moreover, rutin, to some extent, enhanced antibacterial activities of flavonoids against *Bacillus cereus* and *Salmonella enteritidis* (Arima, Ashida and Danno, 2002) and exhibited hepatoprotective effect against paracetamol- and carbontetrachloride-induced hepatotoxicity in rodents (Janbaz, Saeed and Gilani, 2002). The compound also showed significant analgesic (Harborne and Williams, 2000) and hypoglycemic activities in rats (Onunkwo, Akah and Udeala, 1998). Rutin might therefore be useful in the treatment of clinical disorders.

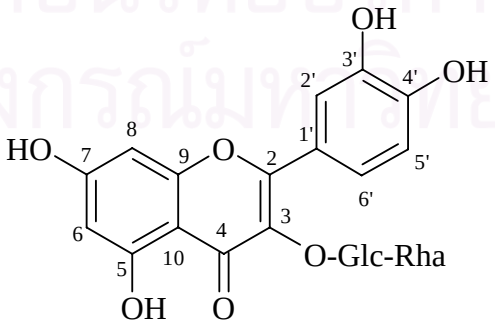

Rutin

Table 20. ^{1}H (300 MHz) and ^{13}C (75 MHz) NMR spectral data of rutin and compound CAR-3 (in DMSO-d_6)

Position	Rutin [a]		CAR-3	
	^{1}H (mult., *J* in Hz)	^{13}C	^{1}H (mult., *J* in Hz)	^{13}C
2	-	156.4	-	156.1
3	-	133.3	-	133.0
4	-	177.4	-	177.0
5	-	161.2	-	160.9
6	6.20 (*d*, *J* = 2.1 Hz)	98.7	6.18 (*br s*)	98.5
7	-	164.1	-	163.8
8	6.39 (*d*, *J* = 2.1 Hz)	93.6	6.37 (*br s*)	93.4
9	-	156.6	-	156.3
10	-	104.0	-	103.7
1′	-	121.2	-	120.9
2′	7.55 (*m*)	115.2	7.51 (*br s*)	115.0
3′	-	144.7	-	144.4
4′	-	148.4	-	148.1
5′	6.85 (*d*, *J* = 8.9 Hz)	116.3	6.83 (*d*, *J* = 8.4 Hz)	116.0
6′	7.55 (*m*)	121.6	7.53 (*d*, *J* = 8.4 Hz)	121.3
Glc-1	5.35 (*d*, *J* = 7.3 Hz)	101.2	5.32 (*d*, *J* = 7.2 Hz)	101.0
Glc-2		74.0		73.9
Glc-3		76.3		76.3
Glc-4		70.6		70.4
Glc-5		75.9		75.8
Glc-6		67.0		66.9
Rha-1	4.40 (*d*, *J* = 1.2 Hz)	100.7	4.37 (*br s*)	100.5
Rha-2		70.4		70.2
Rha-3		70.3		69.9
Rha-4		71.8		71.7
Rha-5		68.2		68.1
Rha-6	1.00 (*d*, *J* = 6.1 Hz)	17.7	0.97 (*d*, *J* = 5.1 Hz)	17.7

[a] De Britto *et al*., 1995

1.4 Identification of Compound CAR-4 (*Epi*-inositol 6-*O*-methyl ether)

Compound CAR-4 was obtained as colorless crystals. Its molecular formula was determined as $C_7H_{14}O_6$ based on its ESIMS quasi-molecular ion peak ($[M+Na]^+$) at *m/z* 217 (**Figure 27**), suggesting a cyclic structure. The IR spectrum (**Figure 26**) exhibited a hydroxyl absorption band at 3336 cm^{-1}, C-H stretching bands at 2940 and 2929 cm^{-1}, and C-O stretching bands in the 1324-1103 cm^{-1} region. The ^{1}H-NMR spectrum (**Figure 28** and **Table 21**) displayed six oxymethine proton signals at δ 3.32 (*ddd*, *J* = 9.3, 4.9, 2.6 Hz, H-1), 3.43 (*ddd*, *J* = 6.6, 5.8, 2.6 Hz, H-2), 3.62 (*ddd*, *J* = 6.6, 3.4, 2.6 Hz, H-3), 3.62 (*ddd*, *J* = 6.6, 3.4, 2.6 Hz, H-4), 3.50 (*ddd*, *J* = 9.3, 6.6, 2.6 Hz, H-5) and 2.99 (*t*, *J* = 9.3 Hz, H-6); five hydroxyl proton doublets at δ 4.48 (*J* = 4.9 Hz, 1-OH), 4.30 (*J* = 5.8 Hz, 2-OH), 4.69 (*J* = 3.4 Hz, 3-OH), 4.60 (*J* = 3.4 Hz, 4-OH) and 4.43 (*J* = 6.4 Hz, 5-OH); and one methoxy singlet at δ 3.43 (*s*, 6-OCH_3).

Seven ^{13}C NMR resonances (**Figure 29** and **Table 21**), corresponding to six oxymethine carbons and a methoxy carbon, appeared at δ 72.5 (C-1), 71.0 (C-2), 72.1 (C-3), 72.7 (C-4), 70.2 (C-5), 83.9 (C-6) and 59.8 (6-OCH_3), respectively. The most downfield resonance at δ 83.9 indicated the site of methylation. Assignments for the five remaining carbon and proton resonances on the cyclitol ring were determined by ^{1}H-^{1}H COSY (**Figure 30**) and HMQC (**Figure 31**) experiments

The orientation of hydroxyl groups and a methoxy group on the cyclohexane ring was determined on the basis of coupling constant analysis. The signals at δ 3.43 (H-2) and 3.62 (H-4) corresponded to the equatorial hydrogens with the small coupling constant characteristic of an H_{ax}-H_{eq}-H_{ax} system The most upfield triplet at δ 2.99 corresponded to the axial hydrogen with the large coupling constant characteristic of an H_{ax}-H_{ax}-H_{ax} transaxial systems on the cyclitol ring (Obendorf *et al*., 2005). The remaining hydrogens also exhibited large coupling constants.

From the above NMR spectral data, together with the information from HMBC (**Figures 32a-32b** and **Table 21**) and NOESY (**Figure 33**) experiments, compound CAR-4 was identified as *epi*-inositol 6-*O*-methyl ether.

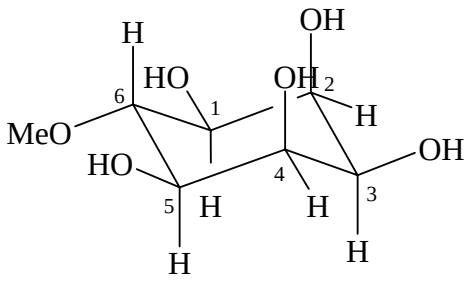

Epi-inositol 6-*O*-methyl ether

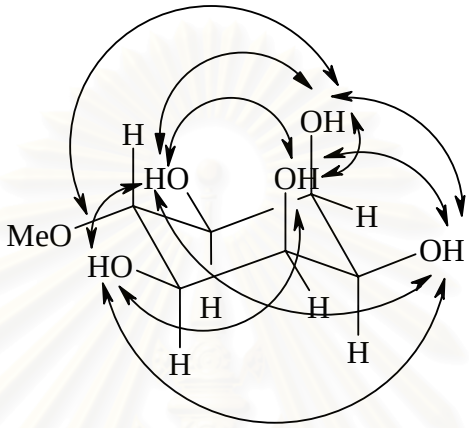

NOESY correlations of *epi*-inositol 6-*O*-methyl ether

Table 21. ^{1}H (500 MHz) and ^{13}C (125 MHz) NMR spectral data of compound CAR-4 with long-range correlations observed in the HMBC spectrum (in DMSO-d_6)

Position	^{1}H (mult., *J* in Hz)	^{13}C	HMBC
1	3.32 (*ddd*, *J* = 9.3, 4.9, 2.6 Hz)	72.5	
2	3.43 (*ddd*, *J* = 6.6, 5.8, 2.6 Hz)	71.0	
3	3.62 (*ddd*, *J* = 6.6, 3.4, 2.6 Hz)	72.1	
4	3.62 (*ddd*, *J* = 6.6, 3.4, 2.6 Hz)	72.7	
5	3.50 (*ddd*, *J* = 9.3, 6.6, 2.6 Hz)	70.2	
6	2.99 (*t*, *J* = 9.3 Hz)	83.9	C-4, C-5, 6-OCH_3
1-OH	4.48 (*d*, *J* = 4.9 Hz)	-	C-1, C-2, C-6
2-OH	4.30 (*d*, *J* = 5.8 Hz)	-	C-2, C-3
3-OH	4.69 (*d*, *J* = 3.4 Hz)	-	C-3, C-4
4-OH	4.60 (*d*, *J* = 3.4 Hz)	-	C-4, C-3
5-OH	4.43 (*d*, *J* = 6.4 Hz)	-	C-1, C-5
6-OCH_3	3.43 (*s*)	59.8	C-6

1.5 Structure Elucidation of Compound CAR-6 (Canarosine)

Compound CAR-6 was obtained as pale yellow needles. The molecular formula of compound CAR-6 was determined as $C_{20}H_{30}N_4O_3$ based on its HRESIMS quasi-molecular ion $[M+H]^+$ at *m/z* 375.2469 (**Figure 35**). Its IR spectrum (**Figure 34**) showed intense C=O (amide) or C=N bands at 1657 and 1613 cm^{-1} and a prominent hydroxy band at 3429 cm^{-1}.

The ^1H spectrum (**Figures 36a-36d**) showed two doublets at δ 1.72 (3H, *d*, *J* = 0.5 Hz, H-9) and 1.76 (3H, *d*, *J* = 0.5 Hz, H-10), corresponding to two methyl groups which attached to a trisubstituted double bond of an isoprene unit. The olefinic proton of this unit, appearing as a multiplet at δ 5.15, also coupled to a methylene resonance at δ 3.94 (2H, *d*, *J* = 6.5 Hz, H-6). Typical resonances of a ferulic amide residue, including two doublets at δ 7.10 (*J* = 1.8 Hz, H-2′) and 6.78 (*J* = 7.8 Hz, H-5′) and a doublet of doublets at δ 7.01 (*J* = 7.8, 1.8 Hz, H-6′) for the aromatic ring; two doublets at δ 7.43 (*J* = 15.6 Hz, H-7′) and 6.40 (*J* = 15.6 Hz, H-8′) for the unsaturated amide *trans*-double bond; and the methoxy singlet at δ 3.86 (3′-OMe), could clearly be observed. The ^1H-^1H COSY spectrum (**Figure 39**) showed the spin system of a four methylene chain (C_1-C_4) between δ 1.57 and 3.34 indicating that it was placed between two nitrogens, one of which was the ferulic amide NH. A spin system of an isoprene unit, from the olefinic H-7 at δ 5.15 to either the methylene H-6 at δ 3.94 and the gem-dimethyls H-9 and H-10 at δ 1.72 and 1.76, respectively, was also confirmed by the COSY spectrum. The downfield shift of the isoprene H-6 suggested its connection to a heteroatom.

The ^{13}C NMR spectrum (**Figure 37**) and DEPT experiments (**Figure 38**) exhibited twenty carbon signals including 3 methyls, 5 methylenes, 6 methines and 6 quaternary carbons. The amide carbonyl (C-9′) appeared as the most downfield signal at δ 169.2, while a quaternary carbon signal resonating at δ 157.5 (C-5) represented the characteristic chemical shift of a guanidine group (Lonsti *et al*., 1998). The chemical shifts in the aromatic amide part of C-2′ and C-5′, at δ 111.5 and 116.7, respectively, confirmed that the methoxy group was at position 3′.

The HMBC spectrum (**Figures 41a-41e**, **Table 22**) showed the linkage between the isoprene unit to the same guanidine nitrogen as the C_1-C_4 methylene chain, as shown by cross peaks between H-4 at δ 3.33 and C-5 (δ 157.5), C-6 (δ 47.5)

and between H-6 at δ 3.94 and C-4 (δ 49.0), C-5. HMBC correlations supporting the linkage of the ferulic amide to the C_1-C_4 chain were those between H-1 at δ 3.34 to C-2 (δ 28.0), C-3 (δ 25.4), C-9′ (δ 169.2) and H-2 at δ 1.57 to C-1 (δ 39.5), C-3, C-4.

These spectral data were further compared with those of fontaineine (see **1.23**, page 15), an acyclic guanidine-type alkaloid isolated from the leaves of *Fontainea pancheri* (family Euphorbiaceae). However, compound CAR-6 differs from fontaineine in that it contains only one isoprene unit and, therefore, was elucidated as a new acyclic guanidine-type alkaloid, trivially named canarosine.

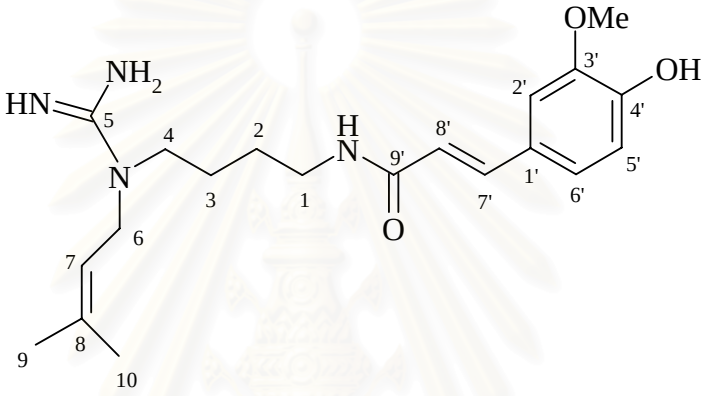

Canarosine

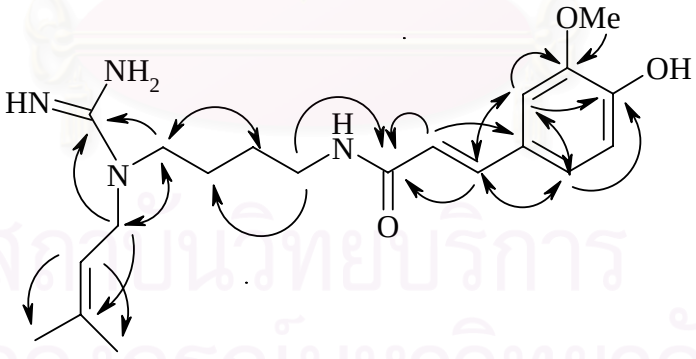

Major HMBC correlations of canarosine

Table 22. ^{1}H (500 MHz) and ^{13}C (125 MHz) NMR assignments of compound CAR-6 (in CD_3OD)

Position	^{1}H (mult., *J* in Hz)	^{13}C	HMBC
1	3.34 (*t*, *J* = 6.3 Hz)	39.5	C-2, C-3, C-9′
2	1.57 (*quintet*, *J* = 6.3 Hz)	28.0	C-1, C-3, C-4
3	1.65 (*m*)	25.4	C-2, C-4
4	3.33 (*m*)	49.0	C-2, C-3, C-5, C-6
5	-	157.5	-
6	3.94 (*d*, *J* = 6.5 Hz)	47.5	C-4, C-5, C-7, C-8
7	5.15 (*m*)	118.6	C-9, C-10
8	-	139.3	-
9	1.71 (*s*)	18.1	C-7, C-8, C-10
10	1.75 (*s*)	25.9	C-7, C-8, C-9
1′	-	127.9	-
2′	7.10 (*d*, *J* = 1.8 Hz)	111.5	C-3′, C-4′, C-6′, C-7′
3′	-	149.1	-
4′	-	149.9	-
5′	6.78 (*d*, *J* = 7.8 Hz)	116.4	C-1′, C-3′, C-4′
6′	7.01 (*dd*, *J* = 7.8, 1.8 Hz)	123.1	C-2′, C-4′, C-7′
7′	7.43 (*d*, *J* = 15.6 Hz)	142.1	C-1′, C-2′, C-6′, C-8′, C-9′
8′	6.40 (*d*, *J* = 15.6 Hz)	118.3	C-1′, C-9′
9′	-	169.2	-
3′-OMe	3.86 (*s*)	56.4	C-3′

2. Structure Determination of Compounds Isolated from *Elateriospermum tapos*

2.1 Identification of Compound ET-S1 (Lupeol 3-acetate)

Compound ET-S1 was obtained as colorless needle crystals, soluble in hexane. The EIMS spectrum (**Figure 43**) of compound ET-S1 exhibited a molecular ion peak at *m/z* 468, consistent with a molecular formula of $C_{32}H_{52}O_2$. Intense mass fragment peaks at *m/z* 189, 191 and 218 were important in showing compound ET-S1 as having

a skeletal structure of the lupane-type triterpenoid (Budzikiewicz, Djerassi and Williams, 1964).

The IR spectrum (**Figure 42**) displayed a strong band at 1734 cm^{-1} indicating carbonyl group and a band at 1246 cm^{-1} representing C-O linkage. It could be concluded that this compound consisted of ester bond.

The ^{1}H NMR spectrum (**Figure 44**) of this compound exhibited characteristic resonances of exomethylene functional group as two one-proton singlets at δ 4.55 and 4.65. Eight methyl signals were also observed. Thirty-two carbon signals in its ^{13}C NMR spectrum (**Figures 45a-45b**) could be differentiated, with the aid of DEPT experiments (**Figure 46**), into those of 8 methyls, 11 methylenes, 6 methines and 7 quaternary carbons. The carbon signals at δ 150.9 (C-20) and 109.4 (C-30) represented disubstituted double bond of a lupane-type triterpenoid. The oxomethine C-3 resonated at δ 81.0, while the carbonyl and methyl resonances at δ 170.8 and 21.4, respectively, were those of the acetyl substituent at this position.

On the basis of the above evidence and by comparison with the literature, compound ET-S1 was identified as lupeol 3-acetate (Sholichin *et al*., 1980) (**Table 23**), which has previously been reported as a constituent of *E. tapos* bark (Chow and Quon, 1970). This triterpenoid was shown to significantly neutralize the damaging effects of *Daboia russellii* venom such as its lethality, haemorrhagic effect and edema. In addition, lupeol 3-acetate potentiated the protection by the antiserum against venom-induced lethality in male albino mice (Chatterjee, Chakravarty and Gomes, 2006). Gupta *et al*. (2005) revealed that this compound at 10 mg/rat/day caused significant reduction in the weight of reproductive organs, i.e. testes, epididymides, seminal vesicle and ventral prostate.

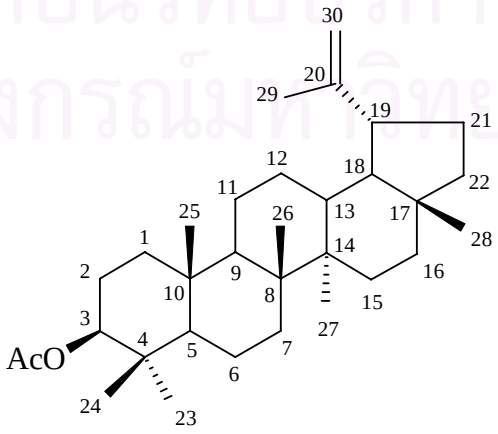

Lupeol acetate

Table 23. ^{13}C NMR spectral data of lupeol 3-acetate and compound ET-S1 (in $CDCl_3$, 75 MHz)

Position	Lupeol 3-acetate [a]	ET-S1	Position	Lupeol 3-acetate [a]	ET-S1
1	38.4	38.5	17	43.0	43.1
2	23.7	23.8	18	48.0	48.1
3	81.0	81.0	19	48.3	48.2
4	37.8	37.9	20	150.9	150.8
5	55.4	55.4	21	29.9	30.0
6	18.2	18.3	22	40.0	40.1
7	34.3	34.3	23	28.0	28.1
8	40.9	40.9	24	16.5	16.6
9	50.4	50.4	25	16.2	16.3
10	37.1	37.2	26	16.0	16.1
11	21.0	21.1	27	14.5	14.7
12	25.1	25.2	28	18.0	18.1
13	38.1	38.1	29	19.3	19.4
14	42.9	42.9	30	109.4	109.3
15	27.5	27.6	-CO-**CH_3**	21.3	21.4
16	35.6	35.7	-**CO**-CH_3	170.8	170.8

[a] Sholichin *et al*., 1980

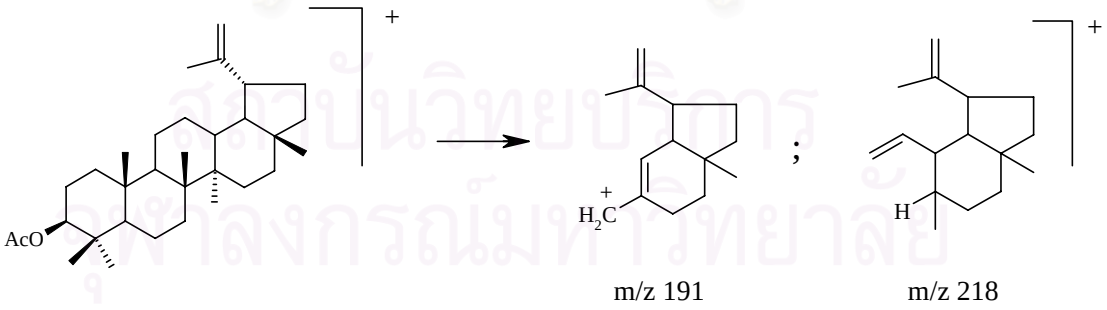

m/z 191 m/z 218

Principal EI mass fragments of lupeol acetate

2.2 Identification of Compound ET-S2 (3-Acetyl aleuritolic acid)

Compound ET-S2 was obtained as colorless needle crystals, soluble in $CHCl_3$. Its ESIMS data (**Figure 48**) showed a quasi-molecular ion $[M+Na]^+$ peak at *m/z* 521, indicating the molecular formula $C_{32}H_{50}O_4$. The IR spectrum (**Figure 47**) displayed

hydroxyl absorption bands at 3434 cm^{-1}, strong carbonyl bands at 1734 and 1688 cm^{-1} and a band at 1246 cm^{-1} representing C-O linkage, suggesting that the compound could consist of carboxylic acid function and ester bond.

The ^{1}H NMR spectrum of this compound (**Figure 49**) exhibited an olefinic proton signal at δ 5.51 (*d*, *J* = 4.8 Hz, H-15), an oxymethine signal at δ 4.44 (*t*, *J* = 8.4 Hz, H-3) and a methyl singlet of an acetyl group at δ 2.02 (-O-CO-C**H_3**). The ^{13}C NMR spectrum (**Figure 50**) and DEPT experiments (**Figure 51**) showed 32 carbon signals including those of 8 methyls, 10 methylenes, 5 methines and 9 quaternary carbons. The carbonyl carbon of a carboxylic acid function resonated at δ 183.7 (C-28), while an ester carbonyl resonated at δ 170.8 (3-O**CO**-CH_3). Two sp^2 carbons of a trisubstituted double bond between C-14 and C-15 gave peaks at δ 160.3 (C-14) and 116.7 (C-15). The oxygenated sp^3 carbon appeared as a peak at δ 80.9 (C-3). These spectral data and other physical properties were very similar to those reported for 3-acetyl aleuritolic acid (McLean *et al*., 1987), a taraxerane-type triterpenoid. Therefore, compound ET-S2 was identified as 3-acetyl aleuritolic acid.

Acetyl aleuritolic acid, isolated from the leaves and root bark of *Alchornea cordifolia*, was reported to have higher anti-inflammatory activity than indomethacin (Mavar-Manga *et al*., 2008). It also exhibited inhibitory activity against *Staphylococcus aureus* and *Salmonella typhimurium* at the minimum inhibitory concentration (MIC) of 0.1 mg/ml (Peres *et al*., 1997).

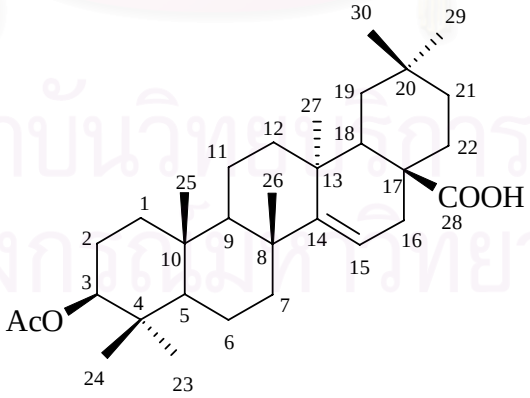

3-Acetyl aleuritolic acid

Table 24. ^{13}C NMR spectral data of 3-acetyl aleuritolic acid and compound ET-S2 (in $CDCl_3$, 75 MHz)

Position	3-Acetyl aleuritolic acid [a]	ET-S2	Position	3-Acetyl aleuritolic acid [a]	ET-S2
1	37.4	37.5	17	51.4	51.5
2	23.4	23.6	18	41.3	41.5
3	80.8	80.9	19	35.2	35.4
4	37.6	37.4	20	29.2	29.4
5	55.5	55.6	21	33.6	33.8
6	18.7	18.9	22	30.6	30.8
7	40.7	40.8	23	27.9	28.1
8	39.0	39.1	24	16.5	16.7
9	49.0	49.1	25	15.6	15.8
10	37.9	38.0	26	26.1	26.3
11	17.2	17.5	27	22.4	22.6
12	33.2	33.4	28	184.2	183.7
13	37.2	37.8	29	31.8	32.0
14	160.5	160.3	30	28.6	28.8
15	116.8	116.7	-**CO**CH_3	170.9	170.8
16	31.3	31.4	-CO**CH_3**	21.2	21.4

[a] McLean *et al*., 1987

2.3 Identification of Compound ET-S3 (Lupeol)

Compound ET-S3 was obtained as colorless needle crystals, soluble in hexane. Its IR spectrum (**Figure 52**) demonstrated an absorption band at 3323 cm^{-1} (O-H stretching), suggesting the presence of hydroxyl group. The EI mass spectrum (**Figure 53**) exhibited a molecular ion peak at *m/z* 426, equivalent to a molecular formula of $C_{30}H_{50}O$, and an $[M\text{-}CH_3]^+$ peak at *m/z* 411. Intense mass fragment peaks at *m/z* 189, 191 and 218 were suggestive of the lupane-type triterpenoid skeletal structure for compound ET-S3 (Budzikiewicz *et al.*, 1964).

The ^1H NMR spectrum (**Figure 54**) exhibited two characteristic singlet signals (at δ 4.55 and 4.65) of the exomethylene function between positions 20 and 30 of a lupane triterpene. Methyl singlets, similar to those of compound ET-S1, could be

observed. However, there were one less methyl group, and the ^{13}C NMR spectrum of compound ET-S3 (**Figure 55**) exhibited only 30 signals, including the olefinic C-20 (δ 150.8) and C-30 (δ 109.2) and the oxomethine C-3 at δ 79.0. The upfield shift of the latter signal and the absence of the acetyl signals helped in identifying this compound as the triterpenoid lupeol, previously isolated from *E. tapos* bark by Chow and Quon (1970). The NMR assignments were further confirmed by comparison with literature values (Sholichin *et al*., 1980) (**Table 25**).

Lupeol has been shown as possessing *in vitro* activity against *Plasmodium falciparum* (Alves *et al*., 1997), anticancer activity against HEp-2 (human larynx epithelial carcinoma) cell line (Badami *et al*., 2003), anti-inflammatory activity (Kuhl *et al.*, 1984) and inhibitory activity against DNA polymerase β (Chaturvedula *et al*., 2004). An abundant source of lupeol in nature might prove to be useful in the development of medicinal agents.

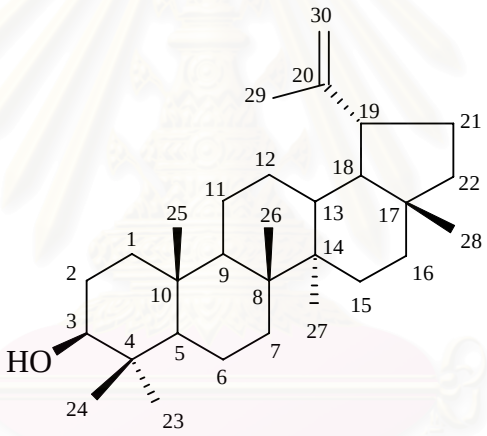

Lupeol

Table 25. ^{13}C NMR spectral data of lupeol and compound ET-S3 (in $CDCl_3$, 75 MHz)

Position	Lupeol [a]	ET-S3	Position	Lupeol [a]	ET-S3
1	38.7	38.8	16	35.6	35.7
2	27.5	27.5	17	43.0	43.1
3	79.0	79.0	18	48.0	48.1
4	38.9	39.0	19	48.3	48.4
5	55.3	55.4	20	150.9	150.8
6	18.3	18.5	21	29.9	30.0
7	34.3	34.4	22	40.0	40.1

Table 25. ^{13}C NMR spectral data of lupeol and compound ET-S3 (in $CDCl_3$, 75 MHz) (continued)

Position	Lupeol [a]	ET-S3	Position	Lupeol [a]	ET-S3
8	40.9	40.9	23	28.0	28.1
9	50.5	50.5	24	15.3	15.5
10	37.2	37.3	25	16.1	16.3
11	21.0	21.1	26	16.0	16.1
12	25.2	25.3	27	14.6	14.7
13	38.1	38.2	28	18.0	18.1
14	42.9	42.9	29	19.3	19.4
15	27.5	27.5	30	109.3	109.2

[a] Sholichin *et al*., 1980

2.4 Identification of Component ET-S4 (β-Sitosterol/stigmasterol Mixture)

Component ET-S4 was obtained as colorless needles, which gave a green color with Liebermann-Burchard test indicating steroid nucleus. The NMR data of compound ET-S4 were in full agreement with the published values of β-sitosterol and stigmasterol mixture. In the ^1H NMR spectrum, the olefinic signals at δ 4.99, 5.13 and 5.32 represented H-22 and H-23 of stigmasterol and H-6 of both β-sitosterol and stigmasterol, respectively. The integration value for H-6 was twice that of either H-22 or H-23 and, therefore, component ET-S4 was identified as a 1:1 mixture of β-sitosterol and stigmasterol, commonly found in numerous plants.

2.5 Identification of Compound ET-S5 (Germanicol palmitate)

Compound ET-S5 was obtained as a white powder. Its IR spectrum (**Figure 57**) exhibited major absorption bands at 2955, 2921, 2851 (C-H stretching), 1725 (C=O) and 1257 (C-O) cm^{-1}, suggestive of ester functional group.

The EI mass spectrum (**Figure 58**) exhibited a molecular ion peak at *m/z* 664 corresponding to the molecular formula $C_{46}H_{80}O_2$. Intense mass fragment peaks at *m/z* 177 and 189 were supportive of compound ET-S5 as being an olean-18-ene triterpenoid (Budzikiewicz *et al.*, 1963). The fragmentation pattern in the mass

spectra showed a loss of 239 mass unit, equivalent to a palmitate moiety, to give an ion peak of the triterpene alcohol at *m/z* 426 (Awasthi and Mitra, 1968).

In ^{1}H NMR spectrum (**Figure 59**), a triplet at δ 4.46 accounted for the 3α-oxymethine proton of the oleanane triterpene. The most downfield resonance was that of an olefinic proton which appeared as a singlet at δ 4.84 (H-18). A group of signals centered at δ 1.23 represented a number of methylene protons within the palmitate chain.

In the ^{13}C NMR spectrum (**Figure 60**), two olefinic carbons which resonated at δ 142.5 and 129.6 could be assigned to C-18 and C-19 of the olean-18-ene skeleton, respectively (Mahato and Kundu, 1994). The most downfield signal at δ 173.5 belongs to carbonyl carbon of the palmitate ester.

Comparison of these spectral data with the literature helped in identifying compound ET-S5 as germanicol palmitate (González *et al*., 1981), a triterpene ester previously isolated from the bark of *E. tapos* (Chow and Quon, 1970).

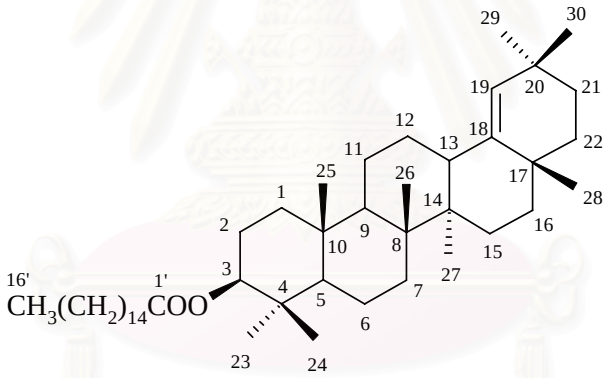

Germanicol palmitate

Table 26. ^{13}C NMR spectral data of germanicol and compound ET-S5 (in $CDCl_3$, 75 MHz)

Position	Germanicol [a]	ET-S5	Position	Germanicol [a]	ET-S5
1	38.5	38.0	19	129.8	129.6
2	27.4	26.3	20	32.3	32.0
3	79.0	80.6	21	33.4	33.4
4	39.0	38.5	22	37.4	37.5
5	55.7	55.6	23	28.0	28.1

Table 26. ^{13}C NMR spectral data of germanicol and compound ET-S5 (in $CDCl_3$, 75 MHz) (continued)

Position	Germanicol [a]	ET-S5	Position	Germanicol [a]	ET-S5
6	18.3	18.3	24	15.4	16.2
7	34.7	35.0	25	16.1	16.8
8	40.8	40.9	26	16.7	16.9
9	51.3	51.2	27	14.6	14.7
10	37.3	37.2	28	25.3	25.3
11	21.2	21.3	29	31.3	31.5
12	26.2	25.4	30	29.2	29.3
13	39.0	38.7	1′	-	173.5
14	43.4	43.4	2′	-	34.4
15	27.6	27.6	3′-13′	-	25.0-29.0
16	37.7	37.8	14′	-	32.5
17	34.4	34.6	15′	-	22.8
18	142.8	142.5	16′	-	14.3

[a] Mahato and Kundu, 1994

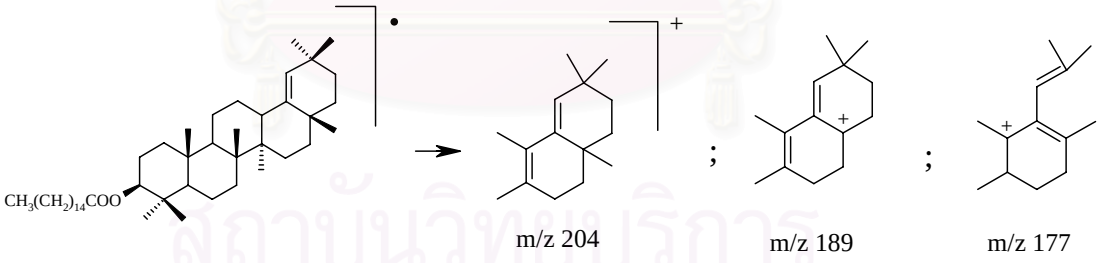

EI mass fragments of germanicol palmitate

2.6 Identification of Compound ET-S6 (Yucalexin B-22)

Compound ET-S6 was obtained as colorless needles. Its molecular formula was determined by TOF-ESIMS (**Figure 62**) as $C_{20}H_{30}O_3$, from its quasi-molecular ion $[M+Na]^+$ peak at *m/z* 341. The IR absorption bands (**Figure 61**) at 3397 and 1706 cm^{-1} indicated the presence of hydroxyl and keto carbonyl groups, respectively.

Its ^{1}H NMR spectrum (**Figure 63**) exhibited four methyl singlets at δ 0.82 (H-19 and H-20), 1.03 (H-18) and 1.07 (H-17). Two olefinic proton signals appeared as doublets at δ 5.60 (1H, *d*, *J* = 5.3 Hz, H-16) and 6.02 (1H, *d*, *J* = 5.3 Hz, H-15), while two adjacent oxymethine protons resonated at δ 3.63 (*m*, H-2) and 2.98 (*d*, *J* = 9.3 Hz, H-3). The large coupling constant between these two oxymethine protons indicated their *trans*-orientaton.

The ^{13}C NMR spectrum of compound ET-S6 (**Figure 64**) displayed twenty carbon signals, indicating its diterpenoid nature. These signals were classified by DEPT experiments (**Figure 65**) into those of one keto carbonyl (the most downfield signal at δ 211.5), four methyl groups (δ 15.4, 16.8, 17.3 and 28.7), five methylene carbons (δ 19.9, 36.2, 36.3, 44.5 and 58.3), six methine carbons (δ 54.6, 54.8, 68.5, 83.5, 136.2 and 139.1) and four quaternary carbons (δ 38.4, 39.3, 49.2 and 57.3). The presence of one disubstituted double bond was supported by the olefinic methine resonances at δ 139.1 (C-15) and 136.2 (C-16), while two oxymethine carbons resonated at δ 68.5 (C-2) and 83.5 (C-3). Since the calculated degree of unsaturation of this compound is six, of which two can be accounted for by a keto carbonyl and a double bond, its skeletal structure should be a tetracyclic diterpenoid.

The positions of different functional groups within the diterpenoid structure were confirmed by the HMBC experiment (**Figures 68a-68b**, **Table 27**). Cross peaks between both H-18 and H-19 and C-3, as well as between H-1 (at δ 0.90 and 1.70) and C-2, established the positions of two hydroxyl substituents at positions 2 and 3. The keto carbonyl could be located at C-12 according to HMBC correlations of both H-11 (δ 2.30, *dd*, *J* = 16.8, 6.5 Hz) and H-17 to this carbon signal. The H-17 methyl signal, through its long-range correlation with C-16, further helped in confirming the position of double bond between C-15 and C-16 on ring D of the *ent*-beyerane structure. The *trans*-orientation of the methine H-2 and H-3 was based on the coupling constant (9.3 Hz) between these protons.

Compound ET-S6 was therefore identified as *ent*-2α,3β-dihydroxybeyer-15-en-12-one or yucalexin B-22, by analysis of the above spectral data and comparison with published data (Sakai and Nakagawa, 1988). The diterpenoid has previously been isolated from the roots of cassava (*Manihot esculenta* Crantz) (Sakai and Nakagawa, 1988), also of the same family as *E. tapos*.

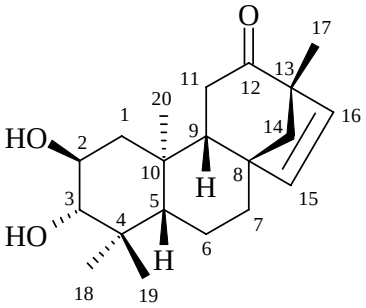

Yucalexin B-22

Table 27. ^{1}H (300 MHz) and ^{13}C (75 MHz) NMR spectral data of yucalexin B-22 and compound ET-S6 (in $CDCl_3$)

Position	Yucalexin B-22 [a]		ET-S6		
	^{1}H (mult., *J* in Hz)	^{13}C	^{1}H (mult., *J* in Hz)	^{13}C	HMBC
1	0.93 (*dd*, *J* =12.0, 12.0 Hz)	44.2	0.90 (*m*)	44.5	C-2
	1.82 (*dd*, *J* = 4.5 Hz)		1.70 (*m*)		C-2, C-3, C-10
2	3.65 (*dd*, *J* = 9.5, 3.5 Hz)	68.5	3.63 (*m*)	68.5	
3	3.00 (*d*, *J* = 4 Hz)	83.6	2.98 (*d*, *J* = 9.3 Hz)	83.5	C-2, C-18, C-19
4	-	39.2	-	39.3	
5	0.97 (*dd*)	54.6	0.97 (overlap)	54.6	
6		19.8	1.74 (overlap)	19.9	
			1.54 (overlap)		
7		36.1	1.86 (overlap)	36.2	C-8
			1.44 (overlap)		
8	-	49.2	-	49.2	
9	1.63 (*dd*, *J* = 10.5, 6.5 Hz)	54.8	1.61 (overlap)	54.8	C-10
10	-	54.6	-	38.4	
11	2.43 (*dd*, *J* = 17.0, 10.5 Hz)	36.2	2.41 (*dd*, *J* = 16.8, 10.7)	36.3	C-9, C-10
	2.30 (*dd*, *J* = 17.0, 10.5 Hz)		2.30 (*dd*, *J* = 16.8, 6.5 Hz)		C-8, C-9, C-12
12	-	211.8	-	211.5	
13	-	57.3	-	57.3	
14	1.62 (*d*, *J* = 11 Hz)	58.3	1.57 (overlap)	58.3	C-9
	1.91 (*d*, *J* = 11 Hz)		1.90 (overlap)		C-8, C-9
15	6.02 (*d*, *J* = 5.5 Hz)	139.3	6.02 (*d*, *J* = 5.3 Hz)	139.1	C-8, C-13, C-16
16	5.62 (*d*, *J* = 5.5 Hz)	136.4	5.60 (*d*, *J* = 5.3 Hz)	136.2	C-8, C-13, C-15

Table 27. ^{1}H (300 MHz) and ^{13}C (75 MHz) NMR spectral data of yucalexin B-22 and compound ET-S6 (in $CDCl_3$) (continued)

Position	Yucalexin B-22 [a]		ET-S6		
	^{1}H (mult., *J* in Hz)	^{13}C	^{1}H (mult., *J* in Hz)	^{13}C	HMBC
17	1.10 (*s*)	17.2	1.07 (*s*)	17.3	C-12, C-16
18	1.11 (*s*)	28.6	1.03 (*s*)	28.7	C-3
19	0.86 (*s*)	16.7	0.82 (*s*)	16.8	C-3, C-4, C-5, C-18
20	0.85 (*s*)	15.2	0.82 (*s*)	15.4	C-1, C-5, C-9, C-10
2-OH	2.05				
3-OH	2.19 (*d*, *J* = 4 Hz)				

[a] Sakai and Nakagawa, 1988

2.7 Identification of Compound ET-S7 (Yucalexin P-17)

Compound ET-S7 was obtained as colorless needles having a molecular formula of $C_{20}H_{30}O_3$ based on its $[M+H]^+$ peak at *m/z* 319 in the TOF-ESI mass spectrum (**Figure 70**). The IR spectrum (**Figure 69**) exhibited a carbonyl absorption band at 1701 cm^{-1} and O-H stretching band at 3459 cm^{-1}.

The ^{1}H NMR spectrum of compound ET-S7 (**Figure 71**) displayed four methyl singlets at δ 0.85 (H-19), 0.91 (H-20), 1.14 (H-17) and 1.18 (H-18). The olefinic proton signals at δ 5.85 (1H, *dd*, *J* = 17.6, 10.5 Hz, H-15), 5.18 (1H, *d*, *J* = 10.5 Hz, H-16*cis*) and 5.04 (1H, *d*, *J* = 17.6 Hz, H-16*trans*) indicated the exomethylene characteristic of the compound. Another olefinic proton singlet at δ 5.10 (H-14) was also observed. An oxymethine broad singlet resonated at δ 3.96 (H-3), while another oxymethine proton appeared as a doublet of doublets at δ 3.46 (*J* = 12.3, 4.2 Hz, H-12).

The ^{13}C NMR (**Figure 72**) and DEPT experiments (**Figure 73**) displayed twenty carbon resonances of the diterpenoid skeleton. These signals could be differentiated as belonging to four methyl groups (δ 15.0, 16.6, 24.9 and 29.2), five methylenes (δ 21.9, 28.4, 34.2, 50.9 and 117.0), six methines (δ 25.0, 52.9, 75.5, 82.5, 128.7 and 141.4) and five quaternary carbons including one keto carbonyl function (δ 43.9, 44.4, 45.6, 139.3 and 210.5). The presence of two double bonds was demonstrated from the carbon signals at δ 141.4 (C-15), 117.0 (C-16), 136.3 (C-8) and 128.7 (C-14). Two oxygenated methine carbons resonated at δ 82.5 (C-3) and

75.5 (C-12), respectively. The calculated six degrees of unsaturation (from the molecular formula of this compound) thus suggested it was a tricyclic diterpene.

The positions of different functional groups within the molecule were confirmed by HMBC experiment (**Figure 76**, **Table 28**). The keto carbonyl could be located at C-2 according to HMBC correlations of both H-1 and H-3 signals to this carbon resonance at δ 210.5. Cross peaks between the signals of both H-18 and H-19 and C-3, and of both H-11 and H-17 and C-12, established the positions of two hydroxyl substitutions at C-3 and C-12. The double bond between positions 8 and 14 was confirmed by long-range coupling between H-11 and C-8, H-14 and C-7, and between H-17 and C-14, while the exomethylene double bond between positions 15 and 16 was proven by cross peaks between H-12, H-14 and H-17 to C-15 and between both *cis* and *trans* H-16 to C-13 (δ 43.9).

By analysis of the above spectral data and comparison with previously reported data, compound ET-S7 was therefore identified as the pimarane diterpene yucalexin P-17 or *ent*-3β,12β-dihydroxypimara-8(14),15-dien-2-one (Sakai and Nakagawa, 1988), which has been reported as a stress metabolite from cassava roots, *Manihot esculenta* (Euphorbiaceae). The ^{13}C NMR assignments of this compound are reported herein for the first time.

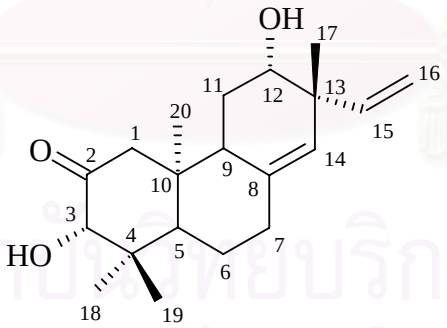

Yucalexin P-17

Table 28. ^{1}H (300 MHz) and ^{13}C (75 MHz) NMR spectral data of yucalexin P-17 and compound ET-S7 (in $CDCl_3$)

Position	Yucalexin P-17 [a]	ET-S7		
	^{1}H (mult., *J* in Hz)	^{13}C	^{1}H (mult., *J* in Hz)	HMBC
1	2.29 (*dd*, *J* = 13, 2 Hz)	50.09	2.25 (*d*, *J* = 13.0 Hz)	C-2, C-3, C-10, C-20
	2.43 (*d*, *J* = 13 Hz)		2.41 (*d*, *J* = 13.0 Hz)	C-2, C-3, C-6, C-9, C-10, C-20
2	-	210.5	-	-
3	3.96 (*dd*, *J* = 5, 2 Hz)	82.5	3.96 (*br s*)	C-2, C-4, C-18, C-19
3-OH	3.43 (*d*, *J* = 5 Hz)		-	
4	-	44.4	-	-
5	1.69 *dd*	52.9	1.69 (overlap)	C-3
6		21.9	1.45 (overlap)	
			1.75 (overlap)	
7		34.2	2.10 (overlap)	
			2.45 (overlap)	
8	-	136.3	-	-
9	2.23 (*dd*, *J* = 12,10 Hz)	52.0	2.20 (overlap)	
10	-	45.6	-	-
11	1.42 (*ddd*, *J* = 12, 10 Hz)	28.4	1.38 (overlap)	C-9, C-10, C-12
	1.61 (*ddd*, *J*= 12, 3.5 Hz)		1.58 (overlap)	C-8, C-9, C-10, C-12
12	3.46 (*ddd*, *J* = 12, 8, 3.5 Hz)	75.5	3.46 (*dd*, *J* = 12.3, 4.2 Hz)	C-15, C-17
12-OH	3.40 (*d*, *J* = 8 Hz)		-	-
13	-	43.9	-	-
14	5.13 *dd*	128.7	5.10 (*s*)	C-7, C-9, C-12, C-15
15	5.88 (*dd*, *J* = 17.5, 11 Hz)	141.4	5.85 (*dd*, *J* = 17.6, 10.5 Hz)	C-12, C-13, C-14, C-17
16	5.21 (*dd*, *J* = 11, 11 Hz)	117.0	5.18 (*d*, *J* = 10.5 Hz)	C-13
	5.07 (*dd*, *J* = 17.5, 11 Hz)		5.04 (*d*, *J* = 17.6 Hz)	C-13
17	1.17 (*s*)	24.9	1.14 (*s*)	C-12, C-14, C-15
18	1.21 (*s*)	29.2	1.18 (*s*)	C-3, C-19
19	0.71 (*s*)	16.6	0.85 (*s*)	C-3
20	0.79 (*s*)	15.0	0.91 (*s*)	C-5, C-9, C-10

[a] Sakai and Nakagawa, 1988

2.8 Identification of Compound ET-S8 (Scopoletin)

Compound ET-S8 was obtained as pale yellow crystals which showed fluorescent spot under UV light. Its IR spectrum (**Figure 78**) showed absorption bands of hydroxyl function at 3338 cm^{-1}, aromatic ring at 1435-1628 cm^{-1} and carbonyl function at 1704 cm^{-1}. The TOF-ESIMS spectrum (**Figure 79**) exhibited a quasi-molecular ion $[M+Na]^+$ peak at *m/z* 215, consistent with a molecular formula of $C_{10}H_8O_4$.

Its ^1H NMR spectrum (**Figure 80**) revealed a methoxyl singlet at δ 3.93. A pair of doublets at δ 6.25 and 7.58 (each 1H, J = 9.3 Hz) represented the *cis*-coupling H-3 and H-4, respectively, of the unsubstituted pyrone ring. This feature is characteristic of a coumarin nucleus (Steck and Mazurek, 1972). A pair of singlets at δ 6.83 and 6.90 corresponded to the *para*-positioned aromatic H-5 and H-8, respectively.

The ^{13}C spectrum (**Figure 81**) showed a lactone carbonyl peak at δ 161.2 (C-2), four methine carbons at δ 113.3 (C-3), 143.1 (C-4), 107.4 (C-5) and 103.1 (C-8), four quaternary carbons at 111.4 (C-5a), 143.8 (C-6), 150.1 (C-7) and 149.5 (C-8a) and one methoxyl carbon at δ 56.5. The deshielded aromatic carbon signal at δ 149.5 was presumably attached to oxygen and, therefore, was assigned to C-8a. All quaternary carbons of compound ET-S8 were assigned according to HMBC experiment (**Figure 84**). The lactone carbonyl C-2 was correlated to both H-3 and H-4, while C-6 was correlated to H-5 and H-9 singlets (δ 3.93). C-7 signal displayed an HMBC cross peak with H-5. The quaternary C-5a was long-range correlated to H-3 and H-8, while C-8a was correlated to both H-5 and H-8.

Compound ET-S8 was identified as scopoletin by analyses of these spectral data and comparison of its ^1H and ^{13}C NMR properties with previously published data (Lin, Yang and Chou, 2002).

Scopoletin is a coumarin previously isolated from several plants of the family Rutaceae e.g. from *Skimmia laureola* aerial parts (Razdan *et al*., 1987), *Eriostemon myoporoides* aerial parts (Sarker *et al*., 1994), *Clausena anisata* roots (Ojewole, 2002), *Zanthoxylum schinifolium* bark (Chang *et al*., 1997), *Pamburus missionnis* fruits (Kumar *et al*., 1994), *Murraya gleinei* leaves (Wickramaratne, Kumar and Balasubramaniam, 1984), *Aegle marmelos* roots (Shoeb, Kapil and Popli, 1973) and *Dictamus angustifolius* root bark (Wu *et al*., 1999). The coumarin was also widely

found in other plant families such as Compositae e.g. *Artemisia dracunculoides* above ground parts (Herz, Bhat and Santhanam, 1970), Leguminosae e.g. *Echinosophora koreensis* roots and stem (Iinuma *et al*., 1993), Apiaceae e.g. *Bupleurum fruticosum* roots (Pistelli *et al*., 1996), Oleaceae e.g. *Olea africana* bark (Tsukamoto *et al*., 1984), Rubiaceae e.g. *Xeromphis obovata* root bark (Sibanda *et al*., 1989), Nyssaceae e.g. *Nyssa sylvatica* wood (Li, Elsohly and Clark, 2000), Meliaceae e.g. *Guarea rhophalocarpa* leaves (Camacho *et al*., 2001) and *Aglaia crassinervia* bark (Su *et al*., 2006), Dipterocarpaceae e.g. *Dipterocarpus hasseltii* bark (Muhtadi *et al*., 2006) and Vahliaceae e.g. *Vahlia capensis* aerial parts (Majinda *et al*., 1995).

Scopoletin has been shown to possess hepatoprotective and antioxidant activities (Kang *et al*., 1998; Shaw *et al*., 2003). Antiproliferative action was also demonstrated on some tumoral cells, inducing apoptosis on PC3 cells (human androgen-independent prostate adenocarcinoma) (Liu *et al*., 2001). It exhibited antitumor activity on P-388 lymphocytic leukemia (Cassady *et al*., 1979). The coumarin suppressed acetylcholine-induced contractures of toad rectus abdominis muscle (Ojewoleand and Adesina, 1983). Kang *et al*. (1999) showed that scopoletin inhibited nitric oxide synthesis in dose-dependent manner in murine macrophage-like RAW 264.7 cell stimulated with interferon-γ plus lipo-polysaccharide. Immunomodulatory effects were reported for noni (*Morinda citrifolia*), a medicinal plant rich in scopoletin, which was found to enhance the host immune system involving macrophages and lymphocytes (Hirazumi *et al*., 1994).

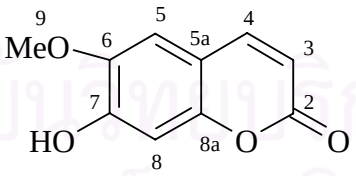

Scopoletin

Table 29. ^{1}H (300 MHz) and ^{13}C (75 MHz) NMR spectral data of scopoletin and compound ET-S8 (in $CDCl_3$)

Position	Scopoletin [a]		ET-S8		
	^{1}H	^{13}C	^{1}H	^{13}C	HMBC
2	-	164.0	-	161.2	
3	6.18 (*d*, *J* = 9.5 Hz)	112.6	6.25 (*d*, *J* = 9.3 Hz)	113.3	C-2, C-5a
4	7.83 (*d*, *J* = 9.5 Hz)	146.1	7.58 (*d*, *J* = 9.3 Hz)	143.1	C-2, C-5, C-8a
5	7.09 (*s*)	110.0	6.83 (*s*)	107.4	C-4, C-6, C-7, C-8a
5a	-	112.6	-	111.4	
6	-	147.1	-	143.8	
7	-	152.9	-	150.1	
8	6.75 (*s*)	104.0	6.90 (*s*)	103.1	C-4, C-5a, C-8a
8a	-	151.4	-	149.5	
9	3.90 (*s*)	56.8	3.93 (*s*)	56.5	C-6

[a] Lin, Yang and Chou, 2002

2.9 Structure Elucidation of Compound ET-S11 (2,3-*Seco*-sonderianol)

The molecular formula of compound ET-S11, $C_{20}H_{26}O_5$, was assigned according to its $[M+Na]^+$ peak at *m/z* 369.1680 in the high resolution ESIMS (**Figure 87**). Its IR spectrum (**Figure 86**) exhibited a strong carbonyl absorption band at 1698 cm^{-1} and O-H stretching band at 3430 cm^{-1}. A band at 927 cm^{-1} could be attributed to the out-of-plane C-H vibration of pentasubstituted aromatic ring.

Its ^{1}H NMR spectrum (**Figure 88**) displayed a broad singlet at δ 8.87 assignable to a phenolic hydroxyl group (12-OH) and a singlet of an aromatic proton located *ortho* to that moiety at δ 6.67 (H-11). Three sets of signals appearing at δ 6.55 (1H, *dd*, *J* = 11.4, 18.0 Hz, H-15), 5.48 (1H, d, *J* = 11.4 Hz, H-16a) and 5.09 (1H, d, *J* = 18.0 Hz, H-16b) were characteristic of an AMX terminal vinyl system. Four methyl singlets were observed, including those of an aromatic methyl at δ 2.01 (H-17), a tertiary methyl at δ 1.38 (H-20), and two geminal methyls at δ 1.11 (H-18) and δ 0.81 (H-19). An AB system at δ 2.56 and 2.33 (each 1H, *d*, *J* = 14.6 Hz, H-1a and H-1b) assignable to the H-1 methylene protons of a 2,3-*seco*-diacid terpenoid was also detected.

The ^{13}C NMR spectrum (**Figure 89**), in combination with DEPT experiments (**Figure 90**), showed the presence of four methyl, four methylene, three methine (1

sp^3 and 2 sp^2) and nine quaternary carbons (2 sp^3 and 7 sp^2, including 2 carbonyls). These data indicated that compound ET-S11 was a cleistanthane diterpene very similar to sonderianol, a diterpene isolated from *Croton sonderianus* (Craveiro and Silveira, 1982), with the only difference being the C-2/C-3 cleavage of its ring A, producing a 2,3-diacid.

HMBC correlations (**Figures 93a-93d**, **Table 30**) of the methylene H-1 to C-2 carbonyl (δ 171.8) and of H-18 and H-19 methyl protons to C-3 carbonyl (δ 180.6) confirmed the bond fission of ring A. The position of the hydroxyl group at C-12 was supported by HMBC cross peaks of the hydroxyl proton at δ 8.87 to C-11 (δ 110.1), C-12 (δ 153.1), and C-13 (δ 119.1). Correlations of both H_3-17 and H_2-16 to C-14 (δ 137.7), and of H-15 to C-8 (δ 124.0) confirmed the position of the double bond in the terminal vinyl between positions 15 and 16.

The NMR assignments of compound ET-S11 were compared with those of sonderianol (Craveiro and Silveira, 1982) and a 2,3-*seco* ring A diterpenoid (Tsichritzis and Jakupovic, 1990). Its relative stereochemistry was assumed to be the same as those of sonderianol and other diterpenes isolated from this plant. The structure of compound ET-S11 was therefore elucidated as *ent*-12-hydroxy-2,3-*seco*-8,11,13,15-cleistanthatetraen-2,3-dioic acid and named 2,3-*seco*-sonderianol.

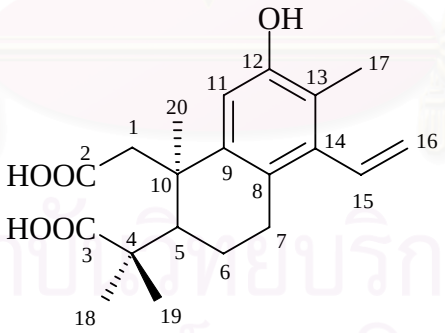

2,3-*Seco*-sonderianol

Table 30. ^{1}H (300 MHz) and ^{13}C (75 MHz) NMR assignments of compound ET-S11 (in DMSO-d_6)

Position	^{13}C	^{1}H (mult., *J* in Hz)	HMBC
1	49.5	2.56 (*d*, *J* = 14.6 Hz)	C-2, C-5, C-6, C-9, C-10
		2.33 (*d*, *J* = 14.6 Hz)	C-2, C-5, C-10
2	171.8	-	-
3	180.6	-	-
4	44.8	-	-
5	42.9	2.71 (*br s*)	C-4, C-6, C-10, C-19
6	20.8	2.01 (overlap)	C-4
		1.77 (*m*)	C-10
7	25.8	2.56 (overlap)	C-5, C-6
8	124.0	-	-
9	142.3	-	-
10	40.7	-	-
11	110.1	6.67 (*s*)	C-8, C-10, C-12, C-13
12	153.1	-	-
13	119.1	-	-
14	137.7	-	-
15	135.7	6.57 (*dd*, *J* = 18.0, 11.4 Hz)	C-8, C-13, C-14, C-16
16	118.9	5.48 (*d*, *J* =11.4 Hz)	C-14
		5.09 (*d*, *J* = 18.0 Hz)	C-14, C-15
17	13.2	2.01 (*s*)	C-12, C-13, C-14
18	27.8	1.11 (*s*)	C-3, C-4, C-5, C-19
19	22.6	0.81 (*s*)	C-3, C-4, C-5, C-18
20	24.3	1.38 (*s*)	C-1, C-5, C-9, C-10
12-OH	-	8.87 (*s*)	C-11, C-12, C-13

2.10 Identification of Compound ET-S12 (Yucalexin P-15)

Compound ET-S12 was obtained as yellow oil. Its molecular formula was determined by TOF-ESI MS as $C_{20}H_{26}O_4$ on the basis of the $[M+H]^+$ peak observed at *m/z* 331 (**Figure 96**). The number of carbon atoms indicated that the compound was a diterpenoid. Its IR spectrum (**Figure 95**) exhibited prominent carbonyl absorption bands at 1718 and 1667 cm^{-1}, and O-H stretching band at 3446 cm^{-1}.

Its ^{1}H NMR spectrum (**Figure 97**) showed four methyl singlets at δ 0.80 (H-19), 1.07 (H-17), 1.19 (H-20) and 1.19 (H-18) which correlated to the carbon signals at δ 16.4, 21.4, 21.4 and 28.1, respectively. The vinylic exomethylene group was represented by olefinic proton signals at δ 6.24 (1H, *dd*, *J* = 18.0, 11.1 Hz, H-15),

5.26 (1H, *d*, *J* = 18.0 Hz, H-16*trans*) and 5.35 (1H, *d*, *J* = 11.1 Hz, H-16*cis*). An olefinic proton appeared as a multiplet at δ 6.40 (H-7), whereas an olefinic singlet could also be observed at δ 5.61 (H-11). Two oxymethine protons resonated as singlets at δ 4.24 (H-14) and 3.95 (H-3).

The ^{13}C NMR spectrum of compound ET-S12 (**Figure 98**) exhibited twenty carbon signals, including those of four methyls (δ 16.4, 21.4, 21.4 and 28.1), three methylenes (δ 24.5, 48.8 and 116.6), six methines (δ 46.6, 78.7, 82.0, 116.4, 134.0 and 137.3), five quaternary carbons (δ 43.0, 44.9, 53.9, 132.1 and 159.1), and two keto carbonyls (δ 200.9 and 208.9). The vinylic double bond gave peaks at δ 137.3 (C-15) and 116.6 (C-16), while two trisubstituted double bonds were represented by carbon signals at δ 134.0 (C-7)/ 132.1 (C-8) and at δ 159.1 (C-9)/ 116.4 (C-11), respectively. Therefore, according to the calculated degree of unsaturation from its molecular formula and these spectral data, compound ET-S12 was a tricyclic diterpene with two carbonyls and three double bonds.

HMBC correlations (**Figure 102**, **Table 31**) from the signals of H-1, H-18 and H-19 to C-3, and from H-14 signal to C-7, C-8, C-9, C-12, C-13 and C-15 established the positions of 3-OH and 14-OH. Two keto carbonyls were located at C-2 (δ 208.9) and C-12 (δ 200.9) according to HMBC correlations of both H-1 and H-3 to C-2 and of H-14 to C-12. The positions of conjugated double bonds at C-7/C-8 and C-9/C-11 could be confirmed by the long-range coupling between H-14 to C-7 and C-8, and between H-11 to C-8. The position of terminal vinyl system at position 13 was likewise confirmed by cross peaks from H-16 signal to C-15 and C-13 signals. This skeletal structure is typical of pimarane-type diterpenoids.

Analysis of these NMR data of compound ET-S12 and comparison with the literature (Sakai and Nakagawa, 1988) led to its identification as *ent*-3β,14α-dihydroxypimara-7,9(11),15-triene-2,12-dione or yucalexin P-15.

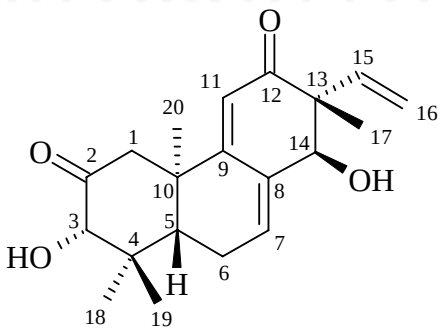

Yucalexin P-15

Table 31. ^{1}H (300 MHz) and ^{13}C (75 MHz) NMR spectral data of yucalexin P-15 and compound ET-S12 (in $CDCl_3$)

Position	Yucalexin P-15 [a]		ET-S12		
	^{13}C	^{1}H (mult., *J* in Hz)	^{13}C	^{1}H (mult., *J* in Hz)	HMBC
1	48.9	2.66 (*dd*, *J* = 12, 1 Hz)	48.8	2.62 (*d*, *J* = 12.6 Hz)	C-2, C-3, C-5, C-10, C-18
		2.71 (*d*, *J* = 12 Hz)		2.72 (*d*, *J* = 12.9 Hz)	C-2, C-3, C-5, C-10, C-18
2	209.3	-	208.9	-	-
3	82.1	3.99 (*dd*, *J* = 5, 1 Hz)	82.0	3.95 (*s*)	C-2, C-4, C-18, C-19
3-OH		3.43 (*d*, *J* = 5 Hz)		-	-
4	45.1	-	44.9	-	-
5	47.1	2.09 (*dd*)	46.6	2.00 (*dd*, *J* = 11.2, 4.7 Hz)	C-4, C-6, C-10, C-18, C-20
6	24.4		24.5	2.34 (*m*)	
				2.53 (*dt*, *J* = 19.5, 5.1 Hz)	
7	116.8		134.0	6.40 (*m*)	C-5, C-13
8	131.0	-	132.1	-	
9	161.7	-	159.1	-	
10	43.2	-	43.0	-	
11	131.6	5.64	116.4	5.61 (*s*)	C-8, C-10
12		-	200.9	-	
13	55.6	-	53.9	-	
14	73.1	4.35 (*m*)	78.7	4.24 (*s*)	C-7, C-8, C-9, C-12, C-13, C-15
14-OH		1.88 (*d*, *J* = 3 Hz)			
15	138.7	5.93 (*dd*, *J* = 17.5, 11 Hz)	137.3	6.24 (*dd*, *J* = 18.0, 11.1 Hz)	C-12
16	118.3	5.47 (*dd*, *J* = 11, 1 Hz)	116.6	5.26 (*d*, *J* = 18.0 Hz)	C-13, C-15
		5.31 (*dd*, *J* = 17.5, 1 Hz)		5.35 (*d*, *J* = 11.1 Hz)	C-13
17	21.2	1.16 (*s*)	21.4	1.07 (*s*)	-
18	28.0	1.23 (*s*)	28.1	1.19 (*s*)	C-3
19	16.3	0.84 (*s*)	16.4	0.80 (*s*)	C-3, C-4, C-5, C-18
20	14.1	1.07 (*s*)	21.3	1.19 (*s*)	C-5, C-10

[a] Sakai and Nakagawa, 1988

2.11 Identification of Compound ET-S14 (Oleic acid)

Compound ET-S14 was obtained as white plates having the molecular formula of $C_{18}H_{34}O_2$, on the basis of its $[M]^+$ peaks at *m/z* 282 in the EI mass spectrum (**Figure 104**). Its IR spectrum (**Figure 103**) exhibited absorption bands of aliphatic C-H at 2918 and 2850 cm^{-1}, and carboxylic acid at 1705 cm^{-1}.

The ^1H NMR spectrum (**Figure 105**) displayed a broad triplet of a methyl group at the end of an aliphatic chain at δ 0.86 (*J* = 6.6 Hz, H-18) which coupled to a methylene signal at δ 1.61 (*m*, H-17). The methylene proton next to a carbonyl group resonated at δ 2.33 (*t*, *J* = 7.5 Hz, H-2), while other aliphatic methylene protons appeared as broad singlet at δ 1.24 (H-4-H-7 and H-11-H-15). The most downfield signal in its ^{13}C NMR spectrum (**Figure 106**) at δ 179.4 ppm belongs to that of the carboxylic carbonyl (C-1). Two olefinic signals at δ 129.6 and 129.9 represented C-9 and C-10, respectively, of the *cis*-double bond. Other signals between δ 29.2-29.9 were those of the methylene C-4 - C-7 and C11 - C-15. Comparison of these data with literature (Kalinowski and Braun, 1988) identified compound ET-S14 as the unsaturated fatty acid, oleic acid.

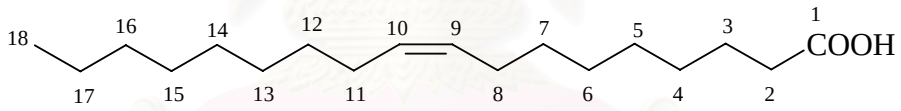

Oleic acid

Table 32. ^{13}C NMR Spectral data of oleic acid and compound ET-S14 (in $CDCl_3$, 75 MHz)

Position	Oleic acid [a]	ET-S14
1	180.1	179.4
2	34.3	34.1
3	25.0	24.8
4	29.3	29.2-29.9
5	29.3	
6	29.3	
7	29.9	
8	27.5	27.3

Table 32. ^{13}C NMR Spectral data of oleic acid and compound ET-S14 (in $CDCl_3$, 75 MHz) (continued)

Position	Oleic acid [a]	ET-S14
9	129.8	129.6
10	130.1	129.9
11	29.5	29.2-29.9
12	29.9	
13	29.6	
14	29.8	
15	29.6	
16	32.3	32.0
17	22.9	22.8
18	14.2	14.2

[a] Kalinowski and Braun, 1988

2.12 Identification of Compound ET-S15

Compound ET-S15 was obtained as colorless needles, which displayed $[M+Na]^+$ peak in its TOF-ESI mass spectrum (**Figure 108**) at *m/z* 205, equivalent to a molecular formula of $C_9H_{10}O_4$. The IR spectrum (**Figure 107**) showed hydroxyl absorption band at 3346 cm^{-1} and α,β-unsaturated carbonyl absorption at 1675 cm^{-1}

The ^1H NMR spectrum (**Figure 109**) showed an aldehydic proton signal at δ 9.80 (*s*). It displayed a singlet signal for two equivalent aromatic protons at δ 7.14 (H-2 and H-6), indicating its symmetrical, tetra-substituted structure. A methoxy singlet at δ 3.96 also represented two symmetrical methoxy groups, which resonated at δ 56.5 (3-OMe and 5-OMe) in the ^{13}C NMR spectrum (**Figure 110**). The carbon spectrum, in combination with DEPT experiments (**Figure 111**), also showed two methine carbon resonances at δ 106.7 (C-2 and C-6), three quaternary carbon resonances at δ 128.5 (C-1), 140.8 (C-3 and C-5) and 147.4 (C-4), and an aldehyde carbonyl peak at δ 190.7.

Therefore, compound ET-S15 was identified as 3,5-dimethoxy-4-hydroxy benzaldehyde or syringaldehyde (Borges-Del-Castillo *et al*., 1983).

Syringaldehyde is a common plant secondary metabolite. The compound has previously been isolated from plants such as *Bulbophyllum odoratissimum* (Orchidaceae) (Chen *et al*., 2008), *Populus lasiocarpa* (Salicaceae) (Greenaway, Scaysbrook and Whatley, 1988), *Rhamnus pubescens* (Rhamnaceae) (Sharp *et al*., 2001) and *Ambrosia cumanensis* (Compositae) (Borges-Del-Castillo *et al*., 1983).

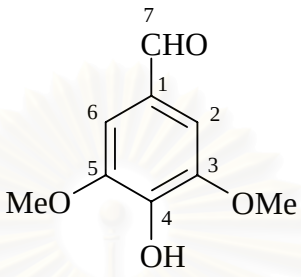

Syringaldehyde

Table 33. ^{1}H NMR spectral data of syringaldehyde and compound ET-S15 (in $CDCl_3$, 300 MHz)

Position	Syringaldehyde [a]	ET-S15		
	^{1}H (mult.)	^{1}H (mult.)	^{13}C	HMBC
1	-	-	128.5	-
2, 6	7.10 (s)	7.14 (*s*)	106.7	C-3, C-4, CHO
3, 5	-	-	140.8	-
3-OMe	3.90 (*s*)	3.96 (*s*)	56.5	C-3
5-OMe	3.90 (*s*)	3.96 (*s*)	56.5	C-5
4	-	-	147.4	-
4-OH	6.55 (*br s*)	6.03 (*s*)	-	C-3, C-4
CHO	9.80 (*s*)	9.80 (*s*)	190.7	C-2, C-6

[a] Borges-Del-Castillo *et al*., 1983

2.13 Identification of Compound ET-S17 (Amentoflavone)

The yellow compound ET-S17 gave orange-red color with Shinoda's test. Its TOF-ESI mass spectrum (**Figure 117**) exhibited the $[M-H]^+$ peak at *m/z* 537, consistent with a molecular formula of $C_{30}H_{18}O_{10}$. This was supported by thirty carbon signals in its ^{13}C NMR spectrum (**Figure 119**), mostly in aromatic region. These properties, especially the number of carbon atoms, indicated compound ET-S17

to be a biflavonoid. The IR spectrum (**Figure 116**) showed signals for hydroxyl group at 3434 cm^{-1} and conjugated carbonyl at 1645 cm^{-1}. The UV spectrum (**Figure 115**) showed absorption maxima at 334, 271 and 215 nm, identical to those of the flavone apigenin, suggesting that the compound was built up of two apigenin units (Garg and Mitra, 1971).

The ^{1}H NMR spectrum (**Figure 118**) showed 12 aromatic proton resonances and two hydrogen-bonded hydroxyl signals at δ 12.99 (5-OH) and 13.15 (5″-OH). Both H-3 and H-3″ of each flavone unit resonated as singlets at δ 6.70 and 6.63, respectively. The signals at δ 6.21 (1H, *br s*) and 6.48 (1H, *br s*) could be assigned to the *meta*-coupled H-6 and H-8, respectively, while another singlet at δ 6.41 was assigned to H-6″, suggesting that the linkage was at C-8″. A proton system of one ring B consists of a two-proton doublet which appeared at δ 7.64 (H-2‴ and H-6‴) and *ortho*-coupled (J = 8.6 Hz) to another two-proton doublet at δ 6.80 (H-3‴ and H-5‴). Another ring B proton system consists of a doublet at δ 7.21 (J = 8.7 Hz, H-5′) which *ortho*-coupled to a doublet of doublets at δ 8.00 (J = 8.7, 2.4 Hz, H-6′) which, in turn, *meta*-coupled to a doublet at δ 8.10 (J = 2.4 Hz, H-2′). Therefore, the linkage of two apigenin units of compound ET-S17 appeared to be between C-3′ and C-8″.

From the above spectral data and by comparison with literature values, compound ET-S17 was identified as the biflavonoid amentoflavone (Markham, Sheppard and Geiger, 1987). This compound has been found from the leaves of *Ginkgo biloba* (Ginkgoaceae) (Bedir *et al*., 2002) and *Podocarpus taxifolia* (Podocarpaceae) (Hameed, *et al*. 1973), and from the leaves and twigs of *Celaennodendron maxicanum* (Euphorbiaceae) (Castaneda *et al*., 1992). This biflavonoid has been reported to have inhibitory effect on phospholipase A2 activity. It inhibited the enzyme cyclooxygenase from guinea-pig epidermis without affecting lipoxygenase (Kim *et al*., 1998). The compound also inhibited phospholipase Cy1 (Lee *et al*., 1996), DNA topoisomerase (Grynberg *et al*., 2002) and the production of aflatoxin by *Aspergillus flavus* (Gonçalez, Felicio and Pinto, 2001).

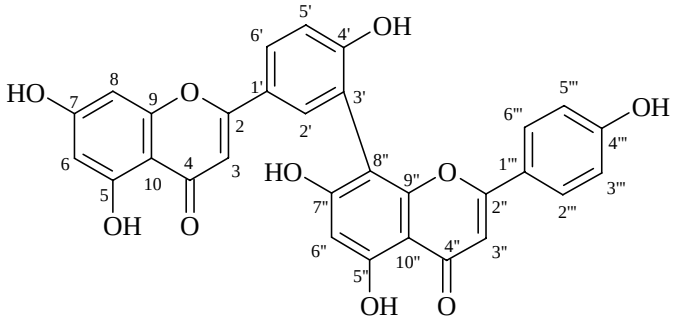

Amentoflavone

Table 34. ^{1}H (300 MHz) and ^{13}C (75 MHz) NMR spectral data of amentoflavone and compound ET-S17 (in acetone-d_6)

Position	Amentoflavone [a]	ET-S17	
	^{13}C	^{1}H (mult., *J* in Hz)	^{13}C
2	164.1	-	165.0
3	103.2	6.70 (*s*)	103.8
4	181.9	-	183.1
5	161.6	-	163.1
5-OH	-	12.99 (*s*)	-
6	98.8	6.21 (*br s*)	99.7
7	163.9	-	164.9
8	94.2	6.48 (*br s*)	94.8
9	157.6	-	159.0
10	104.0	-	105.4
1′	120.3	-	123.3
2′	127.9	8.10 (*d*, *J* = 2.4 Hz)	132.6
3′	121.7	-	121.1
4′	159.6	-	161.8
5′	116.4	7.21 (*d*, *J* = 8.7 Hz)	117.6
6′	131.6	8.00 (*dd*, *J* = 8.7, 2.4 Hz)	128.7
2″	164.3	-	165.1
3″	102.8	6.63 (*s*)	103.8
4″	182.2	-	183.5
5″	160.8	-	160.6
5″-OH	-	13.15 (*s*)	-
6″	99.1	6.41 (*s*)	99.9
7″	161.9	-	163.4
8″	104.1	-	104.3
9″	154.7	-	156.0
10″	104.0	-	105.4
1‴	121.4	-	123.2
2‴, 6‴	128.3	7.64 (*d*, *J* = 8.6 Hz)	129.1
3‴, 5‴	116.0	6.80 (*d*, *J* = 8.6 Hz)	116.7
4‴	161.1	-	162.8

[a] Markham, Sheppard and Geiger, 1987

2.14 Identification of Compound ET-F6 (Putraflavone)

ET-F6 was another yellow compound which gave an orange-red color with Shinoda's test. Its TOF-ESI mass spectrum (**Figure 125**) exhibited $[M+H]^+$ peak at *m/z* 567 consistent with a molecular formula of $C_{32}H_{22}O_{10}$. The IR spectrum (**Figure 124**) showed hydroxyl band at 3407 cm^{-1} and carbonyl bands at 1663 and 1655 cm^{-1}, whereas its UV spectrum (**Figure 123**) showed absorption maxima identical to those of amentoflavone, suggesting compound ET-F6 to be a derivative of amentoflavone.

The ^1H NMR spectrum (**Figure 126**) showed similar resonance pattern to that of amentoflavone, with the additional presence of two methoxy signals at 3.81 (7-OMe) and 3.74 (4‴-OMe). This was supported by two methoxy carbon signals which resonated in the ^{13}C NMR spectrum (**Figure 127**) at δ 56.1 and 55.6, respectively.

The doublet at δ 6.34 was assigned to H-6 of ring A which *meta*-coupled (*J* = 1.8 Hz) with H-8 signal at δ 6.75. The signals at 8.02 (*br s*), 7.14 (*d, J* = 9.3 Hz) and 8.05 (*d, J* = 9.3 Hz) were assigned to H-2′, H-5′ and H-6′of ring B, respectively. The 1,4-disubstituted ring B′ was represented by the signal at δ 7.67 (2H, *d, J* = 8.7 Hz, H-2‴ and H-6‴) which *ortho*-coupled to the signal at δ 6.92 (2H, *d, J* = 8.7 Hz, H-3‴ and H-5‴). The olefinic H-3 resonated at δ 6.90 (s), while H-3″ gave a singlet at δ 6.89. Another singlet at δ 6.39 could be assigned to H-6″. HMBC spectrum (**Figures 131a-131d**) showed long-range correlation between H-2′ and C-8″ (δ 104.2), confirming the linkage between C-3′ of ring B and C-8″ of ring A′ identical to amentoflavone.

The carbon chemical shifts of C-6 (δ 98.1), C-8 (δ 92.7), C-3‴ (δ 114.6) and C-5‴ (δ 114.6) were upfield of those same positions in amentoflavone and may be attributed to the 7-OH and 4‴-OH being methylated. HMBC correlations between C-7 signal and 7-OMe proton signal at δ 3.81 and between C-4‴ and 4‴-OMe signal at δ 3.74 confirmed these assignments. From these data and through comparison with published report (Suárez *et al*, 2003), compound ET-F6 was identified as putraflavone (7,4‴-dimethyl amentoflavone).

Putraflavone was first isolated from the trunk bark and leaves of *Putranjiva roxburghii* of the family Euphorbiaceae (Garg and Mitra, 1971), and later found in the aerial parts of *Podocalyx loranthoides* of the same family (Suárez *et al*., 2003). This

biflavonoid was moderately active against *Leishmania mexicana* promastigotes (Suárez *et al*., 2003).

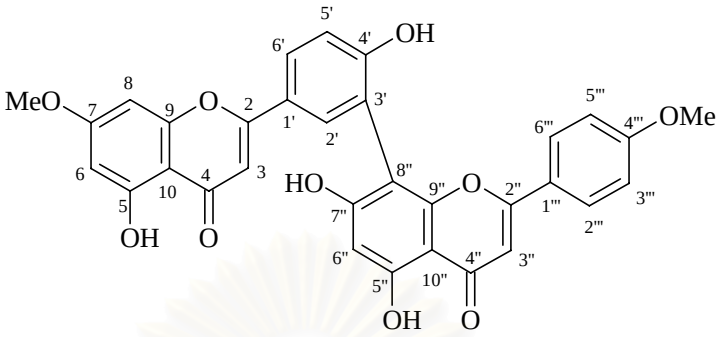

Putraflavone

Table 35. ^{1}H (300 MHz) and ^{13}C (75 MHz) NMR spectral data of putraflavone and compound ET-F6 (in DMSO-d_6)

Position	Putraflavone [a]		ET-F6		
	^{1}H (mult., *J* in Hz)	^{13}C	^{1}H (mult., *J* in Hz)	^{13}C	HMBC
2	-	164.3	-	164.2	
3	6.87 (*s*)	103.5	6.90 (*s*)	103.3	C-1′, C-2, C-4, C-10
4	-	182.3	-	182.0	
5	-	161.1	-	161.2	
5-OH	12.95 (*s*)		12.95 (*s*)	-	C-5, C-6, C-10
6	6.35 (*d*, *J* = 1.8 Hz)	98.3	6.34 (*d*, *J* = 1.8 Hz)	98.1	C-5, C-7, C-8, C-10
7		165.3	-	165.2	
7-OMe	3.82 (*s*)	56.3	3.81 (*s*)	56.1	C-7
8	6.75 (*d*, *J* = 1.8 Hz)	93.0	6.75 (*d*, *J* = 1.8 Hz)	92.7	C-6, C-7, C-9, C-10
9	-	157.6	-	157.4	
10	-	104.9	-	104.8	
1′	-	121.2	-	120.8	
2′	7.96 (*br d*)	128.2	8.02 (*br s*)	128.0	C-8′′
3′	-	120.2	-	120.2	
4′	-	159.8	-	160.0	
5′	7.18 (*d*, *J* = 9.0 Hz)	116.4	7.14 (*d*, *J* = 9.3 Hz)	116.4	C-1′, C-3′
6′	8.04 (*br dd*)	131.6	8.05 (*d*, *J* = 9.3 Hz)	131.5	C-2′
2′′		163.4	-	163.2	
3′′	6.89 (*s*)	103.5	6.89 (*s*)	103.2	C-10, C-2′′, C-4′′, C-1′′′

Table 35. ^{1}H (300 MHz) and ^{13}C (75 MHz) NMR spectral data of putraflavone and compound ET-F6 (in DMSO-d_6) (continued)

Position	Putraflavone [a]		ET-F6		
	^{1}H (mult., *J* in Hz)	^{13}C	^{1}H (mult., *J* in Hz)	^{13}C	HMBC
4″	-	182.1	-	182.8	
5″	-	160.5	-	160.6	
5″-OH	13.07 (*s*)	-	13.05 (*s*)	-	C-5″, C-6″, C-10″
6″	6.45 (*s*)	98.8	6.39 (*s*)	98.9	C-5″, C-7″, C-8″, C-10″, C-4″
7″	-	162.1	-	162.5	
8″	-	104.3	-	104.2	
9″	-	154.8	-	154.6	
10″	-	104.0	-	103.7	
1‴	-	123.2	-	123.0	
2‴	7.66 (*d*, *J* = 8.7 Hz)	128.2	7.67 (*d*, *J* = 8.7 Hz)	128.0	C-2″, -4‴
3‴	6.93 (*d*, *J* = 8.7 Hz)	114.8	6.92 (*d*, *J* = 8.7 Hz)	114.6	C-1‴
4‴	-	162.5	-	162.3	
4‴-OMe	3.76 (*s*)	55.7	3.74 (*s*)	55.6	C-4‴
5‴	6.93 (*d*, *J* = 8.7 Hz)	114.8	6.92 (*d*, *J* = 8.7 Hz)	114.6	
6‴	7.66 (*d*, *J* = 8.7 Hz)	128.2	7.67 (*d*, *J* = 8.7 Hz)	128.0	C-2″, C-4‴

[a] Suárez *et al*, 2003

2.15 Identification of Compound ET-F7 (Ellagic acid 3, 3'-dimethyl ether)

Compound ET-F7 was obtained as pale yellow needles. Its molecular formula was shown to be $C_{16}H_{10}O_8$ according to a molecular ion peak in its EI mass spectrum at *m/z* 330 (**Figure 132**), whereas its ^{13}C NMR spectrum (**Figure 134**) exhibited only 8 carbon signals and, therefore, these signals were doubled. These data suggested symmetry in its skeletal structure.

The ^{1}H NMR spectrum (**Figure 133**) of compound ET-F7 showed a methoxy singlet at δ 4.03 (3-OMe and 3′-OMe), an aromatic proton singlet at δ 7.51 (H-5 and H-5′), and a phenolic hydroxyl signal at δ 10.75 (4-OH and 4′-OH). Eight carbon signals in its carbon spectrum could be differentiated, based on DEPT experiments (**Figure 135**), into those of one methoxy, one methine and six quaternary carbons.

One quaternary carbon which resonated at δ 158.6 (C-7 and C-7′) was a lactone carbonyl. Compound ET-F7 was therefore a dimeric phenolic compound consisting of two penta-substituted phenolic acid arranged symmetrically.

From the above observations and comparison with previously reported data, compound ET-F7 was identified as ellagic acid 3,3'-dimethyl ether (Nawwar, Buddrus and Bauer, 1982). This phenolic derivative has previously been isolated from the roots of *Tamarix nilotica* (Tamaricaceae) (Nawwar, Buddrus and Bauer, 1982) and *Coriaria intermedia* (Coriariaceae) (Chang *et al*., 1996).

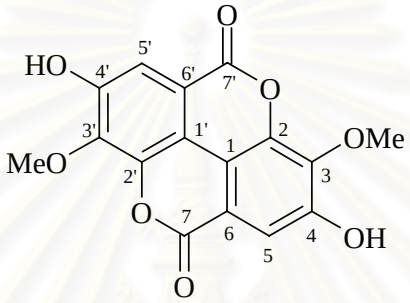

Ellagic acid 3,3′-dimethyl ether

Table 36. ^{1}H (300 MHz) and ^{13}C (75 MHz) NMR spectral data of ellagic acid 3,3′-dimethyl ether and compound ET-F7 (in DMSO-d_6)

Position	Ellagic acid 3,3′-dimethyl ether [a]		ET-F7	
	^{1}H (mult., *J* in Hz)	^{13}C	^{1}H (mult., *J* in Hz)	^{13}C
1, 1′	-	111.8	-	111.8
2, 2′	-	141.1	-	141.3
3, 3′	-	140.2	-	140.3
4, 4′	-	153.0	-	152.3
5, 5′	7.52 (*s*)	111.4	7.51 (*s*)	111.6
6, 6′	-	112.0	-	112.2
7, 7′	-	158.3	-	158.6
4-OH, 4′-OH	10.6 (*br s*)	-	10.7 (*br s*)	-
3-OMe, 3′-OMe	4.08 (*s*)	60.9	4.03 (*s*)	61.1

[a] Nawwar, Buddrus and Bauer, 1982

2.16 Identification of Compound ET-FM3 (Quercetin)

Compound ET-FM3 was obtained as yellow amorphous powder which exhibited a strong conjugated carbonyl absorption band at 1656 cm^{-1} and O-H stretching band at 3420 cm^{-1} in its IR spectrum (**Figure 139**). Its molecular formula

was determined to be $C_{15}H_{10}O_7$ from $[M-H]^+$ peak at *m/z* 301 in the ESI mass spectrum (**Figure 140**). The compound displayed quenching spot under UV light indicative of its flavonoid nature.

The ^1H NMR spectrum of compound ET-FM3 (**Figure 141**) displayed a hydrogen-bonded hydroxyl proton resonance at the most downfield shift of δ 12.16. Two aromatic proton signals could be observed. A pair of broad singlets at δ 6.25 and 6.51 were assigned to the *meta*-coupled H-6 and H-8, respectively, of ring A of a flavonoid structure. The 3′,4′-dihydroxy substituted ring B was represented by the signals at δ 7.81 (1H, *br s*, H-2′), 6.98 (1H, *d*, *J* = 8.4 Hz, H-5′) and 7.68 (1H, *d*, *J* = 8.4 Hz, H-6′). The ^{13}C NMR spectrum of this compound (**Figure 142**) displayed fifteen carbon signals, including that of a carbonyl carbon at δ176.5. These data suggested that the compound was a flavonol with hydroxyl substituents at C-5, C-7, C-3′ and C-4′.

HMBC experiments (**Figure 145**) and comparison with previous published data confirmed compound ET-FM3 as quercetin (Alfonso and Kapetanidis, 1994), a common flavonol.

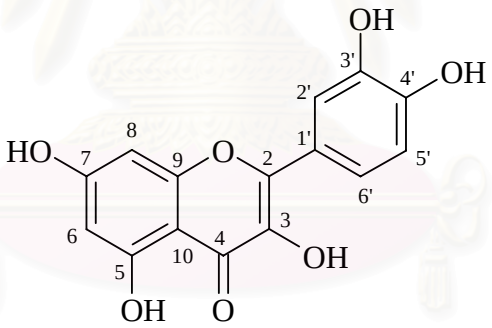

.

Quercetin

Table 37. ^1H (300 MHz) and ^{13}C (75 MHz) NMR spectral data of quercetin and compound ET-FM3 (in acetone-d_6)

Position	Quercetin [a]		ET-FM3		
	^1H (mult., *J* in Hz)	^{13}C	^1H (mult., *J* in Hz)	^{13}C	HMBC
2	-	146.8	-	147.0	
3	-	135.7	-	136.7	
4	-	175.9	-	176.5	
5	-	160.7	-	162.3	
5-OH	-	-	12.16 (*s*)	-	C-5, C-6, C-10

Table 37. ^{1}H (300 MHz) and ^{13}C (75 MHz) NMR spectral data of quercetin and compound ET-FM3 (in acetone-d_6)

Position	Quercetin [a]		ET-FM3		
	^{1}H (mult., *J* in Hz)	^{13}C	^{1}H (mult., *J* in Hz)	^{13}C	HMBC
6	6.17 (*d*, *J* = 2.0 Hz)	98.2	6.25 (*br s*)	99.1	C-5, C-8, C-10
7	-	163.9	-	165.0	
8	6.40 (*d*, *J* = 2.0 Hz)	93.4	6.51 (*br s*)	94.4	C-6, C-9, C-10
9	-	156.2	-	157.8	
10	-	103.0	-	104.1	
1′	-	122.0	-	123.7	
2′	7.66 (*d*, *J* = 2.2 Hz)	115.1	7.81 (*br s*)	115.7	C-2, C-3′, C-4′, C-6′
3′	-	145.1	-	145.8	
4′	-	147.7	-	148.3	
5′	6.84 (*d*, *J* = 8.5 Hz)	115.6	6.98 (*d*, *J* = 8.4 Hz)	116.2	C-1′, C-3′, C-4′
6′	7.53 (*dd*, *J* = 8.5, 2.2 Hz)	120.0	7.68 (*d*, *J* = 8.4 Hz)	121.4	C-2′, C-4′

[a] Alfonso and Kapetanidis, 1994

2.17 Identification of Compound ET-L2 (Hopenol-B)

Compound ET-L2, which was obtained as a colorless needles, exhibited absorption bands in its IR spectrum (**Figure 146**) at 3389 (OH), 1638 and 890 cm^{-1} (terminal methylene). Its EI mass spectrum (**Figure 147**) showed a molecular ion peak at *m/z* 426, corresponding to the molecular formula $C_{30}H_{50}O$. The intense mass fragment peaks at *m/z* 207 and 189 were due to the cleavage of ring C of a hopane triterpenoid skeleton (Matsunaga and Morita, 1983).

The ^{1}H NMR spectrum (**Figure 148**) showed seven methyl signals at δ 0.70 (*d*, *J* = 1.0 Hz, H-28), 0.75 (*s*, H-24), 0.84 (*s*, H-25), 0.96 (*s*, H-23), 0.97 (*s*, H-27), 1.01 (*s*, H-26) and 1.65 (*t*, *J* = 1.0 Hz, H-30). An olefinic, two-proton singlet at δ 4.66 (H-29) indicated the presence of an exomethylene functional group. The α-oriented oxymethine H-3 resonated as a doublet of doublets (*J* = 11.0, 5.5 Hz) at δ 3.11.

The ^{13}C NMR spectrum (**Figures 149a-149b**) exhibited thirty carbon signals of a triterpenoid structure, including two sp^2 carbons (δ 148.4, C-22 and δ 110.1, C-29) and one oxygenated carbon at δ 78.4 (C-3). The carbon resonances could be classified

by DEPT experiment (**Figure 150**) into those of seven methyl (δ 15.4, 16.0, 16.3, 17.0, 17.1, 19.6 and 28.5), eleven methylene (δ 19.1, 21.5, 21.7, 24.6, 27.9, 28.1, 33.3, 34.1, 39.5, 40.7 and 110.1), six methine (δ 48.7, 49.5, 51.2, 54.5, 56.0 and 78.4) and six quaternary carbons (δ 37.8, 39.5, 42.4, 42.9, 44.8 and 148.4). HMBC experiment (**Figures 153a-153h, Table 38**) confirmed the location of the double bond between C-22 and C-29 through correlations observed between the signals of H-29 to C-21, H-30 to C-21 and C-22, and H-17 to C-22.

The ^{1}H and ^{13}C NMR assignments of compound ET-L2 were established by analyses of the COSY (**Figure 151**), HSQC (**Figures 152a-152b**) and HMBC experiments (**Figures 153a-153h**), and comparison with previously reported data (Matsunaga and Morita, 1983). Finally, compound ET-L2 was identified as the hopane triterpenoid hop-22(29)-en-3β-ol or hopenol-B, previously isolated from the whole plant of *Euphorbia supina* Rafin. (family Euphorbiaceae). However, this is the first report of its ^{13}C NMR assignment.

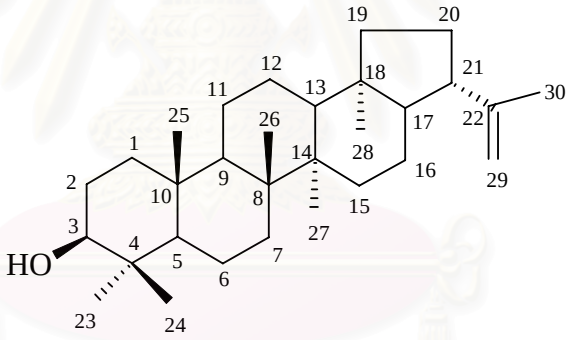

Hopenol-B

Table 38. ^{1}H (500 MHz) and ^{13}C (75 MHz) NMR assignments of compound ET-L2 (in acetone-d_6)

Position	^{13}C	^{1}H (mult., *J* in Hz)	HMBC
1	39.5	0.95 (*m*)	C-2, C-10, C-25
2	28.1	1.56 (*m*)	C-1, C-4, C-10
3	78.4	3.11 (*dd*, *J* = 11.0, 5.5 Hz)	C-4, C-23, C-24
4	39.5	-	-
5	56.0	0.71 (*dd*, *J* = 13.0, 3.0 Hz)	C-3, C-6, C-23, C-24, C-25
6	19.1	1.52 (*m*)	-
7	34.1	1.25 (*m*)	C-6, C-26
		1.52 (*m*)	C-26
8	42.4	-	-

Table 38. ^{1}H (500 MHz) and ^{13}C (75 MHz) NMR assignments of compound ET-L2 (in acetone-d_6) (continued)

Position	^{13}C	^{1}H (mult., *J* in Hz)	HMBC
9	51.2	1.28 (*dd*, *J* = 12.5, 3.0 Hz)	C-1, C-5, C-8, C-10, C-11, C-12, C-14
10	37.8	-	-
11	21.7	1.40 (*m*)	C-12, C-14
12	24.6	1.44 (*m*)	-
13	49.5	1.50 (*m*)	-
14	42.9	-	-
15	33.3	1.20 (*ddd*, *J* = 9.0, 5.0, 3.0 Hz)	C-13, C-14, C-17, C-27
		1.42 (*m*)	C-13, C-14, C-17, C-27
16	21.5	1.40 (*m*)	-
17	54.5	1.08 (*m*)	C-15, C-20, C-21, C-22
18	44.8	-	-
19	40.7	1.08 (*dd*, *J* = 12.0, 2.5 Hz),	C-18, C-28
		1.54 (*m*)	C-13
20	27.9	1.44 (*m*)	-
		1.84 (*m*)	C-17, C-19
21	48.7	2.26 (*ddd*, *J* = 12.0, 10.0, 7.0 Hz)	C-16, C-17, C-20, C-30
22	148.4	-	-
23	28.5	0.96 (*s*)	C-3, C-4, C-24
24	16.0	0.75 (*s*)	C-4, C-5, C-23
25	16.3	0.84 (*s*)	C-1, C-5, C-9, C-10
26	17.1	1.01 (*s*)	C-7, C-8, C-9, C-14
27	17.0	0.97 (*s*)	C-8, C-13, C-14, C-15
28	15.4	0.70 (*d*, *J* = 1.0 Hz)	C-13, C-17, C-18, C-19
29	110.1	4.66 (*br s*)	C-21, C-30
30	19.6	1.65 (*t*, *J* = 1.0 Hz)	C-21, C-22, C-29

2.18 Structure Elucidation of Compound ET-L3 (2,3-*Seco*-taraxer-14-ene-2,3,28-trioic acid 2,3-dimethyl ester)

Compound ET-L3, obtained as a white powder, was assigned the molecular formula $C_{32}H_{50}O_6$ on the basis of its high resolution ESIMS quasi-molecular $[M+Na]^+$ peak at *m/z* 553.3509 (calcd. for $C_{32}H_{50}O_6Na$, 553.3505) (**Figure 155**). The IR spectrum (**Figure 154**) suggested the presence of carboxylic acid (3434 and 1692 cm^{-1}), ester (1729 and 1145 cm^{-1}) and olefinyl (1636 cm^{-1}) groups.

The ^{1}H NMR spectrum (**Figures 156a-156d**) showed seven tertiary methyl singlets (δ 0.91, H-30; 0.93, H-27; 0.94, H-29; 0.96, H-26; 1.00, H-25; 1.20, H-23 and H-24) and two carbomethoxy singlets at δ 3.56 (3-COOMe) and 3.57 (2-COOMe). An olefinic proton on a trisubstituted double bond appeared as a well-defined doublet

of doublets at δ 5.56 (*J* = 8.0, 3.5 Hz, H-15), suggesting that compound ET-L3 was a taraxer-14-ene derivative (Ogihara *et al*., 1987).

The ^{13}C NMR spectrum (**Figures 157a-157b**) exhibited thirty-two carbon signals, including those of three carbonyls (δ 172.0, C-2; 179.0, C-28; 179.8, C-3) and a double bond (δ 117.2, C-15; 161.2, C-14). An AB system in the proton spectrum at δ 2.25 (1H, *d*, *J* = 18.7 Hz) and 2.35 (1H, *d*, *J* = 18.7 Hz) was assigned to the H-1 methylene protons of a 2,3-*seco*-diacid deriving from a taraxerane triterpene with cleaved A ring. Its NMR data were also compared with those of other 2,3-*seco*-terpenoids reported from another euphorbiaceous plant, *Excoecaria agallocha* (Konishi *et al*., 1998; 2003). Both acid moieties at C-2 (δ 172.0) and C-3 (δ 179.8) were methylated, as indicated by HMBC cross-peaks between the carbomethoxy singlet at δ 3.57 and C-2, as well as between another carbomethoxy signal at δ 3.56 and C-3 (**Figures 160a-160h**). The HMBC spectrum also exhibited correlations of H-1 to C-2, C-5, C-10, and C-25, and both H-23 and H-24 to C-3, C-4 and C-5. Another carboxylic group was determined to be at C-28, on the basis of long-range correlations of this carbonyl carbon at δ 179.0 with H-16, H-18 and H-22. The location of the double bond was confirmed by HMBC correlations of H-15 to C-8 (δ 39.3) and C-13 (δ 37.8) and of both H-16 and H-27 to C-14 (δ 161.2). Therefore, the structure of compound ET-L3 was elucidated as 2,3-*seco*-taraxer-14-ene-2,3,28-trioic acid 2,3-dimethyl ester.

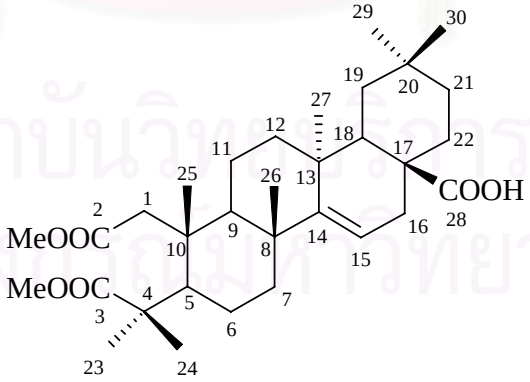

2,3-*Seco*-taraxer-14-ene-2,3,28-trioic acid 2,3-dimethyl ester

Table 39. ^{1}H (500 MHz) and ^{13}C (125 MHz) NMR assignments of compound ET-L3 (in acetone-d_6)

Position	^{13}C	^{1}H (mult., *J* in Hz)	HMBC
1	41.1	2.25 (*d*, *J* = 18.7 Hz)	C-2, C-5, C-9, C-10, C-25
		2.35 (*d*, *J* = 18.7 Hz)	C-2, C-5, C-9, C-10, C-25
2	172.0	-	
3	179.8	-	
4	46.7	-	
5	49.6	2.41 (overlap)	C-6, C-10, C-24, C-25
6	21.7	1.56 (*m*)	
		1.64 (*m*)	
7	41.0	1.32 (*m*)	
		1.92 (*dt*, *J* = 13.0, 3.0 Hz)	
8	39.3	-	
9	41.5	2.58 (*dd*, *J* = 10.5, 9.5 Hz)	C-8, C-10, C-11, C-25, C-26
10	43.0	-	
11	18.3	1.56 (*m*)	
12	34.3	1.63 (*m*)	C-9, C-11, C-13, C-14, C-27
		1.75 (*m*)	C-27
13	37.8	-	
14	161.2	-	
15	117.2	5.56 (*dd*, *J* = 8.0, 3.5 Hz)	C-8, C-13, C-16
16	32.3	1.98 (*dd*, *J* = 14.5, 3.5 Hz)	C-14, C-15, C-17, C-18, C-28
		2.39 (overlap)	C-14, C-15, C-17, C-18, C-28
17	51.4	-	
18	42.3	2.40 (overlap)	C-14, C-17, C-28
19	36.0	1.12 (*dd*, *J* = 13.5, 3.5 Hz)	
		1.32 (*t*, *J* = 13.5 Hz)	C-17, C-18, C-29, C-30
20	29.5	-	
21	34.5	1.07 (*td*, *J* =13.5, 3.0 Hz)	
		1.17 (*dd*, *J* = 5.0, 3.5 Hz)	
22	31.5	1.47 (*td*, *J* = 13.5, 3.0 Hz)	C-21, C-28
		1.70 (*ddd*, *J* = 14.0, 4.5, 3.0 Hz)	
23	28.1	1.20 (*s*)	C-3, C-4, C-5, C-24
24	24.1	1.20 (*s*)	C-3, C-4, C-5, C-23
25	19.5	1.00 (*s*)	C-5, C-9, C-10
26	25.5	0.96 (*s*)	C-7, C-8, C-14
27	21.9	0.93 (*s*)	C-12, C-13, C-14, C-18

Table 39. ^{1}H (500 MHz) and ^{13}C (125 MHz) NMR assignments of compound ET-L3 (in acetone-d_6) (continued)

Position	^{13}C	^{1}H (mult., *J* in Hz)	HMBC
28	179.0	-	
29	32.4	0.94 (*s*)	C-19, C-21, C-30
30	29.2	0.91 (*s*)	C-19, C-20, C-21, C-29
2-COO**Me**	51.0	3.57 (*s*)	C-2
3-COO**Me**	51.9	3.56 (*s*)	C-3

2.19 Structure Elucidation of Compound ET-L5 (2,3-*Seco*-taraxer-14-ene-2,3,28-trioic acid 3-methyl ester)

The molecular formula of compound ET-L5, which was isolated as colorless needles, was determined as $C_{31}H_{48}O_6$ on the basis of its high resolution ESIMS $[M+Na]^+$ peak at *m/z* 539.3346 (calcd. for $C_{31}H_{48}O_6Na$, 539.3349) (**Figure 162**). Its IR spectrum (**Figure 161**) showed absorption bands for carboxylic acid (3433 and 1690 cm^{-1}) and ester moieties (1728 cm^{-1}), nearly identical to those observed in compound ET-L3.

Its ^{1}H NMR spectrum (**Figures 163a-163e**) showed seven methyl singlets at δ 0.83 (H-27), 0.86 (H-30), 0.89 (H-25 and H-26), 0.90 (H-29) and 1.14 (H-23 and H-24) and only one carbomethoxy singlet at δ 3.52 (3-COOMe). The H-15 olefinic proton of a taraxer-14-ene derivative resonated at δ 5.45 (*dd*, *J* = 7.8, 3.3 Hz), while the H-1 methylene protons of a 2,3-*seco*-diacid appeared as an AB system in the proton spectrum at δ 2.10 (1H, *d*, *J* = 19.3 Hz) and 2.20 (1H, *d*, *J* = 19.3 Hz).

The ^{13}C NMR spectrum (**Figure 164**) exhibited thirty-one carbon signals, including those of three carbonyls at δ 172.3 (C-2), 178.7 (C-28) and 178.9 (C-3) and a double bond between C-14 (δ 159.8) and C-15 (δ 115.9). The only methoxy carbon gave a signal at δ 51.6. These data suggested that compound ET-L5 was very similar to compound ET-L3, and the major difference was the presence of only one, instead of two, carbomethoxy moiety in this compound. HMBC correlations of the C-3 carbonyl with the carbomethoxy singlet, H-5, H-23 and H-24 established the esterification at this C-3 position. The location of the double bond was also confirmed by HMBC cross-peaks of H-15 to C-8 (δ 38.0) and C-13 (δ 36.6) and of H-12, H-16, H-18 and H-27 to C-14 (δ 159.8).

Consequently, the structure of compound ET-L5 was determined as 2,3-*seco*-taraxer-14-ene-2,3,28-trioic acid 3-methyl ester.

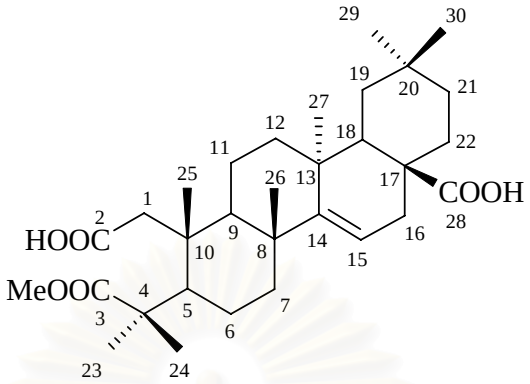

2,3-*Seco*-taraxer-14-ene-2,3,28-trioic acid 3-methyl ester

Table 40. ^{1}H (500 MHz) and ^{13}C (125 MHz) NMR assignments of compound ET-L5 (in acetone-d_6)

Position	^{13}C	^{1}H (mult., *J* in Hz)	HMBC
1	40.2	2.10 (*d*, *J* = 19.3 Hz)	C-2, C-5, C-10, C-25
		2.20 (*d*, *J* = 19.3 Hz)	C-2, C-5, C-10, C-25
2	172.3	-	
3	178.9	-	
4	45.6	-	
5	48.0	2.33 (*dd*, *J* =12.3, 1.8 Hz)	C-3, C-4, C-6, C-10, C-23, C-24, C-25
6	20.6	1.44 (*m*)	C-8
		1.54 (*m*)	C-1, C-14
7	39.7	1.21 (*m*)	
		1.84 (*dt*, *J* = 13.0, 3.0 Hz)	
8	38.0	-	
9	39.7	2.54 (*t*, *J* = 9.8 Hz)	C-8, C-10, C-11, C-14, C-25, C-26
10	41.5	-	
11	17.2	1.44 (*m*)	C-8, C-12
12	33.2	1.55 (*m*)	C-11, C-13, C-14
		1.65 (*m*)	C-13
13	36.6	-	
14	159.8	-	
15	115.9	5.45 (*dd*, *J* = 7.8, 3.3 Hz)	C-8, C-13
16	31.3	1.89 (*dd*, *J* = 14.5, 3.0 Hz)	C-14, C-15, C-17, C-18, C-28
		2.25 (overlap)	C-14, C-15, C-17, C-18, C-28
17	50.1	-	
18	40.9	2.24 (overlap)	C-14, C-17, C-28

Table 40. ^{1}H (500 MHz) and ^{13}C (125 MHz) NMR assignments of compound ET-L5 (in acetone-d_6) (continued)

Position	^{13}C	^{1}H (mult., *J* in Hz)	HMBC
19	35.0	1.04 (*dd*, *J* = 13.5, 3.5 Hz)	
		1.21 (*t*, *J* = 13.5 Hz)	C-29, C-30
20	29.0	-	
21	33.5	0.94 (*td*, *J* = 13.3, 2.8 Hz)	
		1.11 (*t*, *J* = 4.0 Hz)	
22	30.4	1.37 (*td*, *J* = 13.5, 3.0 Hz)	C-17, C-20, C-21, C-28
		1.57 (overlap)	C-20
23	27.2	1.14 (*s*)	C-3, C-4, C-5, C-24
24	23.7	1.14 (*s*)	C-3, C-4, C-5, C-23
25	19.0	0.89 (*s*)	C-1, C-5, C-9, C-10
26	24.9	0.89 (*s*)	C-7, C-8, C-14
27	21.3	0.83 (*s*)	C-12, C-13, C-14, C-18
28	178.7	-	
29	32.0	0.90 (*s*)	C-19, C-20, C-21, C-30
30	28.8	0.86 (*s*)	C-19, C-20, C-21, C-29
3-COO**Me**	51.6	3.52 (*s*)	C-3

2.20 Identification of Compound ET-L12 (Aleuritolic acid)

Compound ET-L12 was obtained as colorless needles. Its molecular formula was determined as $C_{30}H_{48}O_3$ on the basis of $[M-H]^+$ peak in the ESI mass spectrum at *m/z* 455 (**Figure 169**). Its IR spectrum (**Figure 168**) showed absorption bands at 3434 and 1690 cm^{-1}, suggesting the presence of hydroxyl and carbonyl functions, respectively.

The ^{1}H and ^{13}C NMR data of compound ET-L12 (**Table 41**) were similar to those of compound ET-S2. The ^{1}H NMR spectrum (**Figure 170**) showed an olefinic proton signal at δ 5.43 (*d*, *J* = 4.8 Hz, H-15) and an oxymethine proton signal at δ 4.28 (*d*, *J* = 4.5 Hz, H-3), while the ^{13}C NMR spectrum (**Figure 171**) together with DEPT experiments (**Figures 172a-172b**) exhibited 30 carbon signals including those of 7 methyls, 10 methylene, 5 methines and 8 quaternary carbons. The carbonyl carbon of an acid group resonated at δ 178.7 (C-28). Two olefinic carbon signals of C-14 and C-15 appeared at δ 160.0 and 115.9, respectively, while the oxygenated C-3 resonated at δ 77.0. These spectral data were very similar to those of 3-acetyl aleuritolic acid (ET-S2), except acetate signal was absence in this compound.

Compound ET-L12 was identified as the triterpenoid aleuritolic acid (McLean *et al*., 1987). The compound has been shown to be an inhibitor of the enzyme human DNA ligase-1, which was a possible target for anti-tumor agents (Tan *et al*., 1996).

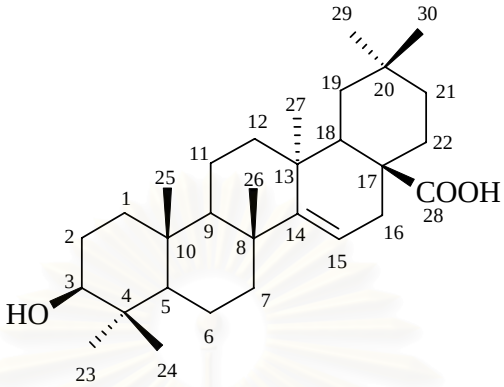

Aleuritolic acid

Table 41. Comparison of ^{13}C NMR spectral data of acetyl aleuritolic acid and compound ET-L12 (in DMSO-d_6, 75 MHz)

Carbon	Acetyl aleuritolic acid [a]	ET-L12	Carbon	Acetyl aleuritolic acid [a]	ET-L12
1	37.4	37.5	17	51.4	50.2
2	23.4	27.0	18	41.3	41.2
3	80.8	77.0	19	35.2	35.1
4	37.6	37.6	20	29.2	29.0
5	55.5	55.2	21	33.6	33.6
6	18.7	18.5	22	30.6	30.6
7	40.7	40.9	23	27.9	28.2
8	39.0	38.5	24	16.5	15.9
9	49.0	48.8	25	15.6	15.3
10	37.9	38.5	26	26.1	25.8
11	17.2	17.0	27	22.4	22.0
12	33.2	33.1	28	184.2	178.7
13	37.2	36.9	29	31.8	32.1
14	160.5	160.0	30	28.6	28.9
15	116.8	115.9	-O-**CO**CH_3	170.9	-
16	31.3	31.5	-O-CO**CH_3**	21.2	-

[a] McLean *et al*., 1987

2.21 Identification of Compound ET-LC4 (Kaempferol)

The yellow compound ET-LC4 displayed an $[M+H]^+$ peak at *m/z* 287 in its ESI mass spectrum (**Figure 175**), consistent with a molecular formula of $C_{15}H_{10}O_6$.

The compound absorbed UV light with maximum peaks at 366, 265 and 210 nm (**Figure 173**).

Its ^{1}H NMR spectrum (**Figure 176**) exhibited a pair of *para*-substituted aromatic signals at δ 7.74 (2H, *d*, *J* = 8.7 Hz, H-2′ and H-6′) and 6.58 (2H, *d*, *J* = 8.7 Hz, H-3′ and H-5′). Two *meta*-coupled aromatic signals at δ 6.06 (1H, *br s*, H-8) and 6.89 (1H, *br s*, H-6) could also be observed.

The ^{13}C NMR (**Figure 177**, **Table 42**) displayed fifteen carbon signals of a flavonol skeleton, including a carbonyl signal at δ 175.4. On the basis of HMQC (**Figure 179**), ^{1}H-^{1}H COSY (**Figure 178**) and HMBC experiments (**Figure 180**) and comparison with literature (Harborne and Mabry, 1982), compound ET-LC4 was identified as kaempferol, a common flavonol aglycone.

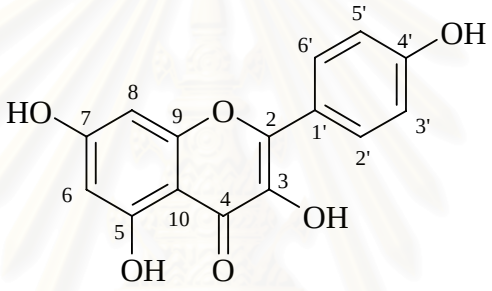

Kaempferol

Table 42. ^{13}C NMR spectral data of kaempferol (in DMSO-d_6, 22.5 MHz) and ^{1}H (300 MHz) and ^{13}C (75 MHz) NMR data of compound ET-LC4 (in CD_3OD + $CDCl_3$)

Position	Kaempferol [a]	ET-LC4		
	^{13}C	^{13}C	^{1}H (mult., *J* in Hz)	HMBC
2	146.8	146.3	-	-
3	135.6	135.2	-	-
4	175.9	175.4	-	-
5	160.7	160.3	-	-
6	98.2	97.8	6.89 (*br s*)	C-5, C-8, C-10
7	163.9	163.4	-	-
8	93.5	93.1	6.06 (*br s*)	C-9, C-10
9	156.2	156.4	-	-
10	103.1	102.5	-	-
1′	121.7	121.9	-	-
2′, 6′	129.5	129.0	7.74 (*d*, *J* = 8.7 Hz)	C-2, C-4′
3′, 5′	115.4	114.7	6.58 (*d*, *J* = 8.7 Hz)	C-1′
4′	159.2	158.4	-	-

[a] Harborne and Mabry, 1982

2.22 Identification of Compound ET-LC7 (Sequoiaflavone)

Compound ET-LC7 was obtained as a pale yellow powder which showed an $[M-H]^+$ peak at *m/z* 551 in its ESI mass spectrum (**Figure 183**), equivalent to a molecular formula of $C_{31}H_{20}O_{10}$. Its IR spectrum (**Figure 182**) exhibited absorption bands at 3367 and 1659 cm^{-1}, suggesting hydroxyl and carbonyl moieties.

The ^1H NMR spectrum (**Figures 184a-184b**) showed the resonances of methoxy protons at δ 3.81 (3H, *s*, 7-OMe), two olefinic protons at δ 6.90 (H-3) and 6.79 (H-3″), two hydrogen-bonded hydroxyl protons at δ 13.11 (5″-OH) and 12.97 (5-OH) and ten aromatic protons which could be separated into 4 sets. The doublet at δ 6.35 (1H, *d*, *J* = 2.2 Hz) was assigned to H-6 of ring A which *meta*-coupled to another one-proton doublet at δ 6.75 (*J* = 2.2 Hz, H-8). The doublet at δ 7.57 (2H, *d*, *J* = 8.8 Hz) represented H-2‴ and H-6‴ of ring B′ and *ortho*-coupled to the signal at δ 6.71 (2H, *d*, *J* = 8.8 Hz, H-3‴ and H-5‴). The 1,3,4-trisubstituted ring B gave the *meta*-coupled signals at δ 8.06 (*d*, *J* = 2.4 Hz, H-2′) and 8.03 (*dd*, *J* = 8.6, 2.4 Hz, H-6′), while the latter signal also *ortho*-coupled to a doublet at δ 7.13 (*d*, *J* = 8.6 Hz, H-5′). The last set consists of only one singlet at δ 6.37 representing H-6″ of ring A′.

The ^{13}C NMR spectrum (**Figures 185a-185c**) displayed 30 carbon signals of two flavone units and one methoxy carbon which resonated at δ 56.5 (7-OMe). HMBC correlation (**Figures 189a-189f**) between the methoxy proton signal and C-7 (δ 165.6) established the position of this methyl ether moiety on ring A. The C-3′/C-8″ linkage was also confirmed by HMBC cross-peak of H-2′ to C-8″ (δ 104.7).

Therefore, compound ET-LC7 was identified as the biflavone 7-*O*-methyl amentoflavone or sequoiaflavone. It has been isolated from the leaves of *Podocarpus taxifolia* (Podocarpaceae) (Hameed *et al*., 1973) and *Cupressus cashmeriana* (Cupressaceae) (Khabir, Khatoon and Ansari, 1987).

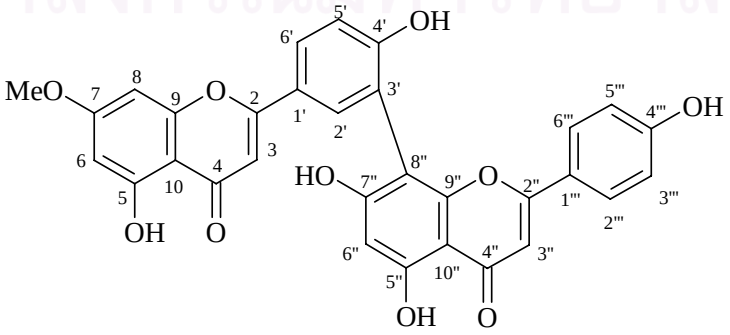

Sequoiaflavone

Table 43. ^{1}H (500 MHz) and ^{13}C (125 MHz) NMR assignments of compound ET-LC7 (in DMSO-d_6)

Position	^{1}H (mult., *J* in Hz)	^{13}C	HMBC
2	-	164.7	-
3	6.90 (*s*)	103.5	C-2, C-4, C-10, C-1′
4	-	182.4	-
5	-	161.6	-
6	6.35 (*d*, *J* = 2.2 Hz)	98.5	C-5, C-7, C-8, C-10
7	-	165.6	-
8	6.75 (*d*, *J* = 2.2 Hz)	93.1	C-6, C-9
9	-	157.8	-
10	-	105.1	-
1′	-	121.0	-
2′	8.06 (*d*, *J* = 2.4 Hz)	131.9	C-2, C-4′, C-6′, C-8″
3′	-	120.8	-
4′	-	160.7	-
5′	7.13 (*d*, *J* = 8.6 Hz)	117.0	C-1′, C-3′, C-4′
6′	8.03 (*dd*, *J* = 8.6, 2.4 Hz)	128.3	C-2, C-2′, C-4′
2″	-	164.1	-
3″	6.79 (*s*)	103.0	C-2″, C-4″, C-10″, C-1‴
4″	-	182.5	-
5″	-	161.0	-
6″	6.37 (*s*)	99.4	C-5″, C-10″
7″	-	163.3	-
8″	-	104.7	-
9″	-	155.0	-
10″	-	103.9	-
1‴	-	121.9	-
2‴	7.57 (*d*, *J* = 8.8 Hz)	128.6	C-2″, C-3‴, C-4‴
3‴	6.71 (*d*, *J* = 8.8 Hz)	116.2	C-1‴, C-4‴
4‴	-	161.5	-
5‴	6.71 (*d*, *J* = 8.8 Hz)	116.2	C-1‴, C-4‴
6‴	7.57 (*d*, *J* = 8.8 Hz)	128.6	C-2″, C-4‴
7-OMe	3.81 (*s*)	56.5	C-7
5-OH	12.97 (*s*)	-	C-5, C-6, C-10
5″-OH	13.11 (*s*)	-	C-5″, C-6″, C-10″

2.23 Identification of Compound ET-LC13 (Ginkgetin)

Compound ET-LC13 was obtained as a pale yellow powder. Its molecular formula was determined by TOF-ESIMS as $C_{32}H_{22}O_{10}$, on the basis of the $[M-H]^+$ peak observed at *m/z* 565 (**Figure 192**). Its IR spectrum (**Figure 191**) exhibited strong carbonyl absorption bands at 1655 and 1606 cm^{-1}, and O-H stretching band at

3435 cm^{-1}. The UV spectrum (**Figure 190**) showed maxima at 333, 270 and 216 nm, identical to those of amentoflavone, suggesting compound ET-LC13 to be amentoflavone derivative.

The ^{1}H (**Figure 193**) and ^{13}C NMR spectra (**Figures 194a-194c**) of compound ET-LC13 were very similar to those of the biflavonoid amentoflavone. The ^{13}C spectrum displayed 30 carbon signals of two flavone units and two methoxy carbons at δ 55.9 (4′-OMe) and 56.5 (7-OMe). The proton spectrum showed the presence of two methoxy signals at δ 3.80 (7-OMe) and 3.72 (4′-OMe), ten aromatic protons, two olefinic protons (H-3 and H-3″), and two chelated hydroxyl protons at δ 13.08 (5″-OH) and 12.97 (5-OH). The proton singlets at δ 6.34 and 6.71 were assignable to H-6 and H-8 of ring A, respectively. The signal at δ 7.69 (2H, *d*, *J* = 9.3 Hz) was clearly that of H-2‴ and H-6‴, which coupled to the signal at δ 6.89 (2H, *d*, *J* = 9.3 Hz) of H-3‴ and H-5‴. Ring B was represented by the signals at δ 8.07 (1H, *d*, *J* = 2.3 Hz, H-2′), 7.12 (1H, *d*, *J* = 8.6 Hz, H-5′) and 8.03 (1H, *dd*, *J* = 8.6, 2.3 Hz, H-6′), whereas only one aromatic proton of ring A″ resonated at δ 6.35 (*s*, H-6″), indicating the C-3′/C-8″ linkage of amentoflavone derivatives. HMBC correlations (**Figures 198a-198e**) of 7-methoxy proton with C-7 at δ 56.5 and of 4′-methoxy proton with C-4′ at δ 55.9 supported the location of these two methyl ethers. Substituent effects on carbon chemical shifts helped confirming the *O*-methylation pattern of this biflavonoid. 7-*O*-Methylation led to an upfield shift of +1.1 ppm for C-8 signal compared with similar signal of amentoflavone (δ 94.2). 4′-*O*-Methylation also led to an upfield shift of +3.2 ppm for C-1′ signal compared to that of amentoflavone (δ 120.3) (Markham, Sheppard and Geiger, 1987).

From the above data and by comparison with published data (Garg and Mitra, 1971; Markham, Sheppard and Geiger, 1987), compound ET-LC13 was identified as the biflavonoid 7, 4″-dimethyl amentoflavone or ginkgetin.

Ginkgetin was first isolated from the leaves of *Ginkgo biloba* (Ginkgoaceae). Later, it was also found in the leaves and twigs of *Celaendendron mexicanum* (Euphorbiaceae) (Castaneda *et al*., 1992) and *Cephalotaxus drupacea* (Cephalotaxaceae) (Hayashi, Hayashi and Morita, 1992), whole plant of *Selaginella moellendorffii* (Selaginellaceae) (Sun *et al*., 1997), and several *Dioon* species e.g. *D. edule, D. spinulosum* and *Zamia augustifolia* (Zamiaceae) (Dossaji and Bell, 1973).

The biflavone possessed various biological activities including anti-herpes simplex virus type-1 (Hayashi, Hayashi and Morita, 1992).

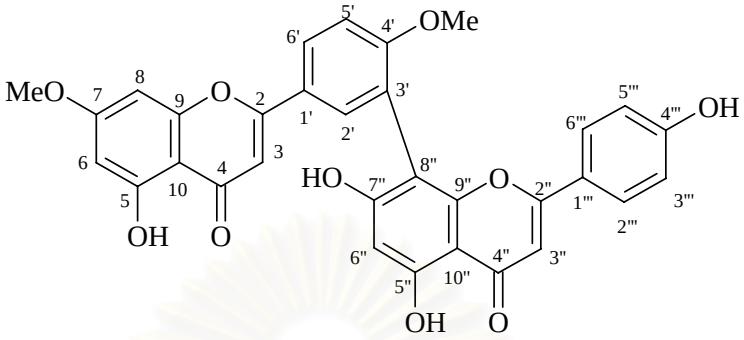

Ginkgetin

Table 44. ^{1}H (500 MHz) and ^{13}C (125 MHz) NMR spectral data of ginkgetin and compound ET-LC13 (in DMSO-d_6)

Position	Ginkgetin [a]		ET-LC13		
	^{13}C	^{1}H	^{13}C	^{1}H (mult., *J* in Hz)	HMBC
2	163.5	-	164.7	-	
3	103.5	6.82	103.7	6.90 (*s*)	C-2, C-10, C-1′
4	181.9	-	182.4	-	
5	161.5	-	161.6	-	
5-O**H**	-	12.96	-	12.97 (*s*)	C-5, C-6, C-10
6	98.5	6.37	98.5	6.34 (*s*)	C-8, C-10
7	165.1	-	165.5	-	
7-O**Me**			56.5	3.80 (*s*)	C-7
8	92.6	6.80	93.1	6.71 (*s*)	C-10
9	157.3	-	157.8	-	
10	104.7	-	105.1	-	
1′	122.3	-	123.5	-	
2′	128.2	8.12	131.9	8.07 (*d*, *J* = 2.3 Hz)	
3′	121.7	-	121.2	-	
4′	160.6	-	162.6	-	
4′-O**Me**			55.9	3.72 (*s*)	C-4′
5′	111.7	7.38	117.3	7.12 (*d*, *J* = 8.6 Hz)	
6′	130.7	8.19	128.2	8.03 (*d*, *J* = 8.6, 2.3 Hz)	
2″	163.6	-	164.7	-	
3″	102.5	7.0	103.4	6.90 (*s*)	C-10″, C-1‴
4″	182.0	-	182.5	-	
5″	160.4	-	161.0	-	
5″-O**H**	-	13.12	-	13.08 (*s*)	C-5″, C-6″, C-10″

Table 44. ^{1}H (500 MHz) and ^{13}C (125 MHz) NMR spectral data of ginkgetin and compound ET-LC13 (in DMSO-d_6) (continued)

Position	Ginkgetin [a]		ET-LC13		
	^{13}C	^{1}H	^{13}C	^{1}H (mult., *J* in Hz)	HMBC
6″	98.6	6.44	99.8	6.35 (*s*)	
7″	161.7	-	160.7	-	
8″	103.8	-	104.2	-	
9″	154.3	-	155.1	-	
10″	103.5	-	103.8	-	
1‴	121.2	-	120.4	-	
2‴, 6‴	128.0	7.51	128.4	7.69 (*d*, *J* = 9.3 Hz)	C-4‴
3‴, 5‴	115.8	6.74	114.9	6.89 (*d*, *J* = 9.3 Hz)	C-4‴, C-2″
4‴	161.0	-	163.5	-	

[a] Markham, Sheppard and Geiger, 1987

3. Bioactivity Evaluation of Compounds Isolated from *Canavalia rosea* and *Elateriospermum tapos*

In the search for biologically active constituents of *Canavalia rosea* and *Elateriospermum tapos*, the 95% ethanol extract of *C. rosea* aerial parts, as well as the hexane, CH_2Cl_2 and MeOH extracts of *E. tapos* stem and flowers and the hexane, CH_2Cl_2 and aqueous extracts of *E. tapos* leaves were subjected to *in vitro* screening for their anti-cancer activities against three cancer cell lines (KB, BC and NCI-H187), antimalarial activity against *Plasmodium falciparum*, antituberculosis activity against *Mycobacterium tuberculosis*, and anti-herpes simplex virus type 1 activity. In addition, screening of the ethanolic extract of *C. rosea* for dopamine-1 receptor inhibitory activity was also performed.

3.1 Bioactivities of Compounds from *Canavalia rosea*

Preliminary bioactivity screening has revealed that the 95% ethanol extract of *C. rosea* aerial parts exhibited inhibitory activity against dopamine-1 receptor at 50% inhibition and cytotoxicity against human small cell lung cancer (NCI-H187) cell line with IC_{50} value of 6.30 μg/ml.

Phytochemical investigation of *C. rosea* aerial parts led to the isolation of a new guanidine type alkaloid named canarosine, *epi*-inositol 6-*O*-methyl ether, rutin, β-sitosterol glucoside and a mixture of β-sitosterol and stigmasterol.

The bioactivities of compounds from *C. rosea* are summarized in **Table 45**.

Table 45. Biological activities of isolated compounds from *C. rosea*

Compound	Cytotoxicity IC_{50} (μg/ml)				Anti HSV-1 IC_{50} (μg/ml)	Anti TB MIC (μg/ml)
	KB	BC	NCI-H187	Vero cell		
β-Sitosterol/ stigmasterol mixture	inactive	inactive	inactive	>50	moderately active	inactive
Rutin	inactive	inactive	inactive	>50	inactive	inactive
Canarosine	inactive	inactive	inactive	>50	moderately active	100
Rifampicin	-	-	-	-	-	0.019
Kanamycin	-	-	-	-	-	1.25
Isoniazid	-	-	-	-	-	0.050
Ellipticine	0.413	0.134	0.521	0.559	-	-
Doxorubicin	0.103	0.140	0.022	-	-	-
Acyclovir	-	-	-	-	4.27	-

3.1.1 Dopamine-1 Receptor Inhibitory Activity

The guanidine-type alkaloid, canarosine at the concentration of 100 μg/ml, was able to inhibit dopamine-1 receptor in the radioligand receptor binding assay at 95% inhibition. The IC_{50} value was 39.4 μM.

3.1.2 Antituberculosis Activity

Canarosine displayed antituberculosis activity against *Mycobacterium tuberculosis* H_{37}Ra at the MIC value of 100 μg/ml.

3.1.3 Antimalarial Activity

Canarosine exhibited antimalarial activity against *Plasmodium falciparum* K1 strain with an IC_{50} value of 4.48 μg/ml. The IC_{50} value of positive control, dihydroartemisinin was 4.2 nM.

3.1.4 Cytotoxic Activity

Canarosine, rutin and β-sitosterol/stigmasterol mixture at the concentration of 20 μg/ml were inactive against the three cancer cell lines tested.

3.1.5 Anti HSV-1 Activity

Canarosine showed moderate anti-HSV-1 activity at the concentration of 50 μg/ml.

3.2 Bioactivities of Compounds from *Elateriospermum tapos*

The hexane extract of *E. tapos* leaves exhibited cytotoxicity against human small cell lung cancer (NCI-H187), breast cancer (BC) and oral human epidermoid carcinoma (KB) cell lines at IC_{50} values of 8.53, 7.69 and 3.29 μg/ml, respectively, as well as antimycobaterial activity against *M. tuberculosis* $H_{37}Ra$ at MIC value of 12.5 μg/ml. Subsequent extraction of the hexane extract of the leaves led to the isolation of two new 2,3-*seco*-taraxerane triterpenoids, 2,3-*seco*-taraxer-14-ene-2,3,28-trioic acid 2,3 dimethyl ester and 2,3-*seco*-taraxer-14-ene-2,3,28-trioic acid 3-methyl ester, and two known triterpenoids, aleuritolic acid and hopenol-B.

Although the CH_2Cl_2 extract of the leaves displayed no detectable activity, further phytochemical investigation was carried out. A flavonoid, kaempferol, and four biflavonoids including amentoflavone, sequoiaflavone, putraflavone and ginkgetin were obtained.

Phytochemical investigation of the *E. tapos* stem yielded four triperpenes, lupeol, lupeol acetate, germanicol palmitate and acetyl aleuritolic acid, four diterpenes including 2,3-*seco*-sonderianol which is a new compound, yucalexin B-22, yucalexin P-15 and yucalexin P-17, a biflavonoid, amentoflavone, scopoletin, syringaldehyde and oleic acid.

Chemical constituents of *E. tapos* flowers were shown to be lupeol, lupeol acetate, quercetin and putraflavone.

The results of the bioactivity evaluation of these isolated compounds are summarized in **Table 46.**

Table 46. Bioactivities of isolated compounds from *E. tapos*

Compound	Cytotoxicity IC_{50} (μg/ml)				Anti HSV-1 IC_{50} (μg/ml)	Anti TB MIC (μg/ml)
	KB	BC	NCI-H187	Vero cell		
Lupeol acetate	inactive	inactive	inactive	>50	inactive	inactive
Acetyl aleuritolic acid	inactive	inactive	inactive	>50	inactive	inactive
Lupeol	inactive	inactive	18.4	13.4	moderately active	50
Yucalexin B22	inactive	inactive	inactive	>50	inactive	ND
Yucalexin P17	inactive	inactive	inactive	>50	3.6	200
Scopoletin	inactive	inactive	inactive	>50	inactive	200
2,3-*seco*-sonderianol	inactive	inactive	inactive	>50	inactive	ND
Yucalexin P15	inactive	inactive	inactive	>50	inactive	ND
Amentoflavone	inactive	inactive	inactive	ND	inactive	100
Hopenol-B	inactive	inactive	inactive	>50	inactive	100
2,3-*seco*-taraxer-14-ene-2,3,28-trioic acid 2,3-dimethyl ester	inactive	7.08	4.65	>50	ND	3.13
2,3-*seco*-taraxer-14-ene-2,3,28-trioic acid 3-methyl ester	inactive	inactive	inactive	>50	ND	50
Aleuritolic acid	inactive	inactive	inactive	ND	inactive	ND
Putraflavone	inactive	16.6	12.3	35.4	inactive	50
Sequoiaflavone	inactive	inactive	inactive	>50	moderately active	200
Ginkgetin	18.5	10.3	inactive	34.8	ND	25
Rifampicin	-	-	-	-	-	0.019
Kanamycin	-	-	-	-	-	1.25
Isoniazid	-	-	-	-	-	0.050
Ellipticine	0.413	0.134	0.521	0.559	-	-
Doxorubicin	0.103	0.140	0.022	-	-	-
Acyclovir	-	-	-	-	4.27	-

ND = not determined

3.2.1 Antituberculosis Activity

Three triterpenoids, 2,3-*seco*-taraxer-14-ene-2,3,28-trioic acid 2,3-dimethyl ester, 2,3-*seco*-taraxer-14-ene-2,3,28-trioic acid 3-methyl ester and hopenol-B

exhibitied antituberculosis activity against *M. tuberculosis* $H_{37}Ra$ at the MIC values of 3.13, 50 and 100 μg/ml, respectively.

The biflavonoids ginkgetin, putraflavone, amentoflavone and sequoiaflavone showed antituberculosis activity at the MIC values of 25, 50, 100 and 200 μg/ml, respectively. These results indicated that 7-*O*-methylation of amentoflavone decreased the activity, while 4′- or 4′′′-*O*-methylation increased this activity. 4′-*O*-methylation of amentoflavone led to more potent anti-TB activity than 4′′′-*O*-methylation derivative.

3.2.2 Antimalarial Activity

None of the isolated compounds showed antimalarial activity at the concentration of 10 μg/ml.

3.2.3 Cytotoxic Activity

2,3-*Seco*-taraxer-14-ene-2,3,28-trioic acid 2,3-dimethyl ester exhibited strong cytotoxicity against NCI-H187 cell line with an IC_{50} value of 4.65 μg/ml and was moderately active against BC cell line with an IC_{50} value of 7.08 μg/ml, while its monomethyl derivative, 2,3-*seco*-taraxer-14-ene-2,3,28-trioic acid 3-methyl ester, was inactive against both cancer cell lines. The structures of both triterpenoids are rather similar except for the difference at C-2, suggesting the importance of 2-methyl ester for the cytotoxic activity

Among the biflavonoids, putraflavone was weakly cytotoxic against BC and NCI-H187 cell lines with IC_{50} values of 16.6 and 12.3 μg/ml, respectively, while ginkgetin showed weak cytotoxic activity against KB and BC cell lines with IC_{50} values of 18.5 and 10.3 μg/ml, respectively. However, putraflavone and ginkgetin were also cytotoxic against Vero cells, their IC_{50} values of 35.4 and 34.8 μg/ml, respectively, therefore their prospect for use as anti-cancer agent might be limited.

3.2.4 Anti HSV-1 Activity

Among the isolated compounds from *E. tapos*, yucalexin P-17 displayed the most potent anti-HSV-1 activity, with IC_{50} value of 3.60 μg/ml, whereas the standard anti-HSV-1 drug, acyclovir, showed inhibitory activity with IC_{50} value of 4.27 μg/ml.

Lupeol and sequoiaflavone showed moderately activity.

Previously reported antiviral activity of ginkgetin concerned its ability to suppress herpes simplex viral protein synthesis by inhibition of transcription and replication of viral DNA (Hayashi, Hayashi and Morita, 1992).

CHAPTER V

CONCLUSION

Phytochemical investigation of the aerial parts of *Canavalia rosea* (Leguminosae) led to the isolation of six compounds including a new guanidine alkaloid named canarosine; rutin, a flavonoid glycoside; *epi*-inositol 6-*O*-methyl ether, cyclitol; β-sitosterol glucoside; and a 2:1 mixture of β-sitosterol and stigmasterol. Canarosine showed inhibitory activity against dopamine-1 receptor with 95% inhibition at the concentration of 100 μg/ml and the IC_{50} value was 39.4 μM. The alkaloid also displayed antimalarial activity against *Plasmodium falciparum* K1 strain with IC_{50} value of 4.48 μg/ml and was moderately active against herpes simplex virus type 1 at the concentration of 50 μg/ml.

Similar study on the chemical constituents of *Elateriospermum tapos* (Euphorbiaceae) led to the isolation of triterpenoids, diterpenoids, coumarins, flavonoids, biflavonoids and an aromatic aldehyde. The stem of this plant yielded fourteen compounds including four triterpenoids i.e. lupeol, lupeol acetate, acetyl aleuritolic acid and germanicol palmitate, a new cleistanthane diterpene named 2,3-*seco*-sonderianol, two pimarane diterpenes (yucalexin P-17 and yucalexin P-15), and a beyerane diterpene (yucalexin B-22). In addition, a biflavonoid (amentoflavone), a coumarin (scopoletin), syringaldehyde, oleic acid and a mixture of β-sitosterol and stigmasterol were also isolated from this plant part. Lupeol, lupeol acetate, β-sitosterol/stigmasterol mixture and amentoflavone were also obtained from its flowers, together with the flavonoid quercetin, another biflavonoid (putraflavone) and ellagic acid 3,3′-dimethyl ether. The leaves of this plant provided thirteen compounds including two new taraxerane triterpenes, 2,3-*seco*-taraxer-14-ene-2,3,28-trioic acid 2,3-dimethyl ester and 2,3-*seco*-taraxer-14-ene-2,3,28-trioic acid 3-methyl ester, two known triterpenes (hopenol-B and aleuritolic acid), β-sitosterol glucoside, β-sitosterol/stigmasterol mixture, four biflavonoids (amentoflavone, sequoiaflavone, putraflavone and ginkgetin), kaempferol and ellagic acid 3,3′-dimethyl ether.

Among the compounds isolated from *E. tapos*, the triterpenoid 2,3-*seco*-taraxer-14-ene-2,3,28-trioic acid 2,3-dimethyl ester exhibited moderate cytotoxicity against BC cell line with IC_{50} value of 7.08 μg/ml, strong cytotoxicity against NCI-H187 cell line with IC_{50} value of 4.65 μg/ml and anti-*Mycobacterium tuberculosis*

with MIC value of 3.13 μg/ml with non-cytotoxic activity against normal cell line, Vero cell. Another triterpene, lupeol, was weakly cytotoxic against NCI-H187 cell line with IC_{50} value of 18.4 μg/ml. Both 2,3-*seco*-taraxer-14-ene 2,3,28-trioic acid 3-methyl ester and lupeol were active against *M. tuberculosis* with the same MIC value of 50 μg/ml. One diterpenoid, yucalexin P-17, displayed anti-herpes simplex virus type 1 activity with IC_{50} value of 3.60 μg/ml. This compound is considered as an interesting anti-HSV-1 agent since it showed their activity as potent as acyclovir and it has no cytotoxic effect on tested cell lines. Among the flavonoids isolated, the biflavone ginkgetin was weakly cytotoxic against KB and BC cell lines with IC_{50} values of 18.5 and 10.3 μg/ml, respectively. However, it was also cytotoxic against Vero cells with IC_{50} value of 34.8 μg/ml. Putraflavone was another biflavone which showed cytotoxicity against BC and NCI-H187 with IC_{50} values of 16.6 and 12.3 μg/ml, respectively and against Vero cells with IC_{50} of 35.4 μg/ml. Ginkgetin, putraflavone, amentoflavone and sequoiaflavone showed antituberculosis activity with MIC values of 25, 50, 100 and 200 μg/ml, respectively.

REFERENCES

ภาษาไทย

ส่วนพฤกษศาสตร์ป่าไม้ สำนักวิชาการป่าไม้ กรมป่าไม้. 2544. ชื่อพรรณไม้แห่งประเทศไทย เต็มสมิตินันท์ ฉบับแก้ไขเพิ่มเติม พ.ศ. 2544. กรุงเทพมหานคร: ประชาชน.

ภาษาอังกฤษ

Addae-Mansah, I., Achenbach, H., Thoithi, G.N., Waibel, R., and Mwangi, J.W. 1992. Epoxychiromodine and other constituents of *Croton megalocarpus*. Phytochemistry 31: 2055-2058.

Ageta, H. and Arai, Y. 1983. Fern constituents: pentacyclic triterpenoids isolated from *Polypodium niponicum* and *P. formosanum*. Phytochemistry 22: 1801-1808.

Alfonso, D. and Kapetanidis, I. 1994. Flavonoids from *Iochroma gesnerioides*. Pharm. Acta Helv. 68: 211-214.

Alves, T.M., Nagem, T.J., Carvalho, L.H., Krettli, A.U., and Zani, C.L. 1997. Antiplasmodial triterpene from *Vernonia brasiliana*. Planta Med. 63: 554-555.

Ambrosio, S.R., Tirapelli, C.R., da Costa, F.B., and de Oliveira, A.M. 2006. Kaurane and pimarane-type diterpenes from the *Viguiera* species inhibit vascular smooth muscle contractility. Life Sci. 79: 925-933.

Anjaneyulu, V. and Ravi, K. 1989. Terpenoids from *Euphorbia antiquorum*. Phytochemistry 28: 1695-1698.

Appendino, G., Belloro, E., Tron, G.C., Jakupovic, J., and Ballero, M. 2000. Polycyclic diterpenes from *Euphorbia characias*. Fitoterapia 71: 134-142.

Arima, H., Ashida, H., and Danno, G. 2002. Rutin-enhanced antibacterial activities of flavonoids against *Bacillus cereus* and *Salmonella enteritidis*. Biosci. Biotech. Biochem. 66: 1009-1014.

Atallah, A.M. and Nicholas, H.J. 1972. Triterpenoids and steroids of *Euphorbia pilulifera*. Phytochemistry 11: 1860.

Awasthi, Y.C. and Mitra, C.R. 1968. *Madhuca butyracea*. Constituents of the fruit-pulp and the bark. Phytochemistry 7: 637-640.

Ayimele, G.A., Tane, P., and Connolly, J.D. 2004. Aulacocarpin A and B, nerlidol and β-sitosterol glucoside from *Aframomum escapum*. Biochem. Syst. Ecol. 32: 1205-1207.

Baas, W.J. 1983. Dihydronyctanthic acid methyl ester and other 3,4-*seco*-pentacyclic triterpenoids from *Hoya lacunosa*. Phytochemistry 22: 2809-2812.

Backer, C.A. and Van Den Brink, R.C.B. 1968. Flora of Java (Spermatophyte only) vol.1. Groningen: Wolters-Noordhoff, p. 633.

Badami, S., Vijayan, P., Mathew, N., Chandrashekhar, R., Godavarthi, A., Dhanaraj, S.A., and Suresh, B. 2003. *In vitro* cytotoxic properties of *Grewia tiliaefolia* bark and lupeol. Indian J. Pharmacol. 35: 250-251.

Bandara, B.M., Wimalasiri, W.R., and Macleod, J.K. 1988. *Ent*-kauranes and oleananes from *Croton lacciferus*. Phytochemistry 27: 869-871.

Bandaranayake, W.M. 1980. Terpenoids of *Canarium zeylanicum*. Phytochemistry 19: 255-257.

Bandopadhyay, M., Dhingra, V.K., Mukerjee, S.K., Pardeshi, N.P., and Seshadri, T.R. 1972. Triterpenoid and other components of *Mallotus philippinensis*. Phytochemistry 11: 1511.

Banerji, A., Nandi, G., and Kundu, A.B. 1988. Investigation of *Croton caudatus* Geisel.-Isolation of stigmastan-3,6-dione,5α. J. Indian. Chem. Soc. 65: 459.

Bani, S., Kaul, A., Khan, B., Ahmad, S.F., Suri, K.A., Satti, N.K., Amina, M., and Qazi, G.N. 2005. Immunosuppressive properties of an ethyl acetate fraction from *Euphorbia royleana*. J. Ethnopharmacol. 99: 185-192.

Beckmann, S., Geiger, H., and De Groot Pfleiderer, W. 1971. Biflavone und 2,3-dihydrobiflavone aus *Metasequoia gyptostroboides*. Phytochemistry 10: 2465-2474.

Bedir, E., Tatli, I.I., Khan, R.A., Zhao, J., Takamatsu, S., Walker, L.A., Goldman, P., and Khan, I.A. 2002. Biologically active secondary metabolites from *Ginkgo biloba*. J. Agric. Food Chem. 50: 3150-3155.

Benn, M.H., Shustov, G., Shustova, L., Majak, W., Bai, Y., and Fairey, N.A. 1996. Isolation and characterization of two guanidines from *Galega orientalis* Lam. Cv. Gale (Fodder Galega). J. Agric. Food Chem. 44: 2779-2781.

Berlinck, R.G.S. 1999. Natural guanidine derivatives. Nat. Prod. Rep. 16: 339-365.

Berlinck, R.G.S. 2002. Natural guanidine derivatives. Nat. Prod. Rep. 19: 617-649.

Berlinck, R.G.S. and Kossuga, M.H. 2005. Natural guanidine derivatives. Nat. Prod. Rep. 516-550.

Beutler, J.A., Kashman, Y., Tischler, M., Cardellina ll, J.H., Gray, G.N., Currens, M.J., Wall, M.E., Wani, M.C., and Boyd, M.R. 1995. A reinvestigation of *Maprounea* triterpenes. J. Nat. Prod. 58: 1039-1046.

Biswas, K.M. and Mallik, H. 1986. Cassiadinine, a chromone alkaloid and (+)-6-hydroxy-mellein, a dihydroisocoumarin from *Cassia siamea*. Phytochemistry 25: 1727-1730.

Bohlmann, F., Jakupovic, J., and Schuster, A. 1985. Germacranolides from *Perymenium klattianum* and *Perymeniopsis ovalifolia*. Phytochemistry 24: 495-499.

Bohlmann, F. and Wegner, P. 1982. *Ent*-beyer-15-ene derivatives from *Nidorella anomala*. Phytochemistry 21: 1175-1177.

Boonyarathanakornkit, L., Che, C.T., Fong, H.H.S., and Farnsworth, N.R. 1988. Constituents of *Croton crassifolius* roots. Planta Med. 54: 61-63.

Borges-Del-Castillo, J., Bradley-Delso, A., Manresa-Ferrero, M.T., Vázquez-Bueno, P., and Rodríguez, L.F. 1983. A sesquiterpenoid lactone from *Ambrosia cumanensis*. Phytochemistry 22: 782-783.

Bouic, P.J.D., Etsebeth, S., Liebenberg, R.W., Albrecht, C.F., Pegel, K., and Jaarsveld, P.P.V. 1996. Beta-sitosterol and beta-sitosterol glucoside stimulate human peripheral blood lymphocyte proliferation: implications for their use as an immunomodulatory vitamin combination. Int. Immunopharmacol. 18: 693-700.

Bradford, M.M. 1976. A rapid and sensitive method for the quantitation of microgram quantities of protein utilizing the principle of protein-dye binding. Anal. Biochem. 72: 248-254.

Brinkmeier, E., Geiger, H., and Zinsmeister, H.D. 1999. Biflavonoids and 4,2′-epoxy-3-phenylcoumarins from the moss *Mnium hornum*. Phytochemistry 52: 297-302.

Brum, R.L., Honda, N.K., Hess, S.C., Cavalheiro, A.J., and Monache, F.D. 1998. Acyl lupeols from *Cnidoscolus vitifolius*. Phytochemistry 49: 1127-1128.

Bryce, T.A., Martin-Smith, M., Osske, G., Schreiber, K., and Subramanian, G. 1967. Sterols and triterpenoids-XI: Isolation of arundoin and sawamilletin from Cuban sugar cane wax. Tetrahedron 23: 1283-1296.

Budzikiewicz, H., Djerassi, C., and Williams, D.H. 1964. Structure elucidation of Natural products by mass spectrometry Vol. II: Steroids, terpenoids, sugars and miscellaneous classes. San Francisco: Holden-Day.

Budzikiewicz, H., Wilson, J.M., and Djerassi, C. 1963. Mass spectrometry in structural and stereochemical problems. XXXII. Pentacyclic triterpenes. J. Am. Chem. Soc. 85: 3688-3699.

Calvo, T.R., Lima, Z.P., Silva, J.S., Ballesteros, K.V.R., Pellizzon, C.H., Hiruma-Lima, C.A., Tamashiro, J., Brito, A.R.M.S., Takahira, R.K., and Vilegas, W. 2007. Constituents and antiulcer effect of *Alchornea glandulosa*: activation of cell proliferation in gastric mucosa during the healing process. Biol. Pharm. Bull. 30: 451-459.

Camacho, M.D.R., Phillipson, J.D., Croft, S.L., Kirby, G.C., Warhurst, D.C., and Solis, P.N. 2001. Terpenoids from *Guarea rhophalocarpa*. Phytochemistry 56: 203-210.

Carneiro, F.J.C., Boralle, N., Silva, D.H.S., and Lopes, L.M.X. 2000. Bi- and tetraflavonoids from *Aristolochia ridicula*. Phytochemistry 55: 823-832.

Casa, L.C., Villegas, I., Alarcon de la Lastra, C., Motilva, V., and Martin Celero, M.J. 2000. Evidence for protective and antioxidant properties of rutin, a natural flavone, against ethanol induced gastric lesions. J. Ethnopharmacol. 71: 45-53.

Cassady, J.M., Ojima, N., Chang, C., and McLaughlin, J.L. 1979. An investigation of the antitumor activity of *Micromelum integerrimun* (Rutaceae). J. Nat. Prod. 42: 274-278.

Castaneda, P., Garcia, M.R., Hernandez, B.E., Torres, B.A., Anaya, A.L., and Mata, R. 1992. Effects of some compounds isolated from *Celaenodendron mexicanum* Standl (Euphorbiaceae) on seeds and phytopathogenic fungi. J. Chem. Ecol. 18: 1025-1037.

Chamy, M.C., Piovano, M., Garbarino, J.A., Miranda, C., and Gambaro, V. 1990. Diterpenes from *Calceolaria lepida*. Phytochemistry 29: 2943-2946.

Chang, C.-T., Doong, S.-L., Tsai, I.-L., and Chen, I.-S. 1997. Coumarins and anti-HBV constituents from *Zanthoxylum schinifolium*. Phytochemistry 45: 1419-1422.

Chang, Y.-S., Lin, M.-S., Jiang, R.-L., Huang, S.-C., and Ho, K.-L. 1996. 20-Epibryonolic acid, phytosterols and ellagic acid from *Coriaria intermedia*. Phytochemistry 42: 559-560.

Chatterjee, I., Chakravarty, A.K., and Gomes, A. 2006. *Daboia russellii* and *Naja kaouthia* venom neutralization by lupeol acetate isolated from the root extract of Indian sarsaparilla *Hemidesmus indicus* R.Br. J. Ethnopharmacol. 106: 38-43.

Chatterjee, A., Kotoky, J., Das, K.K., Banerji, J., and Chakraborty, T. 1984. Abiesin, a biflavonoid of *Abies webbiana*. Phytochemistry 23: 704-705.

Chaturvedula, V.S.P., Zhou, B.-N., Gao, Z., Thomas, S.J., Hecht, S.M., and Kingston, D.G.I. 2004. New lupane triterpenoids from *Solidago canadensis* that inhibit the lyase activity of DNA polymerase β. Bioorg. Med. Chem. 12: 6271-6275.

Chaudhuri, S.K., Fullas, F., Brown, D.M., Wani, M.C., Wall, M.E., Cai, L., Mar, W., Lee, S.K., Luo, Y., and Zaw, K. 1995. Isolation and structural elucidation of pentacyclic triterpenoids from *Maprounea africana*. J. Nat. Prod. 58: 1-9.

Chayamarit, K. and Van Welzen, P.C. 2005. *Elateriospermum tapos* In Flora of Thailand, Vol. 8 Part 1; Santisuk, T., Larsen, K., Eds.; Bangkok: Prachachon, pp. 254-255.

Chen, Y., Xu, J., Yu, H., Qing, C., Zhang Y., Liqin, W., Ying, L., and Wang, J. 2008. Cytotoxic phenolics from *Bulbophyllum odoratissimum*. Food Chem. 107: 169-173.

Chiang, Y.-M., Chang, J.-Y., Kuo, C.-C., Chang, C.-Y., and Kuo, Y.-H. 2005. Cytotoxic triterpenes from the aerial roots of *Ficus microcarpa*. Phytochemistry 66: 495-501.

Chow, Y.L. and Quon, H.H. 1970. Biogenetically related triterpenes from *Elateriospermum tapos* bark. Phytochemistry 9: 1151-1152.

Collins, L.A. and Franzblau, S.G. 1997. Microplate Alamar Blue assay versus BACTEC 460 system for high-throughput screening of compounds against *Mycobacterium tuberculosis* and *Mycobacterium avium*. Antimicrob. Agents Chemother. 41: 1004-1009.

Craveiro, A.A. and Silveira, E.R. 1982. Two cleistanthane type diterpenes from *Croton sonderianus*. Phytochemistry 21: 2571-2574.

Croft, J.A.., Ritchie, E., and Taylor, W.C. 1975. Some extractives from the leaves of *Bosistoa sapindiformis* (Rutaceae). Aust. J. Chem. 28: 2093-2094.

De Britto, J., Manickam, V.S., Gopalakrishnan, S., Ushida, T., and Tanaka, N. 1995. Determination of aglycone chirality in dihydroflavonol 3-*O*-α-L-rhamnosides by ^{1}H-NMR spectroscopy. Chem. Pharm. Bull. 43: 338-339.

De Quesada, T.G., Rodri′guez, B., and Valverde, S. 1974. Diterpenes from *Sideritis lagascana* and *Sideritis valverdei*. Phytochemistry 13: 2008.

Deepak, M., Dipankar, G., Prashanth, D., Asha, M.K., Amit, A., and Venkataraman, B.V. 2002. Tribulosin and β-sitosterol-D-glucoside, the anthelmintic principles of *Tribulus terrestris*. Phytomedicine 9: 753-756.

Dharmaratne, H.R.W. and Wijesinghe, W.M.N.M. 1997. A trioxygenated diprenylated chromenxanthone from *Calophyllum moonii*. Phytochemistry 46: 1293-1295.

Dharmaratne, H.R.W., Sajeevani, J.R.D.M., Marasinghe, G.P.K., and Ekanayake, E.M.H.G.S. 1998. Distribution of pyranocoumarins in *Calophyllum cordato-oblongum*. Phytochemistry 49: 995-998.

Desjardins, R.E., Canfield, C.J., Haynes, J.D., and Chulay, J.D. 1979. Quantitative assessment of antimalarial activity *in vitro* by a semiautomated microdilution technique. Antimicrob. Agents Chemother. 16: 710-718.

Dossaji, S.F. and Bell, E.A. 1973. Biflavones of *Dioon*. Phytochemistry 12: 371-373.

Fabricant, D.S., Nikolic, D., Lankin, D.C., Chen, S.-N., Jaki, B.U., Krunic, A., van Breemen, R.B., Fong, H.H.S., Farnsworth, N.R., and Pauli, G.F. 2005. Cimipronidine, a cyclic guanidine alkaloid from *Cimicifuga racemosa*. J. Nat. Prod. 68: 1266-1270.

Felicio, J.D., Rossi, M.H., Braggio, M.M., Goncalez, E., Pak, A., Cordeiro, I., and Felicio, R.C. 2004. Chemical constituents from *Ouratea parviflora*. Biochem. Syst. Ecol. 32: 79-81.

Felicio, J.D., Rossi, M.H., Park, H.R., Goncalez, E., Braggio, M.M., David, J.M., and Condeiro, I. 2001. Biflavonoids from *Ouratea multiflora*. Fitoterapia 72: 453-455.

Fonseca, F.N., Ferreira, A.J.S., Sartorelli, P., Lopes, N.P., Floh, E.I.S., Handro, W., and Kato, M.J. 2000. Phenylpropanoid derivatives and biflavonoids at different stages of differentiation and development of *Araucaria angustifolia*. Phytochemistry 55: 575-580.

Gadex, P.A. and Quinn, C.J. 1982. Amentoflavone from *Callitris* species. Phytochemistry 21: 248-249.

Gadex, P.A. and Quinn, C.J. 1983. Biflavones of the subfamily Callitroideae, Cupressaceae. Phytochemistry 22: 969-972.

Gadex, P.A. and Quinn, C.J. 1985. Biflavones of the subfamily Cupressoideae, Cupressaceae. Phytochemistry 24: 267-272.

Gadex, P.A. and Quinn, C.J. 1989. Biflavones of Taxodiaceae. Biochem. Syst. Ecol. 17: 365-372.

Gaydou, E.M., Faure, R., and Wollenweber, E. 1996. β-Amyrin acetate epoxide from *Canarina canariensis*. Phytochemistry 42: 1115-1118.

Garg, H.S. and Mitra, C.R. 1971. Putraflavone, a new biflavonoid from *Putranjiva roxburghii*. Phytochemistry 10: 2787-2791.

Geiger, H. and De Groot Pfleiderer, W. 1971. Über 2,3-dihydrobiflavone in *Cycas revoluta*. Phytochemistry 10: 1936-1938.

Geiger, H. and Markham, K.R. 1992. Campylopusaurone, an auronoflavanone biflavonoid from the mosses *Campylopus clavatus* and *Campylopus holomitrium*. Phytochemistry 31: 4325-4328.

Ghisalberti, E.K., Jefferies, P.R., and Sefton, M.A. 1978. *Seco*-beyerene diterpenes from *Beyeria calycina*. Phytochemistry 17: 1961-1965.

Gonçalez, E., Felicio, J.D., and Pinto, M.M. 2001. Biflavonoids inhibit the production of aflatoxin by *Aspergillus flavus*. Braz. J. Med. Biol. Res. 34: 1453-1456.

González, A.G., Fraga, B.M., González, P., Hernandez, M.G., and Ravelo, A.G. 1981. ^{13}C NMR spectra of olean-18-ene derivatives. Phytochemistry 20: 1919-1921.

González, A. G., Lopes, I., Ferro, E.A. Ravelo, A.G., Gutiérrez, J., and Aguilar, M.A. 1986. Taxonomy and chemotaxonomy of some species of Celastraceae. Biochem. Syst. Ecol. 14: 479-480.

Grace, M.H., Jin, Y., Wilson, G.R., and Coates, R.M. 2006. Structures, biogenetic relationships, and cytotoxicity of pimarane-derived diterpenes from *Petalostigma pubescens*. Phytochemistry 67: 1708-1715.

Grande, M., Mancheno, B., and Sanchez, M.J. 1991. Elasclepial and other tetracyclic diterpenoids from *Elaeoselinum asclepium*. Phytochemistry 30: 1977-1982.

Greenaway, W., Scaysbrook, T., and Whatley, F.R. 1988. Phenolic analysis of bud exudates of *Populus lasiocarpa* by GC/MS. Phytochemistry 27: 3513-3515.

Gregoire, J. and Nyembo, L. 1977. Triterpenoides d′ *Agauria salicifolia*. Phytochemistry 10: 1609-1610.

Grinberg, L.N., Rachmilewitz, E.A., and Newmark, H. 1994. Protective effects of rutin against hemoglobin oxidation. Biochem. Pharmacol. 48: 643-649.

Grynberg, N.F., Carvalho, M.G., Velandia, J.R., Oliveira, M.C., Moreira, I.C., Braz-Filho, R., and Echevarria, A. 2002. DNA topoisomerase inhibitors: biflavonoids from *Ouratea* species. Braz. J. Med. Biol. Res. 35: 819-822.

Guerreiro, E., De Fernandez, J., and Giordano, O.S. 1984. Beyerene derivatives and other constituents from *Petunia patagonica*. Phytochemistry 23: 2871-2873.

Gunatilaka, A.A.L., De Silva, A.M.Y.J., Sotheeswaran, S., Balasubramaniam, S., and Wazeer, M.I.M. 1984. Terpenoid and biflavonoid constituents of *Calophyllum calaba* and *Garcinia spicata* from Sri Lanka. Phytochemistry 23: 323-328.

Gupta, M.M. and Verma, R.K. 1991. Lipid constituents of *Cissus quadrangularis*. Phytochemistry 30: 875-878.

Gupta, R.S., Bhatnager, A.K., Joshi, Y.C., Sharma, M.C., Khushalani, V., and Kachhawa, J.B.S. 2005. Induction of antifertility with lupeol acetate in male albino rats. Pharmacology 75: 57-62.

Haba, H., Lavaud, C., Harkat, H., Magid, A.A., Marcourt, L., and Benkhaled, M. 2007. Diterpenoids and triterpenoids from *Euphorbia guyoniana*. Phytochemistry 68: 1255-1260.

Hameed, N., Ilyas, M., Rahman, W., Okigawa, M., and Kawano, N. 1973. Biflavones in the leaves of *Podocarpus taxifolia*. Phytochemistry 12: 1497.

Harborne, J.B. and Mabry, T.J. 1982. The flavonoids: advances in research. Cambridge: Chapman and Hall, p. 83.

Harborne, J.B. and Williams, C.A. 2000. Advances in flavonoid research since 1992. Phytochemistry 55: 481-504.

Hart, N.K., Johns, S.R., Lamberton, J.A., and Willing, R.I. 1970. Alkaloids of *Alchornea javanensis* (Euphorbiaceae): the isolation of hexahydroimidazo[1,2-a]pyrimidines and guanidines. Aust. J. Chem. 23: 1679-1693.

Hayashi, K., Hayashi, T., and Morita, N. 1992. Mechanism of action of the antiherpesvirus biflavone ginkgetin. Antimicrob. Agents Chemother. 36: 1890-1893.

He, K., Timmermann, B.N., Aladesanmi, A.J., and Zeng, L. 1996. A biflavonoid from *Dysoxylum lenticellare* Gillespie. Phytochemistry 42: 1199-1201.

Herath, W.H.M.W., Rajasekera, N.D.S., Sultanbawa, M.U.S., Wannigama, G.P., and Balasubramaniam, S. 1978. Triterpenoid, coumarin and quinone constituents of eleven *Diospyros* species (Ebenaceae). Phytochemistry 17: 1007-1009.

Herz, W., Bhat, S.V., and Santhanam, P.S. 1970. Coumarins of *Artemisia dracunculoides* and 3′,6′-dimethoxy-4′,5,7-trihydroxyflavone in *A. arctica*. Phytochemistry 9: 891-894.

Heupel, R.C., Sauvaire, Y., Le, P.H., Parish, E.J., and Nes, W.D. 1986. Sterol composition and biosynthesis in sorghum: importance to developmental regulation. Lipids 21: 69-75.

Heywood, V.H. 1978. Flowering plants of the world. Oxford: Oxford University Press. pp. 185-187.

Hirazumi, A., Furusawa, E., Chou, S.C., and Hokawa, Y. 1994. Anticancer activity of *Morinda citrifolia* (noni) on intraperitoneally implanted Lewis lung carcinoma in syngeneic mice. Proc. West. Pharmacol. Soc. 37: 145-146.

Hisham, A., Pieters, L.A.C., Claeys, M., Van Den Heuvel, H., Esmans, E., Dommisse, R., and Vlietinck, A.J. 1991. Acetogenins from root bark of *Uvaria narum*. Phytochemistry 30: 2373-2377.

Hui, W., Ko, P.D.S., Lee, Y.-C., Li, M.-M, and Arthur, H.R. 1975. Triterpenoids from ten *Lithocarpus* species of Hong Kong. Phytochemistry 14: 1063-1066.

Hui, W.-H. and Li, M.-M. 1976a. Neutral triterpenoids from *Melaleuca leucadendron*. Phytochemistry 15: 563.

Hui, W.-H. and Li, M.-M. 1976b. Structures of eight new triterpenoids and isolation of other triterpenoids and *epi*-ikshusterol from the stems of *Lithocarpus cornea*. J. Chem. Soc. Perkin. Trans 1. 23-30.

Hui, W.-H. and Li, M.-M. 1977a. Further triterpenoids from the stems of *Lithocarpus polystachya*. Phytochemistry 16: 111-112.

Hui, W.-H. and Li, M.-M. 1977b. Six new triterpenoids and other triterpenoids and steroids from three *Quercus* species of Hong Kong. J. Chem. Soc. Perkin. Trans 1. 897-904.

Hui, W.-H., Ng, K.K., Fukamiya, N., Koreeda, M., and Nakanishi, K. 1971. Isolation and structure of macarangonol, a diterpene ketol from *Macaranga tanarius*. Phytochemistry 10: 1617-1620.

Hui, W.-H. and Sung, M.-L. 1968. An examination of the Euphorbiaceae of Hong Kong II. The occurrence of epitaraxerol and other triterpenoids. Aust. J. Chem. 21: 2137-2140.

Huneck, S., Tonsberg, T., and Bohlmann, F. 1986. (-)-Allo-pertusaric acid and (-)-dihydropertusaric acid from the lichen *Pertusaria albescens*. Phytochemistry 25: 453-459.

Hutchinson, J. 1959. Families of flowering plants vol. 1. Dicotyledons, second edition. Oxford: Clarendon Press, pp. 152-156, 270-271.

Iinuma, M., Ohyama, M., Tanaka, T., Mizuno, M., and Hong, S.-K. 1993. Five flavonoid compounds from *Echinosophora koreensis*. Phytochemistry 33: 1241-1245.

Iribarren, A.M. and Pomilio, A.B. 1985. Sitosterol 3-*O*-α-D-riburonofuranoside from *Bauhinia candicans*. Phytochemistry 24: 360-361.

Ito, K. and Lai, J. 1978. Studies on the constituents of *Marsdenia formosana* Masamune. II. Structures of marsformoxide A and marsformoxide B. Chem. Pharm. Bull. 26: 1908-1911.

Janbaz, K.H., Saeed, S.A., and Gilani, A.H. 2002. Protective effect of rutin on paracetamol- and CCl_4-induced hepatotoxicity in rodents. Fitoterapia 73: 557-563.

Jang, D.S., Cuendet, M., Pawlus, A.D., Kardono, L.B.S., Kawanishi, K., Farnsworth, N.R., Fong, H.H.S., Pezzuto, J.M., and Kinghorn, A.D. 2004. Potential cancer chemopreventive constituents of the leaves of *Macaranga triloba*. Phytochemistry 65: 345-350.

Jiang, J., Li, Y., Chen, Z., Min, Z., and Lou, F. 2006. Two novel C_{29}-5β-sterols from the stems of *Opuntia dillenii*. Steroids 71: 1073-1077.

Juneja, R.K., Sharma, S.C., and Tandon, J.S. 1985. A substituted 1,2-diarylethane from *Cymbidium giganteum*. Phytochemistry 24: 321-324.

Kalinowski, H.-O. and Braun, S. 1988. Carbon-13 NMR Spectroscopy. New York: John Wiley and sons, p. 213.

Kamnaing, P., Free, S.N.Y.F., Fomum, Z.T., Martin, M.-T., and Bodo, B. 1994. Milletonine, a guanidine alkaloid from *Millettia laurentii*. Phytochemistry 36: 1561-1562.

Kang, S.S., Lee, J.Y., Choi, Y.K., Song, S.S., Kim, J.S., Jeon, S.J., Han, Y.N., Son, K.H., and Han, B.H. 2005. Neuroprotective effects of naturally occurring biflavonoids. Bioorg. Med. Chem. Lett. 15: 3588-3591.

Kang, S.Y., Sung, S.H., Park, J.H., and Kim, Y.C. 1998. Hepatoprotective activity of scopoletin, a constituent of *Solanum lyratum*. Arch. Pharm. Res. 21: 718-722.

Kang, T.H., Pae, H.O., Jeong, S.J., Yoo, J.C., Choi, B.M., Jun, C.D., Chung, H.T., Miyamoto, T., Higuchi, R., and Kim, Y.C. 1999. Scopoletin: an inducible nitric oxide synthesis inhibitory active constituent from *Artemisia feddei*. Planta Med. 65: 400-403.

Katti, S.B. and Tandon, J.S. 1979. Chemical investigation of *Daphne papyracea*. Indian J. Chem. Sect. B 18: 189-190.

Kesari, A.N., Gupta, R.K., and Watal, G. 2004. Two aurone glycosides from heartwood of *Pterocarpus santalinus*. Phytochemistry 65: 3125-3129.

Khabir, M., Khatoon, F., and Ansari, W.H. 1987. Flavonoids of *Cupressus sempervirens* and *Cupressus cashmeriana*. J. Nat. Prod. 50: 511-512.

Khalil, M.W. and Idler, D.R. 1980. Sterols of scollop. III. Characterization of some C-24 epimeric sterols by high resolution (220 MHz) nuclear magnetic resonance spectroscopy. Lipids 15: 69-73.

Khuong-Huu, F., Le Forestier, J.-P., and Goutarel, R. 1972. Alchornéine, isoalchornéine et alchornéinone, produits isolés de I′ *Alchornea floribunda* Muell. Arg. Tetrahedron 28: 5207-5220.

Kim, H.K., Son, K.H., Chang, H.W., Kang, S.S., and Kim, H.P. 1998. Amentoflavone, a plant biflavone: a new potential anti-inflammatory agent. Arch. Pharm. Res. 21: 406-410.

Kobayashi, J., Suzuki, H., Shimbo, K., Takeya, K., and Morita, H. 2001. Celogentins A-C, new antimitotic bicyclic peptides from the seeds of *Celosia argentea*. J. Org. Chem. 66: 6626-6633.

Kojima, H., Sato, N., Hatano, A., and Ogura, H. 1990. Sterol glucosides from *Prunella vulgaris*. Phytochemistry 29: 2351-2355.

Kokpol, U. and Chavasiri, W. 1990. Taraxeryl *cis*-*p*-hydroxycinnamate, a novel taraxeryl from *Rhizophora apiculata*. J. Nat. Prod. 53: 953-955.

Konishi, T., Fujiwara, Y., Konoshima, T., and Kiyosawa, S. 1998. Five new labdane-type diterpenes from *Excoecaria agallocha*. IV. Chem. Pharm. Bull. 46: 1393-1398.

Konishi, T., Yamazoe, K., Konoshima, T., and Fujiwara, Y. 2003. *Seco*-labdane type diterpenes from *Excoecaria agallocha*. Phytochemistry 64: 835-840.

Krishnaswamy, N.R. and Prasanna, S. 1975. α- and β-Amyrin esters and sitosterol glucoside from *Spilanthes acmella*. Phytochemistry 14: 1666-1667.

Kuhl, P., Shiloh, R., Jha, H., Murawsk, U., and Zilhhen, F. 1984. 6,7,4′-Trihydroxyisoflavan: a potent and selective inhibitor of 5-lipoxygenase in human and porcine peripheral blood leukocytes. Prostaglandins 28: 783-804.

Kumar, V., Bulumulla, H.N.K., Wimalasiri, W.R., and Reisch, J. 1994. Coumarins and an indole alkaloid from *Pamburus missionnis*. Phytochemistry 36: 879-881.

Lal, A.R., Cambie, R.C., Rutledge, P.S., and Woodgate, P.D. 1990. *Ent*-pimarane and *ent*-abietane diterpenes from *Euphorbia fidjiana*. Phytochemistry 29: 2239-2246.

Laphookhieo, S., Karalai, C., and Ponglimanont, C. 2004. New sesquiterpenoid and triterpenoids from the fruits of *Rhizophora mucronata*. Chem. Pharm. Bull. 52: 883-885.

Lee, H.S., Oh, W.K., Kim, B.Y., Ahn, S.C., Kang, D.O., Shin, D.I., Kim, J., Mheen, T.-I., and Ahn, J.S. 1996. Inhibition of phospholipase Cy1 activity by amentoflavone isolated from *Selaginella tamariscina*. Planta Med. 62: 293-296.

Lee, M.K., Lim, S.W., Yang, H., Sung, S.H., Lee, H.-S., Park, M.J., and Kim, Y.C. 2006. Osteoblast differentiation stimulating activity of biflavonoids from *Cephalotaxus koreana*. Bioorg. Med. Chem. Lett. 16: 2850-2854.

Li, W.-S. and Duh, C.-H. 1993. Sesquiterpene lactones from *Neolitsea villosa*. Phytochemistry 32: 1503-1507.

Li, X.-C., Elsohly, H.N., and Clark, A.M. 2000. 7-Caffeoylsedoheptulose from *Nyssa sylvatica*. Phytochemistry 53: 1033-1037.

Lima, E.M.C., Medeiros, J.M.R., and Davin, L.B. 2003. Pentacyclic triterpenes from *Euphorbia stygiana*. Phytochemistry 63: 421-425.

Lin, L.C., Yang, L.L., and Chou, C.J. 2002. Constituents from the stems of *Ecdysanthera rosea*. J. Chin. Med. 13: 191-195.

Lin, Y.-M., Flavin, M.T., Cassidy, C.S., Mar, A., and Chen, F.-C. 2001. Biflavonoids as novel antituberculosis agents. Bioorg. Med. Chem. Lett. 11: 2101-2104.

Ling, S.K., Fukumori, S., Tomii, K., Tanaka, T., and Kouno, I. 2006. Isolation, purification and identification of chemical constituents from *Elateriospermum tapos*. J. Trop. Forest Sci. 18: 81-85.

Liu, X.-L., Zhang, L., Fu, X.-L., Chen, K., and Qian, B.-C. 2001. Effect of scopoletin on PC 3 cell proliferation and apoptosis. Acta Pharmacol. Sin. 22: 929-933.

Lobstein, A., Haan-Archipoff, G., Englert, J., Kuhry, J.-G., and Anton, R. 1999. Chemotaxonomical investigation in the genus *Viburnum*. Phytochemistry 59: 1175-1180.

Lonsti, D., Martin, M.T., Litaudon, M., Sèvenet, T., and Païs, M. 1998. Fontaineine, a new alkaloid from *Fontainea pancheri*. J. Nat. Prod. 61: 953-954.

Machado, M. and Lopes, L.M.X. 2005. Chalcone-flavone tetramer and biflavones from *Aristolochia ridicula*. Phytochemistry 66: 669-674.

Maciel, M.A.M., Pinto, A.C., Brabo, S.N., and Silva, M.N.D. 1998. Terpenoids from *Croton cajucara*. Phytochemistry 49: 823-828.

Mahato, S.B. and Kundu, A.P. 1994. ^{13}C NMR spectra of pentacyclic triterpenoids – a compilation and some salient features. Phytochemistry 37: 1517-1575.

Majinda, R.R.T., Gray, A.I., Waigh, R.D., and Waterman, P.G. 1995. A *seco*-olean-18-ene triterpene acid from *Vahlia capensis*. Phytochemistry 38: 461-463.

Manguro, L.O.A., Okwiri, S.O., and Lemmen, P. 2006. Oleanane-type triterpenes of *Embelia schimperi* leaves. Phytochemistry 67: 2641-2650.

Markham, K.R., Anderson, Q.M., and Viotto, E.S. 1988. Unique biflavonoid types from the moss *Dicranoloma robustum*. Phytochemistry 27: 1745-1749.

Markham, K.R., Sheppard, C., and Geiger, H. 1987. ^{13}C NMR studies of some naturally occurring amentoflavone and hinokiflavone biflavonoids. Phytochemistry 26: 3335-3337.

Markstadter, C., Federle, W., Jetter, R., Riederer, M., and Holldobler, B. 2000. Chemical composition of the slippery epicuticular wax blooms on *Macaranga* (Euphorbiaceae) ant-plants. Chemoecology 10: 33-40.

Mar′quez, C., Panizo, F.M., Rodri′quez, B., and Valverde, S. 1975. A new diterpenoid acetate from *Sideritis reverchonii*. Phytochemistry 14: 2713-2714.

Mar′tin, A. S., Rovirosa, J., and Castillo, M. 1983. Diterpenoids from *Baccharis tola*. Phytochemistry 22: 1461-1463.

Matsunaga, S. and Morita, R. 1983. Hopenol-B, a triterpene alcohol from *Euphorbia supina*. Phytochemistry 22: 605-606.

Matsunaga, S., Tanaka, R., and Akagi, M. 1988. Triterpenoids from *Euphorbia maculata*. Phytochemistry 27: 535-537.

Matsugana, S., Tanaka, R., Takaoka, Y., In, Y., Ishida, T., Rahmani, M., and Ismail, H.B.M. 1993. 26-Nor-D-α-friedooleanane triterpenes from *Phyllanthus watsonii*. Phytochemistry 32: 165-170.

Mavar-Manga, H., Haddad, M., Pieters, L, Baccelli, C., Penge, A., and Quetin-Leclercq, J. 2008. Anti-inflammatory compounds from leaves and root bark of *Alchornea cordifolia* (Schumach. & Thonn.) Müll. Arg. J. Ethnopharmacol. 115: 25-29.

McLean, M., Perpick-Dupont, M., Reynolds, W.F., Jacobs, H., and Lachmansing, S.S. 1987. Unambiguous structural and nuclear magnetic resonance spectral characterization of two triterpenoids of *Maprounea guianensis* by two-dimensional nuclear magnetic resonance spectroscopy. Can. J. Chem. 65: 2519-2525.

Merfort, I., Buddrus, J., Nawwar, M.A.H., and Lambert, J. 1992. A triterpene from the bark of *Tamarix aphylla*. Phytochemistry 31: 4031-4032.

Misra, D.R. and Khastgir, H.N. 1970. Terpenoids and related components-XI: Chemical investigation of *Aleurite mantana* and the structure of aleuritolic acid – a new triterpene acid. Tetrahedron 26: 3017-3021.

Misra, G. and Mitra, C.R. 1966. *Mimusops hexandra* – II. Constituents of bark and seeds. Phytochemistry 5: 535-538.

Misra, G. and Mitra, C.R. 1968. *Mimusops hexandra*-III. Constituents of root, leaves and mesocarp. Phytochemistry 7: 2173-2176.

Misra, T.N., Singh, R.S., Upadhyay, J., and Srivastava, R. 1984. Chemical constituents of *Vernonia cinerea*. Isolation and structure elucidation of a new pentacyclic triterpenoid. J. Nat. Prod. 47: 865-867.

Mizushina, Y., Nakanishi, R., Kuriyama, I., Kamiya, K., Satake, T., Shimazaki, N., Koiwai, O., Uchiyama, Y., Yonezawa, Y., Takemura, M., Sakaguchi, K., and Yoshida, H. 2006. β-Sitosterol-3-*O*-β-D-glucopyranoside: a eukaryotic DNA polymerase λ inhibitor. J. Steroid Biochem. Mol. Biol. 99: 100-107.

Muhtadi, H.E.H., Juliawaty, L.D., Syah, Y.M., Achmad, S.A., Latip, J., and Ghisalberti, E.L. 2006. Cytotoxic resveratrol oligomers from the tree bark of *Dipterocarpus hasseltii*. Fitoterapia 77: 550-555.

Nawwar, M.A.M., Buddrus, J., and Bauer, H. 1982. Dimeric phenolic constituents from the roots of *Tamarix nilotica*. Phytochemistry 21: 1755-1758.

Ngamga, D., Free, S.N.Y.F., and Fomum, Z.Y. 1994. A new guanidine alkaloid from *Millettia laurentii*. J. Nat. Prod. 57: 1022-1024.

Ngamga, D., Free, S.N.Y.F., Tane, P., and Fomum, Z.T. 2007. Millaurine A, a new guanidine alkaloid from seeds of *Millettia laurentii*. Fitoterapia 78: 276-277.

Obendorf, R.L., McInnis, C.E., Horbowicz, M., Keresztes, I., and Lahuta, L.B. 2005. Molecular structure of lathyritol, a galactosylbornesitol from *Lathyrus odoratus* seeds, by NMR. Carbohydrate Res. 340: 1441-1446.

Ofman, D.J., Markham, K.R., Vilain, C., and Molloy, B.P.J. 1995. Flavonoid profiles of New Zealand kauri and other species of *Agathis*. Phytochemistry 38: 1223-1228.

Ogihara, K., Higa, M., Hokama, K., and Suga, T. 1987. Triterpenes from the leaves of *Parsonsia laevigata*. Phytochemistry 26: 783-785.

Ojewoleand, J.A.O. and Adesina, S.K. 1983. Cardiovascular and neuromuscular action of scopoletin from fruit of *Tetrapleura tetraptera*. Planta Med. 49: 99-102.

Ojewole, J.A.O. 2002. Hypoglycaemic effect of *Clausena anisata* (Willd) Hook. methanolic root extract in rats. J. Ethnopharmacol. 81: 231-237.

On′okoko, P. and Vanhaelen, M. 1980. Two new diterpene-based alkaloids from *Icacina guesfeldtii*. Phytochemistry 19: 303-305.

On′okoko, P., Vanhaelen, M., Vanhaelen-Fastr′e, R., Declercq, J. P., and Meerssche, M. V. 1985. Icacenone, a furanoditerpene with a pimarane skeleton from *Icacina mannii*. Phytochemistry 24: 2452-2453.

Onunkwo, G.C., Akah, P.A., and Udeala, O.K. 1998. Studies on *Bridelia ferruginea* leaves (1). Stability and hypoglycemic actions of the leaf extracts. Phytother. Res. 10: 418-420.

Padmaja, V., Thankamany, V., and Hisham, A. 1993. Antibacterial, antifungal and anthelmintic activities of root barks of *Uvaria hookeri* and *Uvaria narum*. J. Ethnopharmacol. 40: 181-186.

Page, G., Peeters, M., Maloteaux, J.M., and Hermans, E. 2000. Increases dopamine uptake in striatal synaptosomes after treatment of rats with amantadine. Eur. J. Pharmacol. 403: 75-80.

Pegel, K.H. and Rogers, C.B. 1968. Constituents of *Bridelia micrantha*. Phytochemistry 7: 655-656.

Pegnyemb, D.E., Mbing, J.N., de Théodore Atchadé, A., Tih, R.G., Sondengam, B.L., Blond, A., and Bodo, B. 2005. Antimicrobial biflavonoids from the aerial parts of *Ouratea sulcata*. Phytochemistry 66: 1922-1926.

Peres, M.T.L.P., Monache, F.D., Cruz, A.B., Pizzolatti, M.G., and Yunes, R.A. 1997. Chemical composition and antimicrobial activity of *Croton urucurana* Baillon (Euphorbiaceae). J. Ethnopharmacol. 56: 223-226.

Perry, L.M. and Metzger, J. 1980. Medicinal plants of East and Southeast Asia. Cambridge: MIT Press, p. 209.

Pertino, M., Schmeda-Hirschmann, G., Rodríguez, J.A., and Theoduloz, C. 2007. Gastroprotective effect and cytotoxicity of terpenes from the Paraguayan crude drug "yagua rova" (*Jatropha isabelli*). J. Ethnopharmacol. 111: 553-559.

Pinto, A.C., Antunes, O.A.C., Rezende, C.M., and Correia, C.R.D. 1995. Minor cleistanthane and tetranorfriedolabdane from *Vellozia flavans*. Phytochemistry 38: 1269-1271.

Pinto, A.C., De A Epifanio, R., and Pizzolatii, M.G. 1992. Diterpenoids from *Vellozia declinans*. Phytochemistry 31: 4241-4243.

Pinto, A.C., Peixoto, E.M., and Fiorani, N.G.M. 1984. Diterpenes with pimarane and cleistanthane skeletons from *Vellozia piresiana*. Phytochemistry 23: 1293-1296.

Pinto, A.C., Zocher, D.H.T., Queiroz, P.P.S., and Kelecom, A. 1987. Diterpenoids from *Vellozia flavicans*. Phytochemistry 26: 2409-2411.

Pistelli, L., Bertoli, A., Bilia, A.R., and Morelli, I. 1996. Minor constituents from *Bupleurum fruticosum* roots. Phytochemistry 41: 1597-1582.

Porter, C.L. 1967. Taxonomy of flowering plants, 2nd edition San Francisco: W.H. Freeman and company, pp. 298-306.

Plumb, J.A., Milroy, A., and Kaye, S.B. 1989. Effect of the pH dependence of 3-(4,5-dimethylthiazol-2 yl)-2,5-diphenyltetrazolium bromide-formazan absorption on chemosensitivity determinated by a novel tetrazolium-based assay. Cancer Res. 49: 4435-4440.

Pradhan, B.P., Amer Nath, S.D., and Shoolery, J.N. 1984. Triterpenoid acids from *Sapium sebiferum*. Phytochemistry 23: 2593-2595.

Prasad, R.B.N., Müller, E., and Gülz, P.-G. 1990. Epicuticular waxes from leaves of *Quercus robur*. Phytochemistry 29: 2101-2103.

Rampendahl, C., Seeger, T., Geiger, H., and Zinsmeister, H.D. 1996. The biflavonoids of *Plagiomnium undulatum*. Phytochemistry 41: 1621-1624.

Rani, M.S., Venkata Rao, C., Gunasekar, D., Blond, A., and Bodo, B. 1998. A biflavonoid from *Cycas beddomei*. Phytochemistry 47: 319-321.

Rao, P.S., Sachdev, G.P., Seshadri, T.R., and Singh, H.B. 1968. Isolation and constitution of oblongifoliol, a new diterpene of *Croton oblongifolius* L. Tetrahedron Lett. 9: 4685-4688.

Rasool, N., Khan, A.Q., and Malik, A. 1989. A taraxerane type triterpene from *Euphorbia tirucalli*. Phytochemistry 28: 1193-1195.

Rathore, A., Sharma, S.C., and Tandon, J.S. 1986. Flavones from *Polygonum nepalense*. Phytochemistry 25: 2223-2225.

Ray, T.K., Misra, D.R., and Khastgir, H.N. 1975. Phytosterols in Euphorbiaceae and Rutaceae. Phytochemistry 14: 1876-1877.

Razdan, T.K., Harkar, S., Kachroo, V., and Koul, G.L. 1982. Phytolaccanol and epiacetylaleuritolic acid, two triterpenoids from *Phytolacca acinosa*. Phytochemistry 21: 2339-2342.

Razdan, T.K., Qadri, B., Harkar, S., and Waight, E.S. 1987. Chromones and coumarins from *Skimmia laureola*. Phytochemistry 26: 2063-2069.

Riehl, C.A.S. and Pinto, A.C. 2000. A cleistanthane diterpene lactone from *Vellozia compacta*. Phytochemistry 53: 917-919.

Rizk, A.M. and Rimpler, H. 1972. Isolation of daphnoretin and β-sitosterol-β-D-glucoside from *Thymelea hirsuta*. Phytochemistry 11: 473-475.

Roy, S.K., Qasim, M.A., Kamil, M., and Ilyas, M. 1987. Biflavones from the genus *Podocarpus*. Phytochemistry 26: 1985-1987.

Sacilotto, A.C.B.C., Vichnewski, W., and Herz, W. 1997. *Ent*-kaurene diterpenes from *Gochnatia polymorpha* var. *polymorpha*. Phytochemistry 44: 659-661.

Saha, B., Naskar, D.B., Misra, D.R., Pradhan, B.P., and Khastgir, H.N. 1977. Baccatin, a novel nortriterpene peroxide isolated from *Sapium baccatum* Roxb. Tetrahedron Lett. 35: 3095-3098.

Sakai, T. and Nakagawa, Y. 1988. Diterpenic stress metabolites from cassava roots. Phytochemistry 27: 3769-3779.

Sakurai, N., Yaguchi, Y., and Inoue, T. 1987. Triterpenoids from *Myrica rubra*. Phytochemistry 26: 217-219.

Sannomiya, M., Fonseca, V.B., de Silva, M.A., Rocha, L.R.M., dos Santos, L.C., Hiruma-Lima, C.A., Brito, A.R.M.S., and Vilegas, W. 2005. Flavonoids and antiulcerogenic activity from *Brysonima crassa* leaves extracts. J. Ethnopharmacol. 97: 1-6.

Sarker, S.D., Armstrong, J.A., Gray, A.I., and Waterman, P.G. 1994. Sesquiterpenyl coumarins and geranyl benzaldehyde derivatives from the aerial parts of *Eriostemon myoporoides*. Phytochemistry 37: 1287-1294.

Seeger, T., Geiger, H., Zinsmeister, H.D., and Rozdzinski, W. 1993. Biflavonoids from the moss *Homalothecium lutescens*. Phytochemistry 34: 295-296.

Setzer, W.N., Shen, X., Bates, R.B., Burns, J.R., McClure, K.J., Zhang, P., Moriarity, D.M., and Lawton, R.O. 2000. Phytochemical investigation of *Alchornea latifolia*. Fitoterapia 71: 195-198.

Sharp, H., Latif, Z., Bartholomew, B., Thomas, D., Thomas, B., Sarker, S.D., and Nash, R.J. 2001. Emodin and syringaldehyde from *Rhamnus pubescens* (Rhamnaceae). Biochem. Syst. Ecol. 29: 113-115.

Shaw, C.Y., Chen, C.H., Hsu, C.C., Chen, C.C., and Tsai, Y.C. 2003. Antioxidant properties of scopoletin isolated from *Sinomonium acutum*. Phytother. Res. 17: 823-825.

Sheth, K., Constantine Jr., G.H., Williams, D.K., and Catalfomo, P. 1968. Root triterpenes of *Vaccinium* species. Phytochemistry 7: 1379-1383.

Shin, Y.K., Sohn, U.D., Choi, M.S., Kum, C., Sim, S.S., and Lee, M.Y. 2002. Effects of rutin and harmaline on rat reflux oesophagitis. Auton. Autacoid. Pharmacol. 22: 47-55.

Shinozaki, Y., Fukamiya, N., Uchiyama, C., Okano, M., Tagahara, K., Bastow, K.F., and Lee, K.H. 2002. Multidrug resistant cancer cell susceptibility to cytotoxic taxane diterpenes from *Taxus yunnanensis* and *Taxus chinensis*. Bioorg. Med. Chem. Lett. 12: 2785-2788.

Shoeb, A., Kapil, R.S., and Popli, S.P. 1973. Coumarins and alkaloids of *Aegle marmelos*. Phytochemistry 12: 2071-2072.

Sholichin, M., Yamasaki, K., Kasai, R., and Tanaka, O. 1980. ^{13}C nuclear magnetic resonance of lupane-type triterpenes, lepeol, betulin and betulinic acid. Chem. Pharm. Bull. 28: 1006-1008.

Si, D., Zhong, D., Sha, Y., and Li, W. 2001. Biflavonoids from the aerial part of *Stephania tetrandra*. Phytochemistry 58: 563-566.

Siani, A.C. and Ribeiro, M.N. de S. 1995. Podocarpusflavone A from the leaves of *Trattinnickia glaziovii*. Biochem. Syst. Ecol. 23: 879.

Sibanda, S., Ndengu, B., Multari, G., Pompi, V., and Galeffi, C. 1989. A coumarin glucoside from *Xeromphis obovata*. Phytochemistry 28: 1550-1552.

Siems, K., Jakupovic, J., Castro, V., and Poveda, L. 1993. Rigidol, an unusal diterpene from *Sapium rigidifolium*. Phytochemistry 33: 1465-1468.

Silva, G.L., Chai, H., Gupta, M.P., Farnsworth, N.R., Cordell, G.A., Pezzuto, J.M., Beecher, C.W.W., and Kinghorn, A.D. 1995. Cytotoxic biflavonoids from *Selaginella willdenowii*. Phytochemistry 40: 129-134.

Singh, B., Sahu, P.M., and Sharma, M.K. 2002. Anti-inflammatory and antimicrobial activities of triterpenoids from *Strobilanthes callosus* Nees. Phytomedicine 9: 355-359.

Skehan, P., Storeng, R., Scudiero, D., Monks, A., McMahon, J., Vistica, D., Warren, J.T., Bokesch, H., Kenny, S., and Boyd, M.R. 1990. New colorimetric cytotoxicity assay for anticancer-drug screening. J. Natl. Cancer Inst. 82: 1107-1112.

Smith, K.I., Dornish, J.M., Malterud, K.E., Hvistendahl, G., Romming, C., Bockman, O.C., Kolsaker, P., Stenstrom, Y., and Nordal, A. 1996. Cytotoxic triterpenoids from the leaves of *Euphorbia pulcherrima*. Planta Med. 62: 322-325.

Smith, T.A. and Best, G.R. 1978. Distribution of the hordatines in barley. Phytochemistry 17: 1093-1098.

Southon, I.W. and Buckingham, J. 1989. Dictionary of alkaloids. New York: Chapman and Hall, p. 989.

Stankovic, S.K., Bastic, M.B., and Jovanovic, J.A. 1985. Composition of the triterpene alcohol fraction of horse chestnut seed. Phytochemistry 24: 119-121.

Steck, W. and Mazurek, M. 1972. Identification of natural coumarins by NMR Spectroscopy. J. Nat. Prod. 35: 418-438.

Steele, J.C.P., Warhurst, D.C., Kirby, G.C., and Simmonds, M.S.J. 1999. *In vitro* and *in vivo* evaluation of betulinic acid as an antimalarial. Phytother. Res. 3: 115-119.

Stierle, D.B., Stierle, A.A., and Larsen, R.D. 1988. Terpenoid and flavone constituents of *Polemonium viscosum*. Phytochemistry 27: 517-522.

Suárez, A.I., Diaz M., B., Monache, F.D., and Compagnone, R.S. 2003. Biflavonoids from *Podocalyx loranthoides*. Fitoterapia 74: 473-475.

Su, B.-N., Chai, H., Mi, Q., Riswan, S., Kardono, L.B.S., Afriastini, J.J., Santarsiero, B.D., Mesecar, A.D., Farnsworth, N.R., Cordell, G.A., Swanson, S.M., and

Kinghorn, A.D. 2006. Activity-guided isolation of cytotoxic constituents from the bark of *Aglaia crassinervia* collected in Indonesia. Bioorg. Med. Chem. Lett. 14: 960-972.

Sun, C.-M., Syu, W.-J., Huang, Y.-T., Chen, C.-C., and Ou, J.-C. 1997. Selective cytotoxicity of ginkgetin from *Selagnella moellendorffii*. J. Nat. Prod. 60: 382-384.

Sutthivaiyakit, S., Na Nakorn, N., Kraus, W., and Sutthivaiyakit, P. 2003. A novel 29-nor-3,4-*seco*-friedelane triterpene and a new guaiane sesquiterpene from the roots of *Phyllanthus oxyphyllus*. Tetrahedron 59: 9991-9995.

Sutthivaiyakit, S., Nareeboon, P., Ruangrangsi, N., Ruchirawat, S., Pisutjaroenpong, S., and Mahidol, C. 2001. Labdane and pimarane diterpenes from *Croton joufra*. Phytochemistry 56: 811-814.

Suzuki, H., Morita, H., Iwasaki, S., and Kobayashi, J. 2003. New antimitotic bicyclic peptides, celogentins D-H, and J, from the seeds of *Celosia argentea*. Tetrahedron 59: 5307-5315.

Svenningsen, A.B., Madsen, K.D., Liljefors, T., Stafford, G.I., Van Staden, J., and Jager, A.K. 2006. Biflavones from *Rhus* species with affinity for the $GABA_A$/benzodiazepine receptor. J. Ethnopharmacol. 103: 276-280.

Takeda, Y., Matsumoto, T., Terao, H., Shingu, T., Futatsuishi, Y., Nohara, T., and Kajimoto, T. 1993. Orthosiphol D and E, minor diterpenes from *Orthosiphon stamineus*. Phytochemistry 33: 411-415.

Talapatra, B., Basak, A., and Talapatra, S.K. 1981. Careaborin, a new triterpene ester from the leaves of *Careya arborea*. J. Indian Chem. Soc. 58: 814-815.

Tan, G.T., Lee, S., Lee, I.-S., Chen, J., Leitner, P., Besterman, J.M., Kinghorn, A.D., and Pezzuto, J.M. 1996. Natural-product inhibitors of human DNA ligase-I. Biochem. J. 314: 993-1000.

Tanaka, R., Ida, T., Takaoka, Y., Kita, S., Kamisako, W., and Matsunaga, S. 1994. 3,4-*Seco*-oleana-4(23),18-dien-3-oic acid and other triterpenes from *Euphorbia chamaesyce*. Phytochemistry 36: 129-132.

Tanaka, R. and Matsunaga, S. 1988. Triterpene constituents from *Euphorbia supina*. Phytochemistry 27: 3579-3584.

Tao, J., Morikawa, T., Toguchida, I., Ando, S., Matsuda, H., and Yoshikawa, M. 2002. Inhibitors of nitric oxide production from the bark of *Myrica rubra*: structures of new biphenyl type diarylheptanoid glycosides and taraxerane type triterpene. Bioorg. Med. Chem. Lett. 10: 4005-4012.

Tarus, P.K., Machocho, A.K., Lang'at-Thoruwa, C.C., and Chhabra, S.C. 2002. Flavonoids from *Tephrosia aequilata*. Phytochemistry 60: 375-379.

Tatsumi, M., Jansen, K., Blakely, R., and Richelson, E. 1999. Pharmacological profile of neuroleptics at human monoamine transporters. Eur. J. Pharmacol. 368: 277-283.

Trager, W. and Jensen, J.B. 1976. Human malaria parasites in continuous culture. Science 193: 673-675.

Tsichritzis, F. and Jakupovic, J. 1990. Diterpenes and other constituents from *Relhania* species. Phytochemistry 29: 3173-3187.

Tsukamoto, H., Hisada, S., Nishibe, S., Roux, D.G., and Rourke, J.P. 1984. Coumarins from *Olea africana* and *Olea carpensis*. Phytochemistry 23: 699-700.

Uddin, Q., Malik, A., Azam, S., Hadi, N., Azmi, A.S., Parveen, N., Khan, N.U., and Hadi, S.M. 2004. The biflavonoid, amentoflavone degrades DNA in the presence of copper ions. Toxicol. *in Vitro* 18: 435-440.

Urones, J.G., Marcos, I.S., Diez, D., and Cubilla, R.L. 1998. Tricyclic diterpenes from *Hyptis dilatata*. Phytochemistry 48: 1035-1038.

Wannan, B.S. and Quinn, C.J. 1988. Biflavonoids in the Julianiaceae. Phytochemistry 27: 3161-3162.

Wang, Z.-T., Ma, G.-Y., Tu, P.-F., Xu, G.-J., and Ng, T.-B. 1995. Chemotaxonomic study of *Codonopsis* (Family Campanulaceae) and its related genera. Biochem. Syst. Ecol. 23: 809-812.

Weniger, B., Vonthron-Sénécheau, C., Kaiser, M., Brun, R., and Anton, R. 2006. Comparative antiplasmodial, leishmanicidal and antitrypanosomal activities of several biflavonoids. Phytomedicine 13: 176-180.

Wickramaratne, D.B.M., Kumar, V., and Balasubramaniam, S. 1984. Murragleinin, a coumarin from *Murraya gleinei* leaves. Phytochemistry 23: 2964-2966.

Wiedemann, B., Lerche, H., Lotter, H., Neszmelyi, A., Wagner, H., and Müller, A.A. 1999. Two novel triterpenoids from the stemwood of *Herrania cuatrecasana*. Phytochemistry 52: 333-337.

Williams, C.A., Harborne, J.B., and Tomas-Barberan, F.A. 1987. Biflavonoids in the primitive monocots *Isophysis tasmanica* and *Xerophyta plicata*. Phytochemistry 26: 2553-2555.

Witherup, K.M., Ransom, R.W., Graham, A.C., Bernard, A.M., Salvatore, M.J., Lumma, W.C., Anderson, P.S., Pitzenberger, S.M., and Varga, S.L. 1995. Martinelline and martinellic acid, novel G-protein linked receptor antagonists from the tropical plant *Martinella iquitosensis* (Bignoniaceae). J. Am. Chem. Soc. 117: 6682-6685.

Won, S.W. and Sam, S.K. 1985. Triterpenoids and sterols from seeds of *Phytolacca esculanta*. Phytochemistry 24: 1116-1117.

Woo, W.S. and Wagner, H. 1977. 3-Acetylaleuritolic acid from the seeds of *Phytolacca americana*. Phytochemistry 16: 1845-1846.

Wu, T.-S., Li, C.-Y., Leu, Y.-L., and Hu, C.-Q. 1999. Limonoids and alkaloids of the root bark of *Dictamnus angustifolius*. Phytochemistry 50: 509-512.

Wright, J.L.C., Mclnnes, A.G., Shimizu, S., Smith, D.G., and Walter, J.A. 1978. Identification of C-24 alkyl epimers of marine sterols by ^{13}C nuclear magnetic resonance spectroscopy. Can. J. Chem. 56: 1898-1903.

Yamaguchi, L.F., Vassao, D. G., Kato, M. J., and Mascio, P. D. 2005. Biflavonoids from Brazilian pine *Araucaria angustifolia* as potential protective agents against DNA damage and lipoperoxidation. Phytochemistry 66: 2238-2247.

Yeung, H.W., Kong, Y.C., Lay, W.P., and Cheng, K.F. 1977. The structure and biological effect of leonurine. Planta Med. 31: 51-56.

Yoshida, T. 1976. A new amine, stizolamine, from *Stizolobium hassjoo*. Phytochemistry 15: 1723-1725.

Zdero, C., Bohlmann, F., and Schmeda-Hirschmann, G. 1987. Beyerene derivatives and other terpenoids from *Stevia aristata*. Phytochemistry 26: 463-466.

Zhi-Da, M., Mizuno, M., Tanaka, T., Iinuma, M., Guang-Yi, X., and Qing, H. 1989. A diterpene from *Euphorbia antiquorum*. Phytochemistry 28: 553-555.

Zuco, V., Supino, R., Righetti, S.C., Cleris, L., Marchesi, E., Gambacorti-Passerini, C., and Formelli, F. 2002. Selective cytotoxicity of betulinic acid on tumor cell lines, but not on normal cells. Cancer Lett. 175: 17-25.

APPENDICES

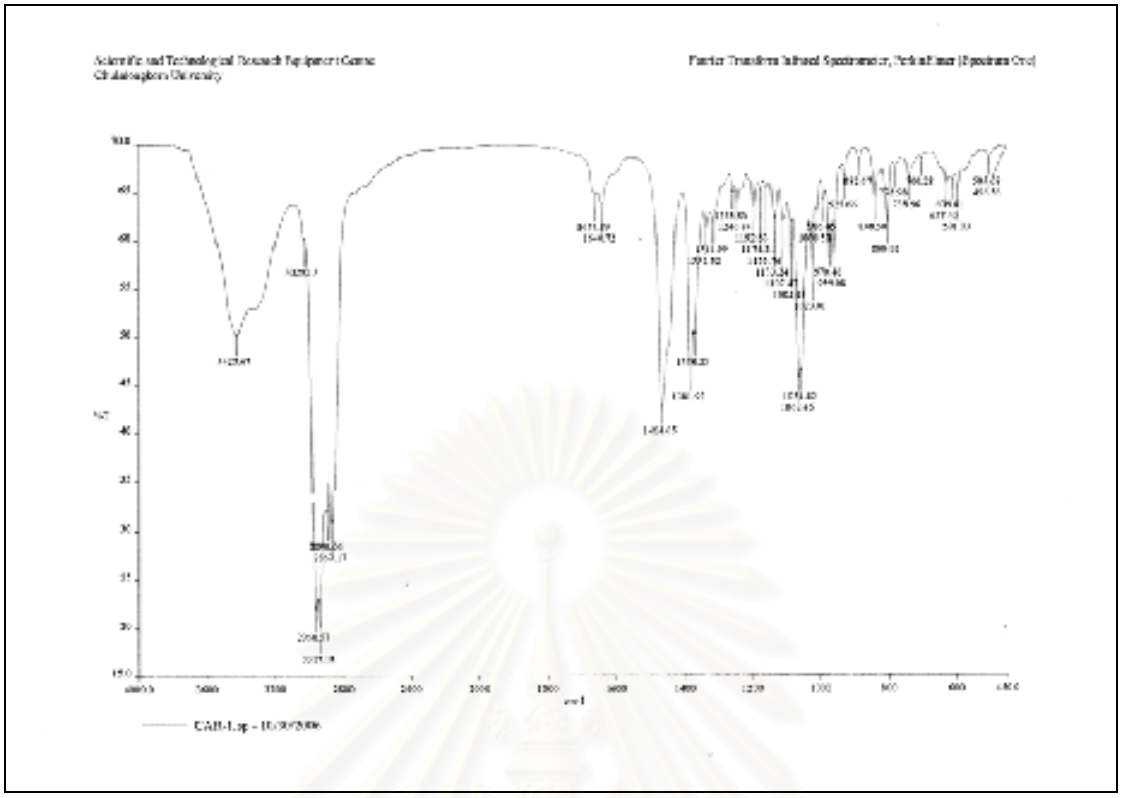

Figure 12. IR Spectrum of component CAR-1 (KBr disc)

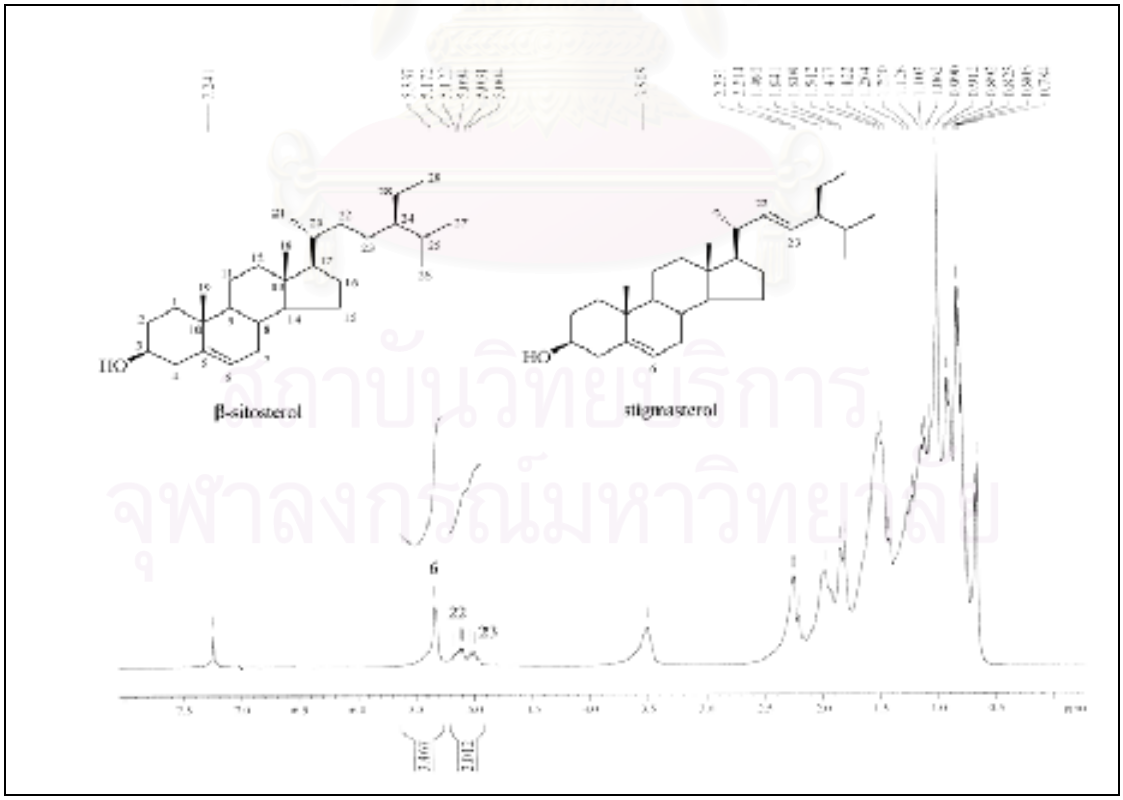

Figure 13. ^{1}H NMR (300 MHz) Spectrum of component CAR-1 (in $CDCl_3$)

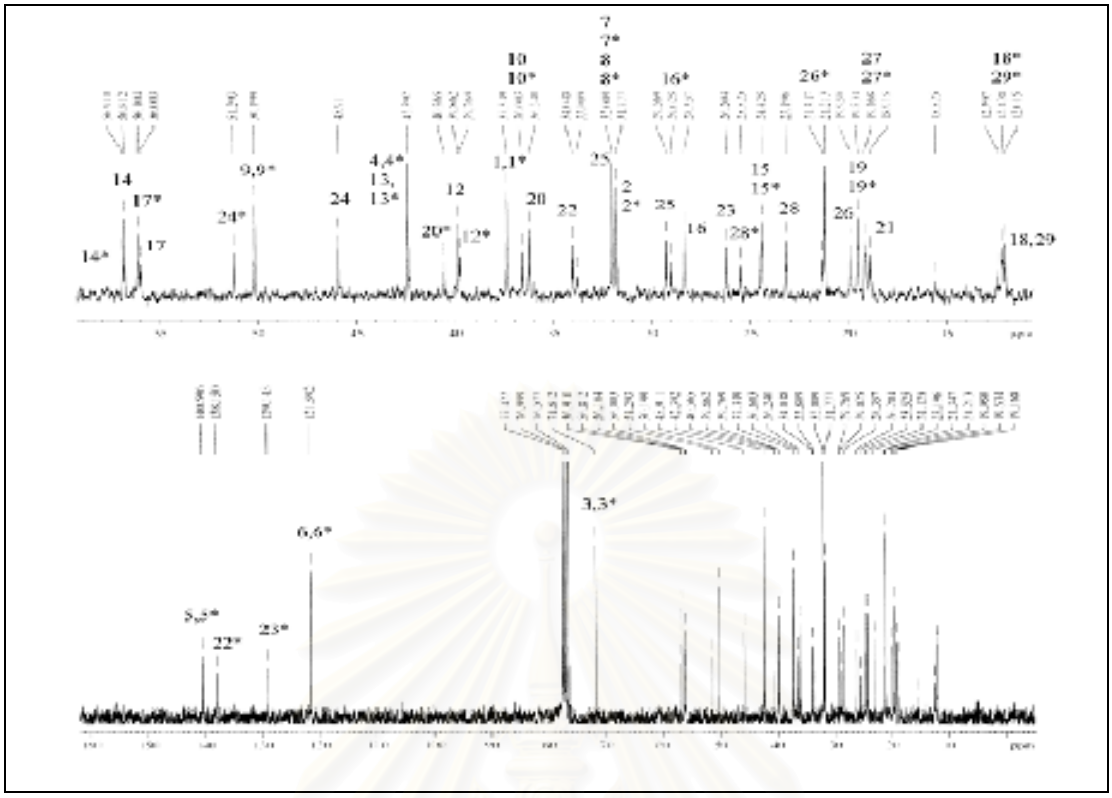

Figure 14. ^{13}C NMR (75 MHz) Spectrum of component CAR-1 (in $CDCl_3$)

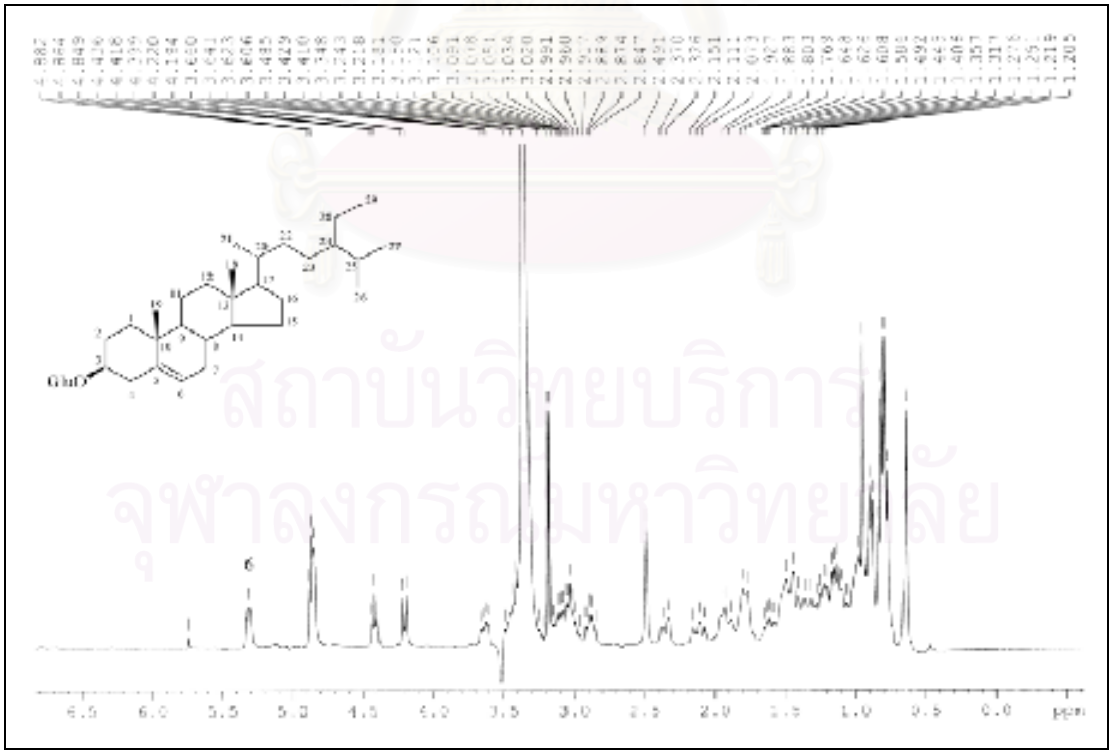

Figure 15. ^{1}H NMR (300 MHz) Spectrum of compound CAR-2 (in DMSO-d_6)

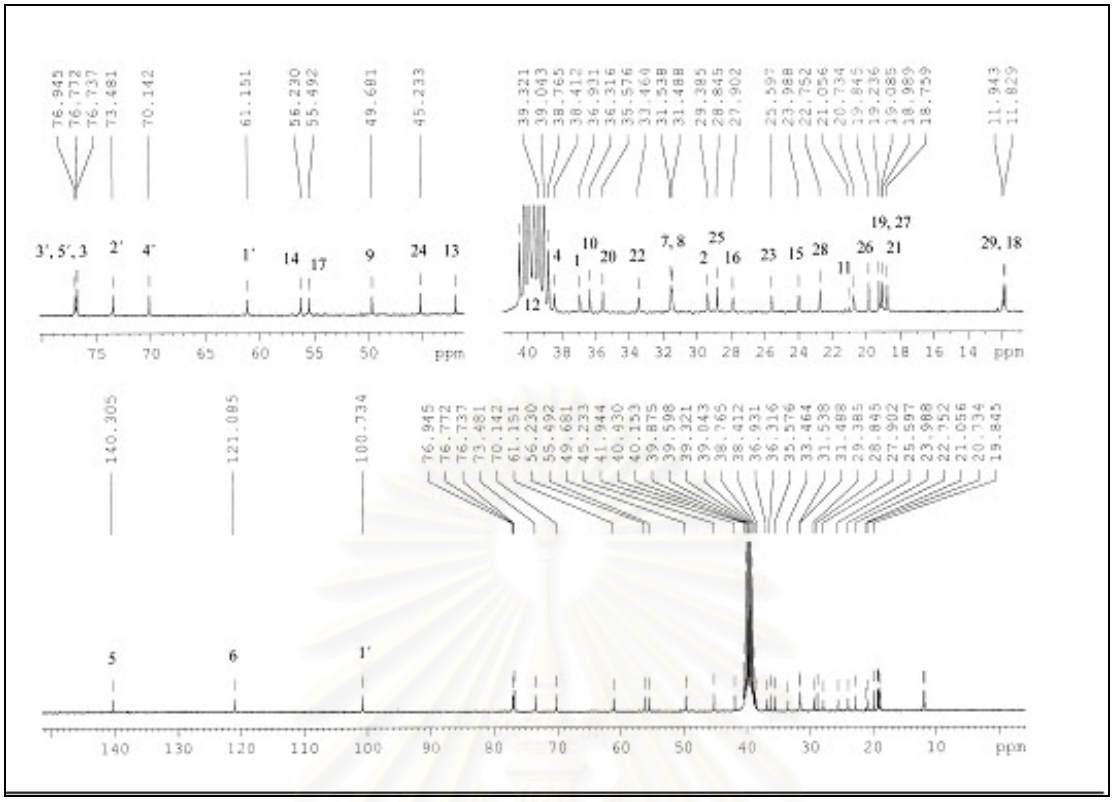

Figure 16. ^{13}C NMR (75 MHz) Spectrum of compound CAR-2 (in DMSO-d_6)

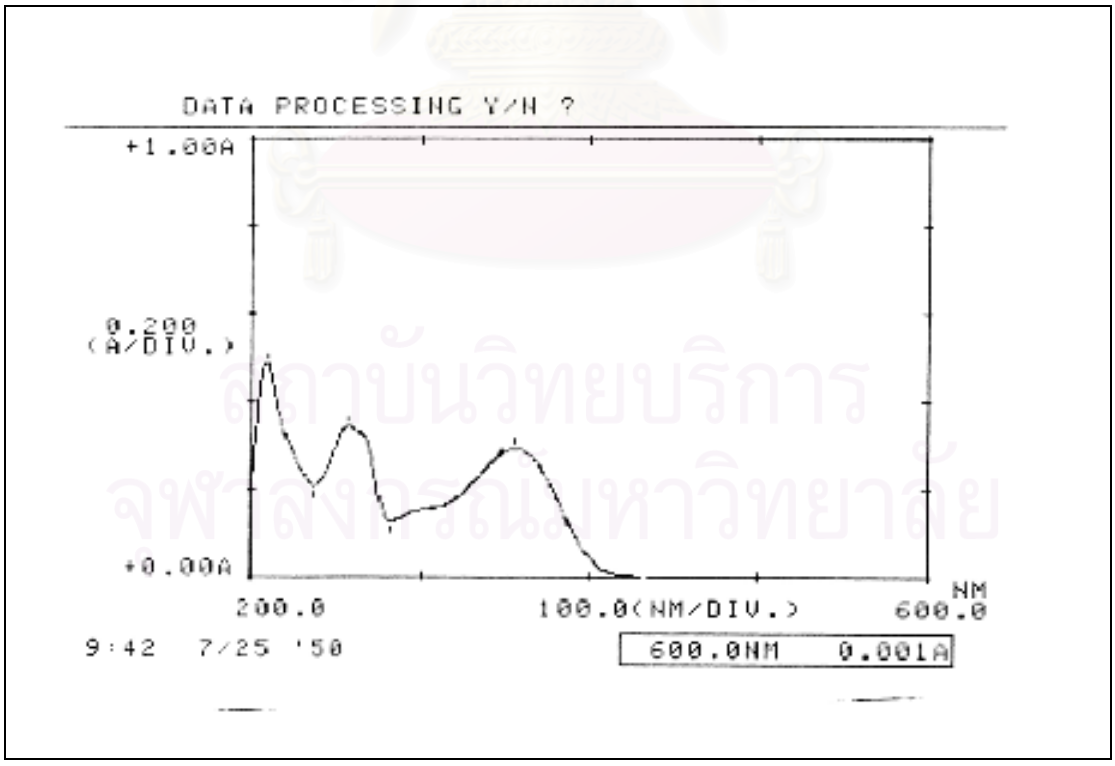

Figure 17. UV Spectrum of compound CAR-3 (in MeOH)

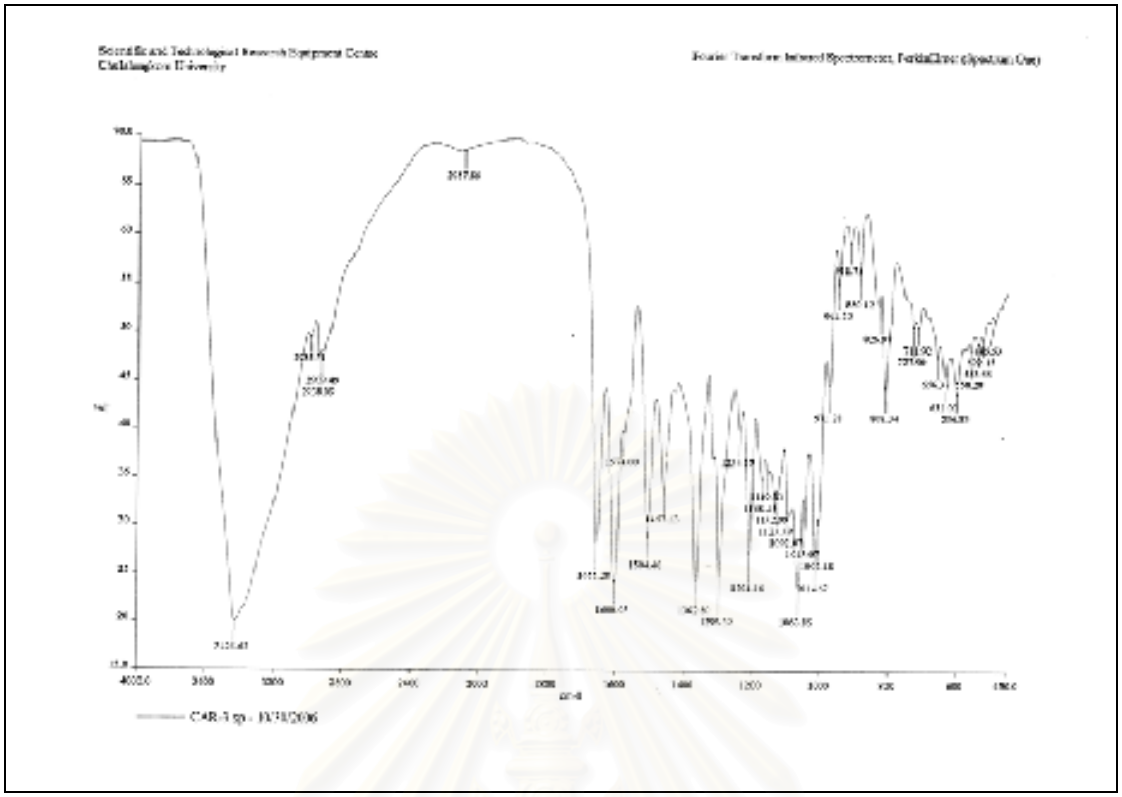

Figure 18. IR Spectrum of compound CAR-3 (KBr disc)

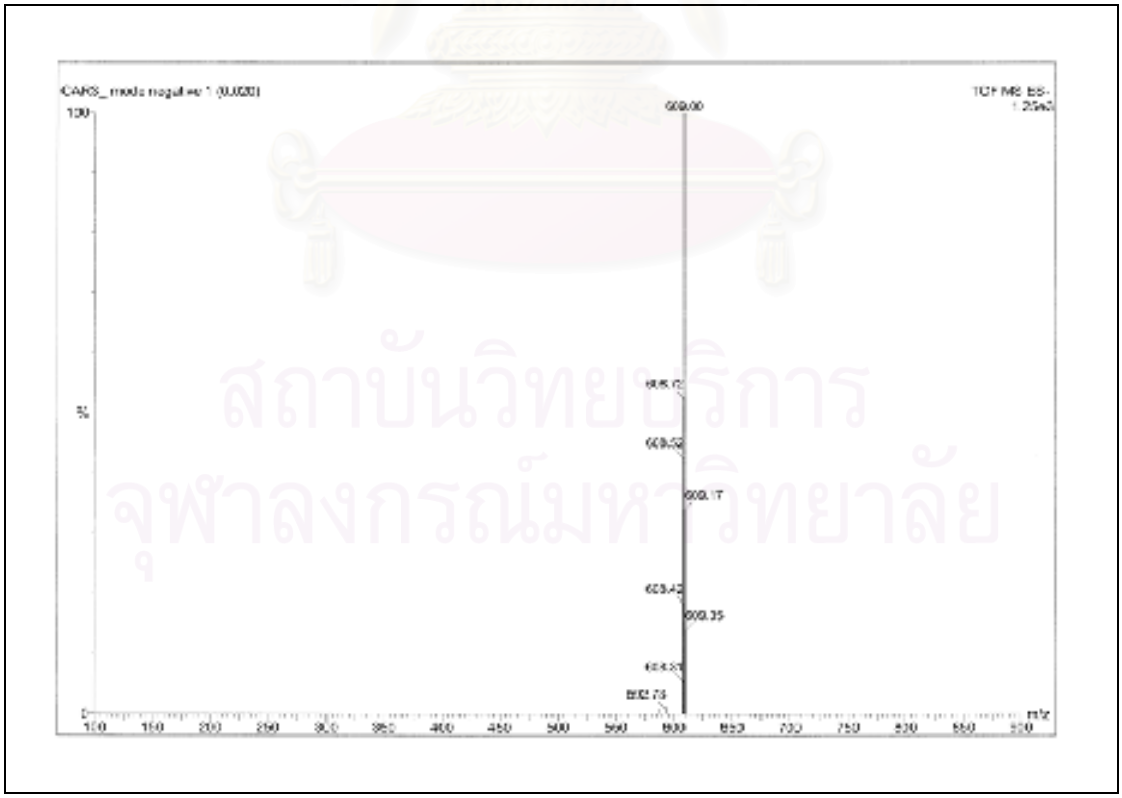

Figure 19. ESI Mass spectrum of compound CAR-3

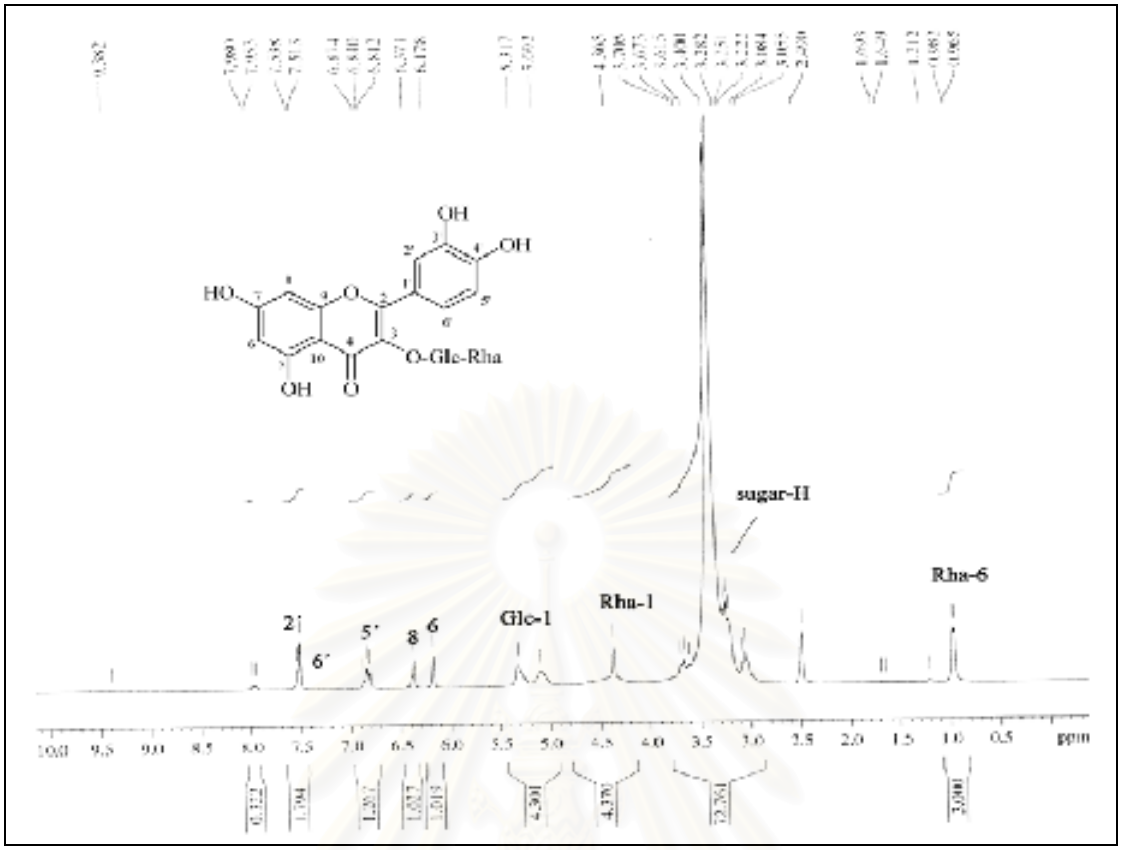

Figure 20. ^{1}H NMR (300 MHz) Spectrum of compound CAR-3 (in DMSO-d_6)

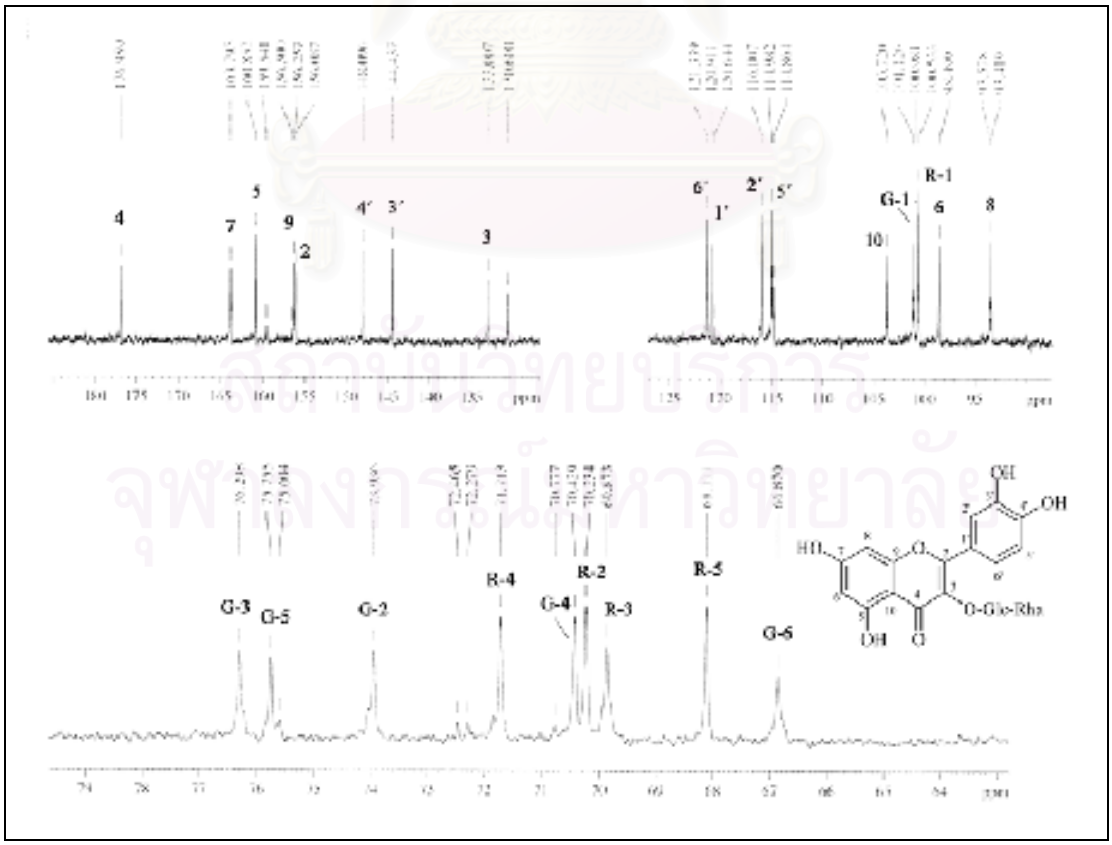

Figure 21. ^{13}C NMR (75 MHz) Spectrum of compound CAR-3 (in DMSO-d_6)

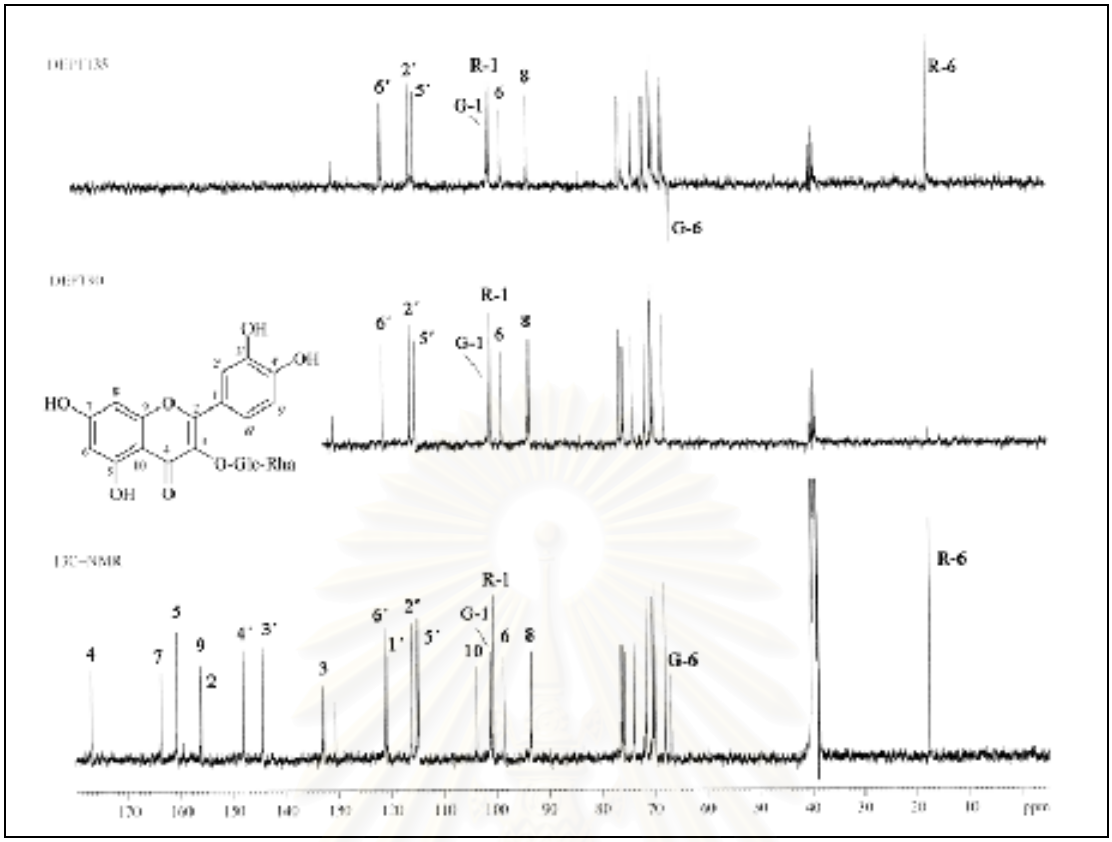

Figure 22. DEPT 135, DEPT 90 and ^{13}C NMR Spectrum of compound CAR-3

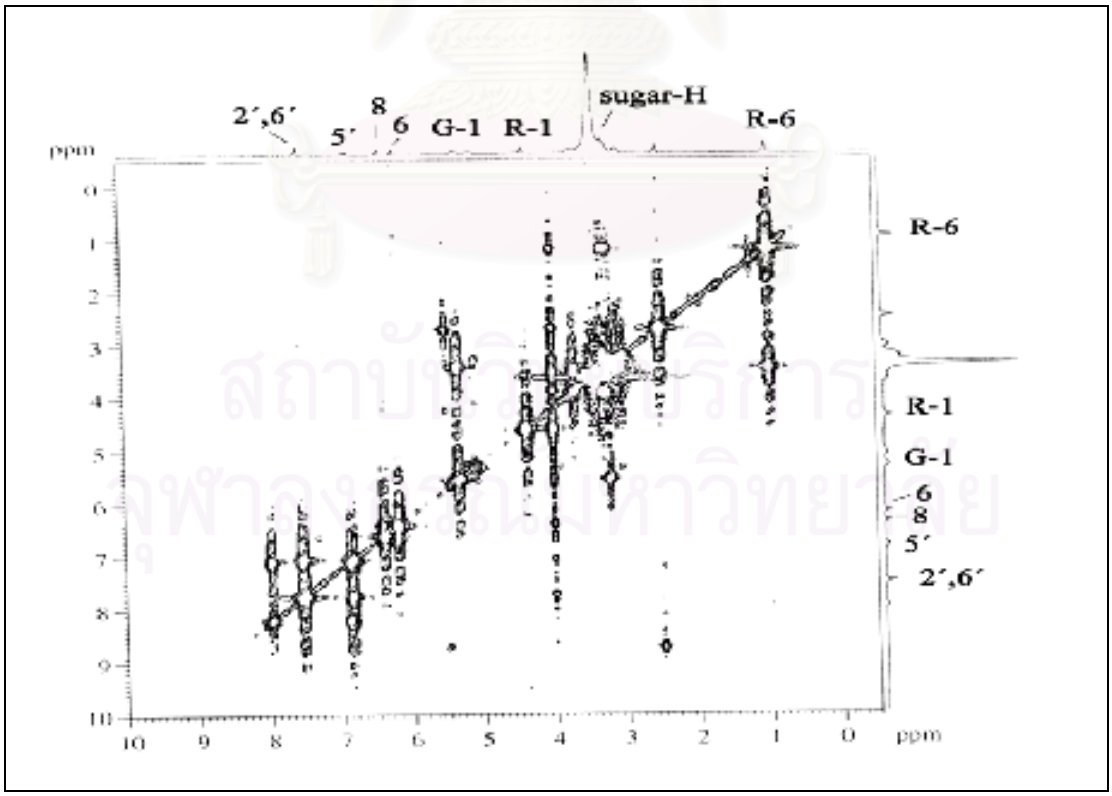

Figure 23. ^{1}H-^{1}H COSY Spectrum of compound CAR-3

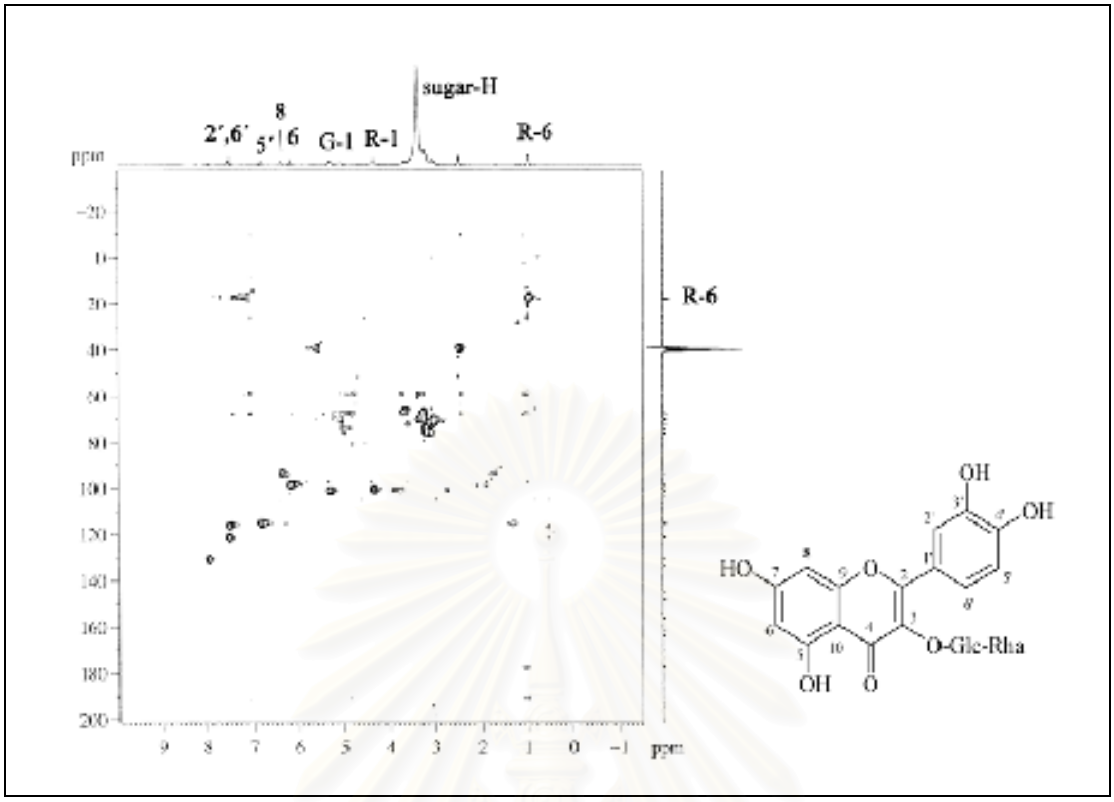

Figure 24. HMQC Spectrum of compound CAR-3

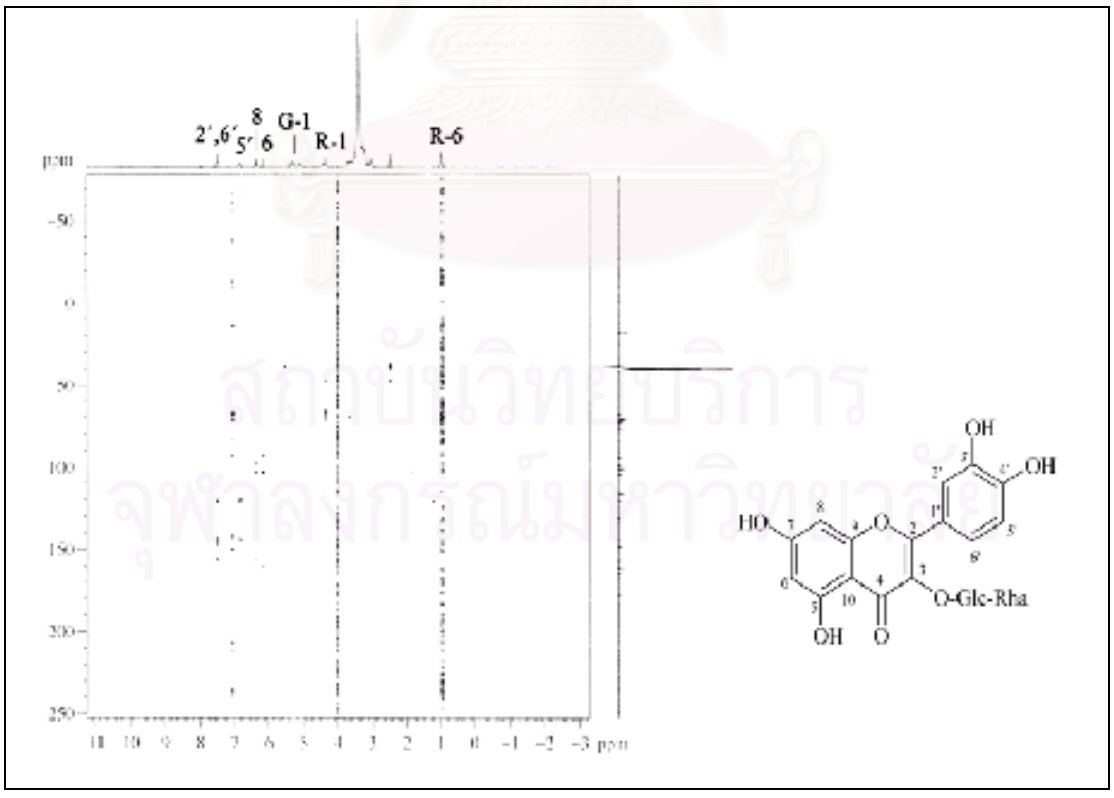

Figure 25. HMBC Spectrum of compound CAR-3

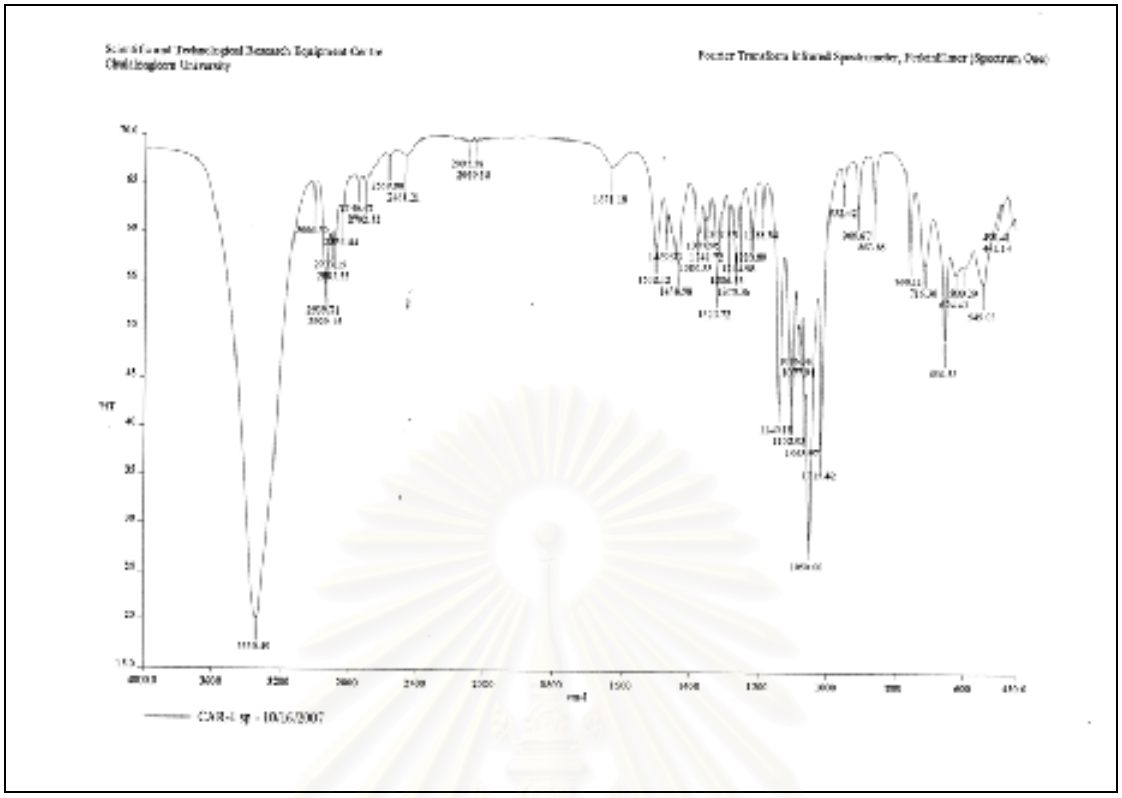

Figure 26. IR Spectrum of compound CAR-4 (KBr disc)

Figure 27. ESI Mass spectrum of compound CAR-4

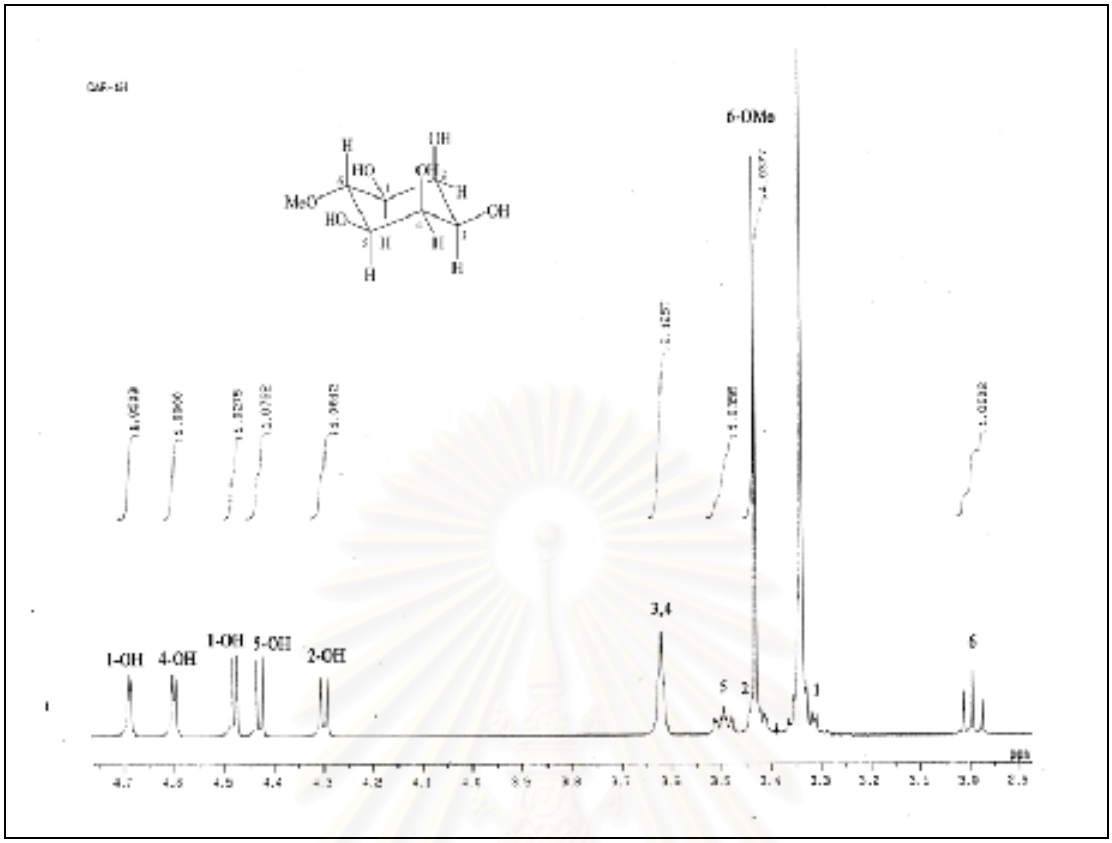

Figure 28. ^{1}H NMR (500 MHz) Spectrum of compound CAR-4 (in DMSO-d_6)

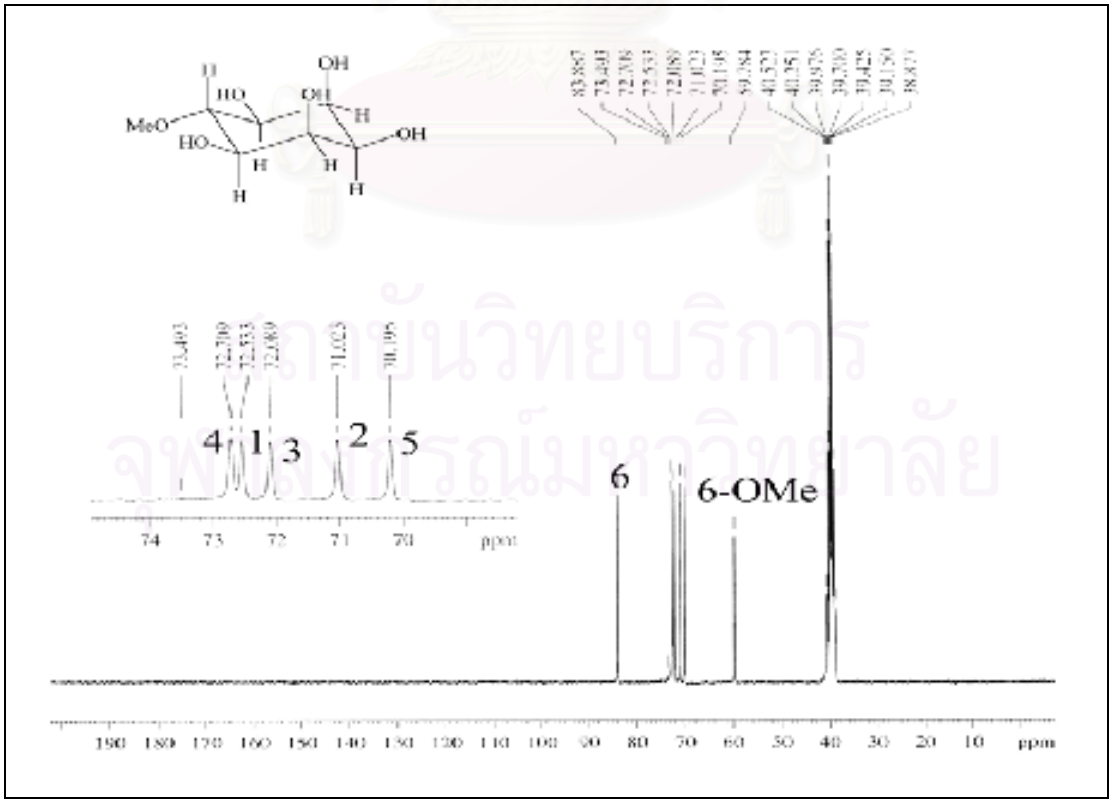

Figure 29. ^{13}C NMR (75 MHz) Spectrum of compound CAR-4 (in DMSO-d_6)

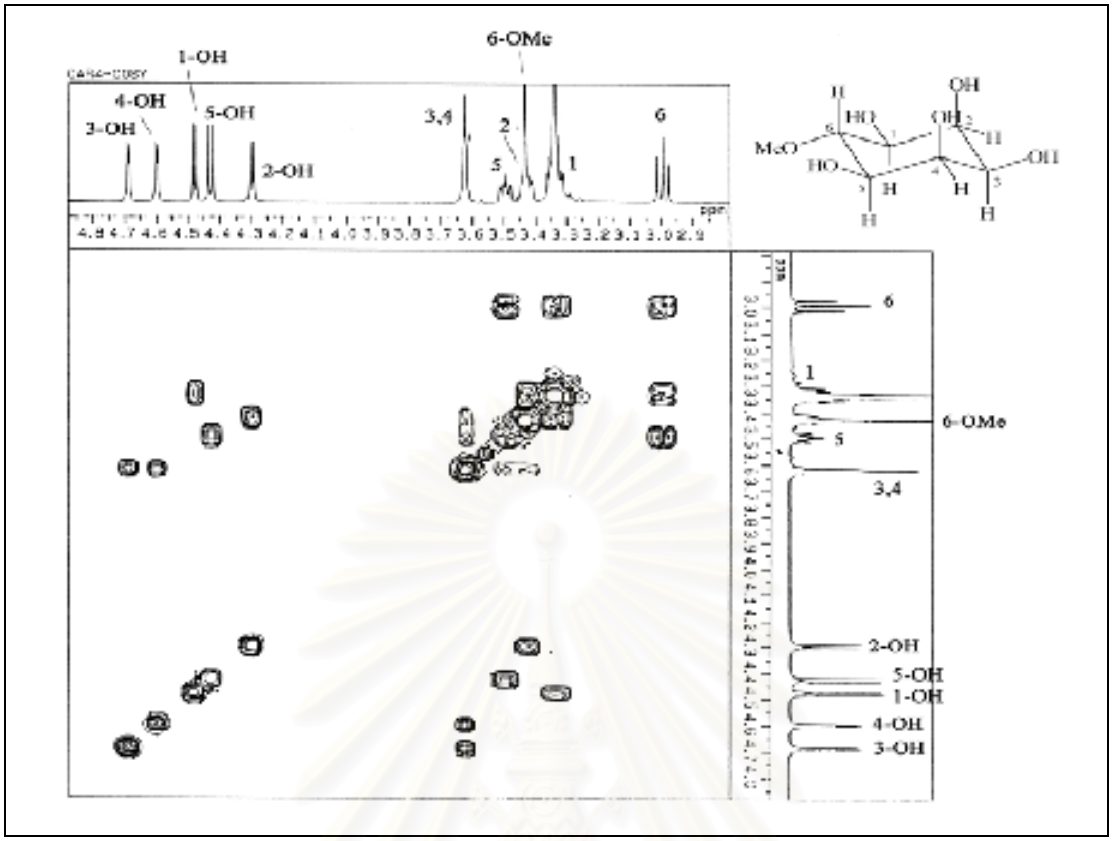

Figure 30. ^{1}H-^{1}H COSY Spectrum of compound CAR-4

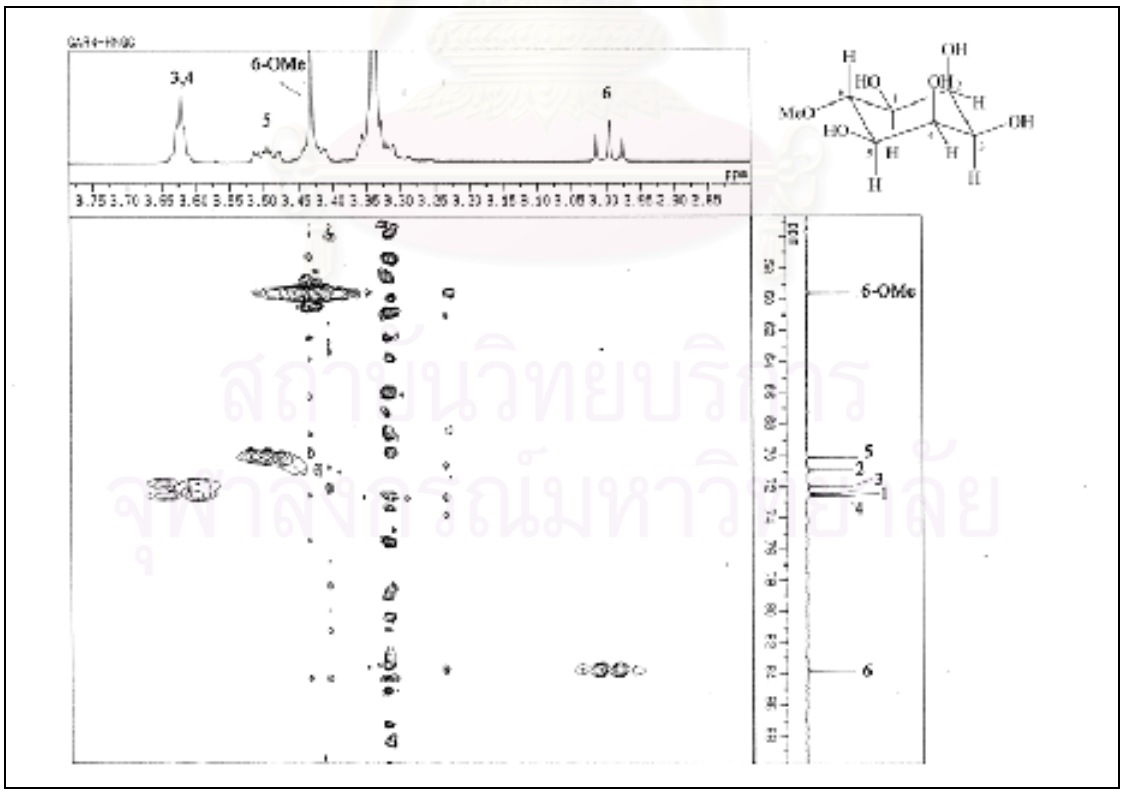

Figure 31. HMQC Spectrum of compound CAR-4
(δ_H 2.85-3.75 ppm, δ_C 56-90 ppm)

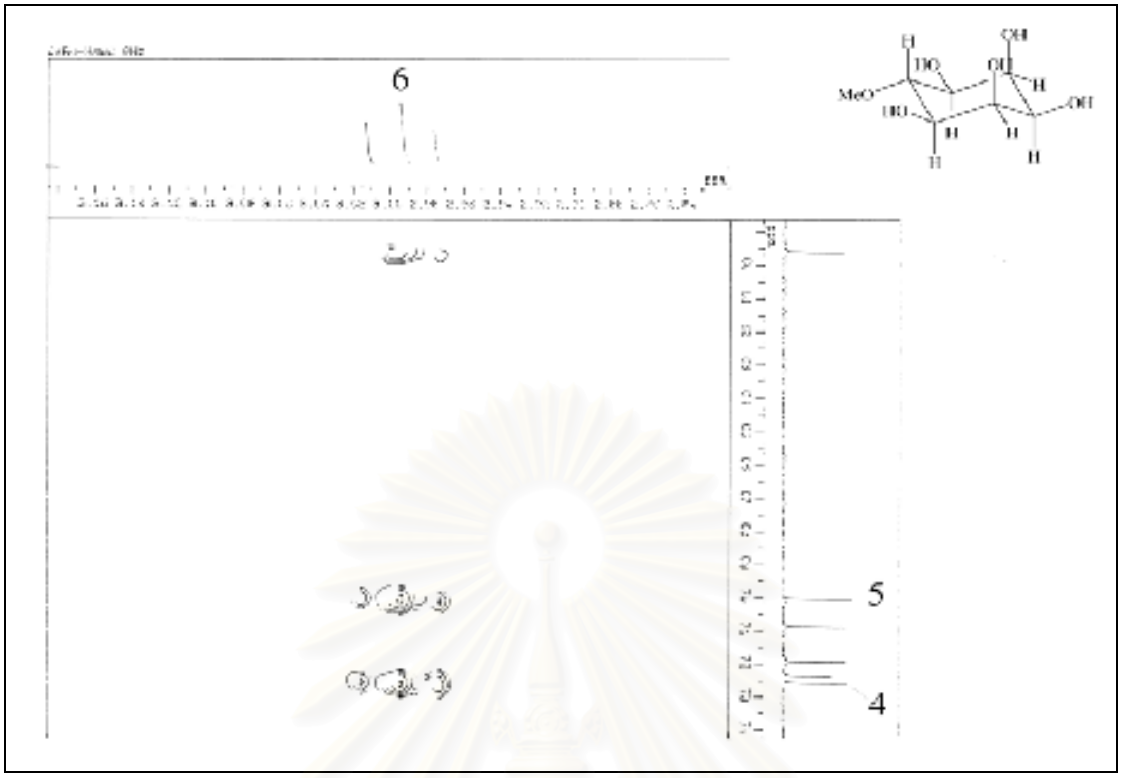

Figure 32a. HMBC Spectrum of compound CAR-4 (δ_H 2.8-3.18 ppm, δ_C 59-74 ppm)

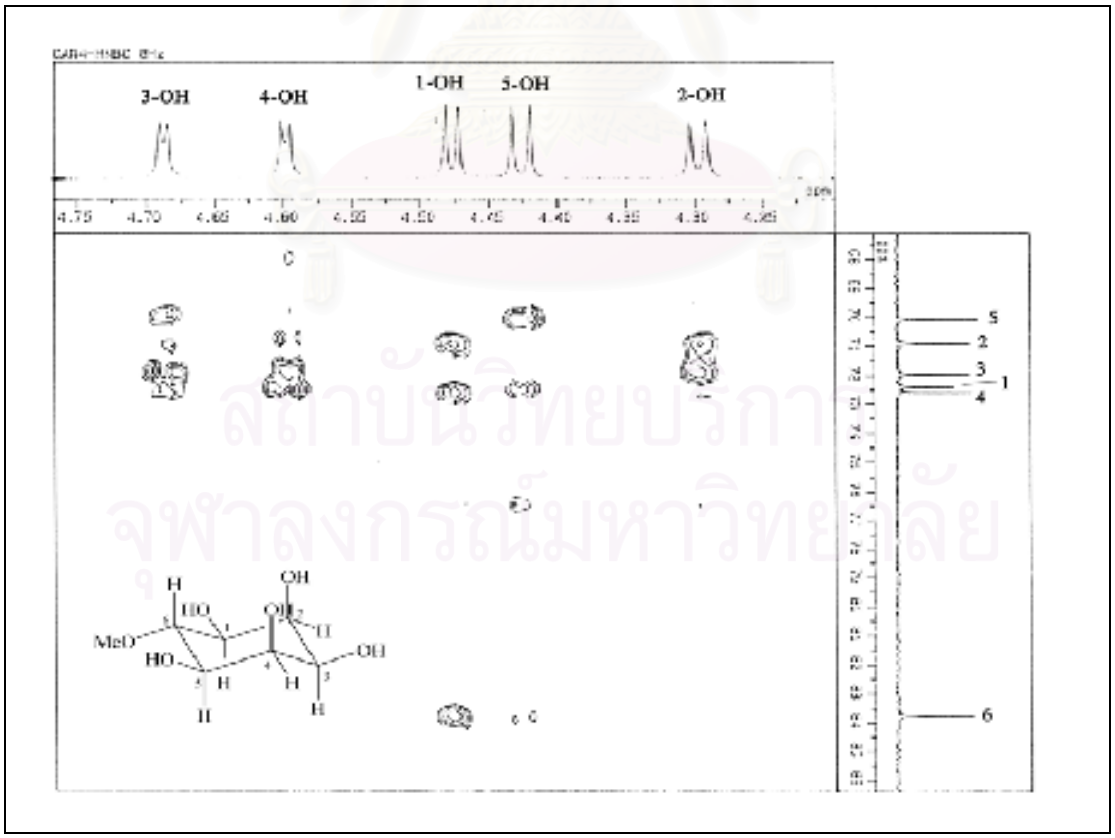

Figure 32b. HMBC Spectrum of compound CAR-4
(δ_H 4.20-4.75 ppm, δ_C 68-86 ppm)

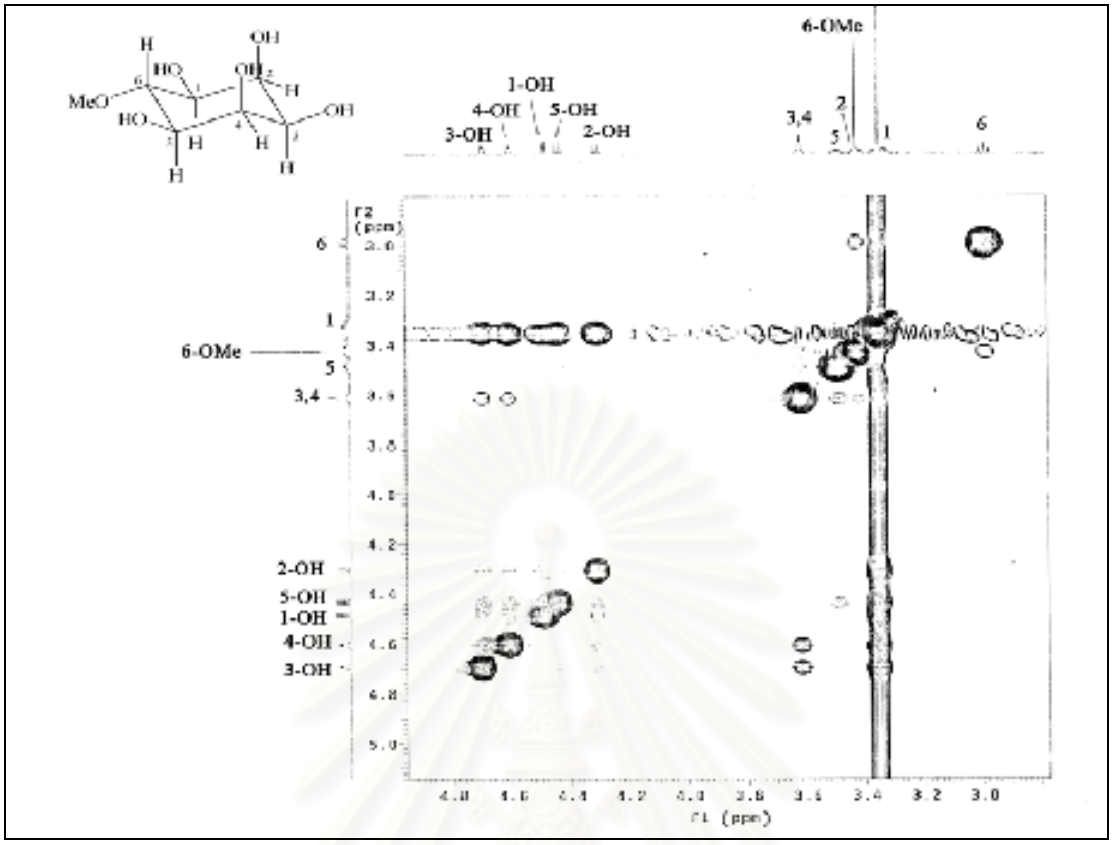

Figure 33. NOESY Spectrum of compound CAR-4

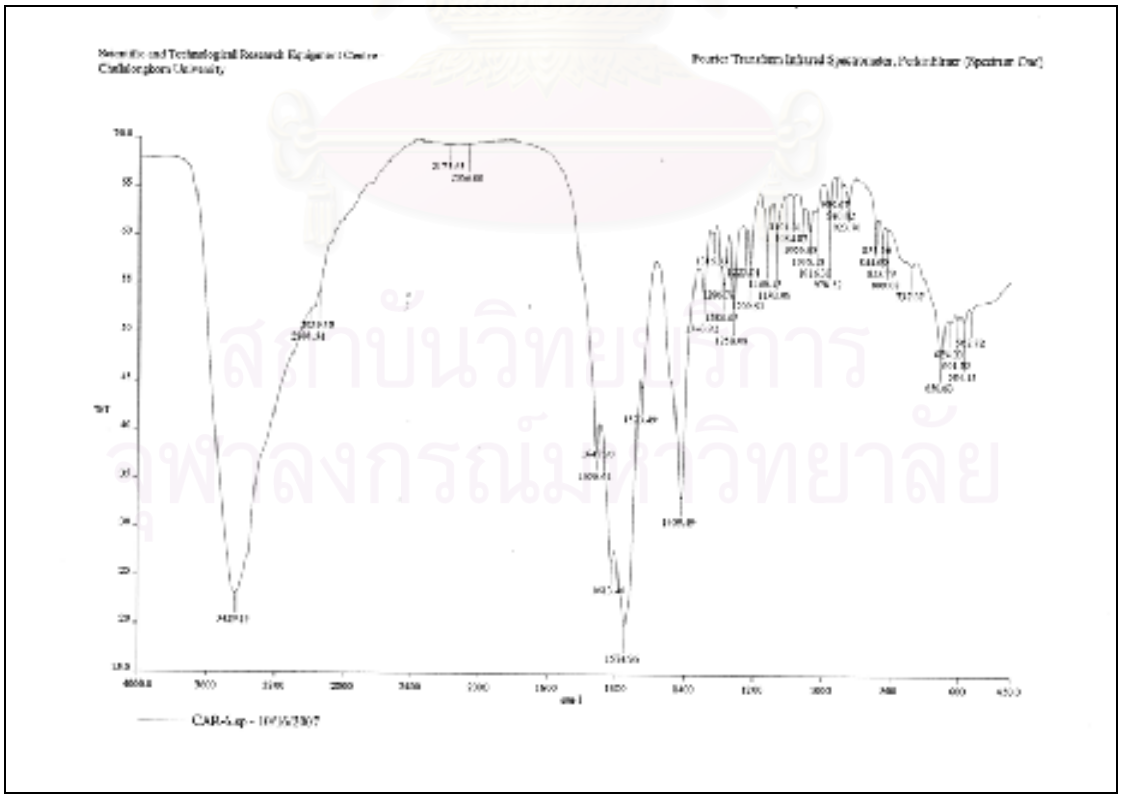

Figure 34. IR Spectrum of compound CAR-6 (KBr disc)

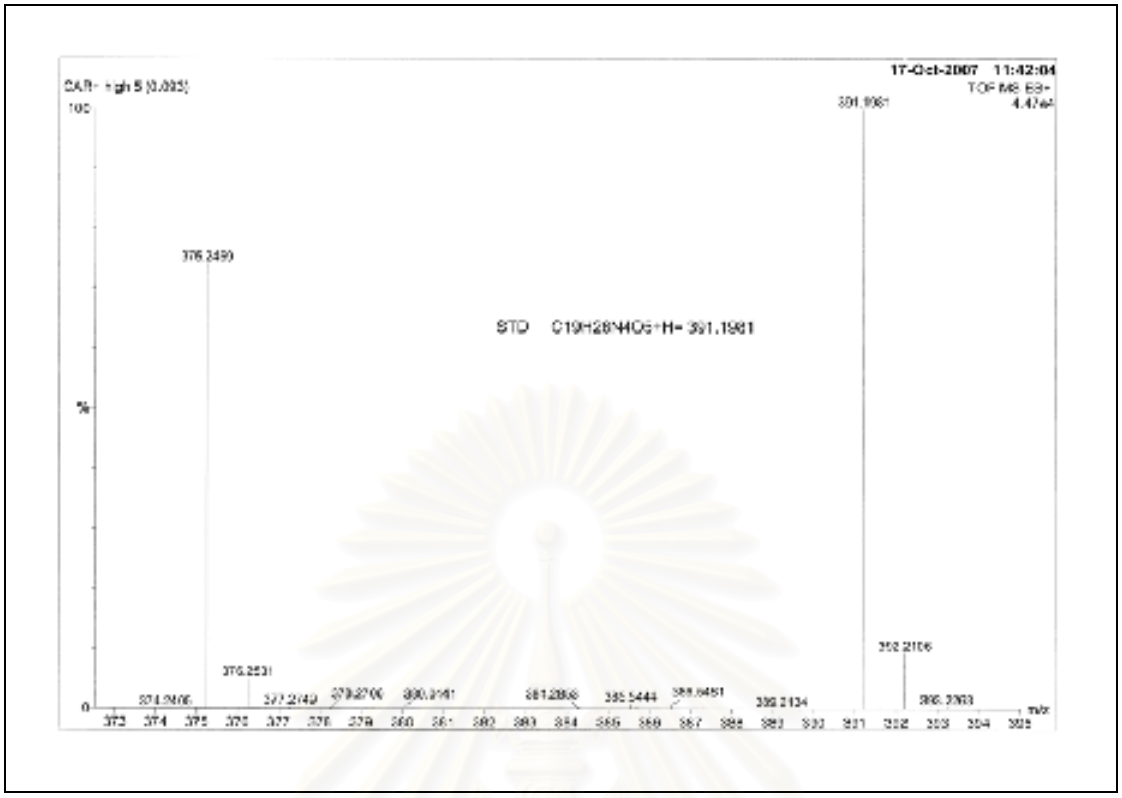

Figure 35. HR ESI Mass spectrum of compound CAR-6

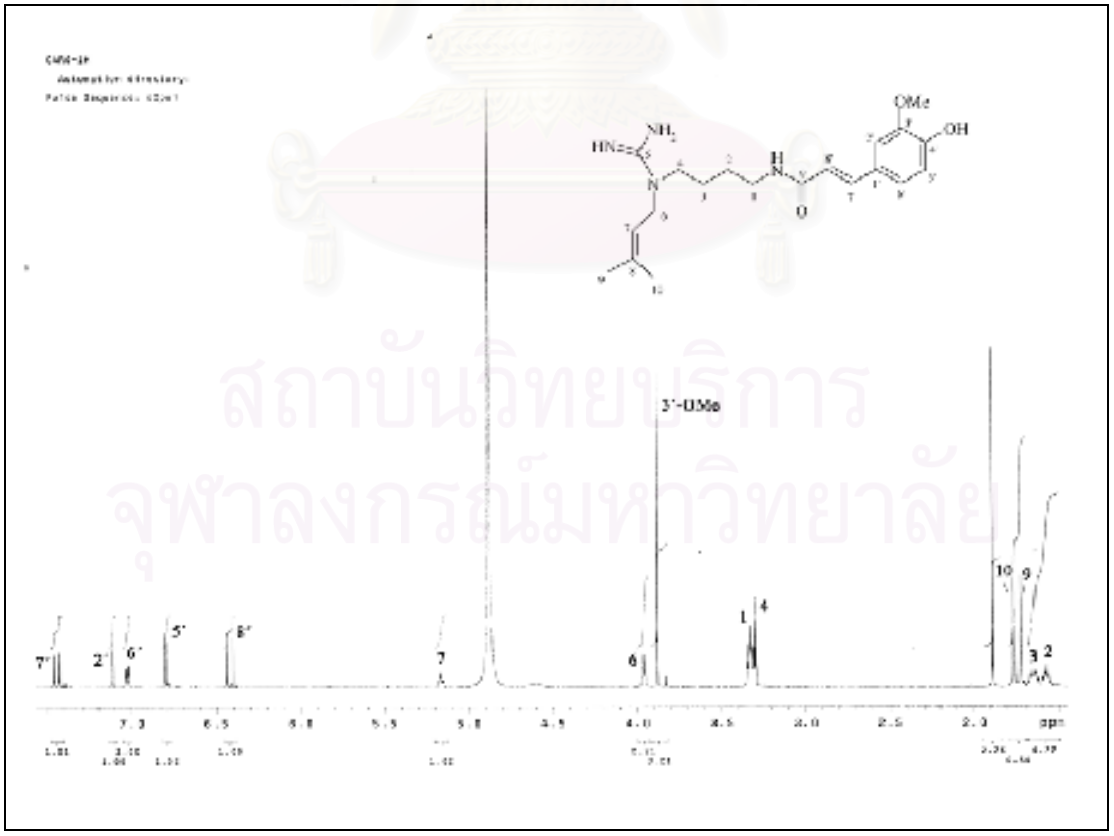

Figure 36a. ^{1}H NMR (500 MHz) Spectrum of compound CAR-6 (in CD_3OD)

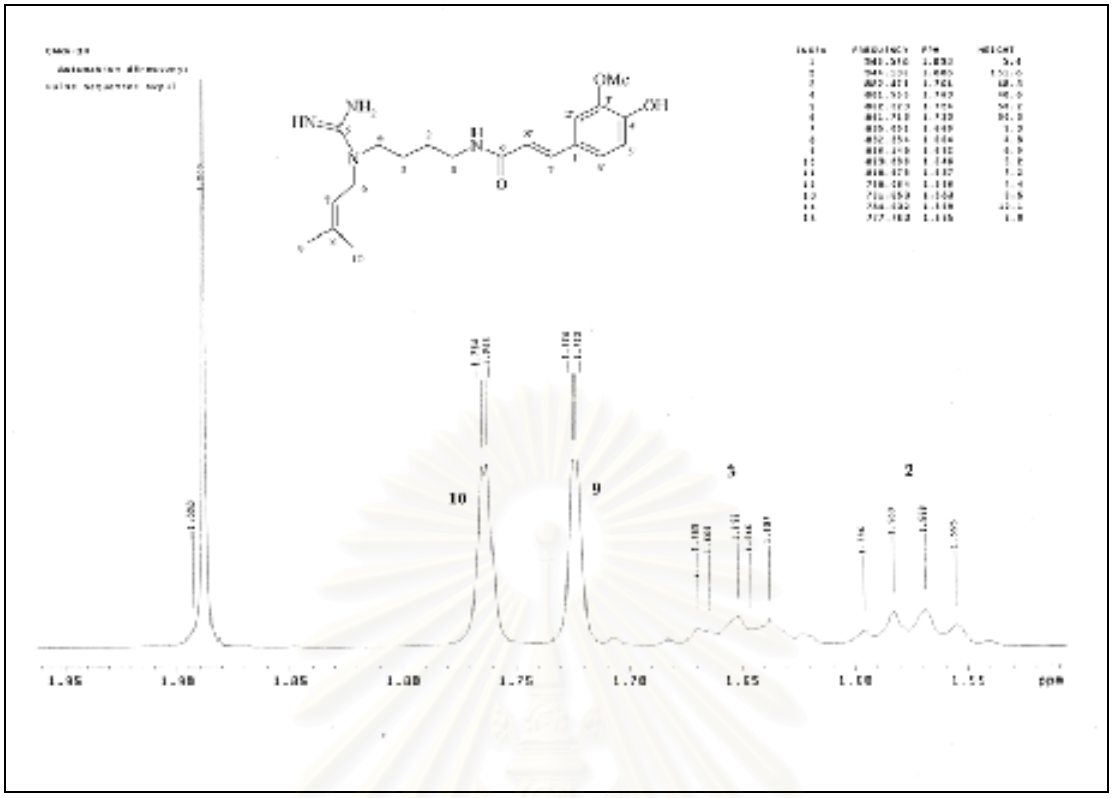

Figure 36b. ^{1}H NMR (500 MHz) Spectrum of compound CAR-6 (δ_H 1.50-1.95 ppm)

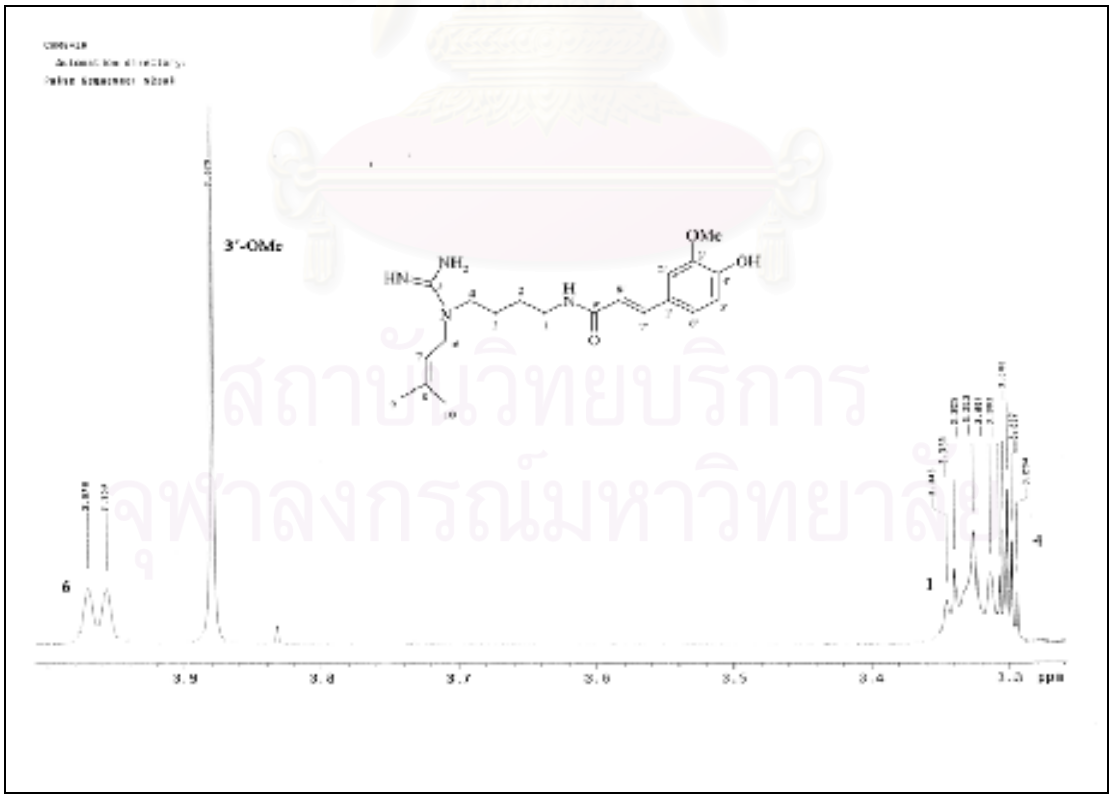

Figure 36c. ^{1}H NMR (500 MHz) Spectrum of compound CAR-6 (δ_H 3.2-4.0 ppm)

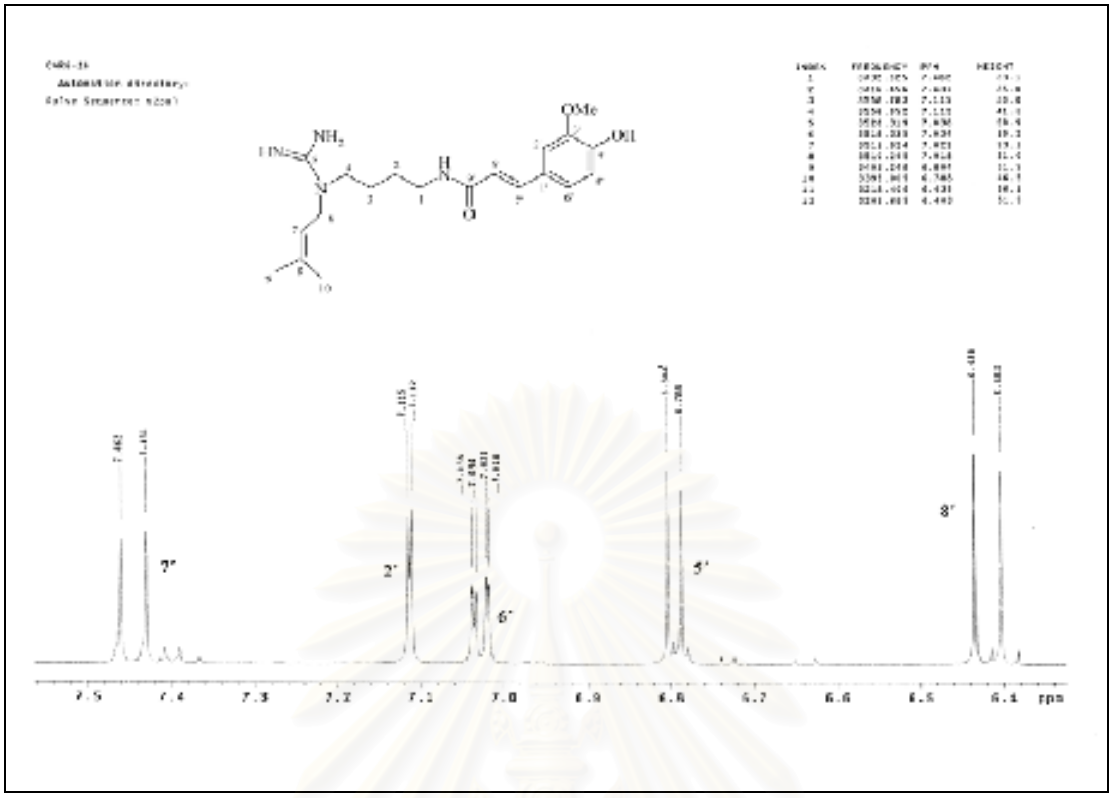

Figure 36d. ^{1}H NMR (500 MHz) Spectrum of compound CAR-6 (δ_H 6.3-7.6 ppm)

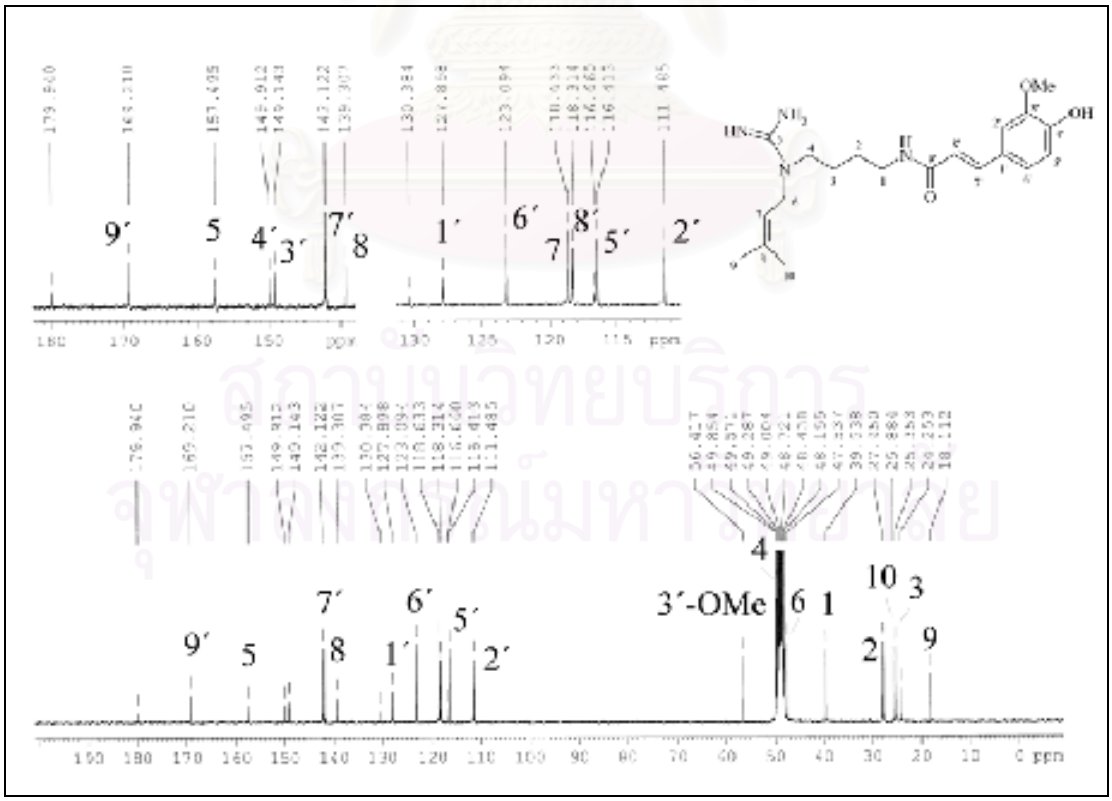

Figure 37. ^{13}C NMR (75 MHz) Spectrum of compound CAR-6 (in CD_3OD)

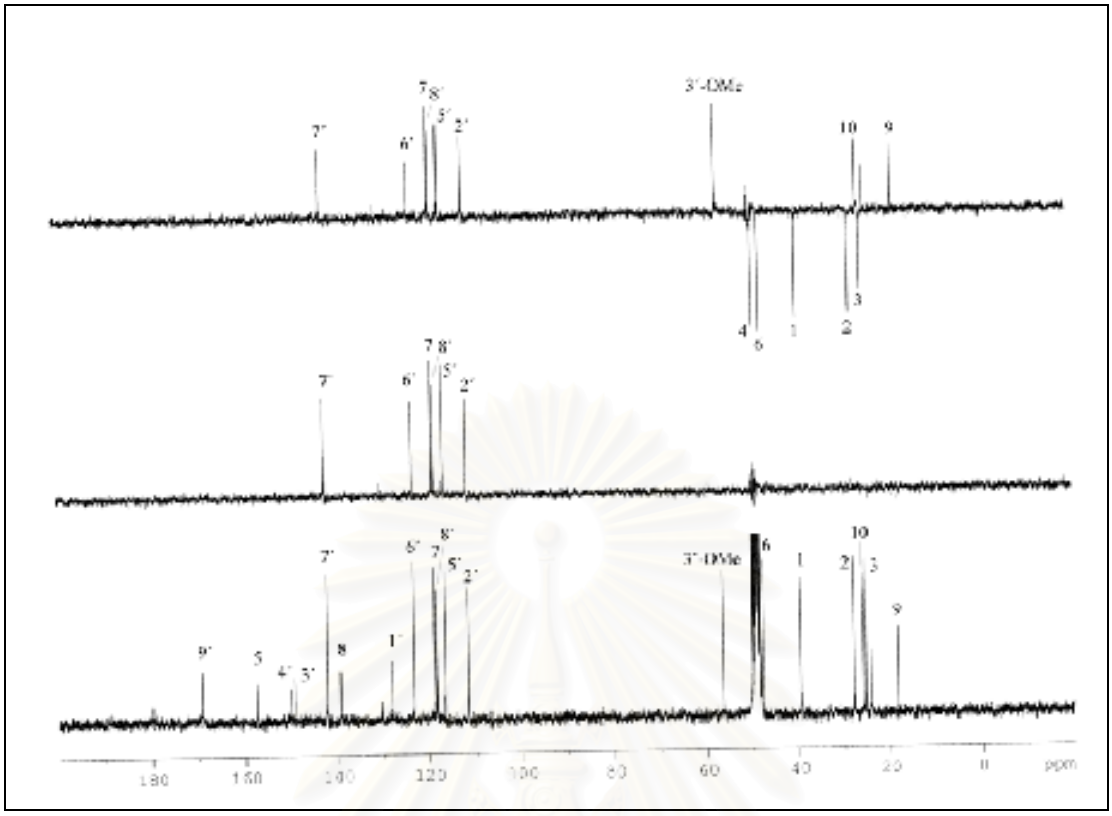

Figure 38. DEPT 135, DEPT 90 and ^{13}C NMR Spectrum of compound CAR-6

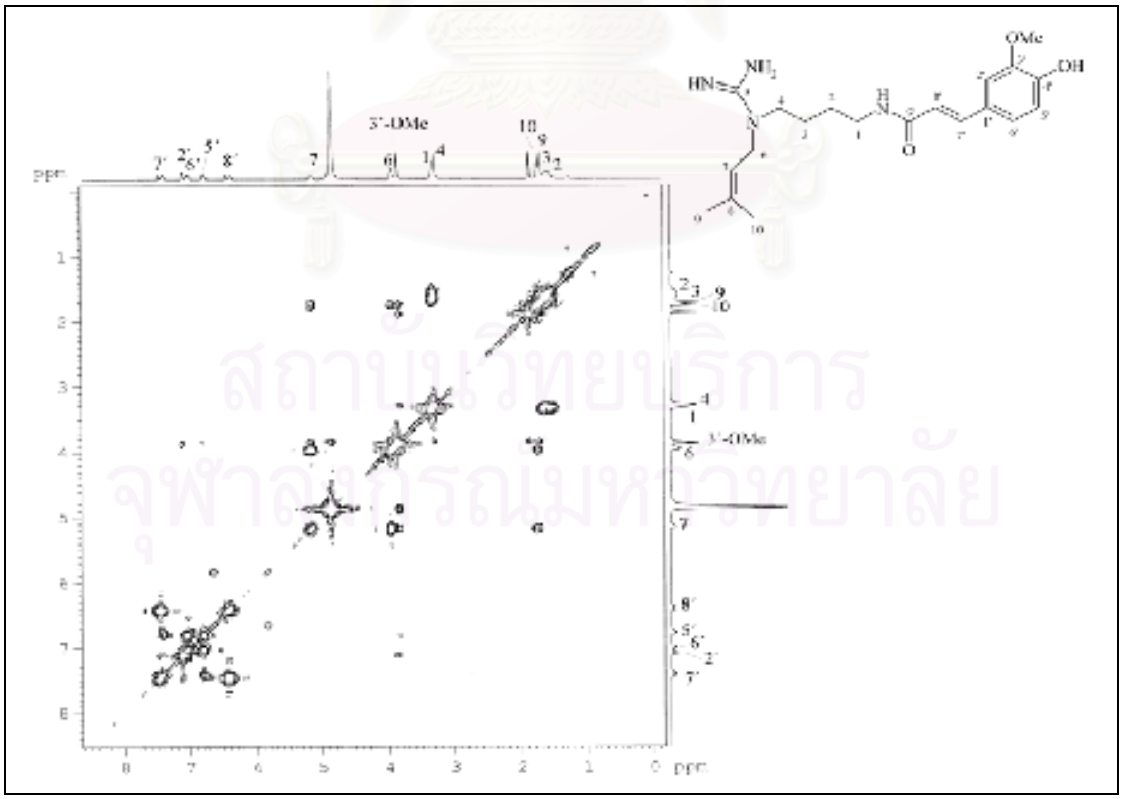

Figure 39. ^{1}H-^{1}H COSY Spectrum of compound CAR-6

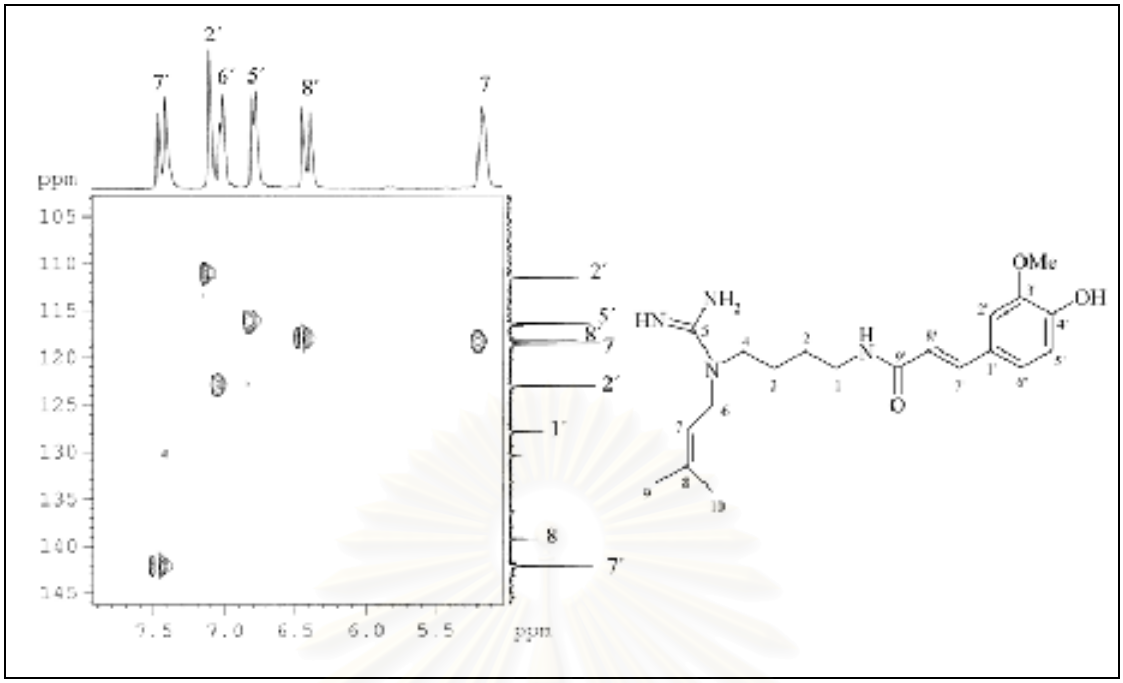

Figure 40a. HMQC Spectrum of compound CAR-6
(δ_H 3.2-4.2 ppm, δ_C 105-145 ppm)

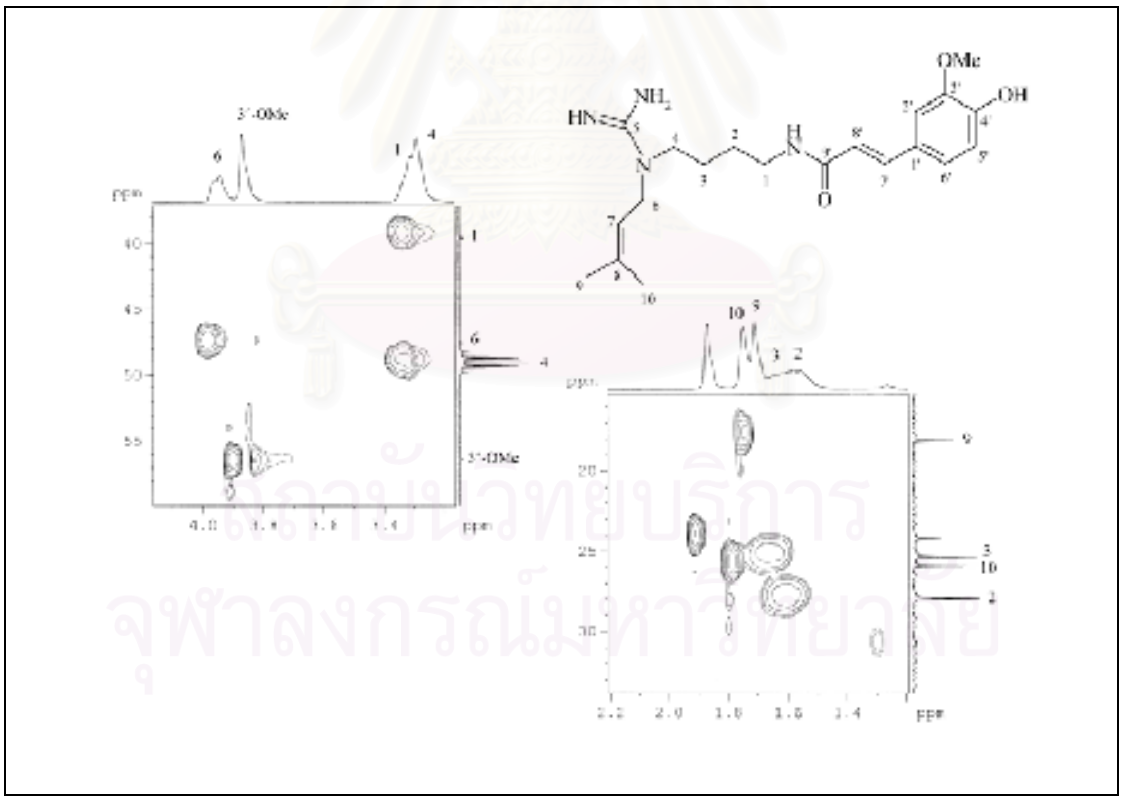

Figure 40b. HMQC Spectrum of compound CAR-6
(δ_H 3.2-4.2 ppm, δ_C 37-60 ppm and δ_H 1.2-2.2 ppm, δ_C 15-35 ppm)

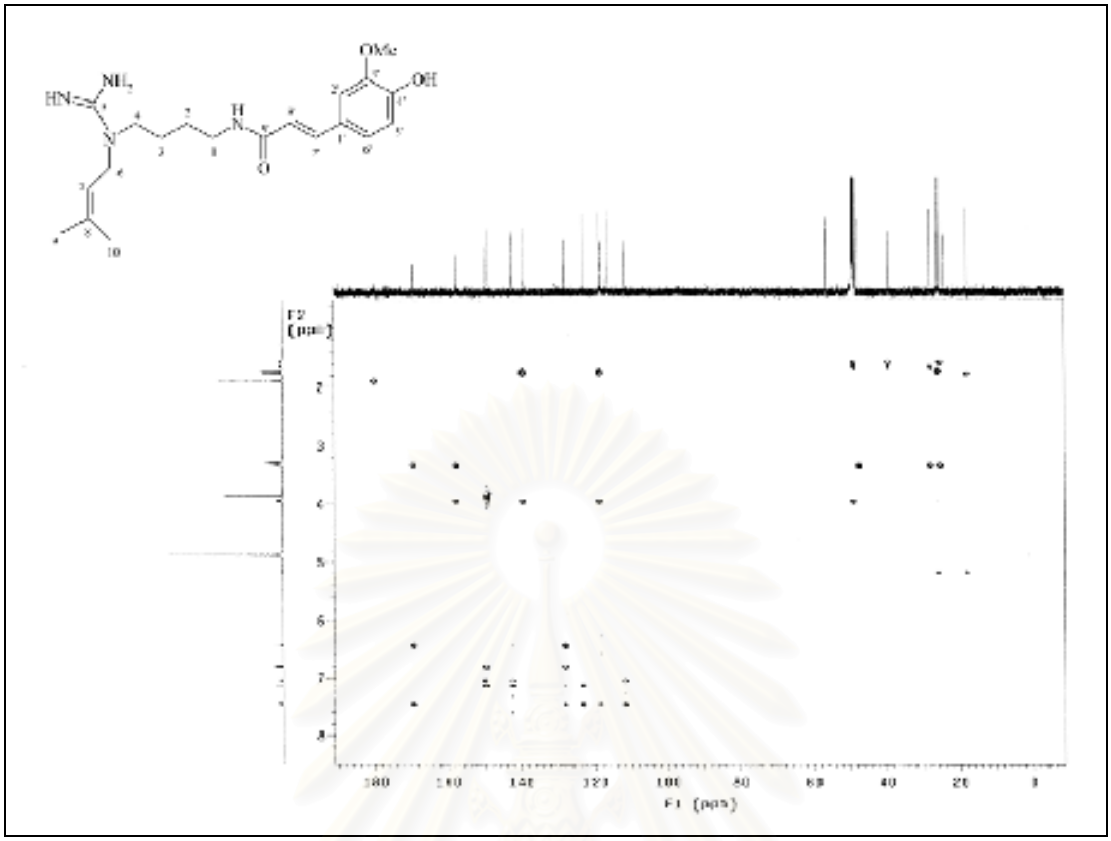

Figure 41a. HMBC Spectrum of compound CAR-6

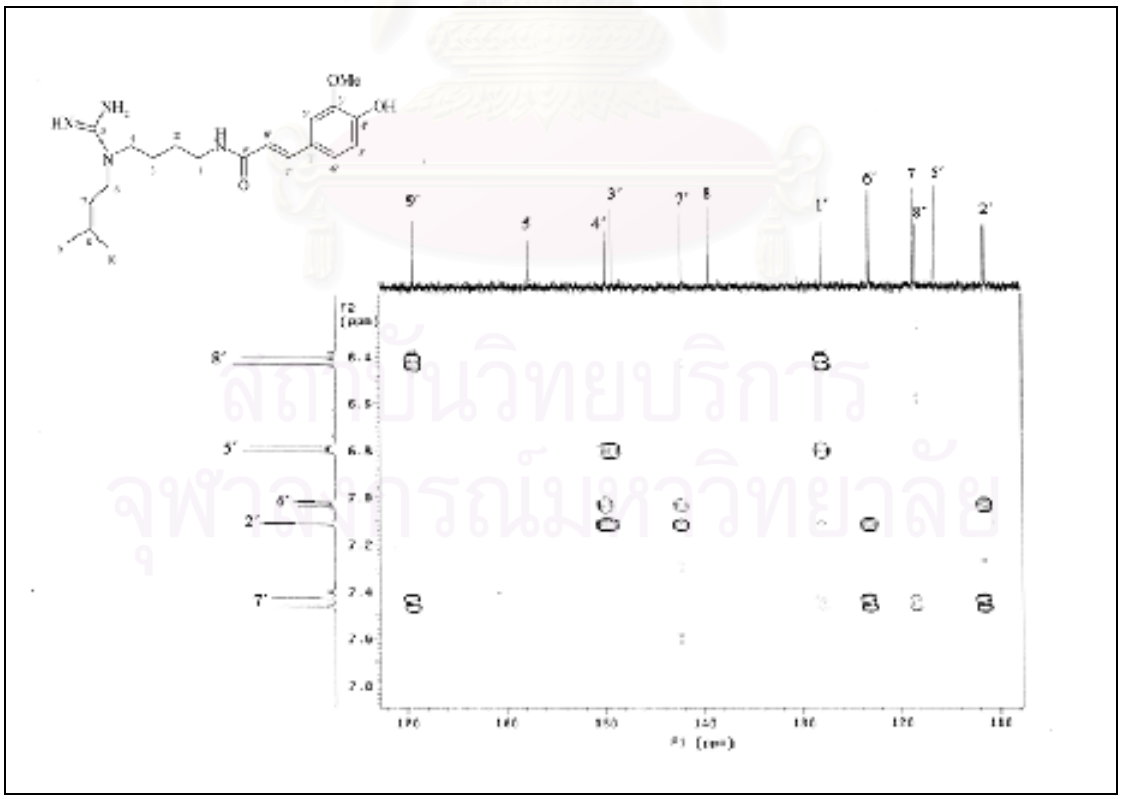

Figure 41b. HMBC Spectrum of compound CAR-6
(δ_H 6.2-7.8 ppm and δ_C 108-170 ppm)

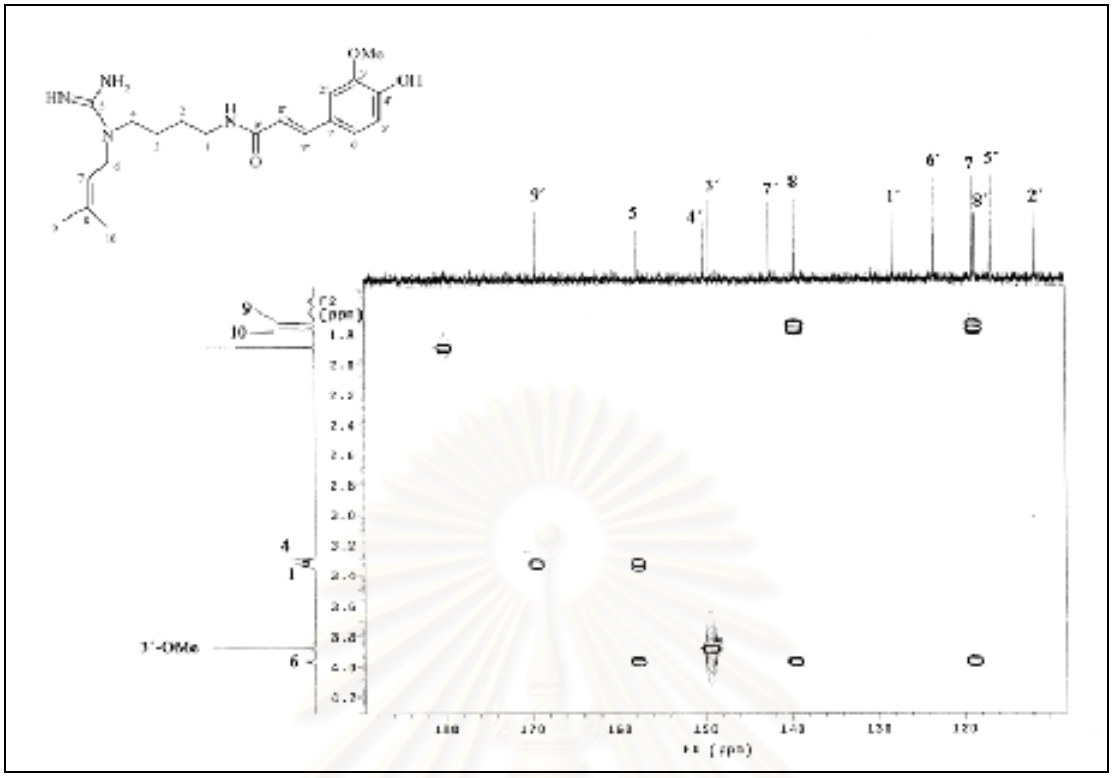

Figure 41c. HMBC Spectrum of compound CAR-6
(δ_H 1.6-4.2 ppm, δ_C 110-190 ppm)

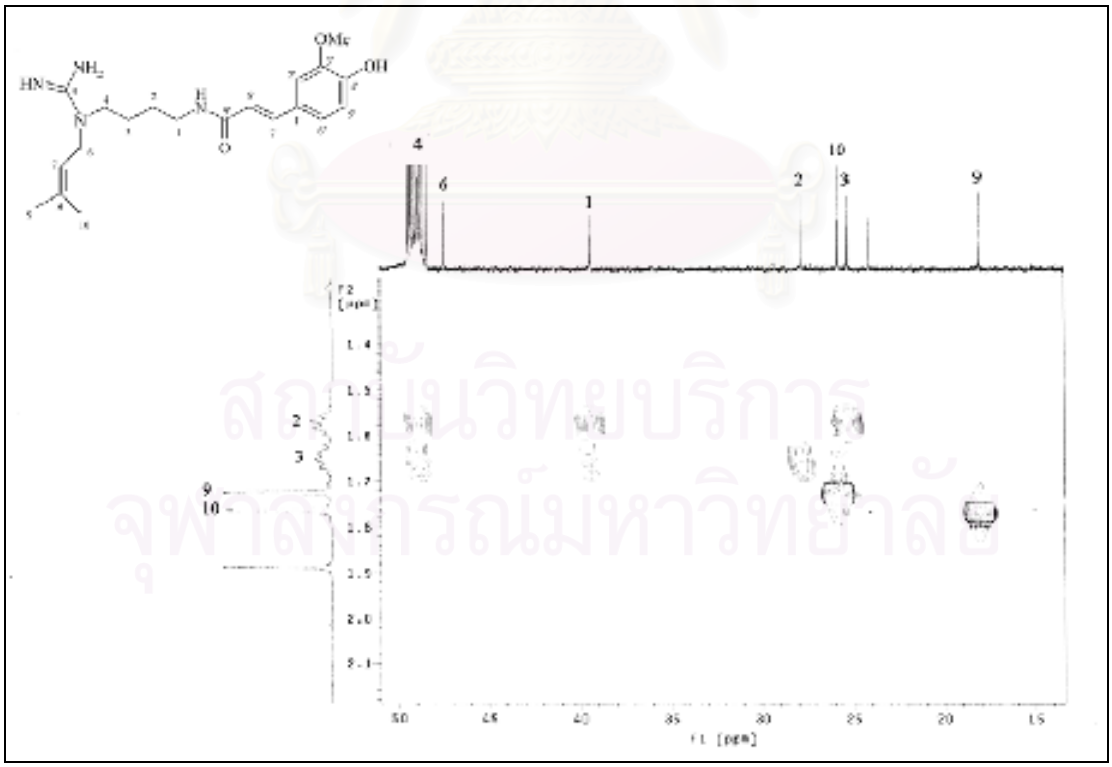

Figure 41d. HMBC Spectrum of compound CAR-6 (δ_H 1.2-2.2 ppm, δ_C 15-50 ppm)

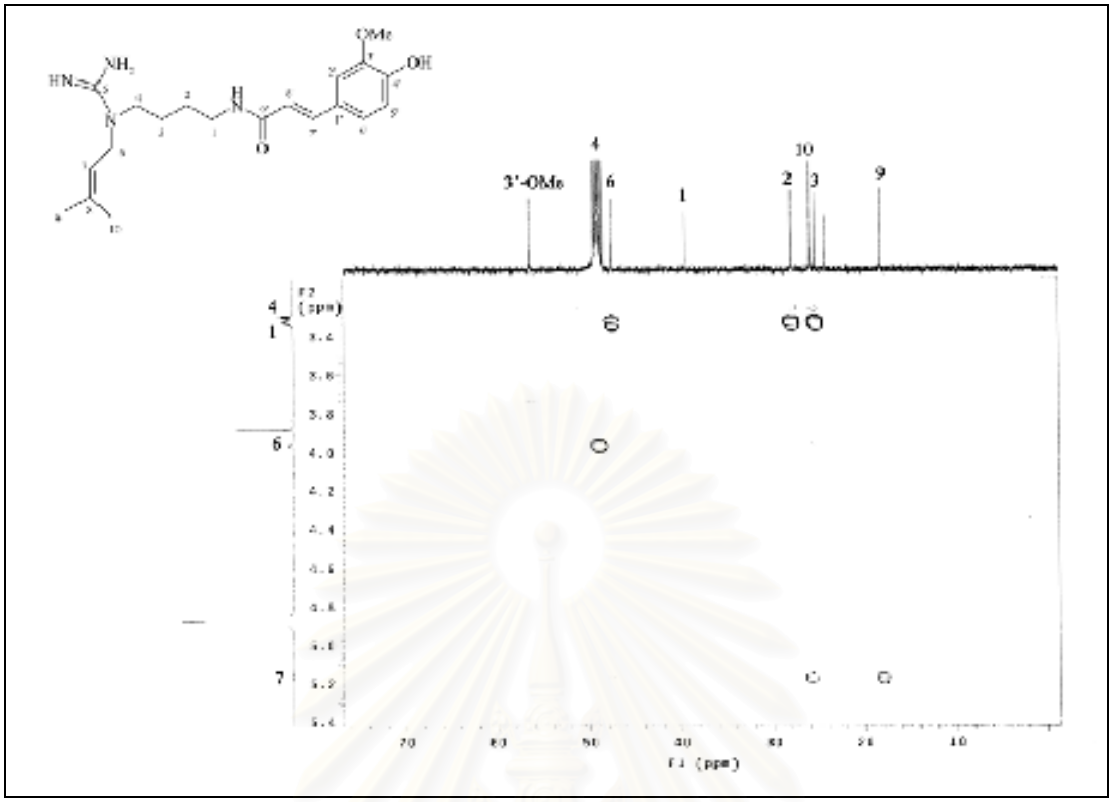

Figure 41e. HMBC Spectrum of compound CAR-6 (δ_H 3.2-5.4 ppm, δ_C 0-75 ppm)

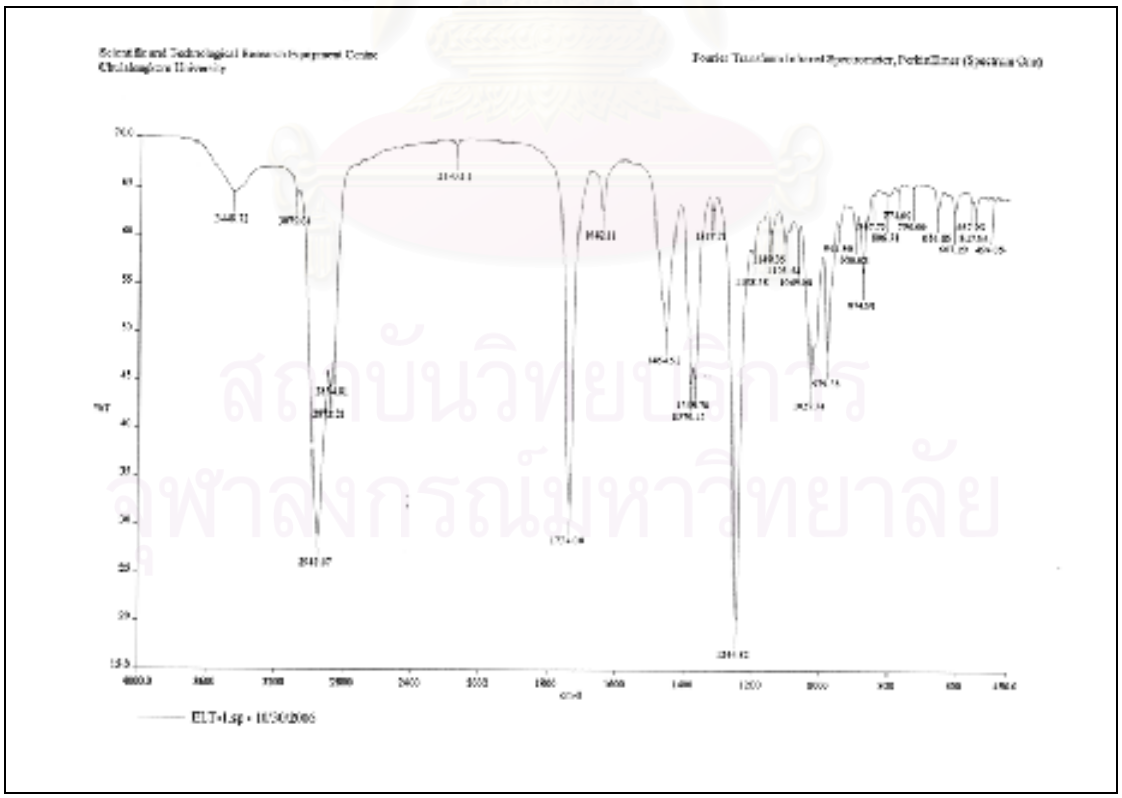

Figure 42. IR Spectrum of compound ET-S1 (KBr disc)

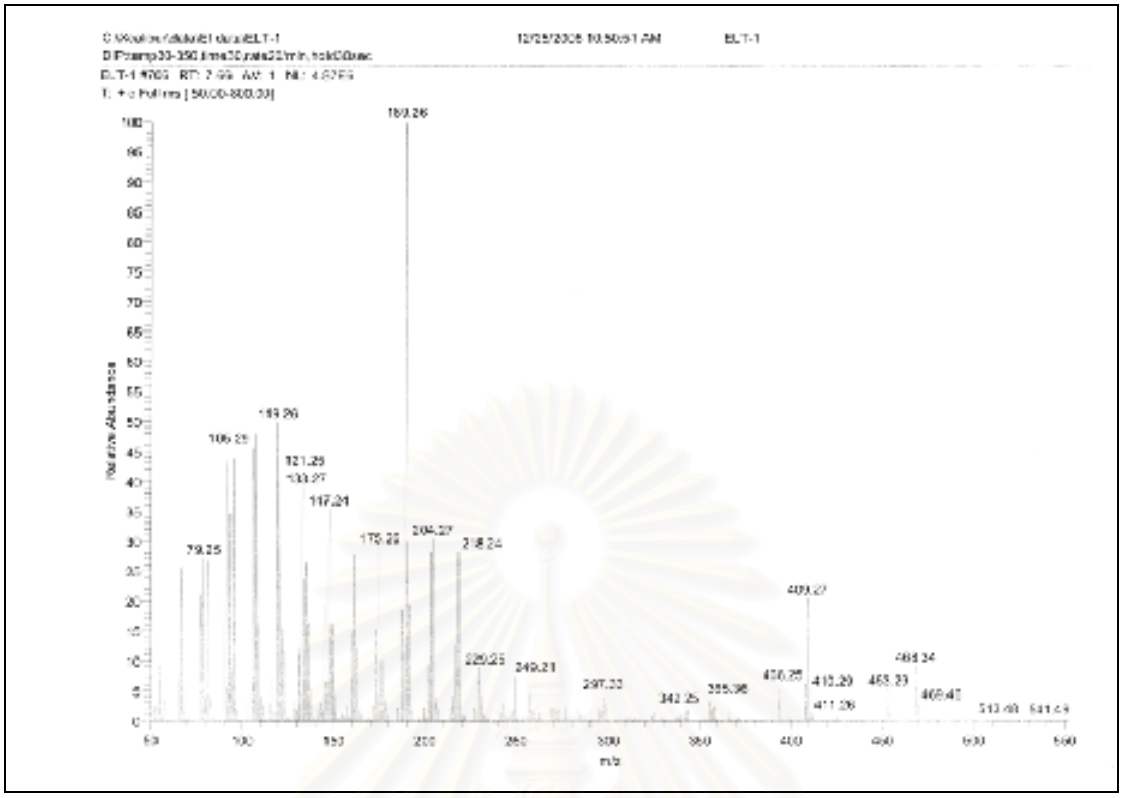

Figure 43. EI Mass spectrum of compound ET-S1

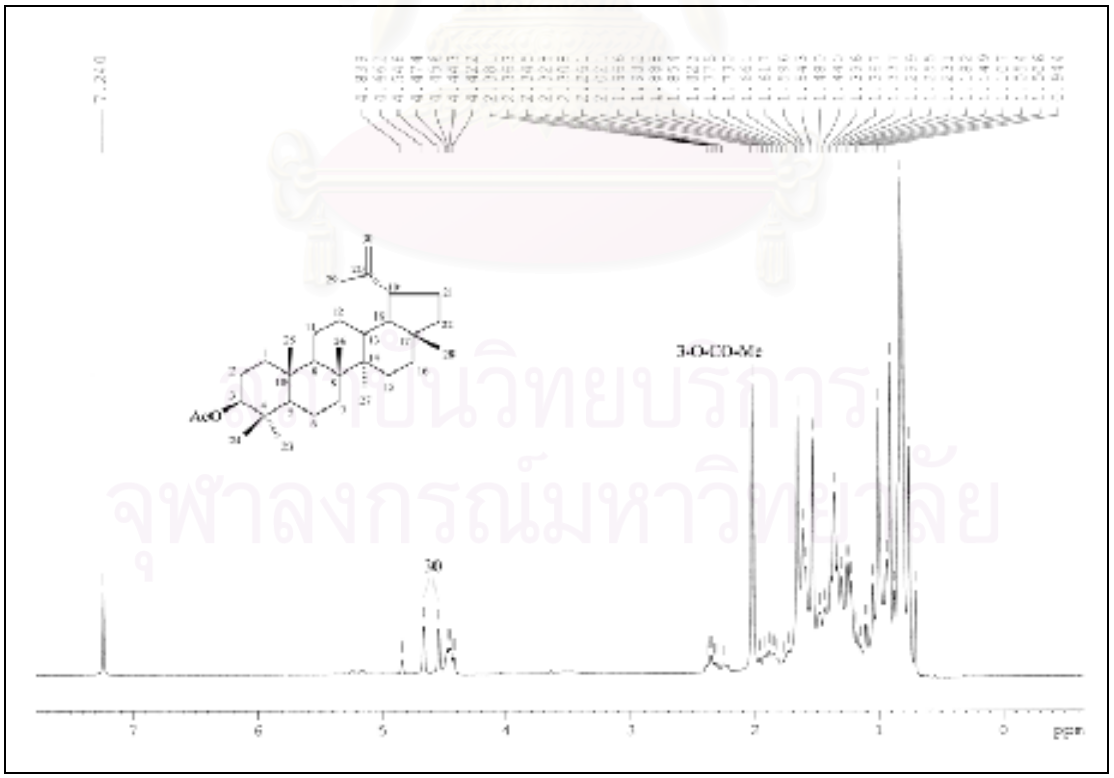

Figure 44. ^{1}H NMR (300 MHz) Spectrum of compound ET-S1 (in $CDCl_3$)

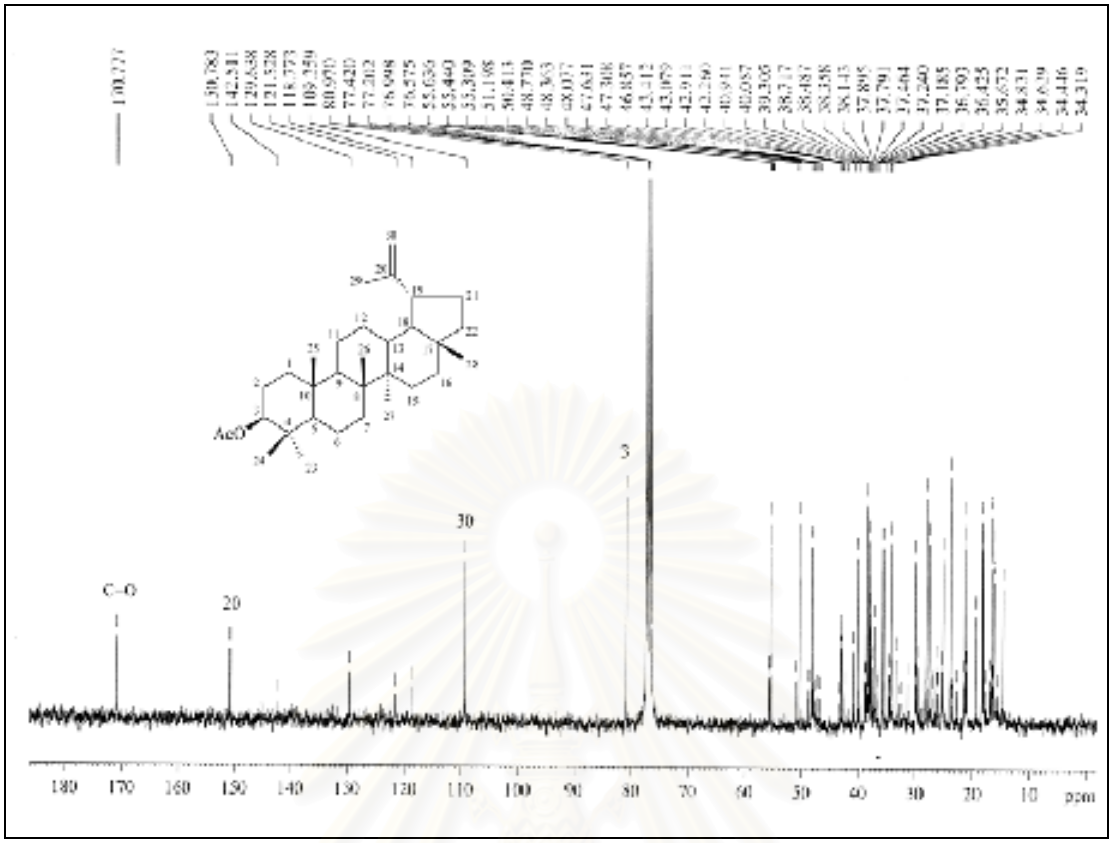

Figure 45a. ^{13}C NMR (75 MHz) Spectrum of compound ET-S1 (in $CDCl_3$)

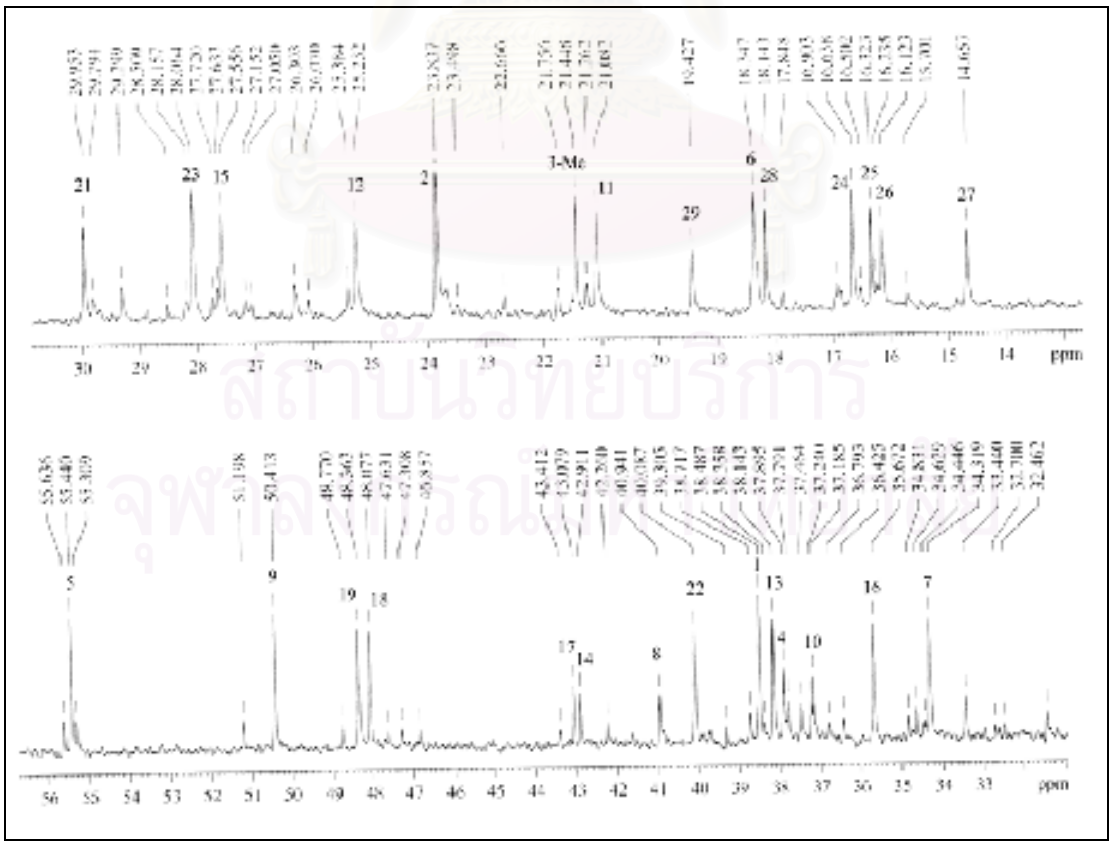

Figure 45b. ^{13}C NMR (75 MHz) Spectrum of compound ET-S1 (δ_C 13-56 ppm)

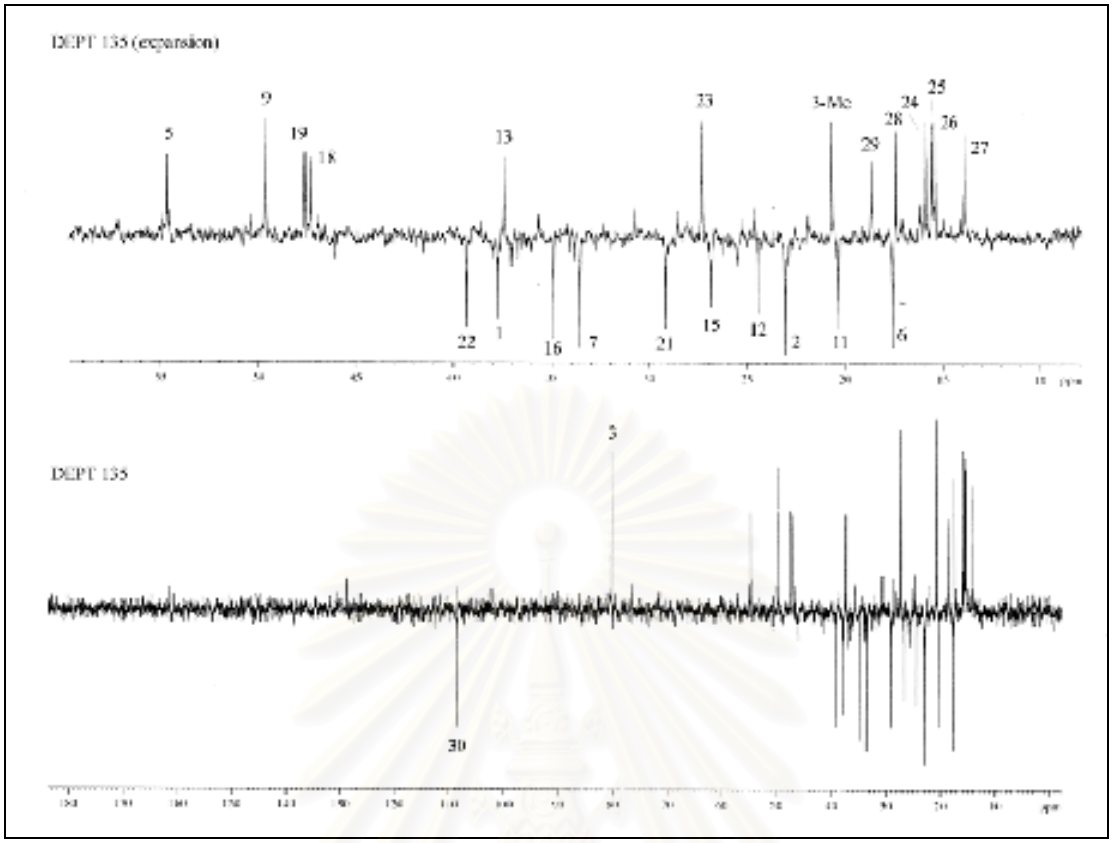

Figure 46. DEPT 135 Spectrum of compound ET-S1

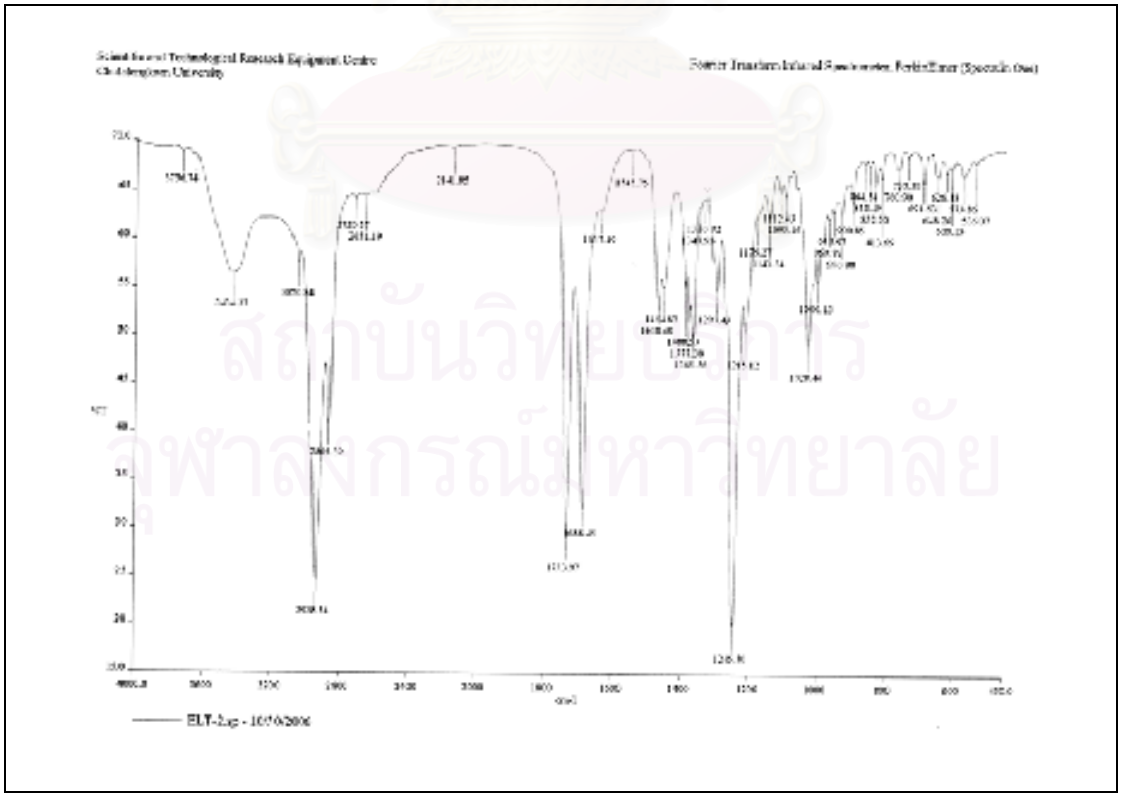

Figure 47. IR Spectrum of compound ET-S2 (KBr disc)

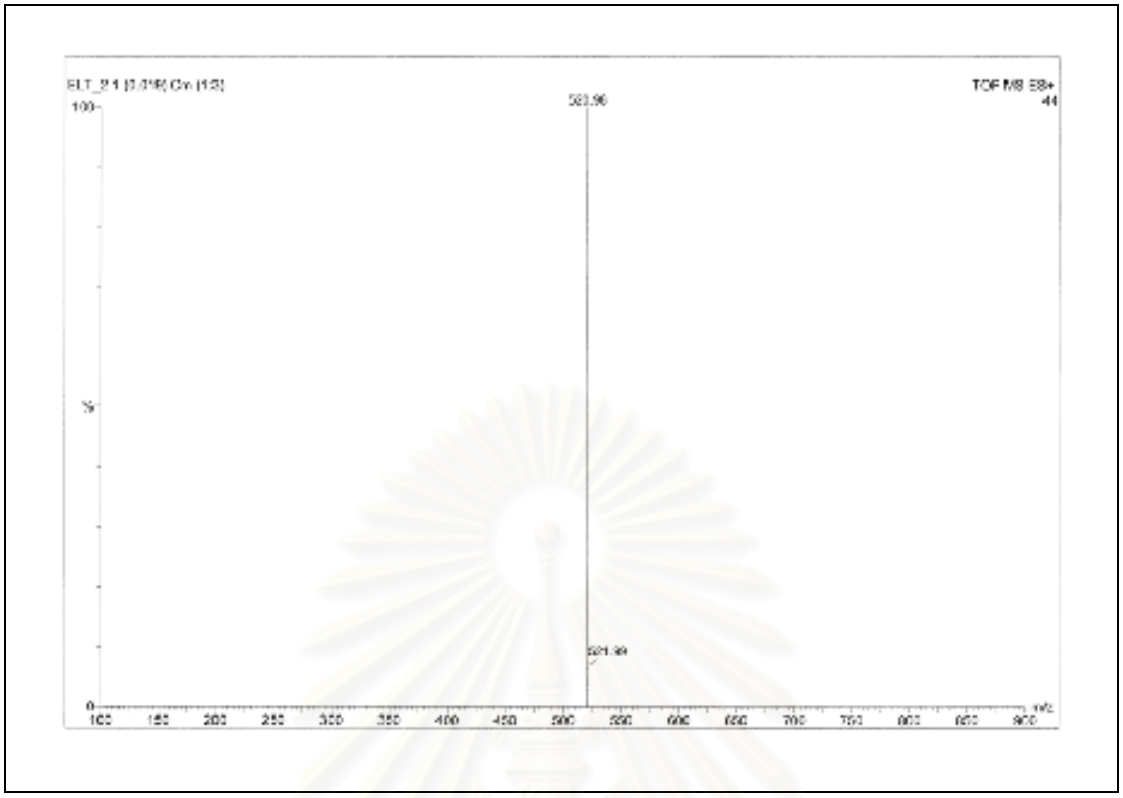

Figure 48. ESI Mass spectrum of compound ET-S2

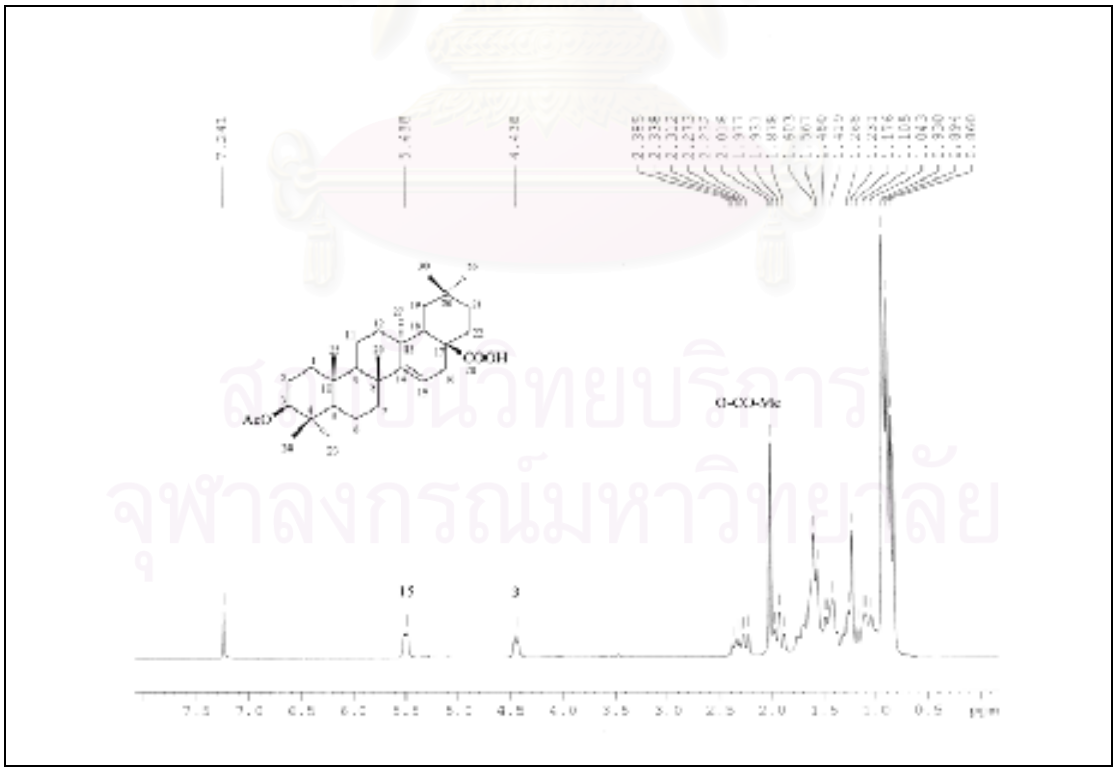

Figure 49. ^{1}H NMR (300 MHz) Spectrum of compound ET-S2 (in $CDCl_3$)

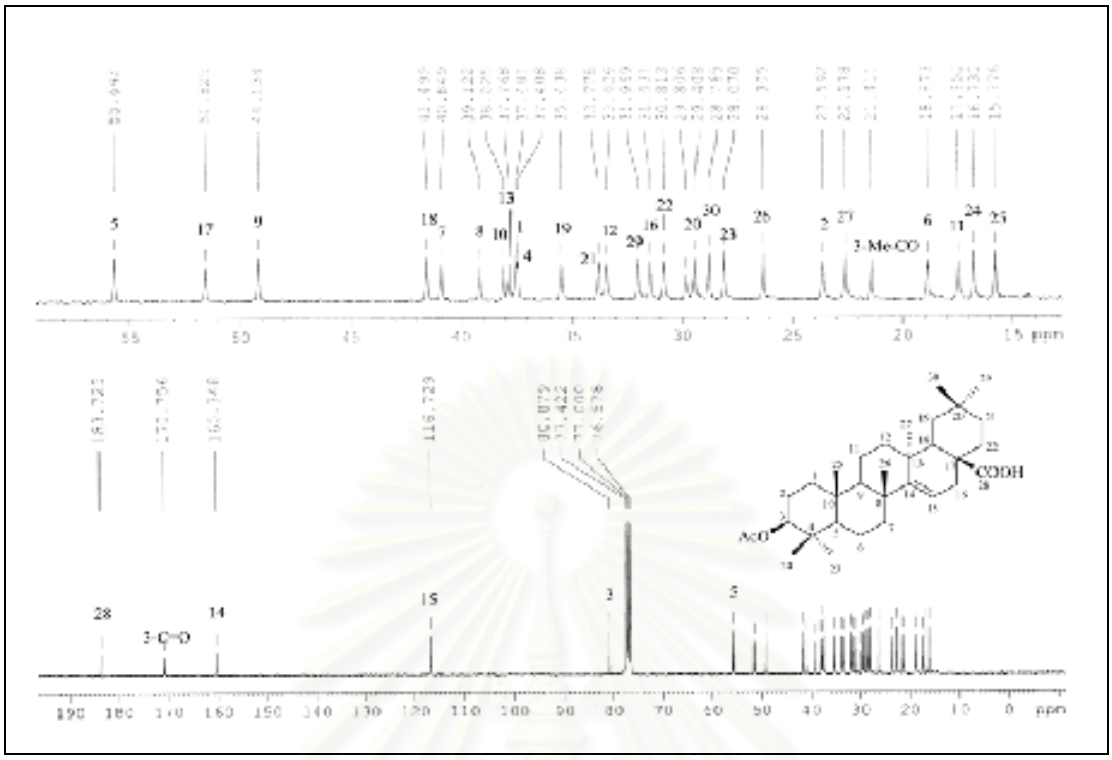

Figure 50. ^{13}C NMR (75 MHz) Spectrum of compound ET-S2 (in $CDCl_3$)

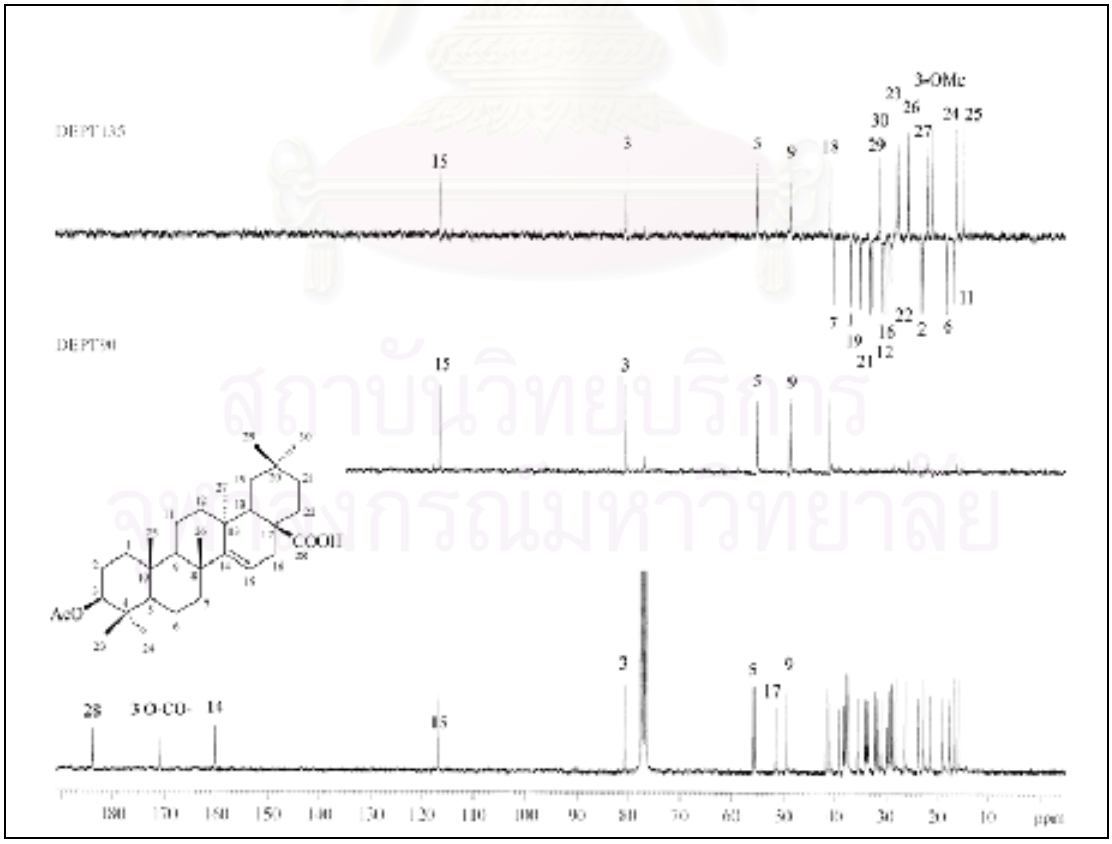

Figure 51. DEPT 135, DEPT 90 and ^{13}C NMR Spectrum of compound ET-S2

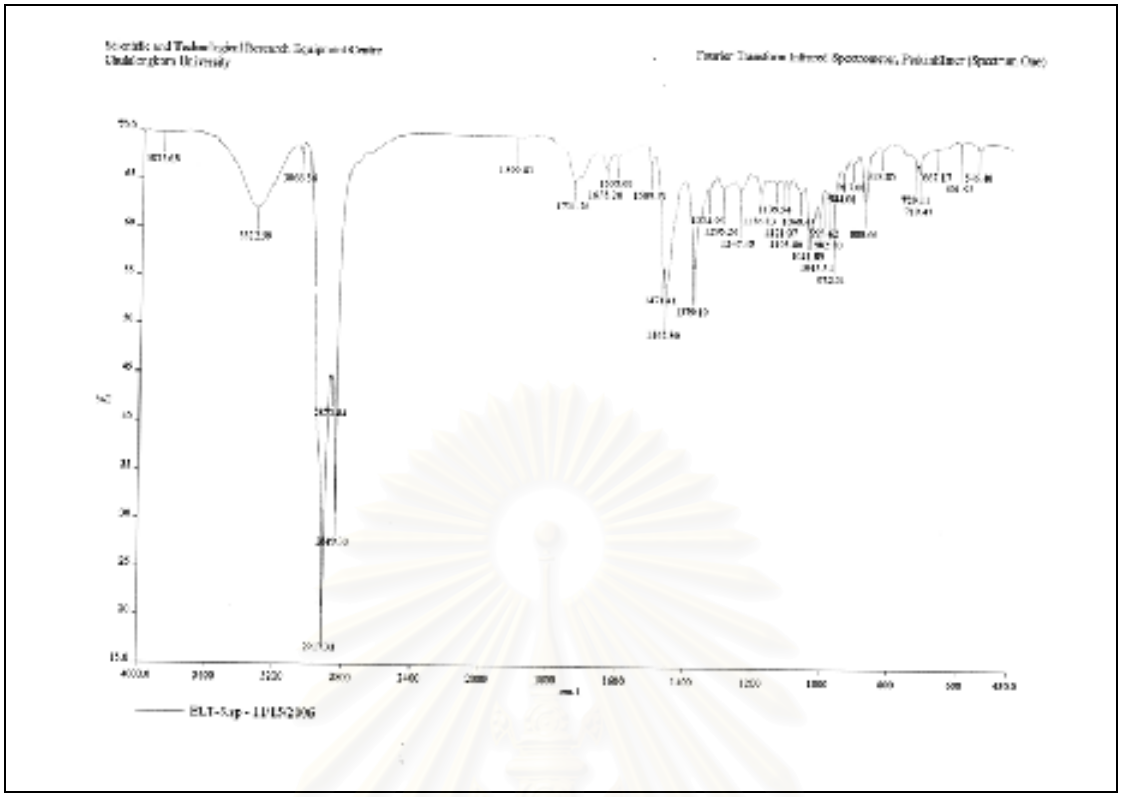

Figure 52. IR Spectrum of compound ET-S3 (KBr disc)

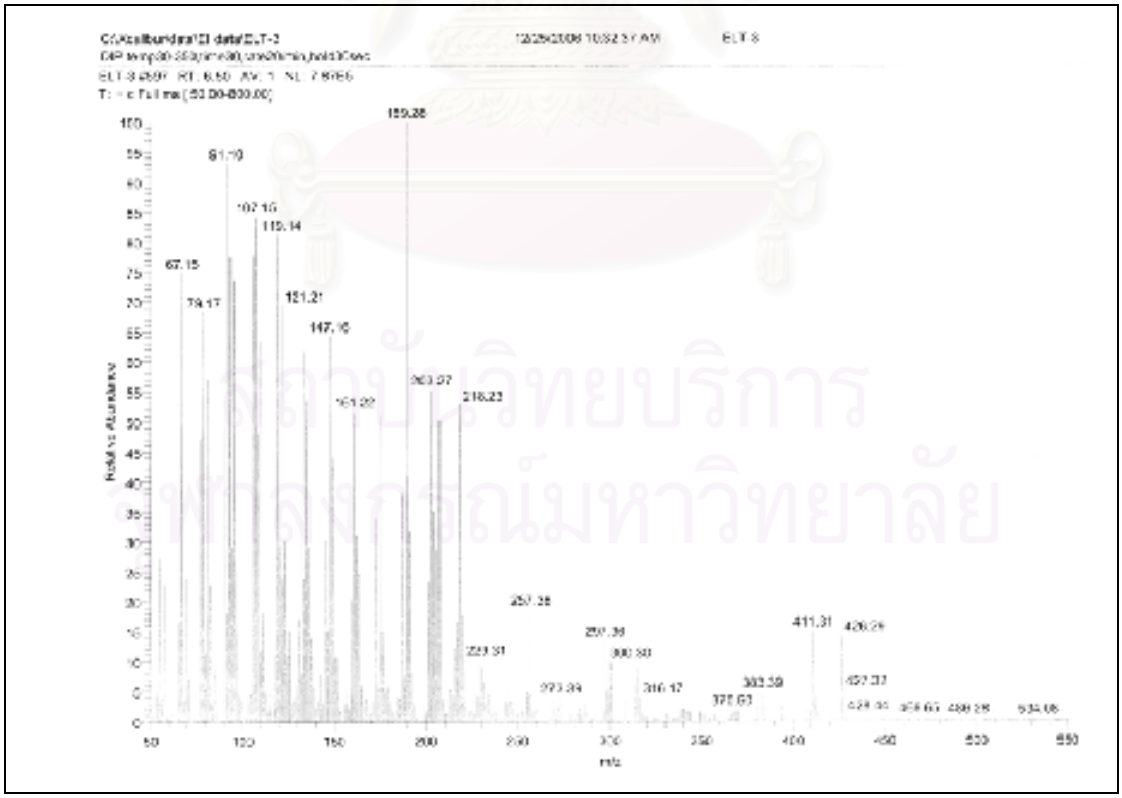

Figure 53. EI Mass spectrum of compound ET-S3

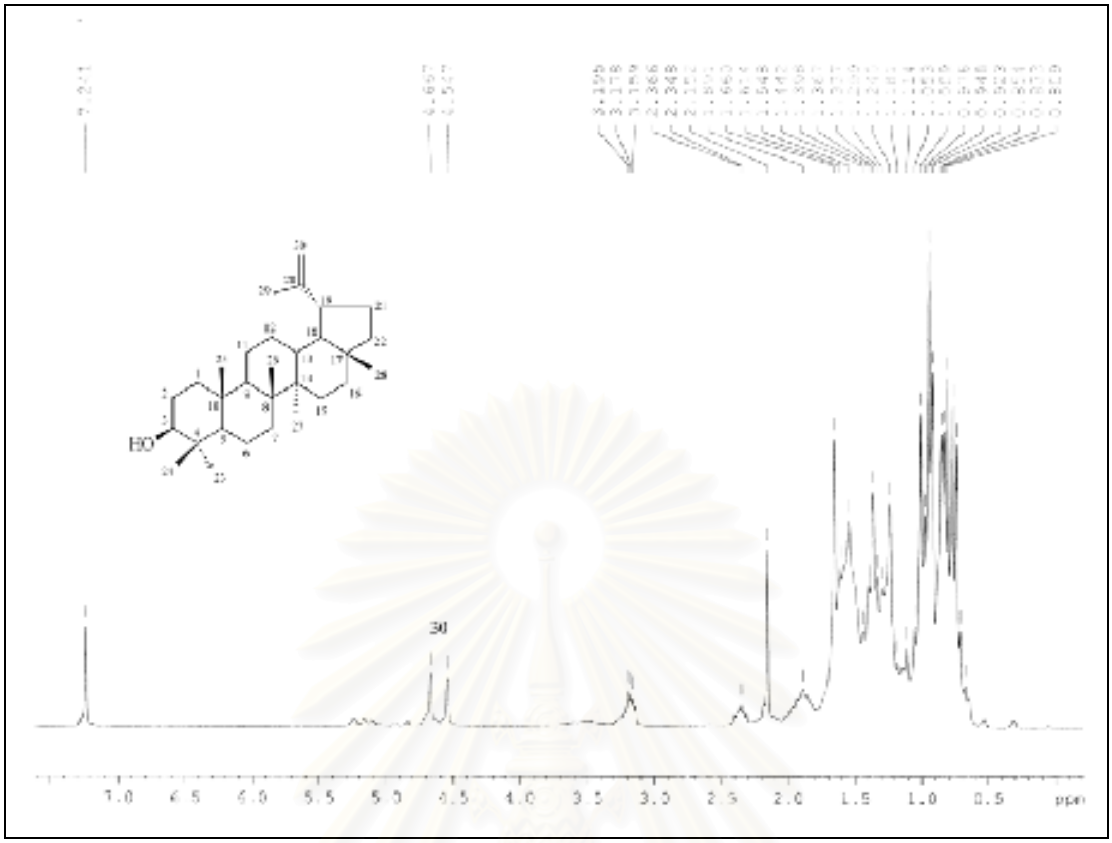

Figure 54. ^{1}H NMR (300 MHz) Spectrum of compound ET-S3 (in $CDCl_3$)

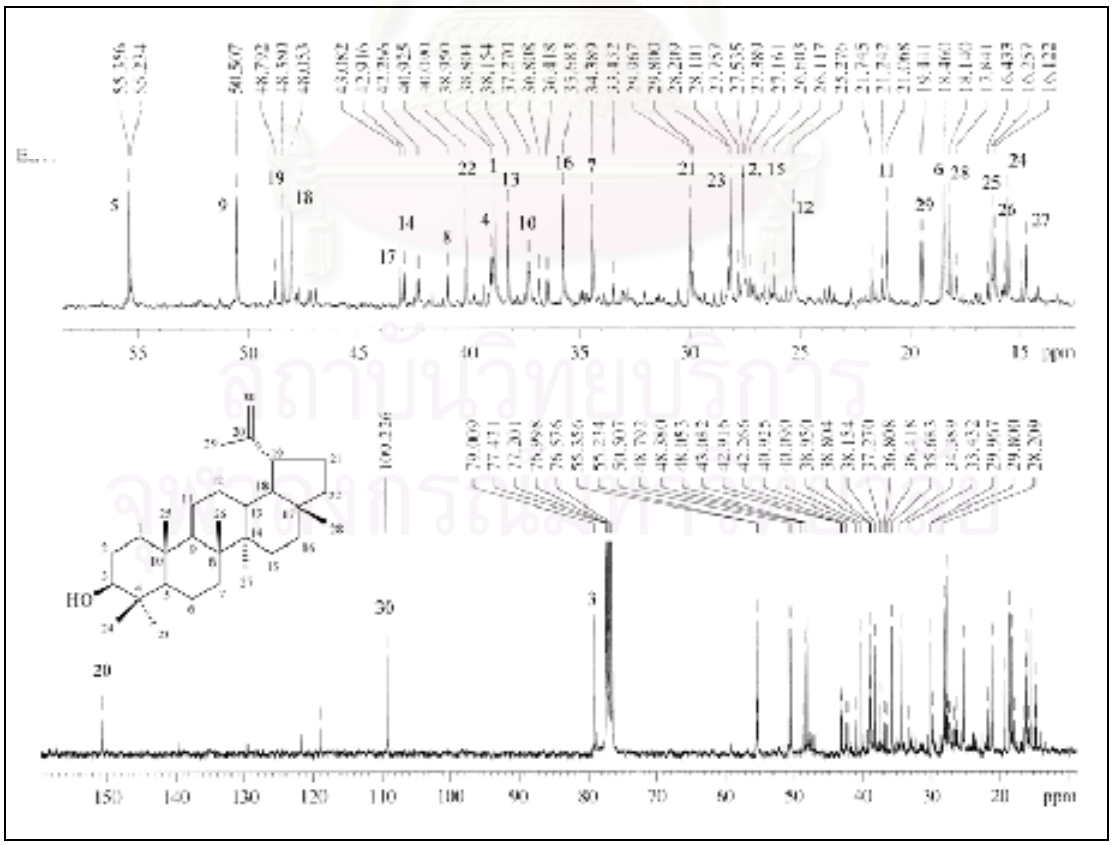

Figure 55. ^{13}C NMR (75 MHz) Spectrum of compound ET-S3 (in $CDCl_3$)

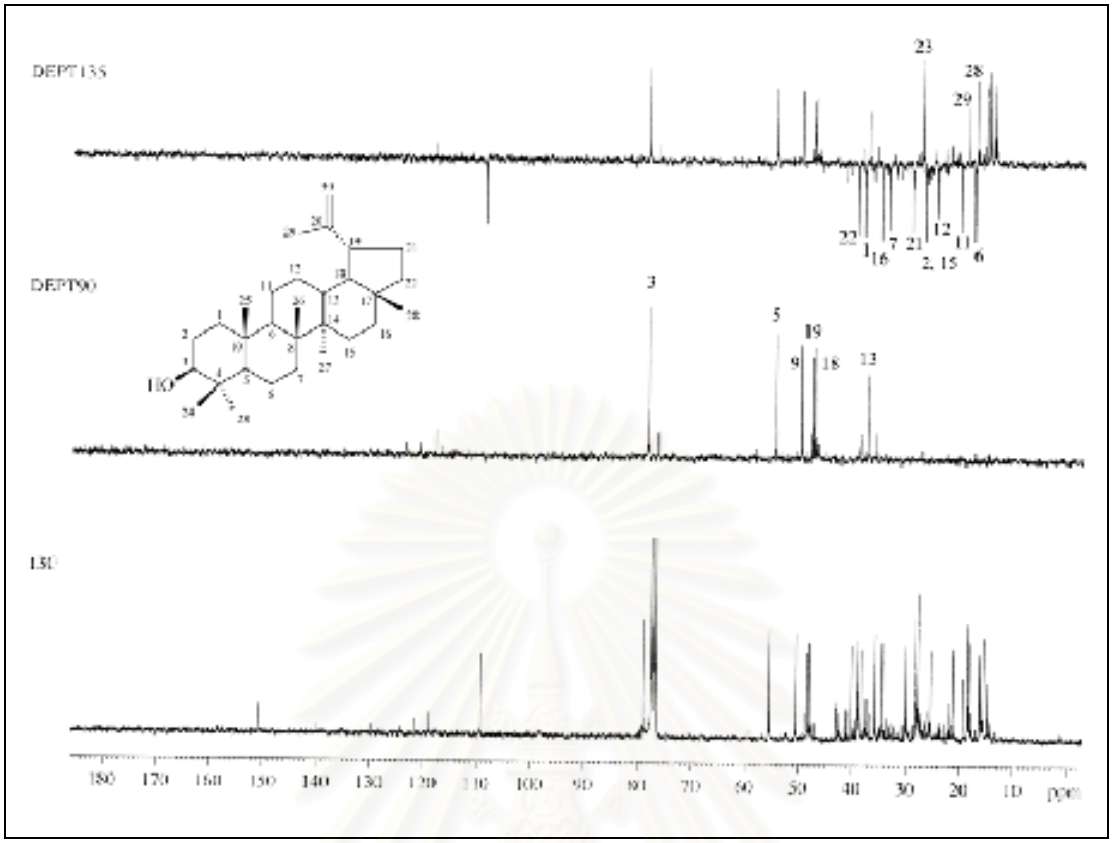

Figure 56. DEPT 135, DEPT 90 and ^{13}C NMR Spectrum of compound ET-S3

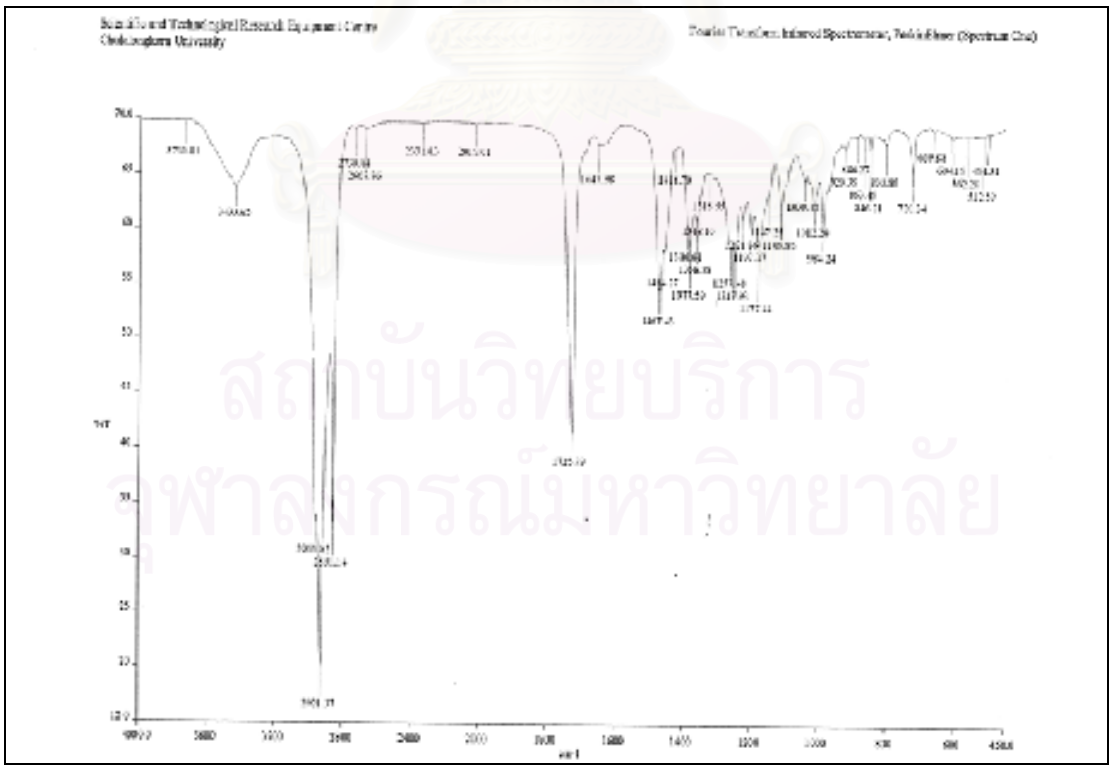

Figure 57. IR Spectrum of compound ET-S5 (KBr disc)

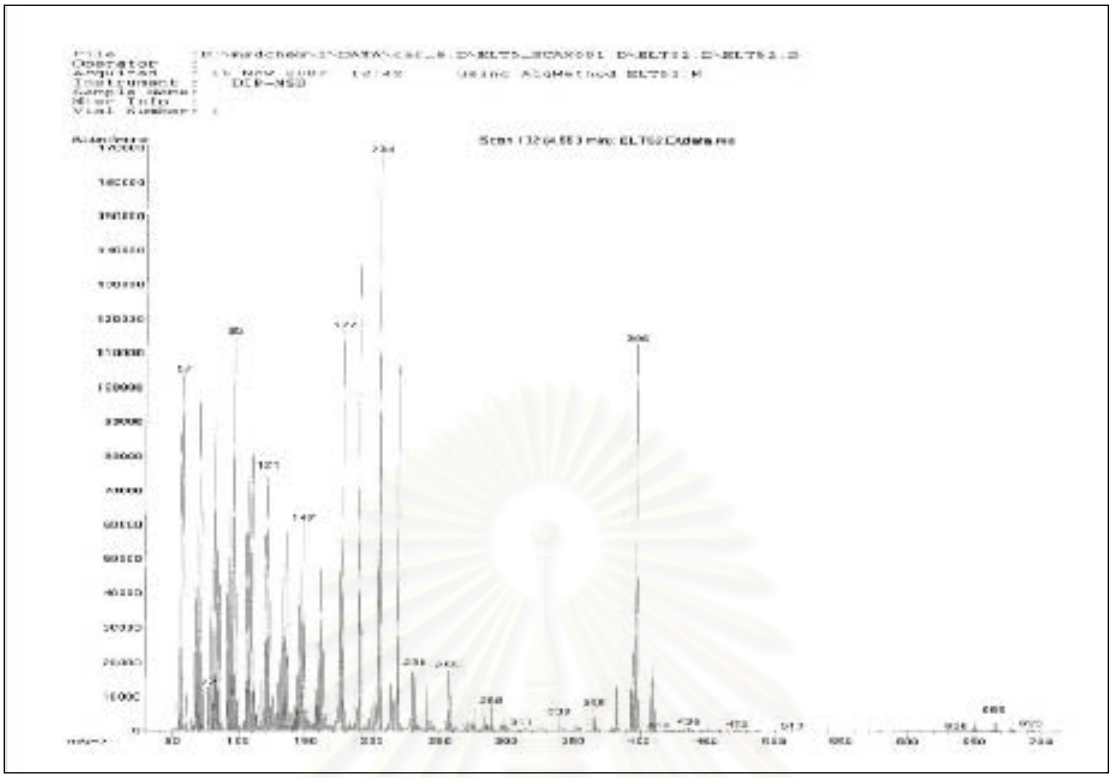

Figure 58. EI Mass spectrum of compound ET-S5

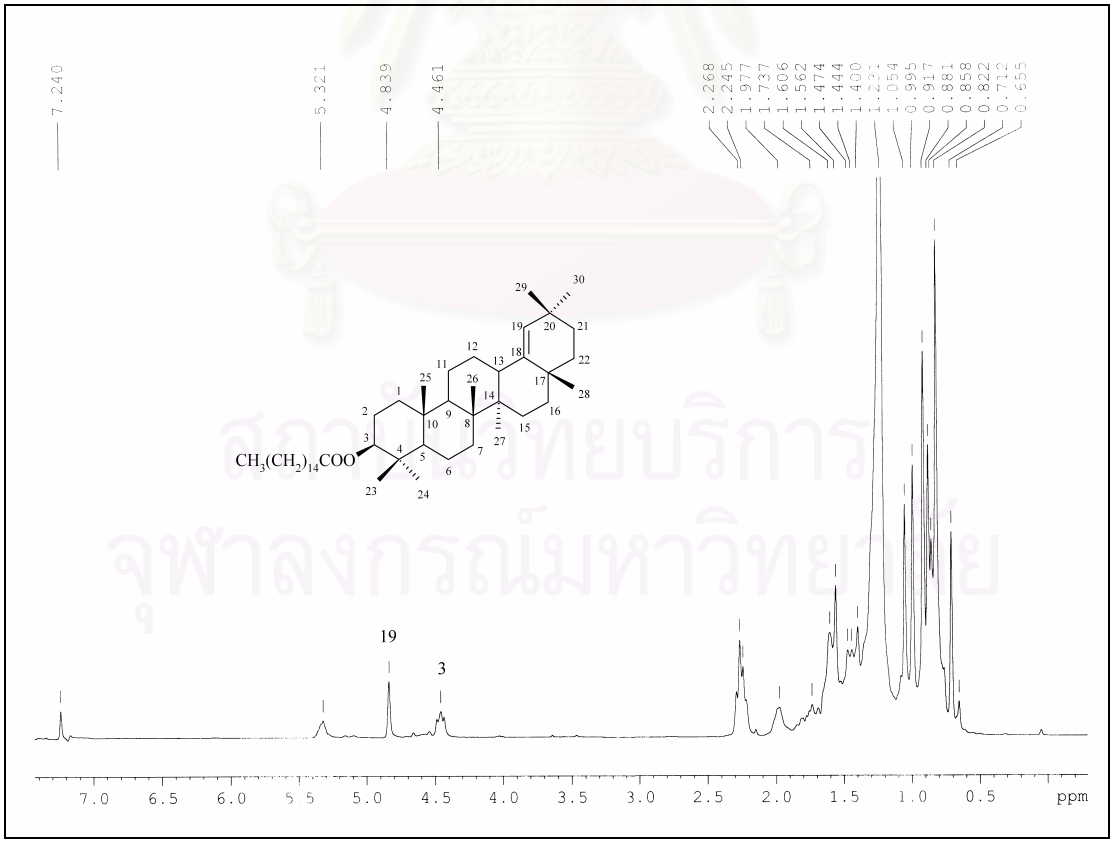

Figure 59. ^{1}H NMR (300 MHz) Spectrum of compound ET-S5 (in $CDCl_3$)

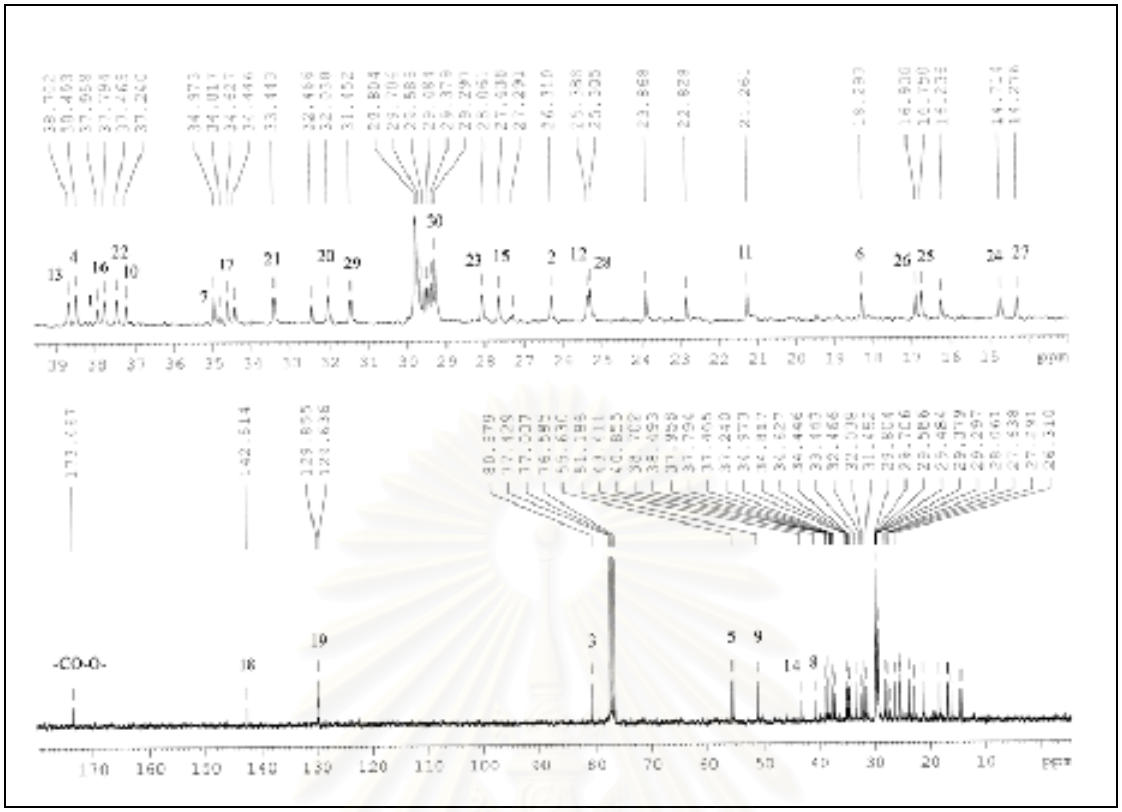

Figure 60. ^{13}C NMR (75 MHz) Spectrum of compound ET-S5 (in $CDCl_3$)

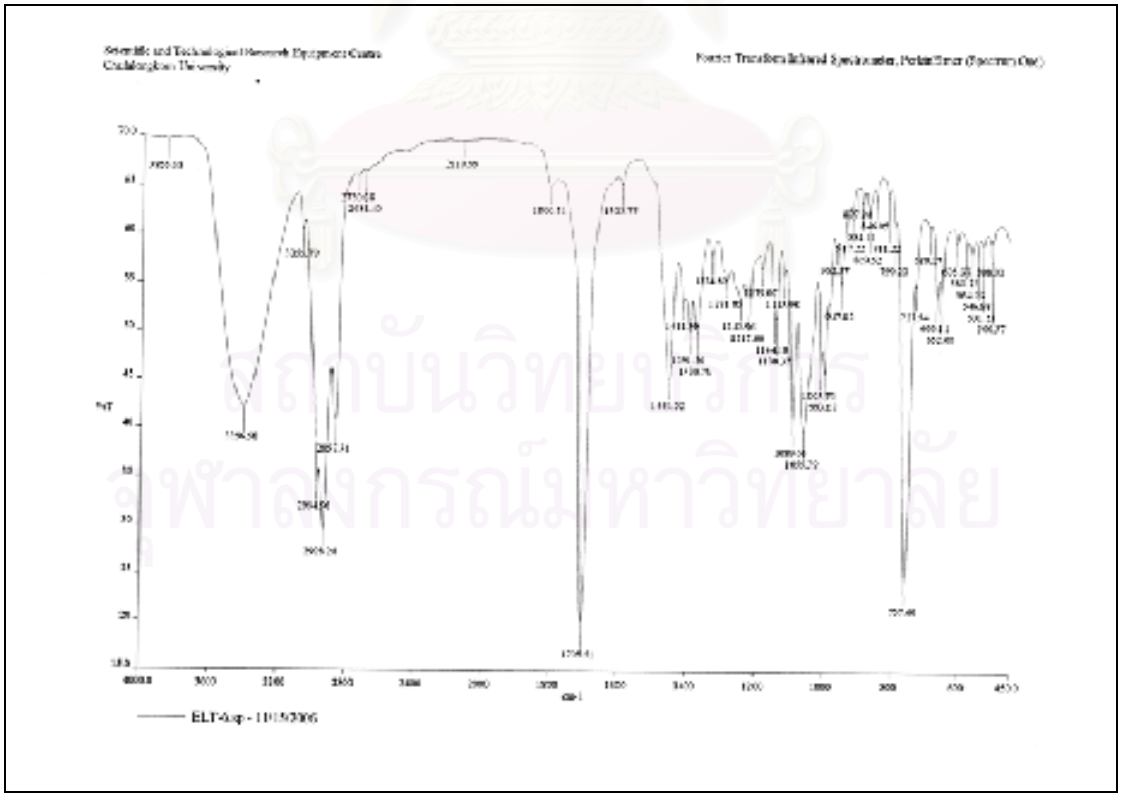

Figure 61. IR Spectrum of compound ET-S6 (KBr disc)

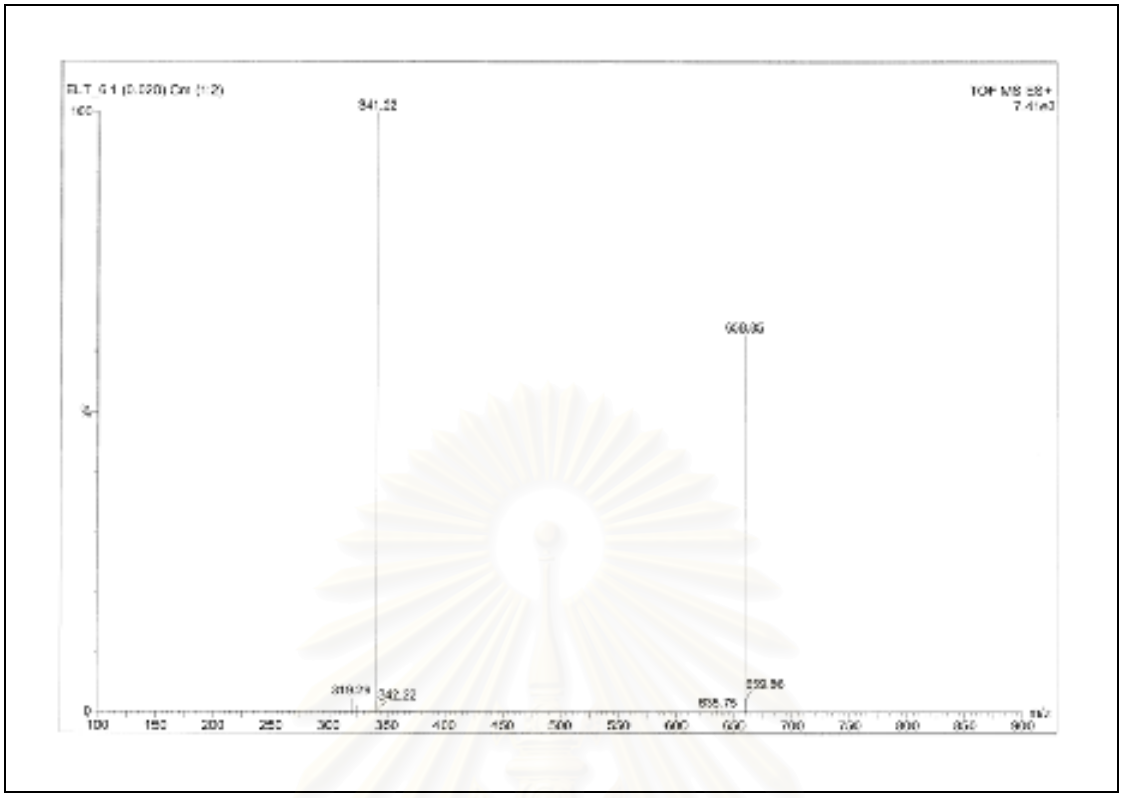

Figure 62. ES Mass spectrum of compound ET-S6

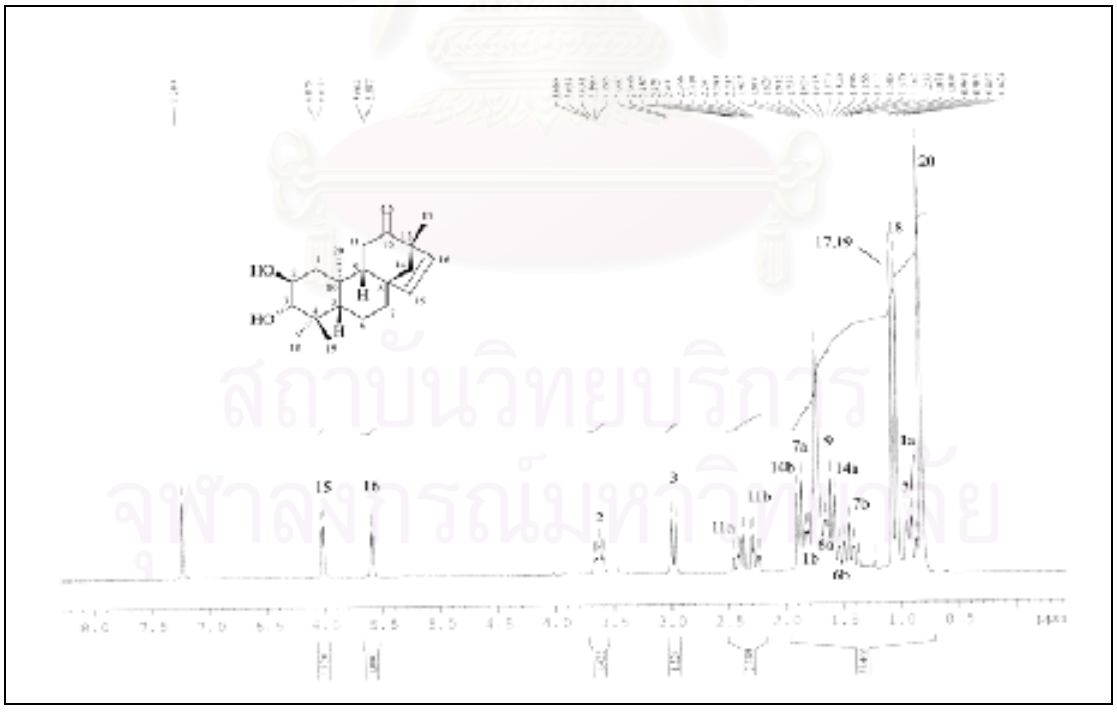

Figure 63. ^{1}H NMR (300 MHz) Spectrum of compound ET-S6 (in $CDCl_3$)

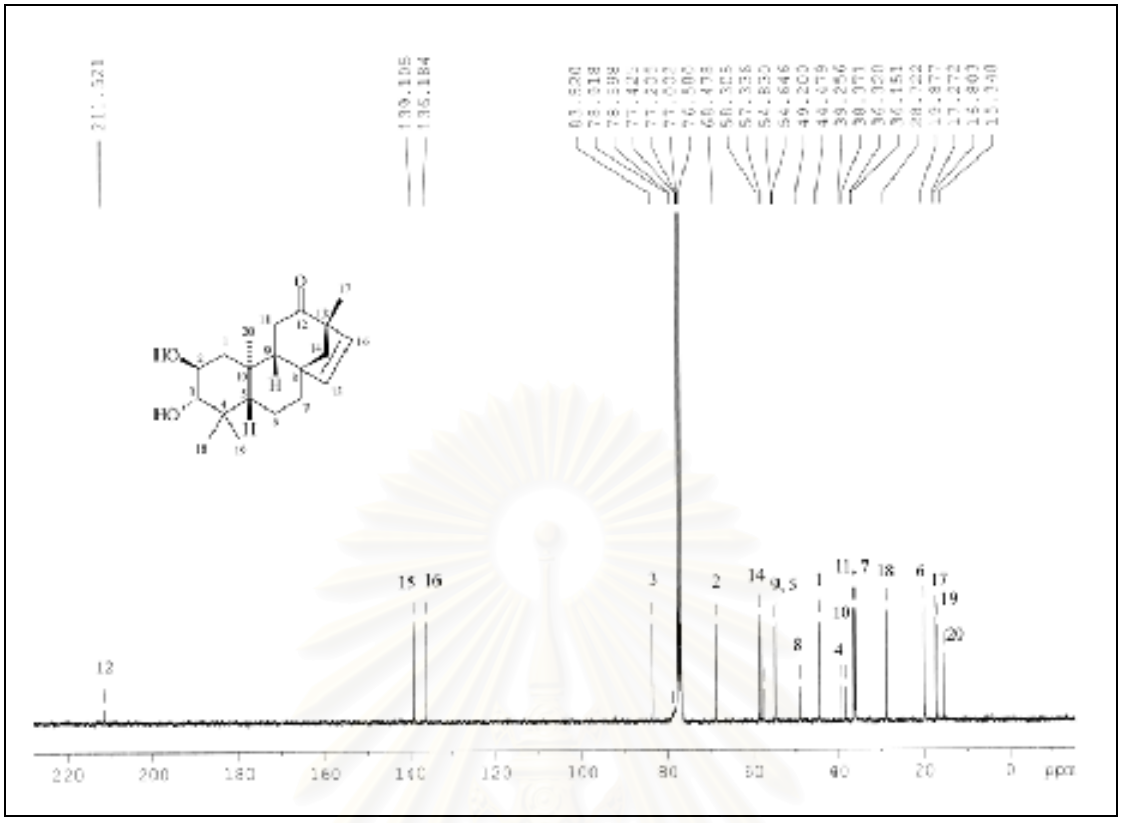

Figure 64. ^{13}C NMR (75 MHz) Spectrum of compound ET-S6 (in $CDCl_3$)

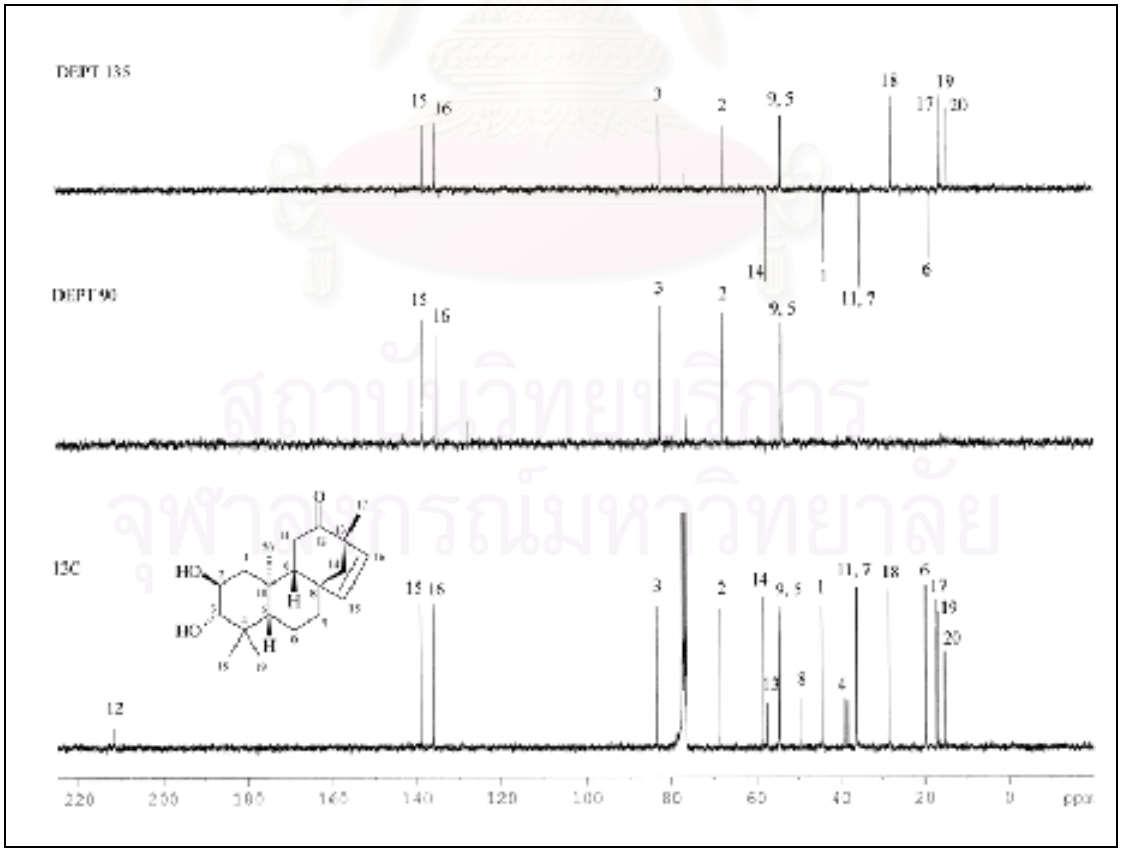

Figure 65. DEPT 135, DEPT 90 and ^{13}C NMR Spectrum of compound ET-S6

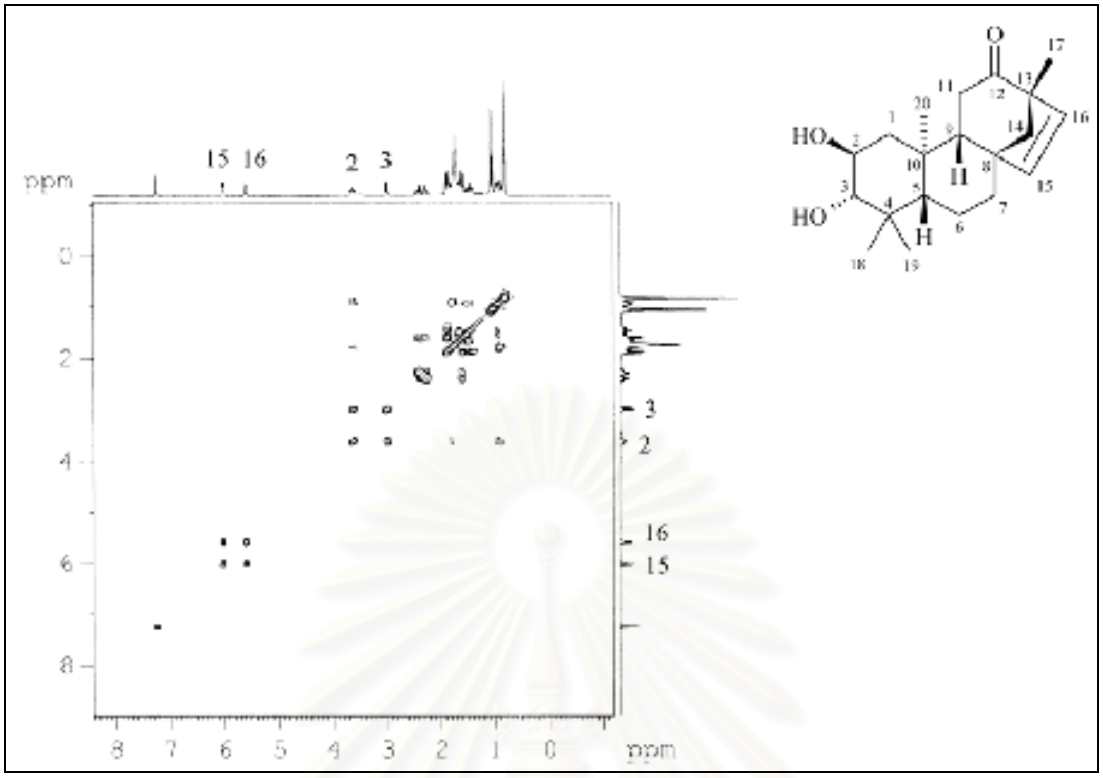

Figure 66a. ^{1}H-^{1}H COSY Spectrum of compound ET-S6

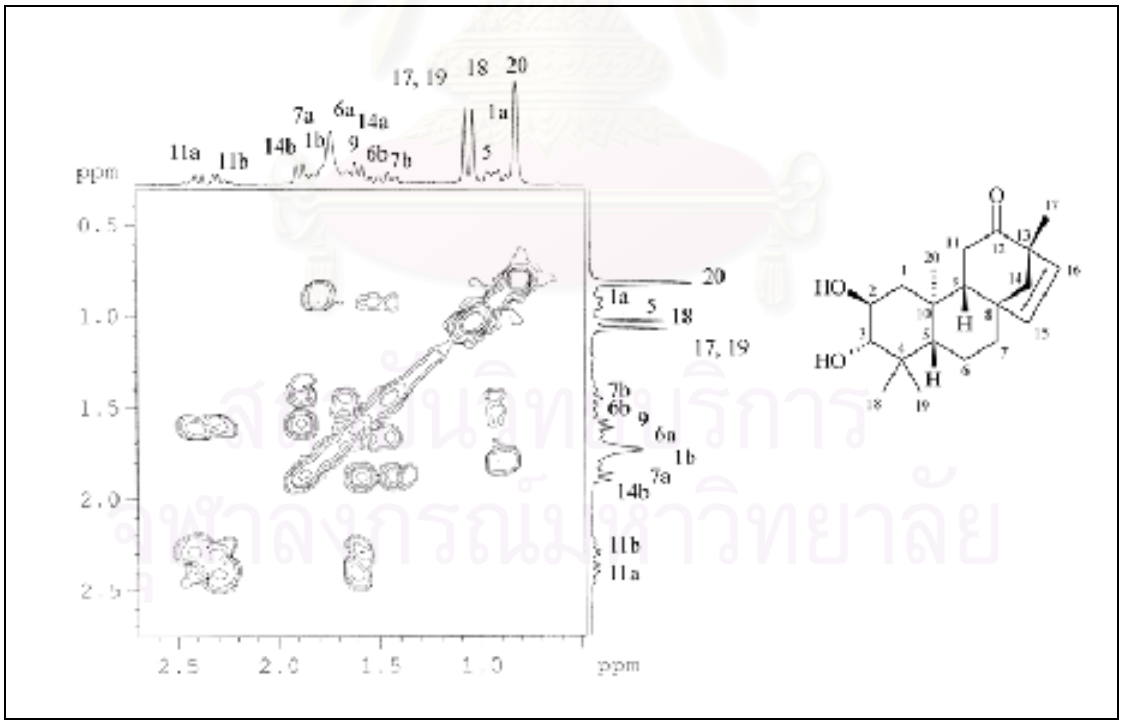

Figure 66b. ^{1}H-^{1}H COSY Spectrum of compound ET-S6 (δ_H 0.5-2.7 ppm)

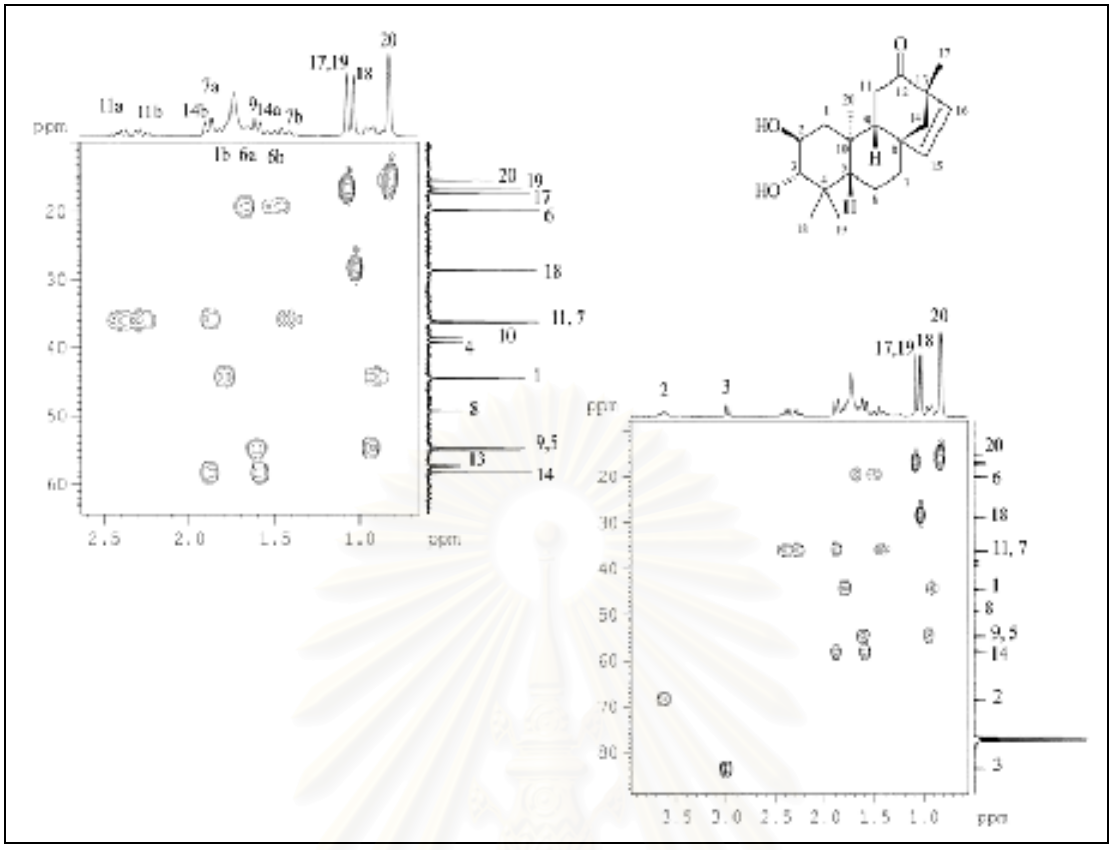

Figure 67. HMQC Spectrum of compound ET-S6
(δ_H 0.5-2.6ppm, δ_C 0-65 ppm and δ_H 0.5-4.0 ppm, δ_C10-90 ppm)

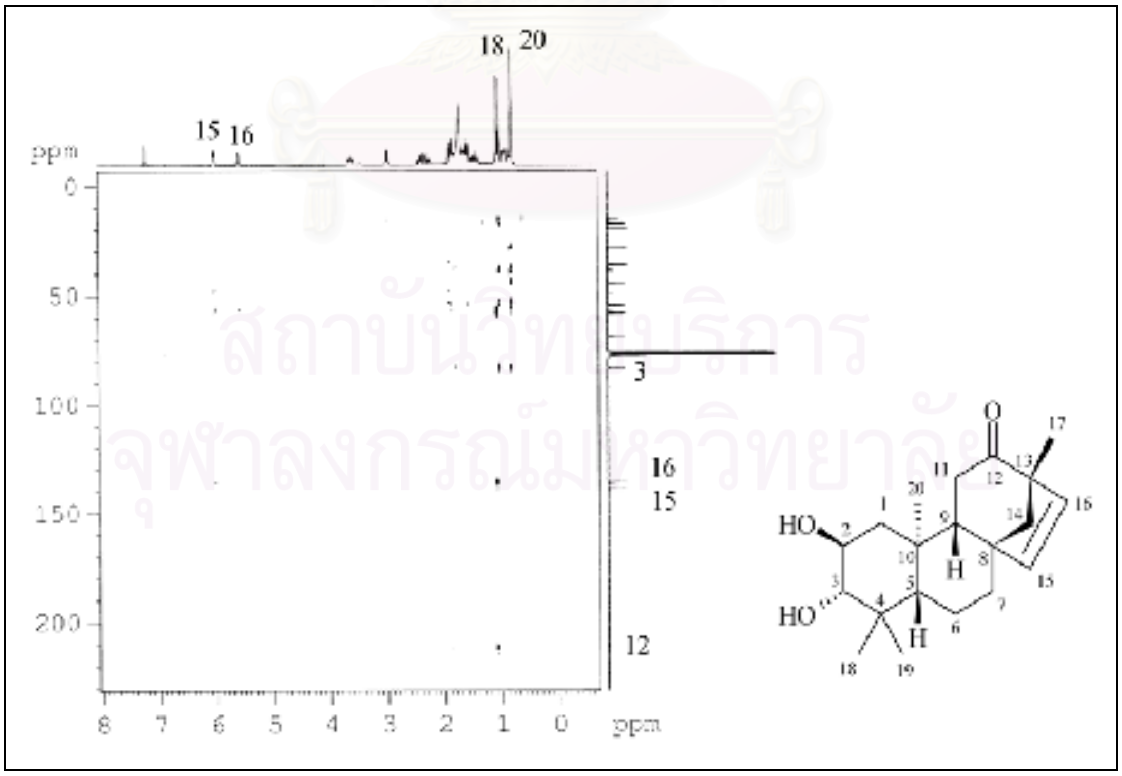

Figure 68a. HMBC Spectrum of compound ET-S6

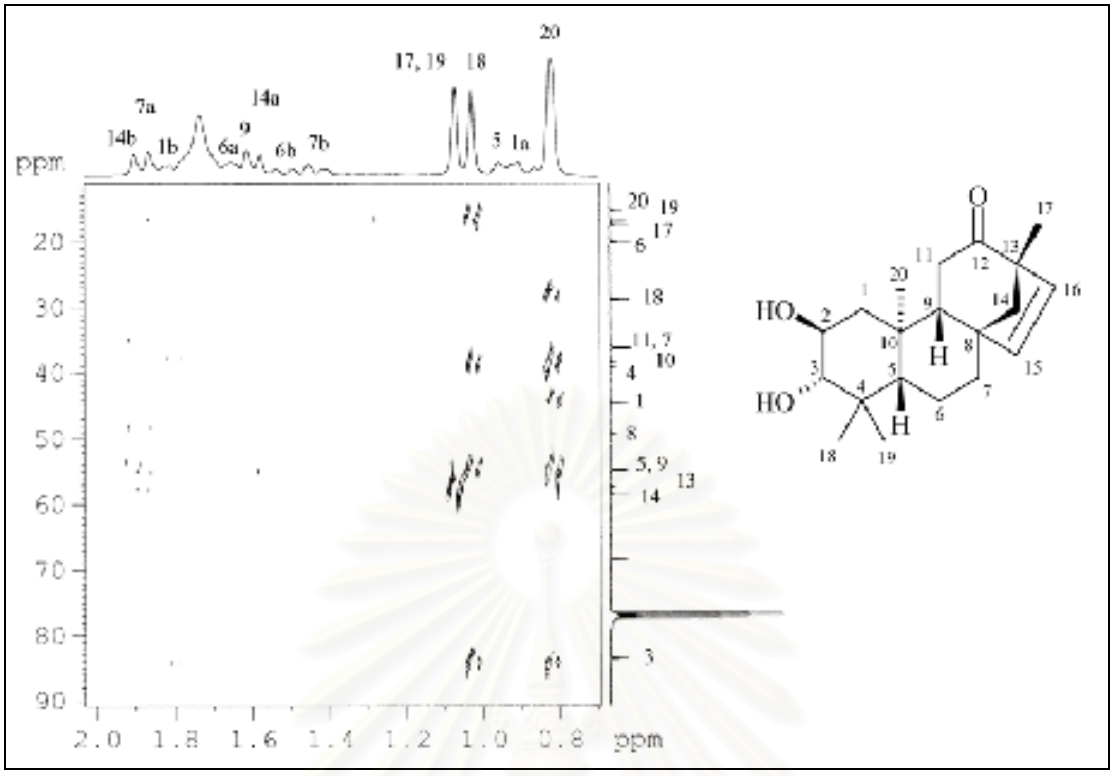

Figure 68b. HMBC Spectrum of compound ET-S6 (δ_H 0.7-2.0 ppm, δ_C 10-90 ppm)

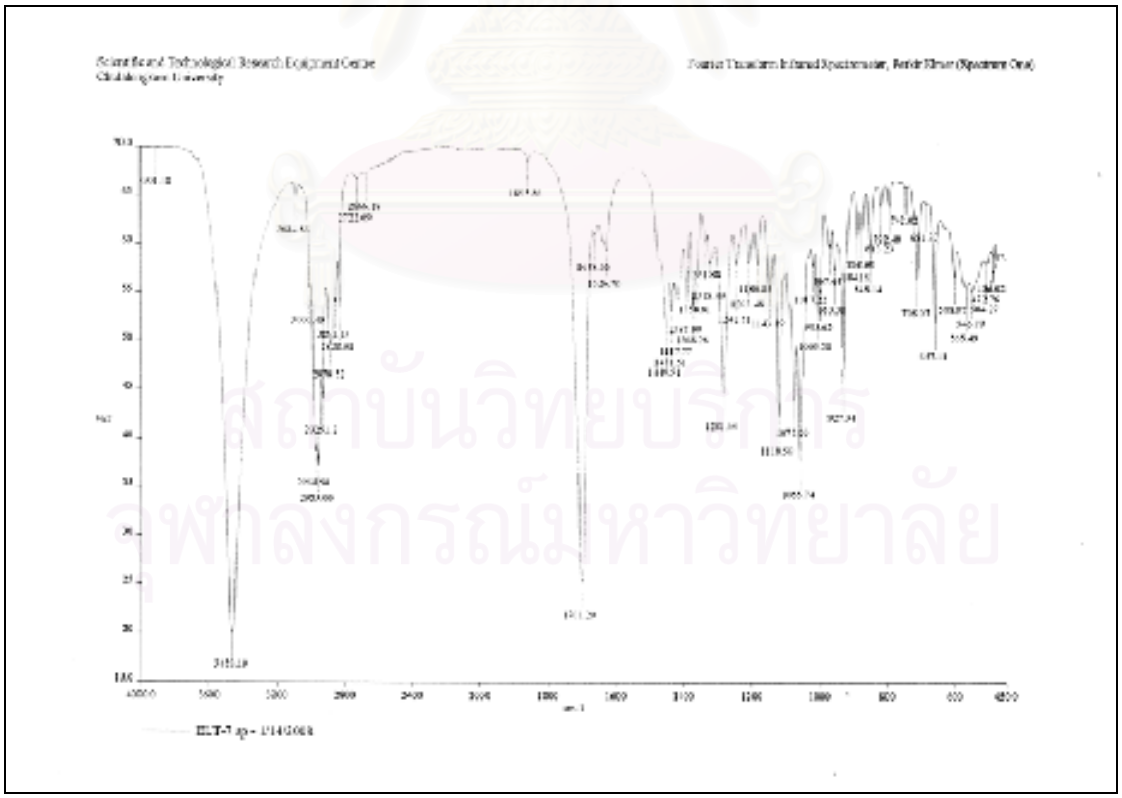

Figure 69. IR Spectrum of compound ET-S7 (KBr disc)

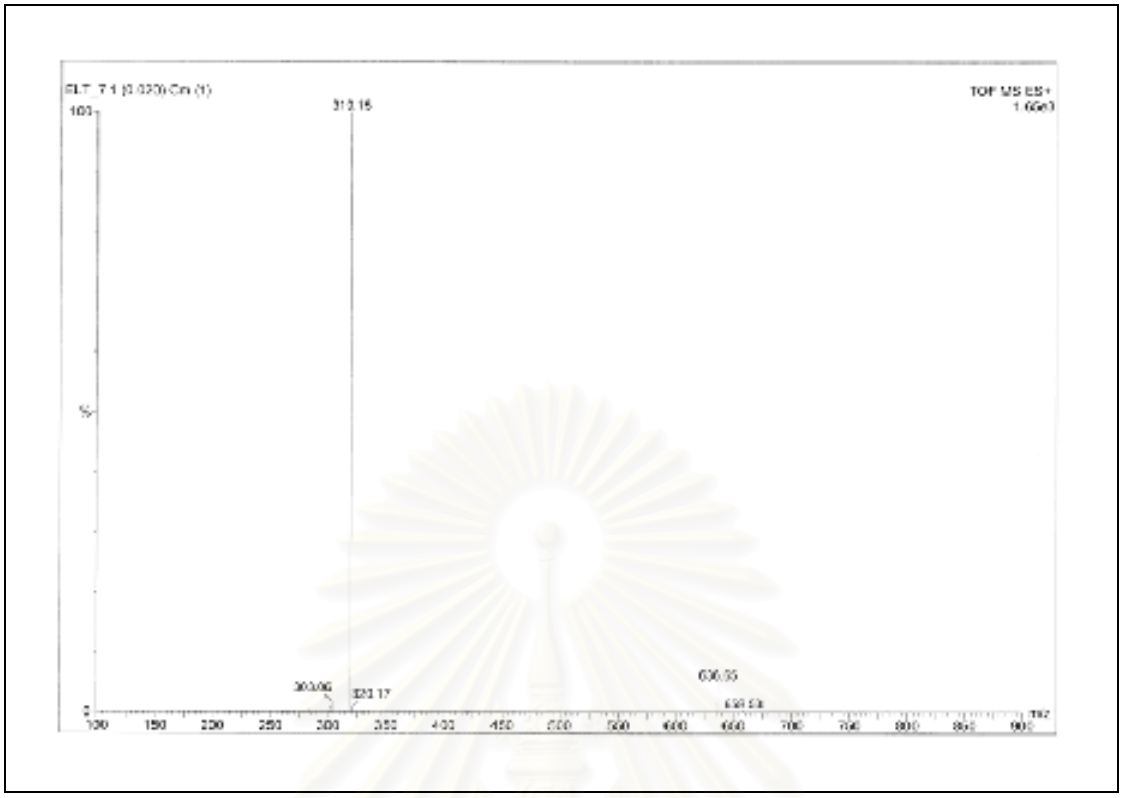

Figure 70. ESI Mass spectrum of compound ET-S7

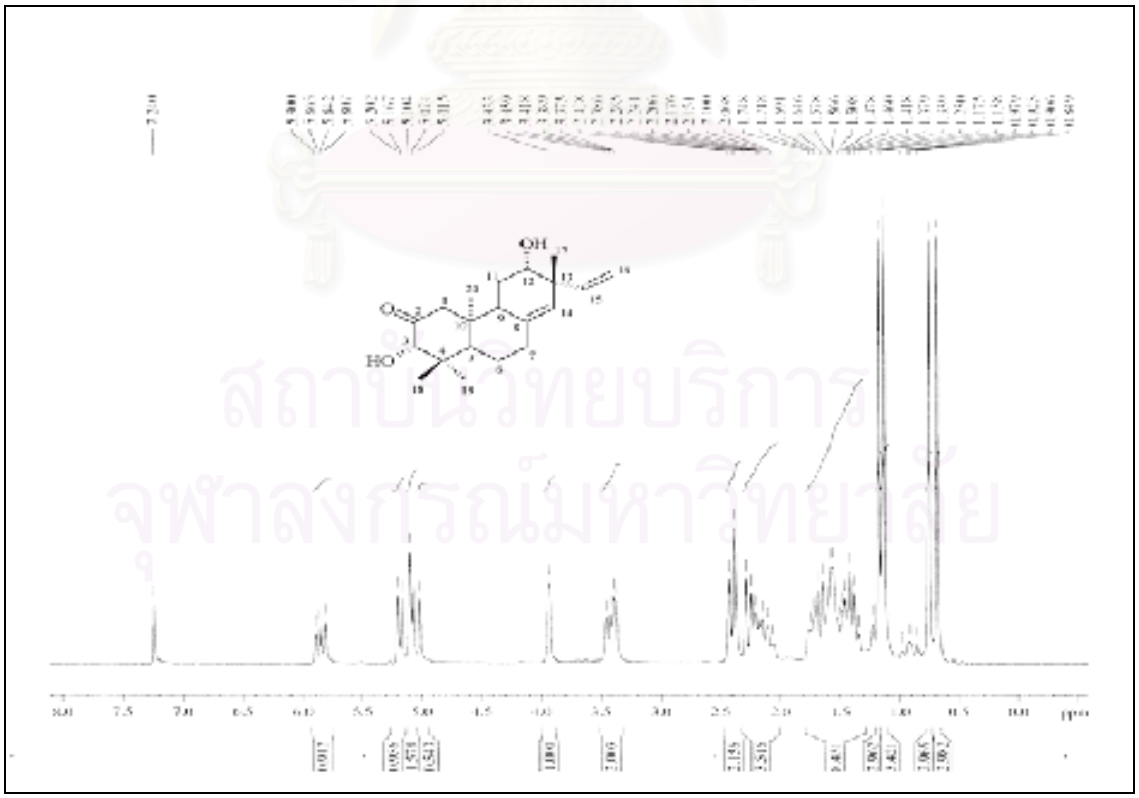

Figure 71. ^{1}H NMR (300 MHz) Spectrum of compound ET-S7 (in $CDCl_3$)

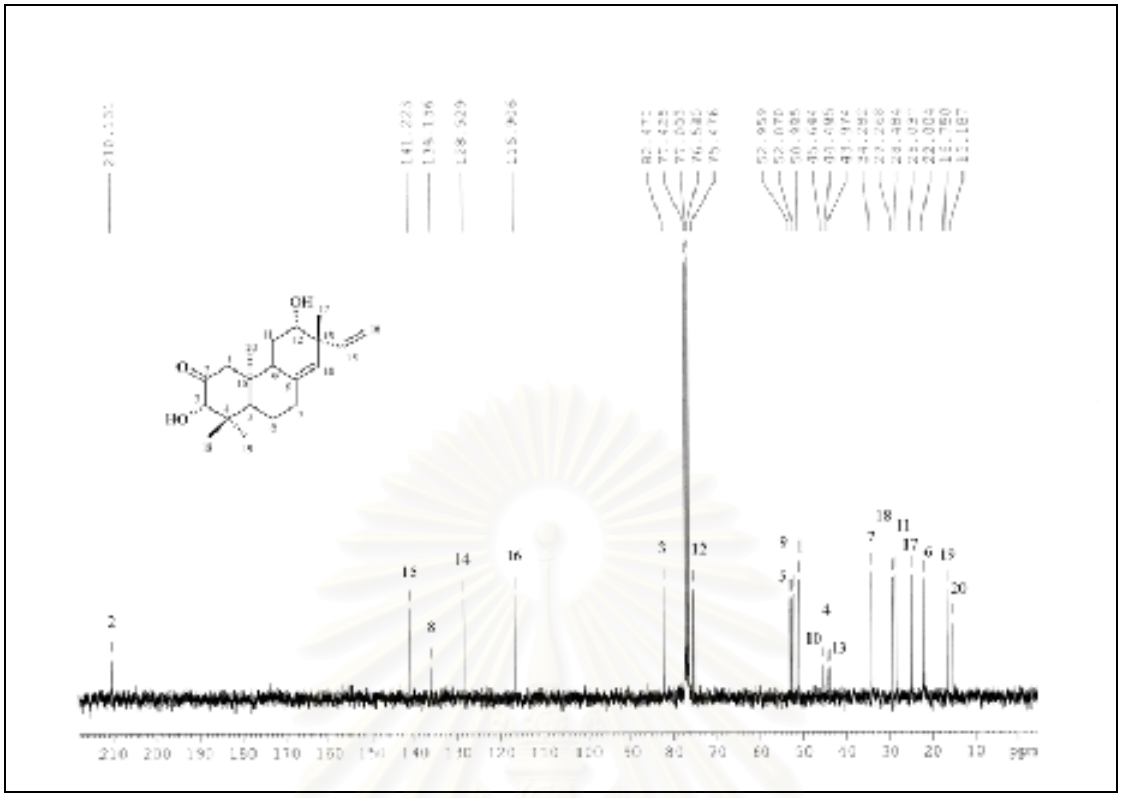

Figure 72. ^{13}C NMR (75 MHz) Spectrum of compound ET-S7 (in $CDCl_3$)

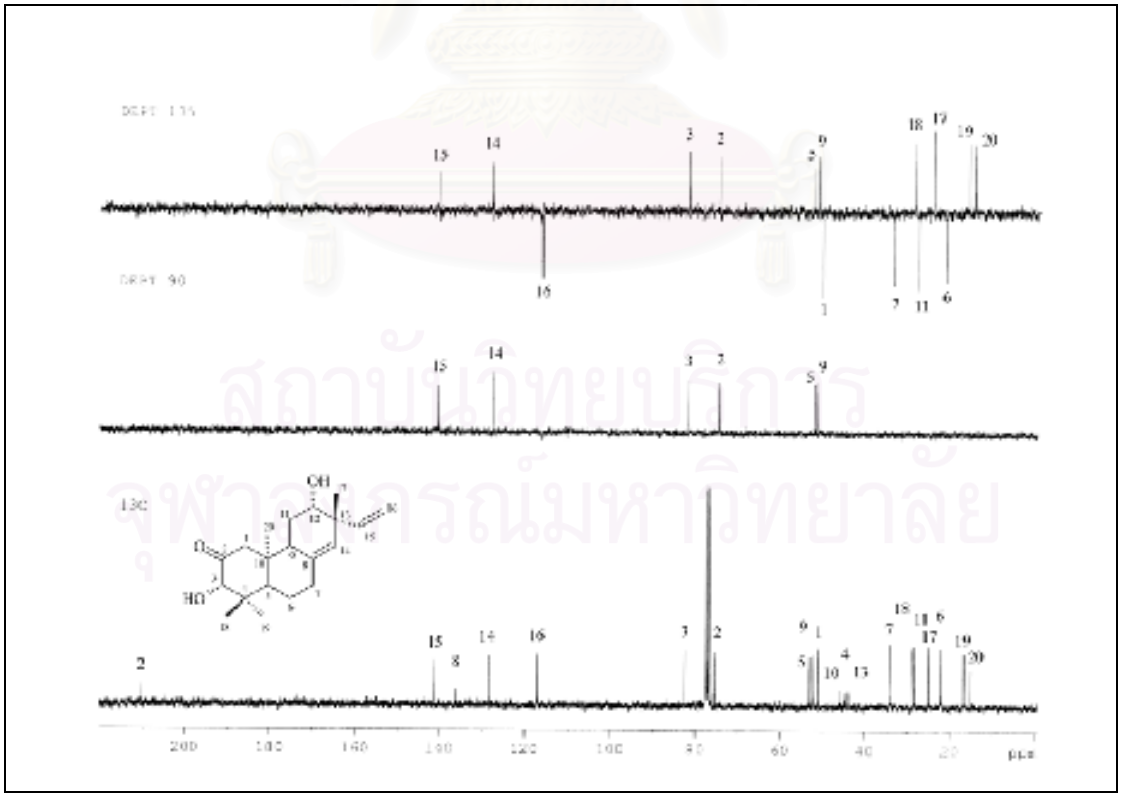

Figure 73. DEPT 135, DEPT 90 and ^{13}C NMR spectrum of compound ET-S7

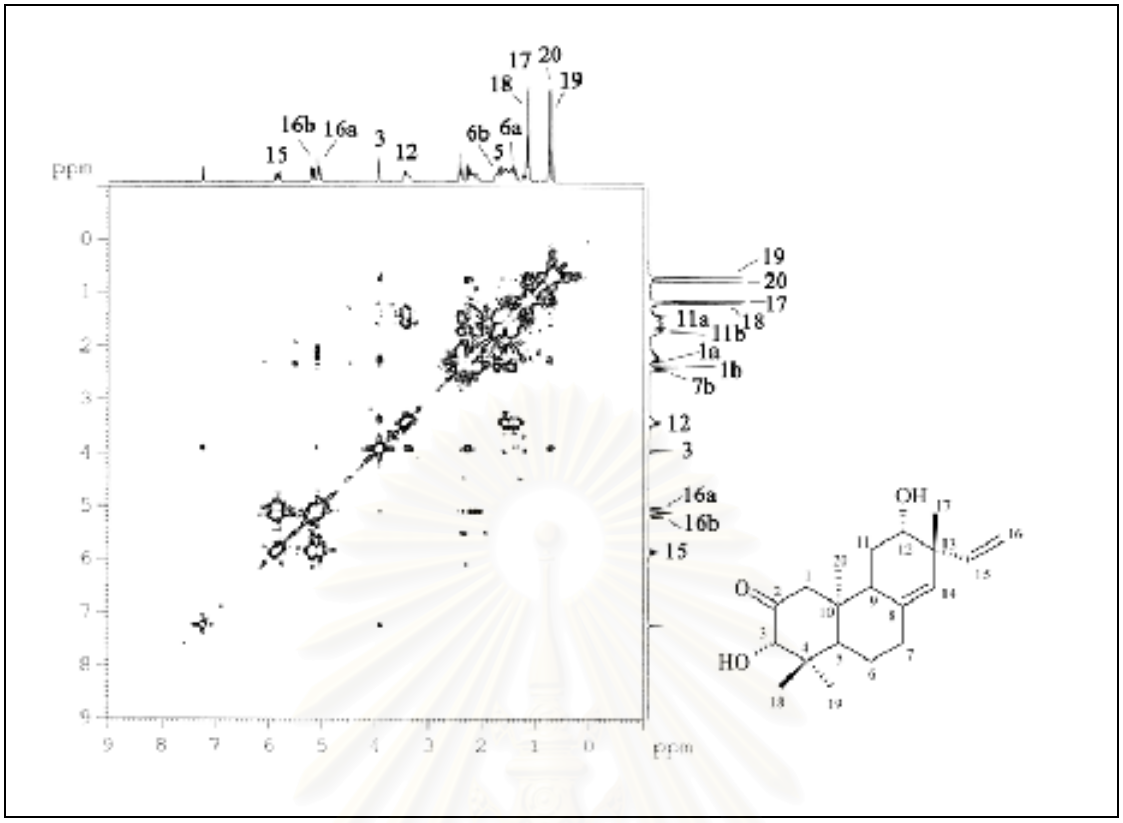

Figure 74. ^{1}H-^{1}H COSY Spectrum of compound ET-S7

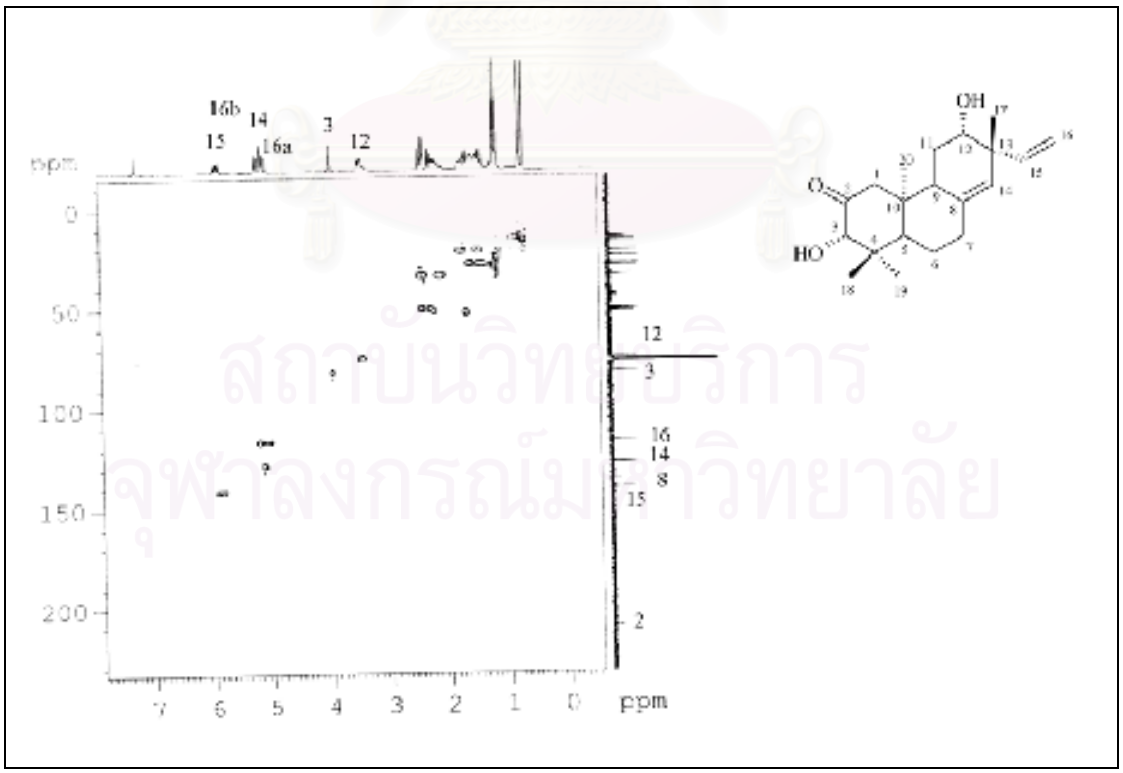

Figure 75a. HMQC Spectrum of compound ET-S7

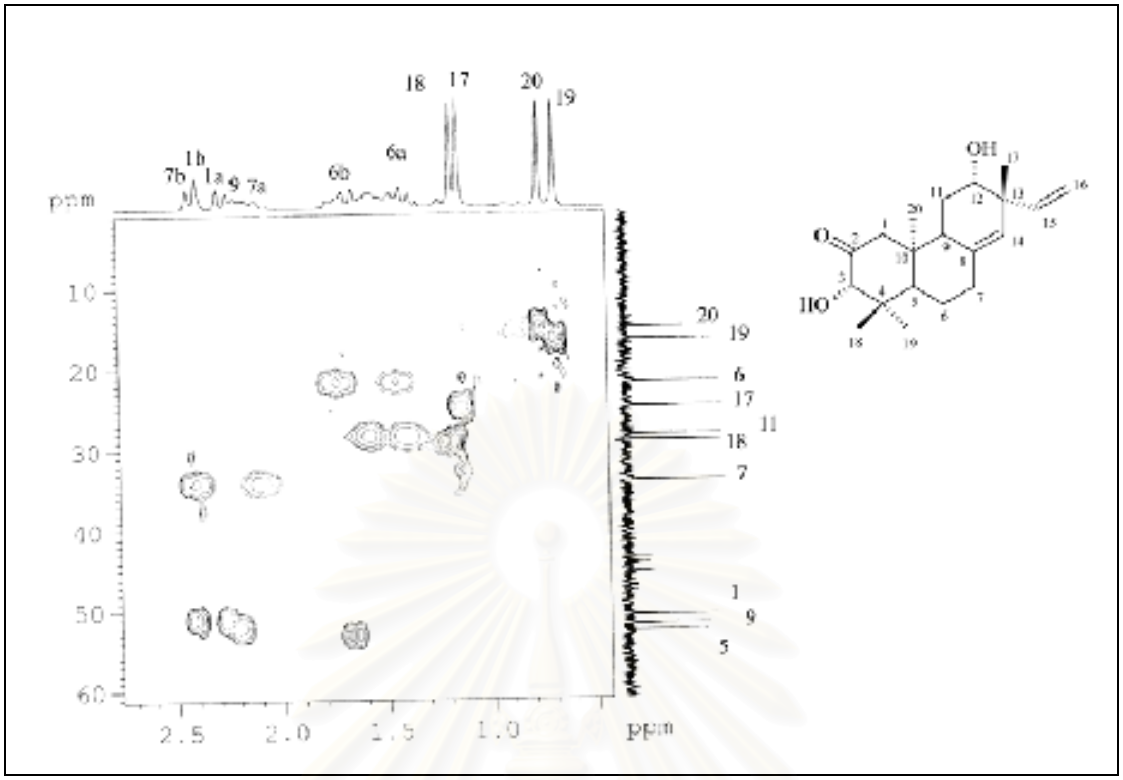

Figure 75b. HMQC Spectrum of compound ET-S7 (δ_H 0.5-2.8 ppm, δ_C 0-60 ppm)

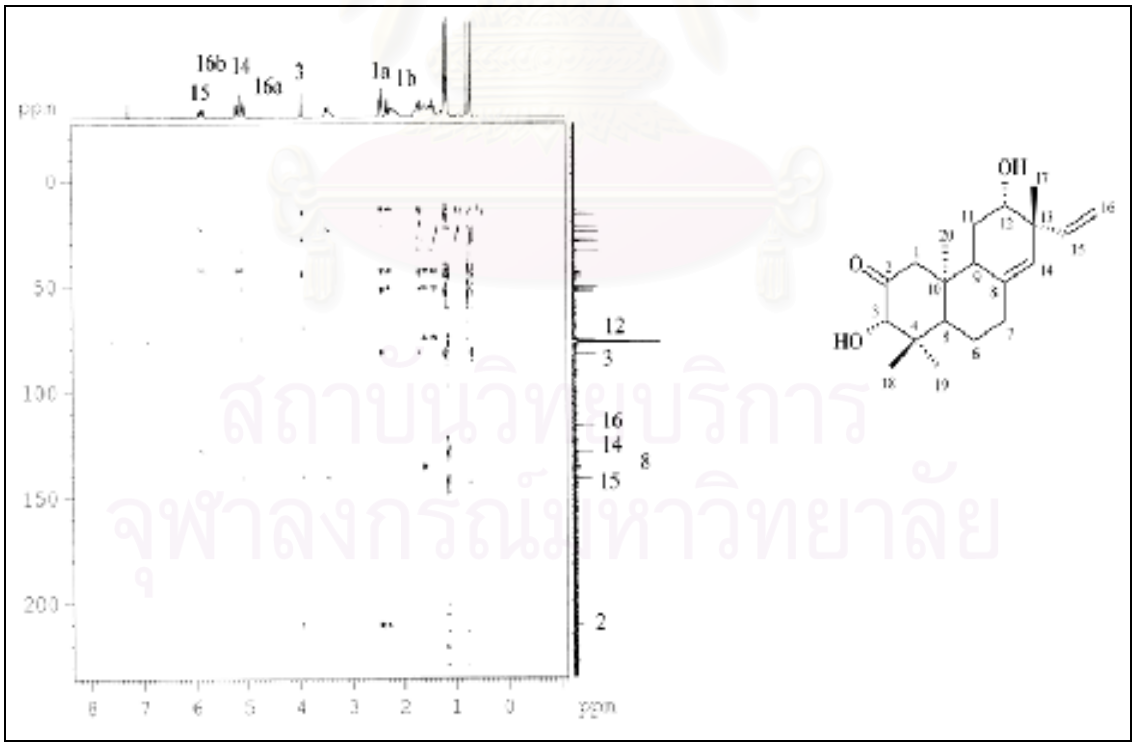

Figure 76. HMBC Spectrum of compound ET-S7

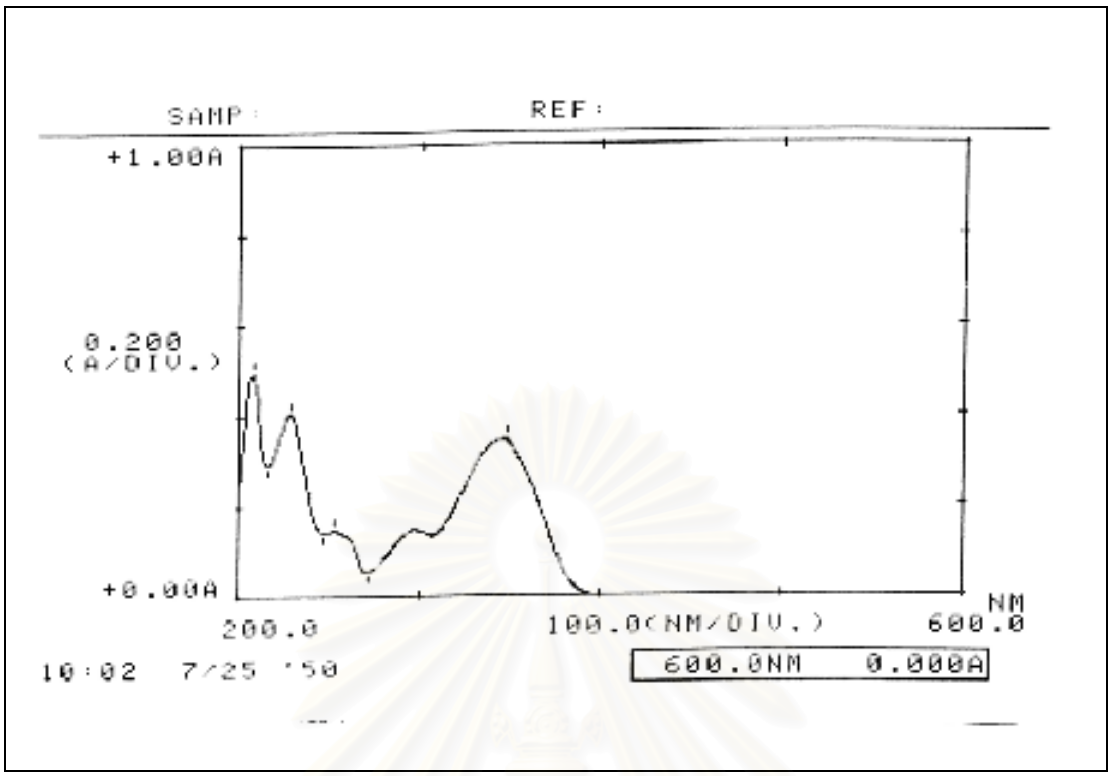

Figure 77. UV Spectrum of compound ET-S8 (in MeOH)

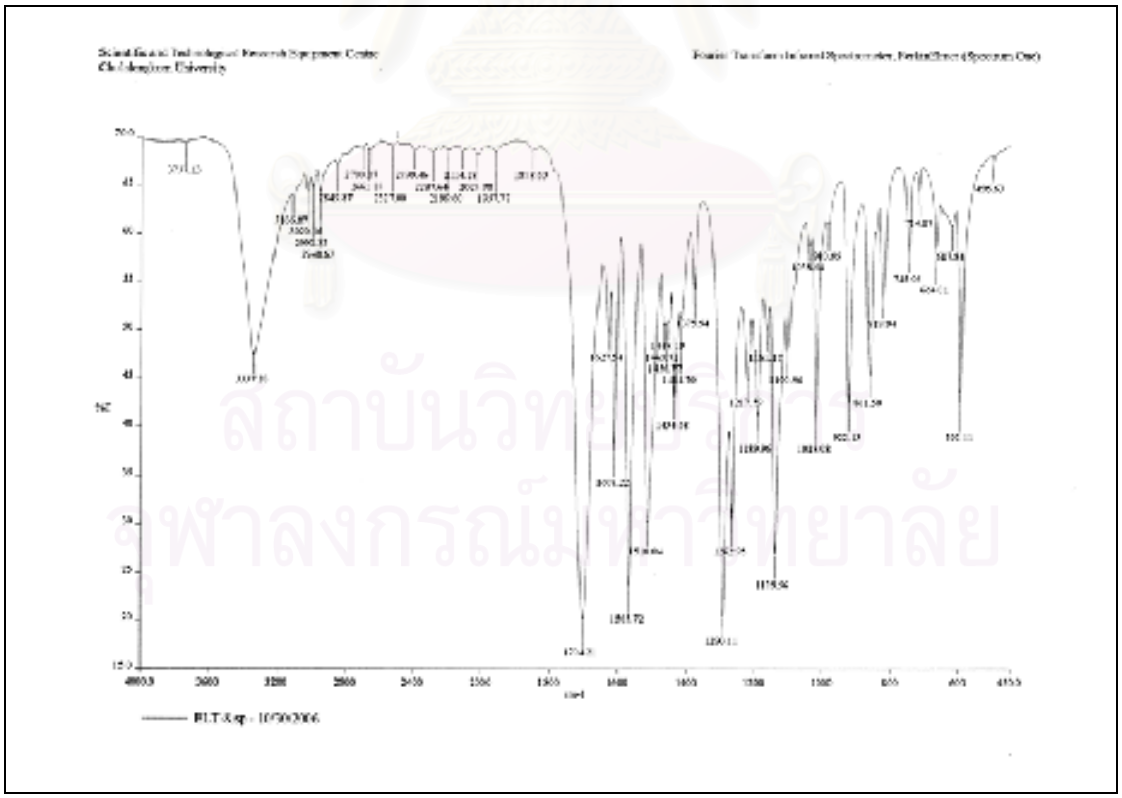

Figure 78. IR Spectrum of compound ET-S8 (KBr disc)

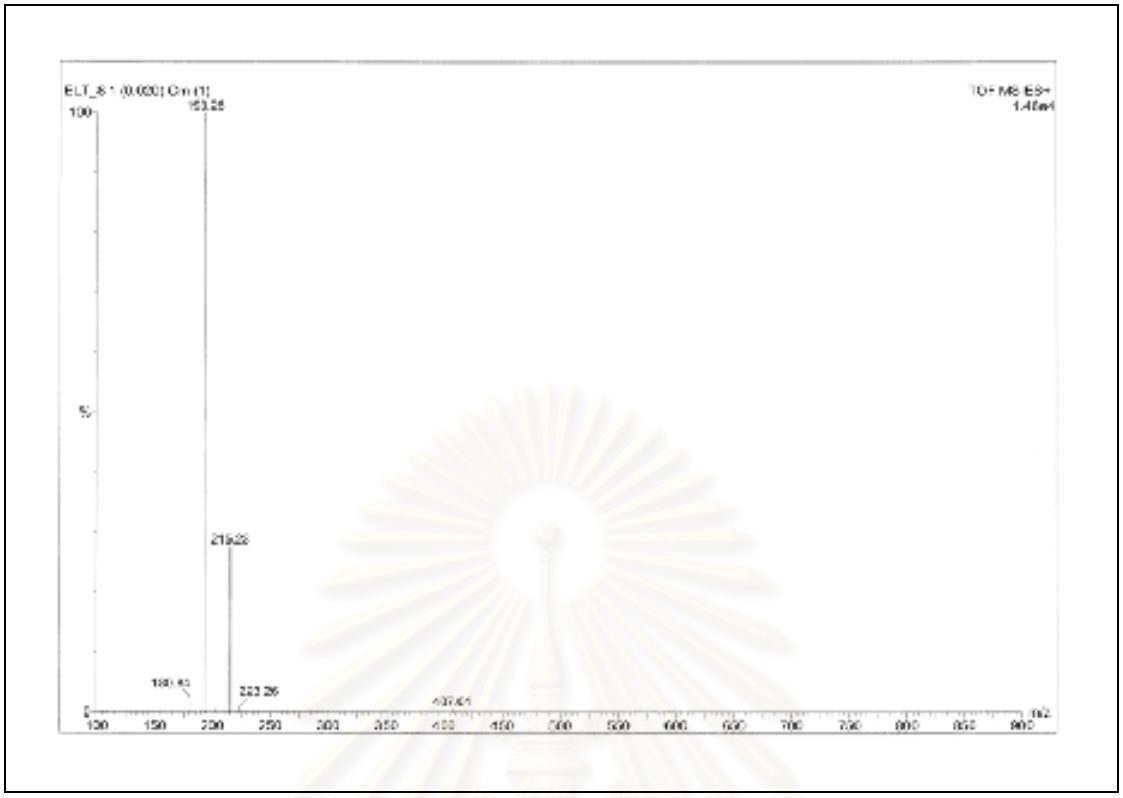

Figure 79. ESI Mass spectrum of compound ET-S8

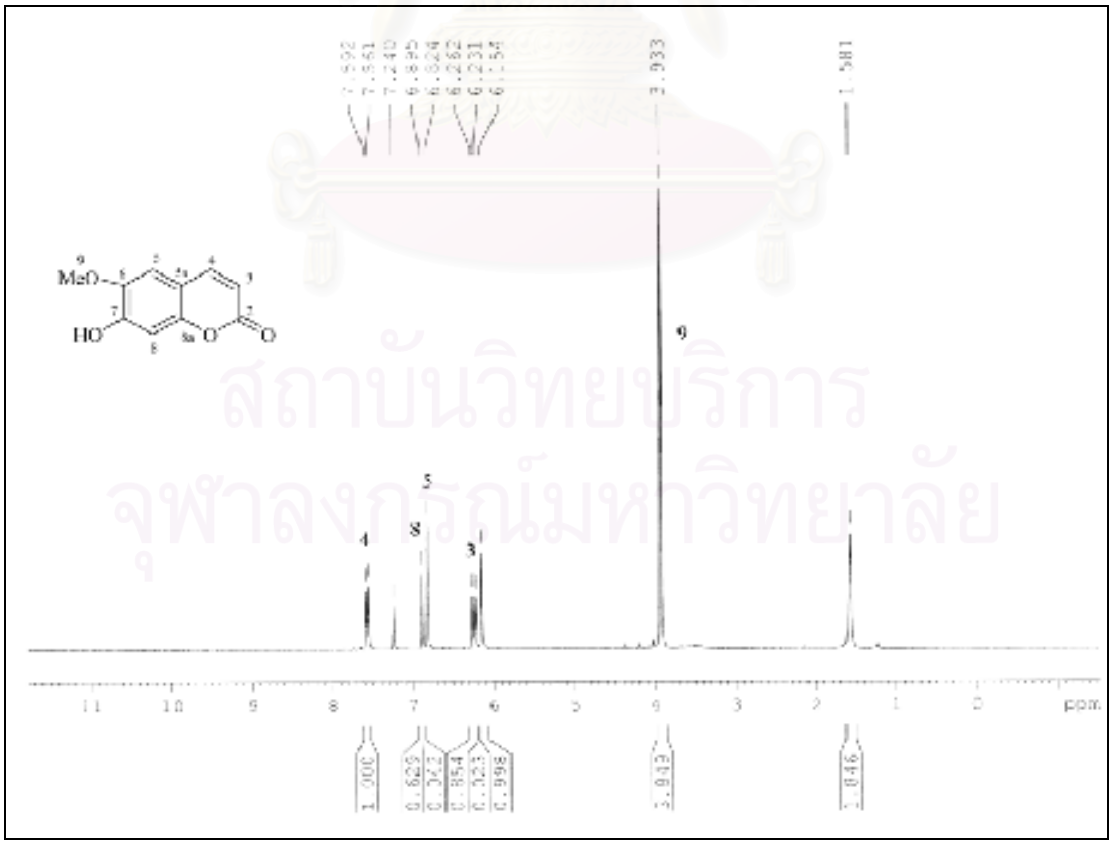

Figure 80. ^{1}H NMR (300 MHz) Spectrum of compound ET-S8 (in $CDCl_3$)

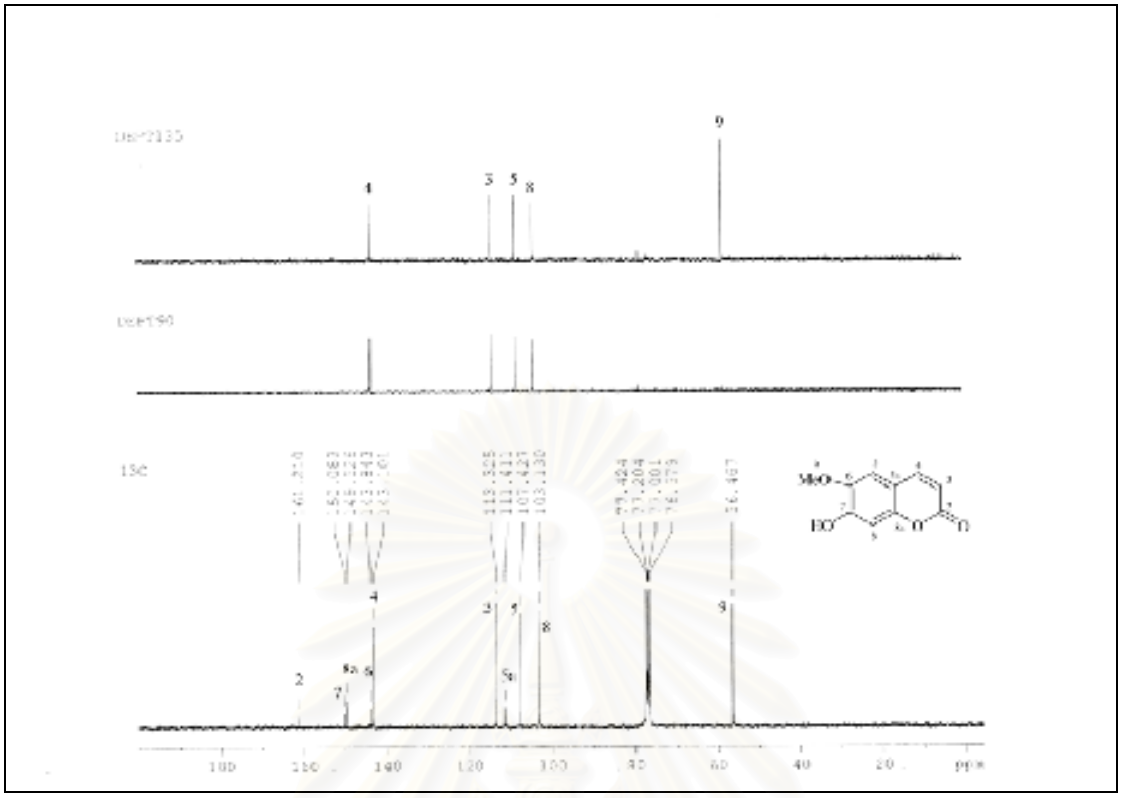

Figure 81. DEPT 135, DEPT 90 and ^{13}C NMR Spectrum of compound ET-S8

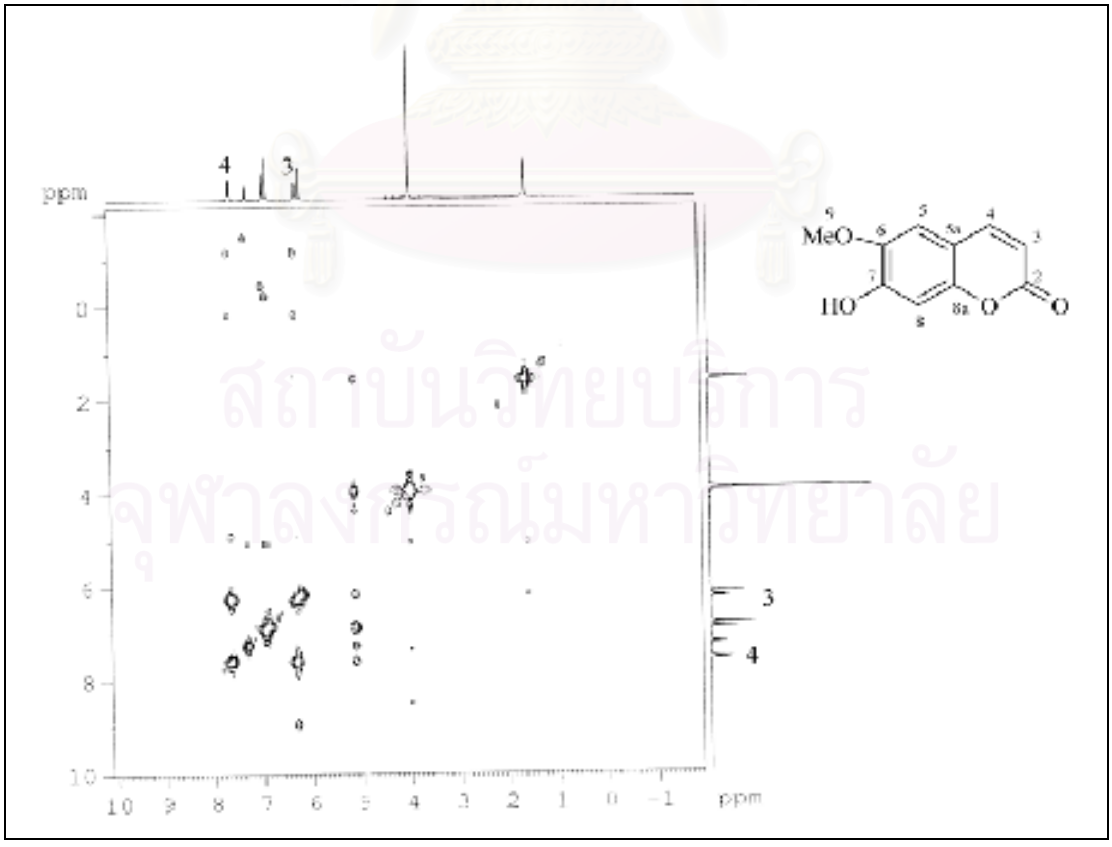

Figure 82. ^{1}H-^{1}H COSY Spectrum of compound ET-S8

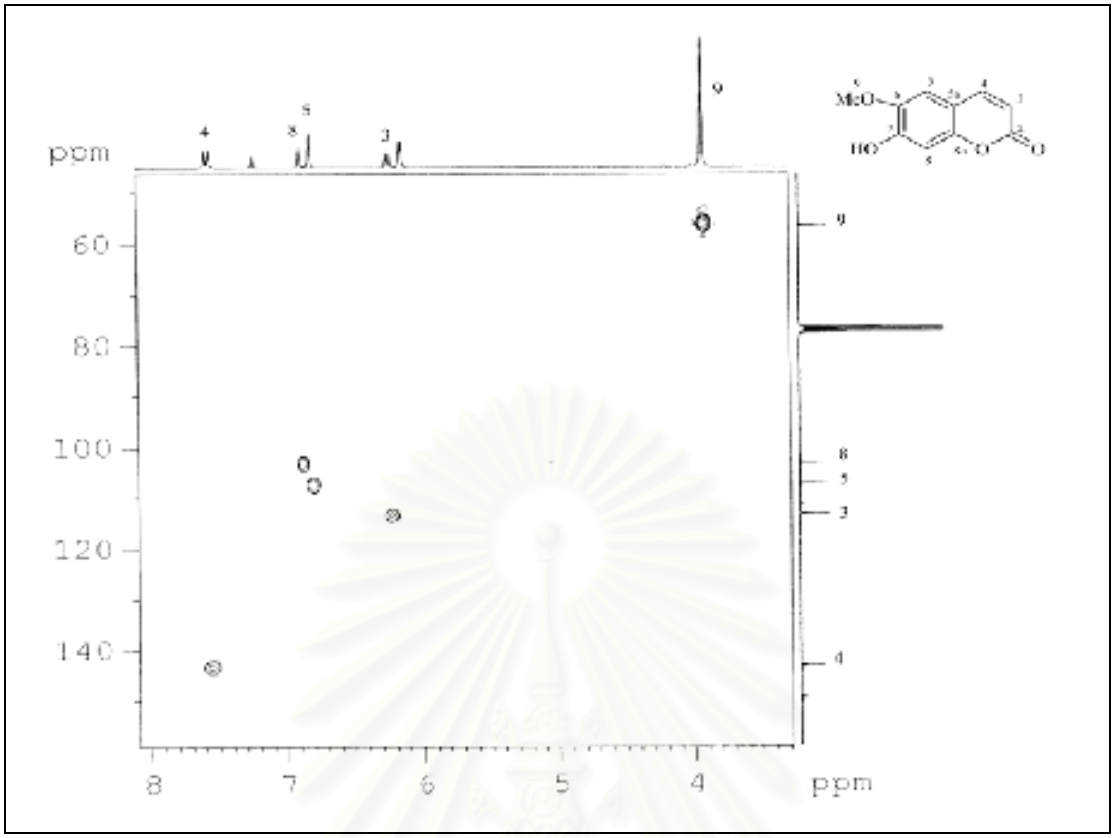

Figure 83. HMQC Spectrum of compound ET-S8

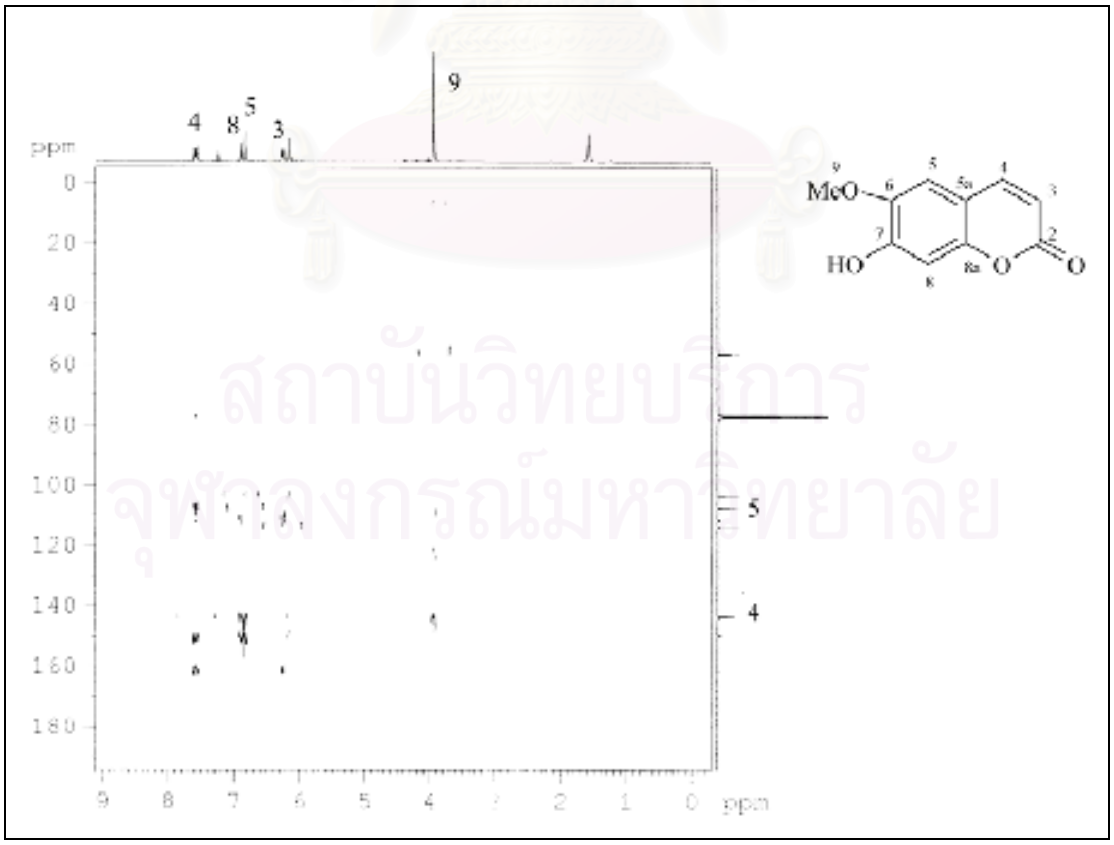

Figure 84. HMBC Spectrum of compound ET-S8

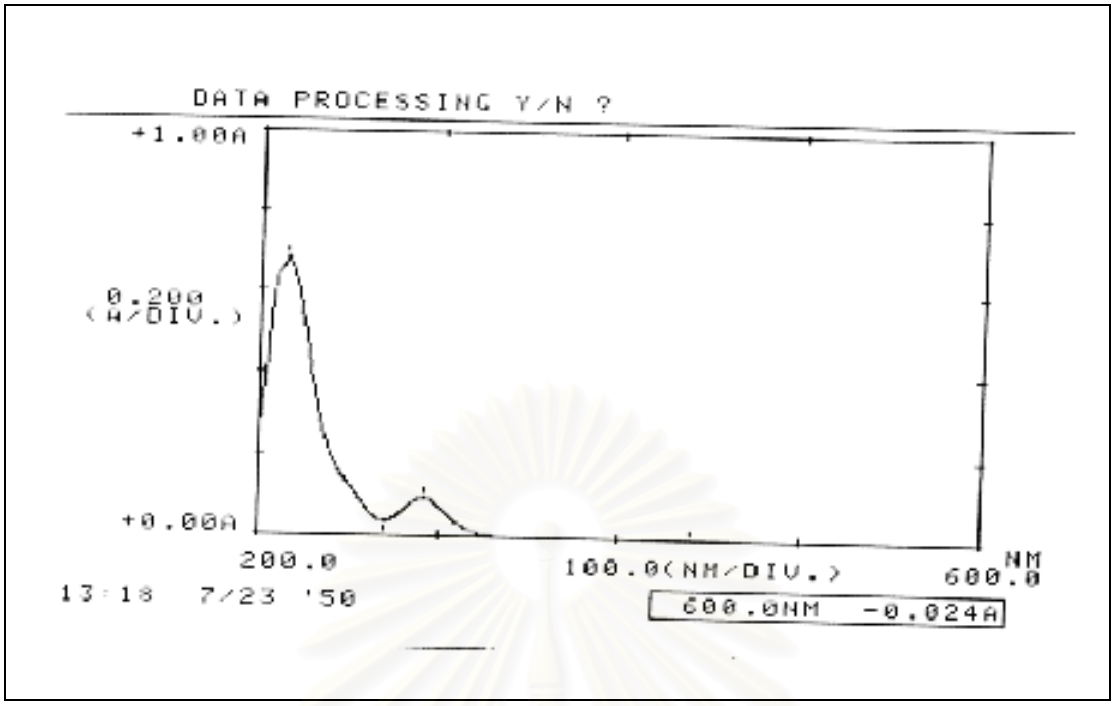

Figure 85. UV Spectrum of compound ET-S11 (in MeOH)

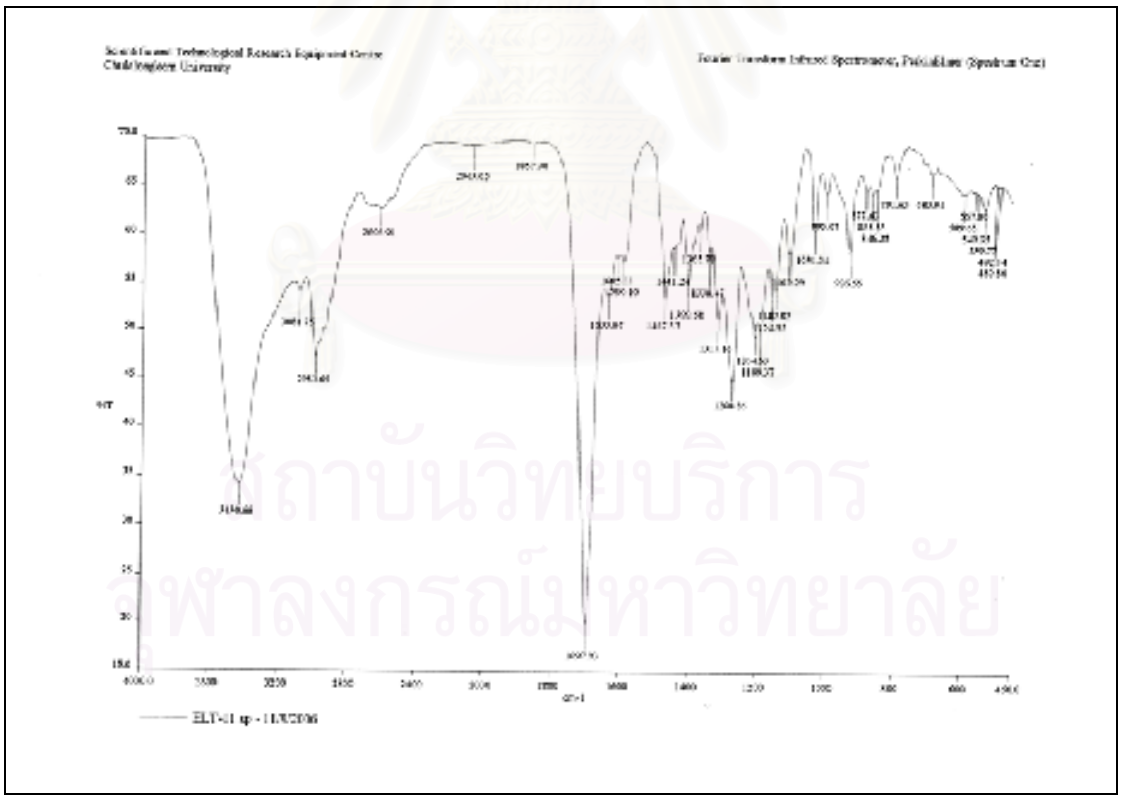

Figure 86. IR Spectrum of compound ET-S11 (KBr disc)

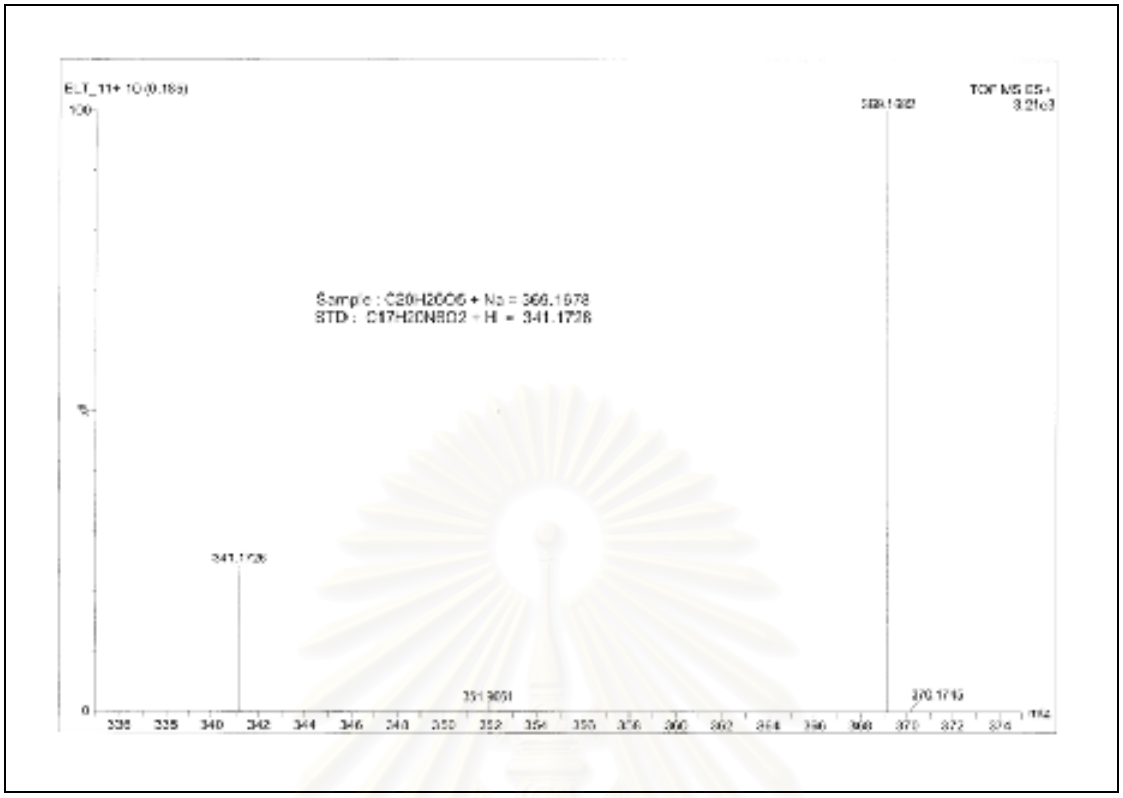

Figure 87. HR ESI Mass spectrum of compound ET-S11

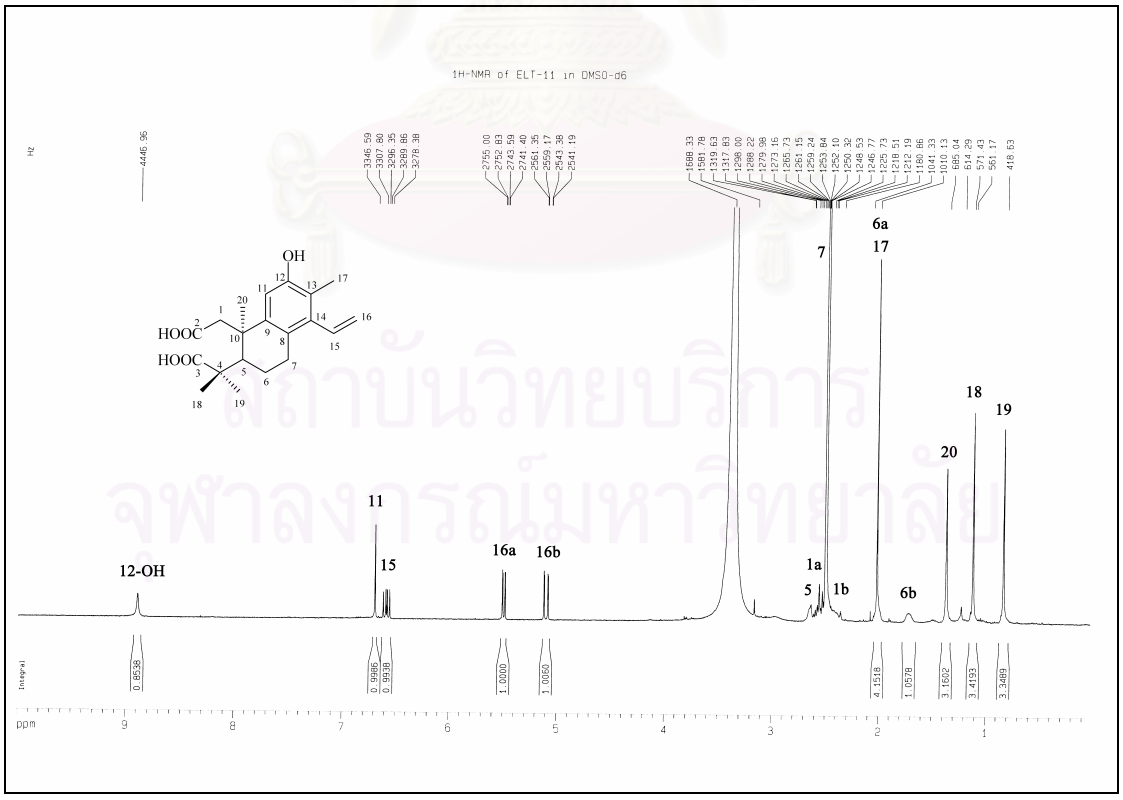

Figure 88. ^{1}H NMR (500 MHz) Spectrum of compound ET-S11 (in DMSO-d_6)

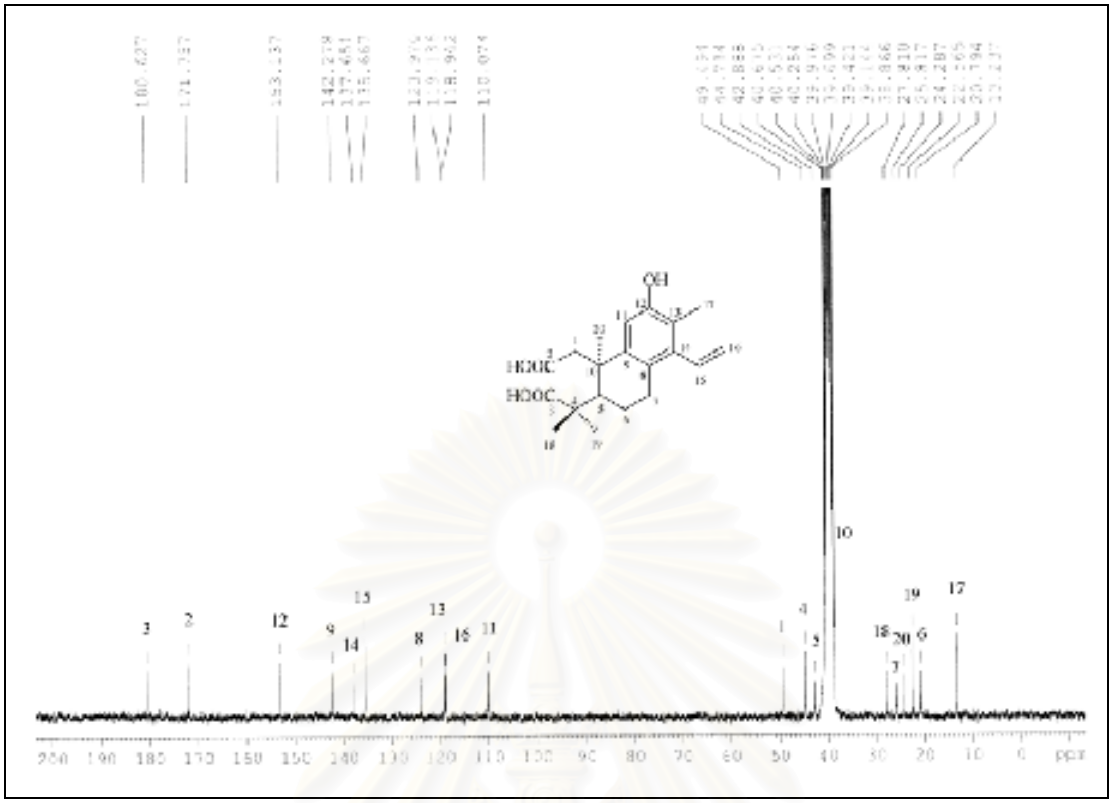

Figure 89. ^{13}C NMR (125 MHz) Spectrum of compound ET-S11 (in DMSO-d_6)

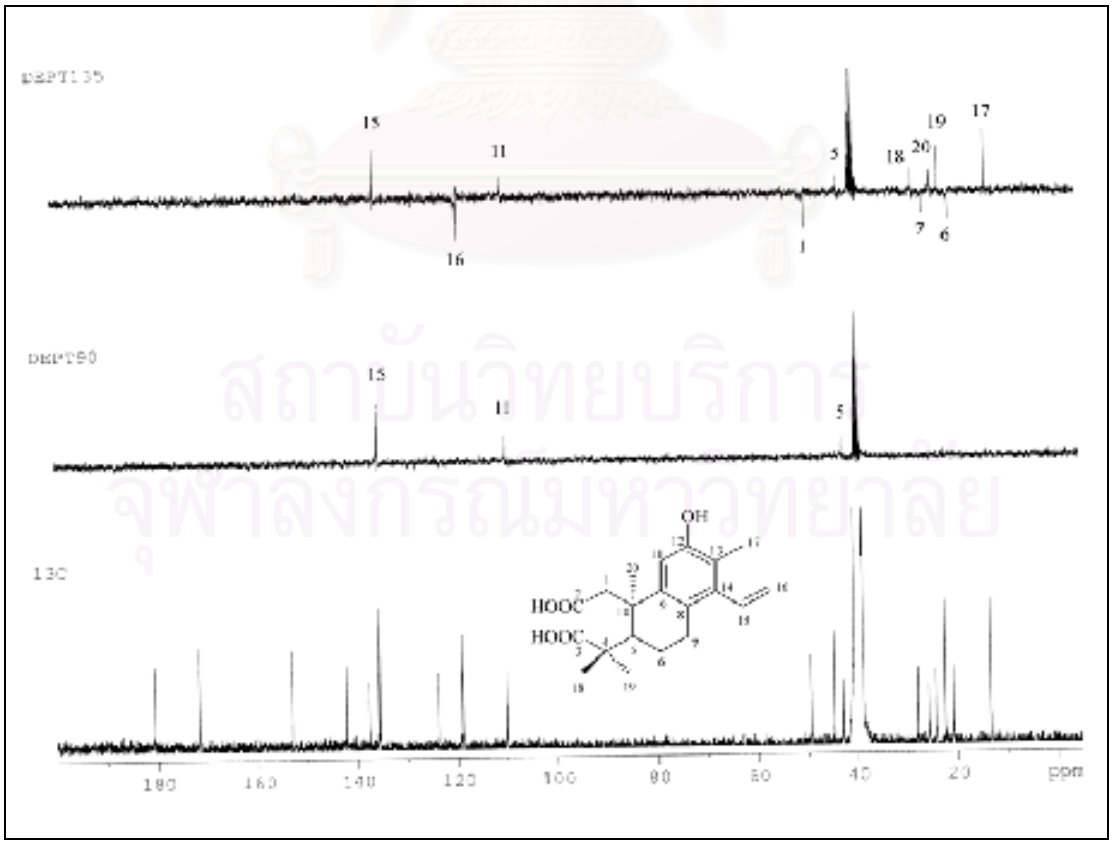

Figure 90. DEPT 135, DEPT 90 and ^{13}C NMR of compound ET-S11

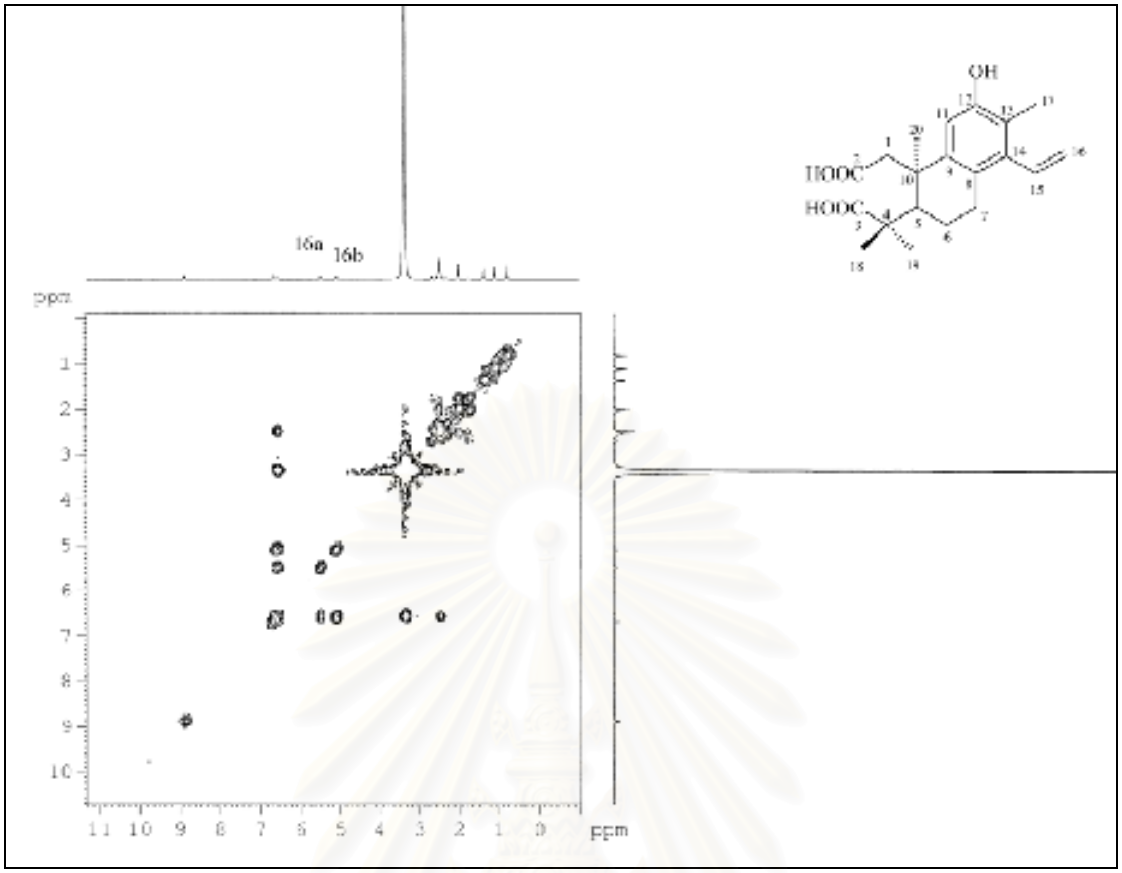

Figure 91a. ^{1}H-^{1}H COSY Spectrum of compound ET-S11

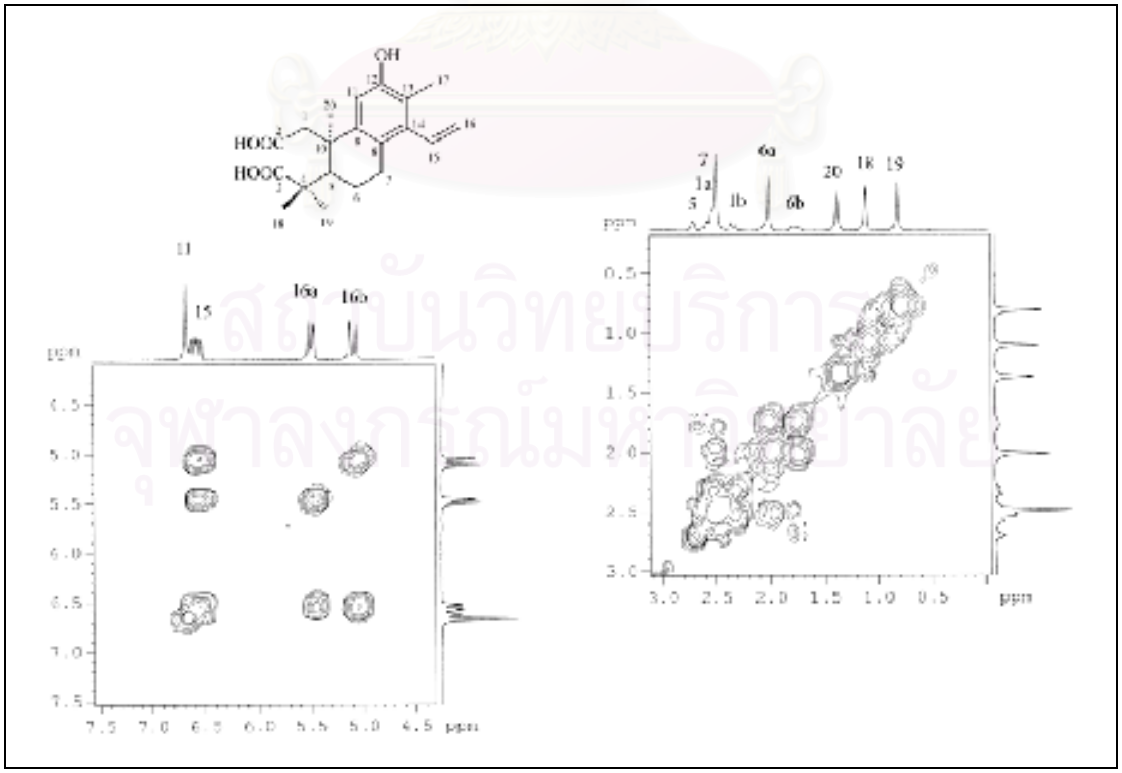

Figure 91b. ^{1}H-^{1}H COSY Spectrum of compound ET-S11 (expansion)

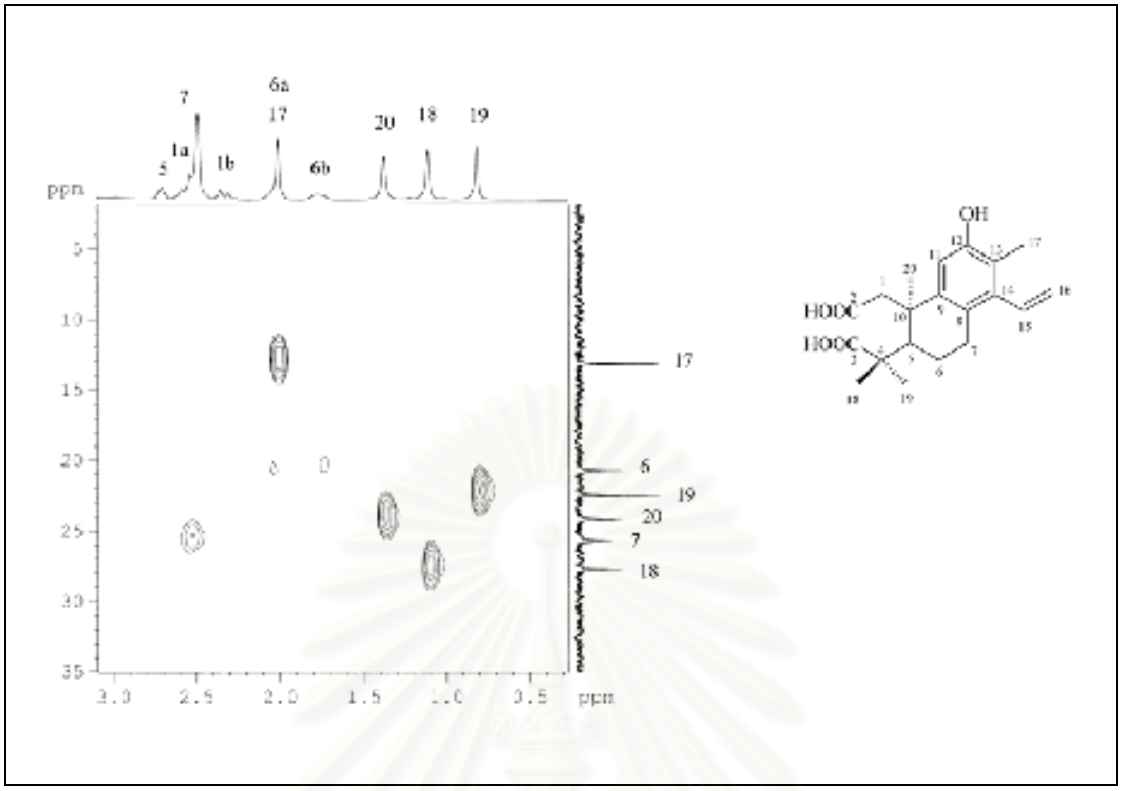

Figure 92a. HMQC Spectrum of compound ET-S11 (δ_H 0.3-3.1 ppm, δ_C 2-35 ppm)

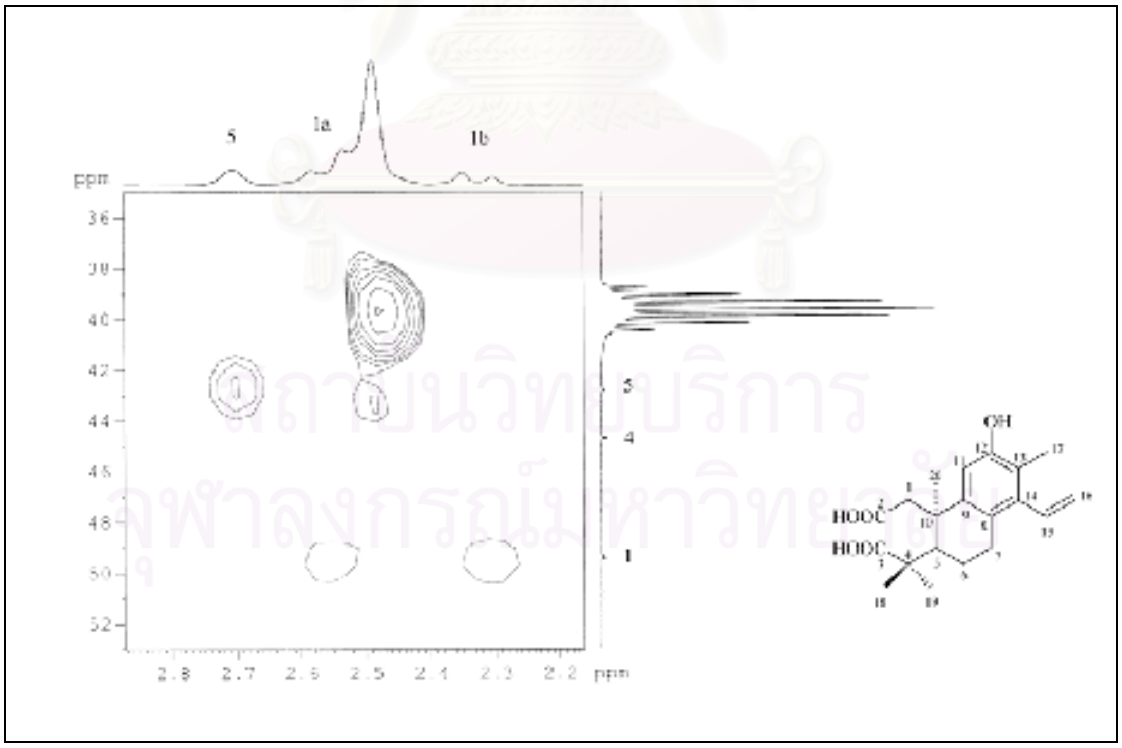

Figure 92b. HMQC Spectrum of compound ET-S11 (δ_H 2.2-2.9 ppm, δ_C 36-52 ppm)

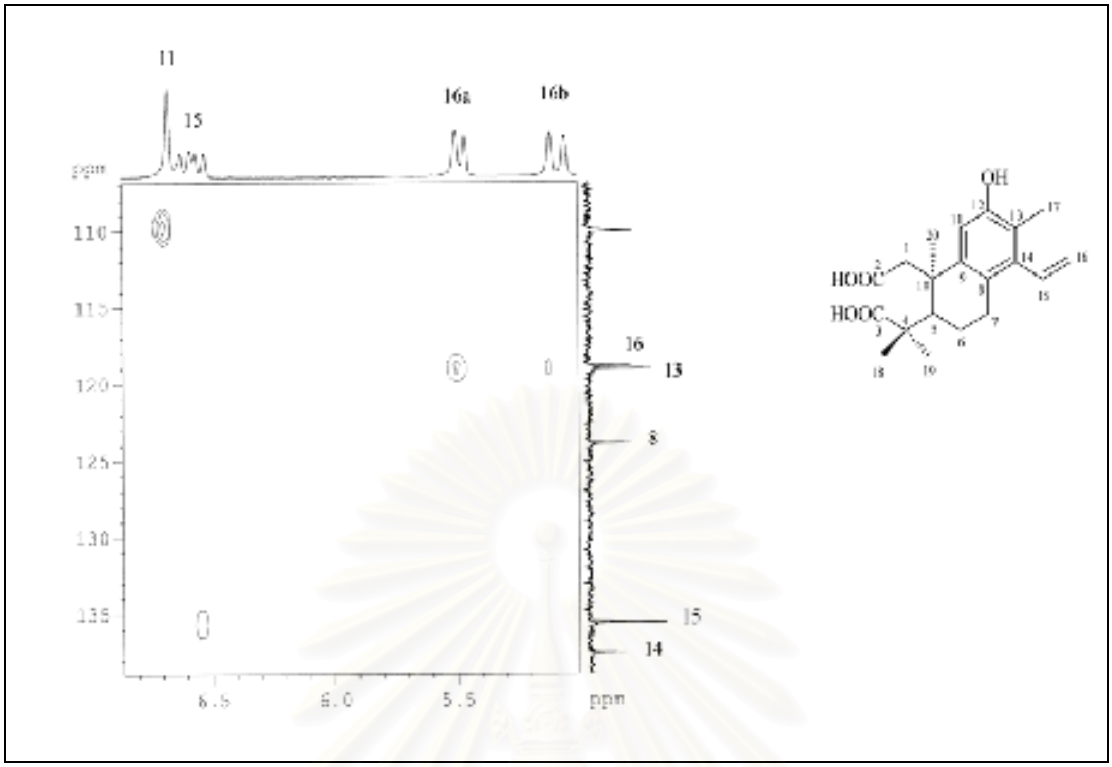

Figure 92c. HMQC Spectrum of compound ET-S11
(δ_H 5.0-6.8 ppm, δ_C 107-139 ppm)

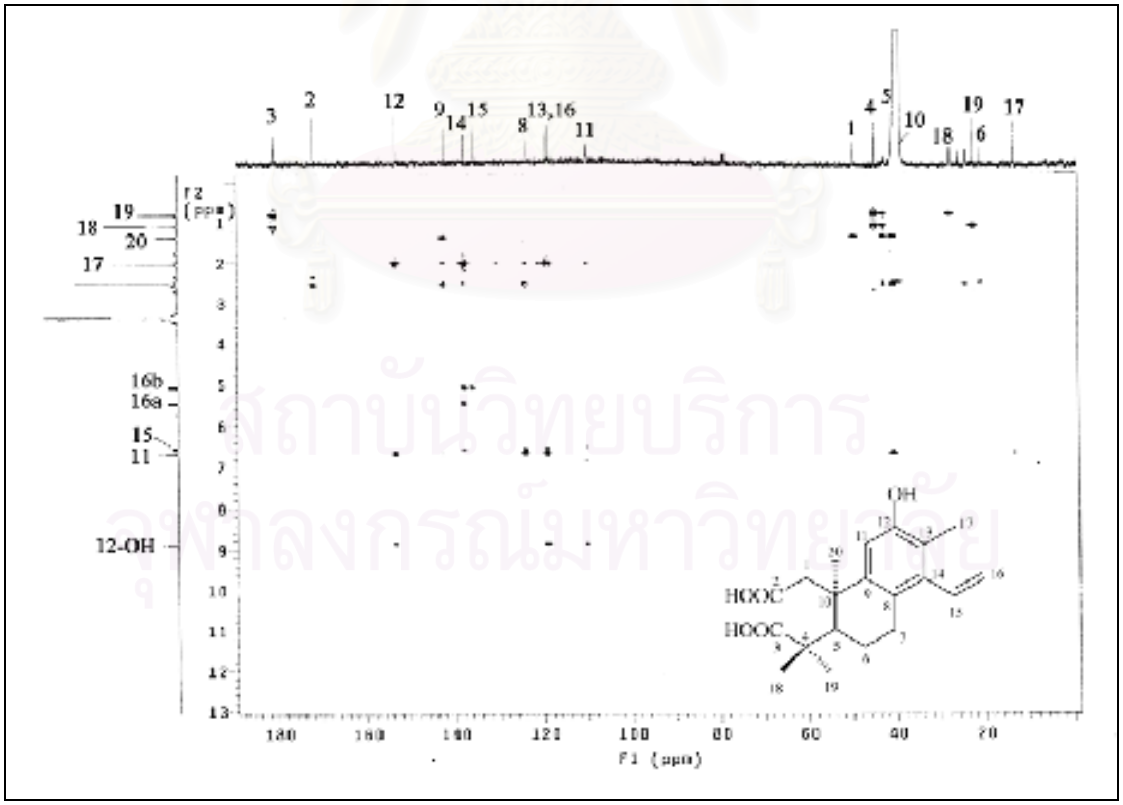

Figure 93a. HMBC Spectrum of compound ET-S11

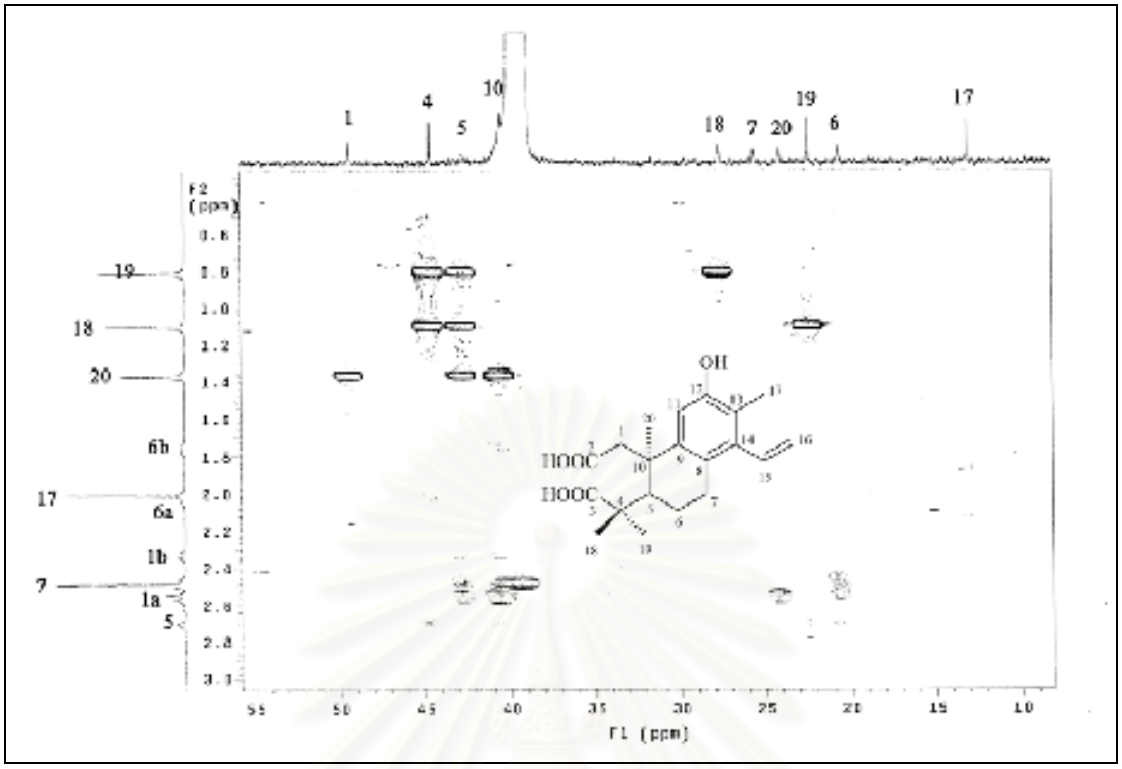

Figure 93b. HMBC Spectrum of compound ET-S11 (δ_H 0.4-3.0 ppm, δ_C 10-55 ppm)

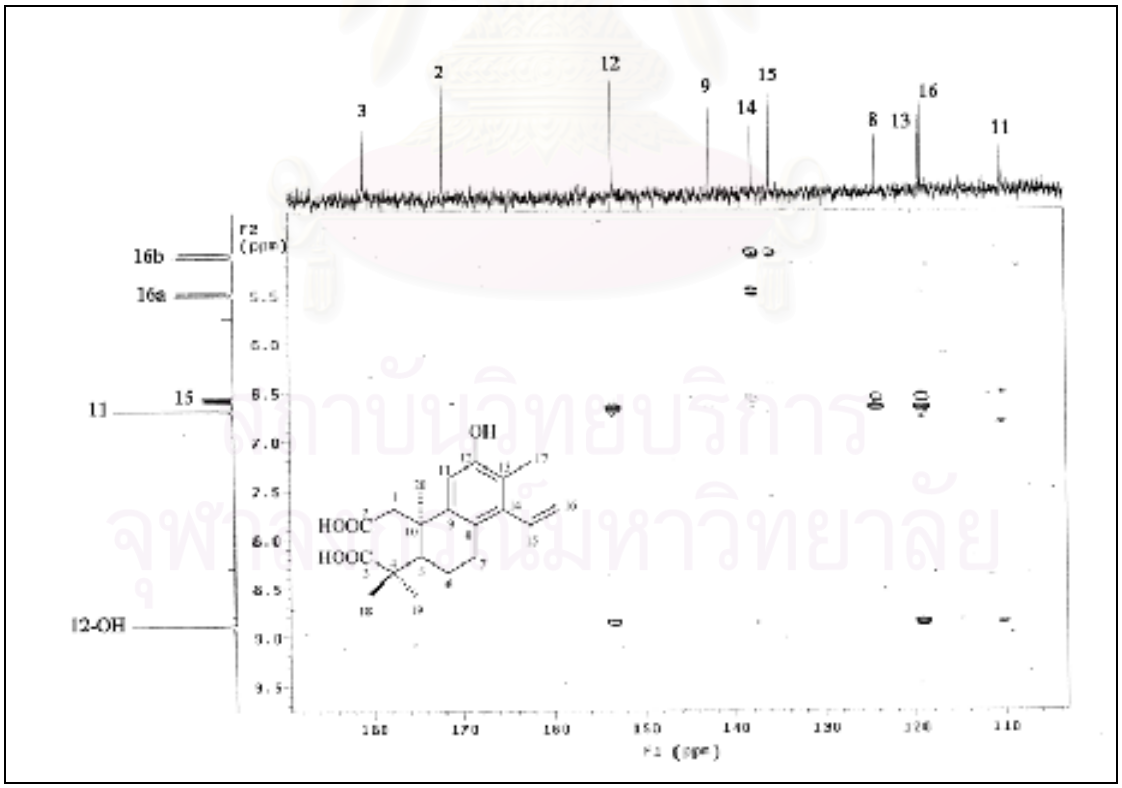

Figure 93c. HMBC Spectrum of compound ET-S11
(δ_H 4.5-9.7 ppm, δ_C 105-190 ppm)

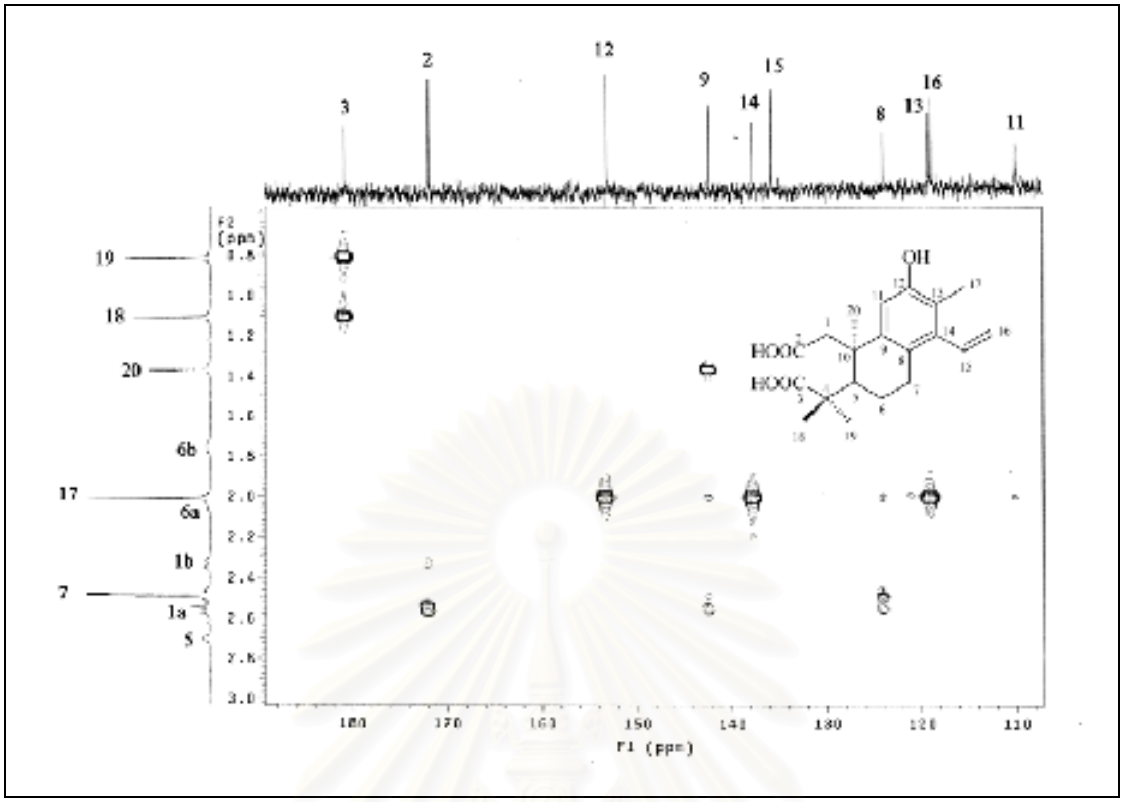

Figure 93d. HMBC Spectrum of compound ET-S11
(δ_H 0.6-3.0 ppm, δ_C 110-190 ppm)

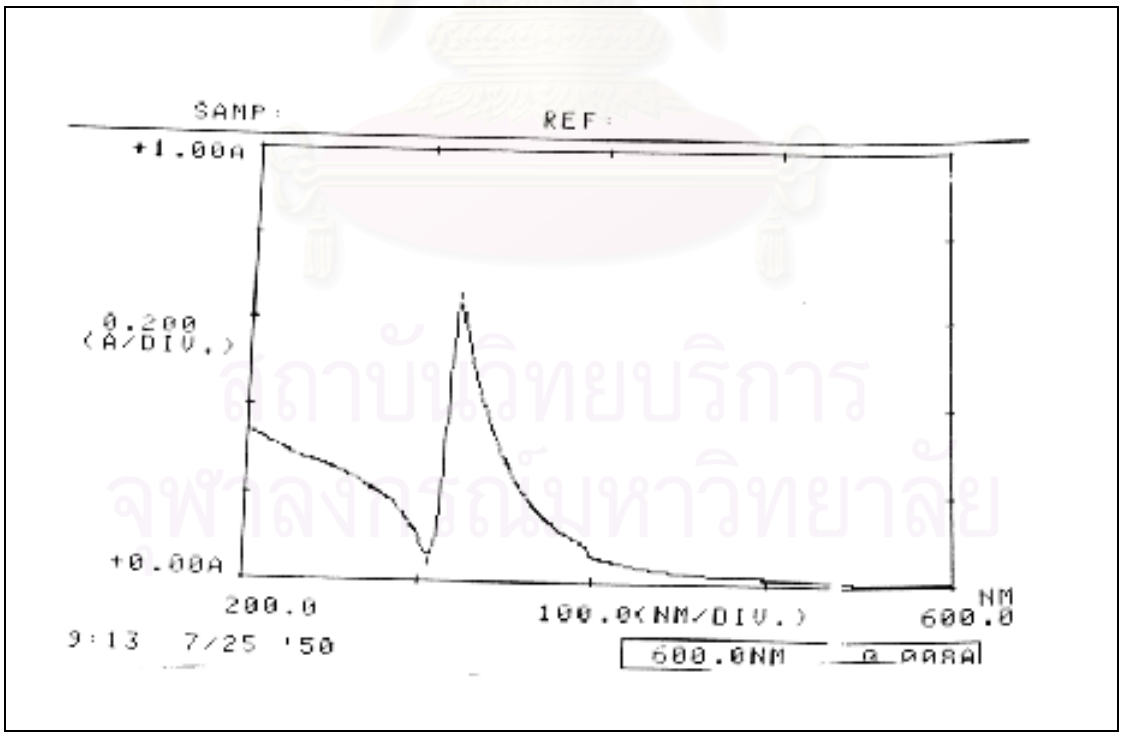

Figure 94. UV Spectrum of compound ET-S12 (in $CHCl_3$)

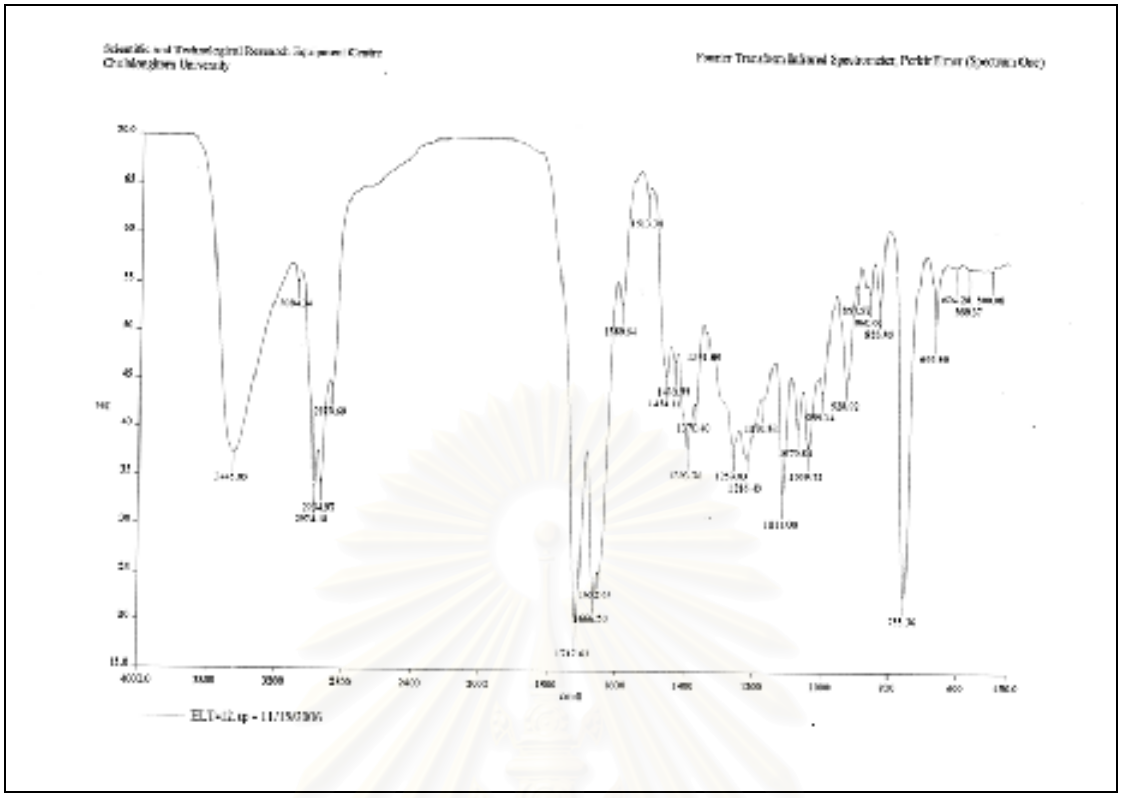

Figure 95. IR Spectrum of compound ET-S12 (KBr disc)

Figure 96. ESI Mass spectrum of compound ET-S12

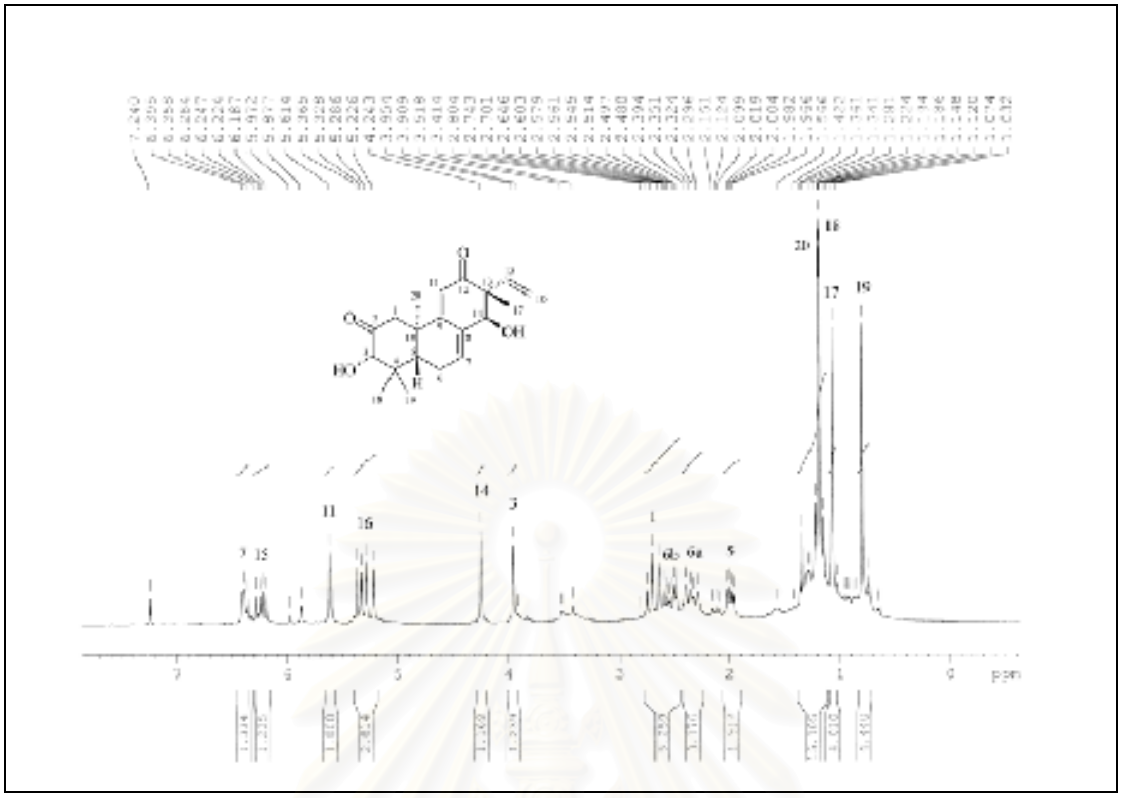

Figure 97. ^{1}H NMR (300 MHz) Spectrum of compound ET-S12 (in $CDCl_3$)

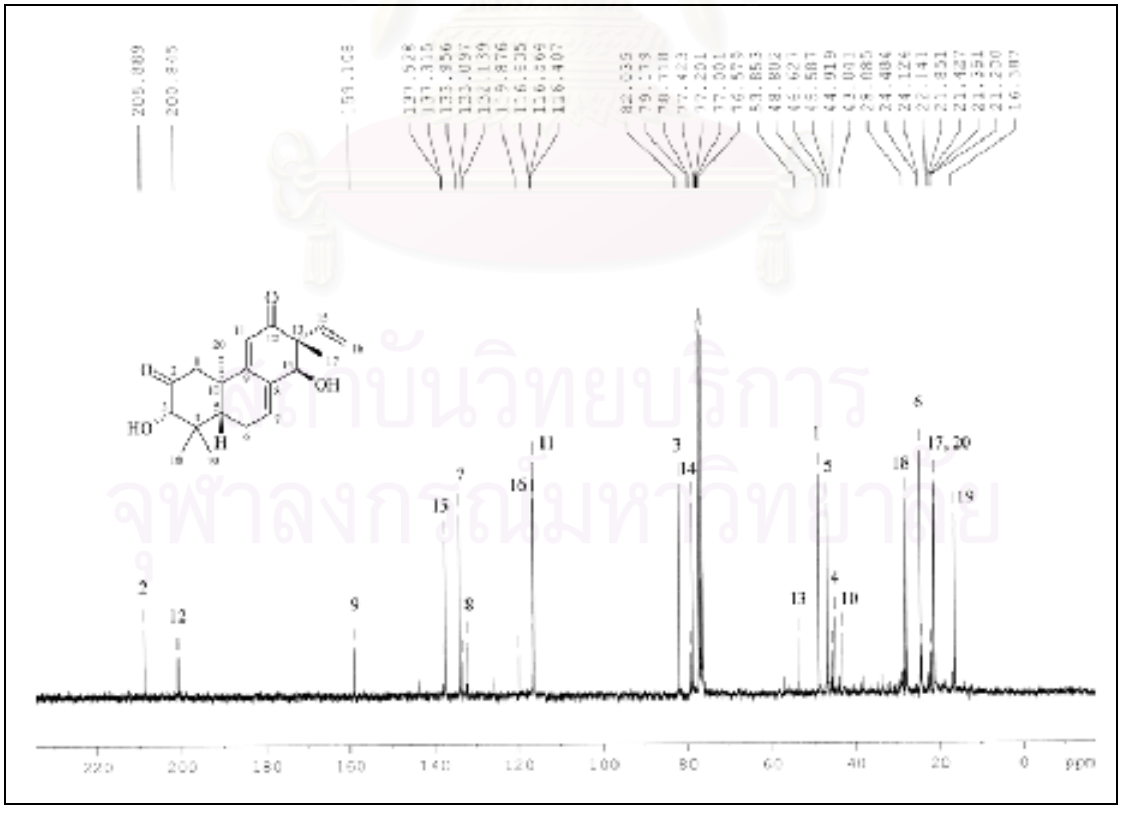

Figure 98. ^{13}C NMR (75 MHz) Spectrum of compound ET-S12 (in $CDCl_3$)

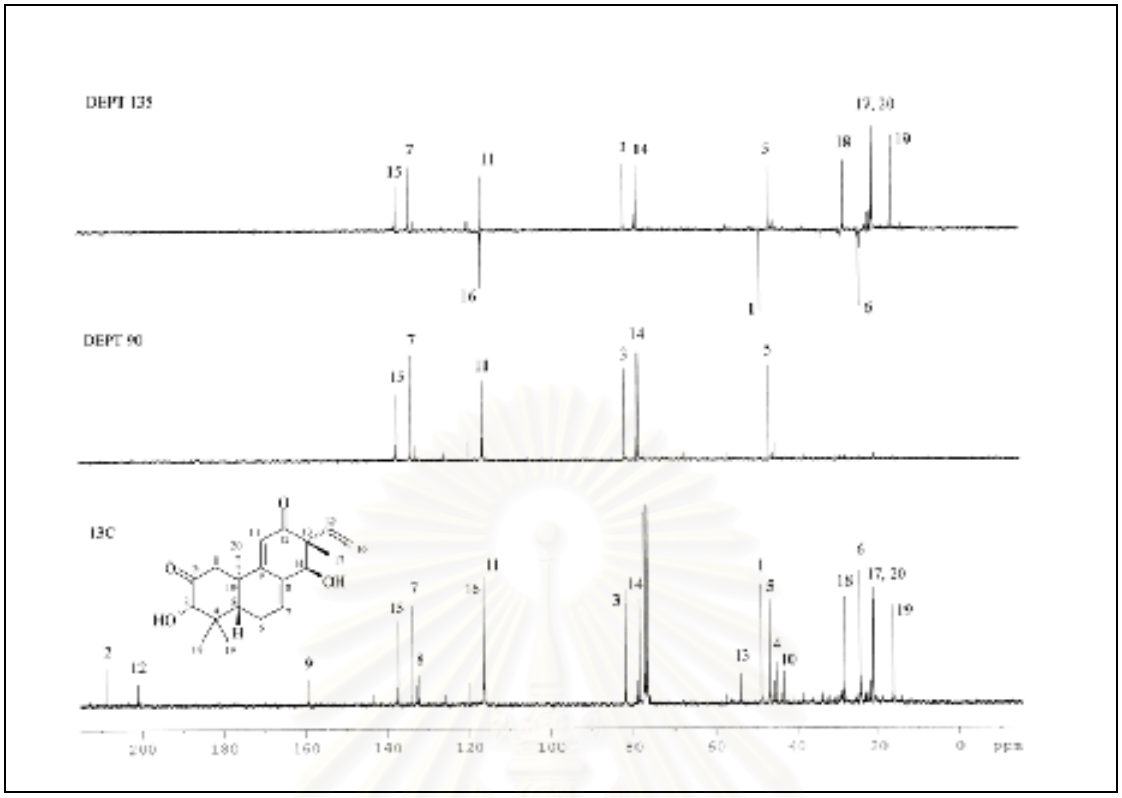

Figure 99. DEPT 135, DEPT 90 and ^{13}C NMR Spectrum of compound ET-S12

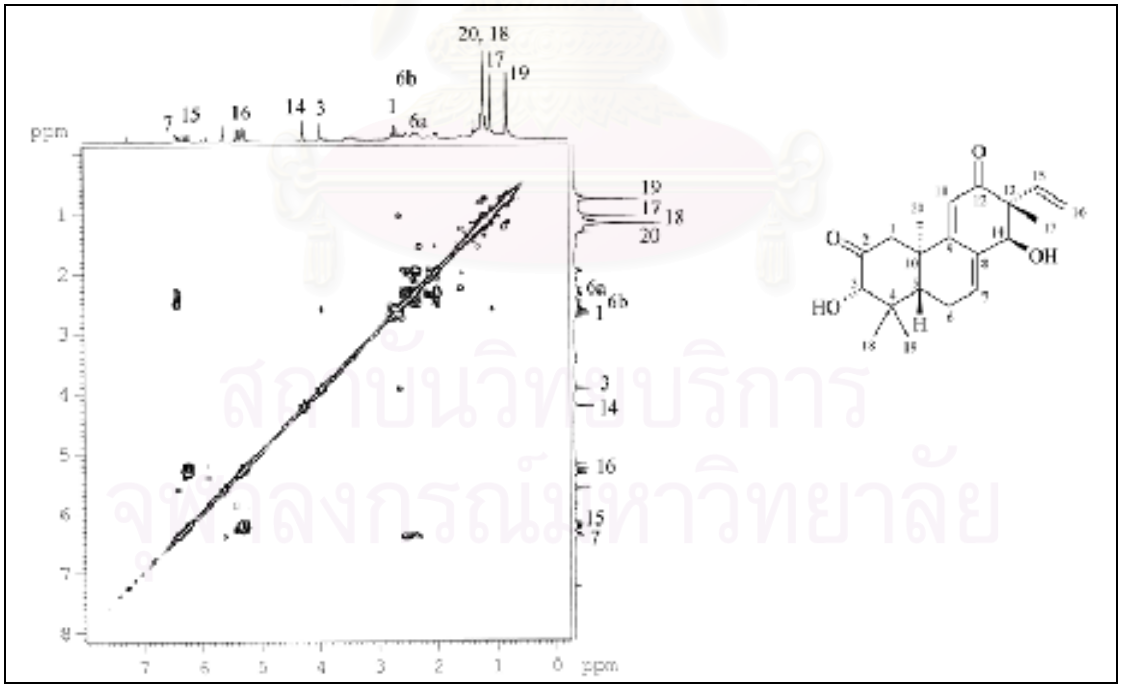

Figure 100. ^{1}H-^{1}H COSY Spectrum of compound ET-S12

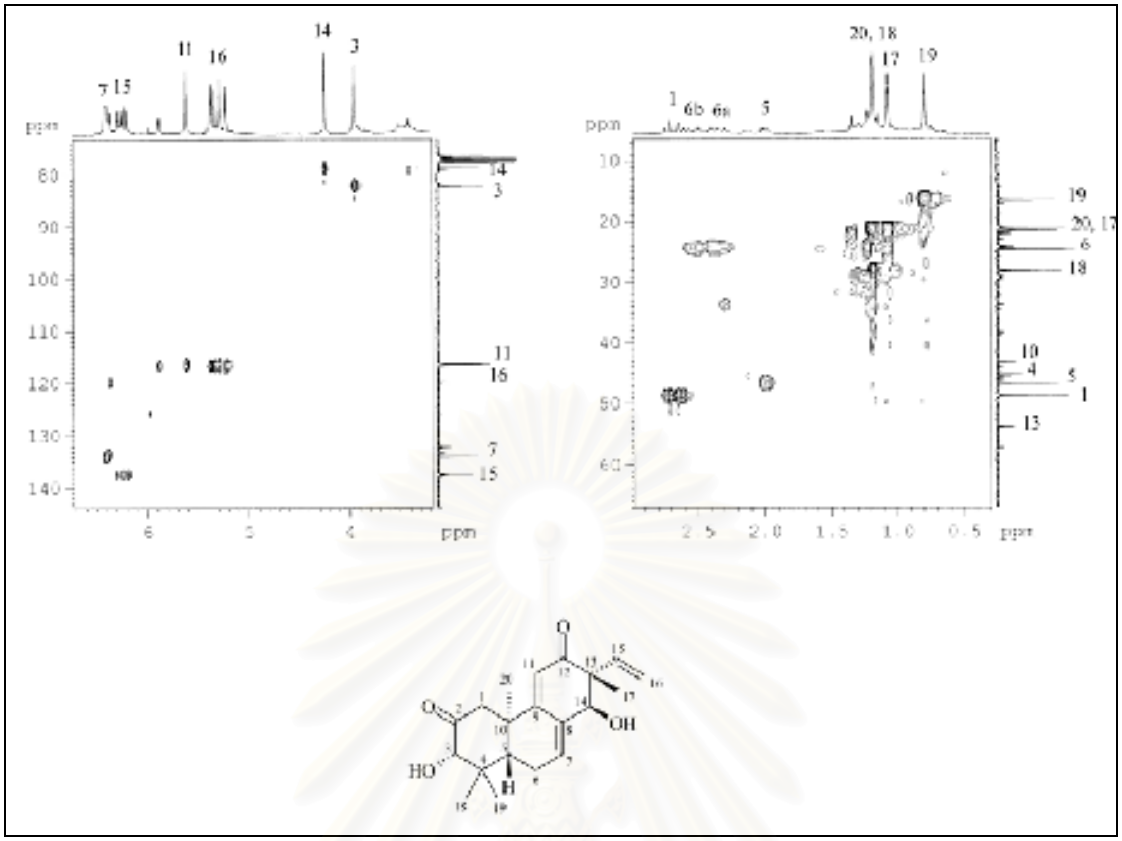

Figure 101. HMQC Spectrum of compound ET-S12

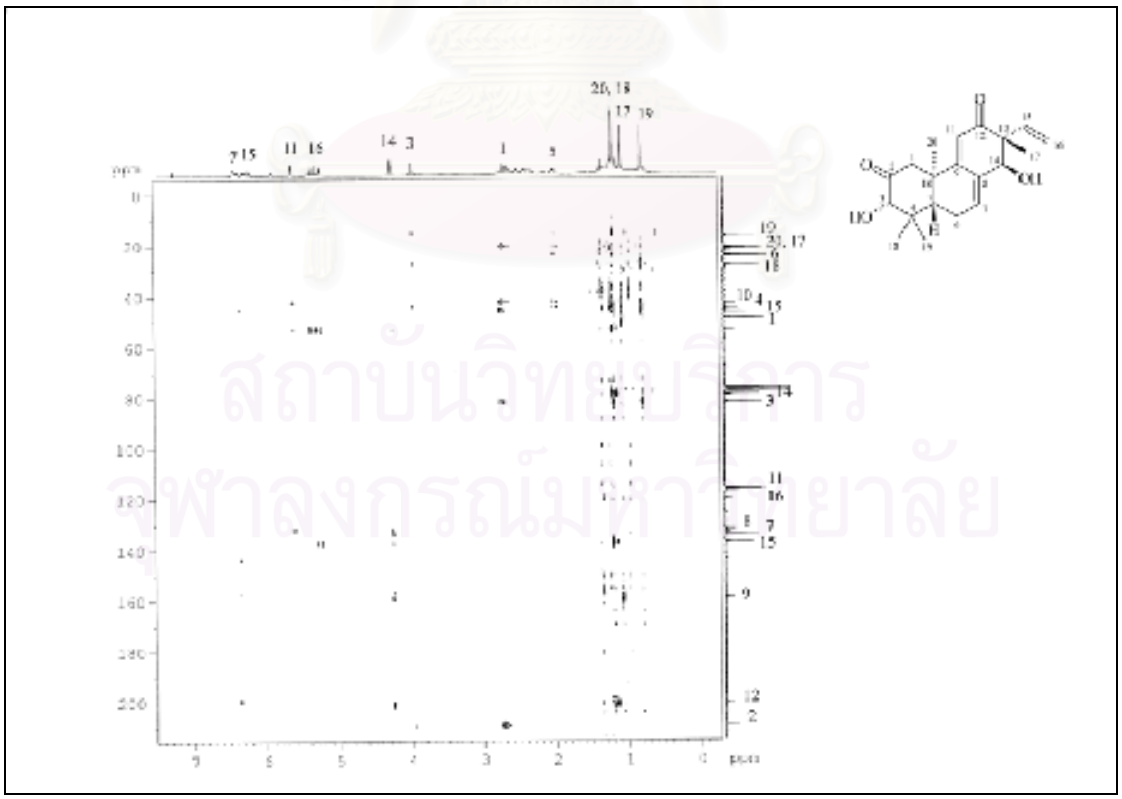

Figure 102. HMBC Spectrum of compound ET-S12

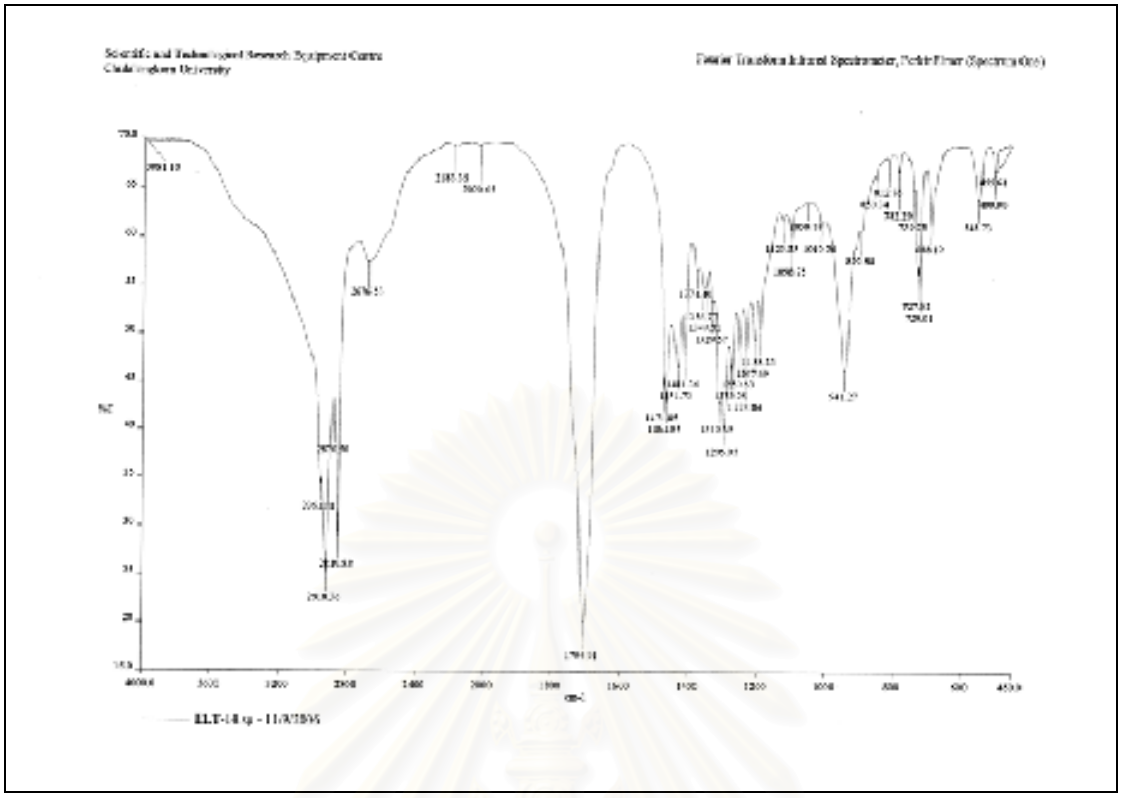

Figure 103. IR Spectrum of compound ET- S14 (KBr disc)

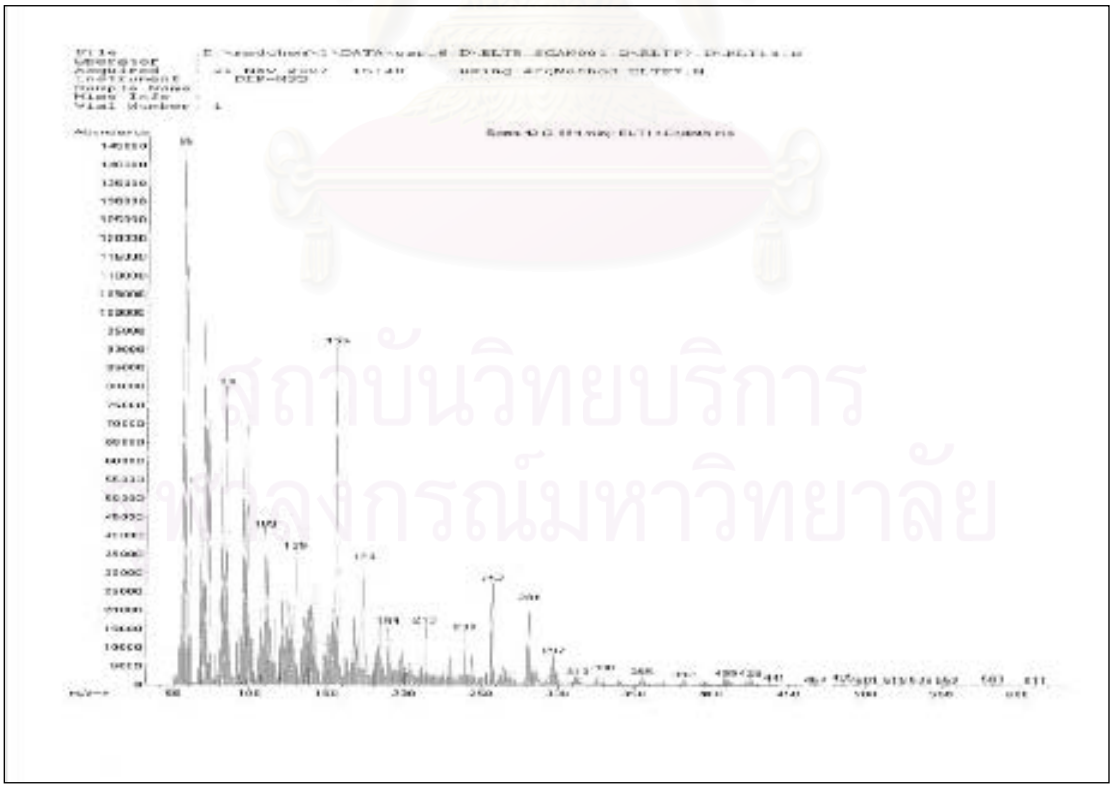

Figure 104. EI Mass spectrum of compound ET-S14

Figure 105. ^{1}H NMR (300 MHz) Spectrum of compound ET-S14 (in $CDCl_3$)

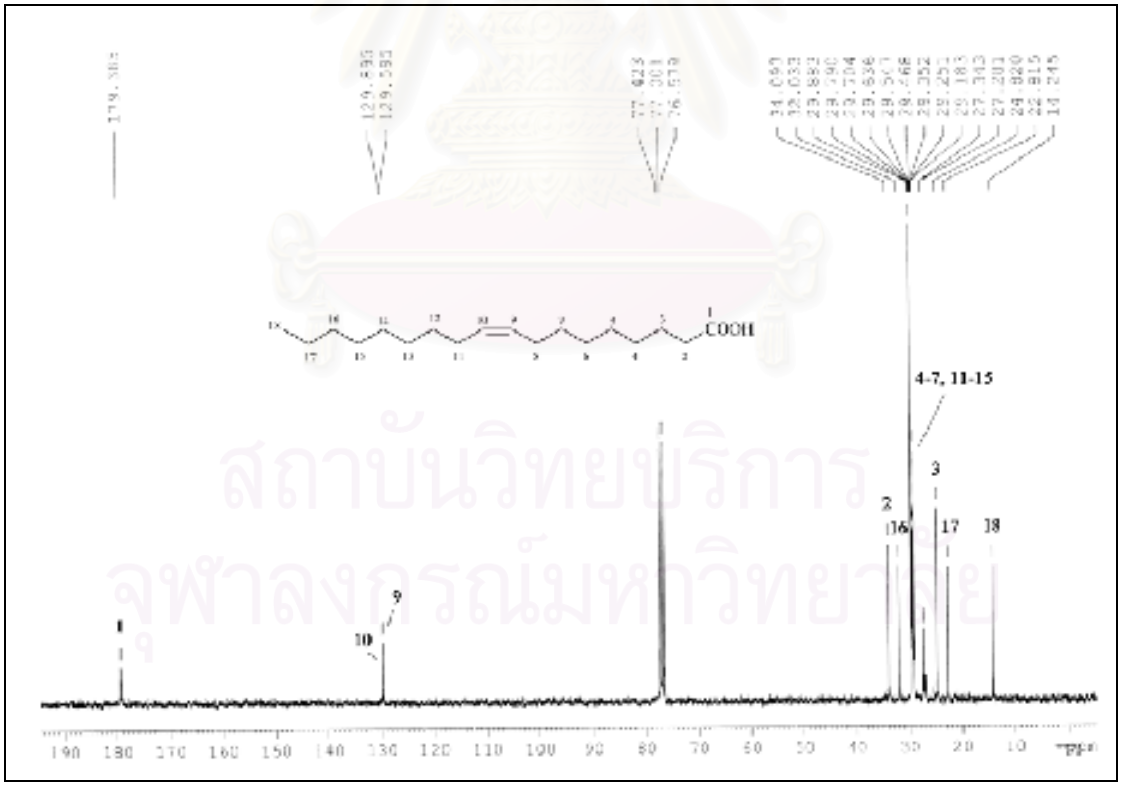

Figure 106. ^{13}C NMR (75 MHz) Spectrum of compound ET-S14 (in $CDCl_3$)

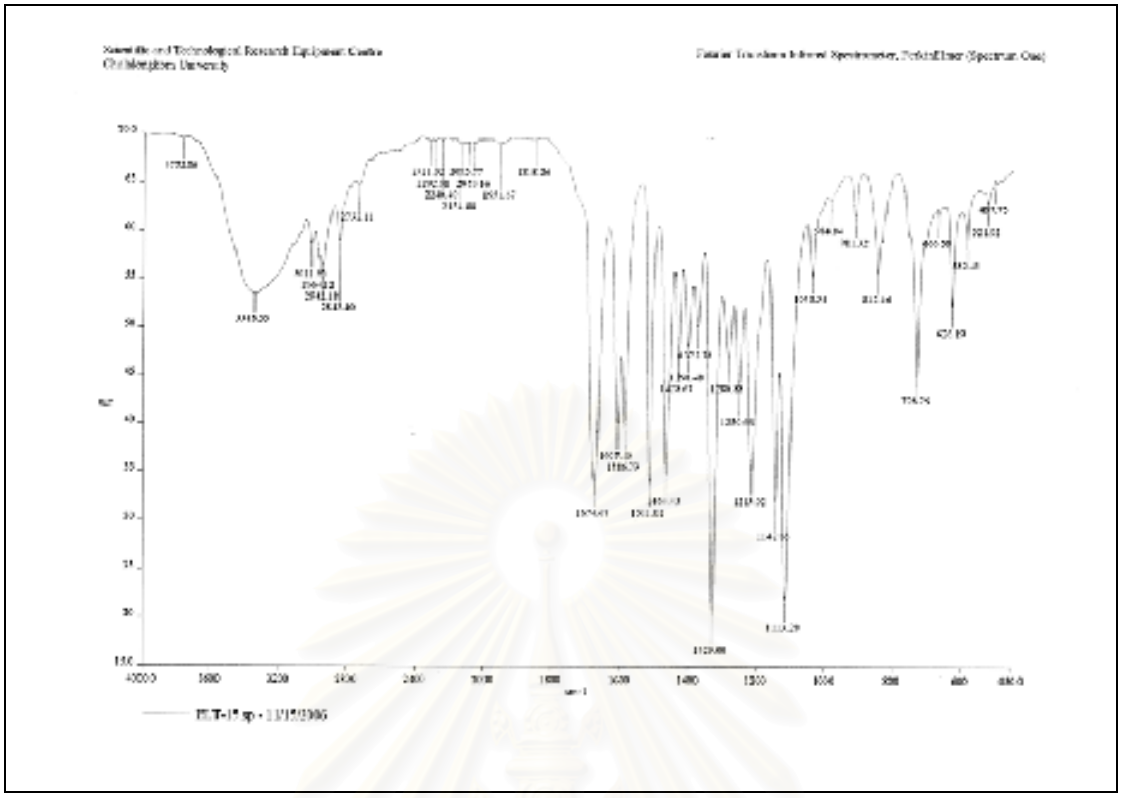

Figure 207. IR Spectrum of compound ET-S15 (KBr disc)

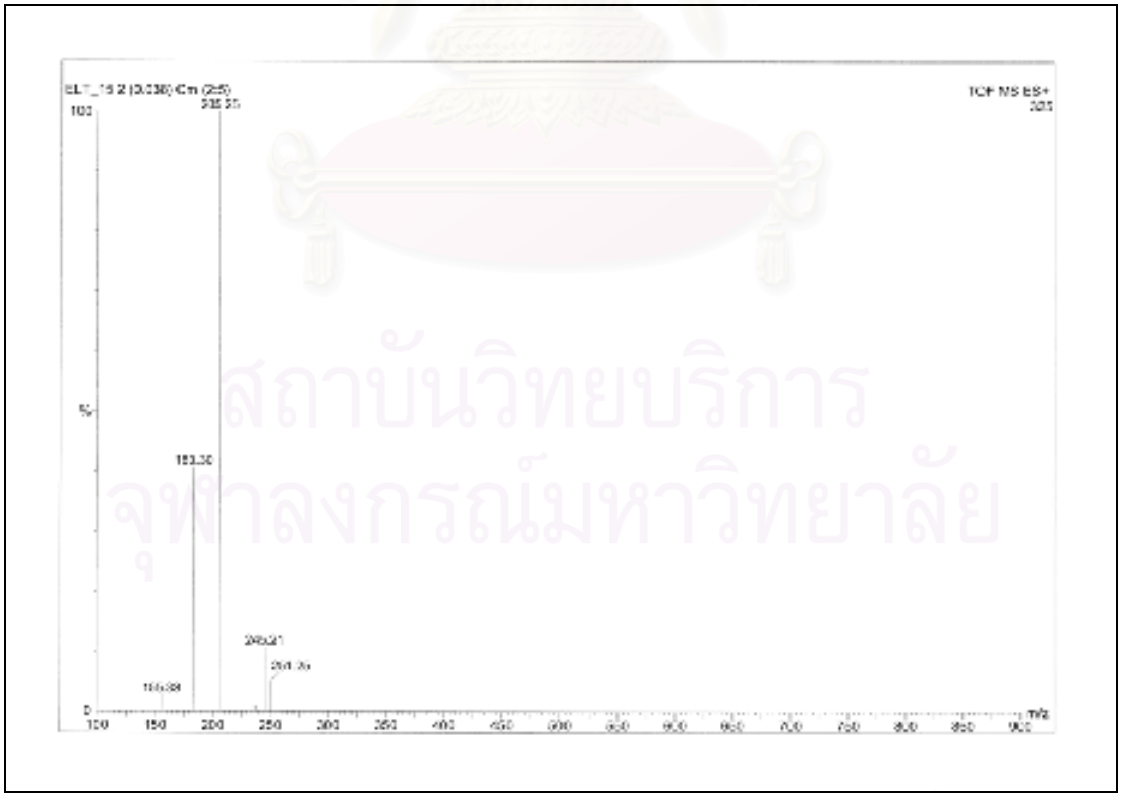

Figure 108. ESI Mass spectrum of compound ET-S15

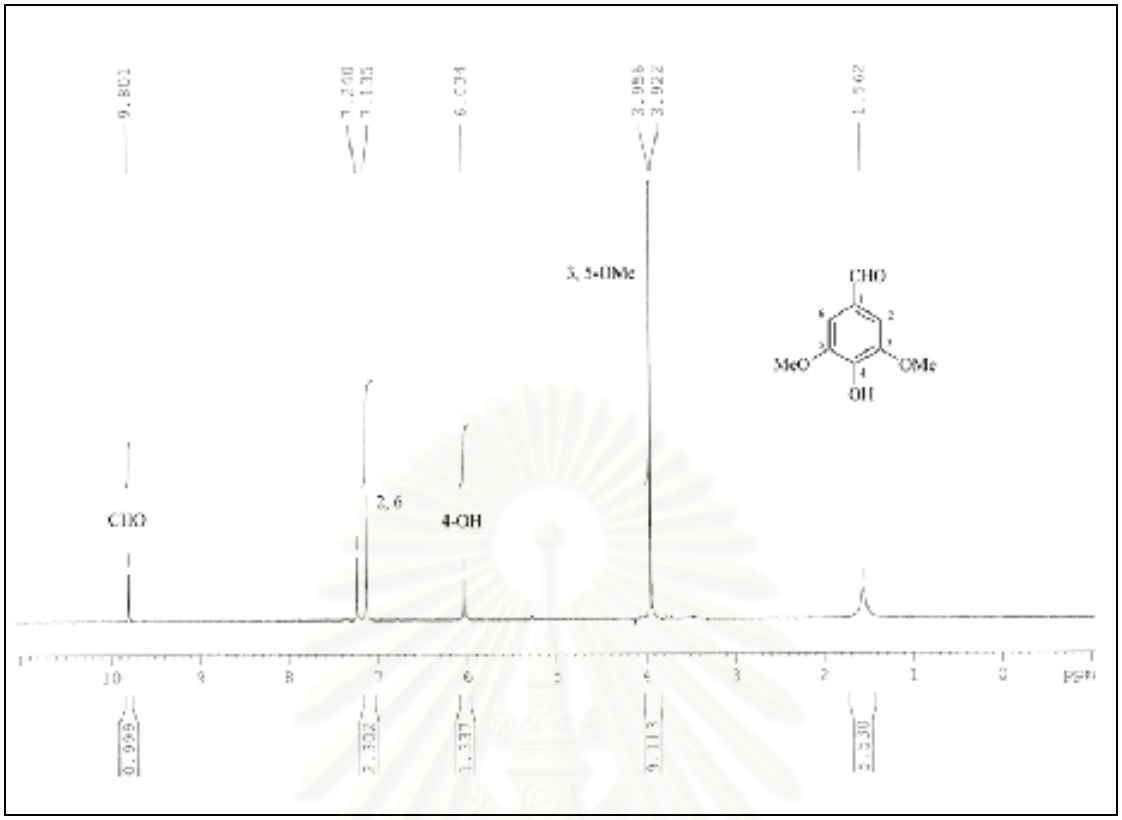

Figure 109. ^{1}H NMR (300 MHz) Spectrum of compound ET-S15 (in $CDCl_3$)

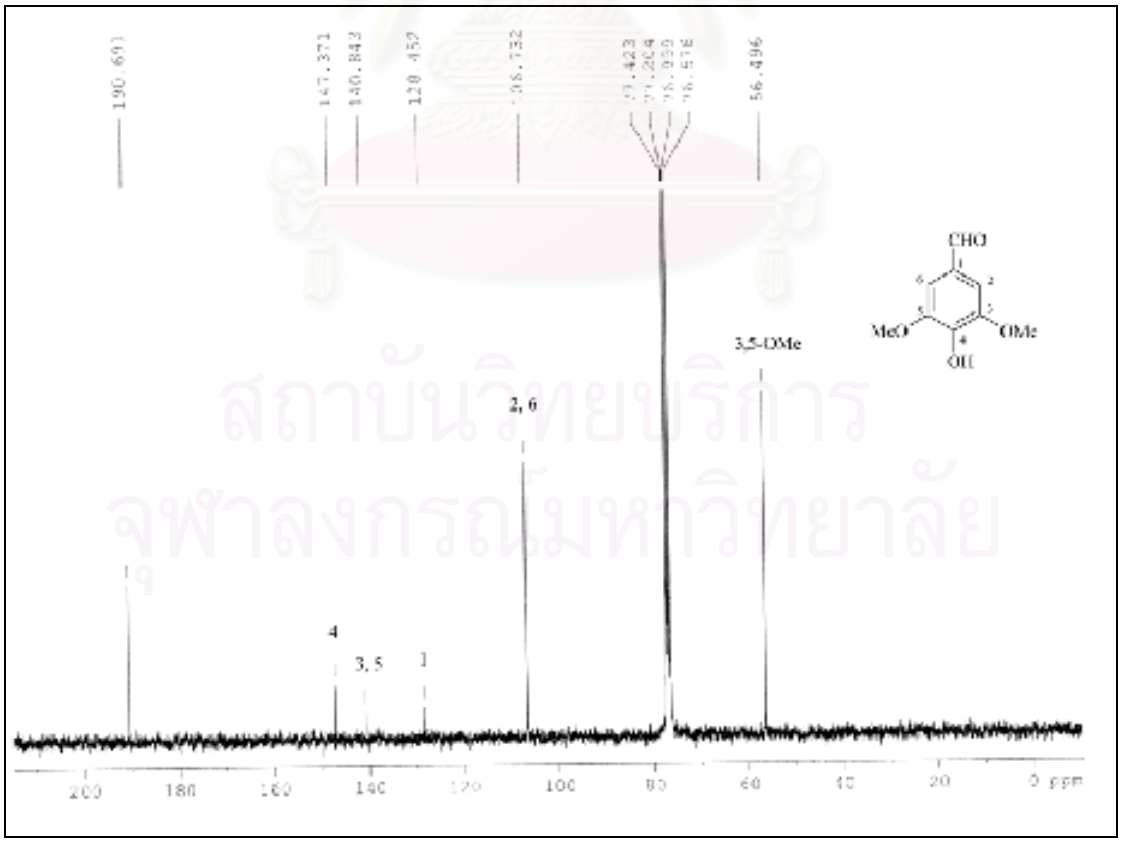

Figure 110. ^{13}C NMR (75 MHz) Spectrum of compound ET-S15 (in $CDCl_3$)

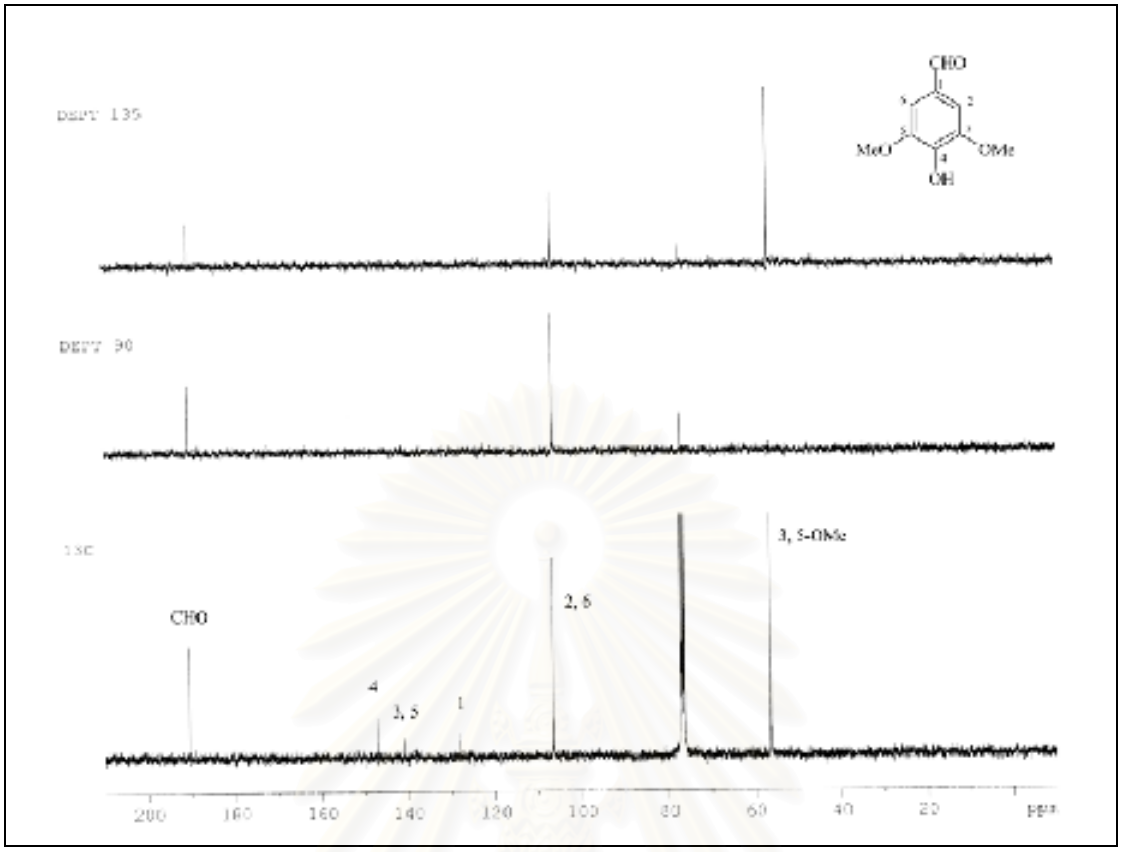

Figure 111. DEPT 135, DEPT 90 and ^{13}C NMR Spectrum of compound ET-S15

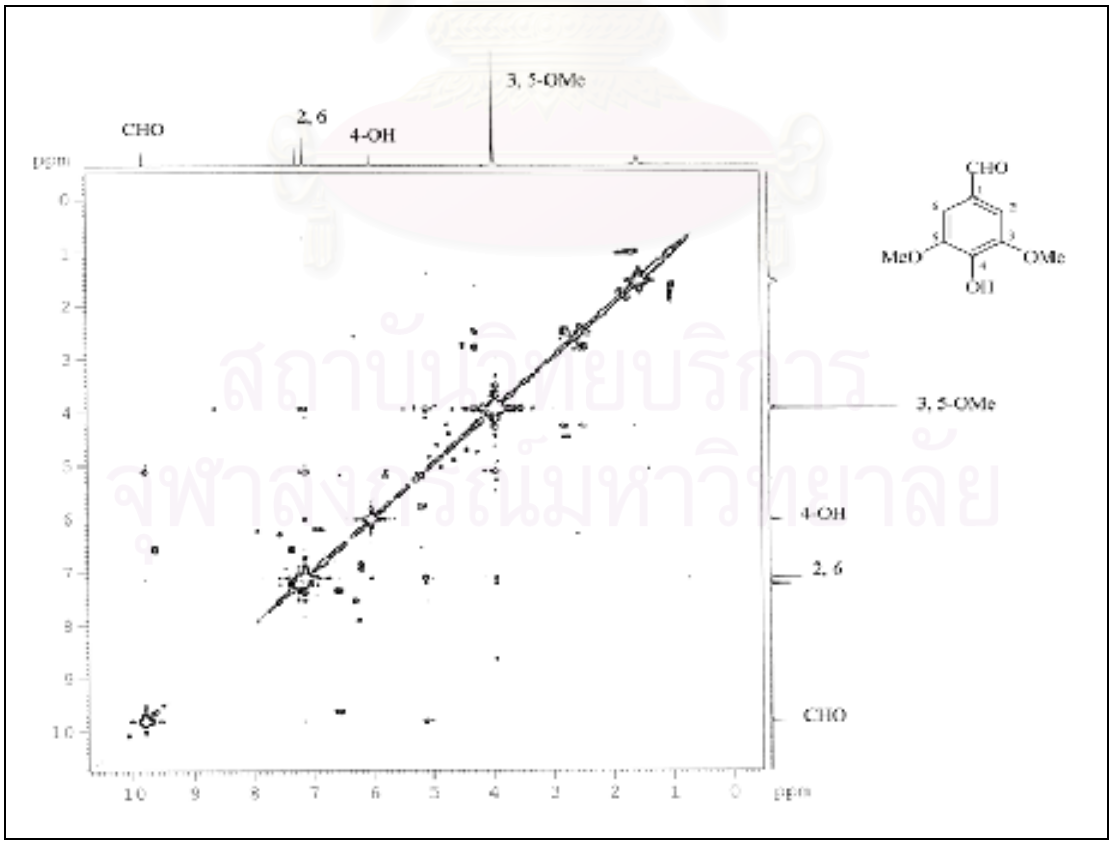

Figure 112. ^{1}H-^{1}H COSY Spectrum of compound ET-S15

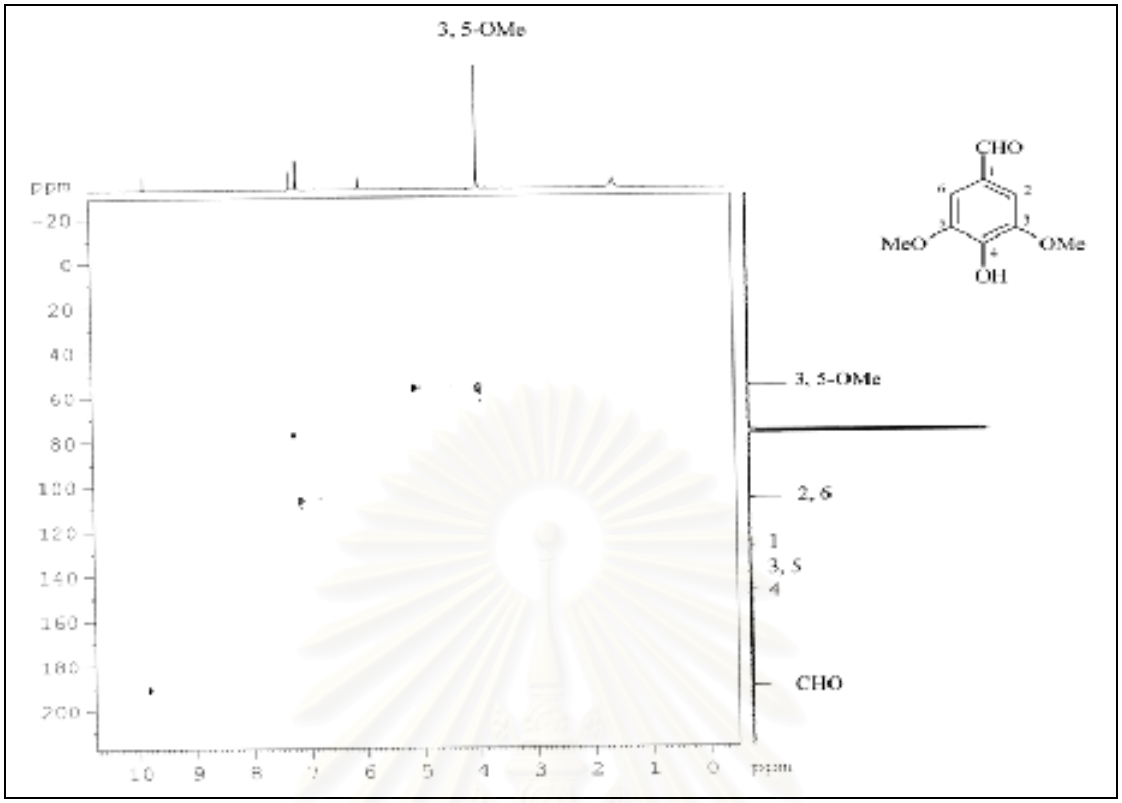

Figure 113. HMQC Spectrum of compound ET-S15

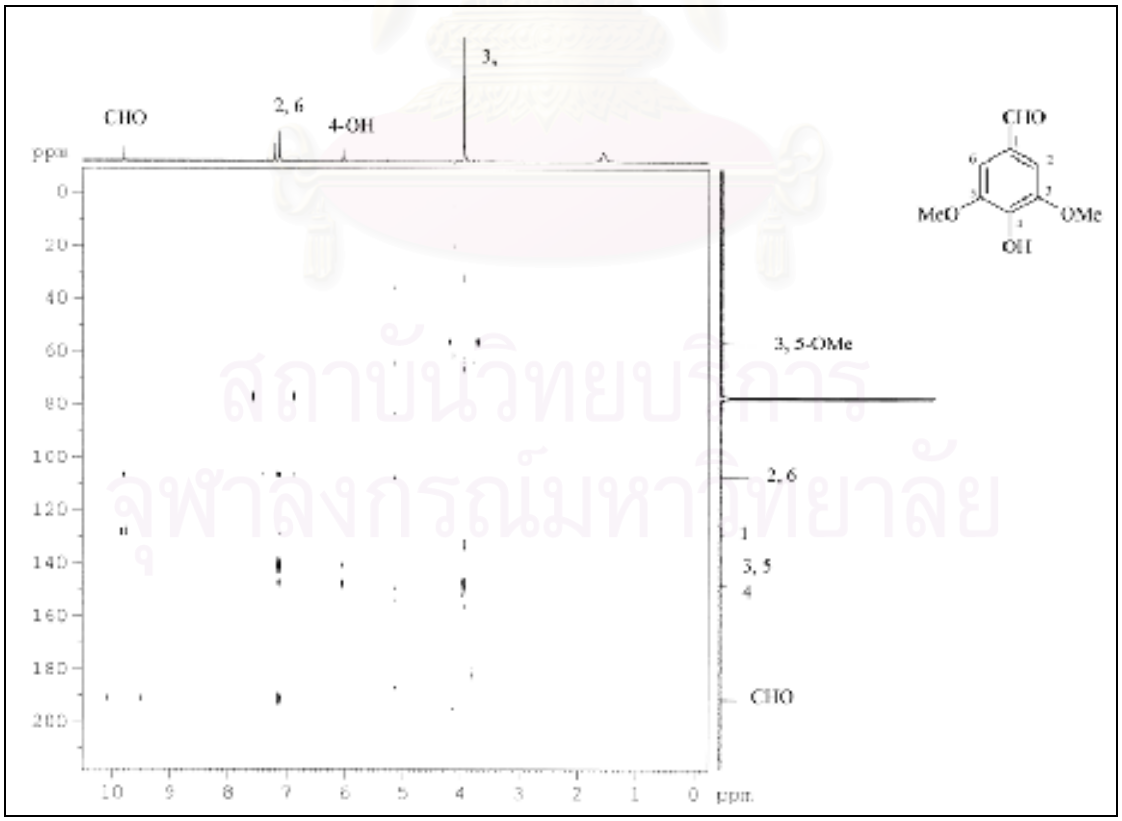

Figure 114. HMBC Spectrum of compound ET-S15

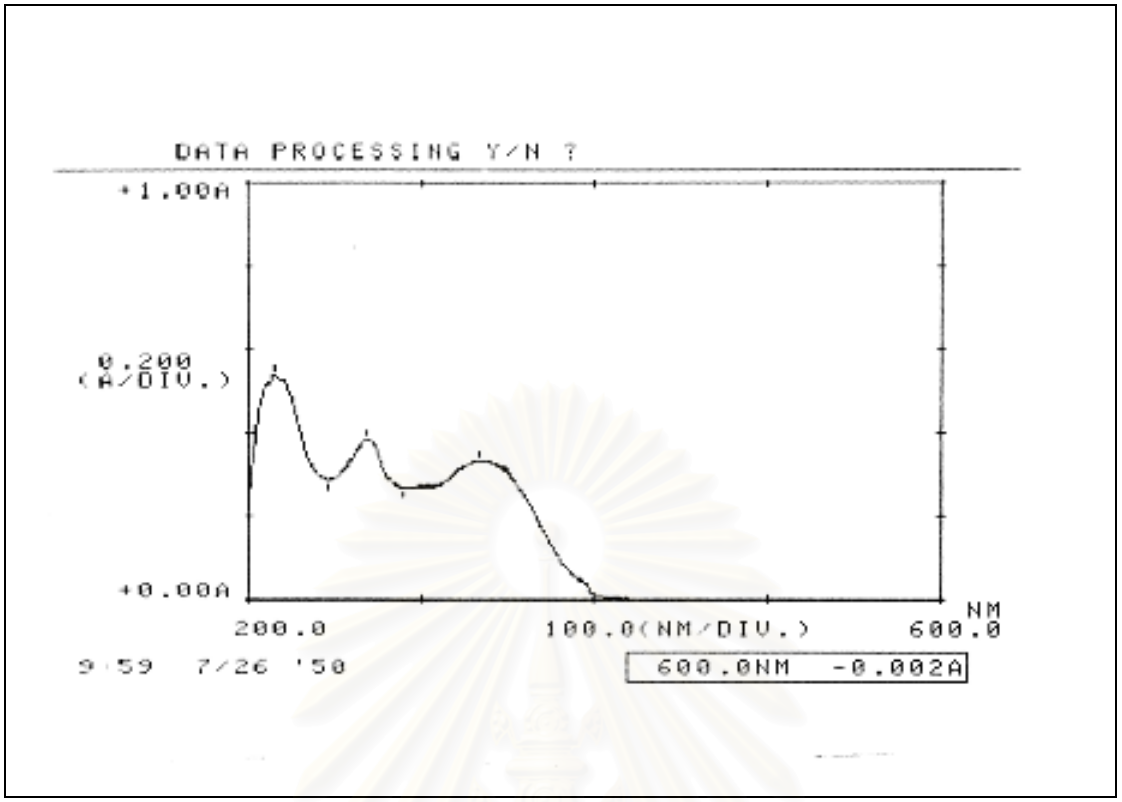

Figure 115. UV Spectrum of compound ET-S17 (in MeOH)

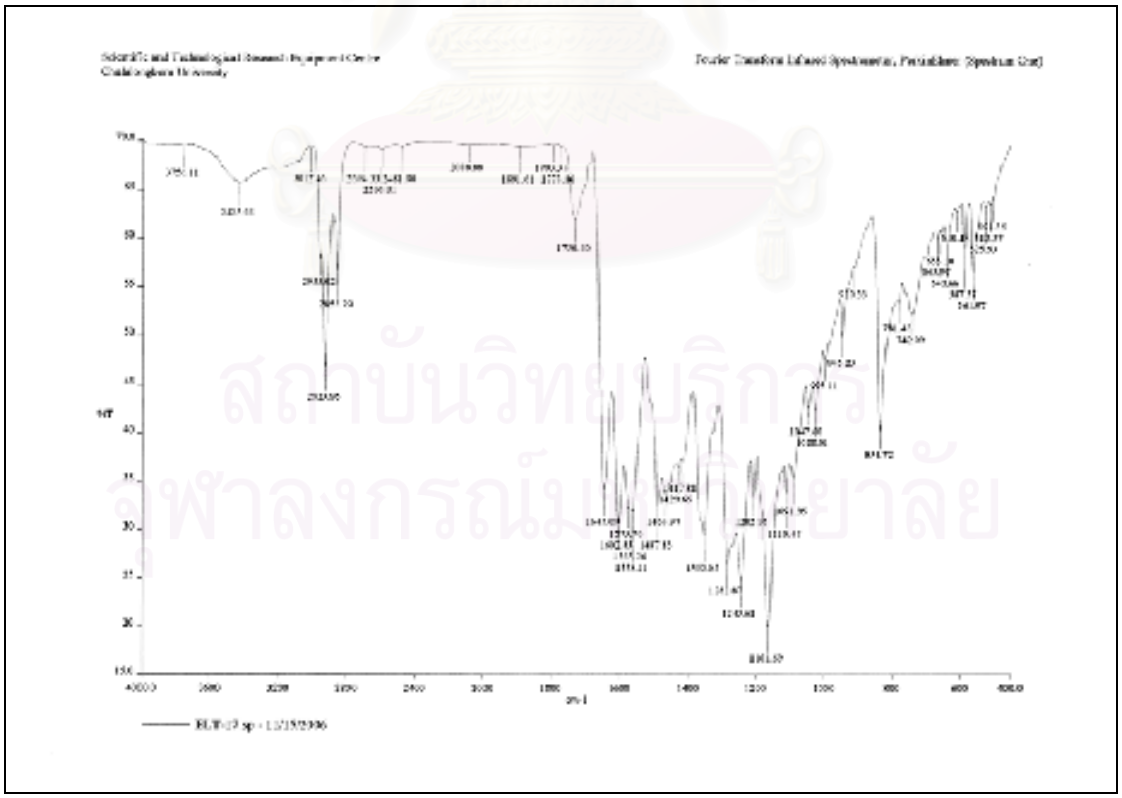

Figure 116. IR Spectrum of compound ET-S17 (KBr disc)

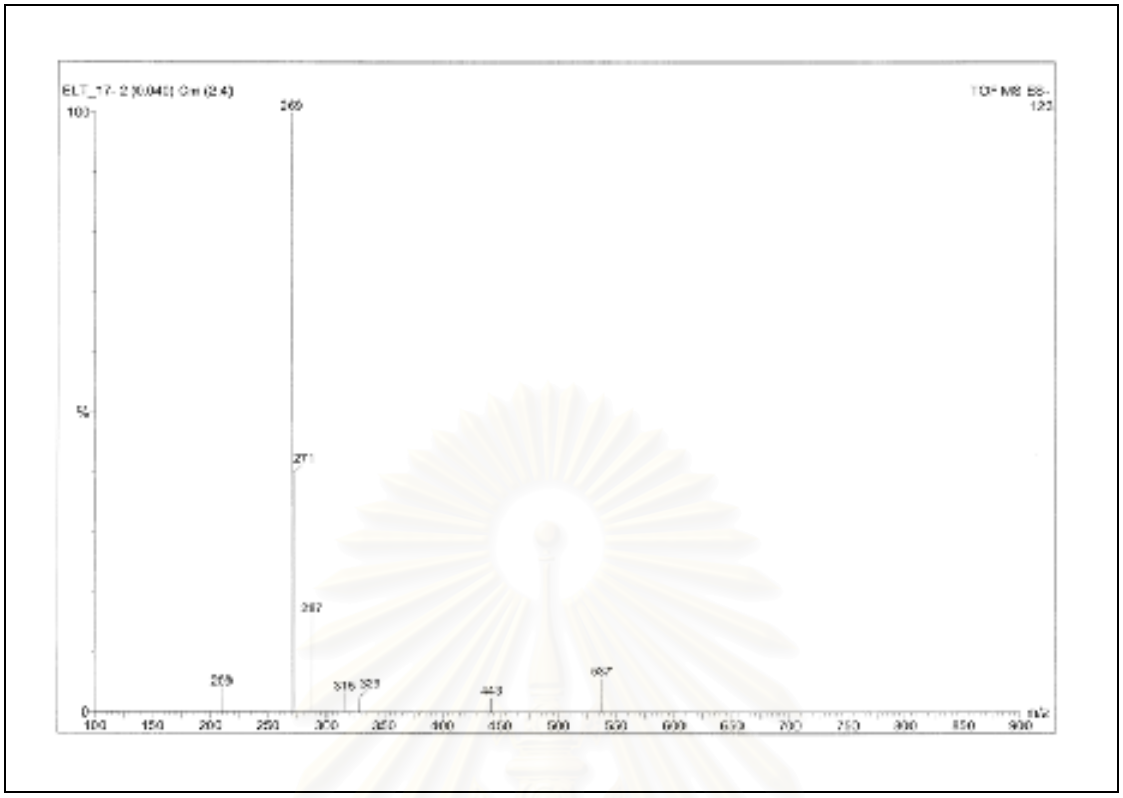

Figure 117. ESI Mass spectrum of compound ET-S17

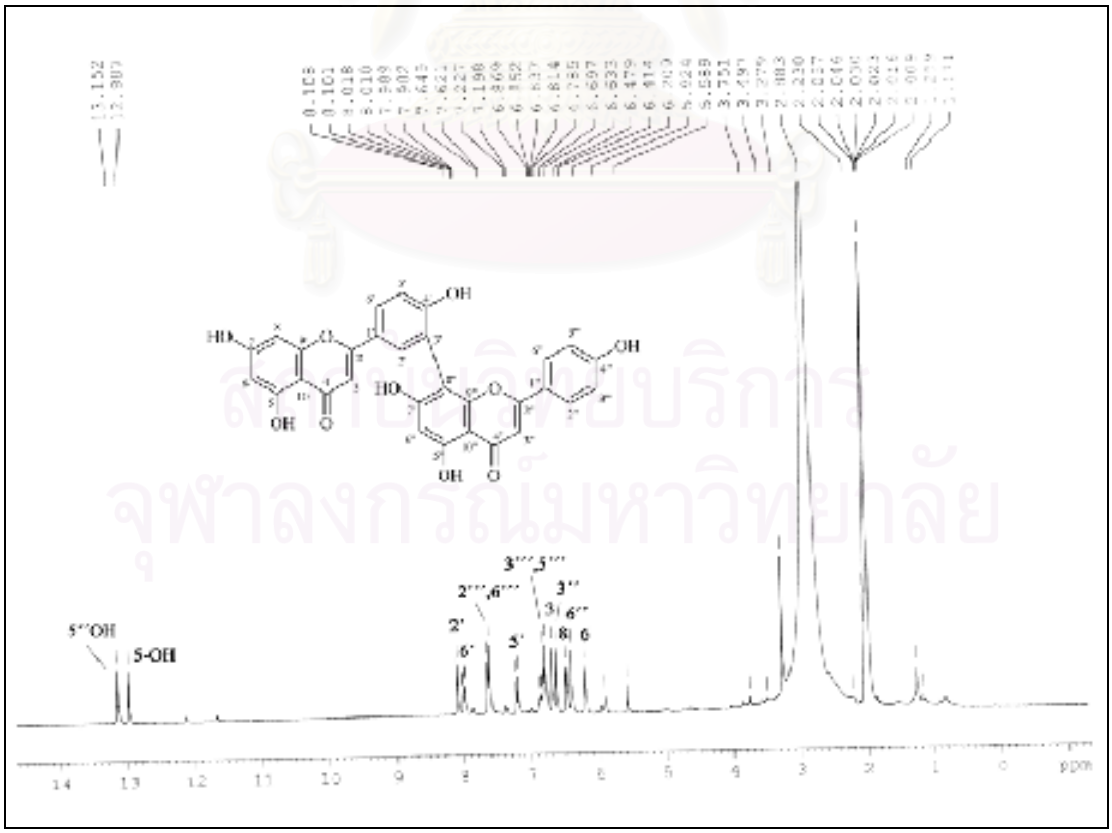

Figure 118. ^{1}H NMR (300 MHz) Spectrum of compound ET-S17 (in acetone-d_6)

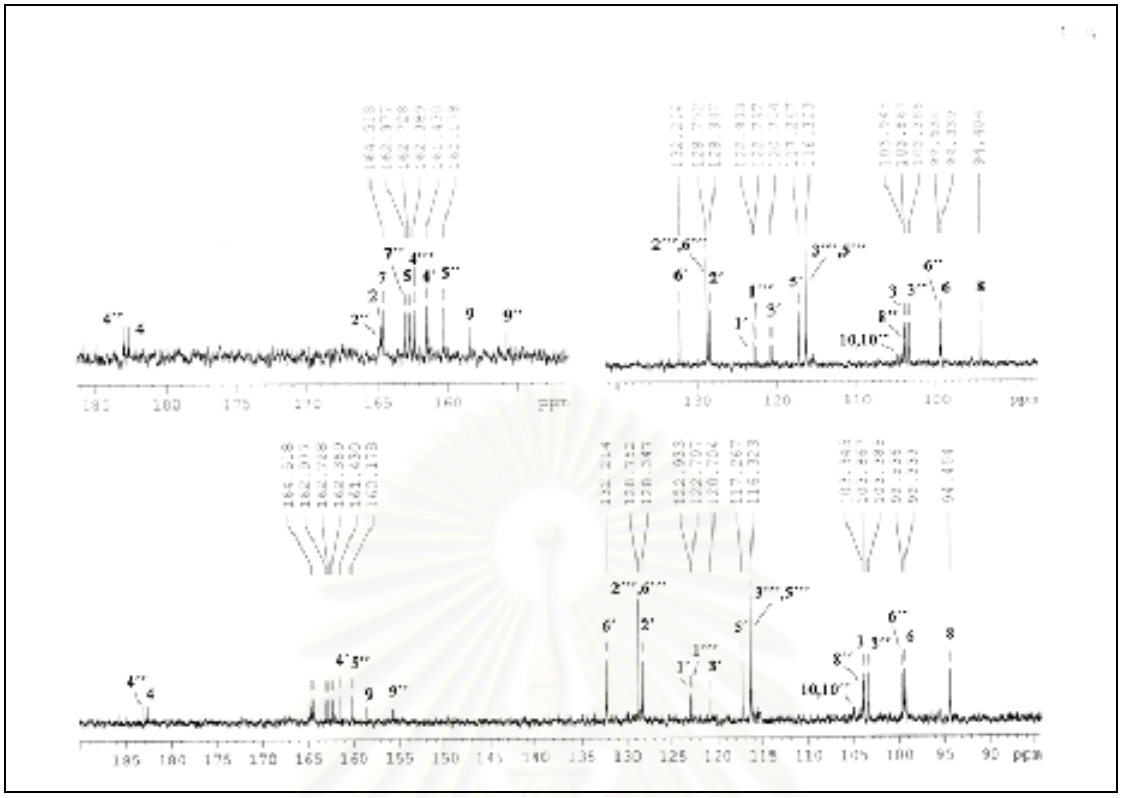

Figure 119. ^{13}C NMR (75 MHz) Spectrum of compound ET-S17 (in acetone-d_6)

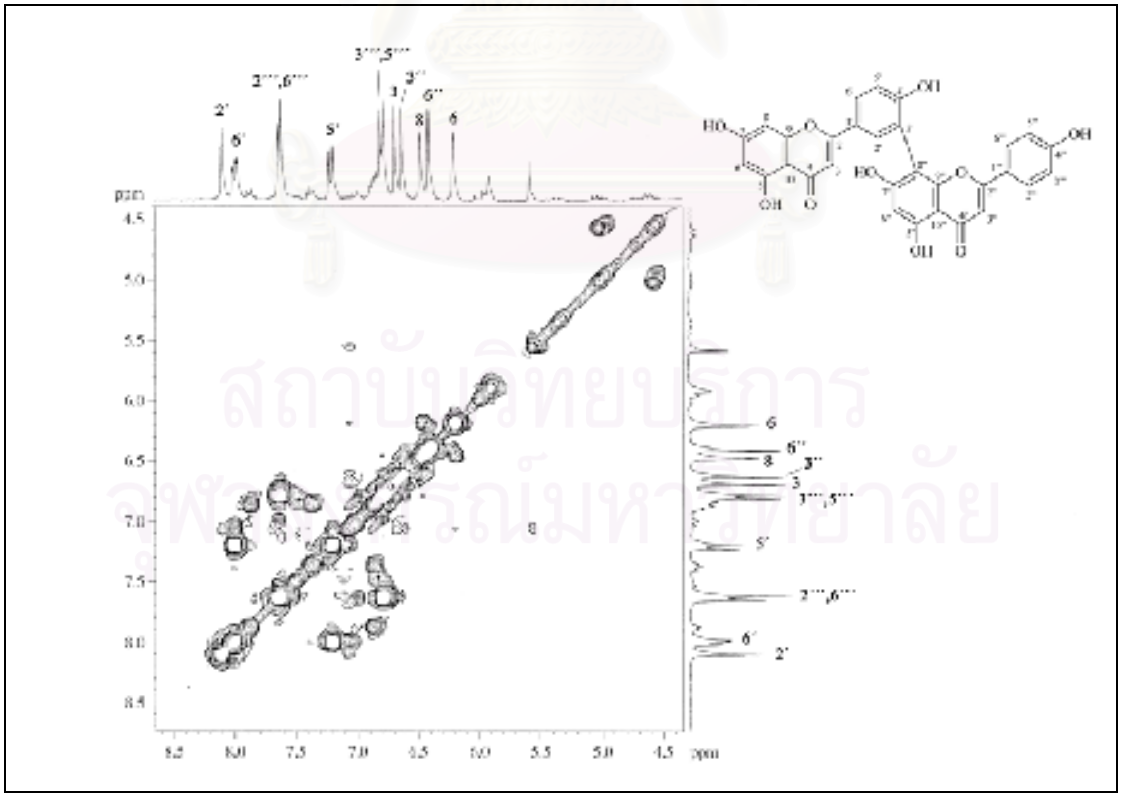

Figure 120. ^{1}H-^{1}H COSY Spectrum of compound ET-S17 (δ_H 4.5-8.5 ppm)

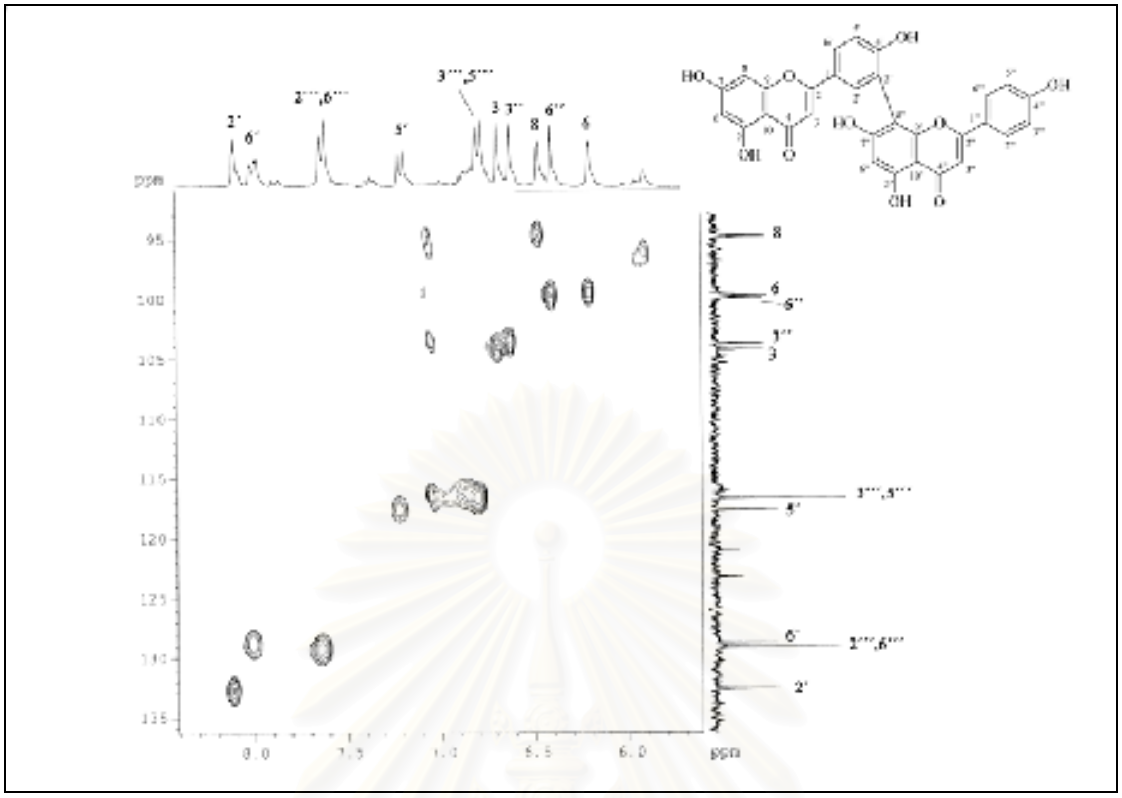

Figure 121. HMQC Spectrum of compound ET-S17

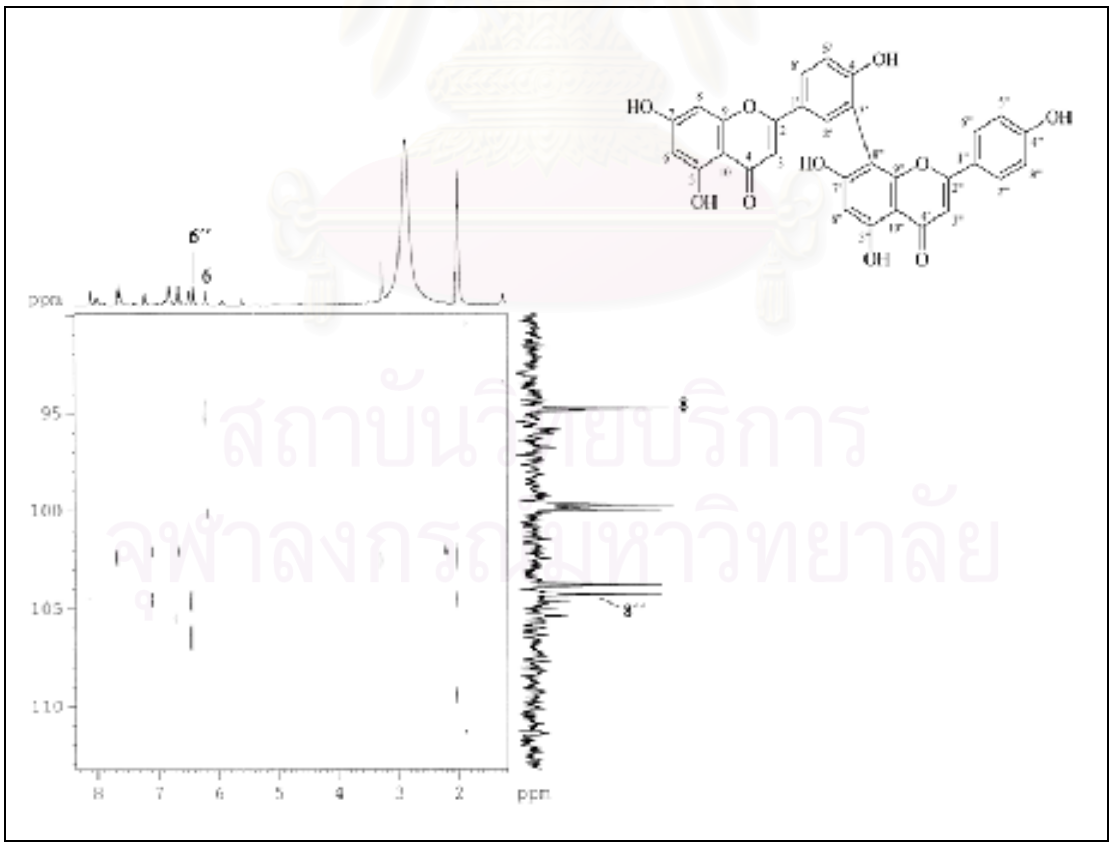

Figure 122a. HMBC Spectrum of compound ET-S17
(δ_H 0-8 ppm, δ_C 90-115 ppm)

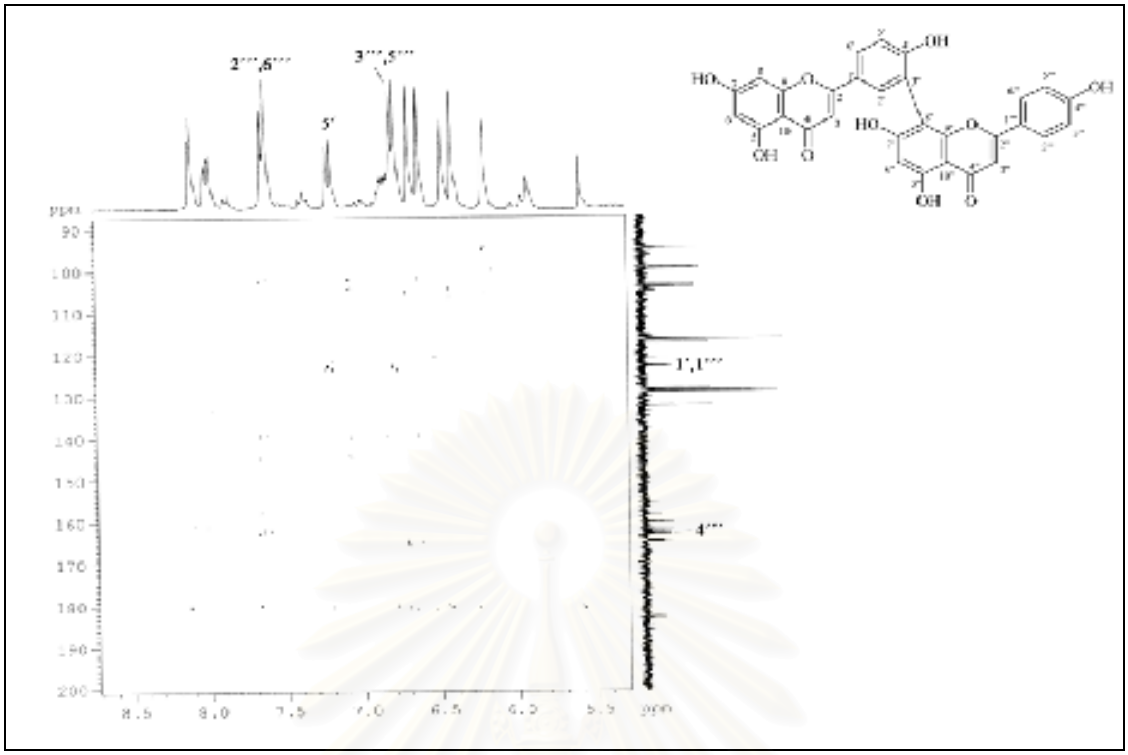

Figure 122b. HMBC Spectrum of compound ET-S17
(δ_H 5.5-8.5 ppm, δ_C 90-200 ppm)

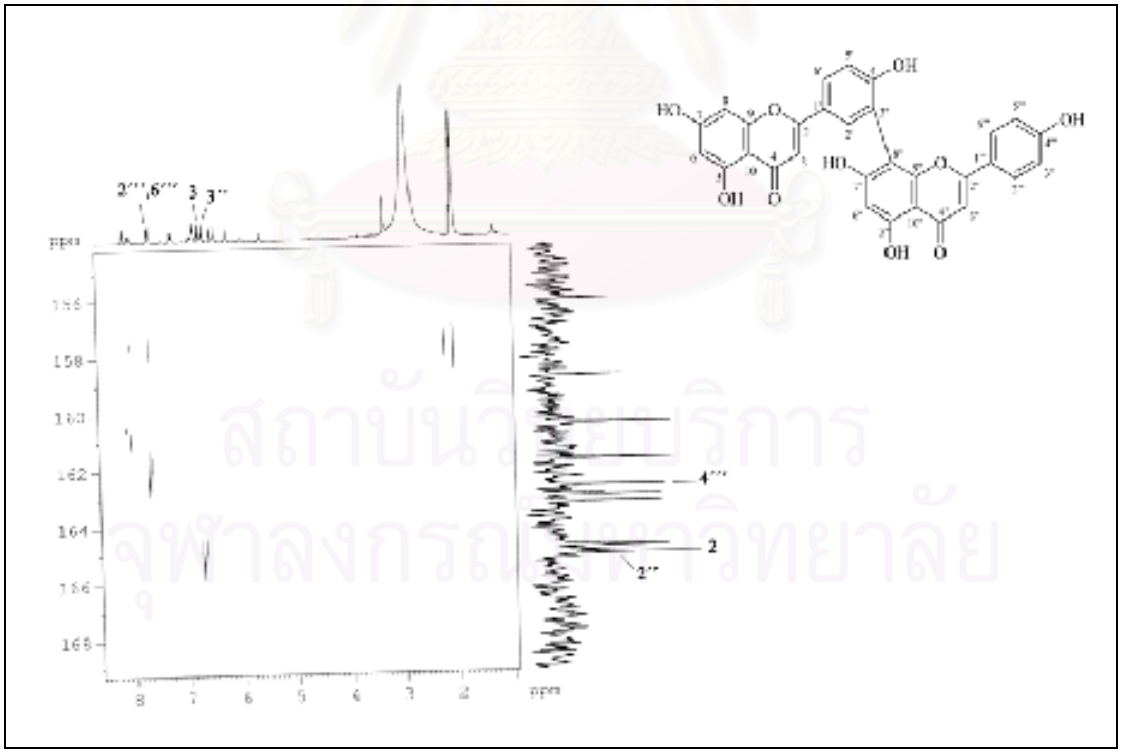

Figure 122c. HMBC Spectrum of compound ET-S17
(δ_H 1-8.5 ppm, δ_C 154-169 ppm)

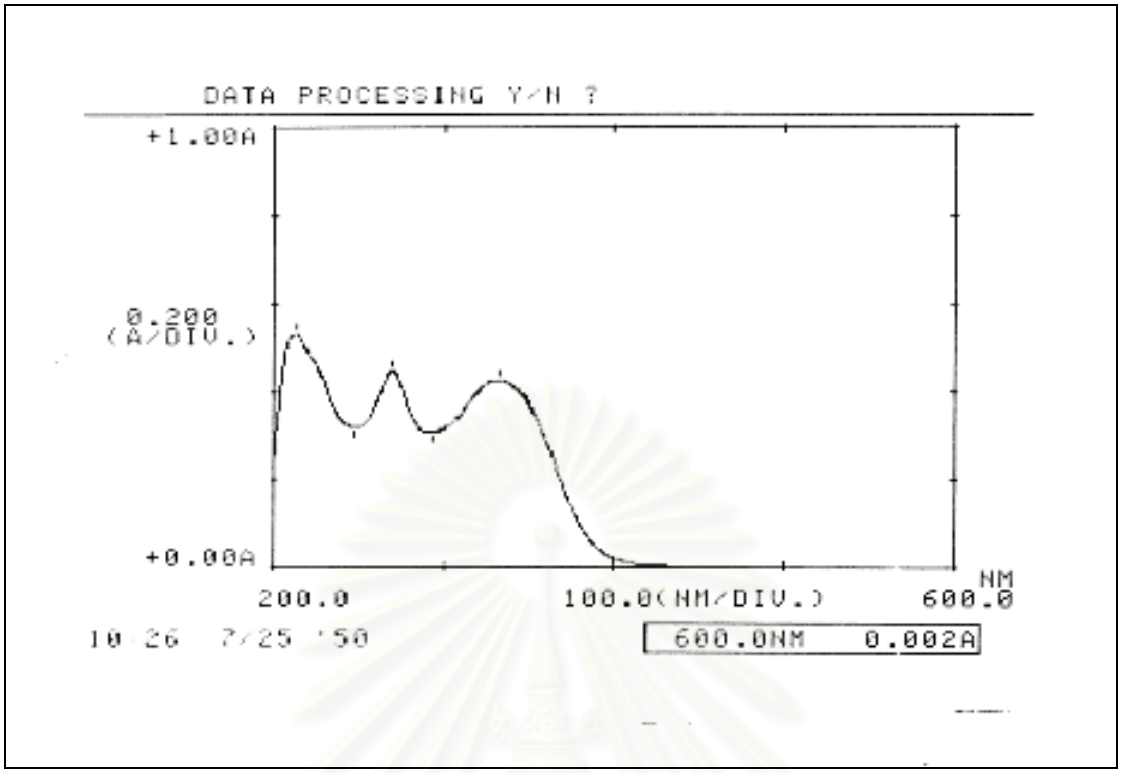

Figure 123. UV Spectrum of compound ET-F6 (in MeOH)

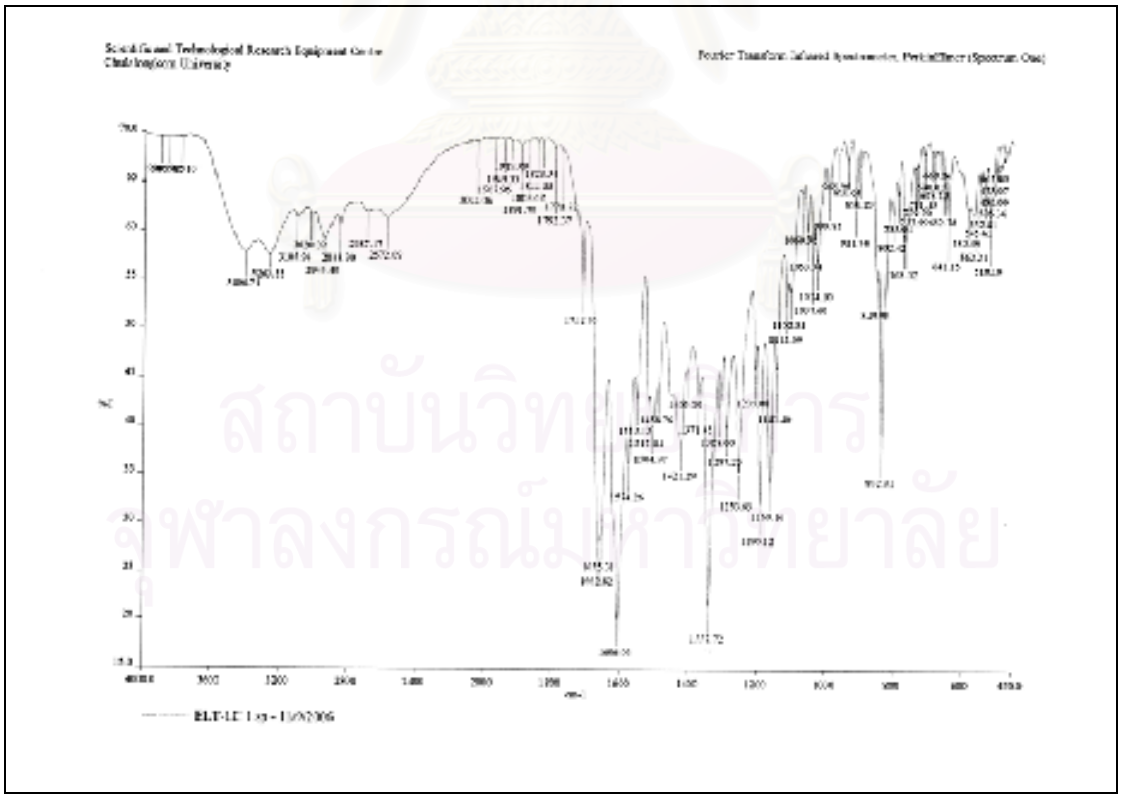

Figure 124. IR Spectrum of compound ET-F6 (KBr disc)

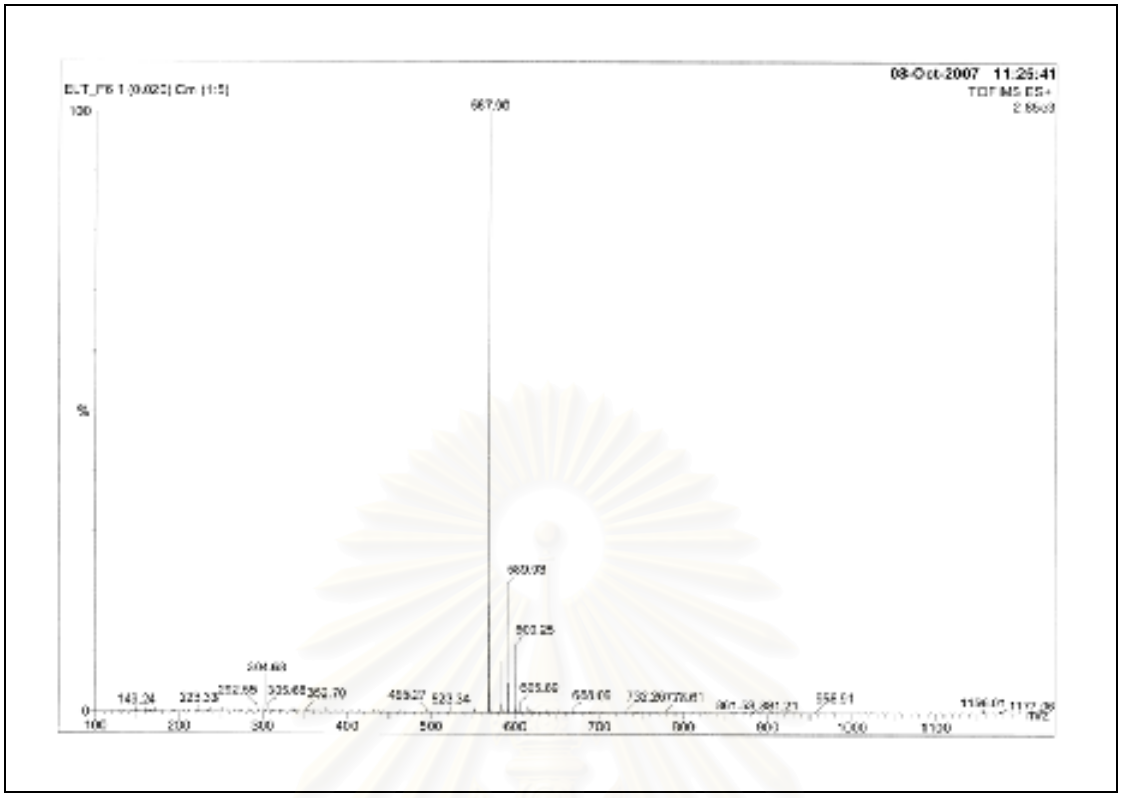

Figure 125. ESI Mass spectrum of compound ET-F6

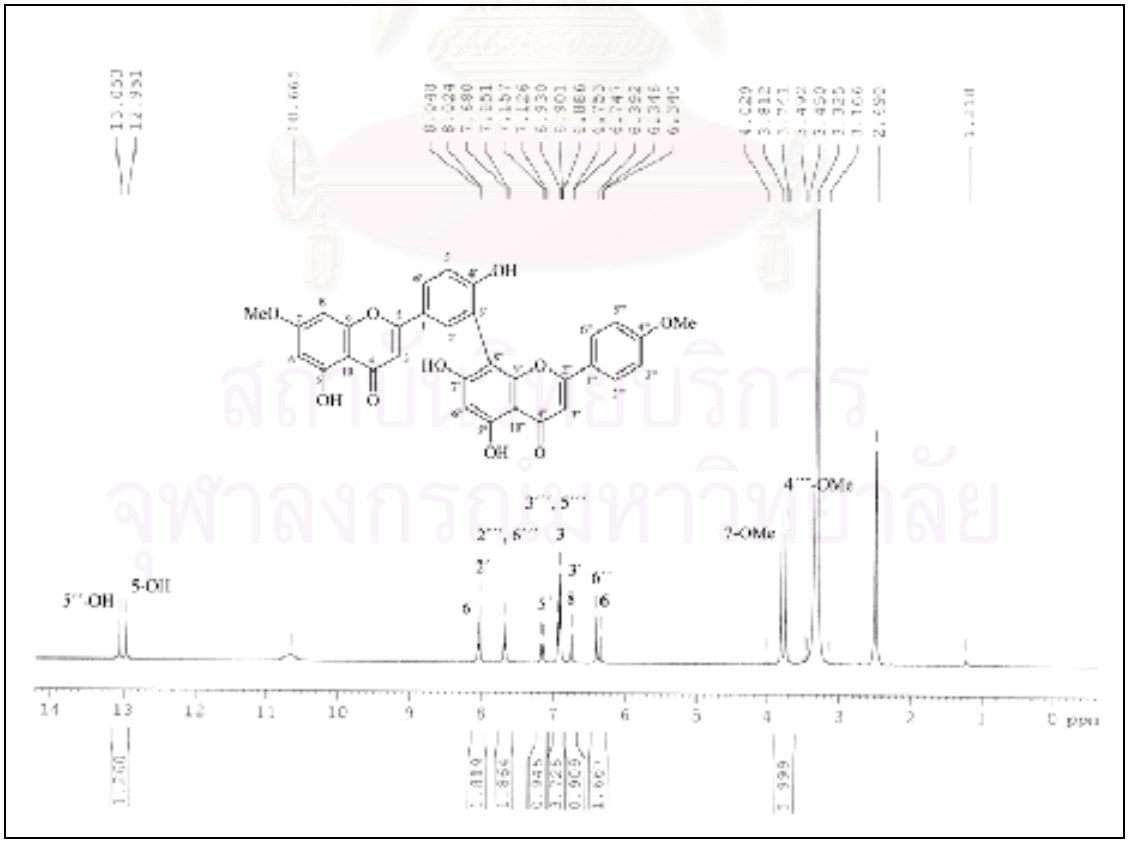

Figure 126. ^{1}H NMR (300 MHz) Spectrum of compound ET-F6 (in DMSO-d_6)

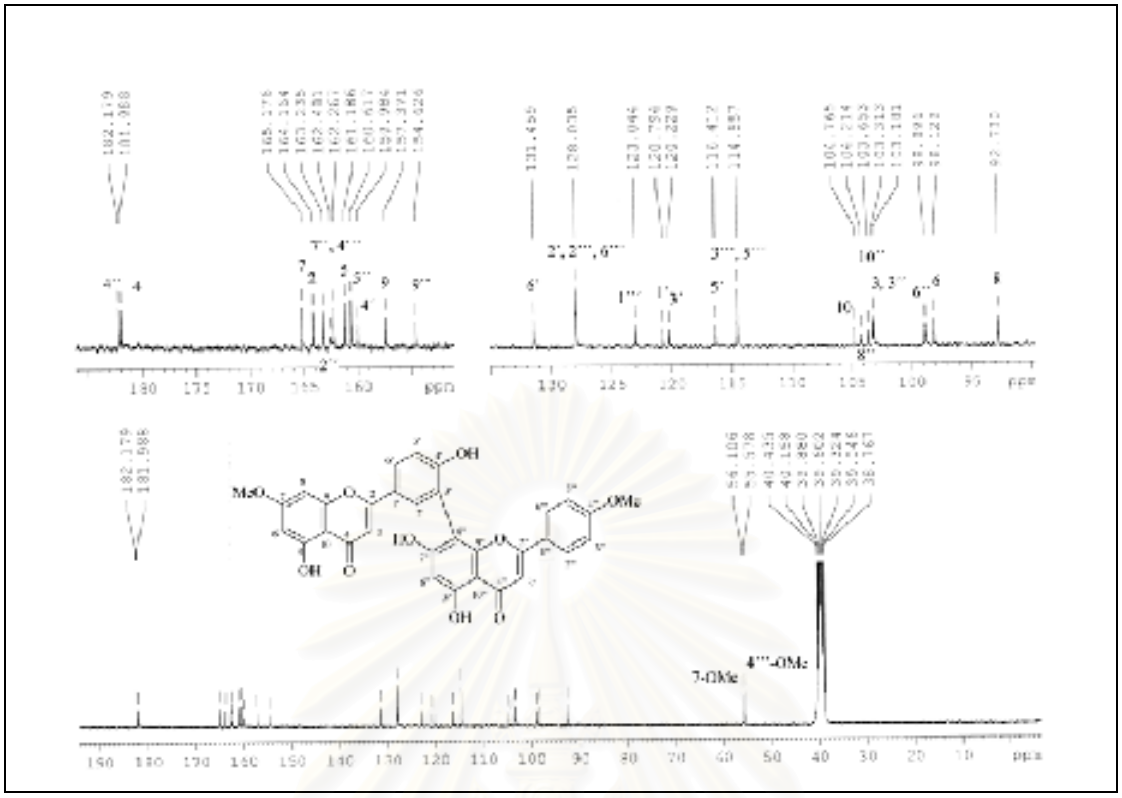

Figure 127. ^{13}C NMR (75 MHz) Spectrum of compound ET-F6 (in DMSO-d_6)

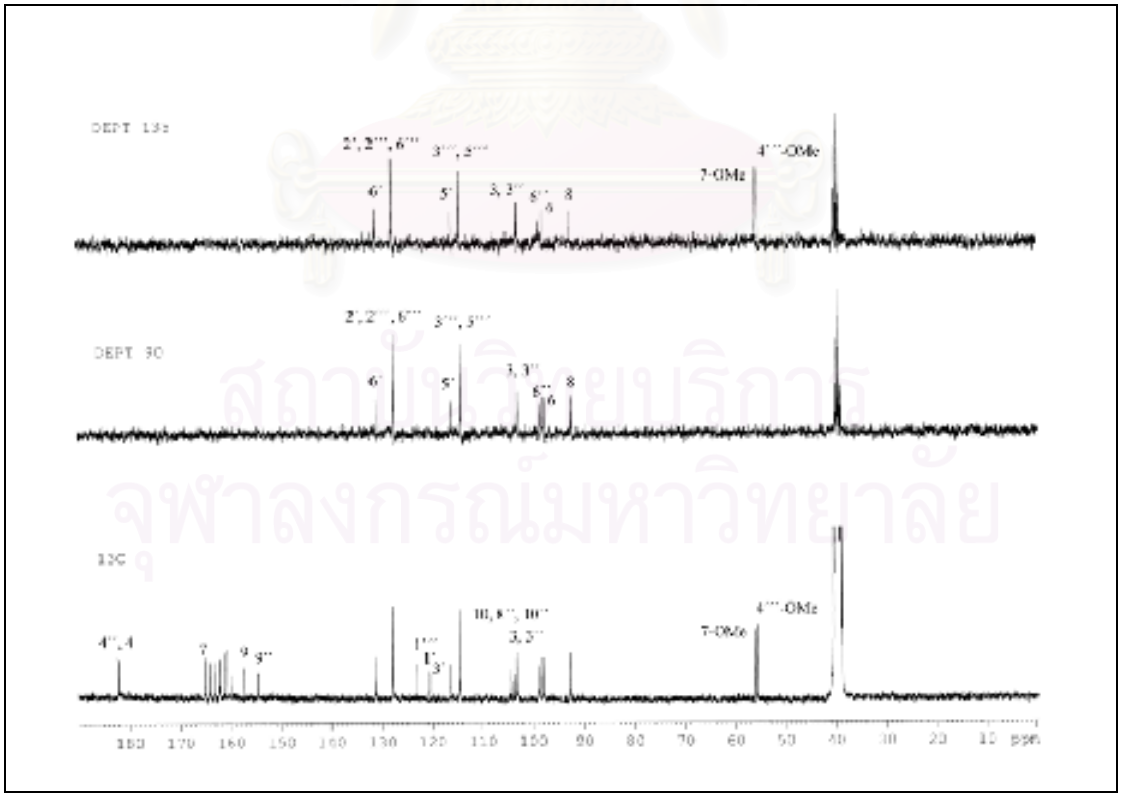

Figure 128. DEPT 135, DEPT 90 and ^{13}C NMR Spectrum of compound ET-F6

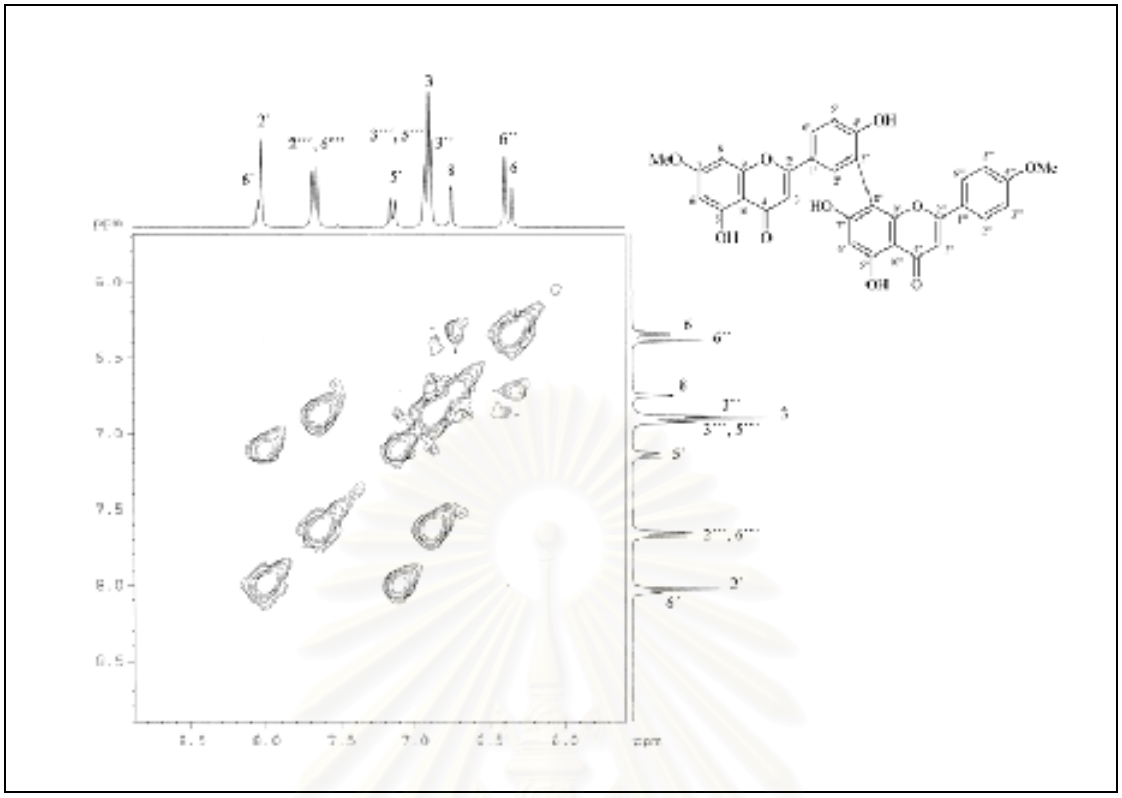

Figure 129. ^{1}H-^{1}H COSY spectrum of compound ET-F6 (δ_H 5.5-9.0 ppm)

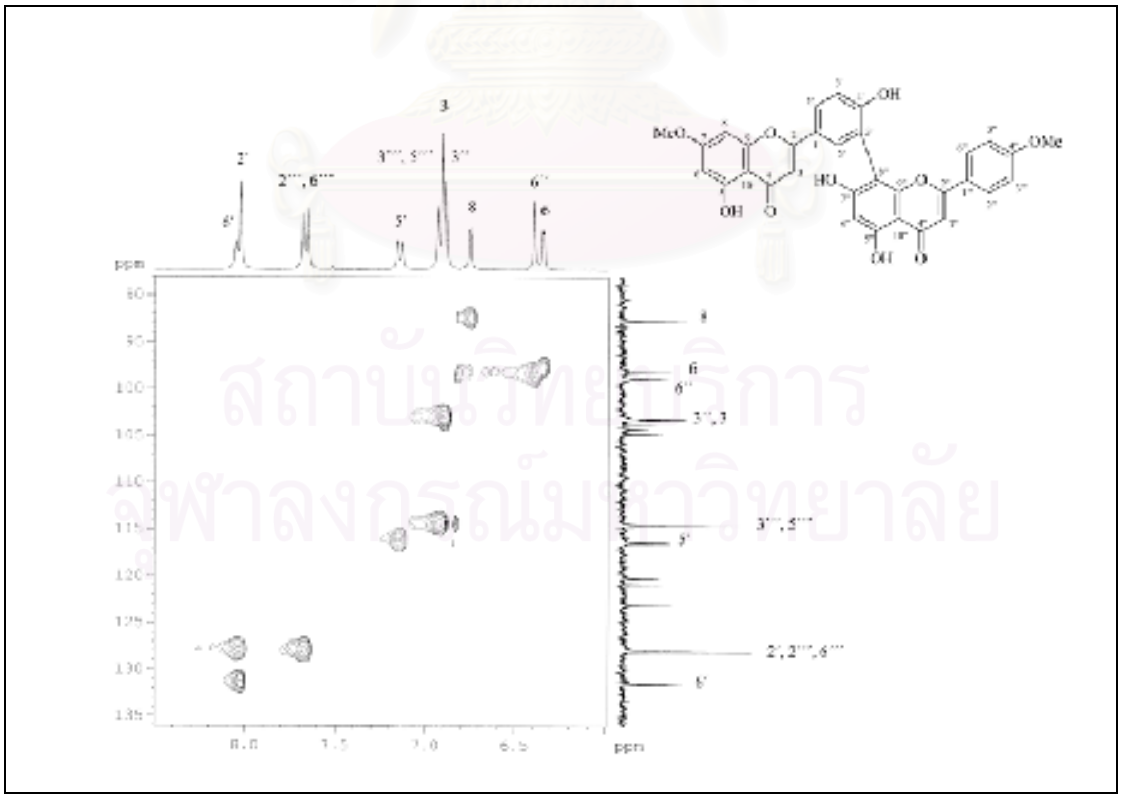

Figure 130a. HMQC Spectrum of compound ET-F6
(δ_H 6.0-8.5 ppm, δ_C 88-136 ppm)

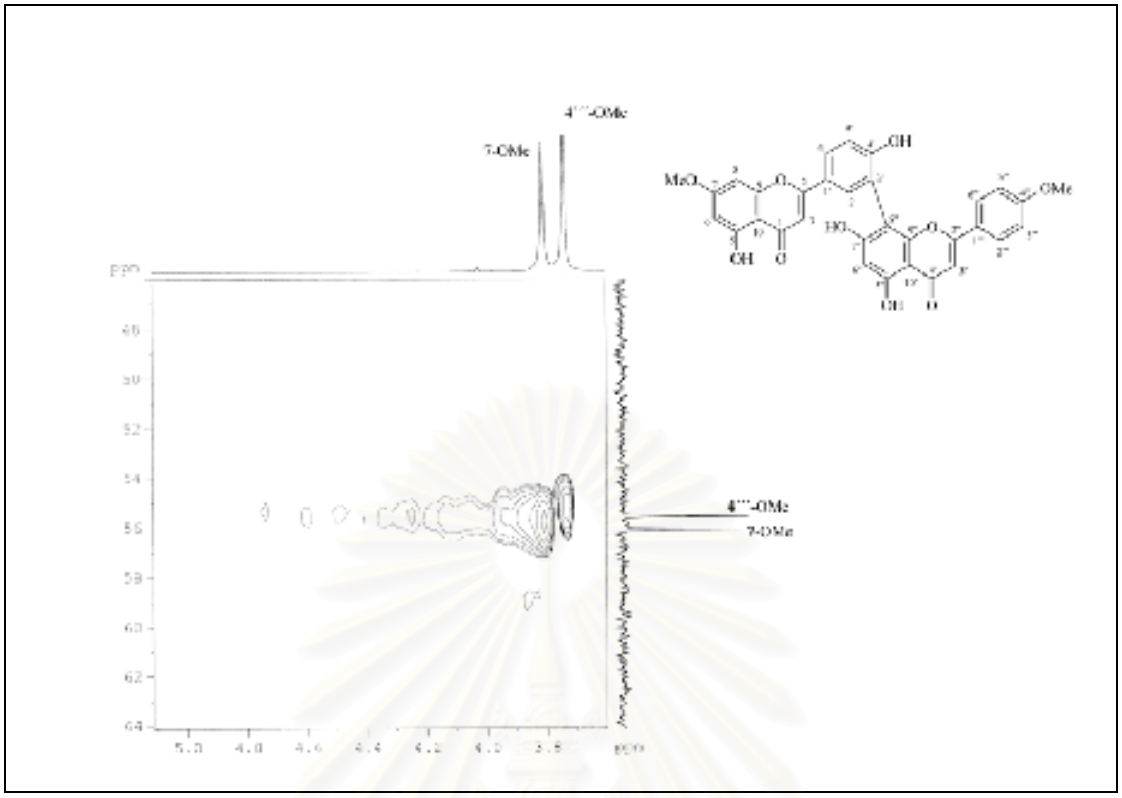

Figure 130b. HMQC Spectrum of compound ET-F6 (δ_H 3.6-5.1 ppm, δ_C 46-64 ppm)

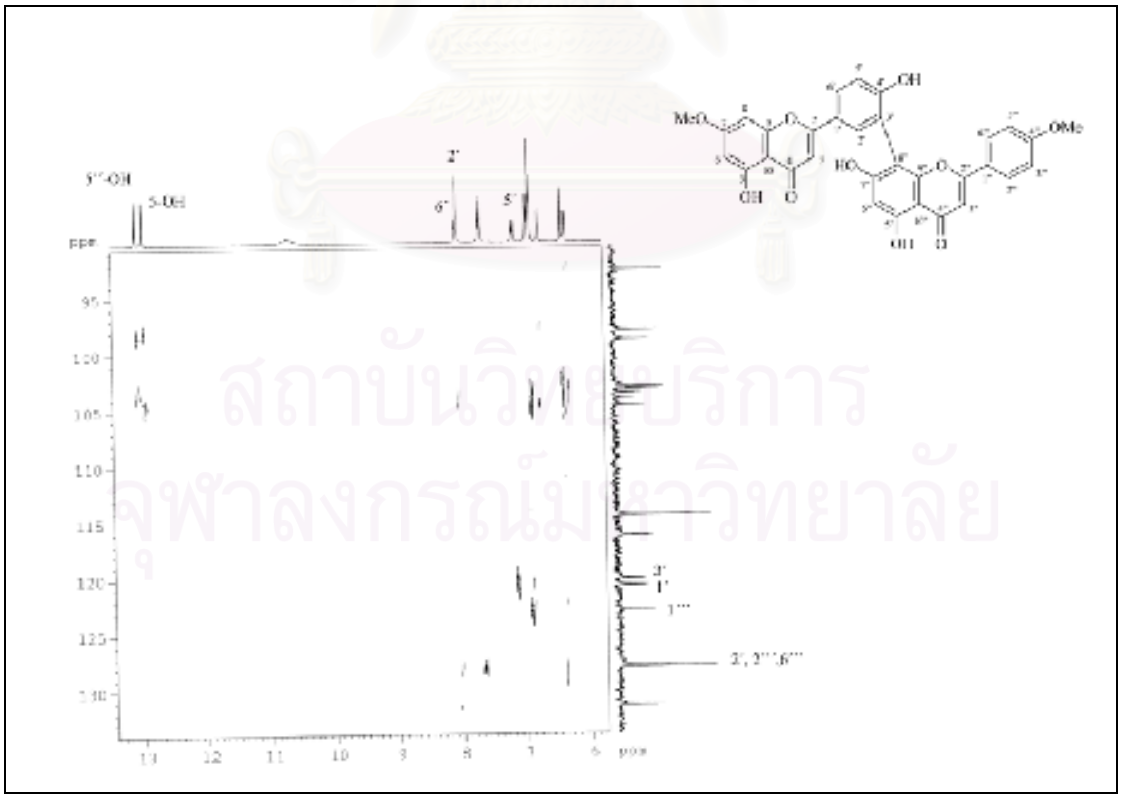

Figure 131a. HMBC Spectrum of compound ET-F6
(δ_H 6-13 ppm, δ_C 90-134 ppm)

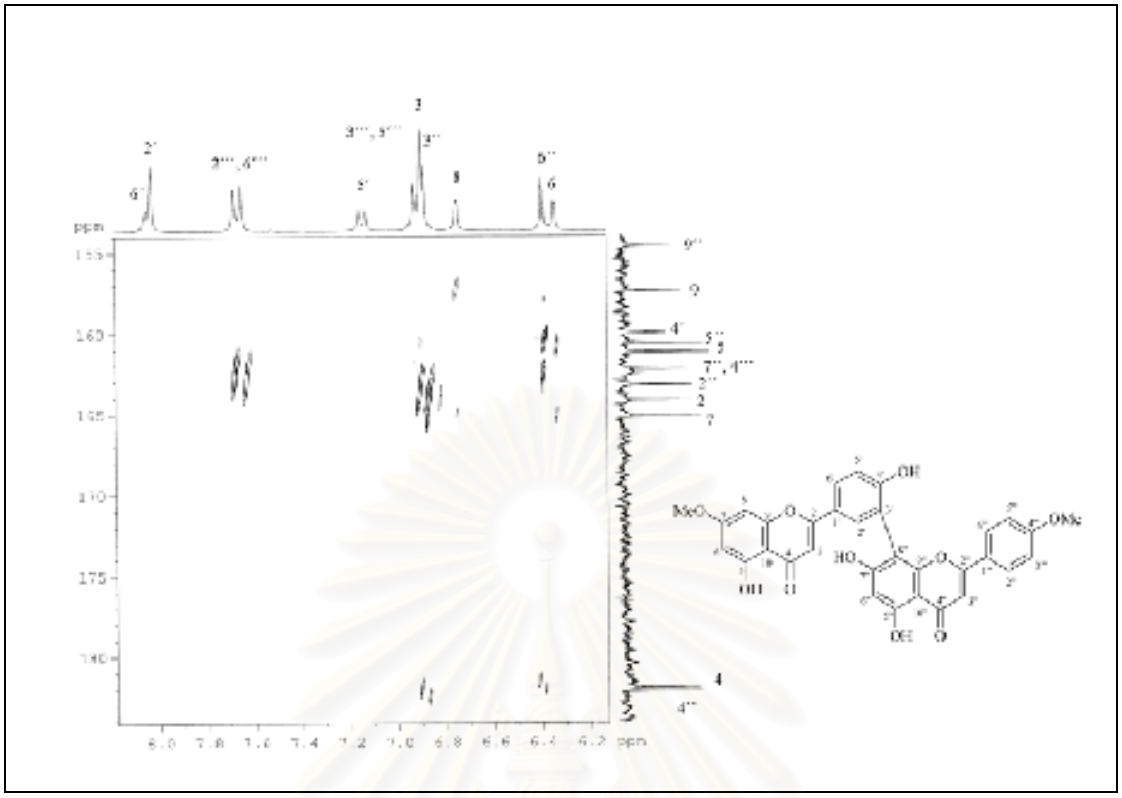

Figure 131b. HMBC Spectrum of compound ET-F6
(δ_H 6.2-8.1 ppm, δ_C 155-185 ppm)

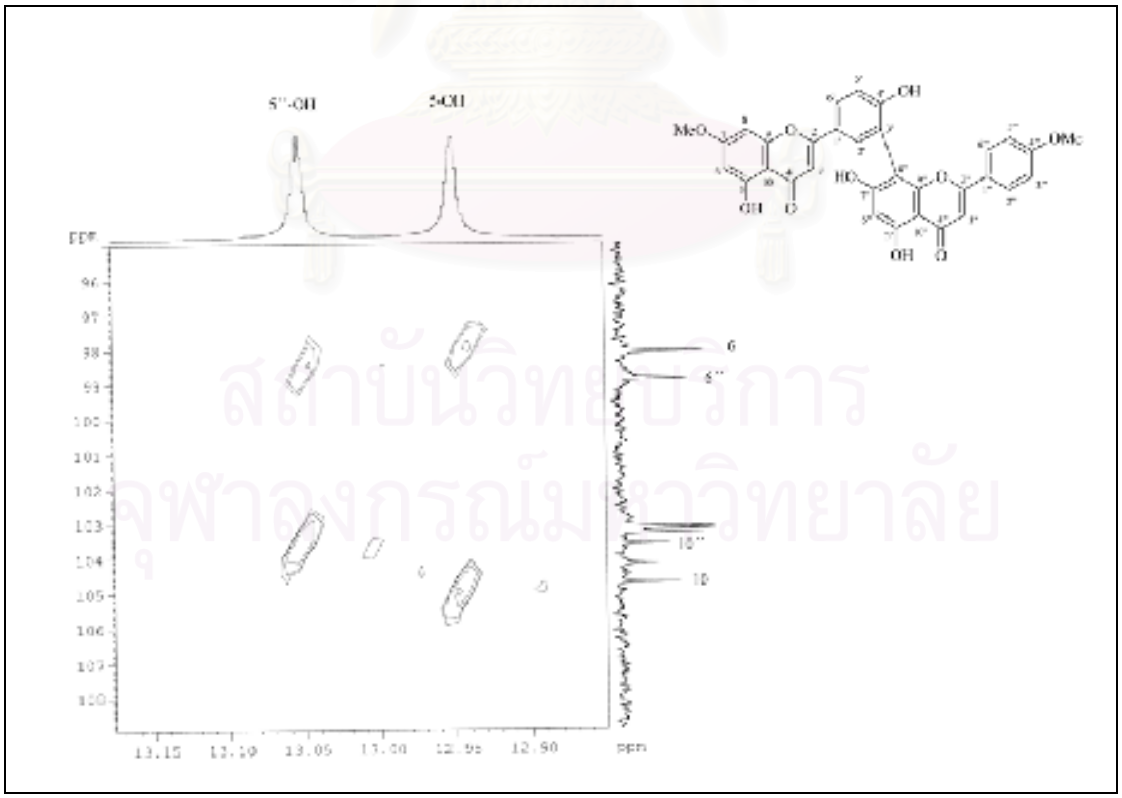

Figure 131c. HMBC Spectrum of compound ET-F6
(δ_H 12.85-13.18 ppm, δ_C 95-109 ppm)

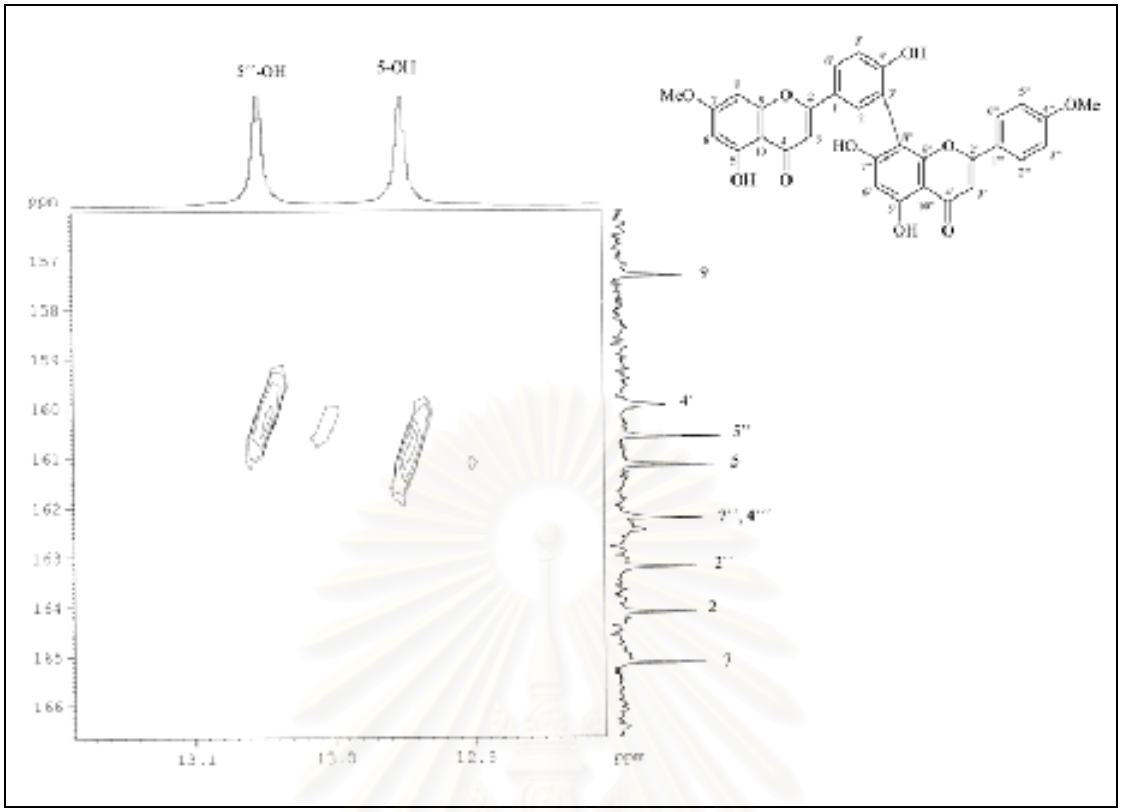

Figure 131d. HMBC Spectrum of compound ET-F6
(δ_H 12.8-13.2 ppm, δ_C 156-167 ppm)

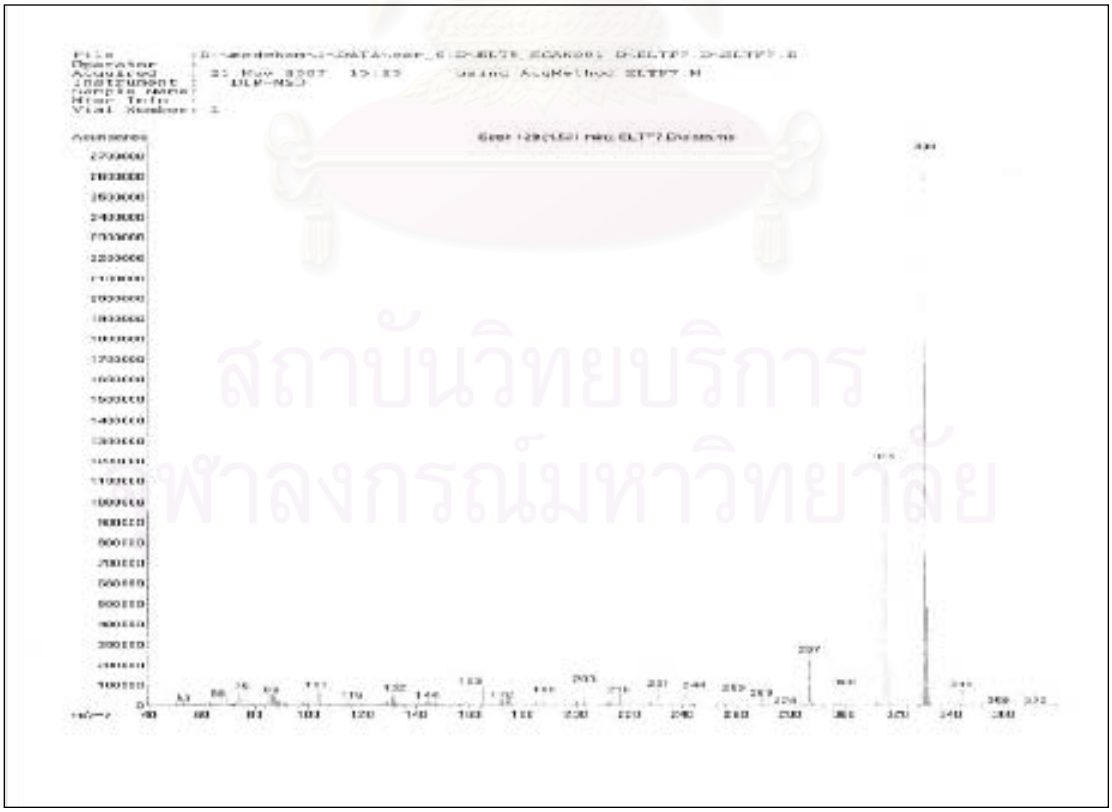

Figure 132. EI Mass spectrum of compound ET-F7

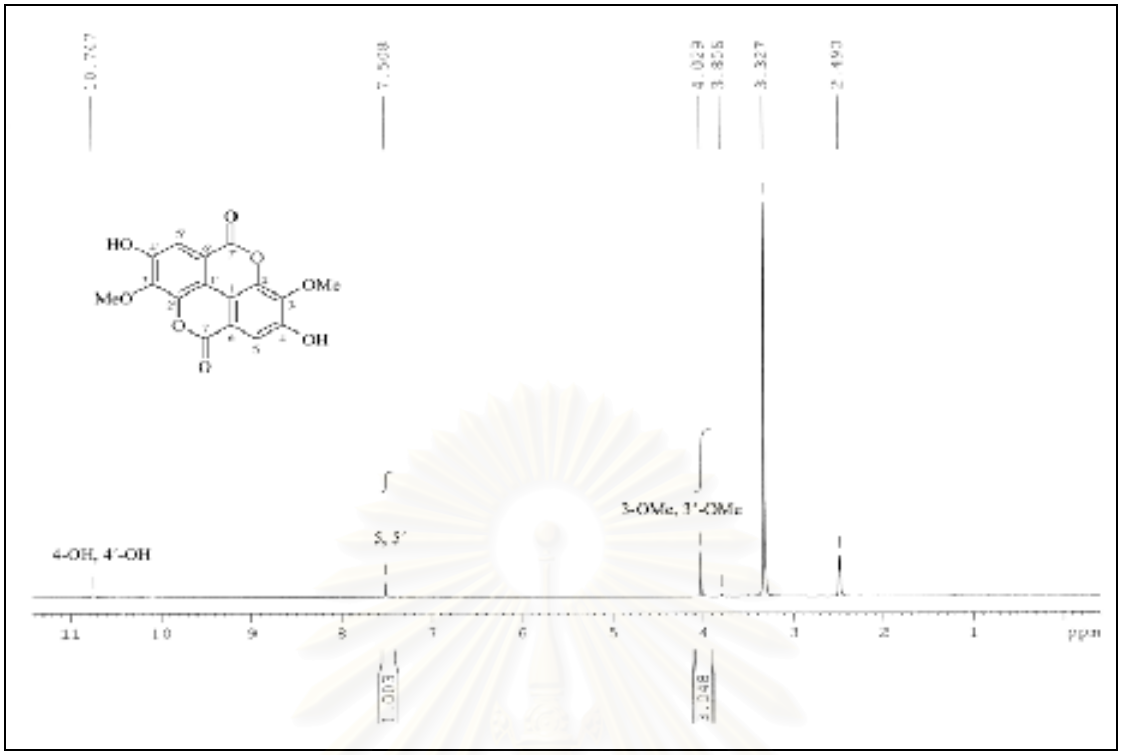

Figure 133. ^{1}H NMR (300 MHz) Spectrum of compound ET-F7 (in DMSO-d_6)

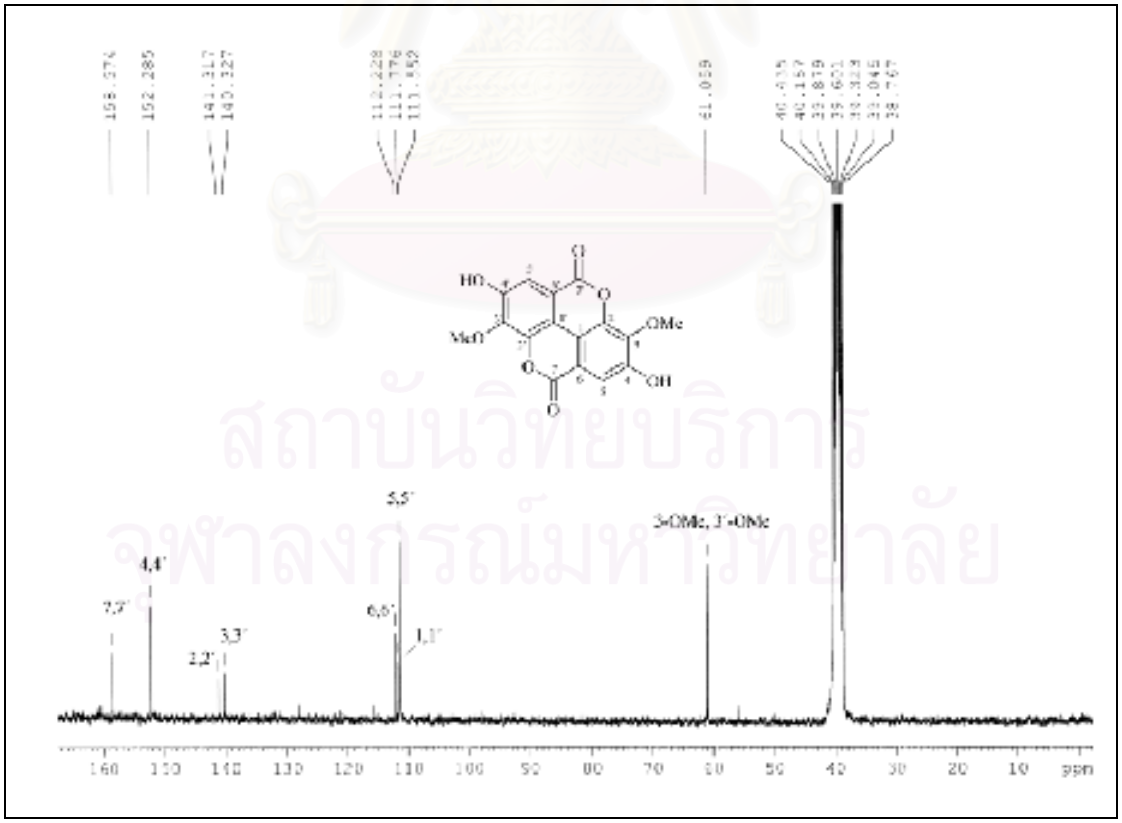

Figure 134. ^{13}C NMR (75 MHz) Spectrum of compound ET-F7 (in DMSO-d_6)

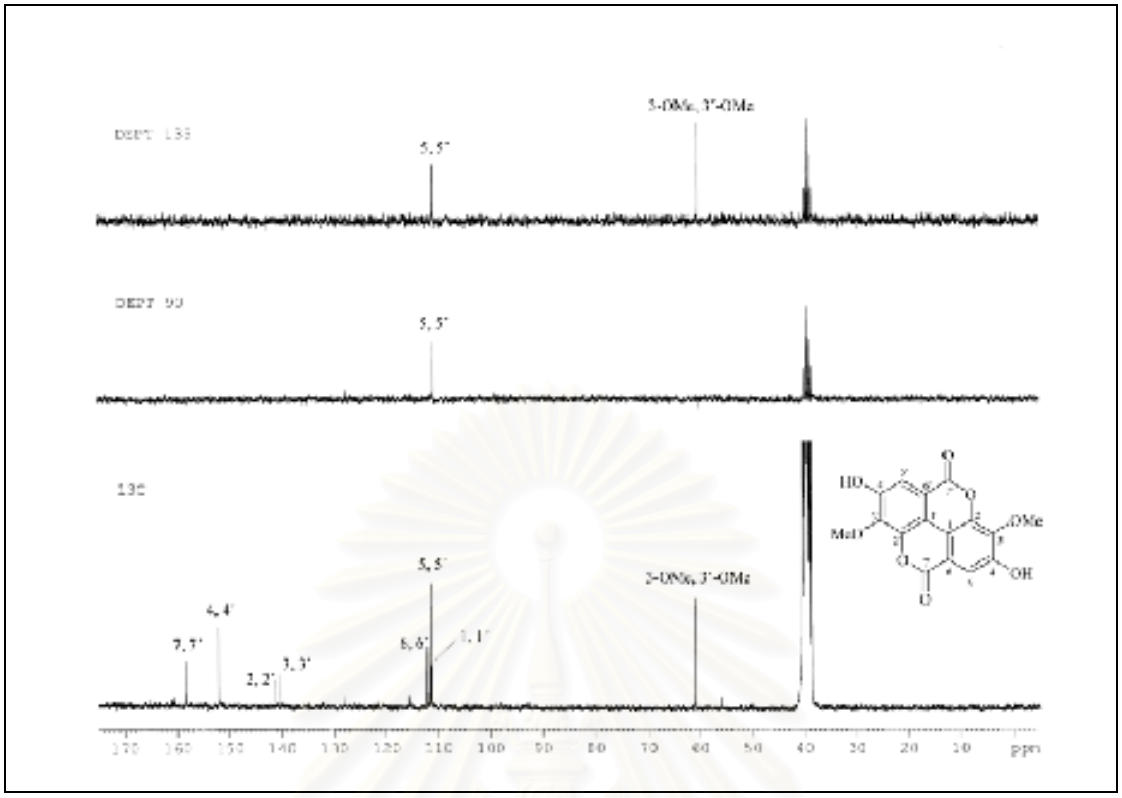

Figure 135. DEPT 135, DEPT 90 and ^{13}C NMR Spectrum of compound ET-F7

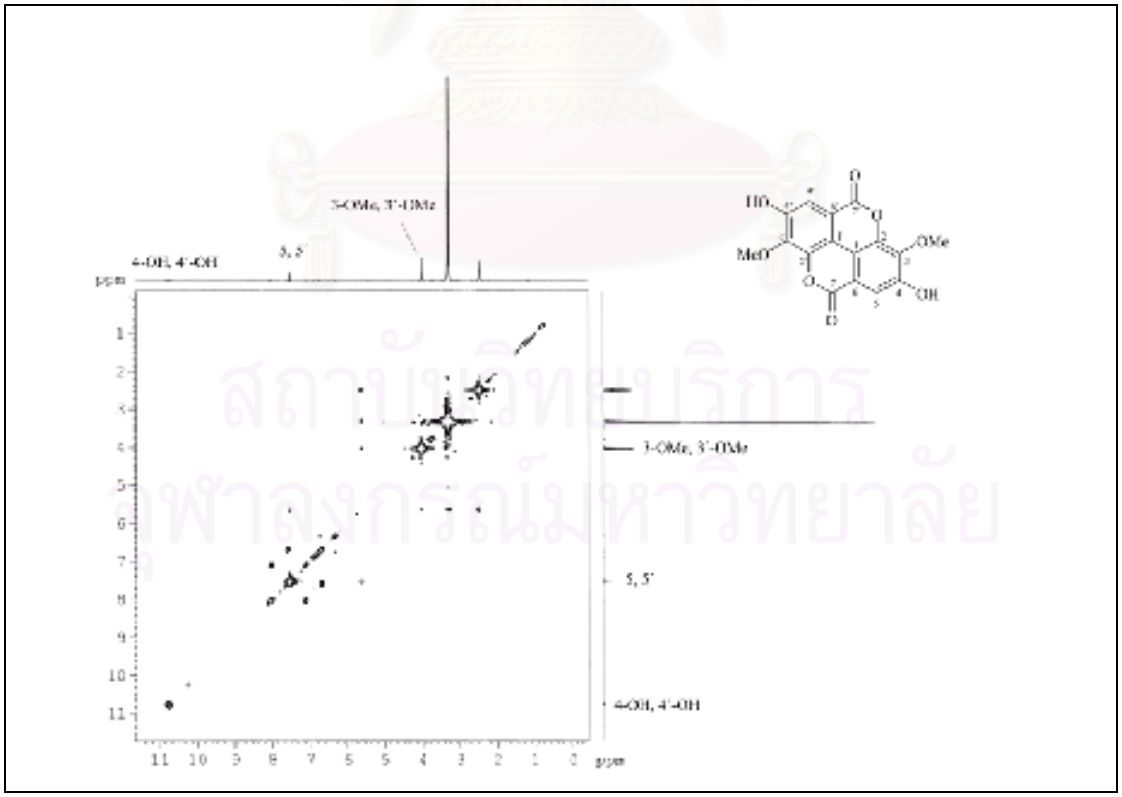

Figure 136. ^{1}H-^{1}H COSY Spectrum of compound ET-F7

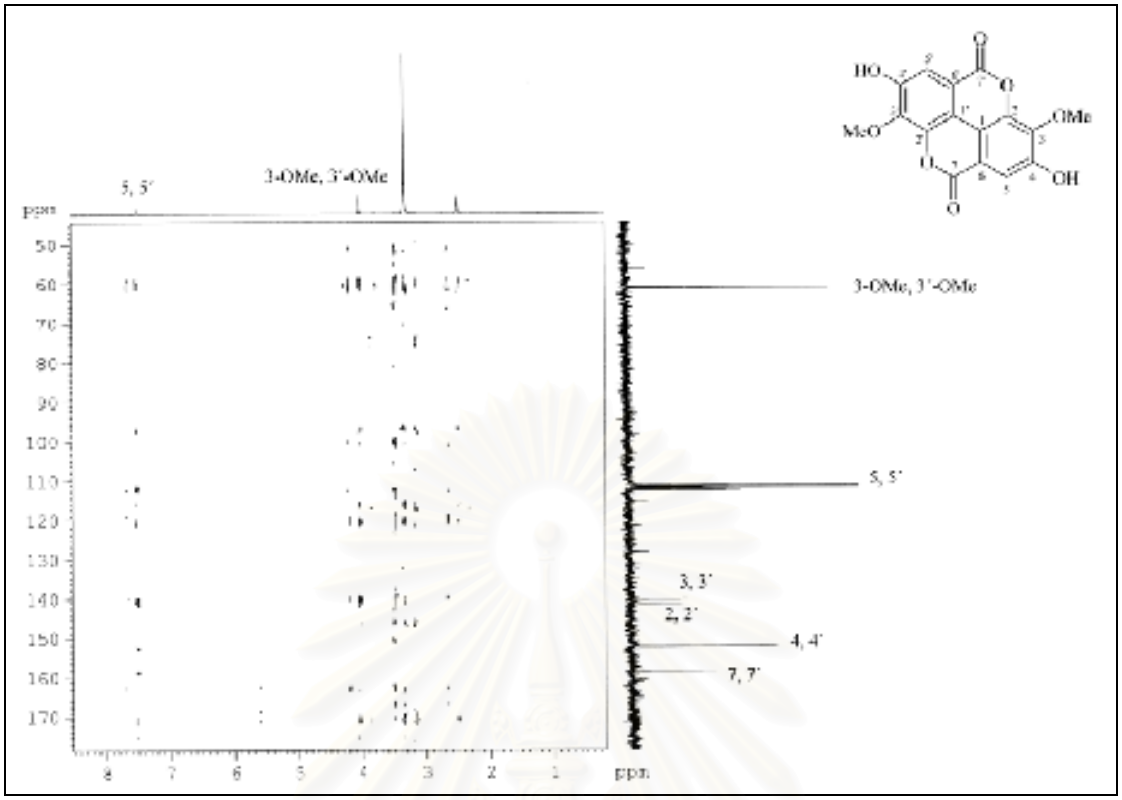

Figure 137. HMBC Spectrum of compound ET-F7 (δ_H 0-8.5 ppm, δ_C 50-170 ppm)

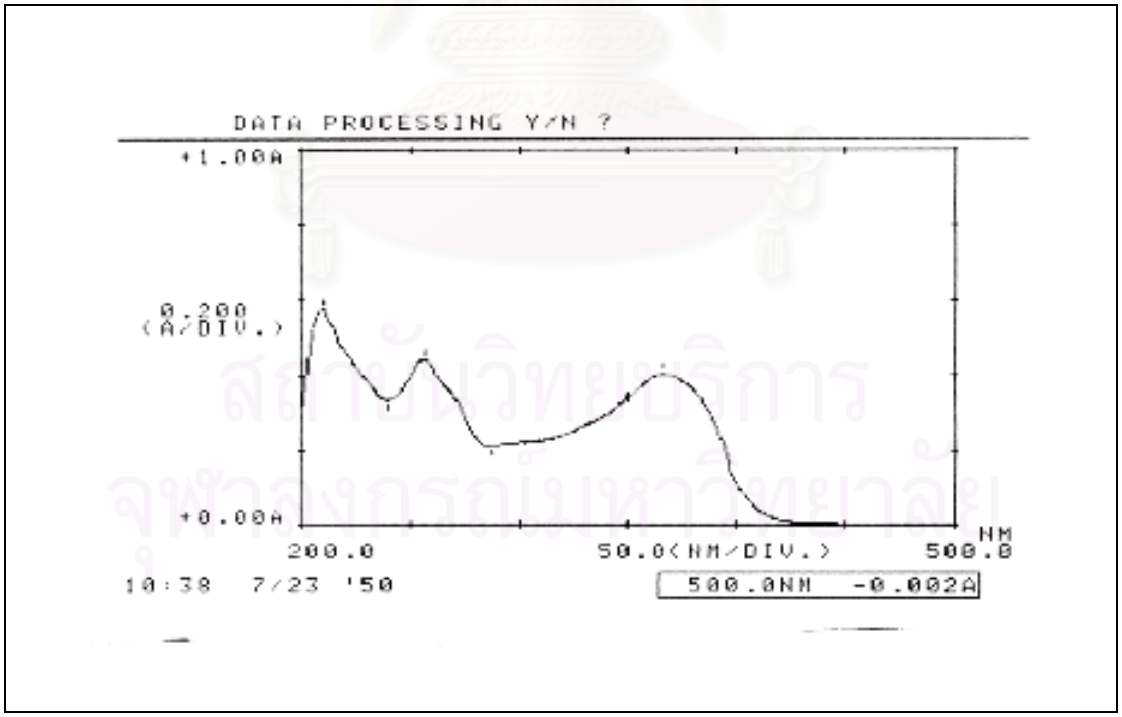

Figure 138. UV Spectrum of compound ET-FM3 (in MeOH)

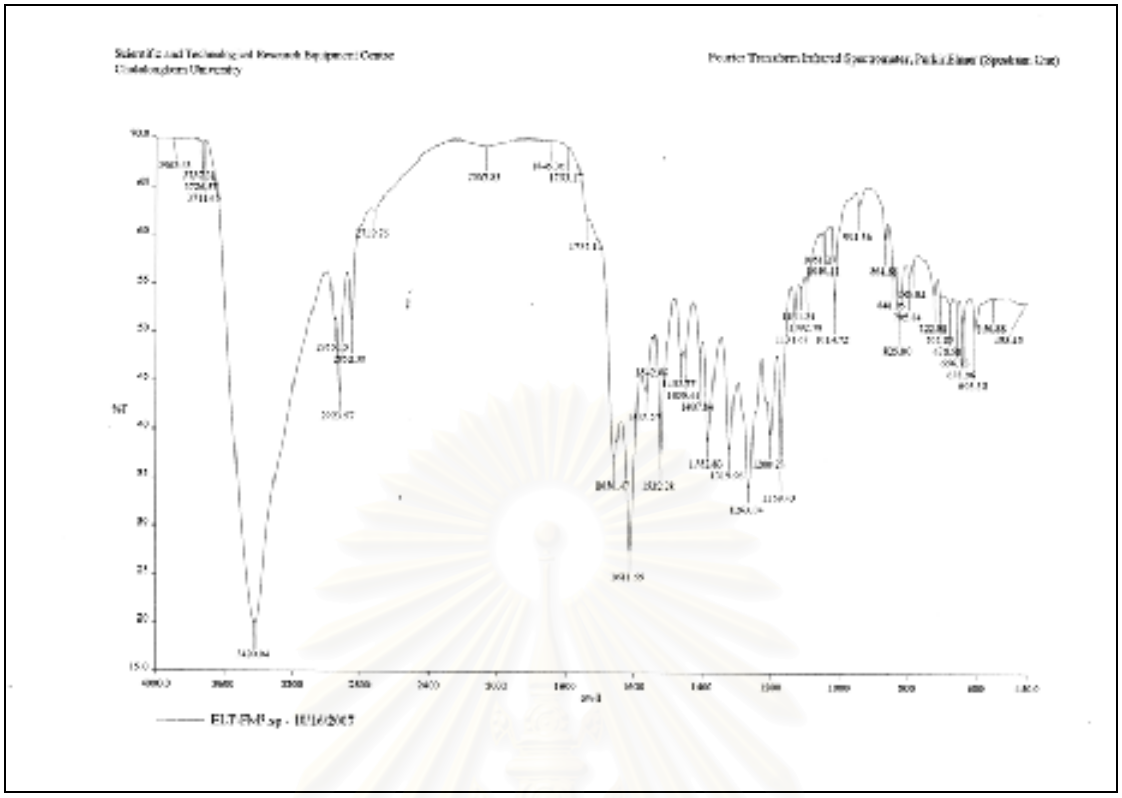

Figure 139. IR Spectrum of compound ET-FM3 (KBr disc)

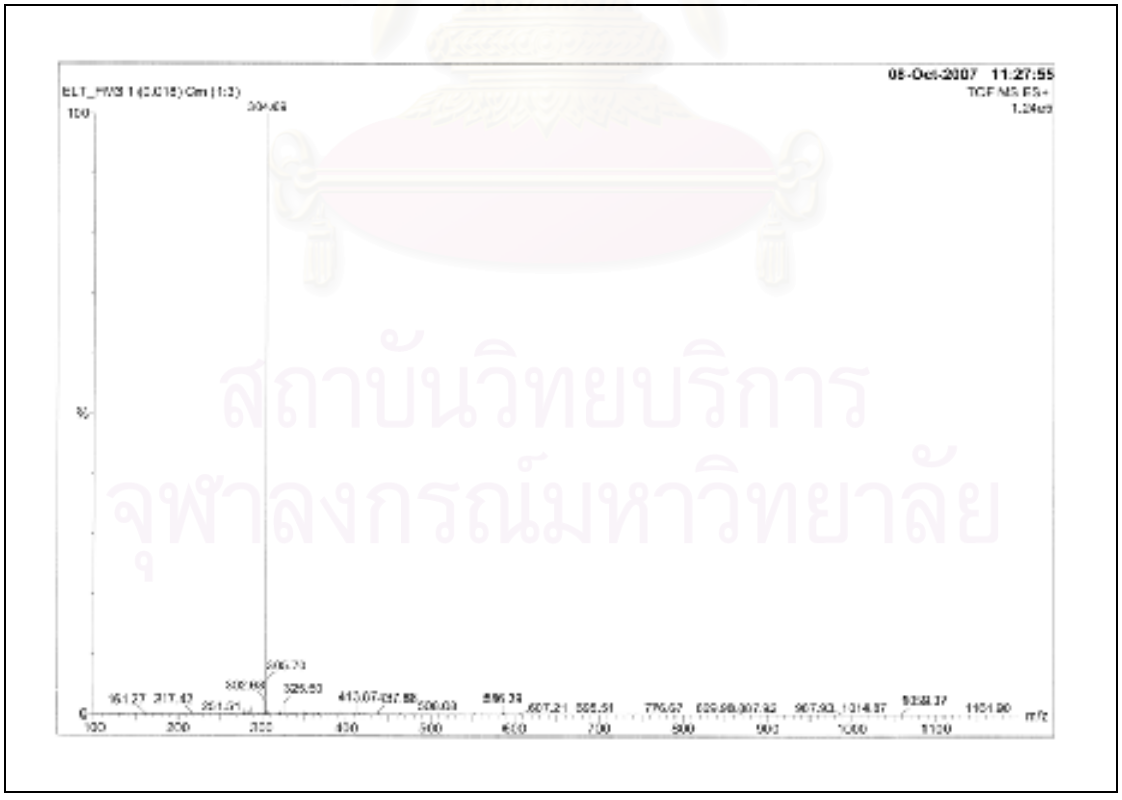

Figure 140. ESI Mass spectrum of compound ET-FM3

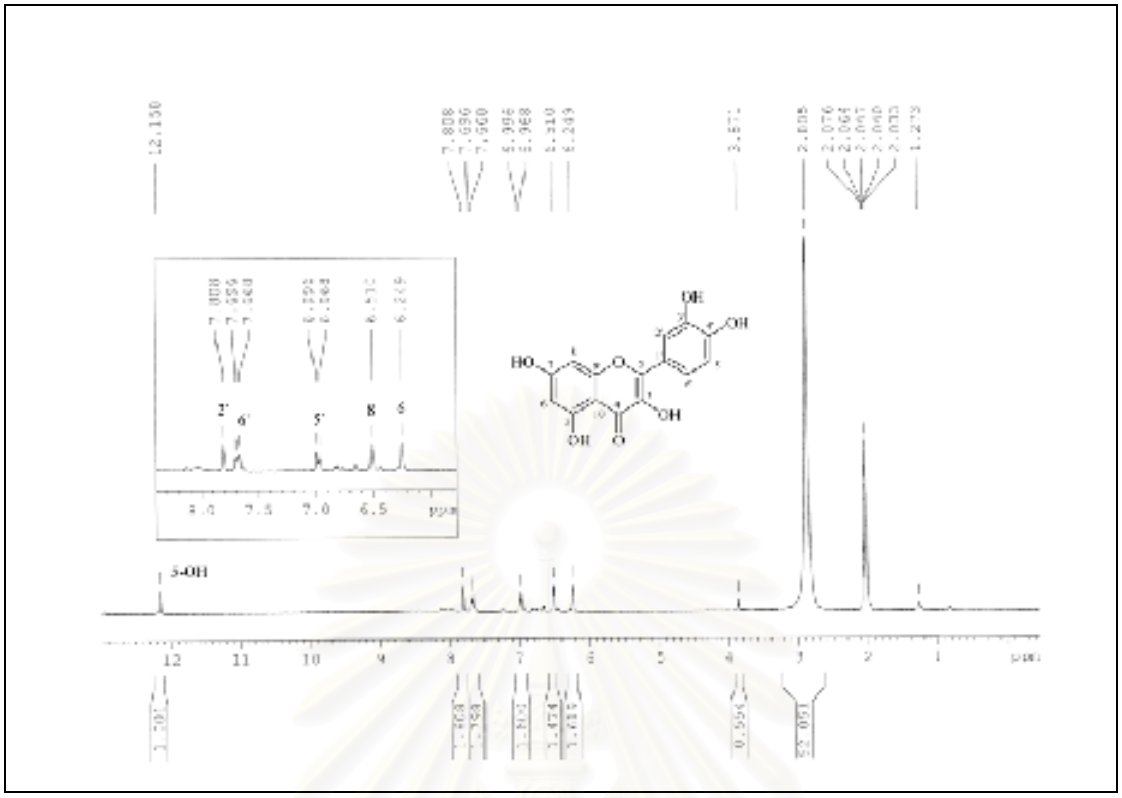

Figure 141. ^{1}H NMR (300 MHz) Spectrum of compound ET-FM3 (in acetone-d_6)

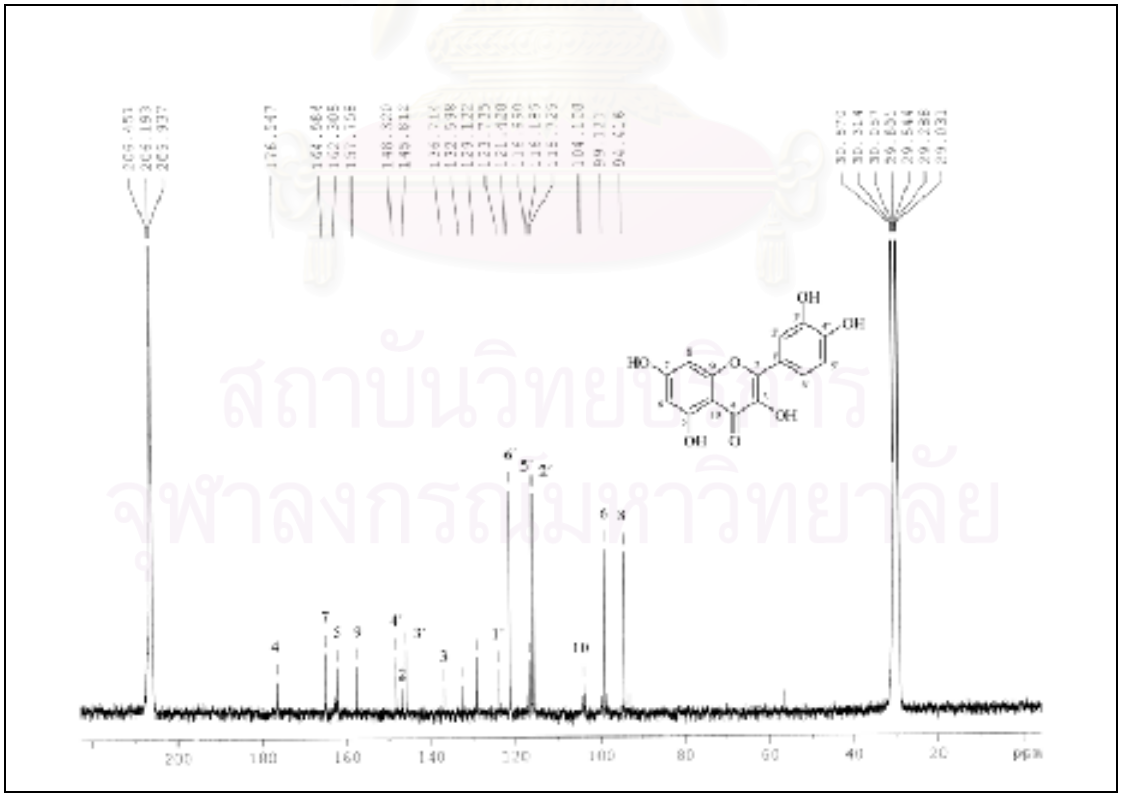

Figure 142. ^{13}C NMR (75 MHz) Spectrum of compound ET-FM3 (in acetone-d_6)

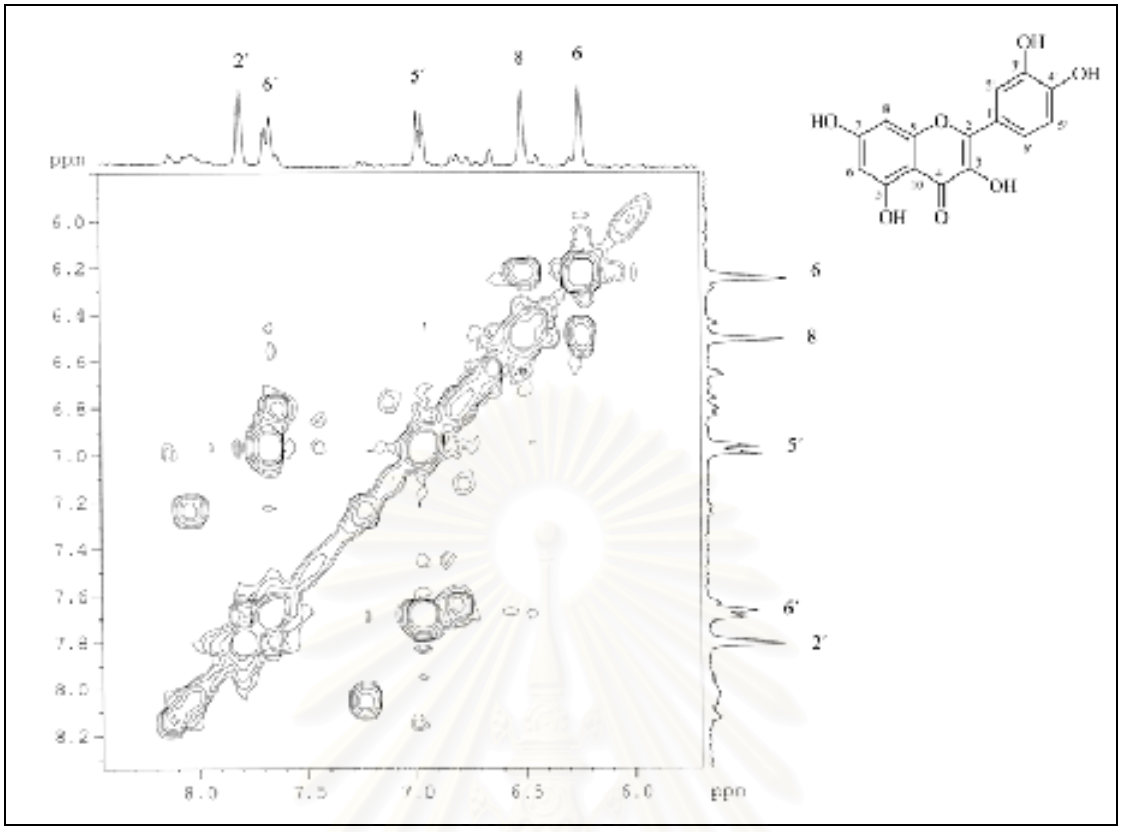

Figure 143. ^{1}H-^{1}H COSY spectrum of compound ET-FM3 (δ_H 5.8-8.5 ppm)

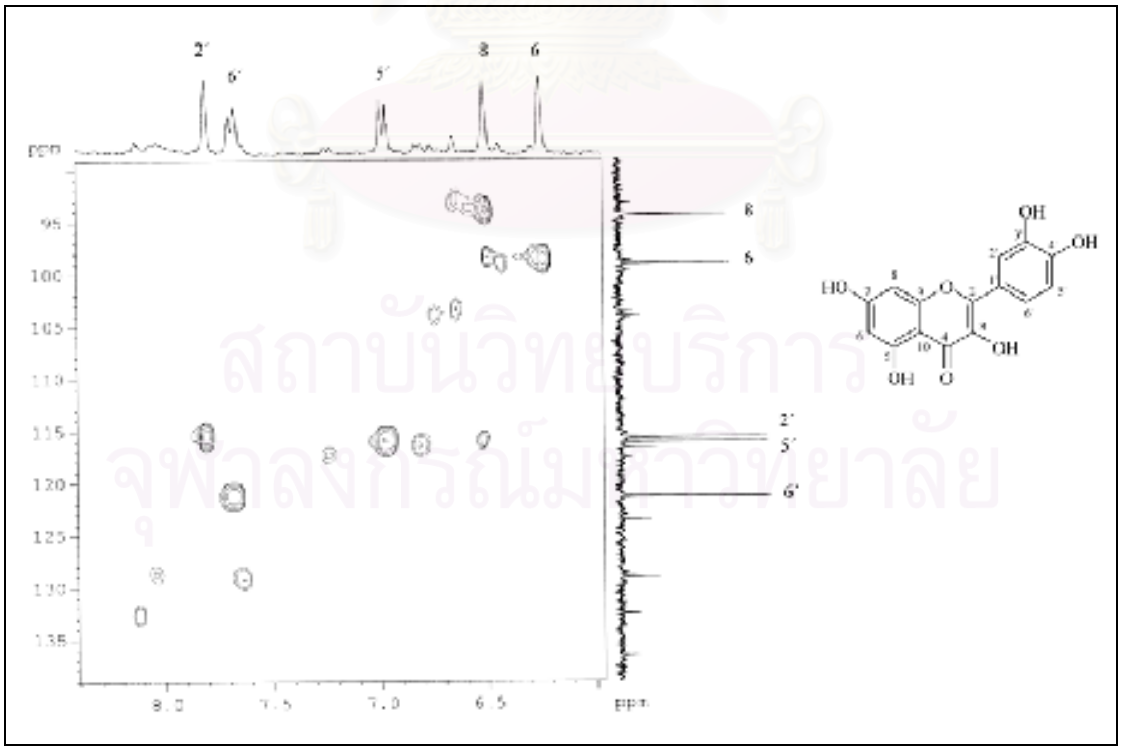

Figure 144. HMQC Spectrum of compound ET-FM3
(δ_H 6.0-8.5 ppm, δ_C 90-140 ppm)

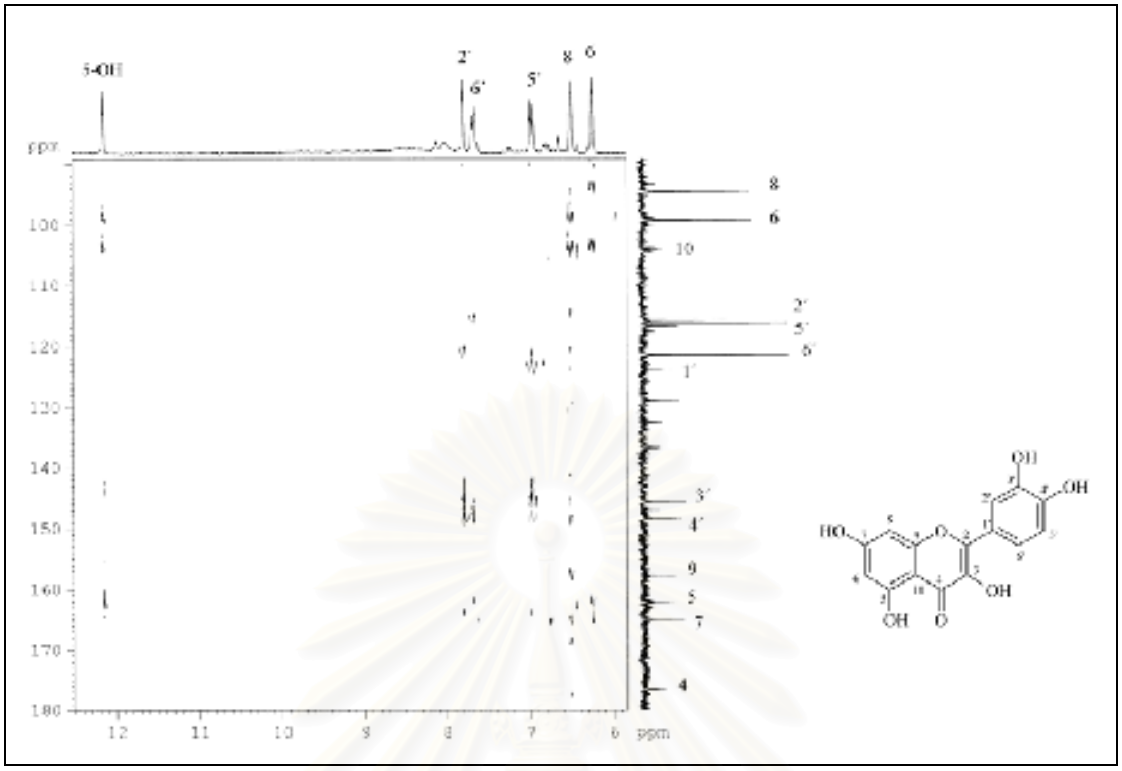

Figure 145. HMBC Spectrum of compound ET-FM3
(δ_H 6.0-12.5 ppm, δ_C 90-180 ppm)

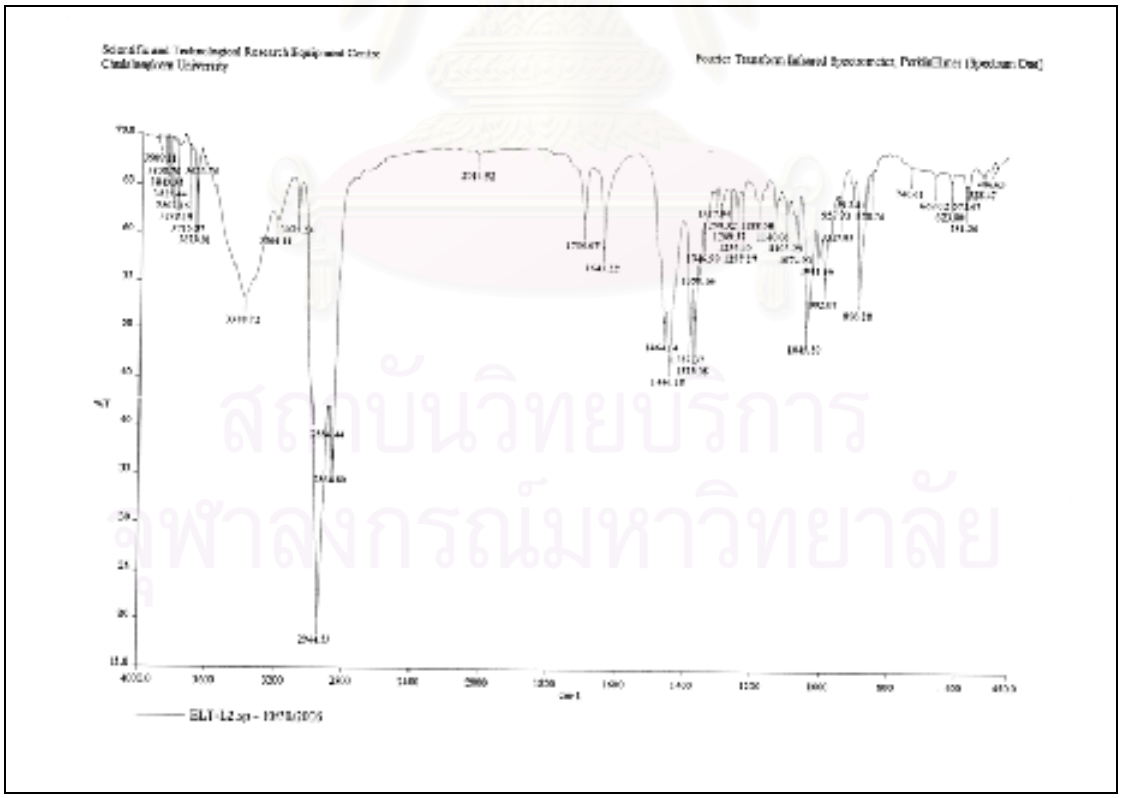

Figure 146. IR Spectrum of compound ET-L2 (KBr disc)

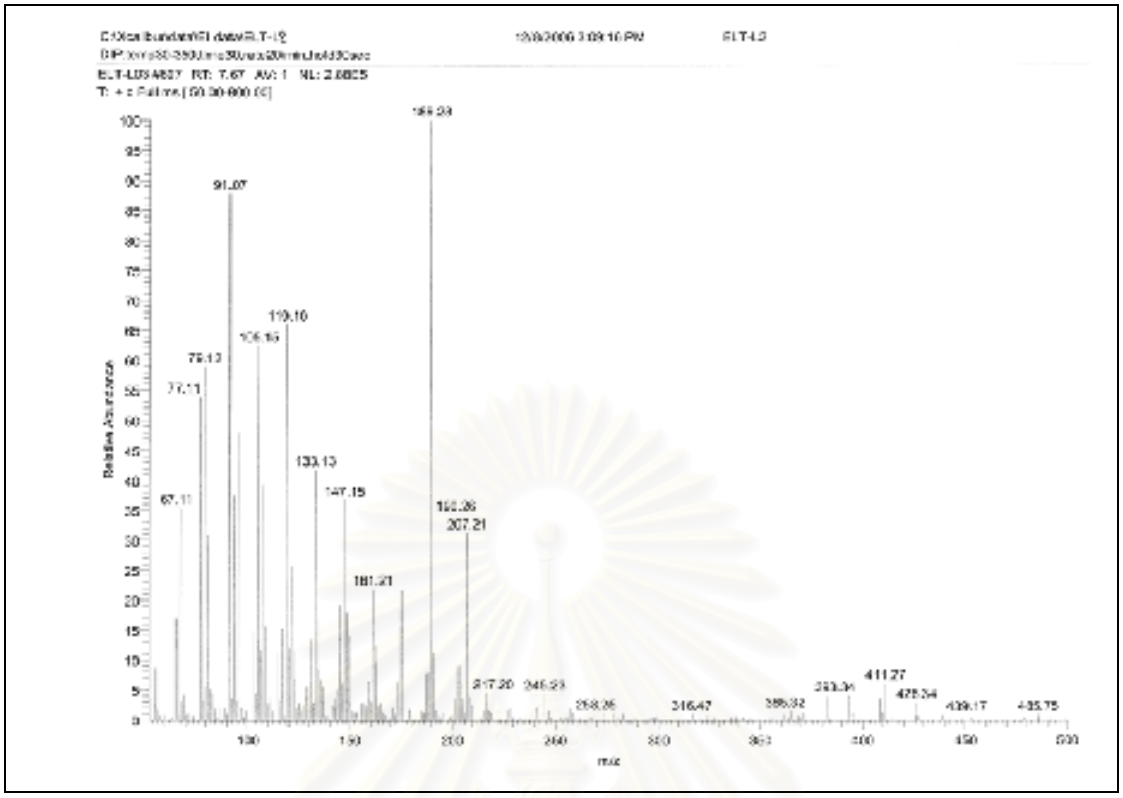

Figure 147. EI Mass spectrum of compound ET-L2

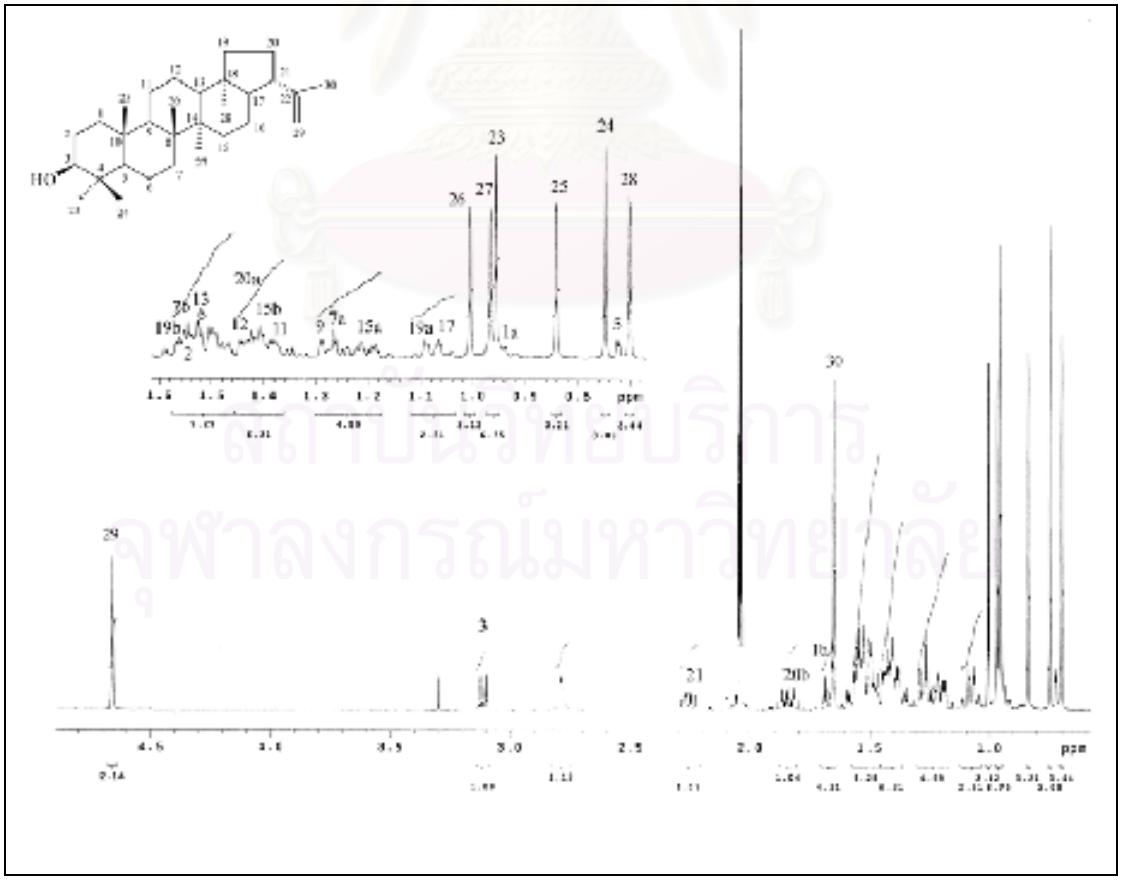

Figure 148. ^{1}H NMR (500 MHz) Spectrum of compound ET-L2 (in acetone-d_6)

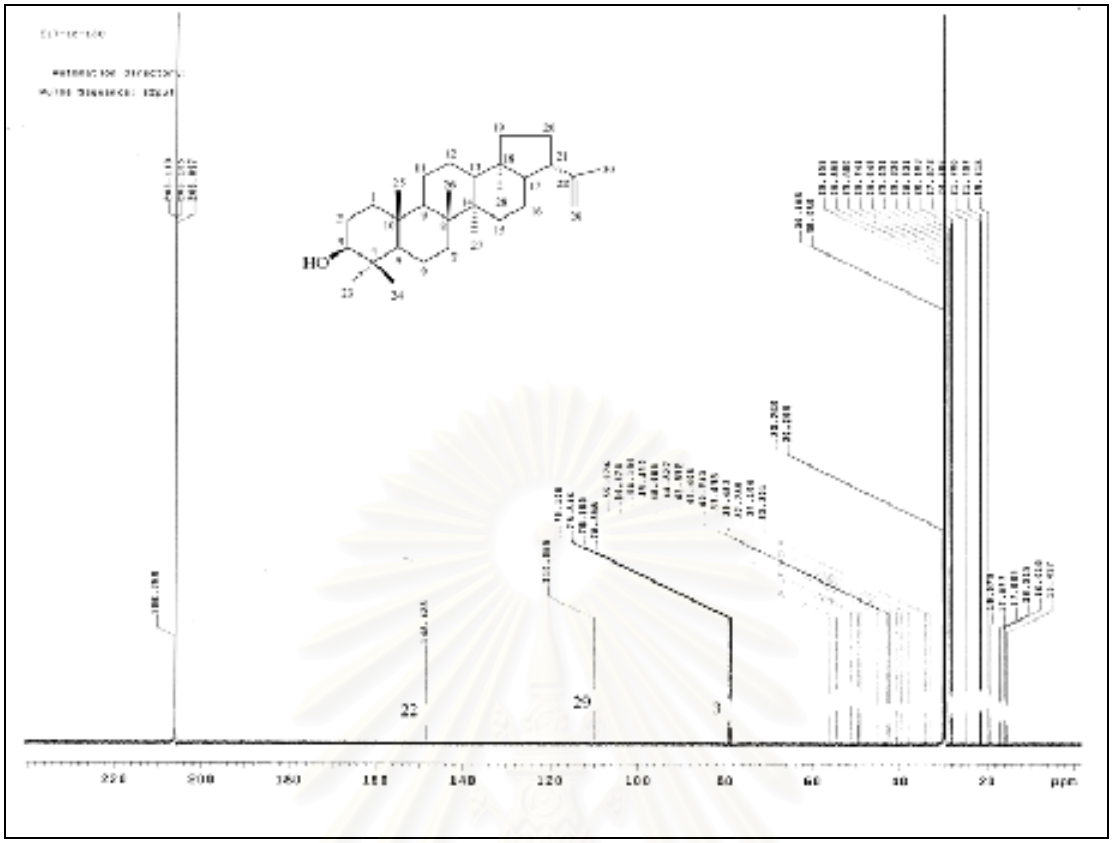

Figure 149a. ^{13}C NMR (125 MHz) Spectrum of compound ET-L2 (in acetone-d_6)

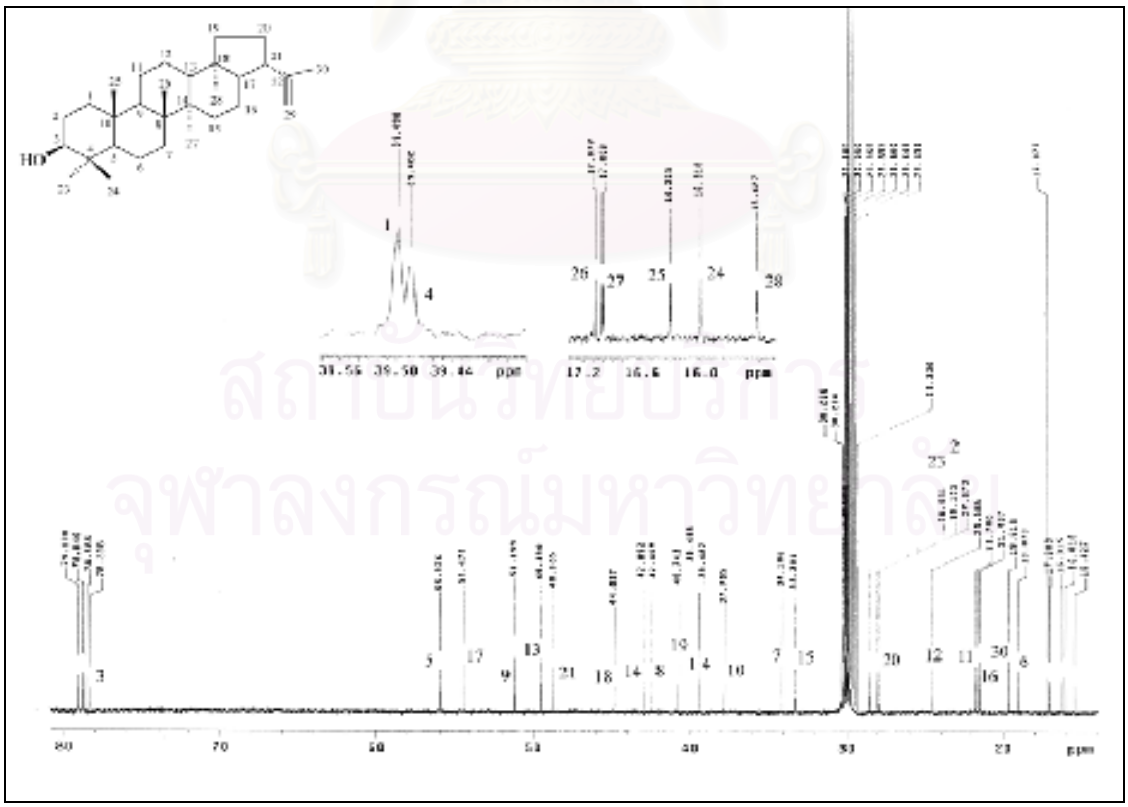

Figure 149b. ^{13}C NMR (125 MHz) Spectrum of compound ET-L2 (δ_C 14-80 ppm)

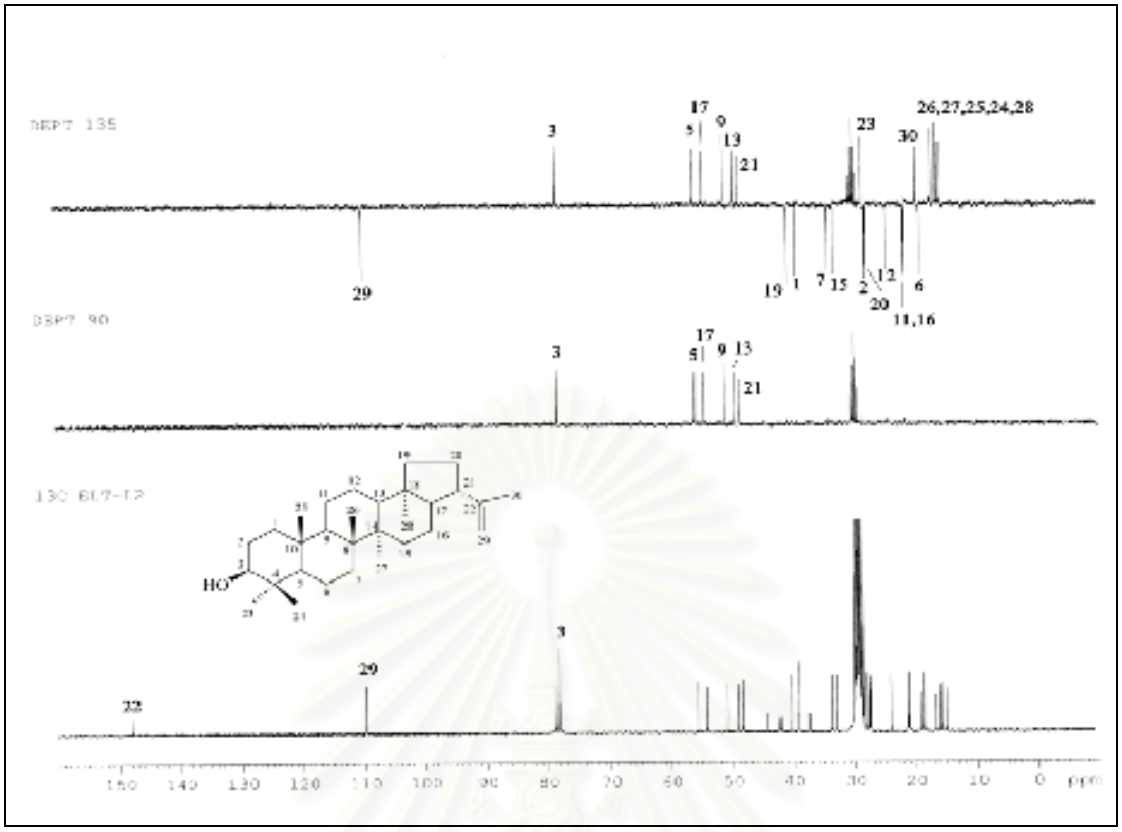

Figure 150. DEPT 135, DEPT 90 and ^{13}C NMR Spectrum of compound ET-L2

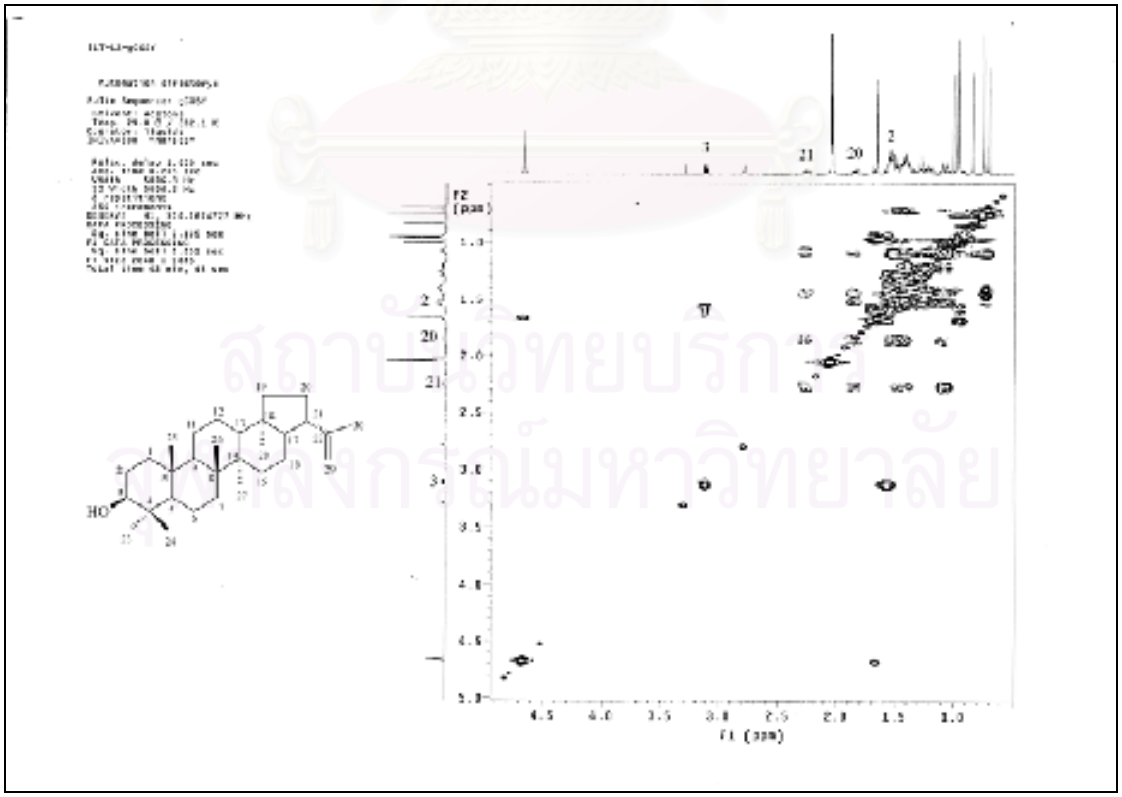

Figure 151. ^{1}H-^{1}H COSY Spectrum of compound ET-L2

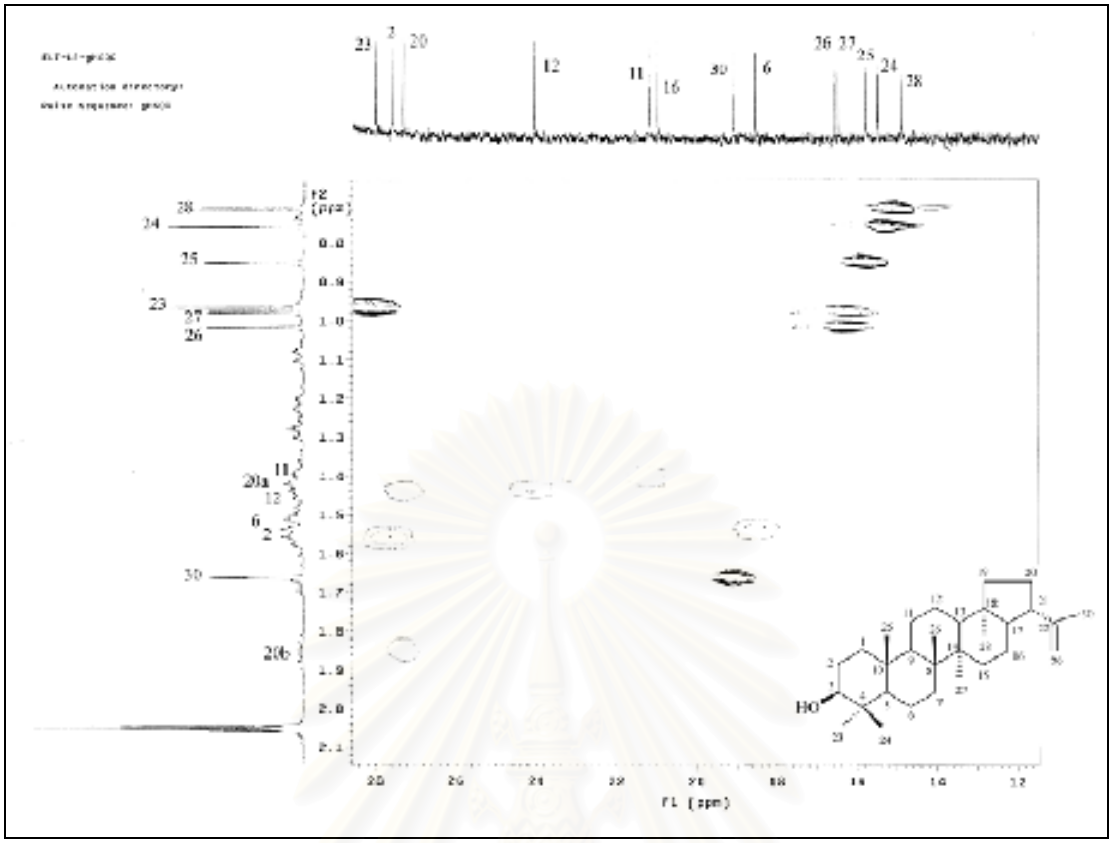

Figure 152a. HSQC Spectrum of compound ET-L2 (δ_H 0.7-2.1 ppm, δ_C 12-28 ppm)

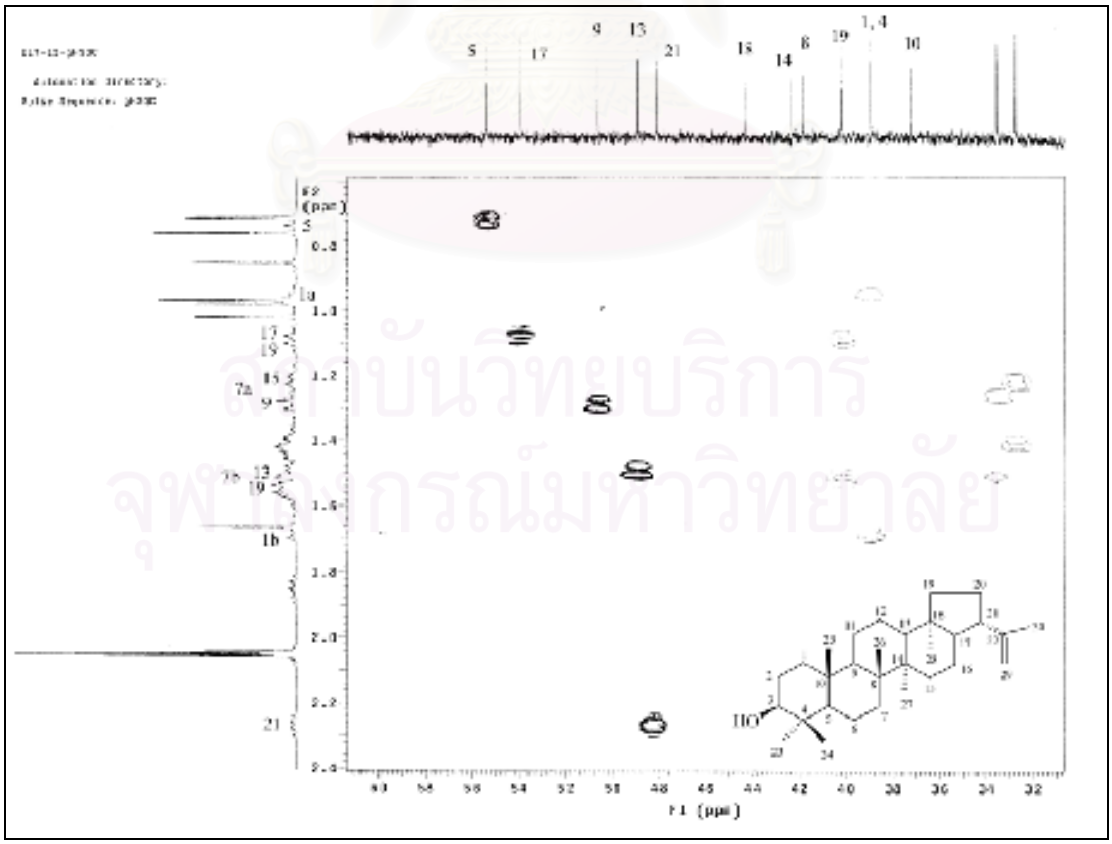

Figure 152b. HSQC Spectrum of compound ET-L2 (δ_H 0.6-2.4 ppm, δ_C 31-61 ppm)

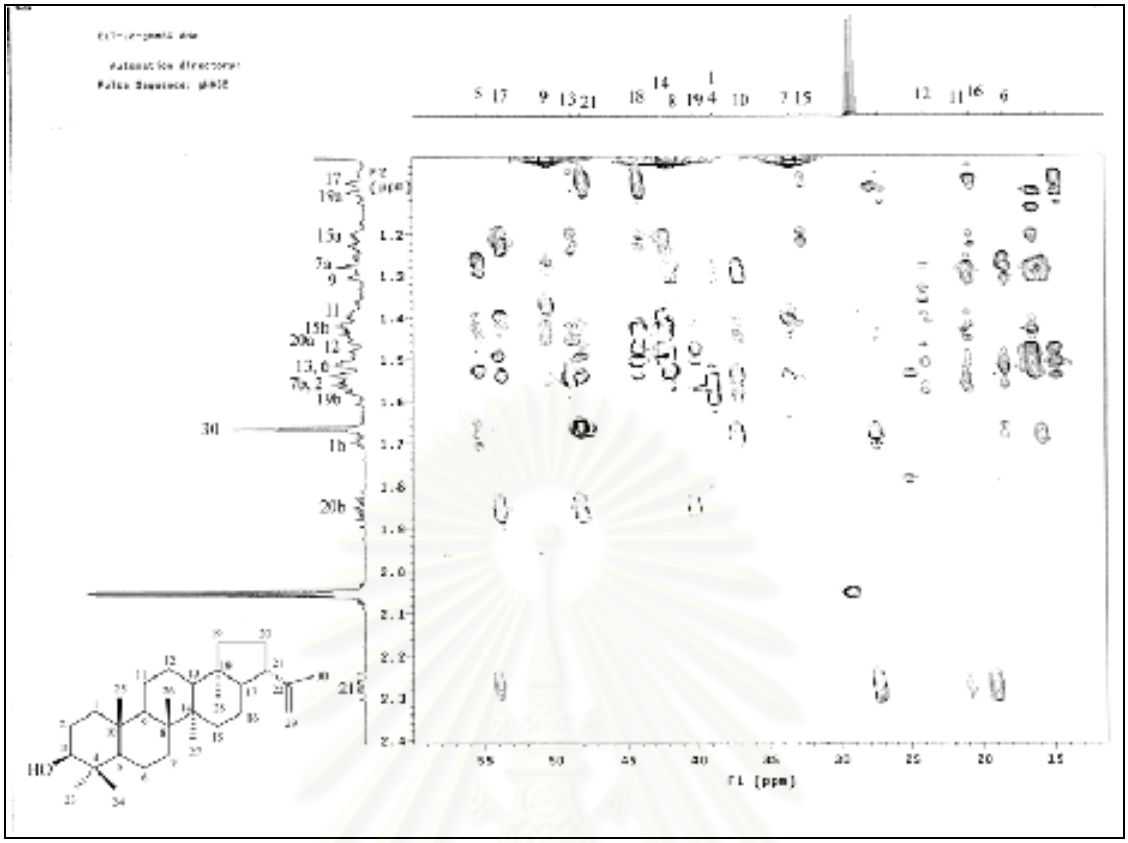

Figure 153a. HMBC Spectrum of compound ET-L2 (δ_H 1.1-2.4 ppm, δ_C 12-60 ppm)

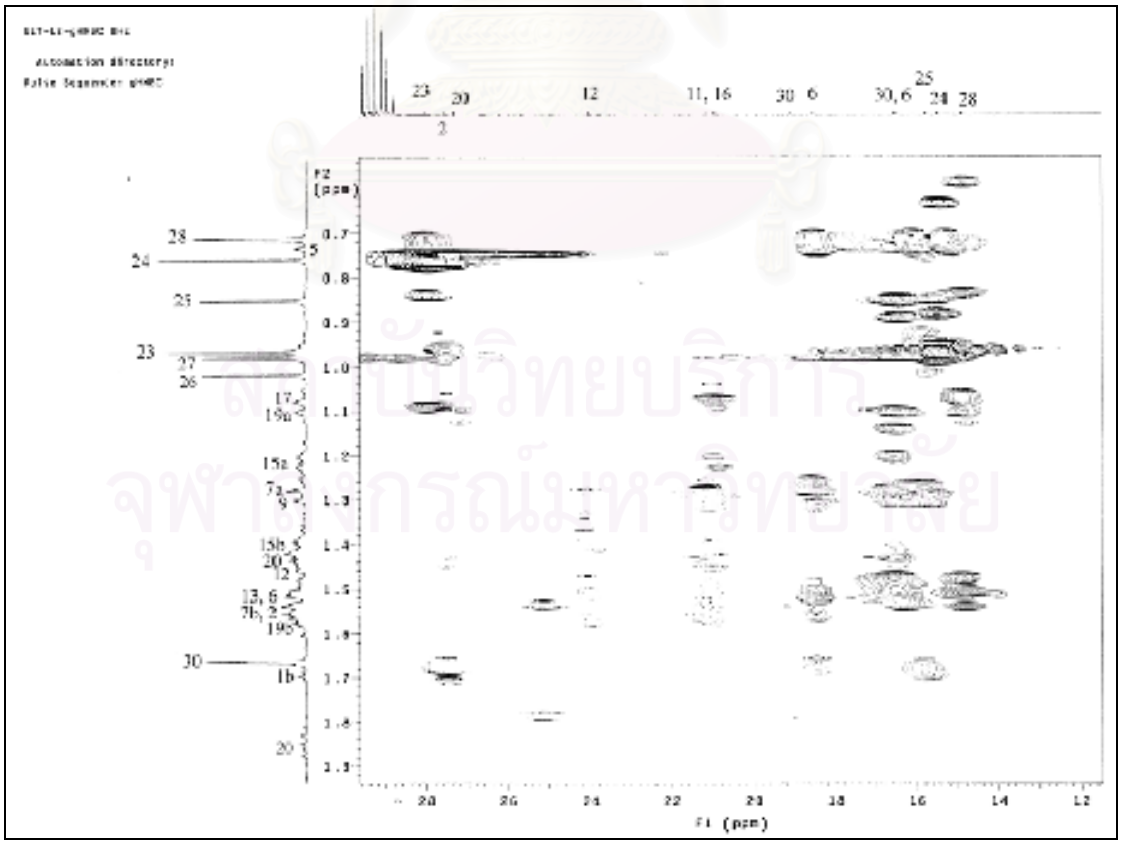

Figure 153b. HMBC Spectrum of compound ET-L2 (δ_H 0.6-1.9 ppm, δ_C 12-30 ppm)

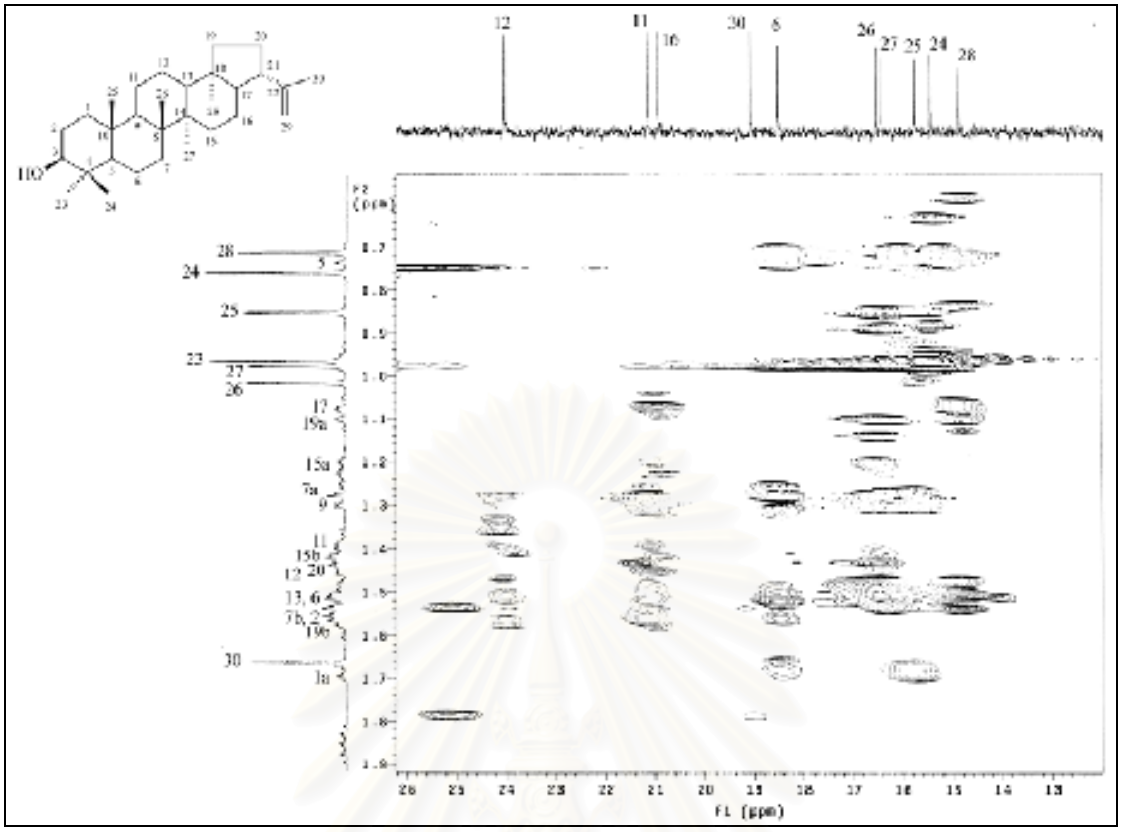

Figure 153c. HMBC Spectrum of compound ET-L2 (δ_H 0.6-1.9 ppm, δ_C 12-26 ppm)

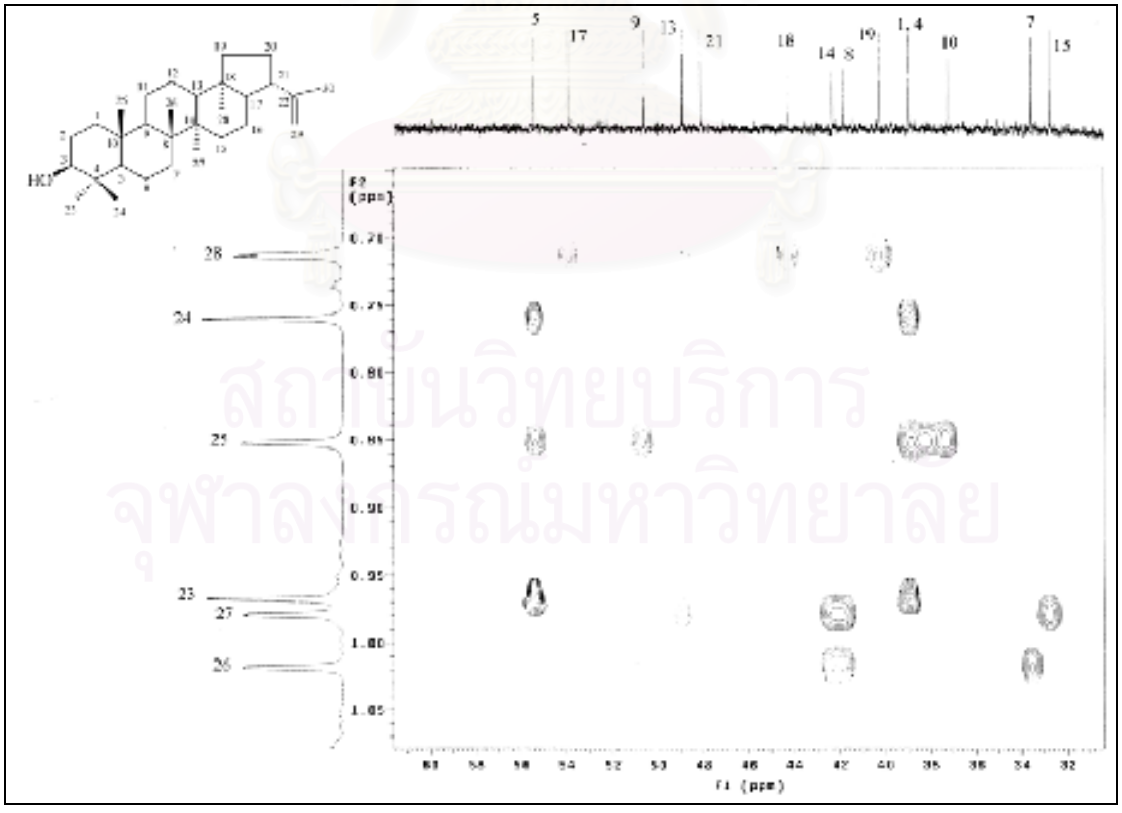

Figure 153d. HMBC Spectrum of compound ET-L2
(δ_H 0.65-1.05 ppm, δ_C 30-61 ppm)

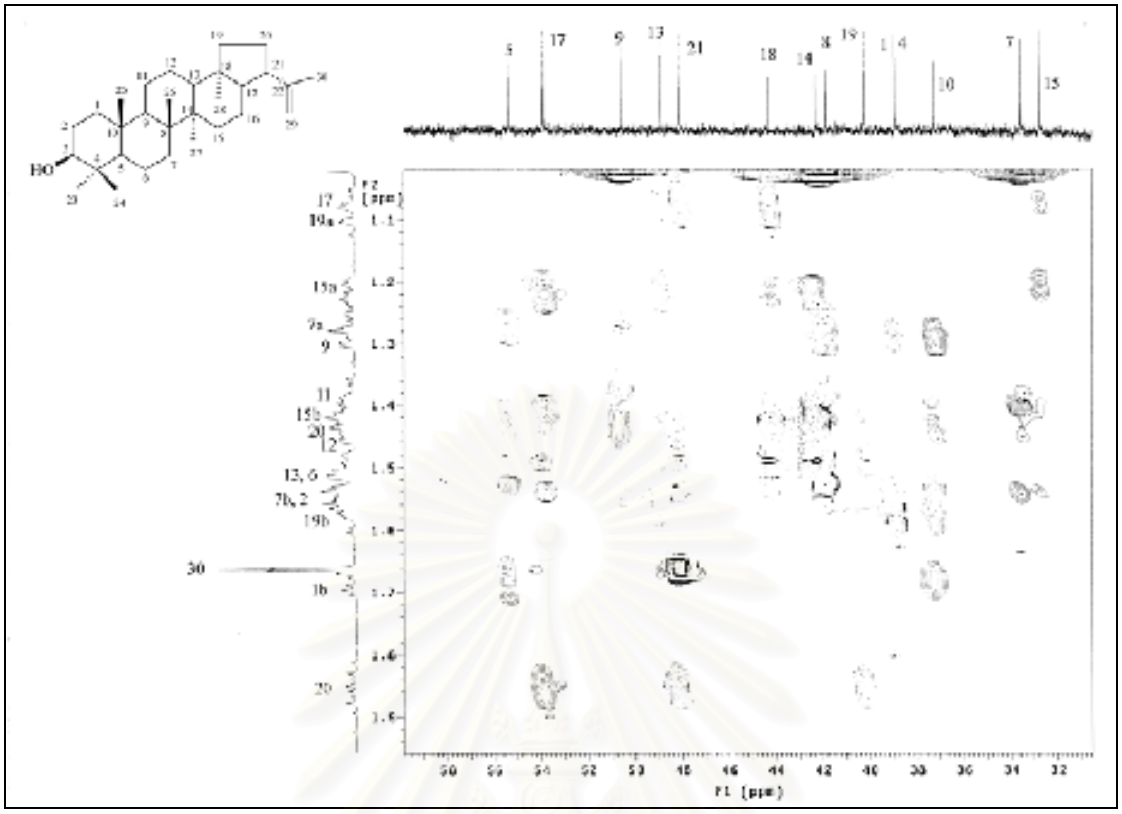

Figure 153e. HMBC Spectrum of compound ET-L2 (δ_H 1.0-1.93 ppm, δ_C 31-60 ppm)

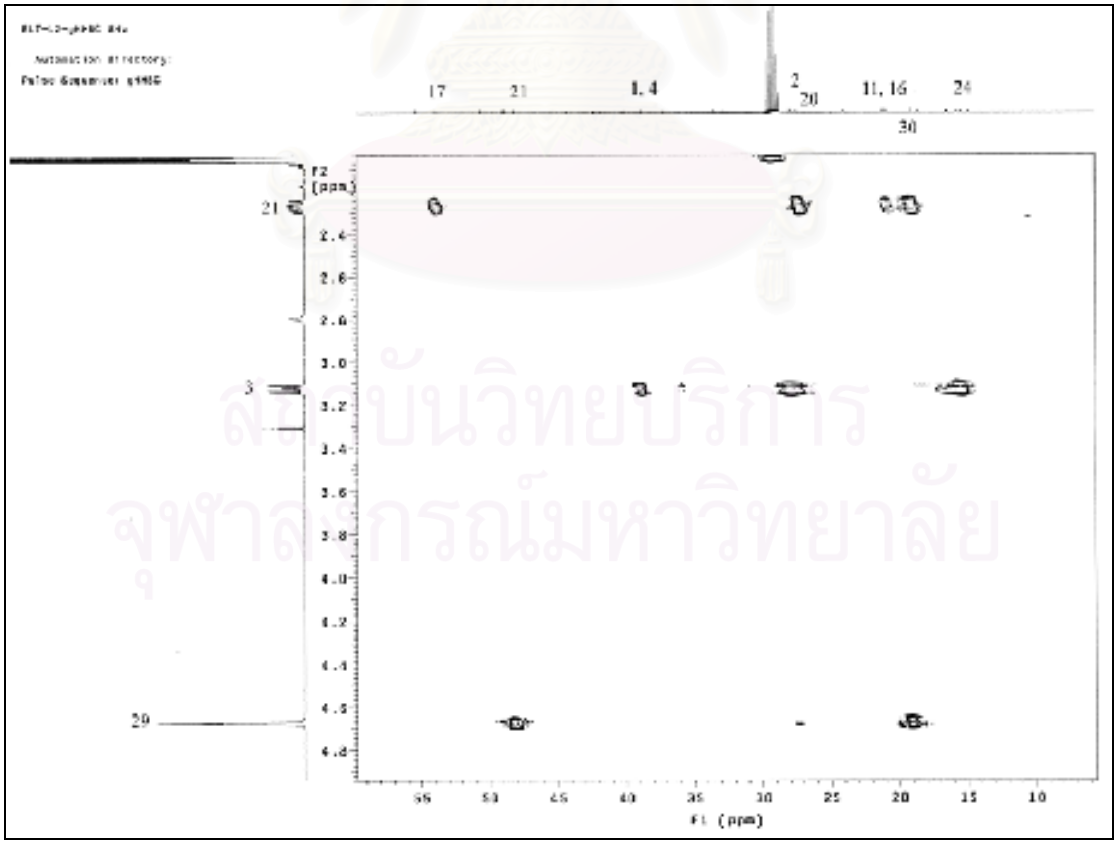

Figure 153f. HMBC Spectrum of compound ET-L2 (δ_H 2.0-4.9 ppm, δ_C 5-60 ppm)

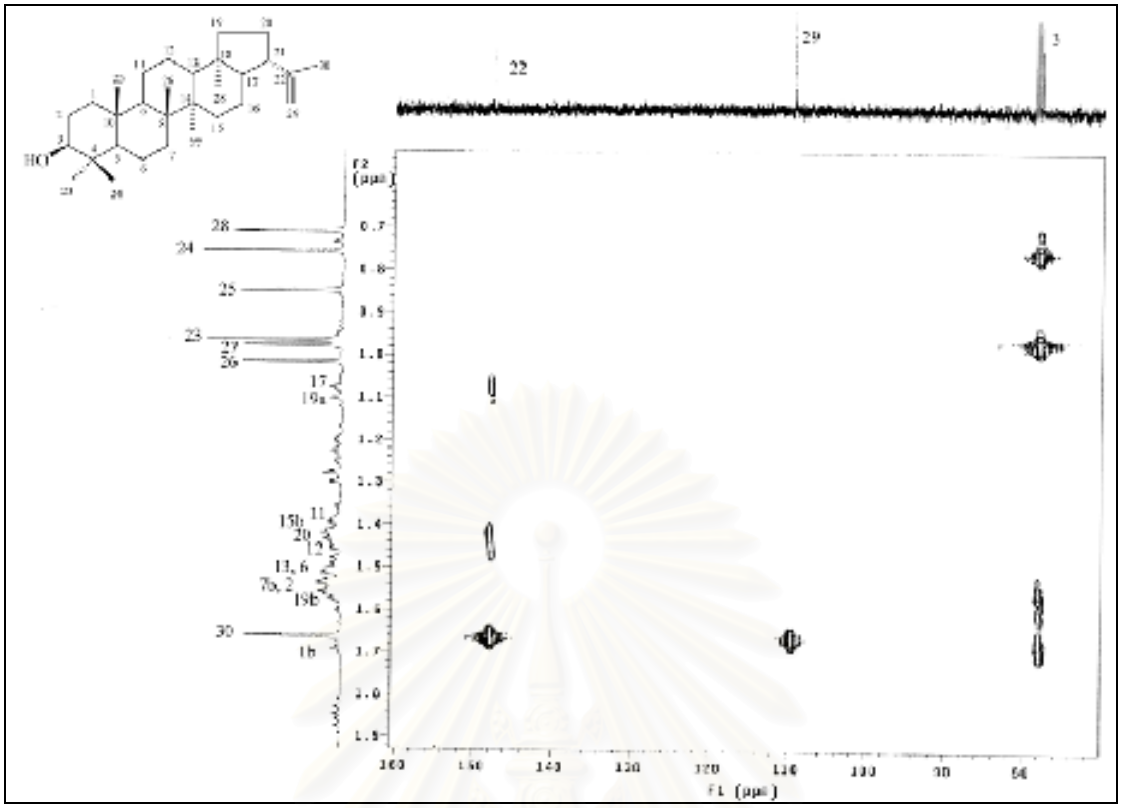

Figure 153g. HMBC Spectrum of compound ET-L2 (δ_H 0.5-1.9 ppm, δ_C 70-160 ppm)

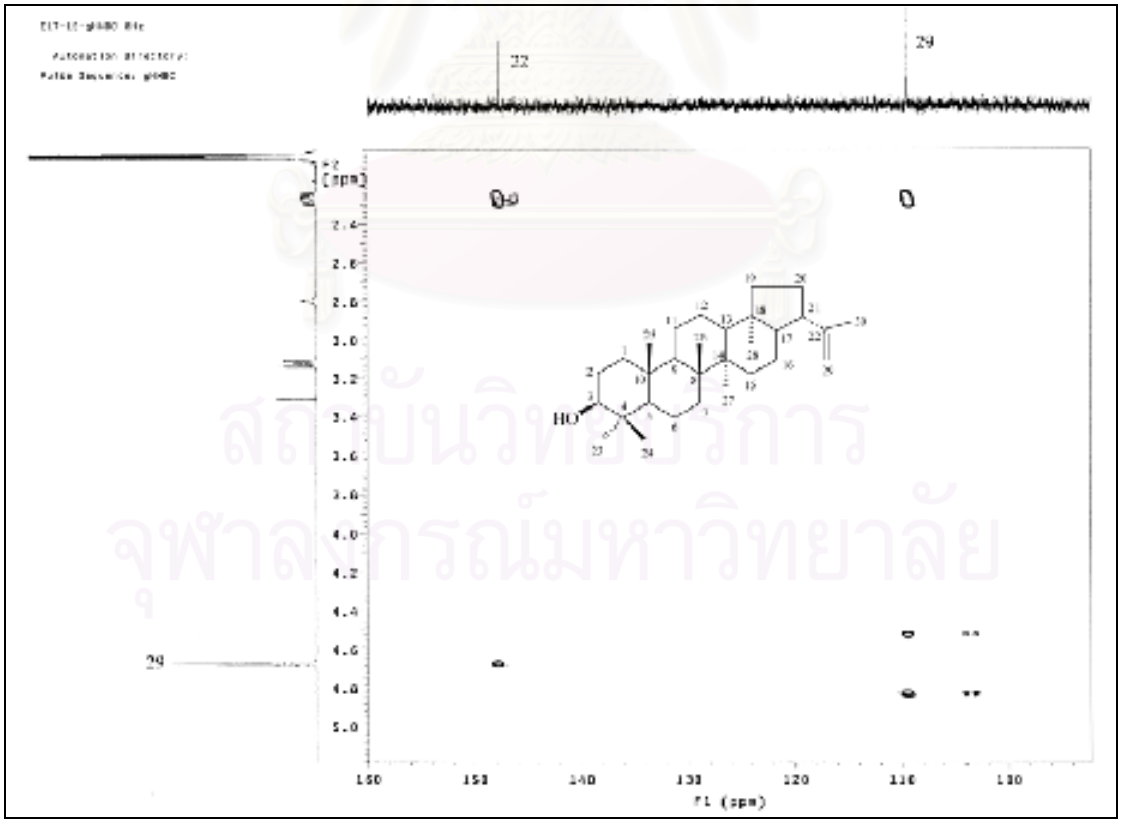

Figure 153h. HMBC Spectrum of compound ET-L2
(δ_H 2.0-5.2 ppm, δ_C 90-160 ppm)

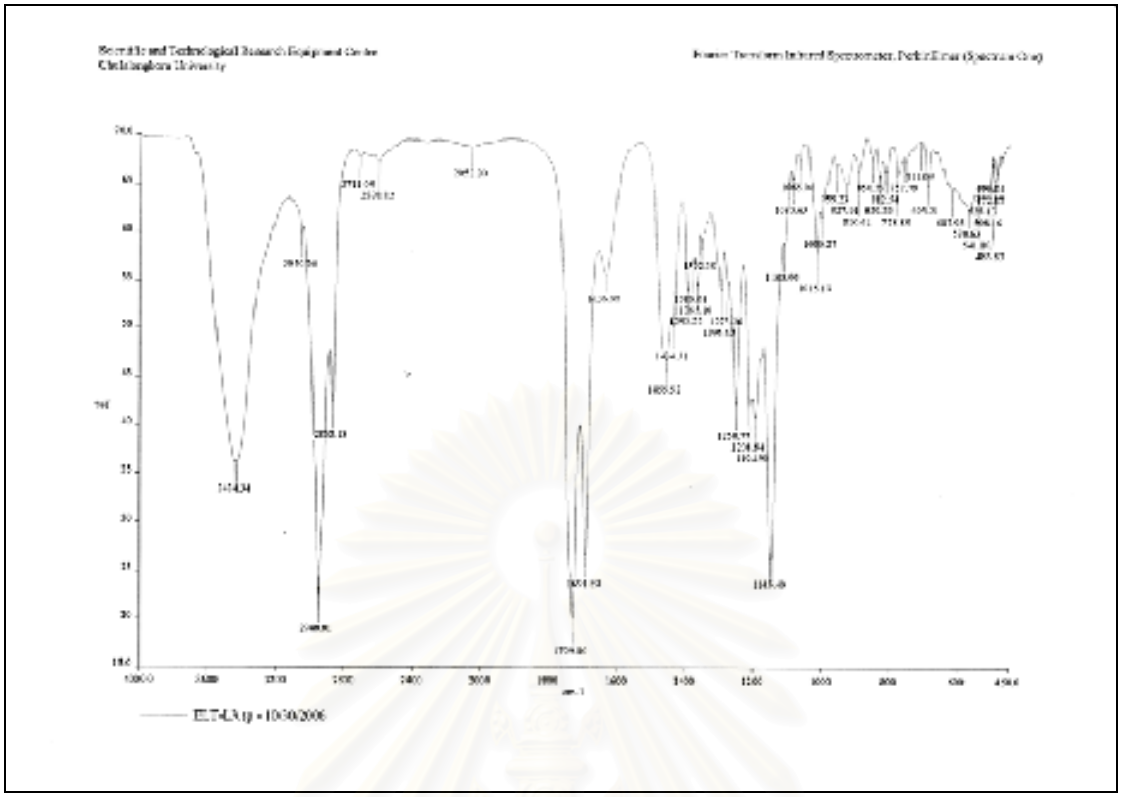

Figure 154. IR Spectrum of compound ET-L3 (KBr disc)

Figure 155. HR ESI Mass spectrum of compound ET-L3

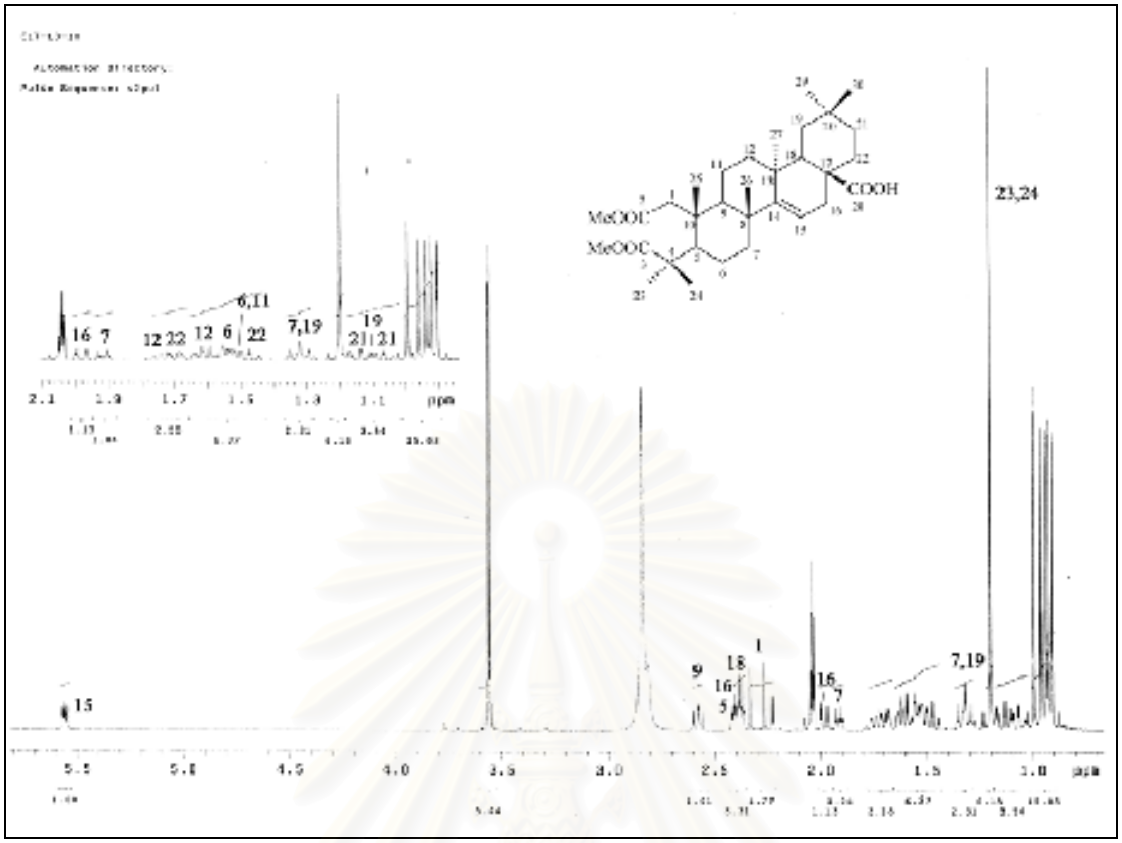

Figure 156a. ^{1}H NMR (500 MHz) Spectrum of compound ET-L3 (δ_H 0.5-6.0 ppm)

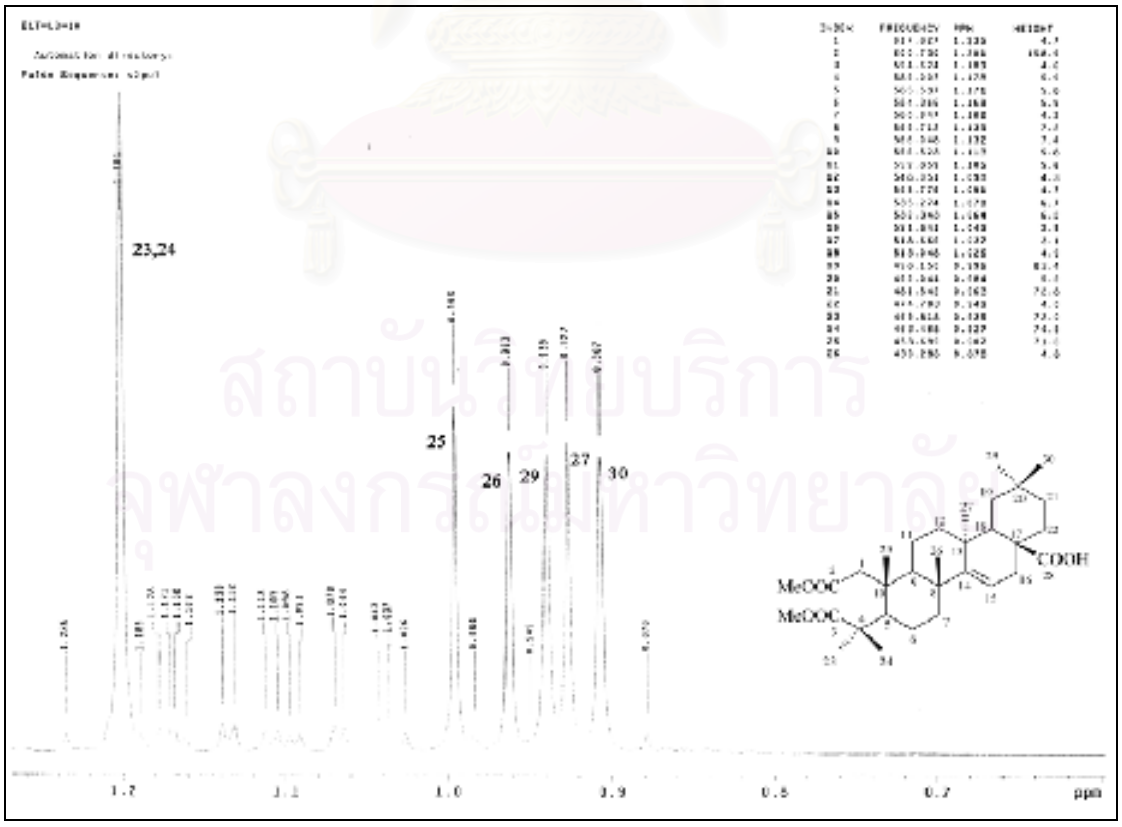

Figure 156b. ^{1}H NMR (500 MHz) Spectrum of compound ET-L3 (δ_H 0.6-1.3 ppm)

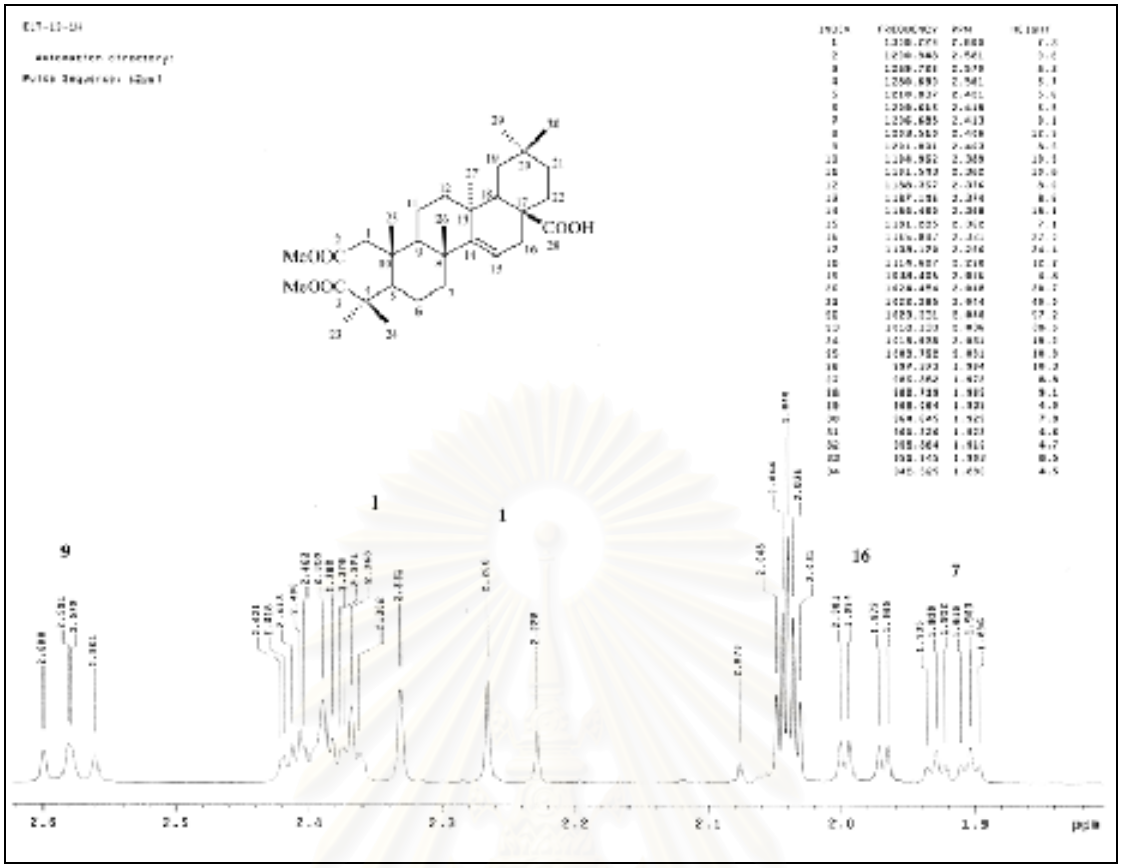

Figure 156c. ^{1}H NMR (500 MHz) Spectrum of compound ET-L3 (δ_H 1.8-2.6 ppm)

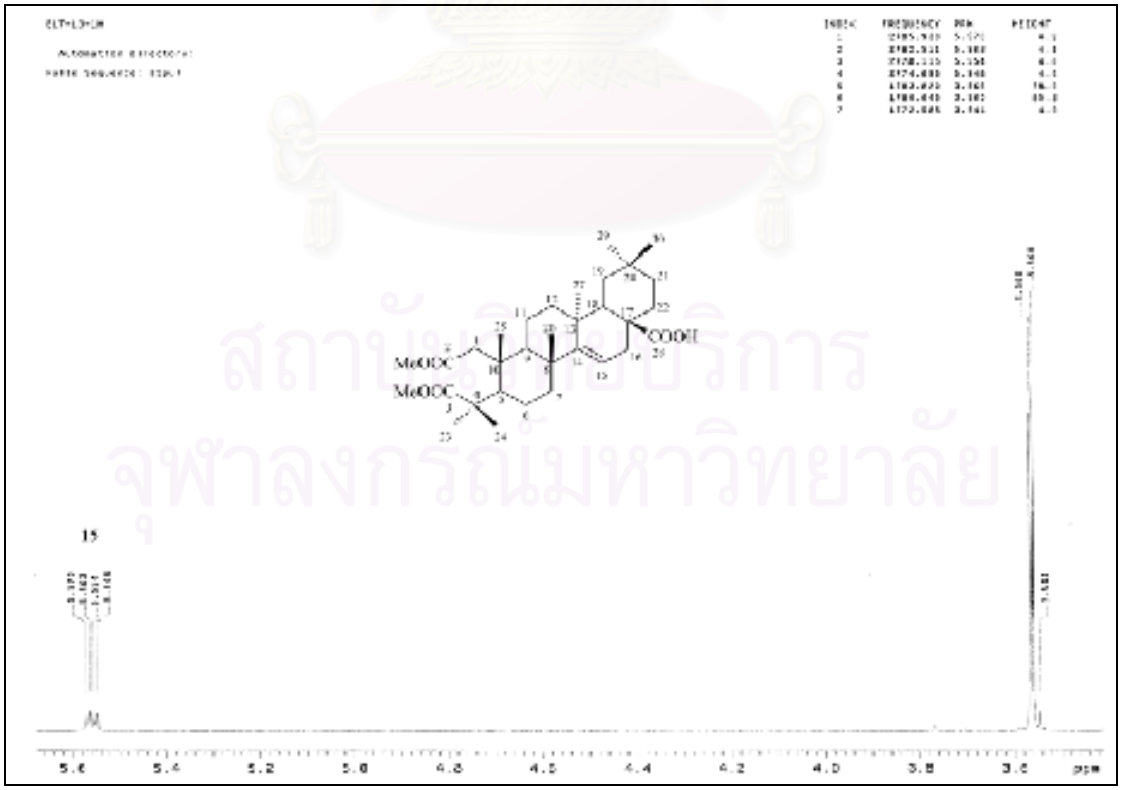

Figure 156d. ^{1}H NMR (500 MHz) Spectrum of compound ET-L3 (δ_H 3.4-5.6 ppm)

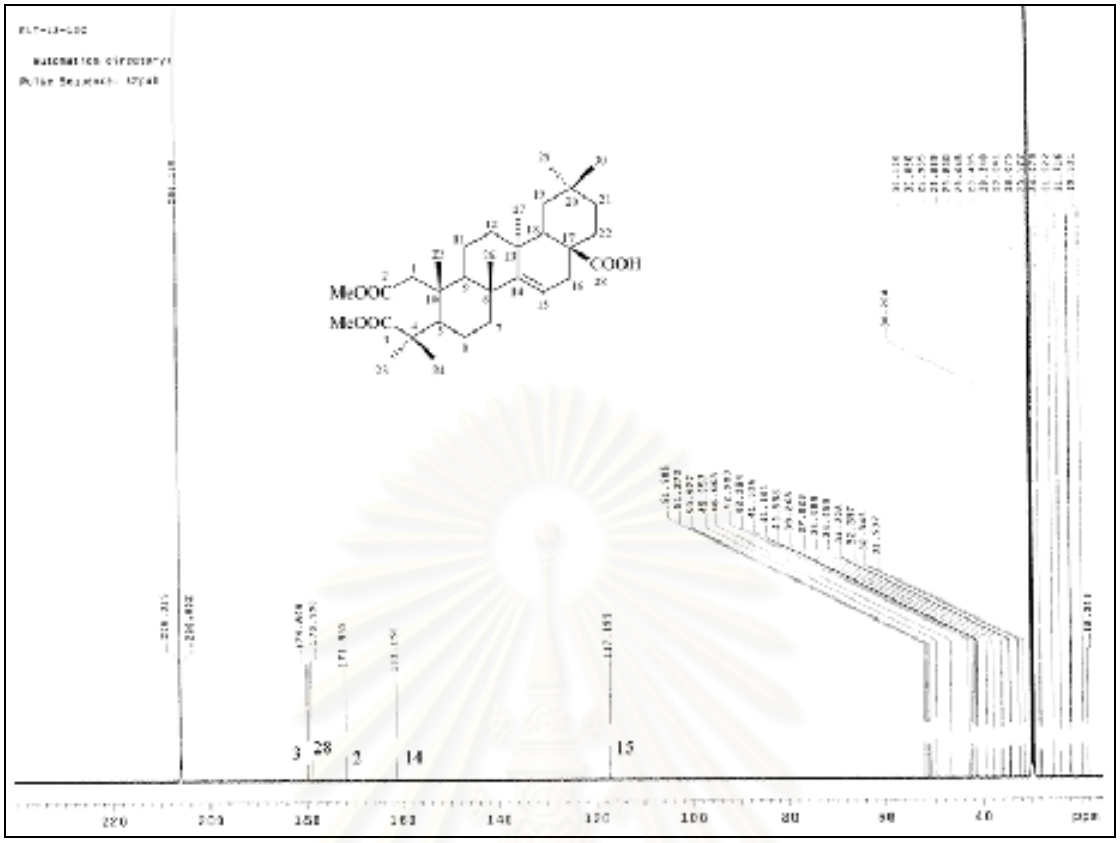

Figure 157a. ^{13}C NMR (125 MHz) Spectrum of compound ET-L3 (in acetone-d_6)

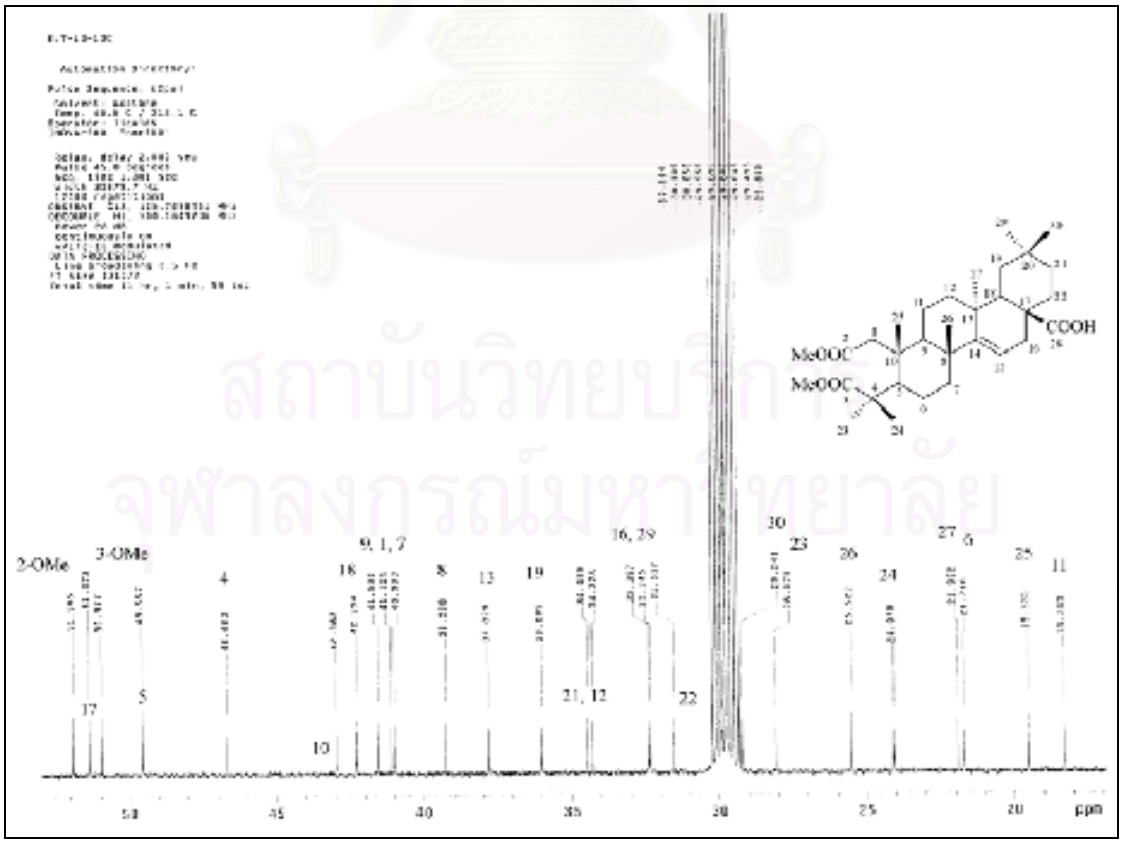

Figure 157b. ^{13}C NMR (125 MHz) Spectrum of compound ET-L3 (δ_C 17-53 ppm)

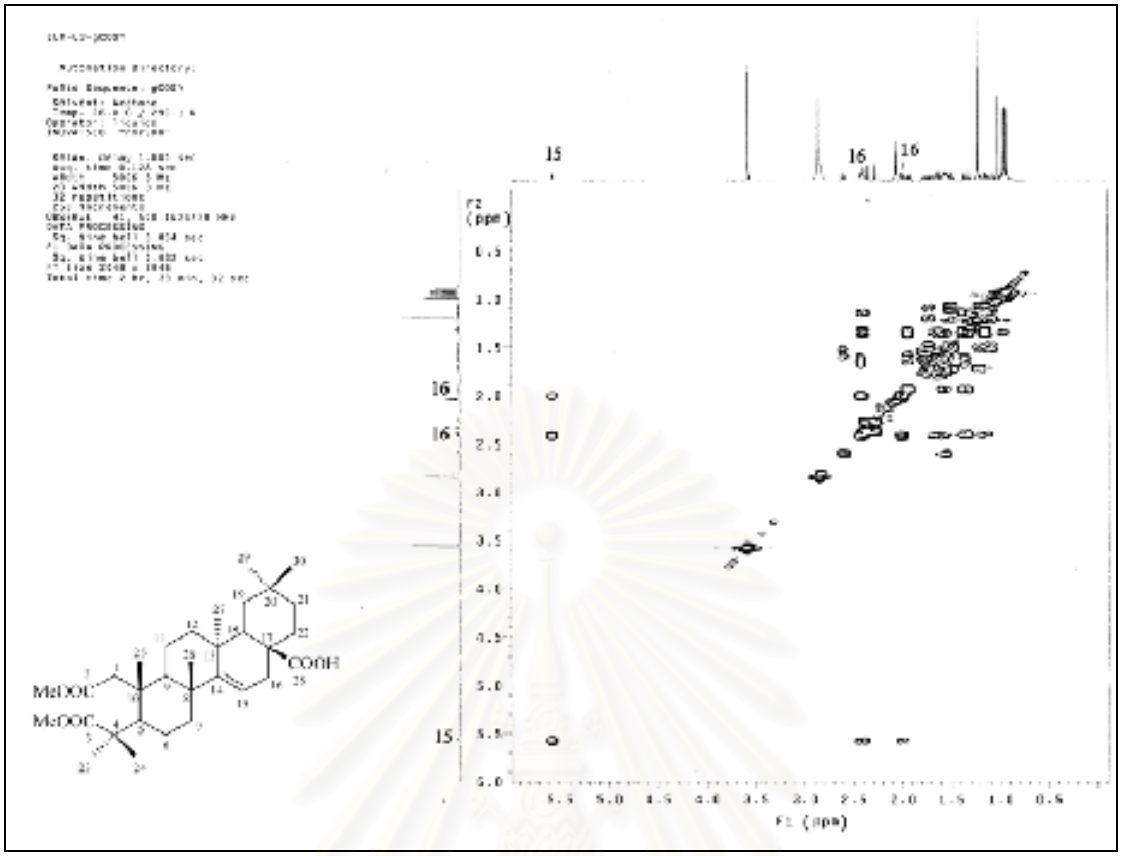

Figure 158a. ^{1}H-^{1}H COSY Spectrum of compound ET-L3

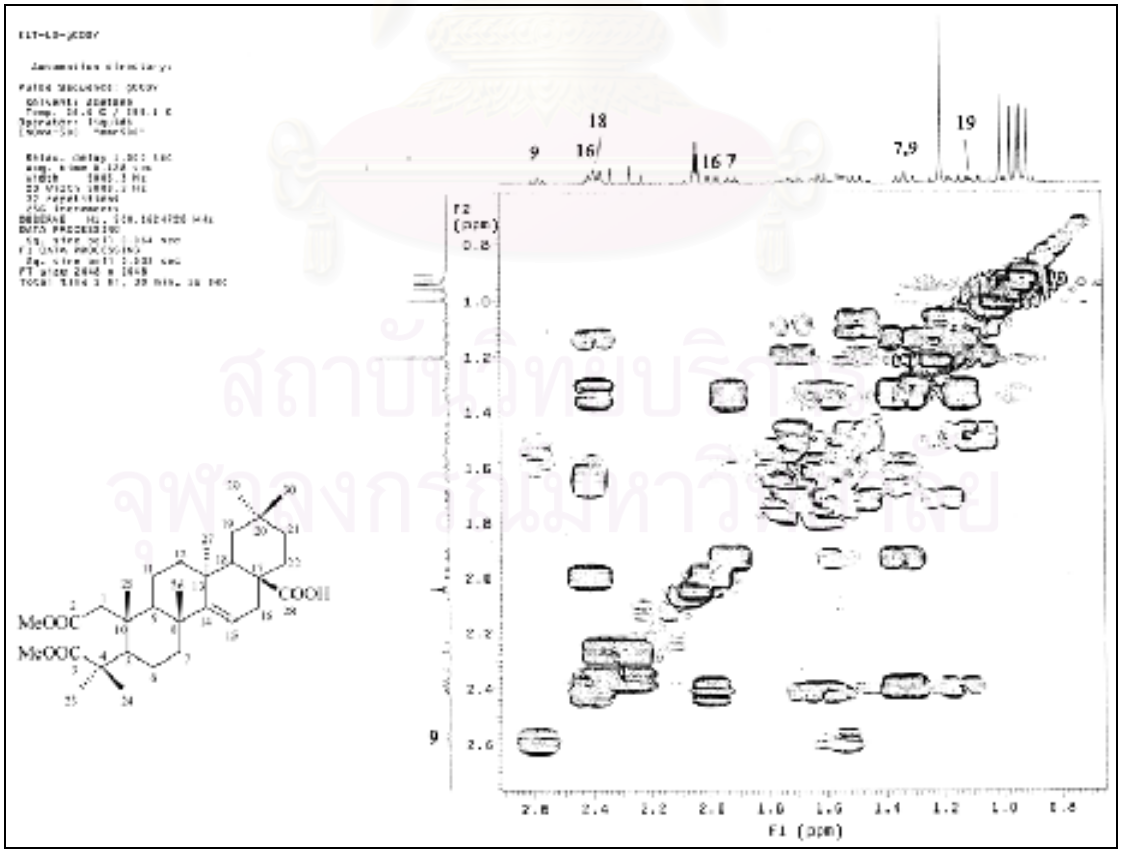

Figure 158b. ^{1}H-^{1}H COSY Spectrum of compound ET-L3 (δ_H 0.7-2.7 ppm)

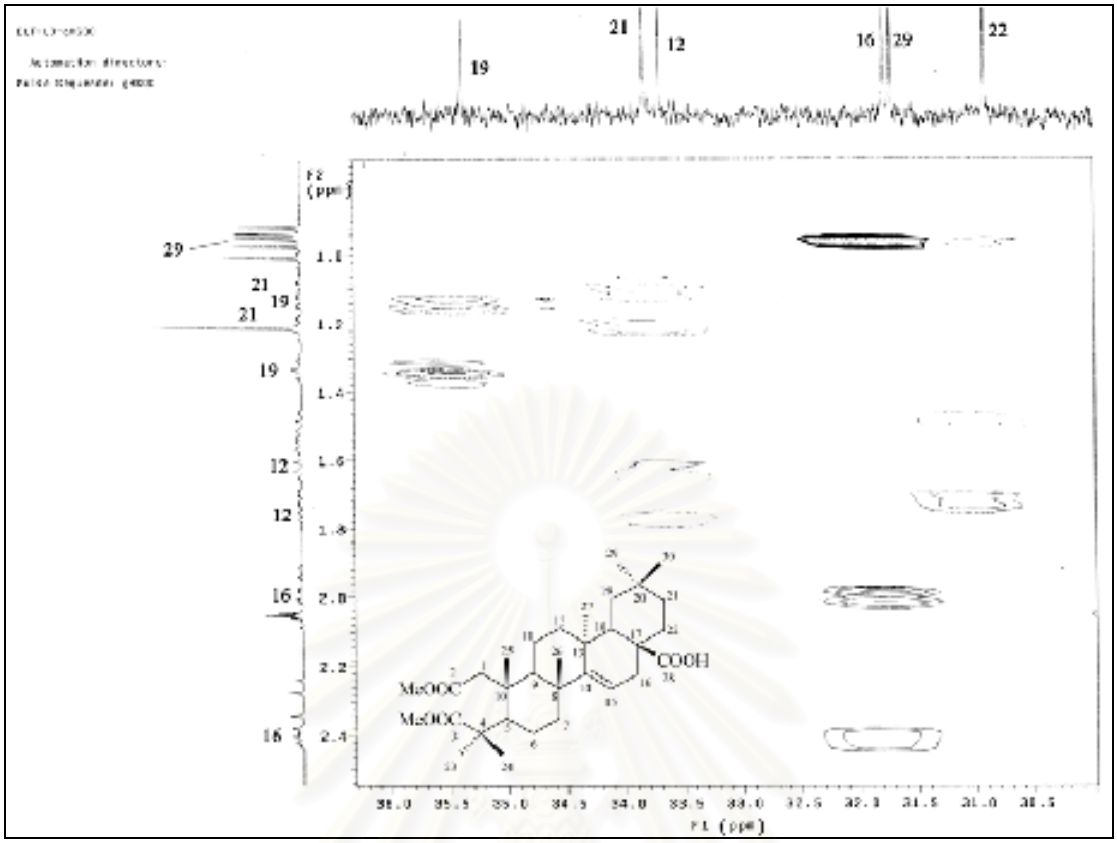

Figure 159a. HSQC Spectrum of compound ET-L3 (δ_H 0.8-2.5 ppm, δ_C 30-36 ppm)

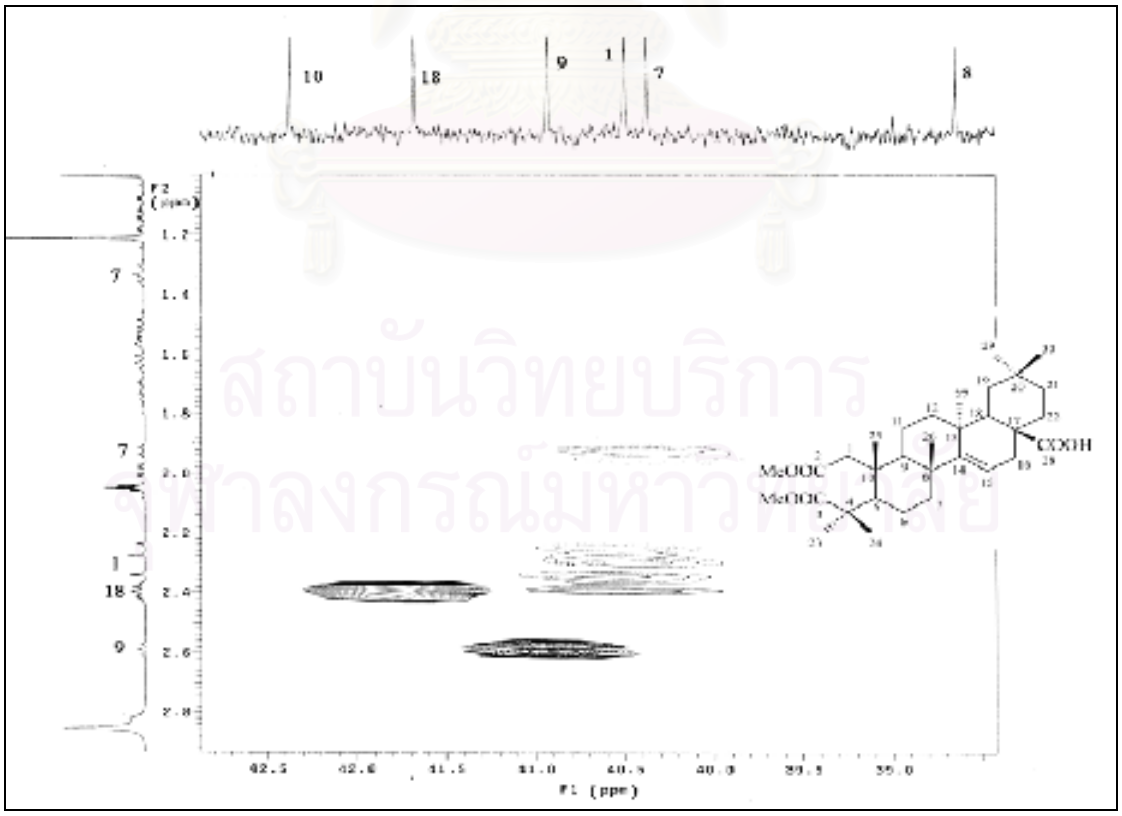

Figure 159b. HSQC Spectrum of compound ET-L3 (δ_H 1.0-2.9 ppm, δ_C 38-43 ppm)

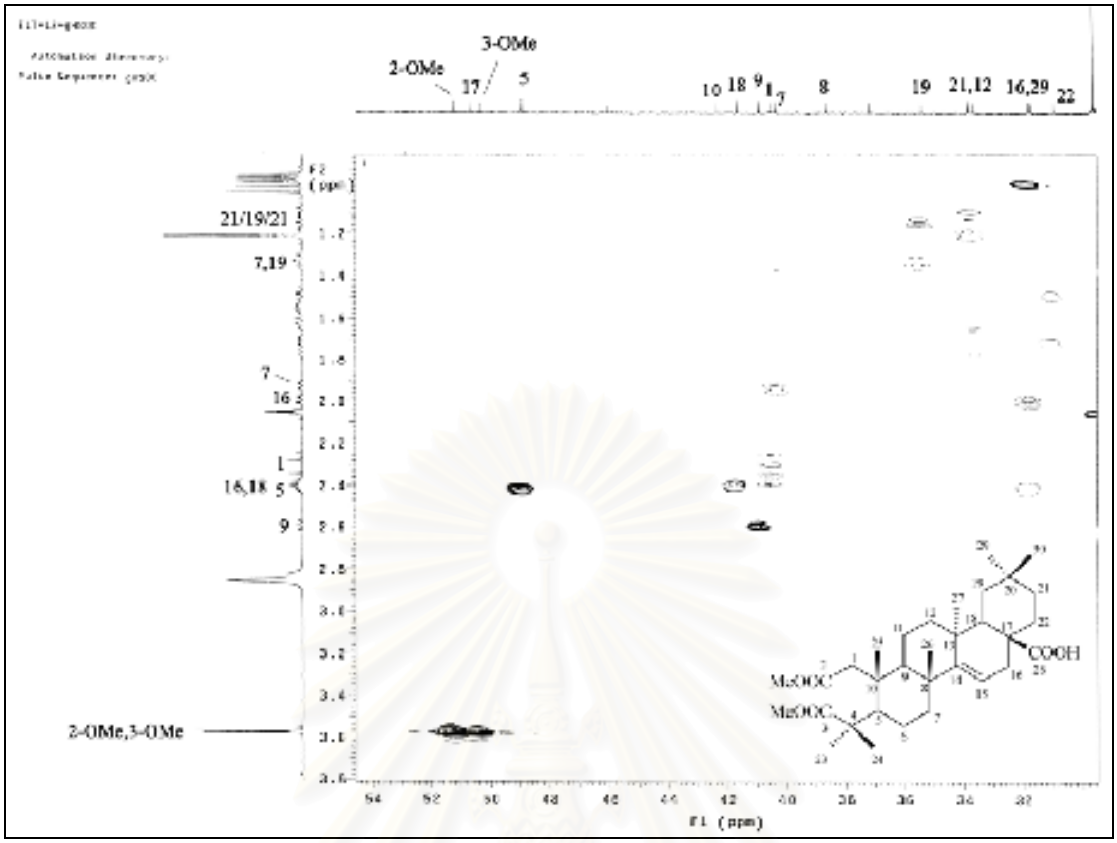

Figure 159c. HSQC Spectrum of compound ET-L3 (δ_H 0.9-3.8 ppm, δ_C 30-54 ppm)

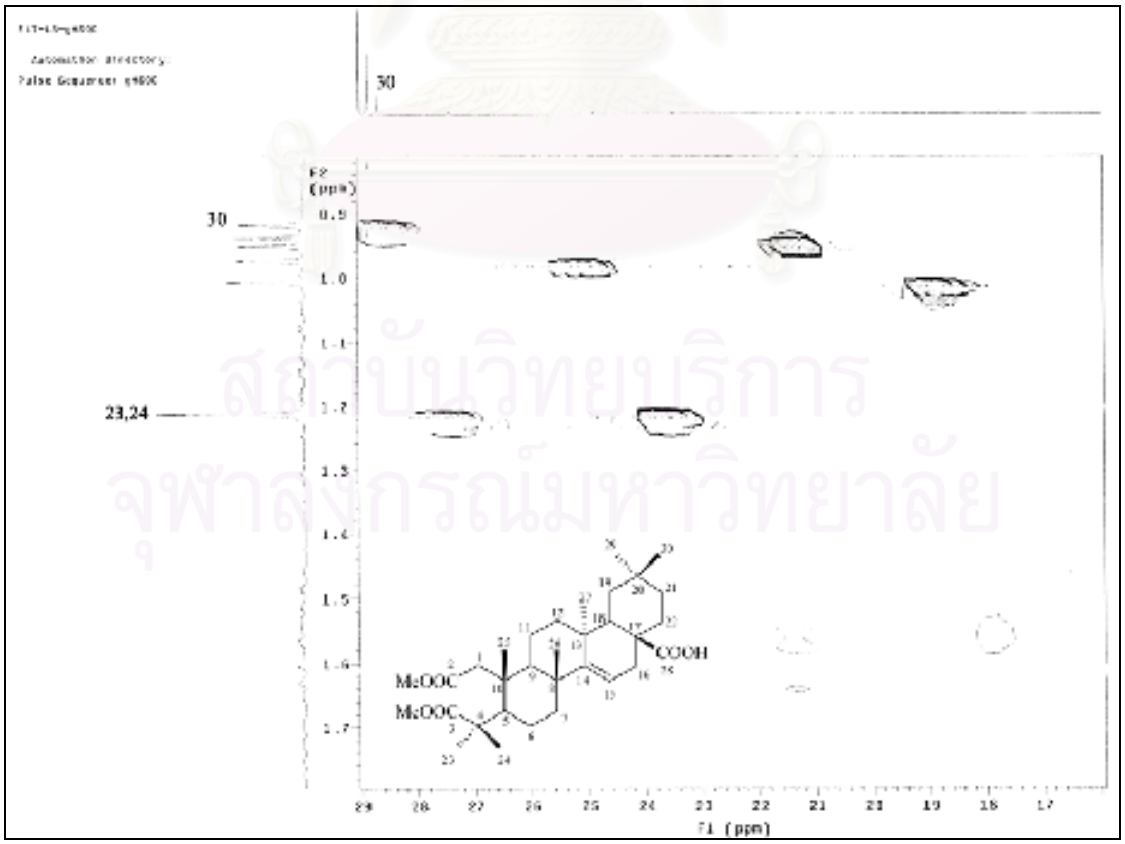

Figure 159d. HSQC Spectrum of compound ET-L3 (δ_H 0.8-1.8 ppm, δ_C 16-29 ppm)

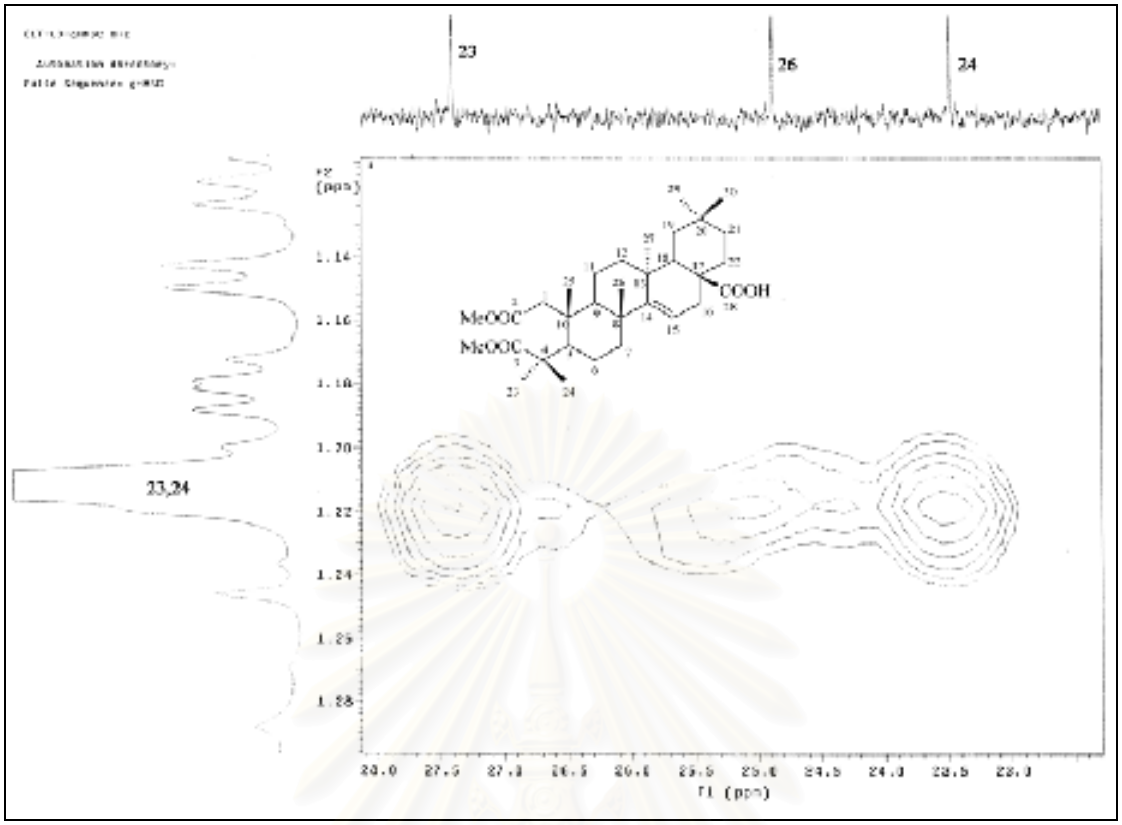

Figure 160a. HMBC Spectrum of compound ET-L3
(δ_H 1.12-1.30 ppm, δ_C 22.5-28 ppm)

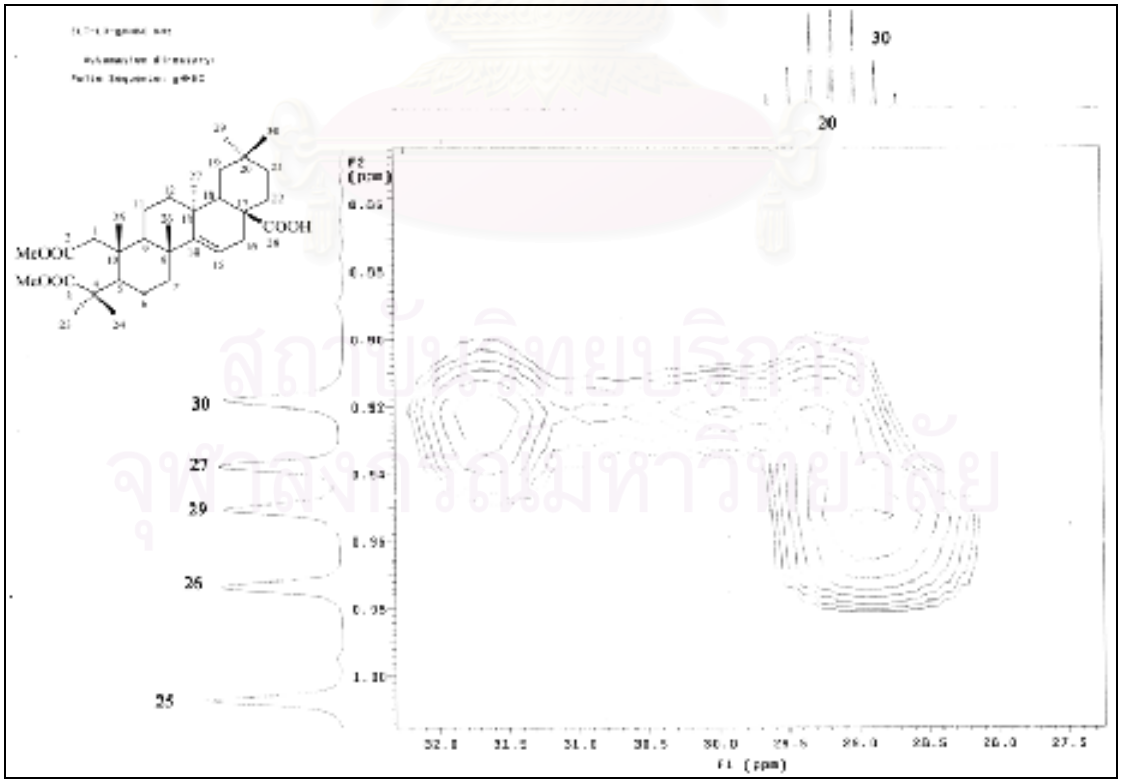

Figure 160b. HMBC Spectrum of compound ET-L3
(δ_H 0.84-1.02 ppm, δ_C 27.5-32.5 ppm)

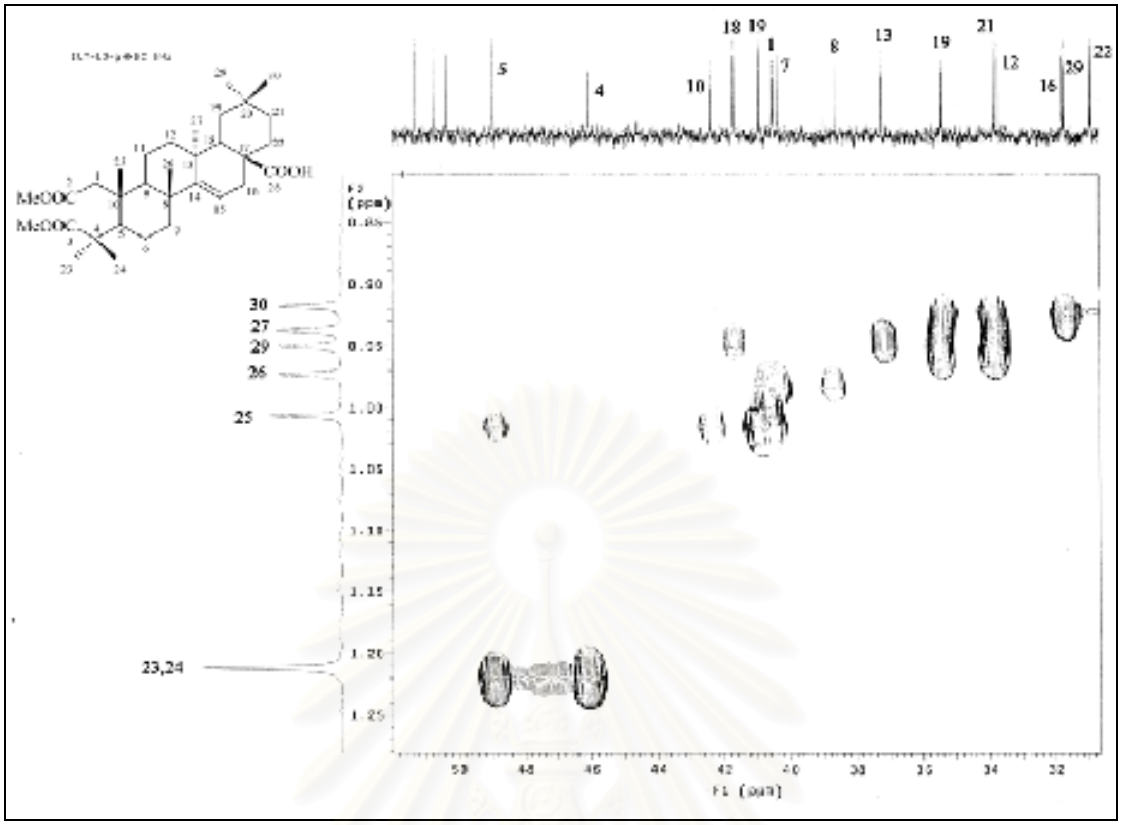

Figure 160c. HMBC Spectrum of compound ET-L3
(δ_H 0.80-1.28 ppm, δ_C 31-52 ppm)

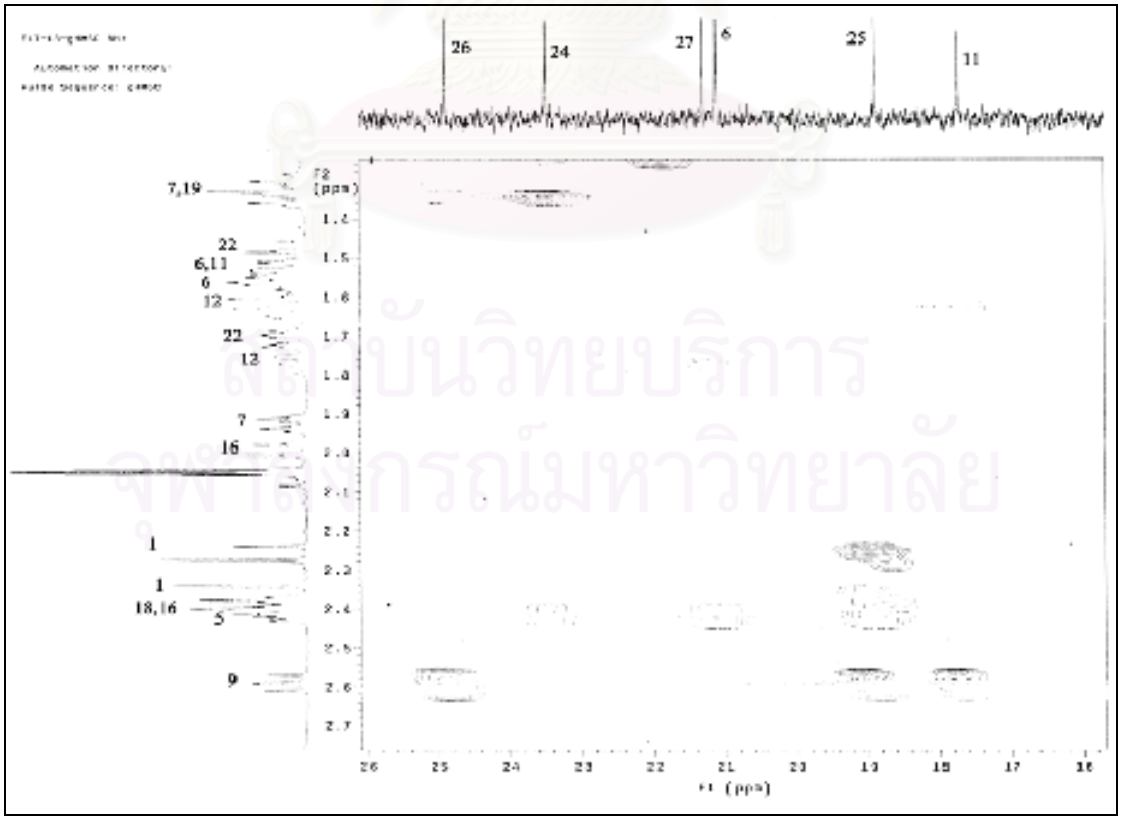

Figure 160d. HMBC Spectrum of compound ET-L3 (δ_H 1.2-2.7 ppm, δ_C 16-26 ppm)

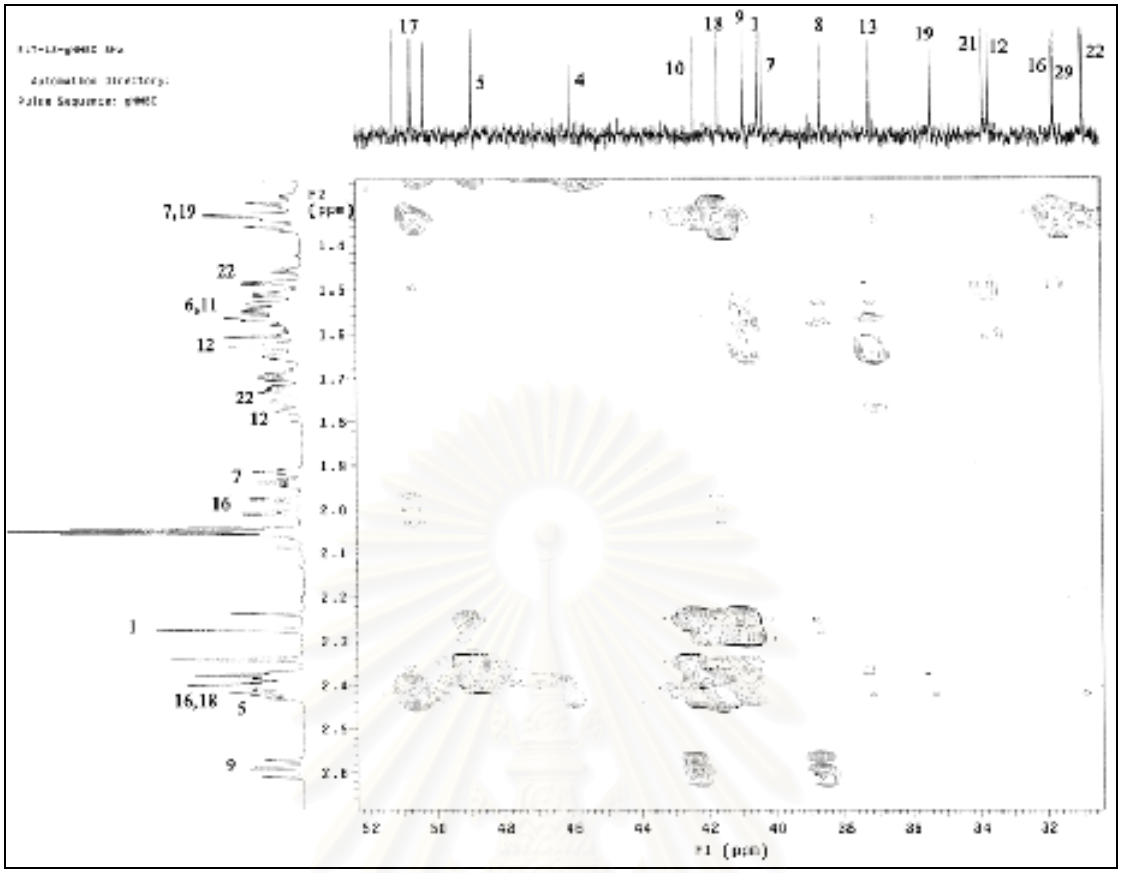

Figure 160e. HMBC Spectrum of compound ET-L3 (δ_H 1.2-2.7 ppm, δ_C 30-52 ppm)

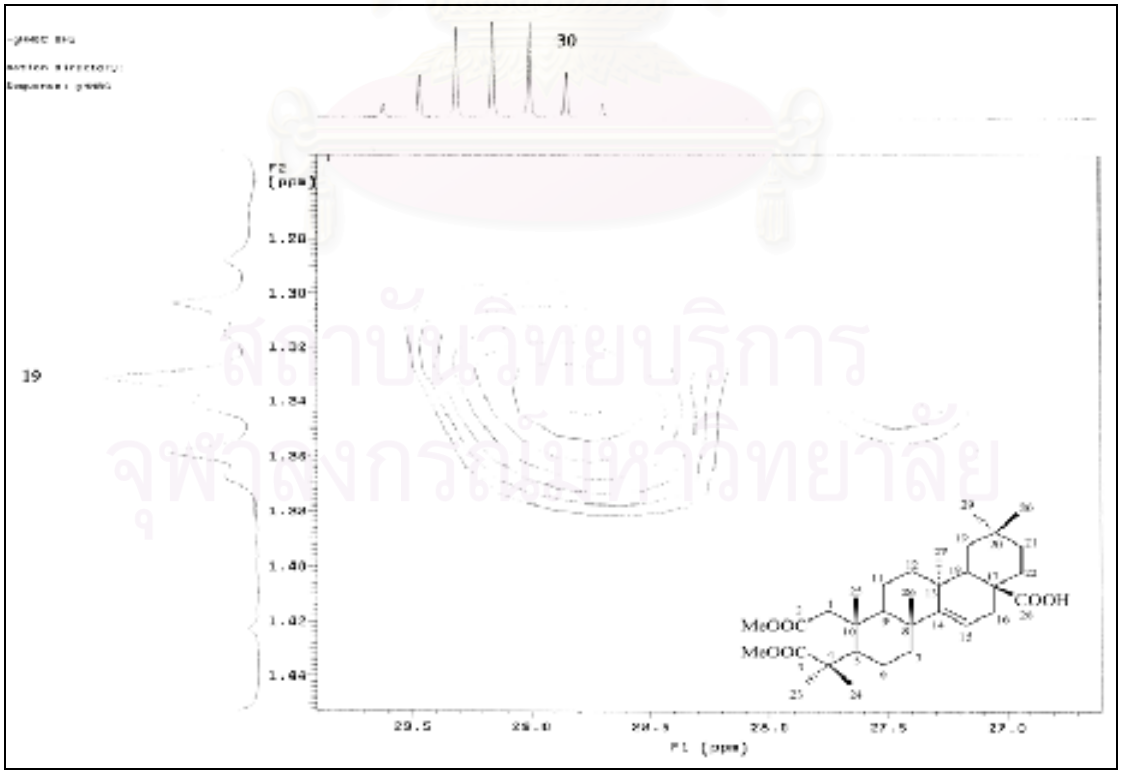

Figure 160f. HMBC Spectrum of compound ET-L3
(δ_H 1.26-1.44 ppm, δ_C 26.5-30 ppm)

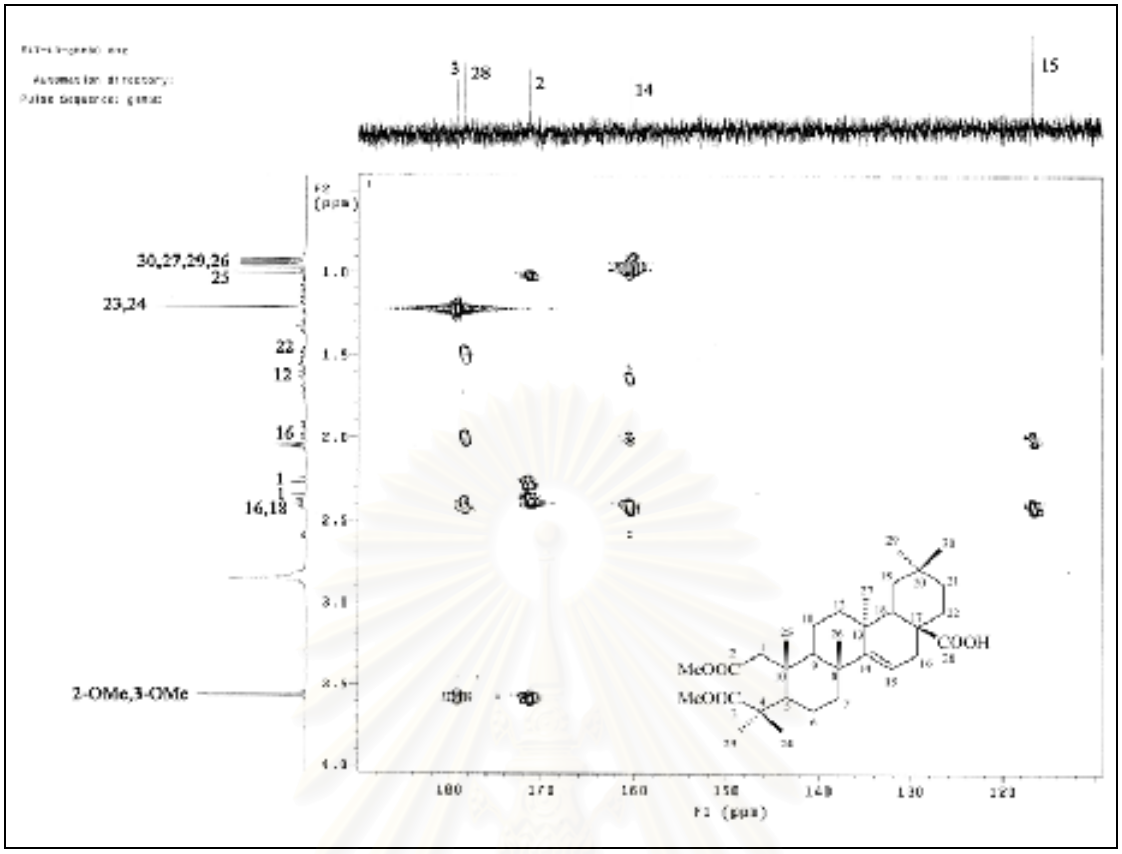

Figure 160g. HMBC Spectrum of compound ET-L3
(δ_H 0.5-4.0 ppm, δ_C 110-190 ppm)

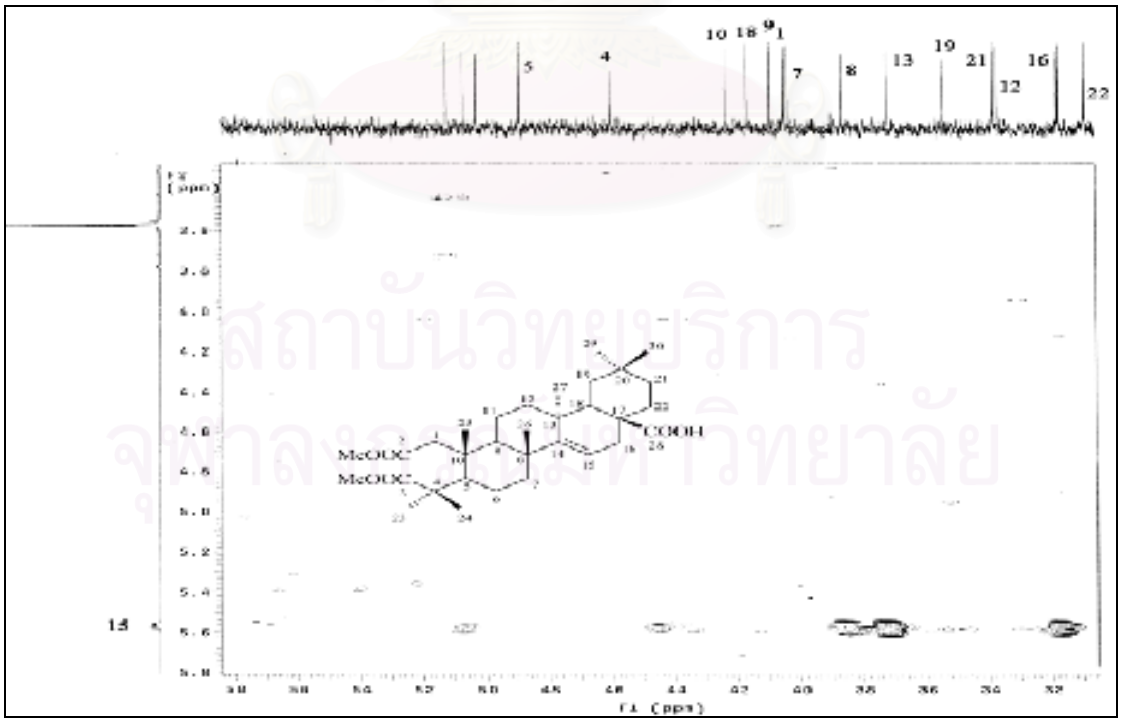

Figure 160h. HMBC Spectrum of compound ET-L3
(δ_H 3.2-5.8 ppm, δ_C 30-58 ppm)

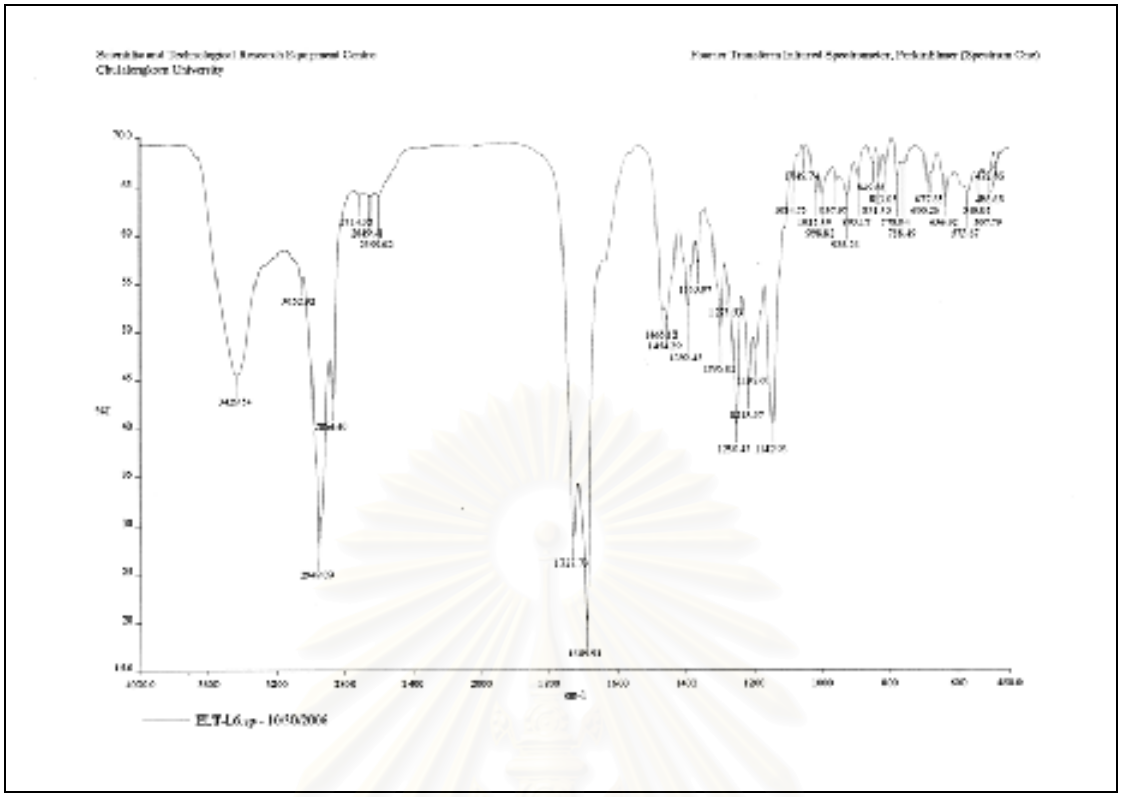

Figure 161. IR Spectrum of compound ET-L5 (KBr disc)

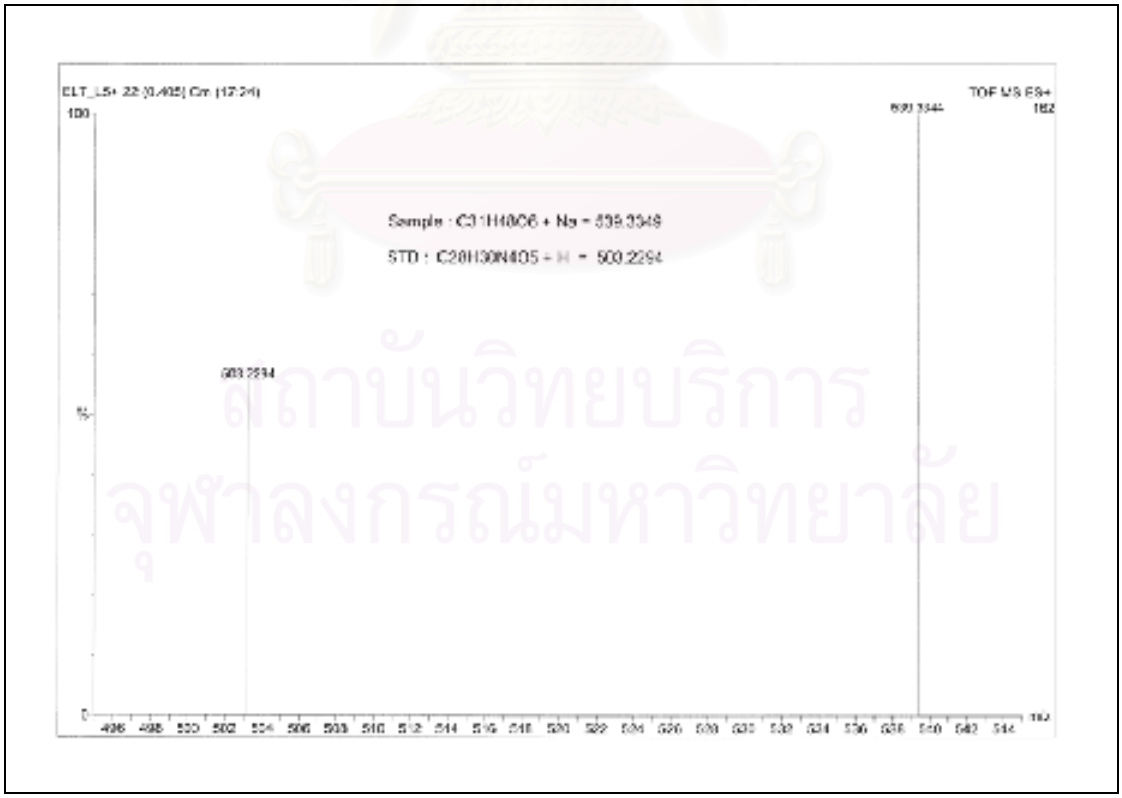

Figure 162. HR ESI Mass spectrum of compound ET-L5

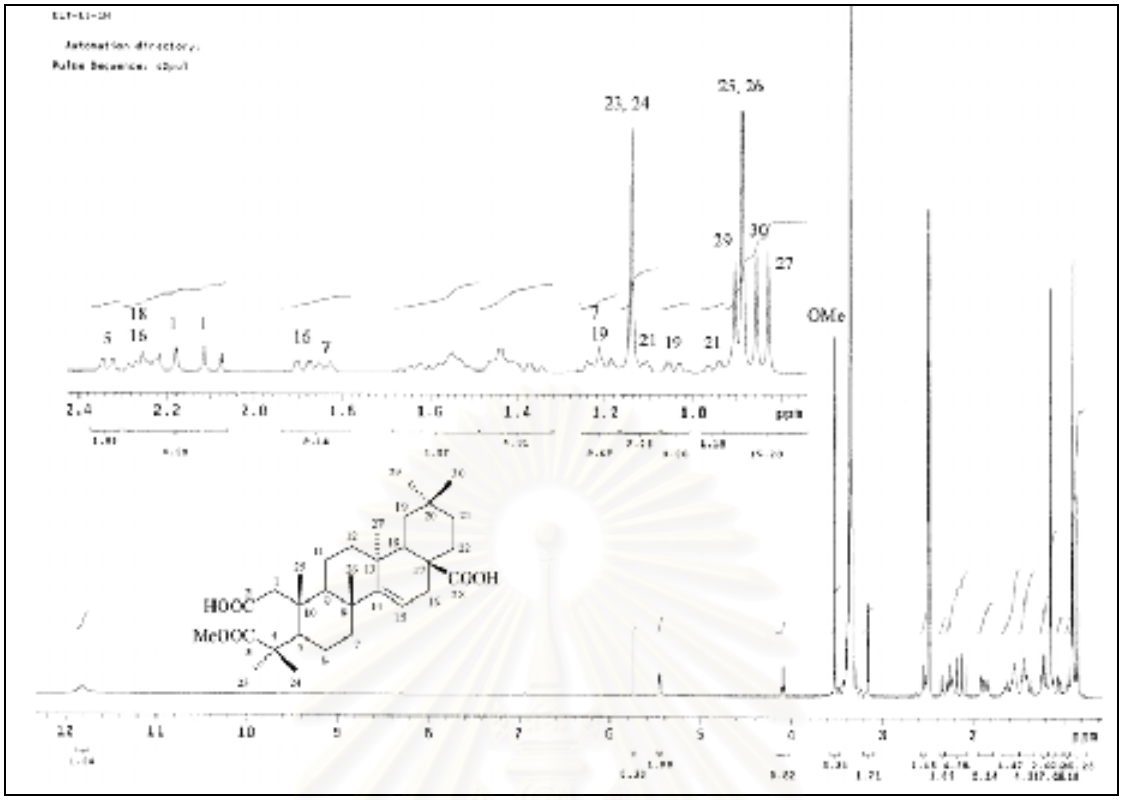

Figure 163a. ^{1}H NMR (500 MHz) Spectrum of compound ET-L5 (in DMSO-d_6)

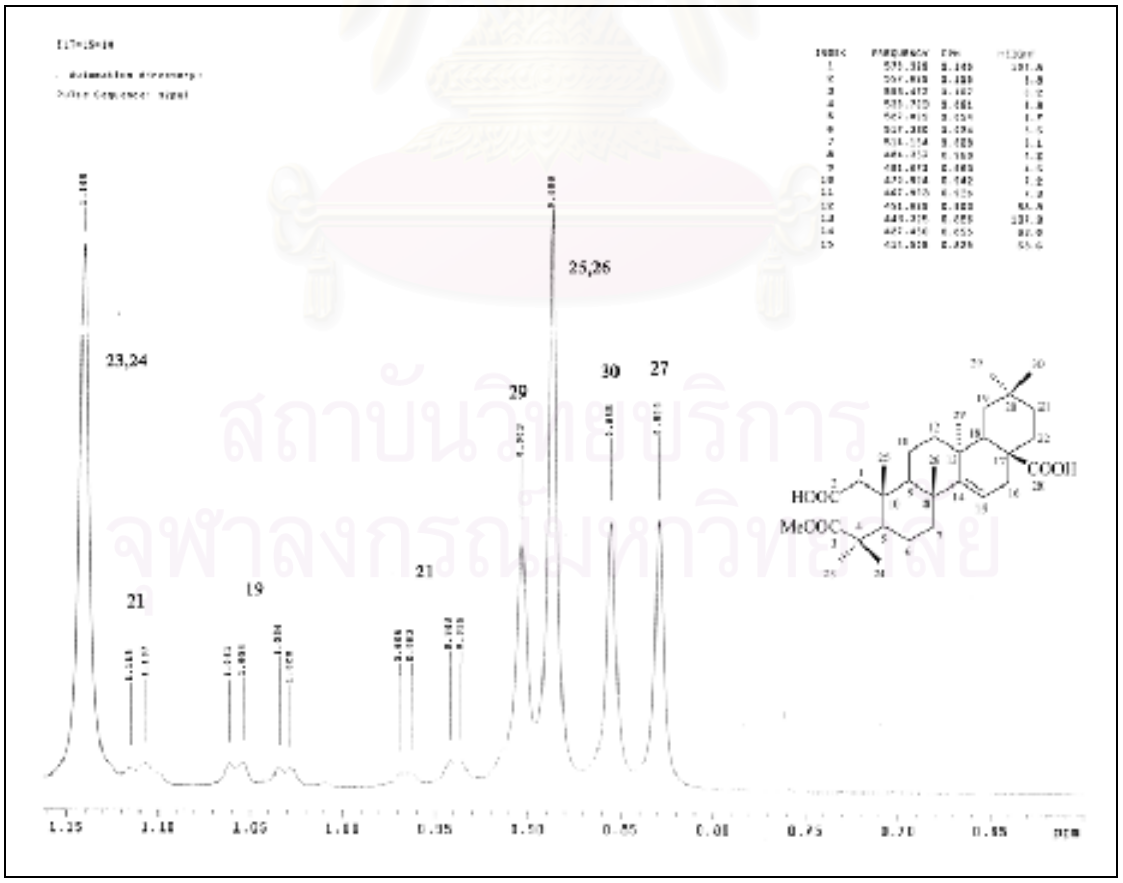

Figure 163b. ^{1}H NMR (500 MHz) Spectrum of compound ET-L5 (δ_H 0.60-1.16 ppm)

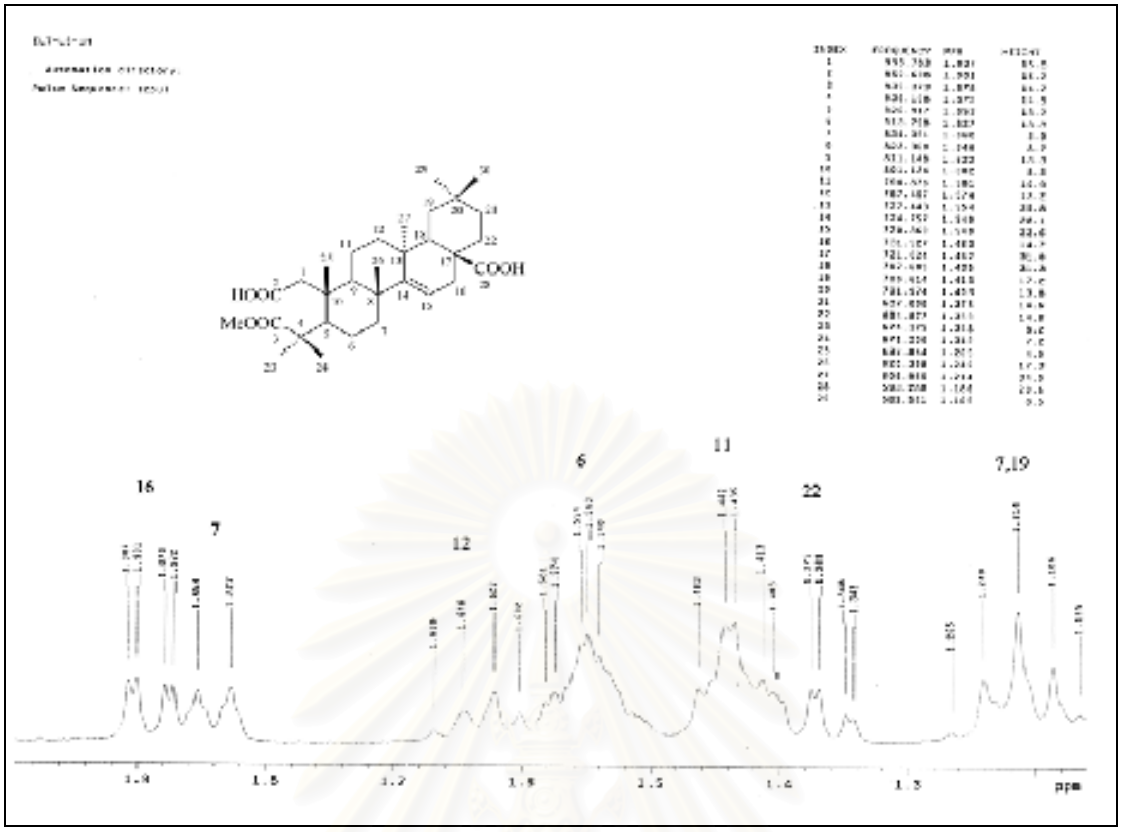

Figure 163c. ^{1}H NMR (500 MHz) Spectrum of compound ET-L5 (δ_H 1.16-2.0 ppm)

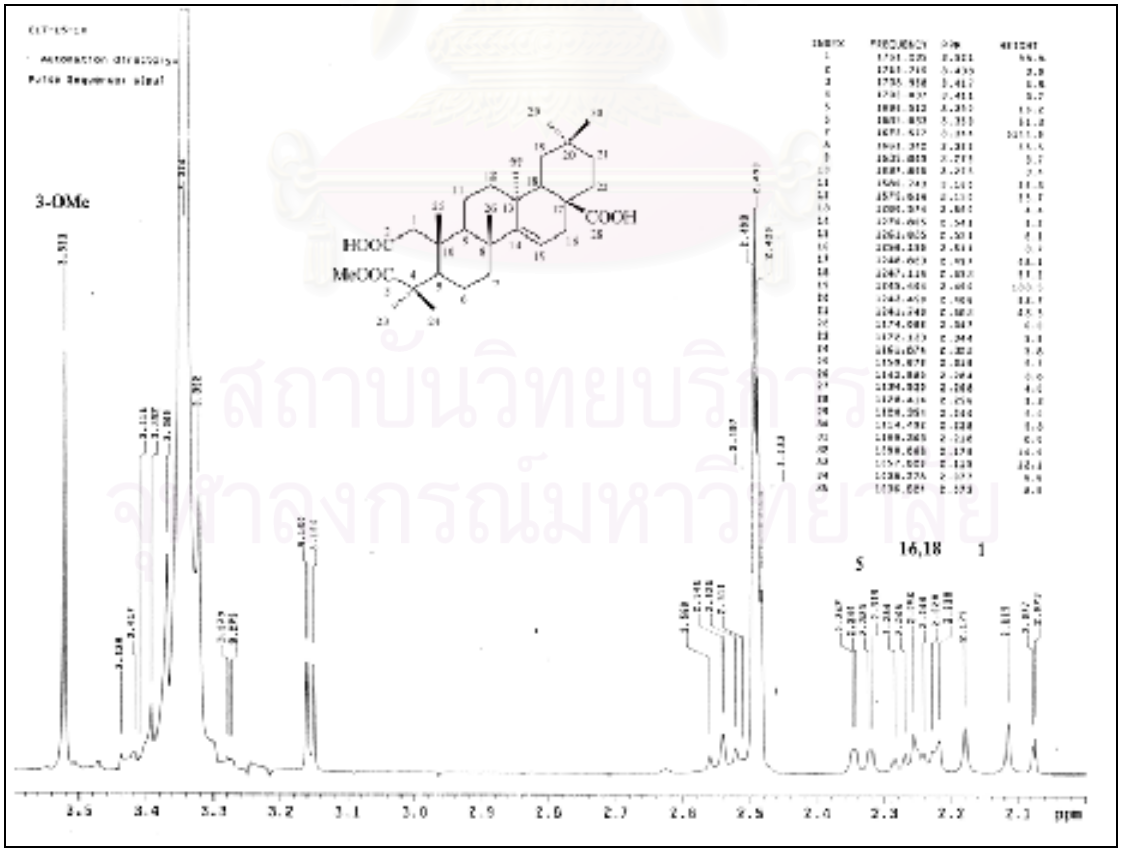

Figure 163d. ^{1}H NMR (500 MHz) Spectrum of compound ET-L5 (δ_H 2.0-3.6 ppm)

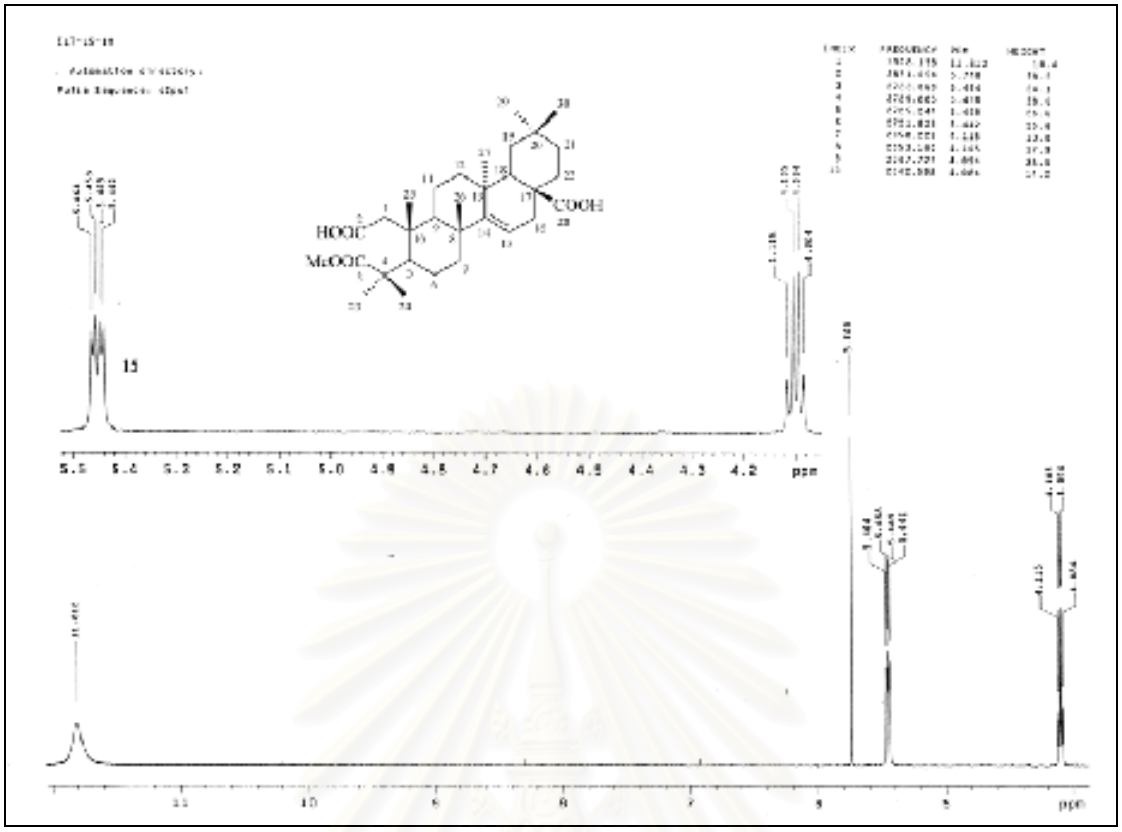

Figure 163e. ^{1}H NMR (500 MHz) Spectrum of compound ET-L5 (δ_H 4-12 ppm)

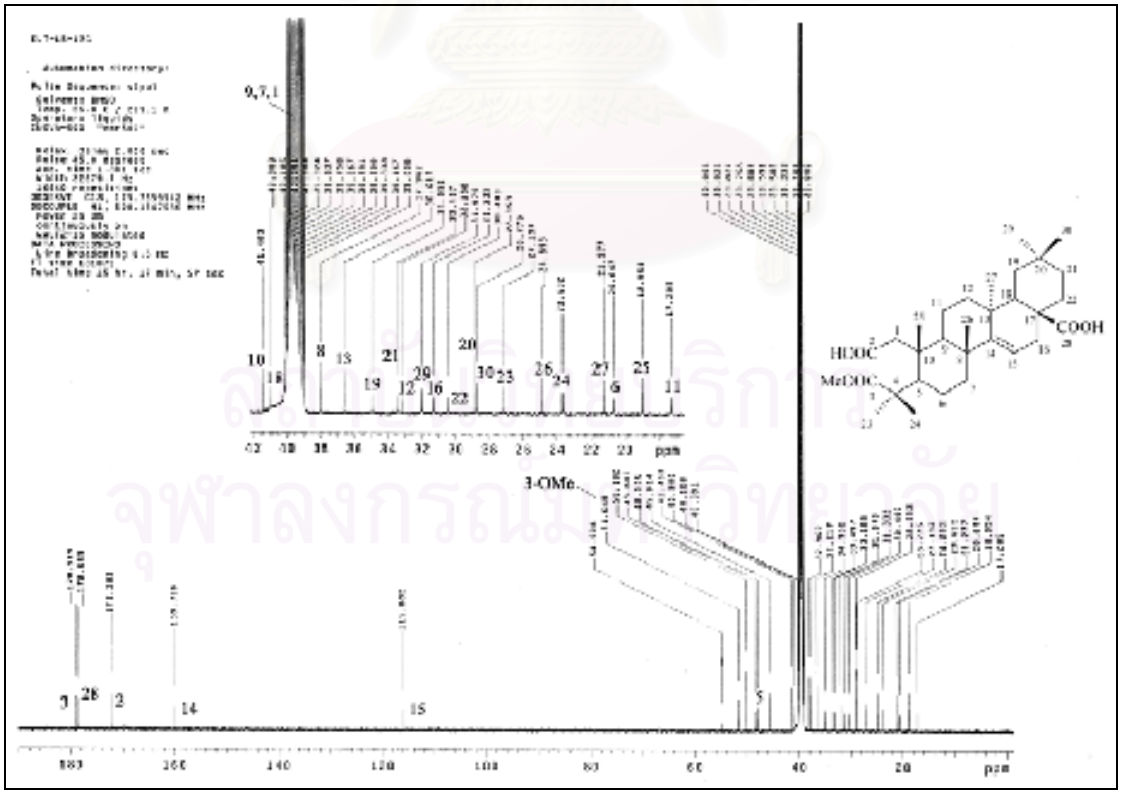

Figure 164. ^{13}C NMR (125 MHz) Spectrum of compound ET-L5 (in DMSO-d_6)

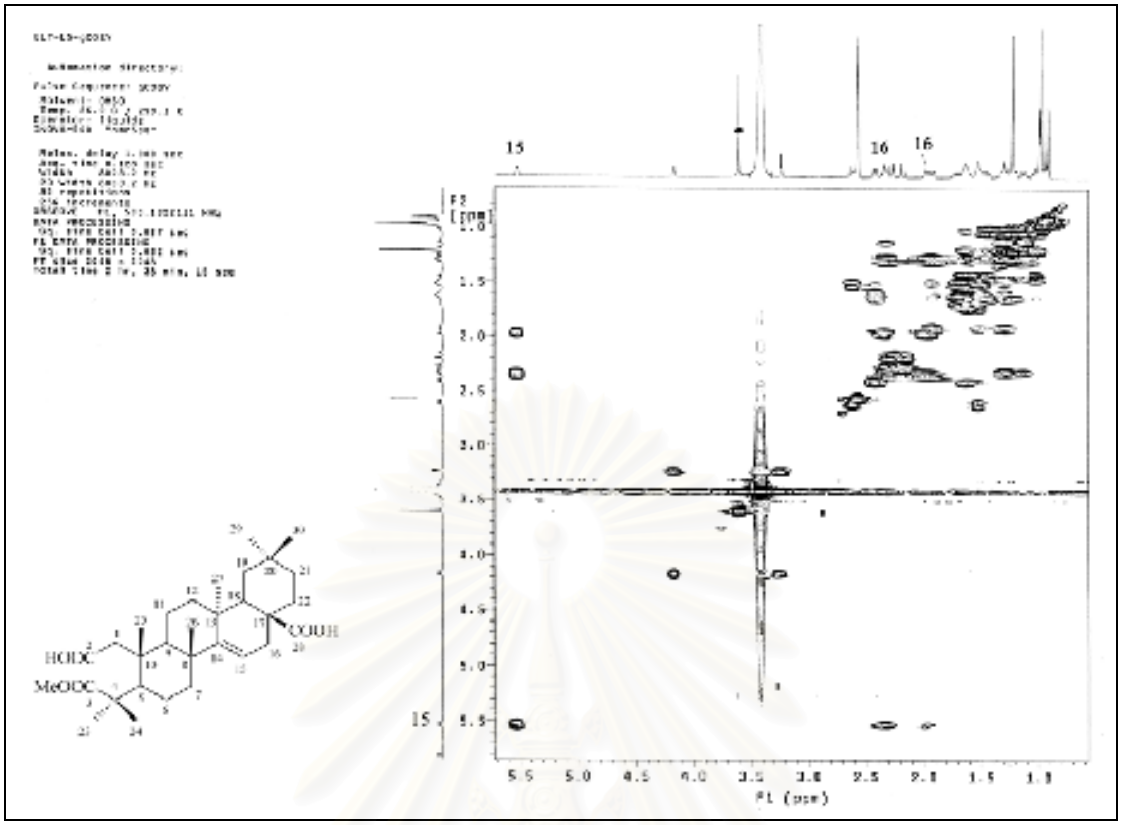

Figure 165. ^{1}H-^{1}H COSY Spectrum of compound ET-L5

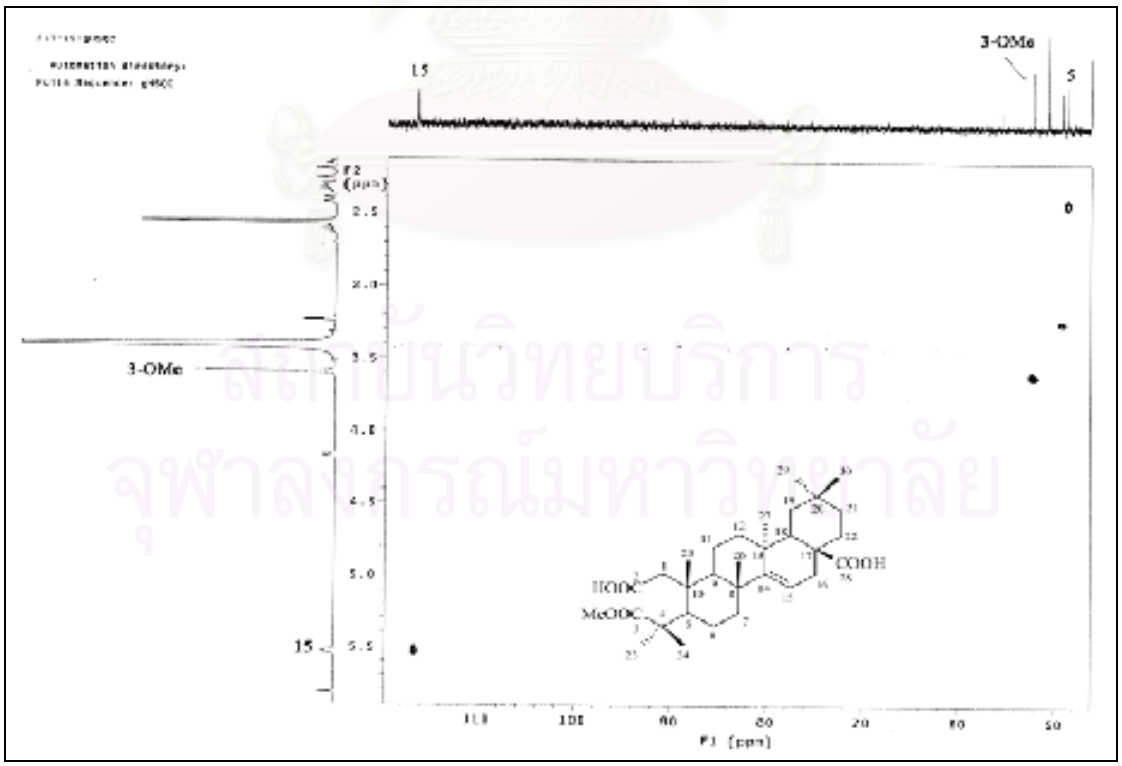

Figure 166a. HSQC Spectrum of compound ET-L5
(δ_H 2.0-6.0 ppm, δ_C 46-120 ppm)

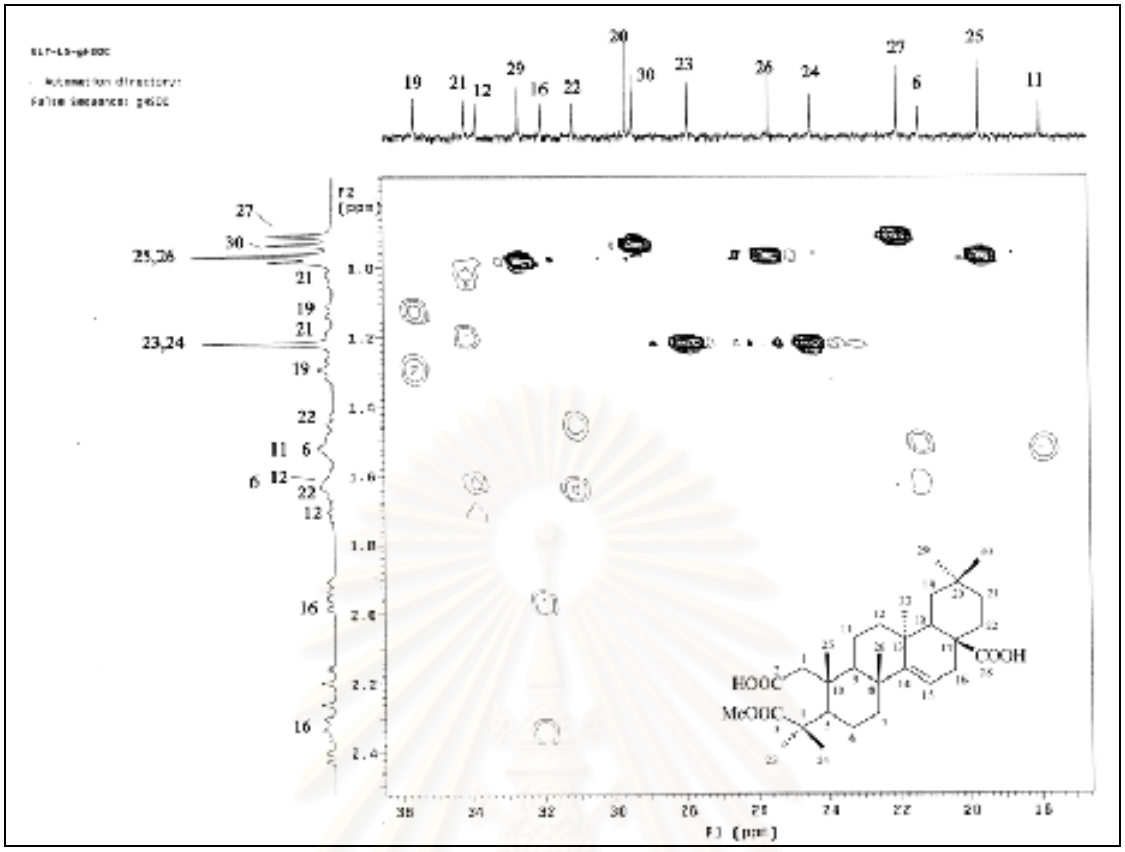

Figure 166b. HSQC Spectrum of compound ET-L5 (δ_H 0.6-2.6 ppm, δ_C 16-36 ppm)

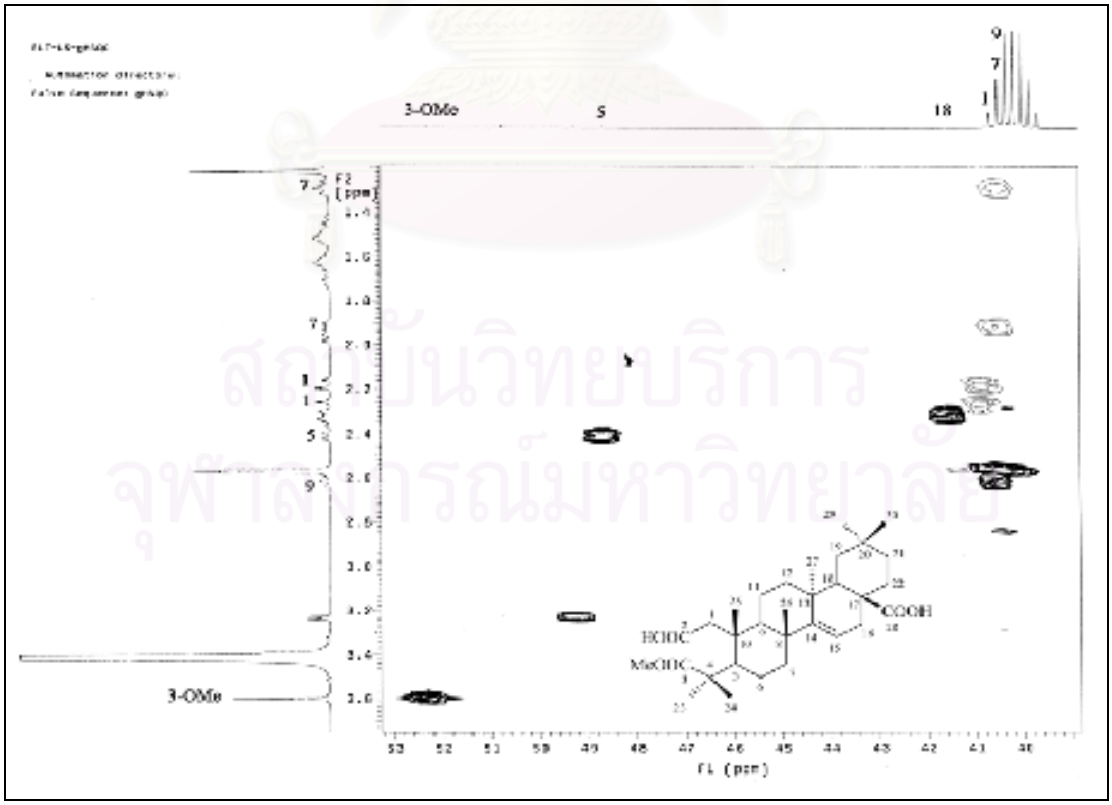

Figure 166c. HSQC Spectrum of compound ET-L5 (δ_H 1.2-3.6 ppm, δ_C 39-53 ppm)

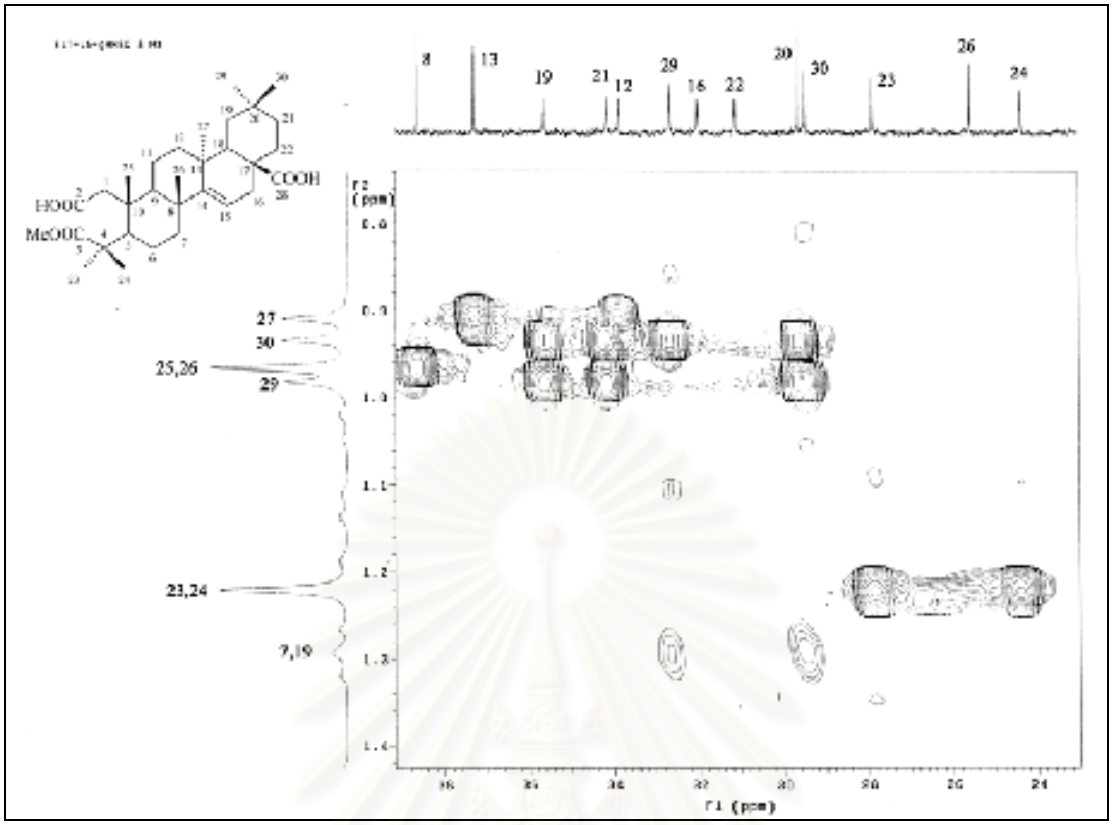

Figure 167a. HMBC Spectrum of compound ET-L5 (δ_H 0.8-1.4 ppm, δ_C 23-39 ppm)

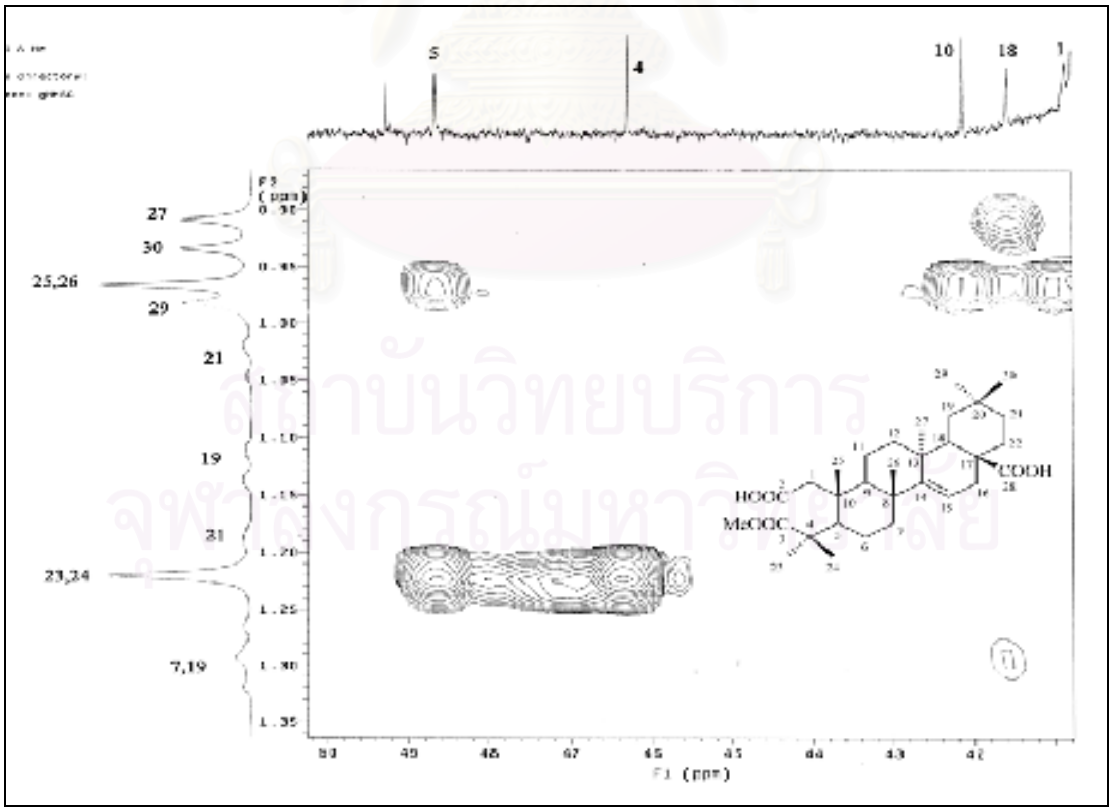

Figure 167b. HMBC Spectrum of compound ET-L5
(δ_H 0.85-1.35 ppm, δ_C 41-50 ppm)

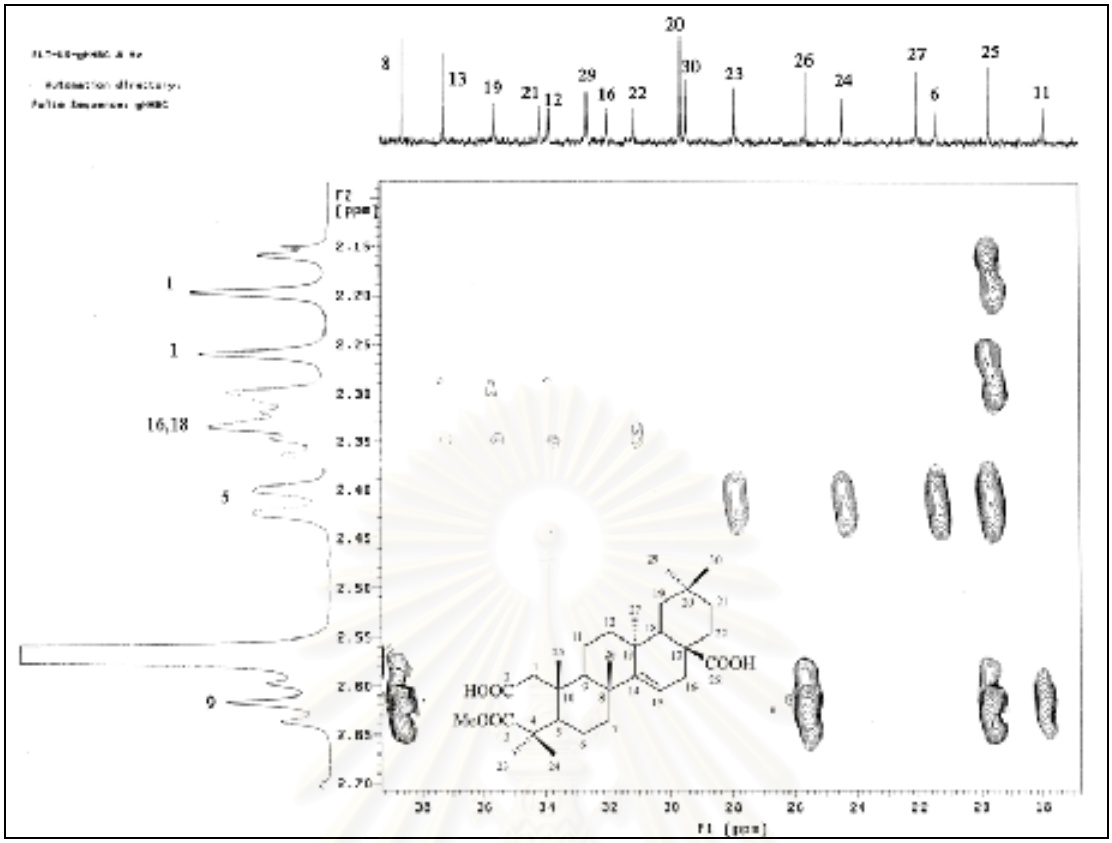

Figure 167c. HMBC Spectrum of compound ET-L5
(δ_H 2.10-2.70 ppm, δ_C 17-39 ppm)

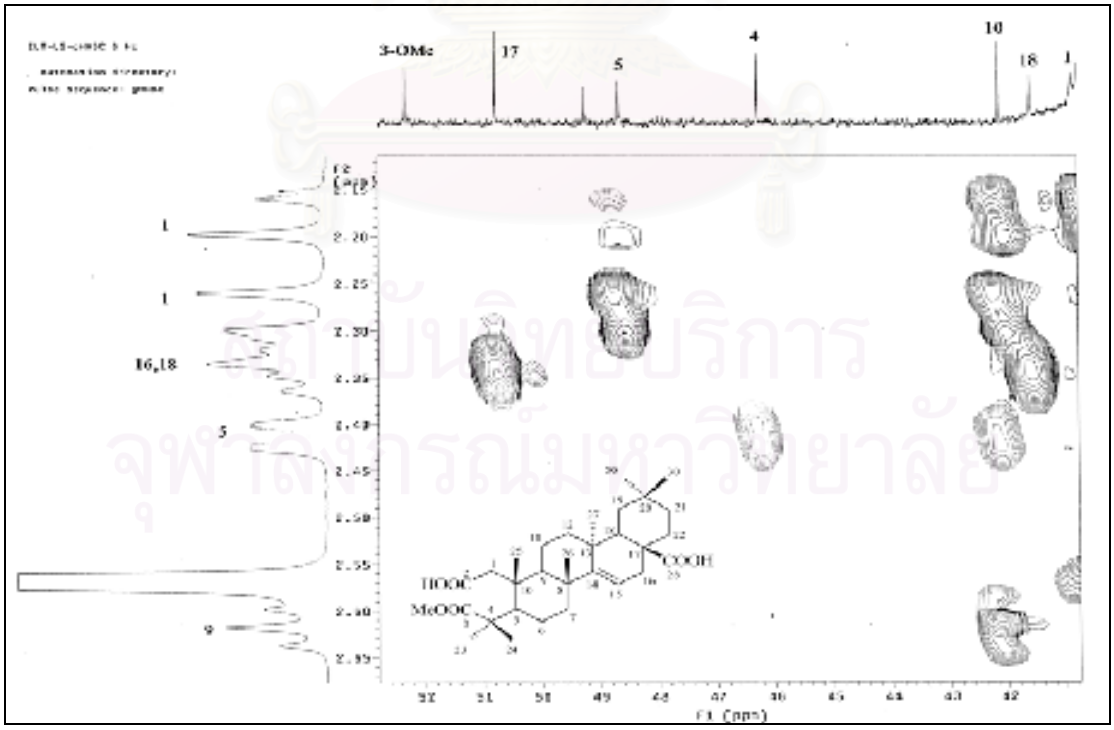

Figure 167d. HMBC Spectrum of compound ET-L5
(δ_H 2.10-2.65 ppm, δ_C 41-53 ppm)

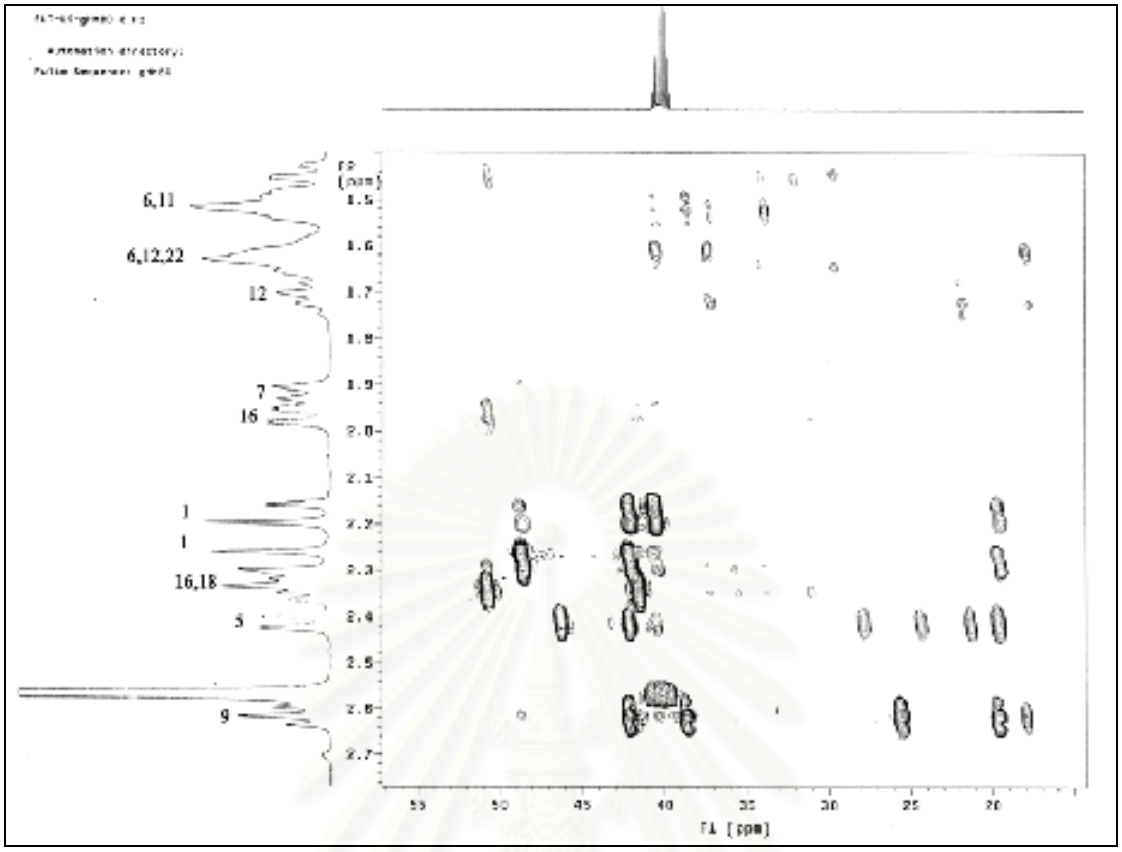

Figure 167e. HMBC Spectrum of compound ET-L5
(δ_H 1.4-2.76 ppm, δ_C 15-57 ppm)

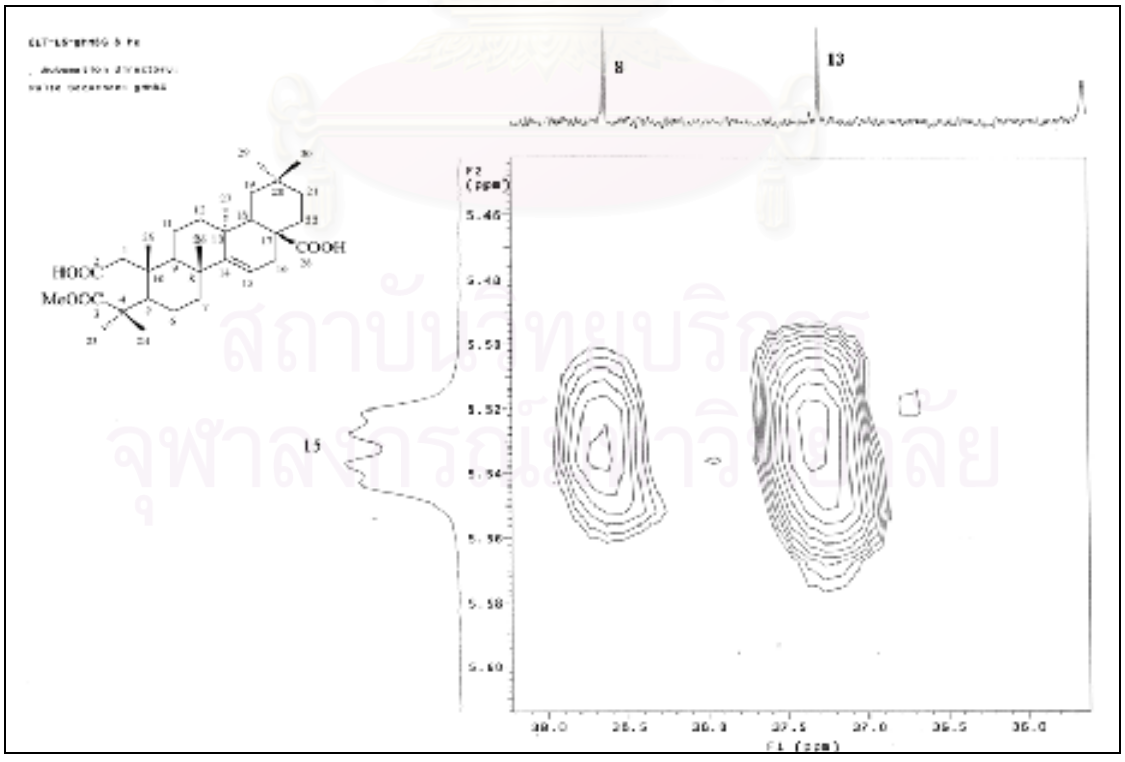

Figure 167f. HMBC Spectrum of compound ET-L5
(δ_H 5.44-5.62 ppm, δ_C 35.5-39.2 ppm)

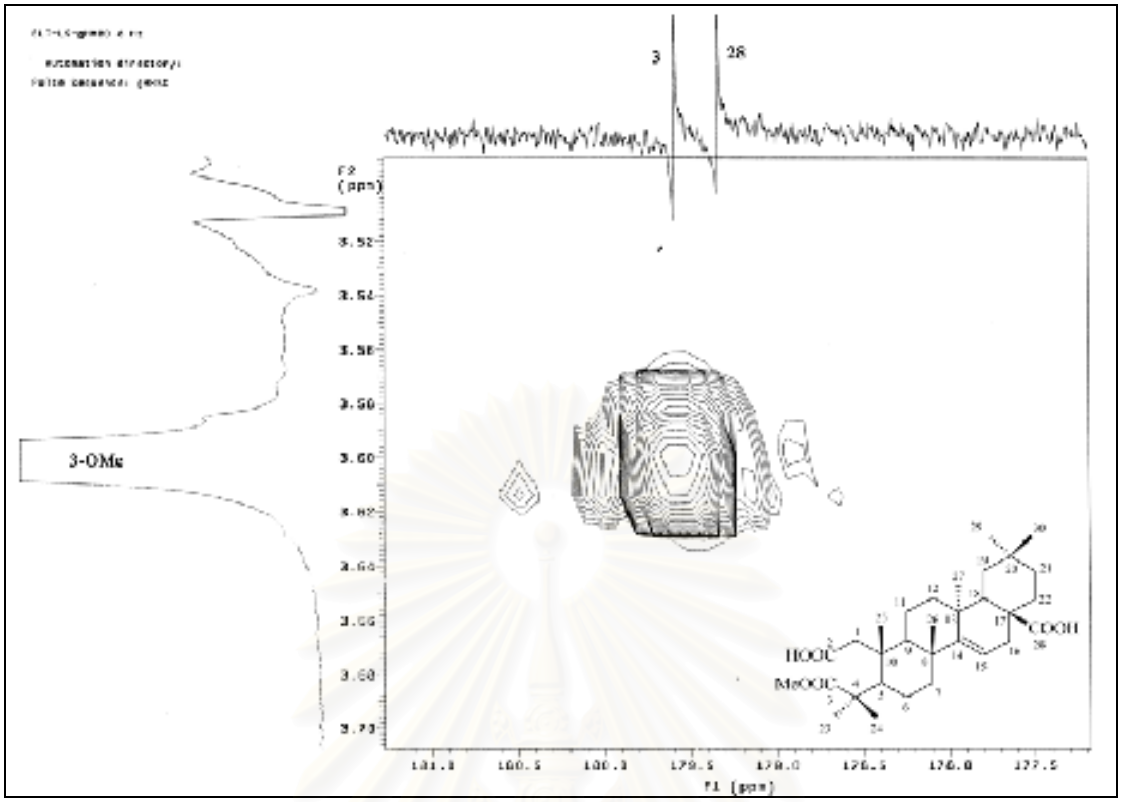

Figure 167g. HMBC Spectrum of compound ET-L5
(δ_H 3.50-3.75 ppm, δ_C 177.2-181.3 ppm)

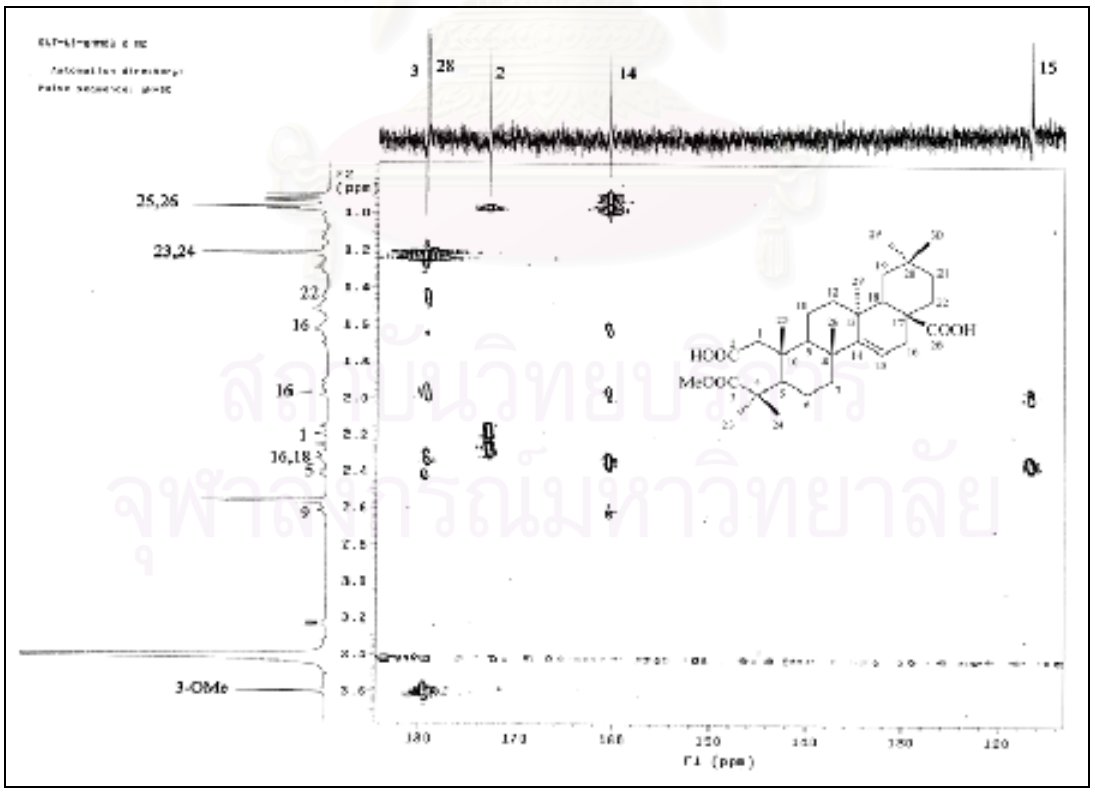

Figure 167h. HMBC Spectrum of compound ET-L5
(δ_H 0.8-3.8 ppm, δ_C 114-184 ppm)

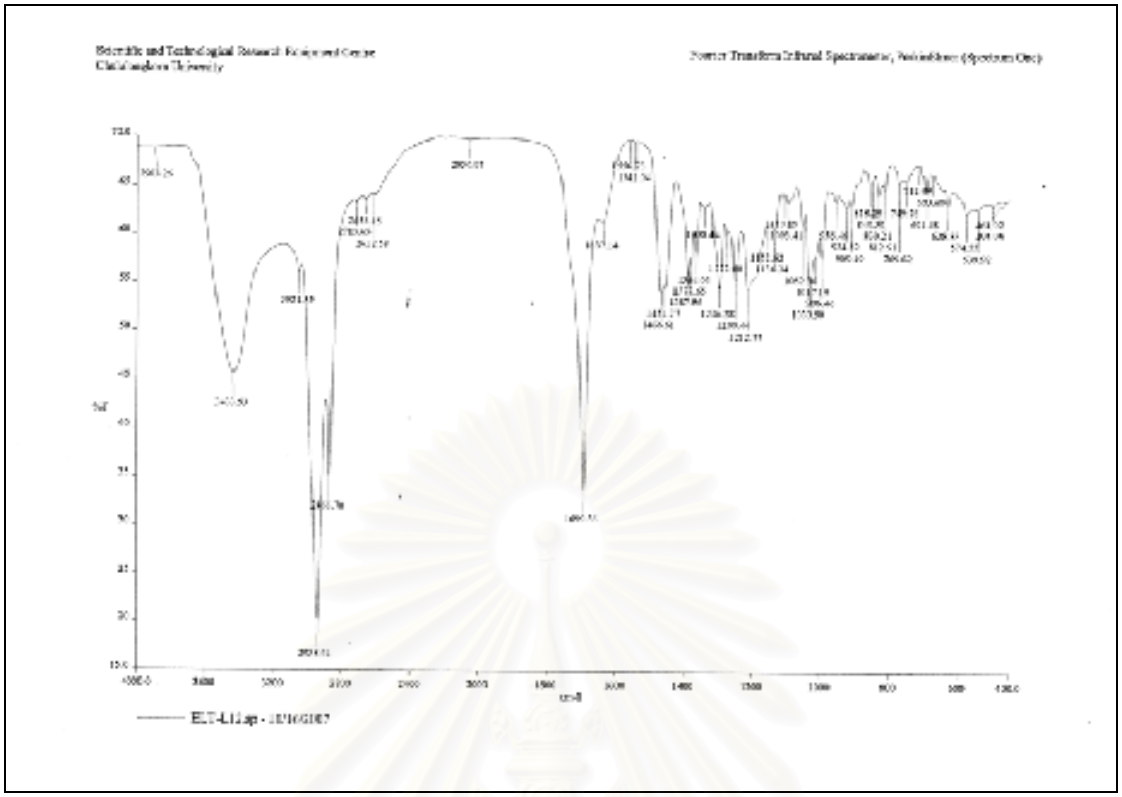

Figure 168. IR Spectrum of compound ET-L12 (KBr disc)

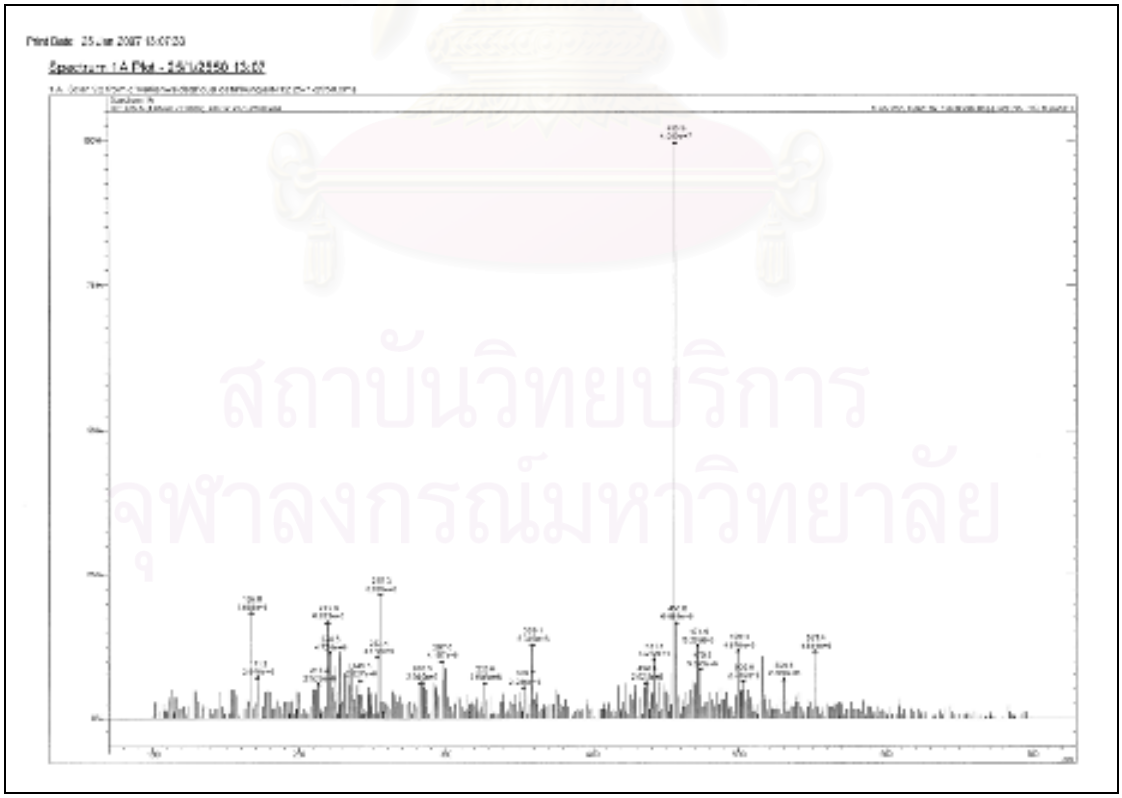

Figure 169. ESI Mass spectrum of compound ET-L12

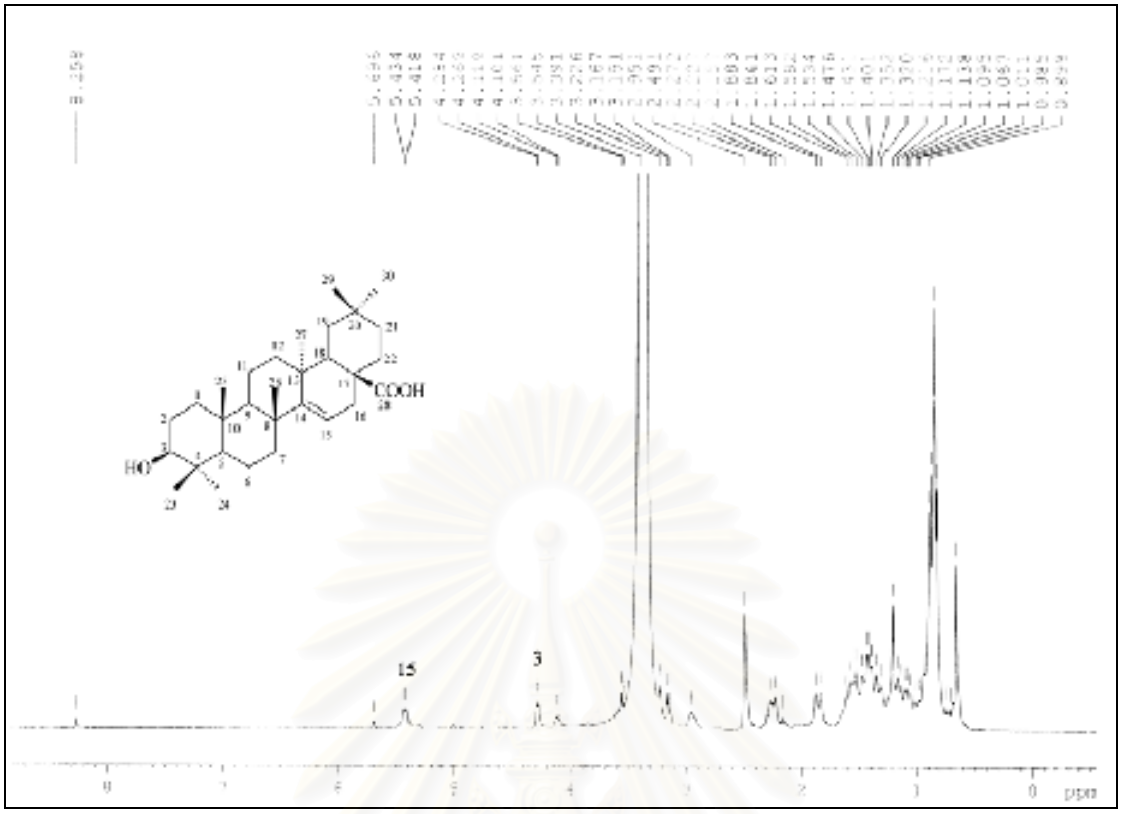

Figure 170. ^{1}H NMR (300 MHz) Spectrum of compound ET-L12 (in DMSO-d_6)

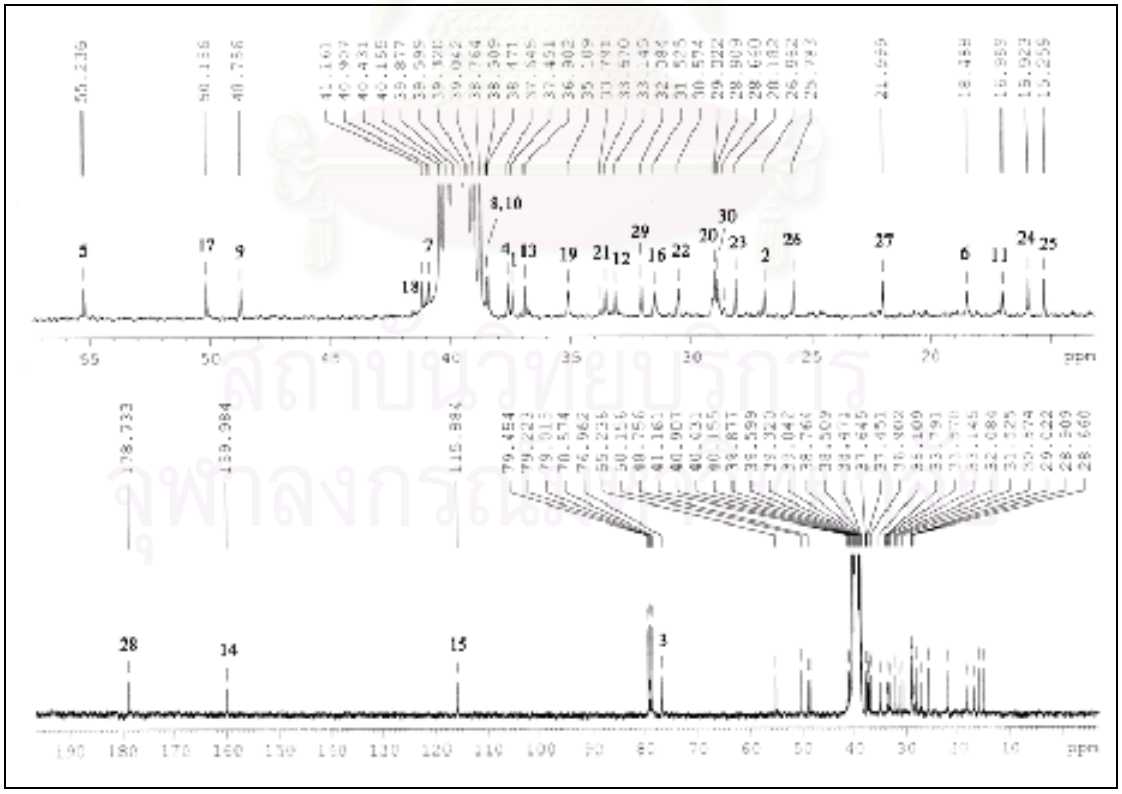

Figure 171. ^{13}C NMR (75 MHz) Spectrum of compound ET-L12 (in DMSO-d_6)

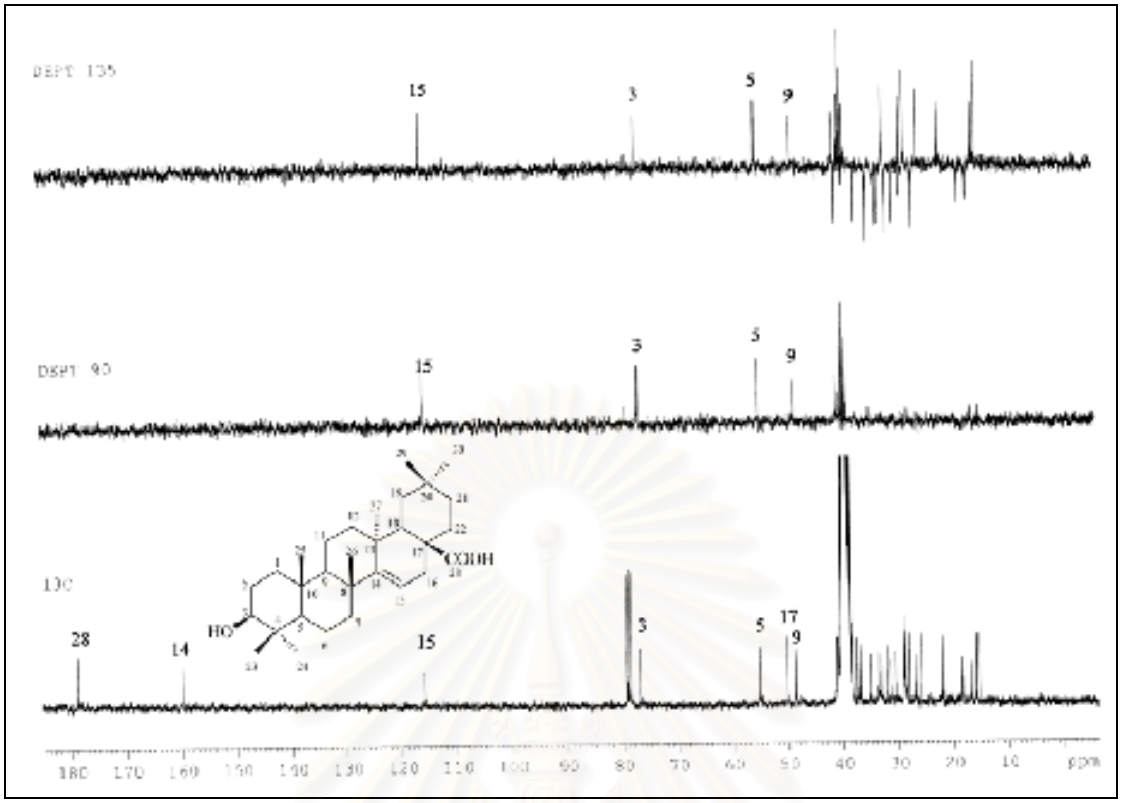

Figure 172a. DEPT 135, DEPT 90 and ^{13}C NMR Spectrum of compound ET-L12

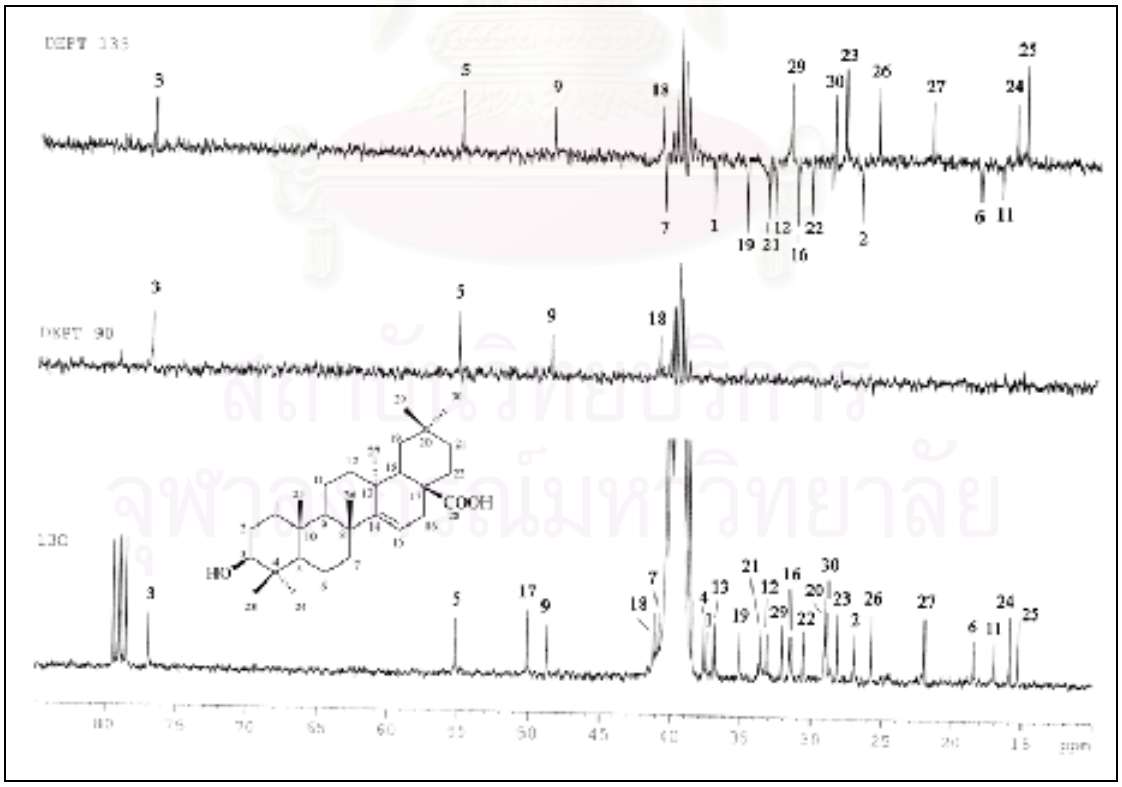

Figure 172b. DEPT 135, DEPT 90 and ^{13}C NMR Spectrum of compound ET-L12 (expansion)

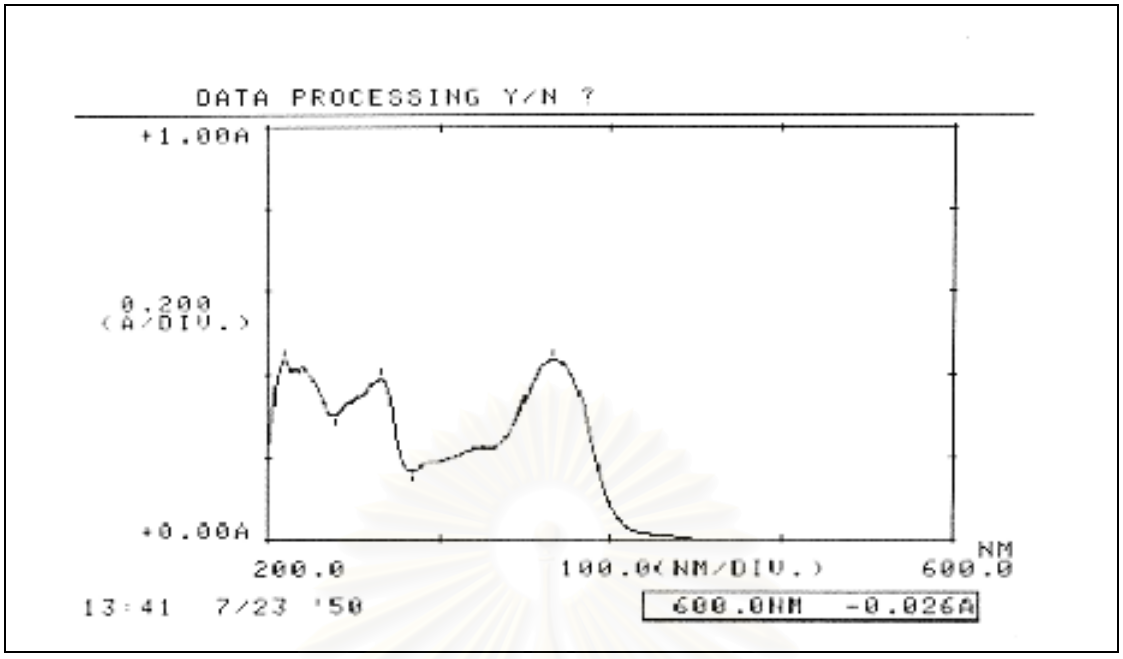

Figure 173. UV Spectrum of compound ET-LC4 (in MeOH)

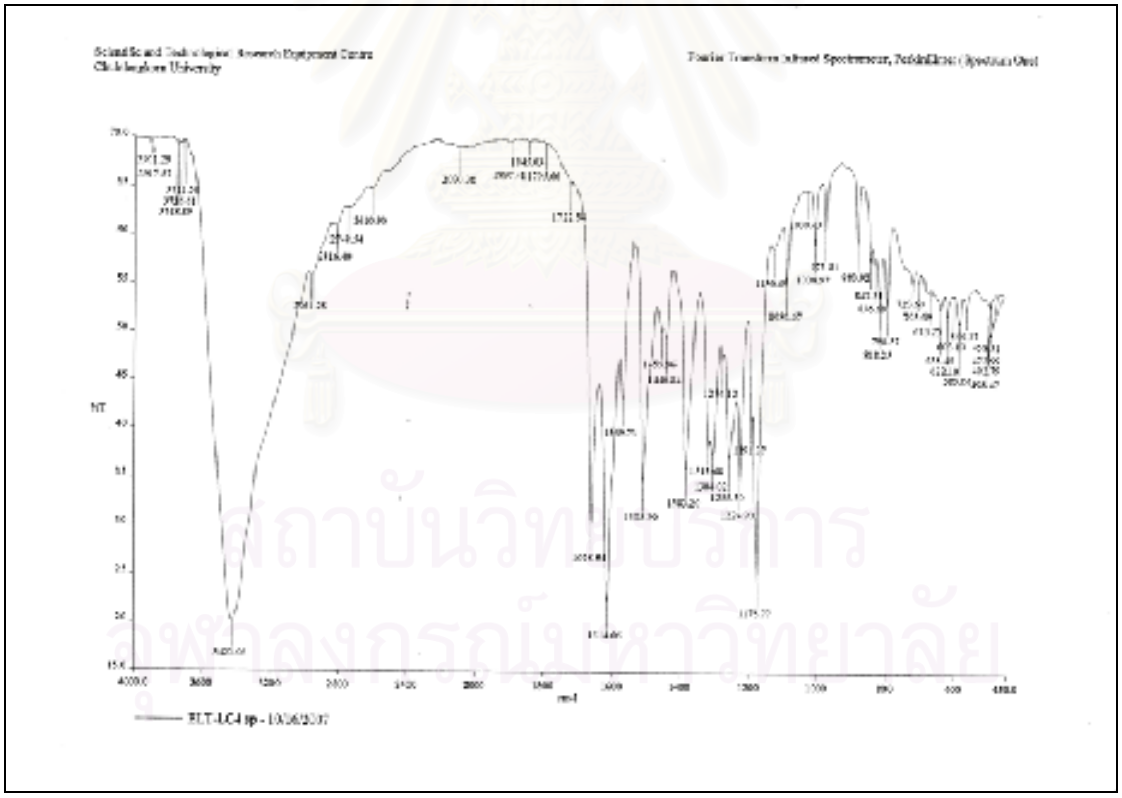

Figure 174. IR Spectrum of compound ET-LC4 (KBr disc)

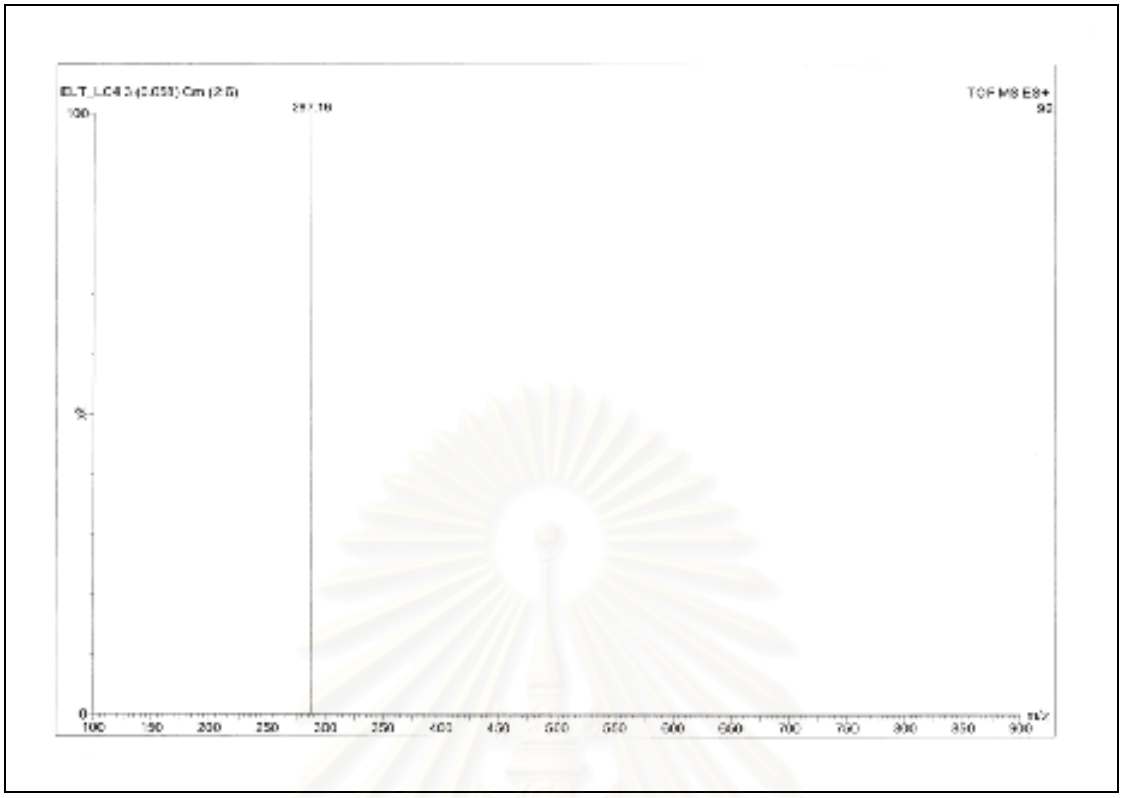

Figure 175. ESI Mass spectrum of compound ET-LC4

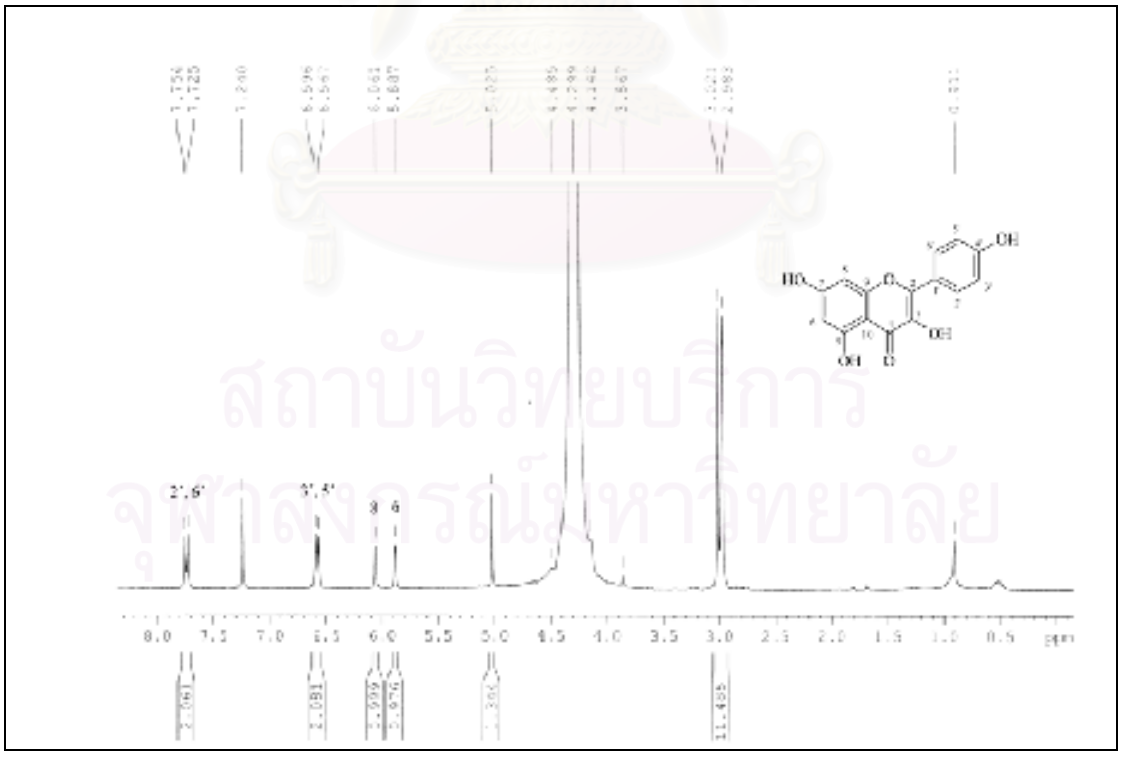

Figure 176. ^{1}H NMR (300 MHz) Spectrum of compound ET-LC4 (in $CD_3OD+CDCl_3$)

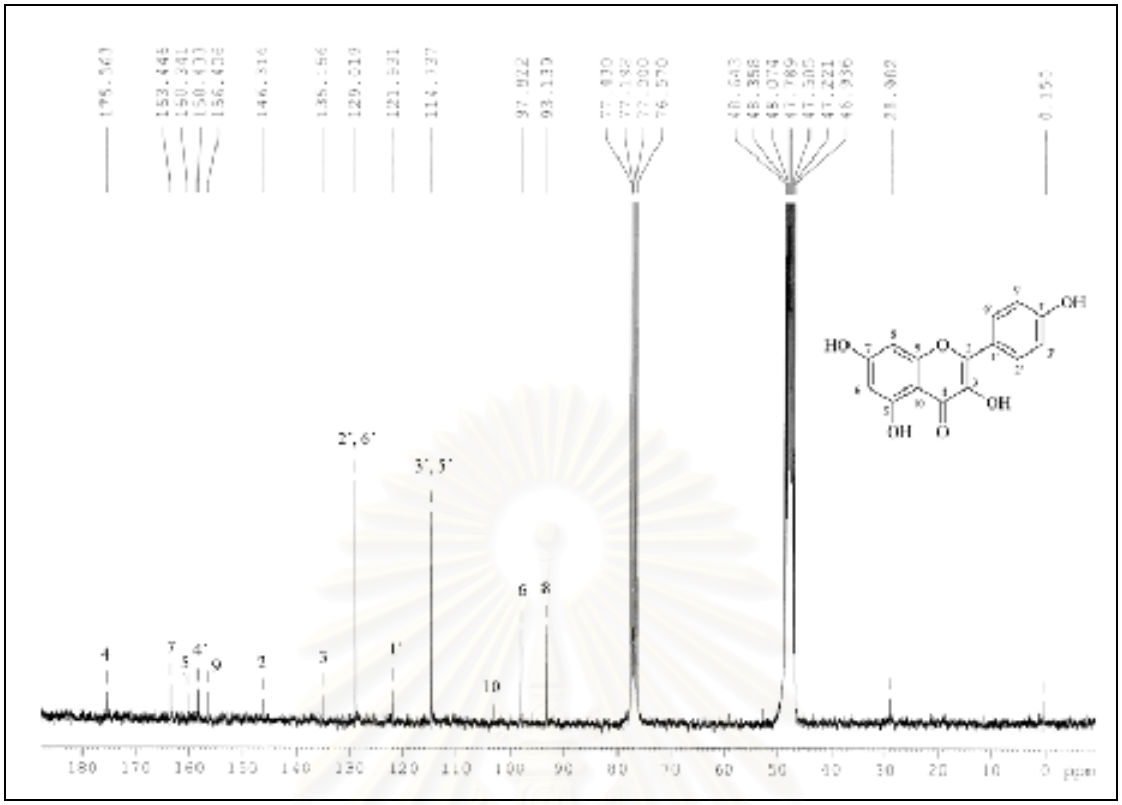

Figure 177. ^{13}C NMR (75 MHz) Spectrum of compound ET-LC4 (in $CD_3OD+CDCl_3$)

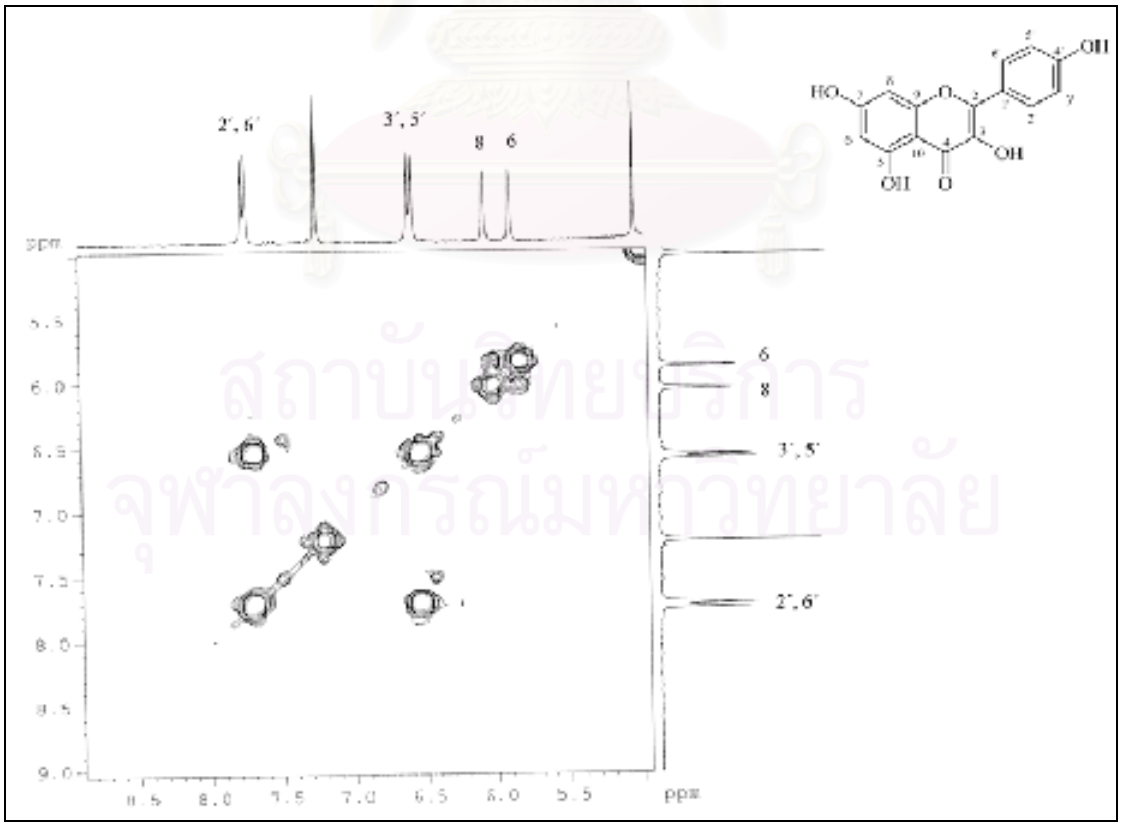

Figure 178. ^{1}H-^{1}H COSY Spectrum of compound ET-LC4 (δ_H 5.0-9.0 ppm)

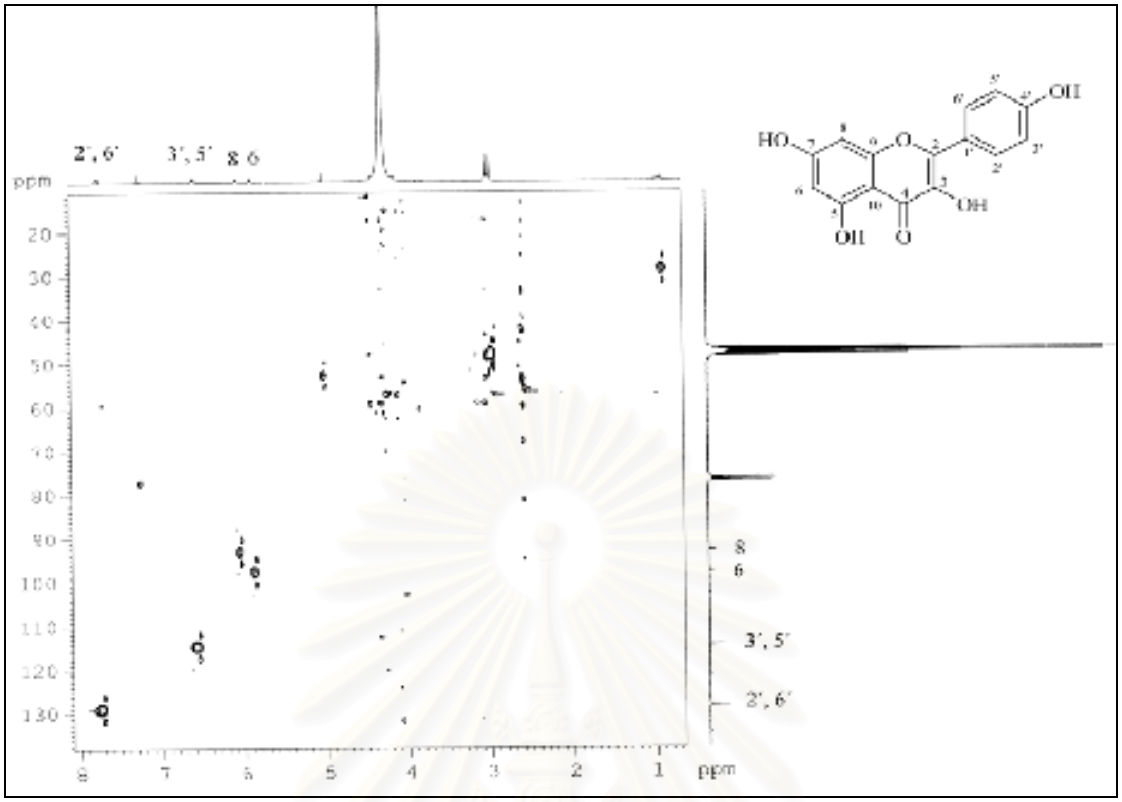

Figure 179. HMQC Spectrum of compound ET-LC4

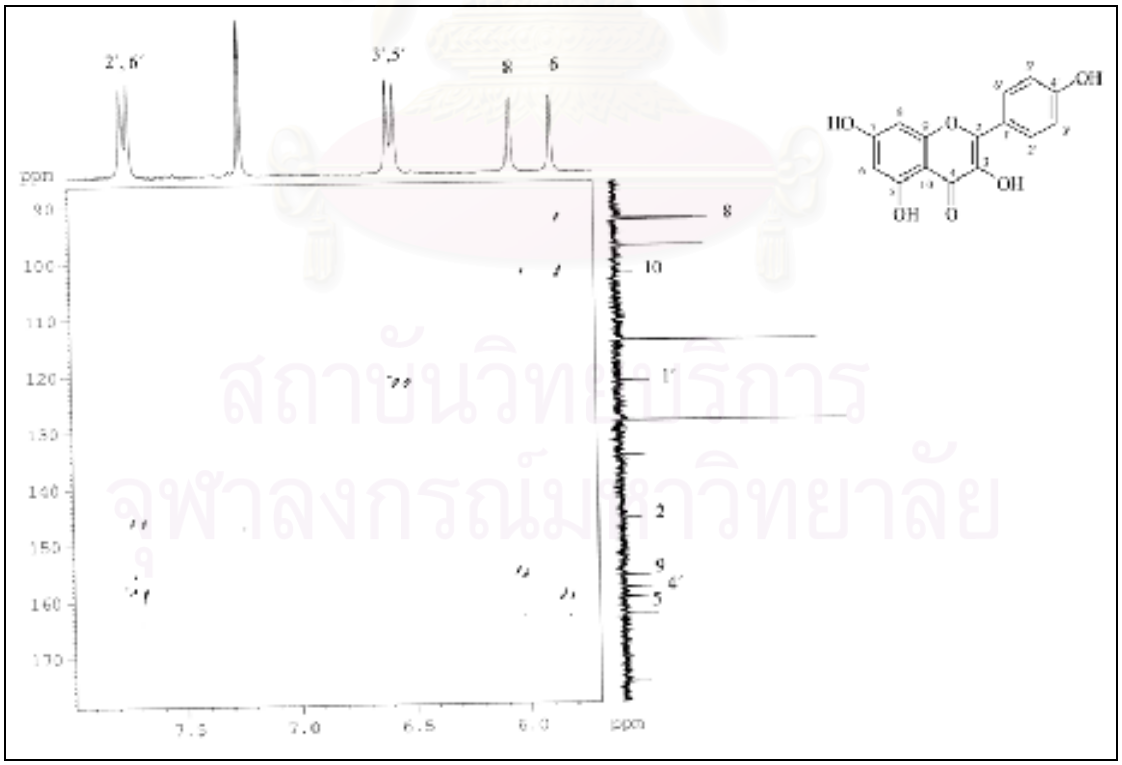

Figure 180. HMBC Spectrum of compound ET-LC4
(δ_H 5.7-8.0 ppm, δ_C 90-180 ppm)

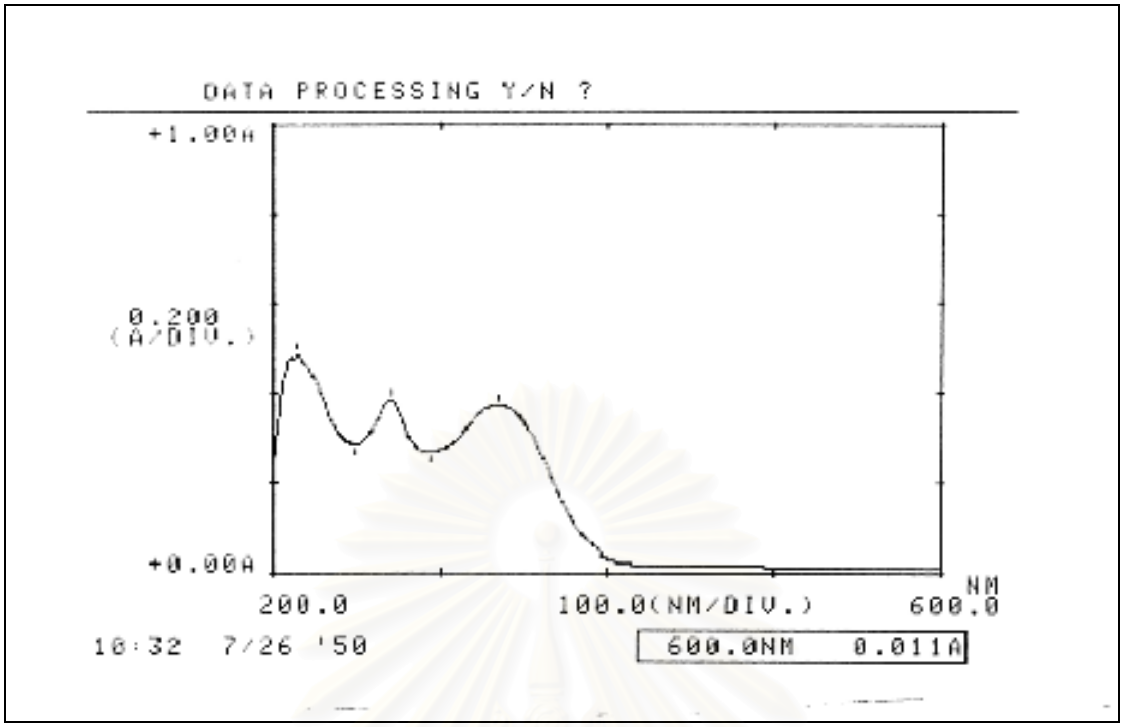

Figure 181. UV Spectrum of compound ET-LC7 (in MeOH)

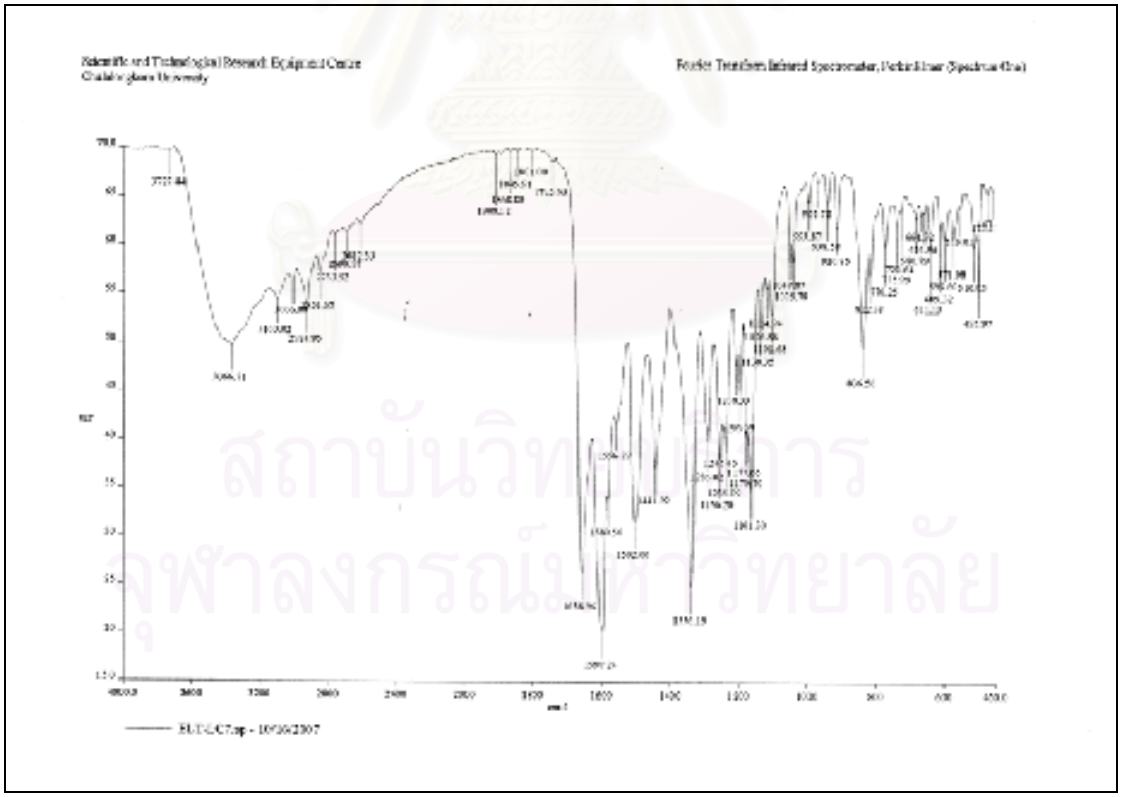

Figure 182. IR Spectrum of compound ET-LC7 (KBr disc)

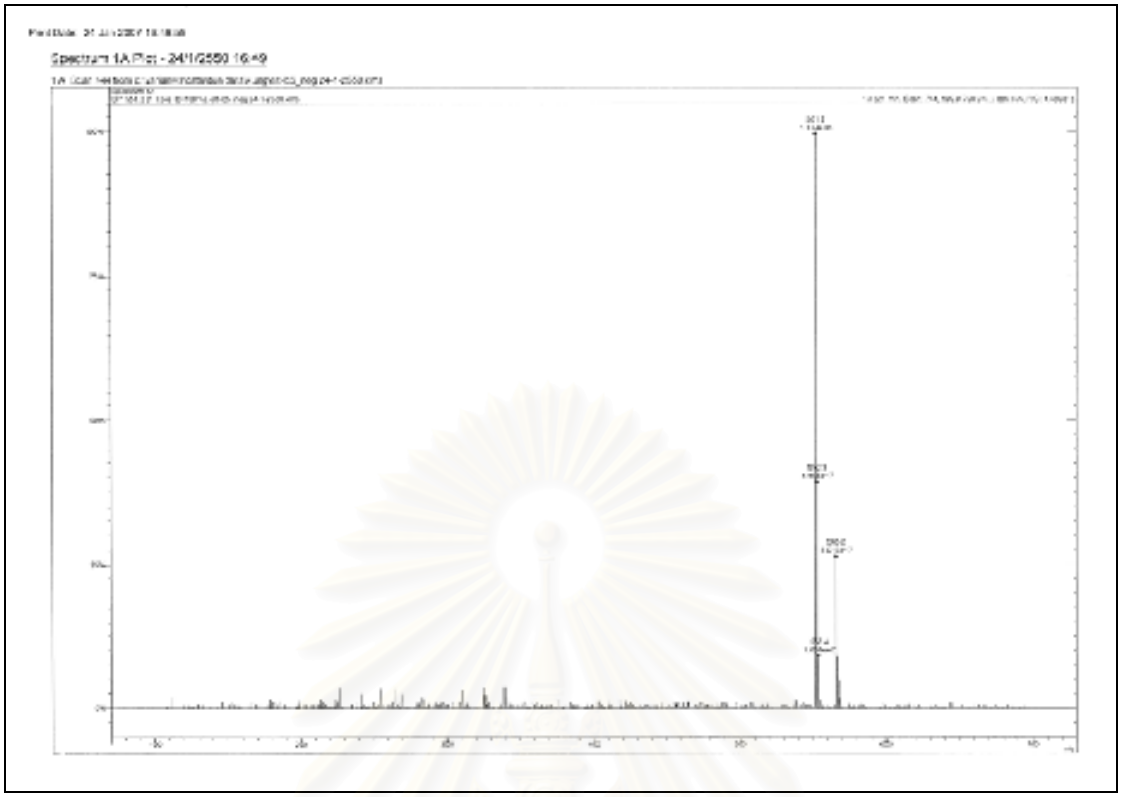

Figure 183. ESI Mass spectrum of compound ET-LC7

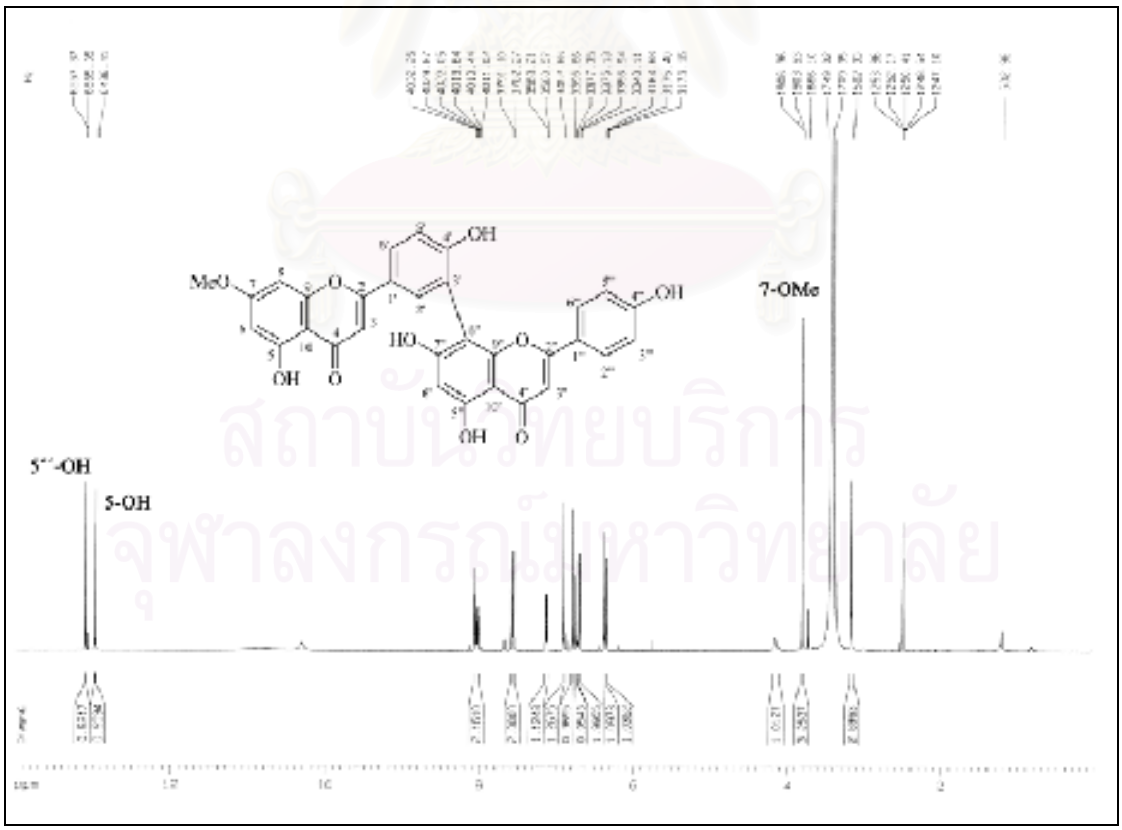

Figure 184a. ^{1}H NMR (500 MHz) Spectrum of compound ET-LC7 (in DMSO-d_6)

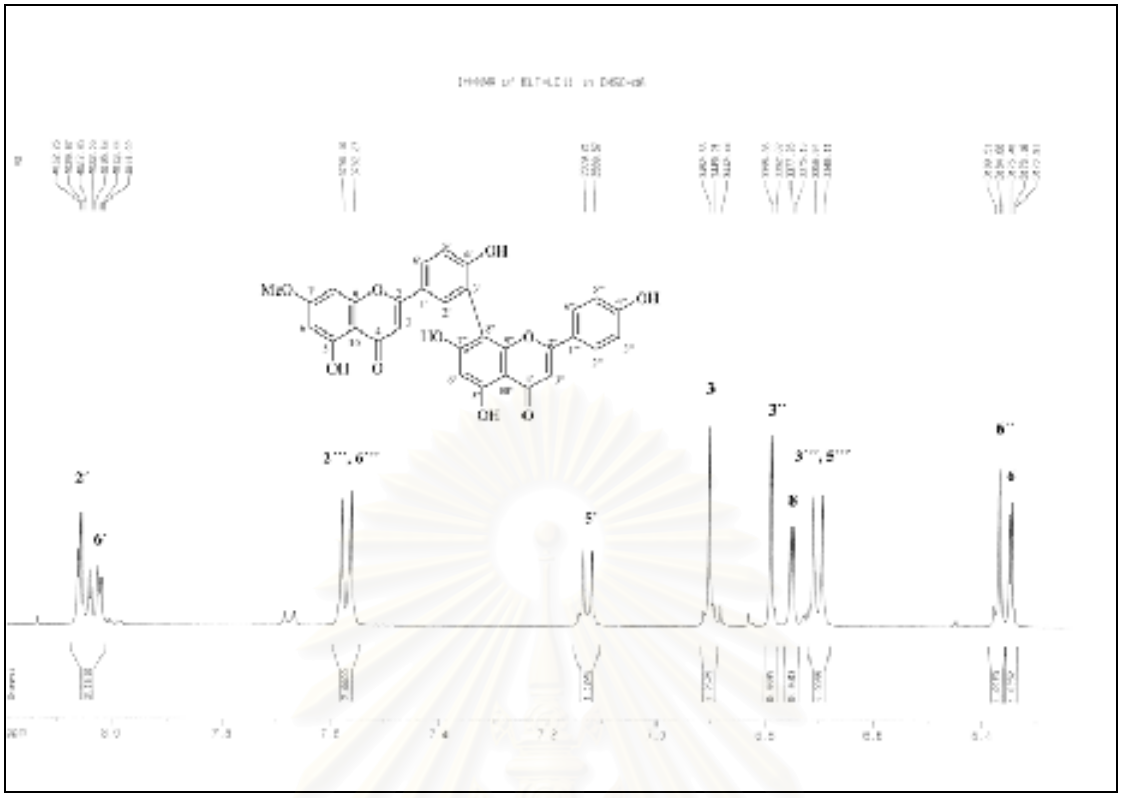

Figure 184b. ^{1}H NMR (500 MHz) Spectrum of compound ET-LC7 (δ_H 6.3-8.2 ppm)

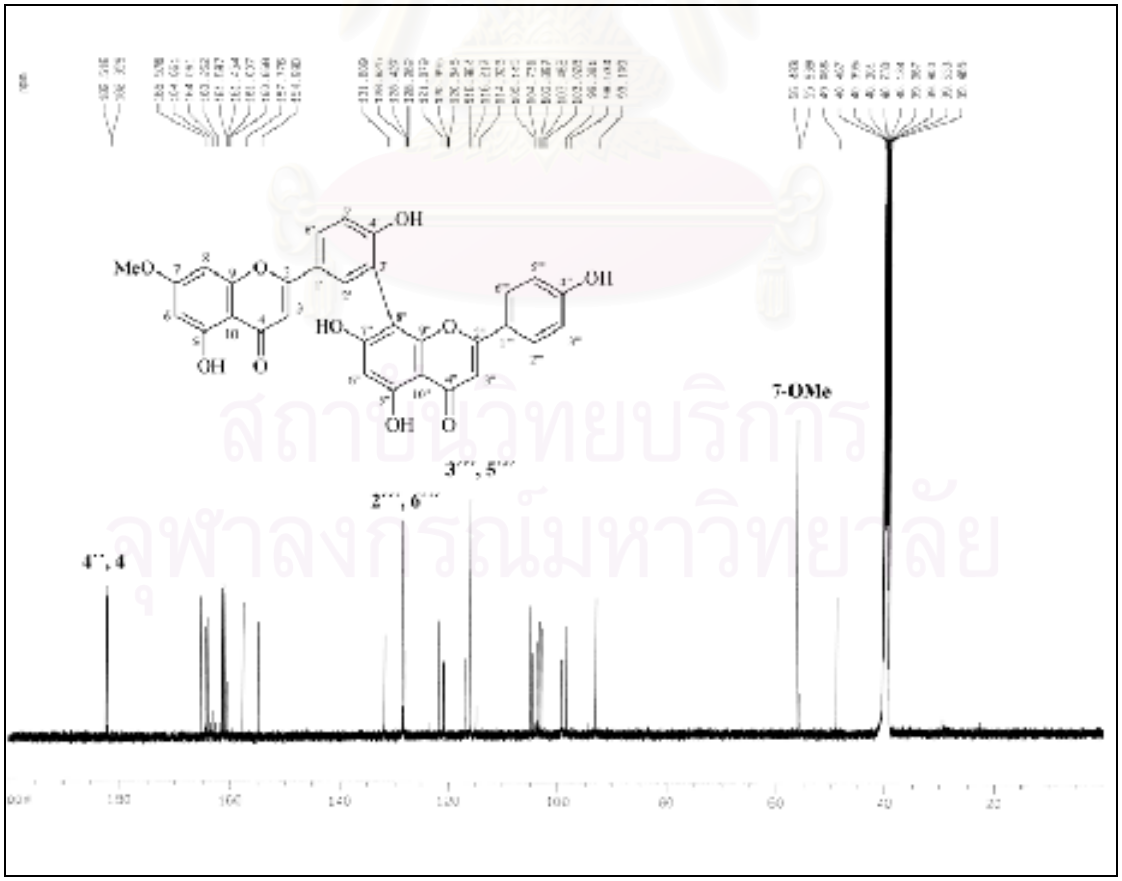

Figure 185a. ^{13}C NMR (125 MHz) Spectrum of compound ET-LC7 (in DMSO-d_6)

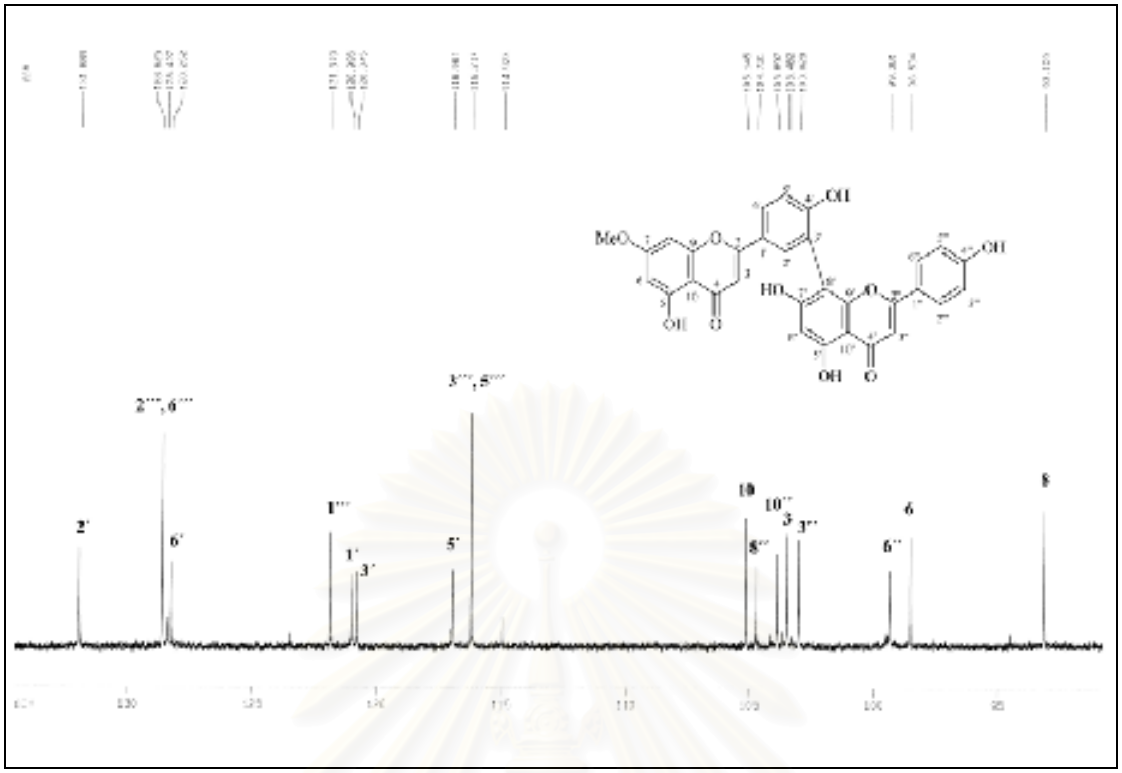

Figure 185b. ^{13}C NMR (125 MHz) Spectrum of compound ET-LC7 (δ_C 90-135 ppm)

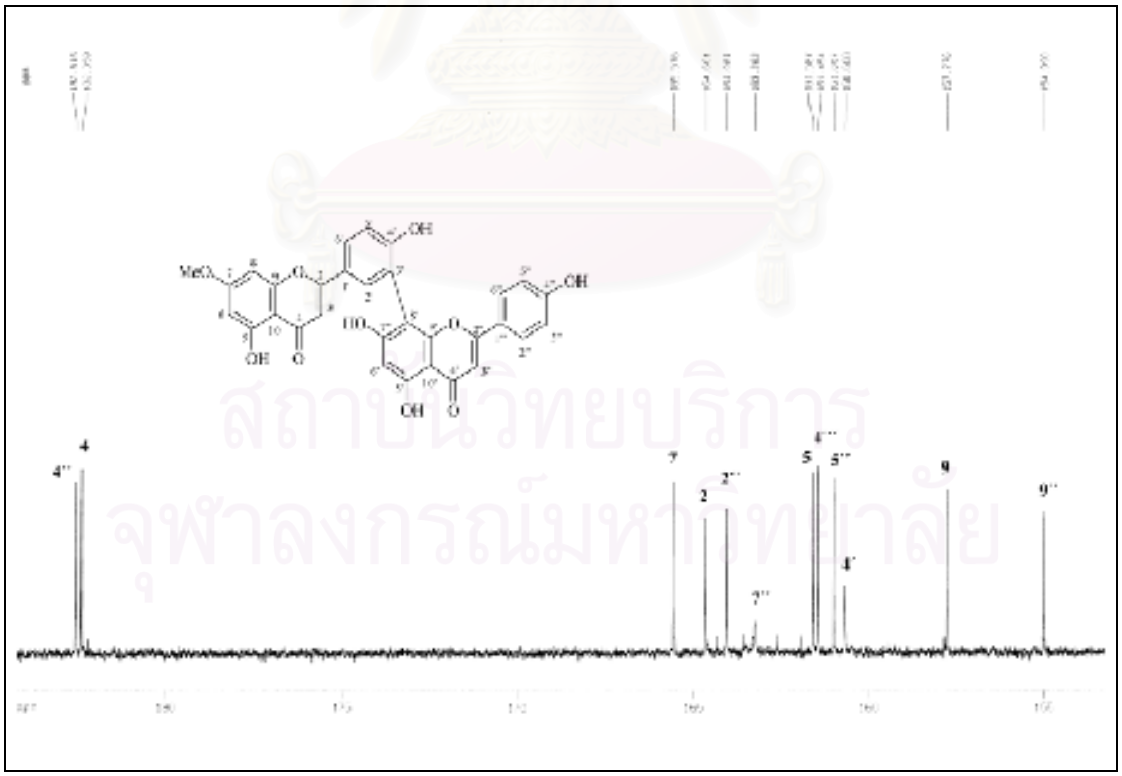

Figure 185c. ^{13}C NMR (125 MHz) Spectrum of compound ET-LC7 (δ_C 155-185 ppm)

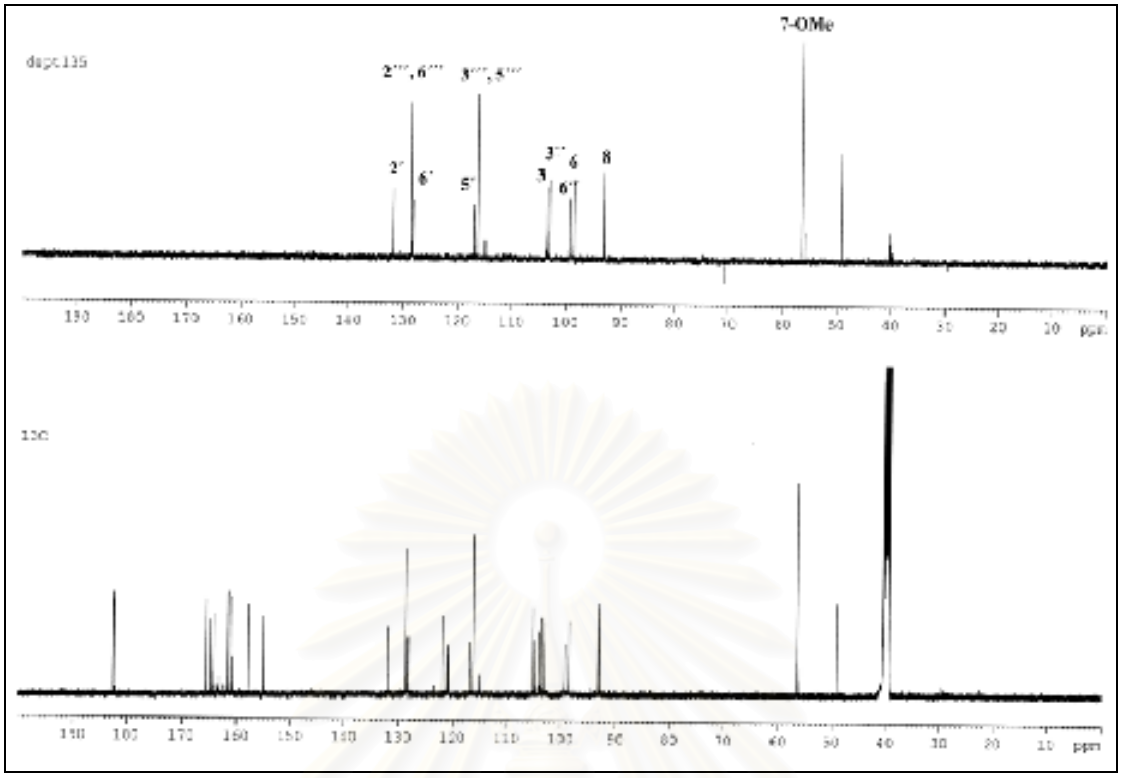

Figure 186. DEPT 135 and ^{13}C NMR Spectrum of compound ET-LC7

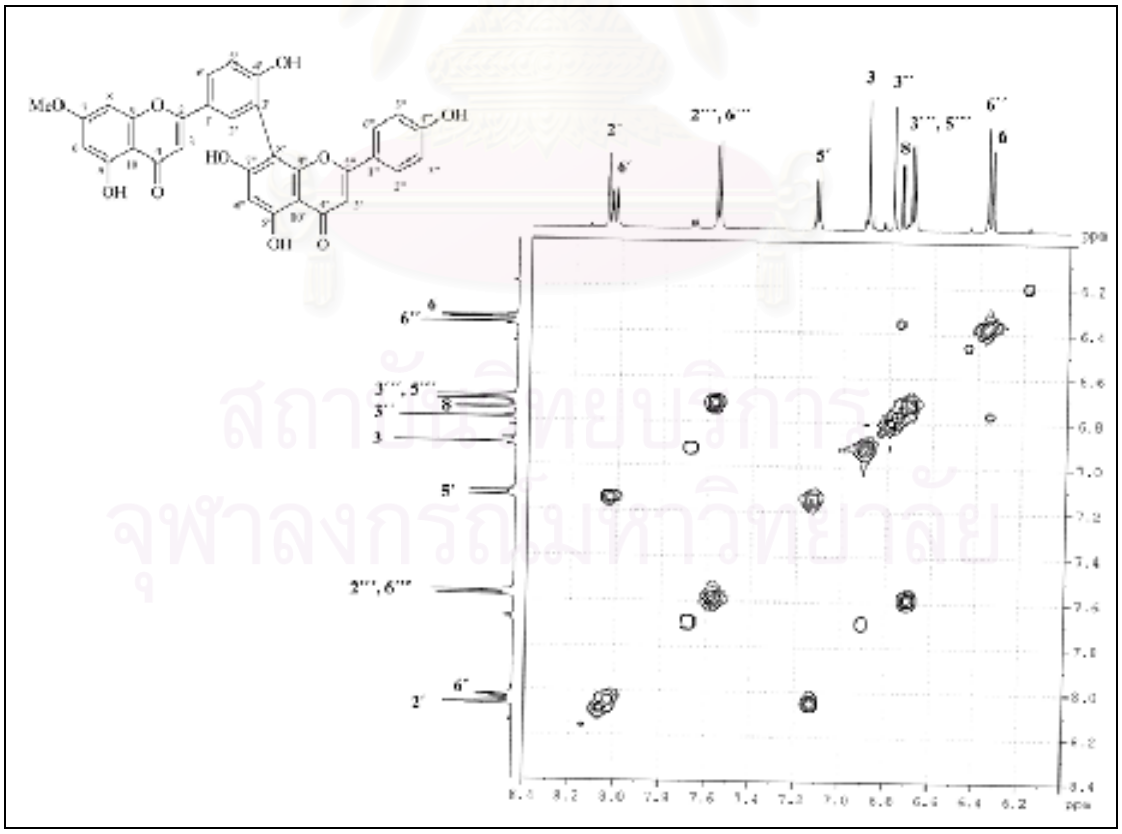

Figure 187. ^{1}H-^{1}H COSY Spectrum of compound ET-LC7 (δ_H 6.0-8.4 ppm)

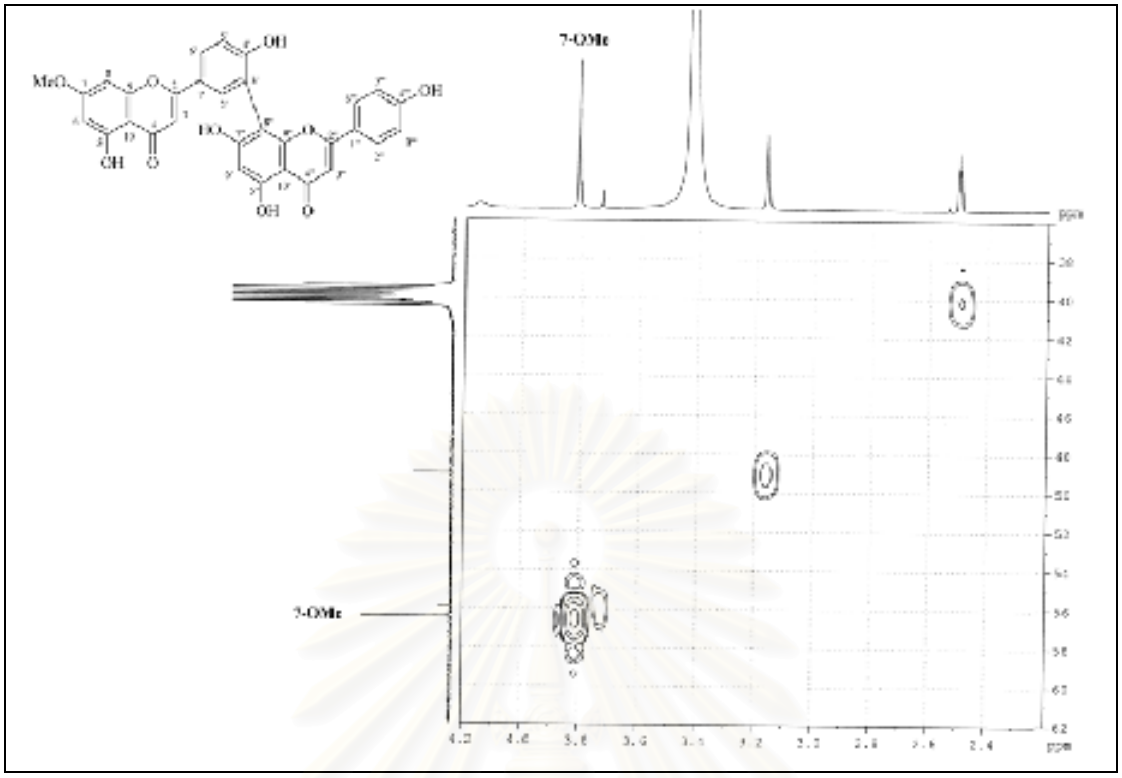

Figure 188a. HMQC Spectrum of compound ET-LC7
(δ_H 2.2-4.2 ppm, δ_C 36-62 ppm)

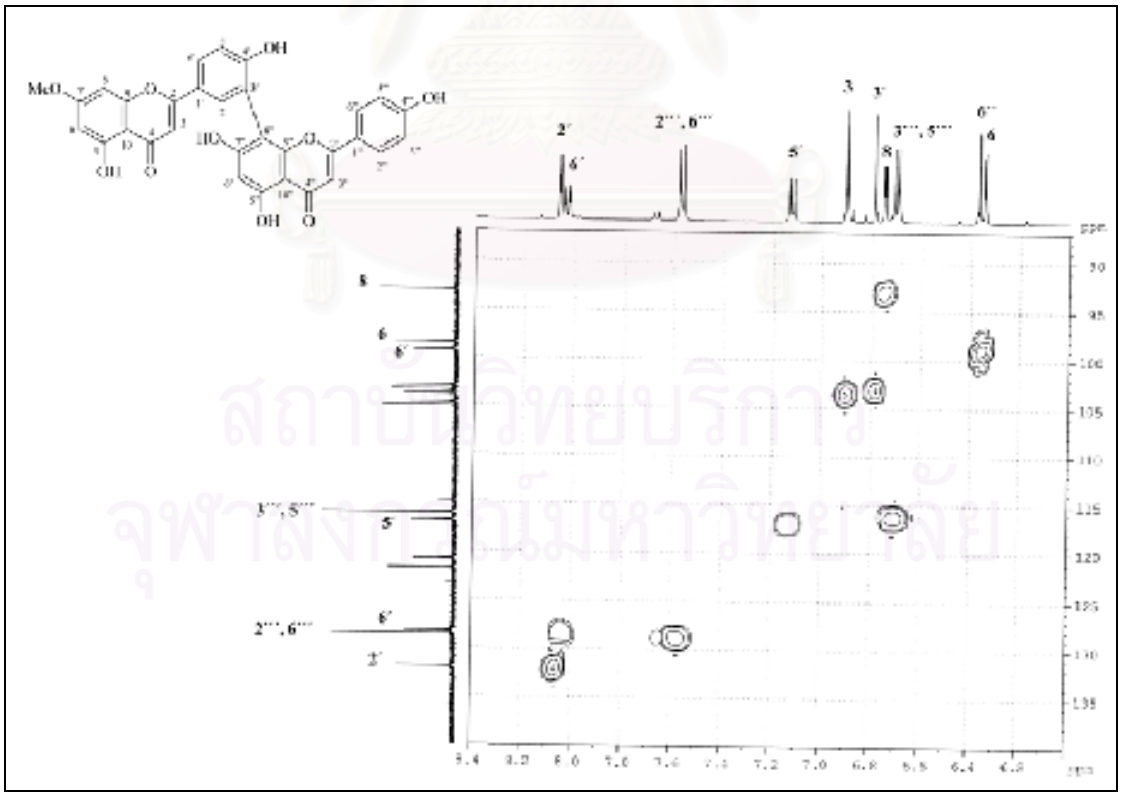

Figure 188b. HMQC Spectrum of compound ET-LC7
(δ_H 6.0-8.4 ppm, δ_C 90-140 ppm)

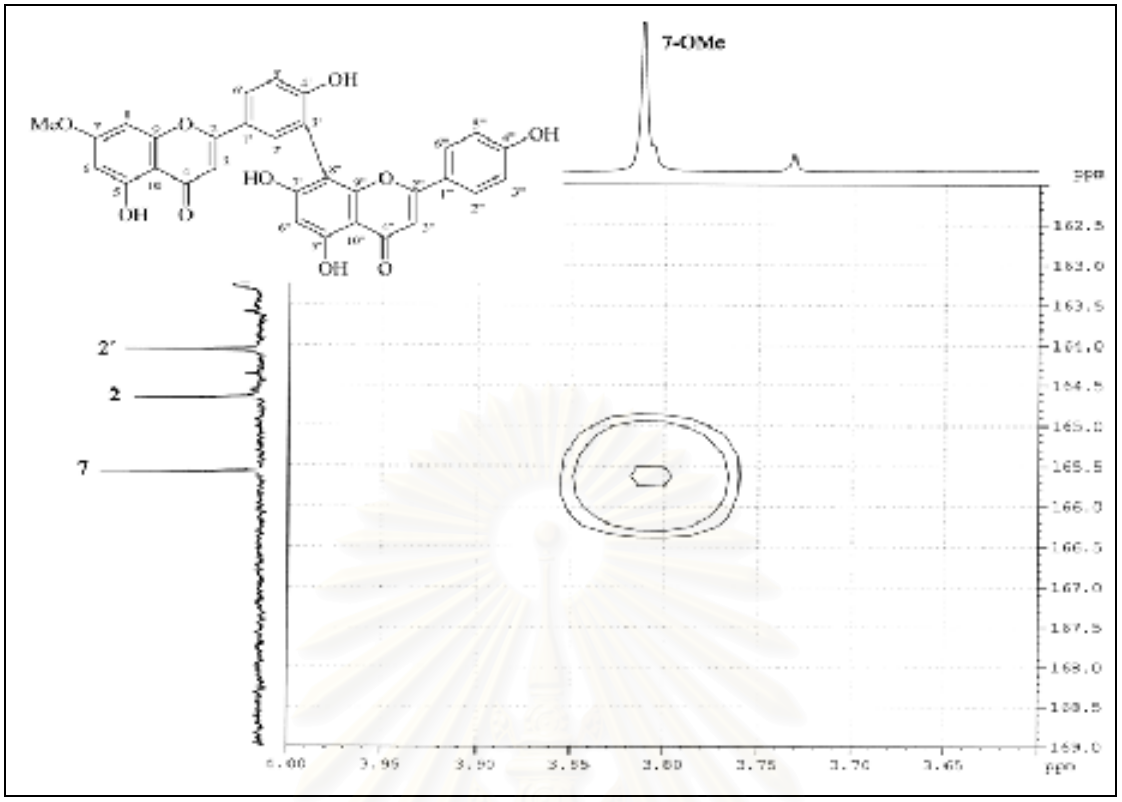

Figure 189a. HMBC Spectrum of compound ET-LC7
(δ_H 3.60-4.00 ppm, δ_C 162-169 ppm)

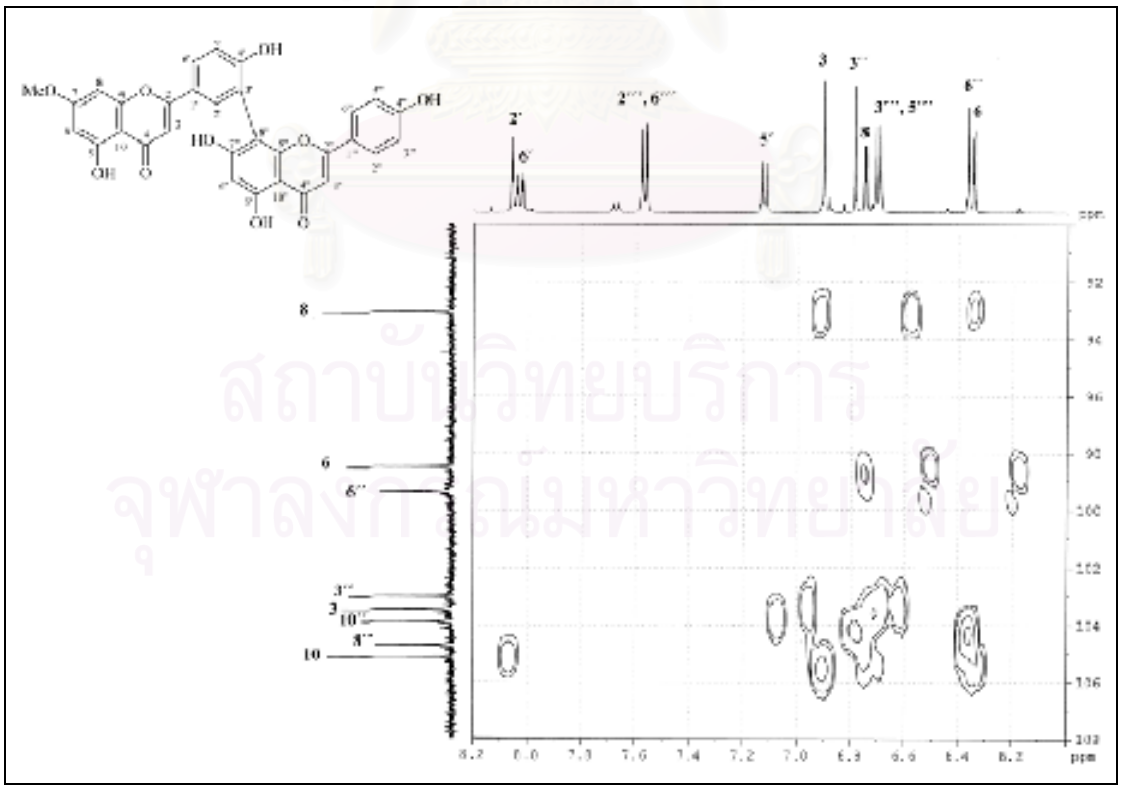

Figure 189b. HMBC Spectrum of compound ET-LC7
(δ_H 6.0-8.2 ppm, δ_C 90-108 ppm)

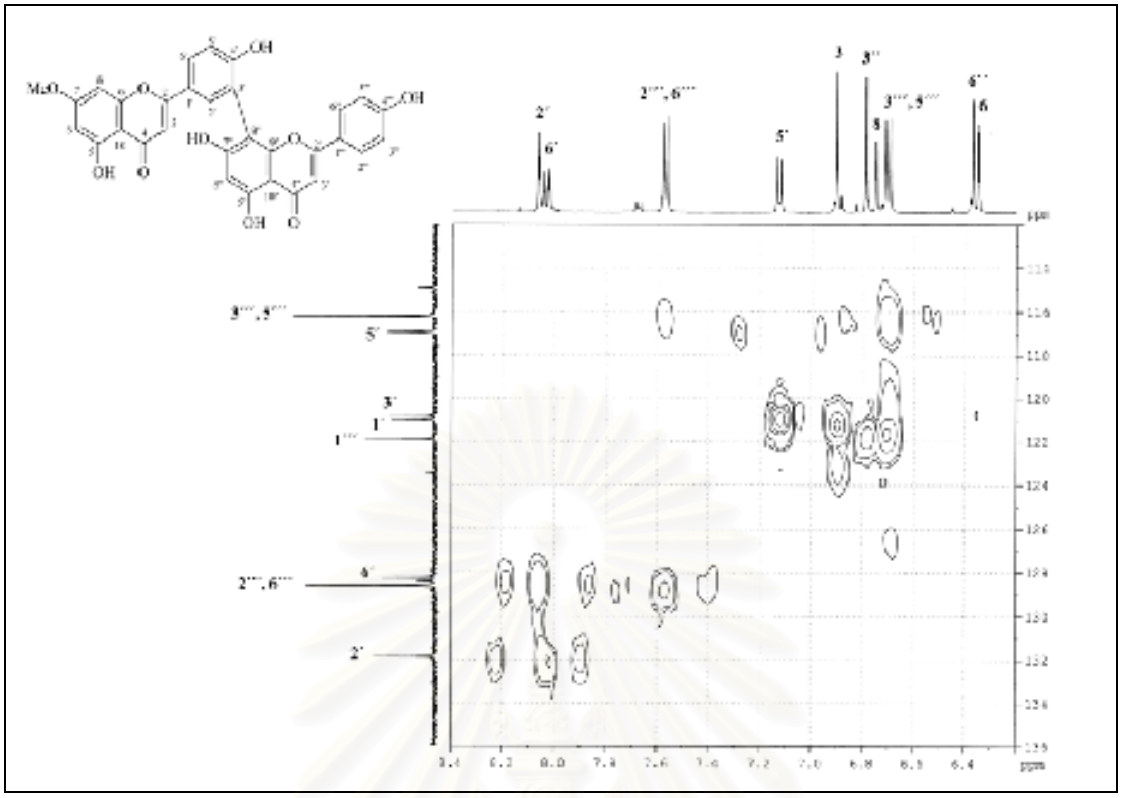

Figure 189c. HMBC Spectrum of compound ET-LC7
(δ_H 6.2-8.4 ppm, δ_C 112-136 ppm)

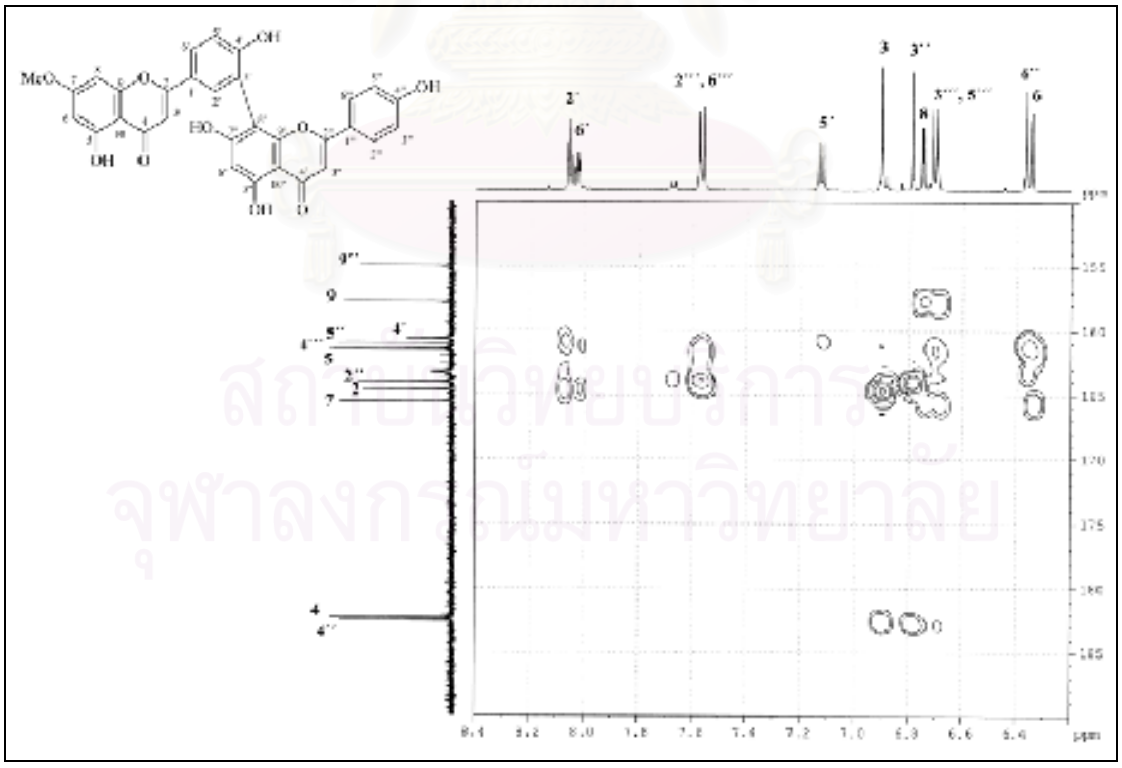

Figure 189d. HMBC Spectrum of compound ET-LC7
(δ_H 6.2-8.4 ppm, δ_C 150-190 ppm)

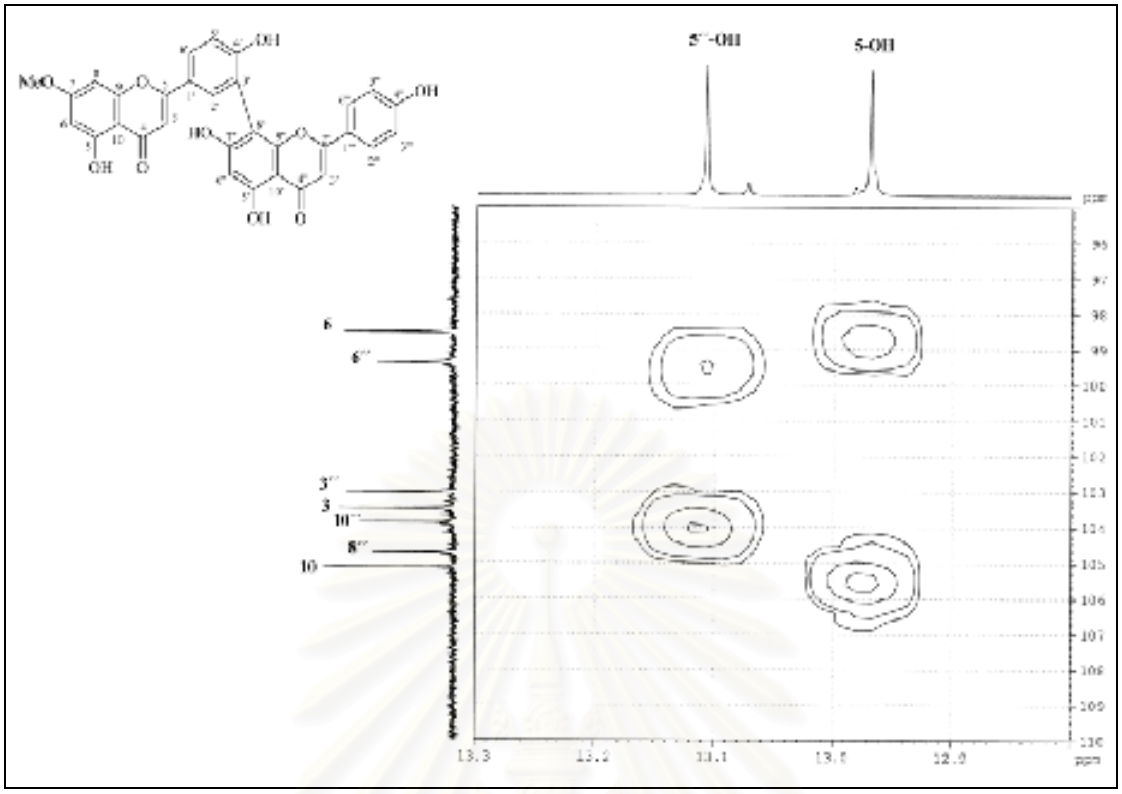

Figure 189e. HMBC Spectrum of compound ET-LC7
(δ_H 12.8-13.3 ppm, δ_C 95-110 ppm)

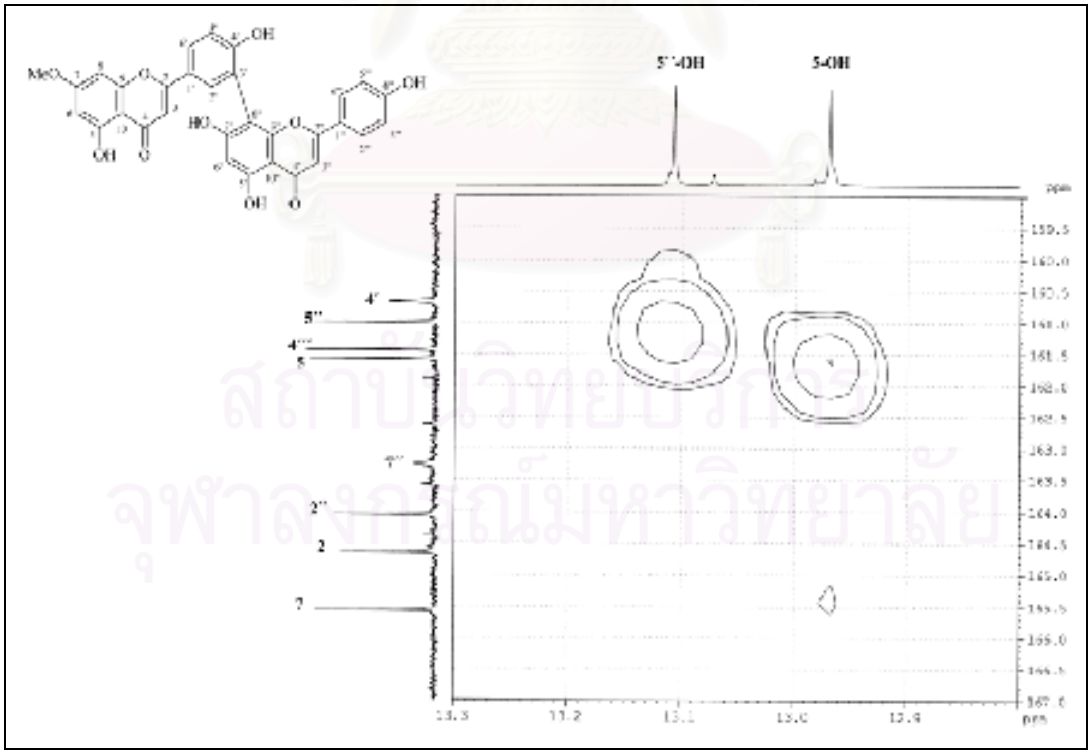

Figure 189f. HMBC Spectrum of compound ET-LC7
(δ_H 12.8-13.3 ppm, δ_C 159-167 ppm)

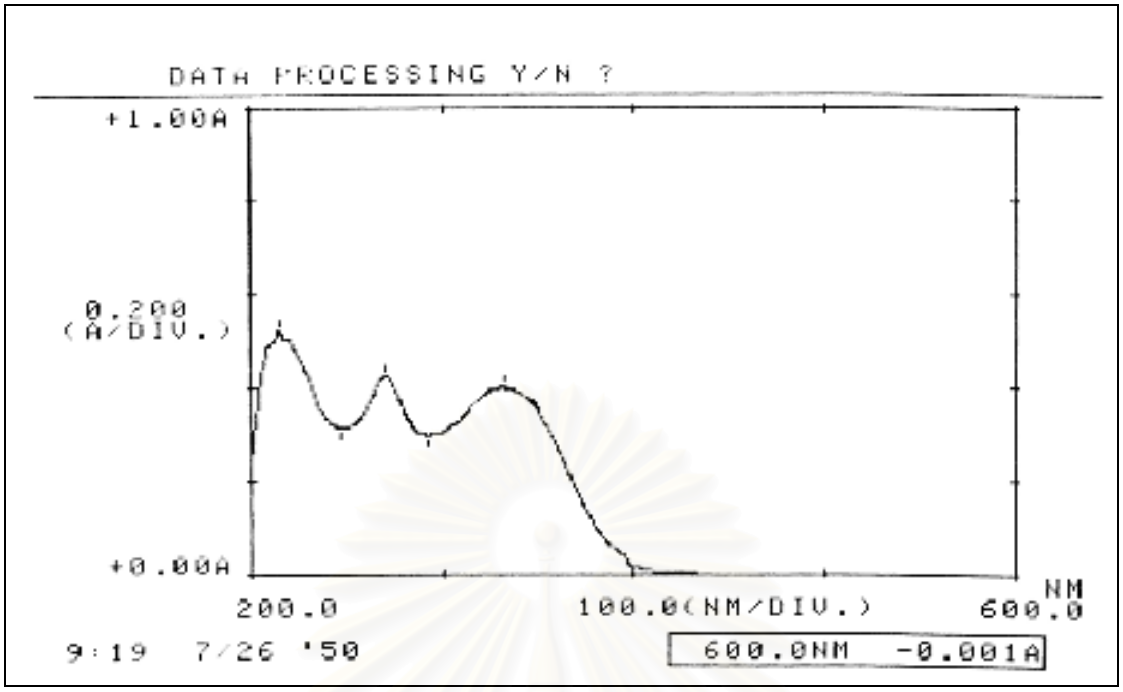

Figure 190. UV spectrum of compound ET-LC13 (in MeOH)

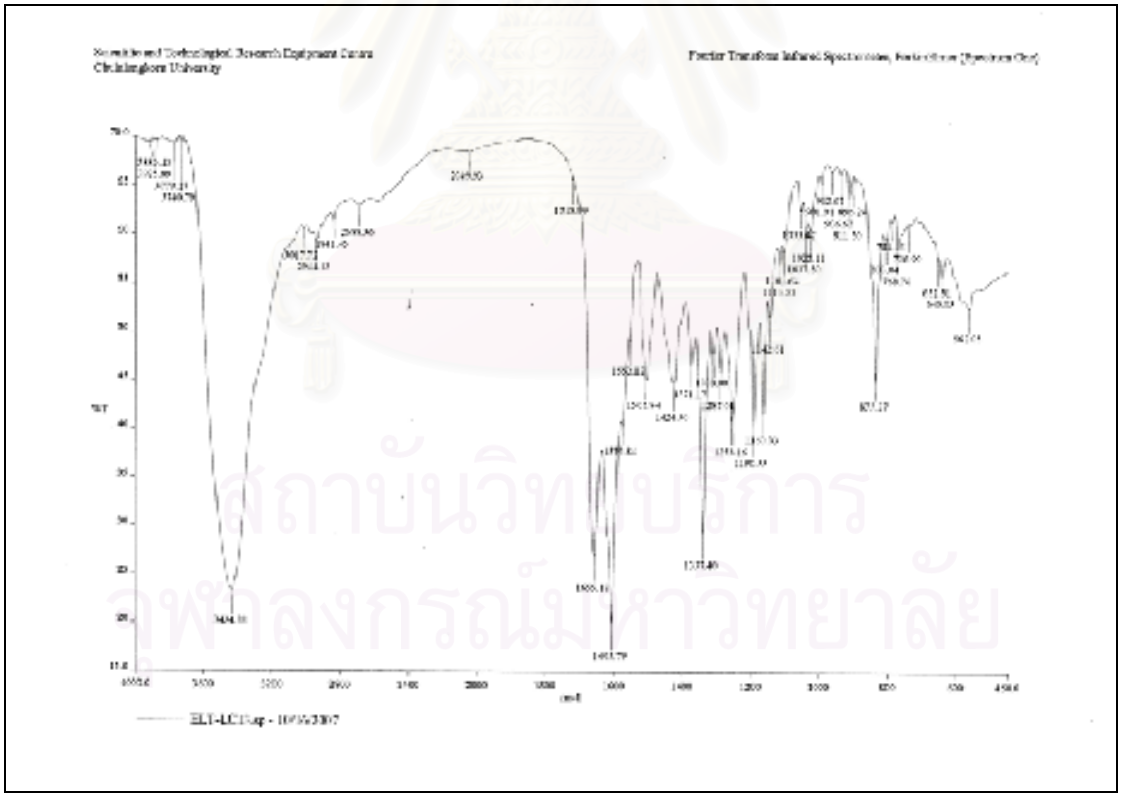

Figure 191. IR Spectrum of compound ET-LC13 (KBr disc)

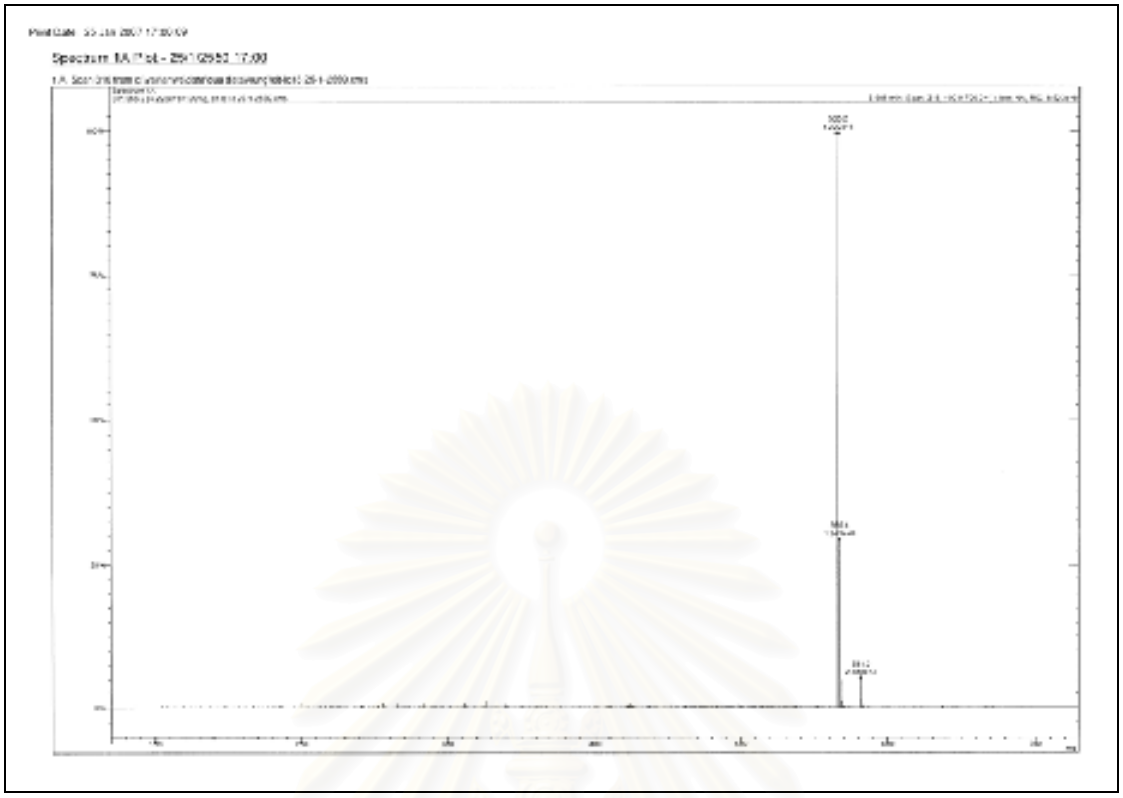

Figure 192. ESI Mass spectrum of compound ET-LC13

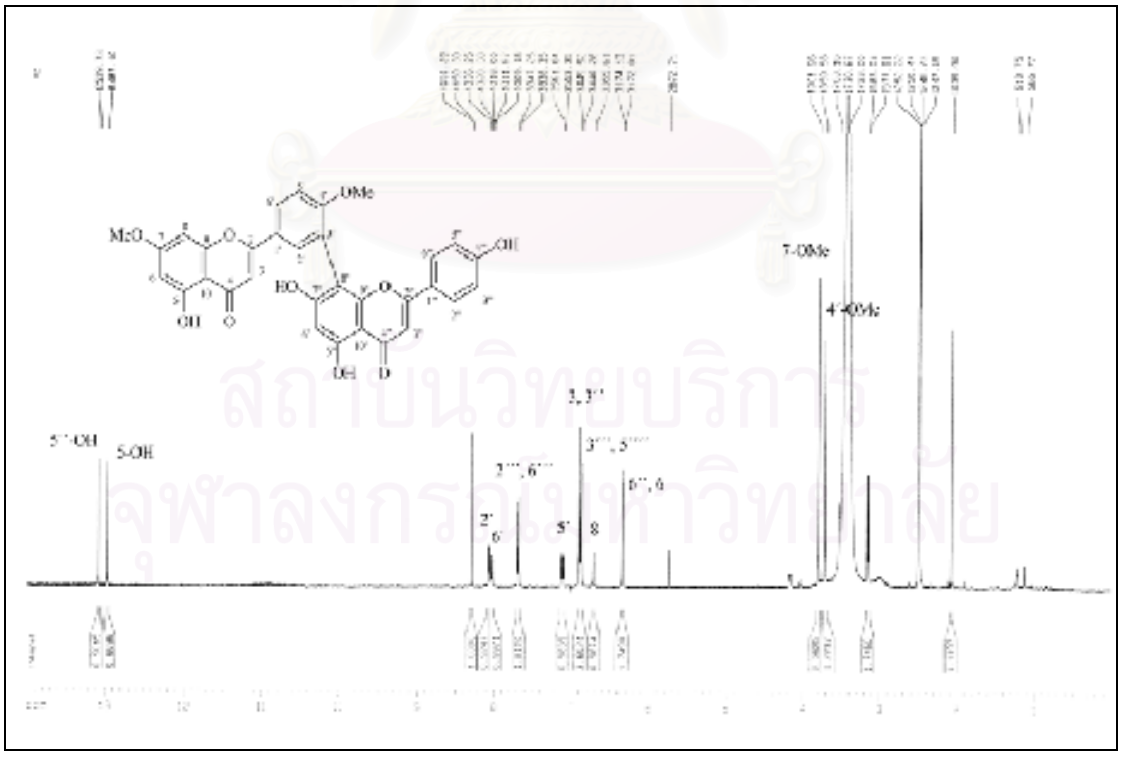

Figure 193. ^{1}H NMR (500 MHz) Spectrum of compound ET-LC13 (in DMSO-d_6)

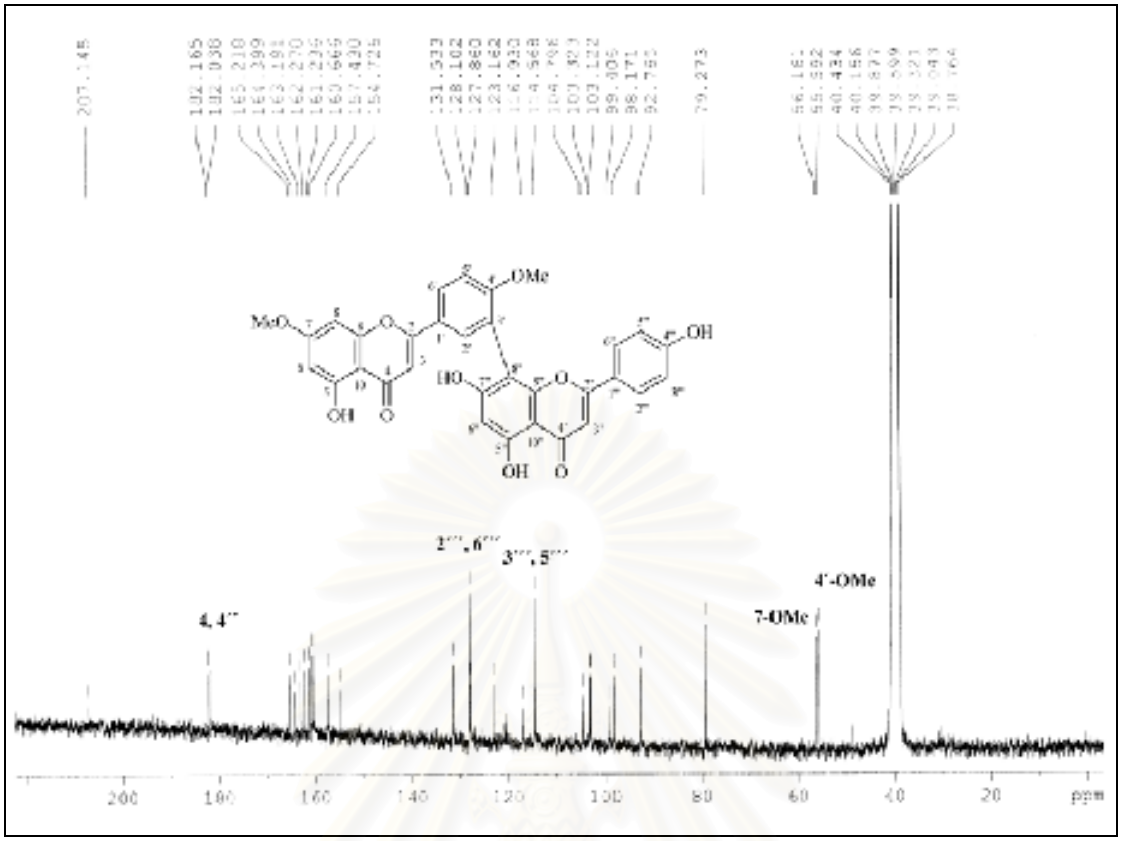

Figure 194a. ^{13}C NMR (125 MHz) Spectrum of compound ET-LC13 (in DMSO-d_6)

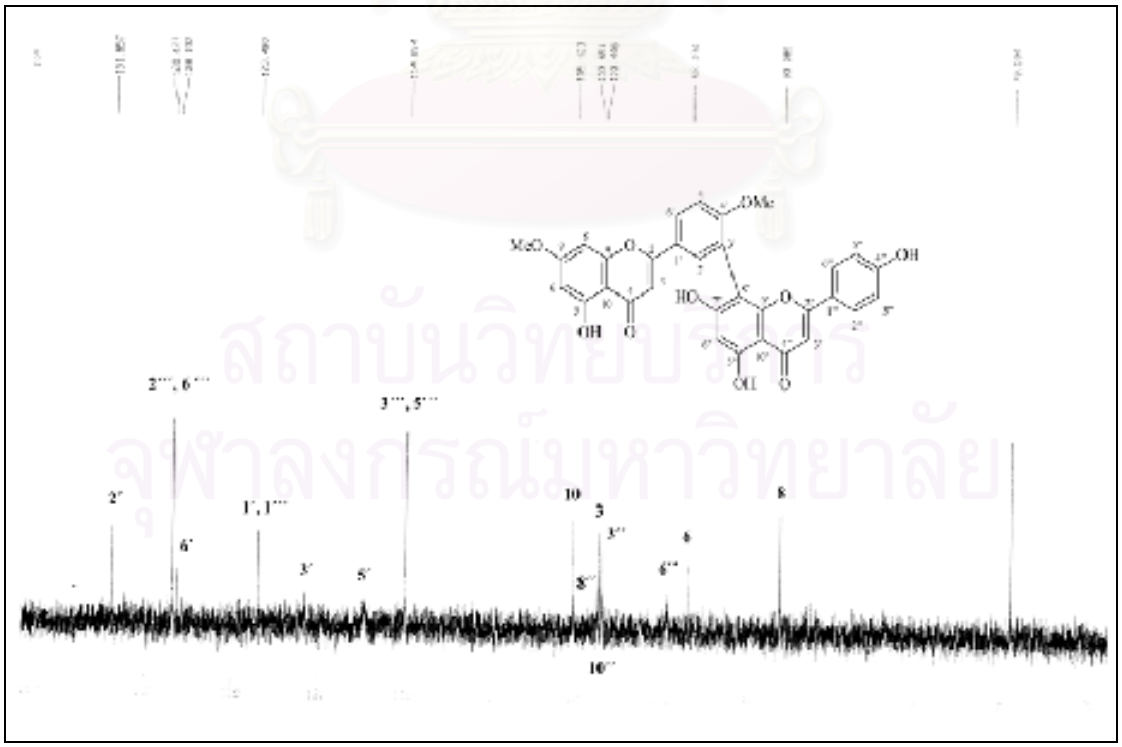

Figure 194b. ^{13}C NMR (125 MHz) Spectrum of compound ET-LC13 (δ_C 90-135 ppm)

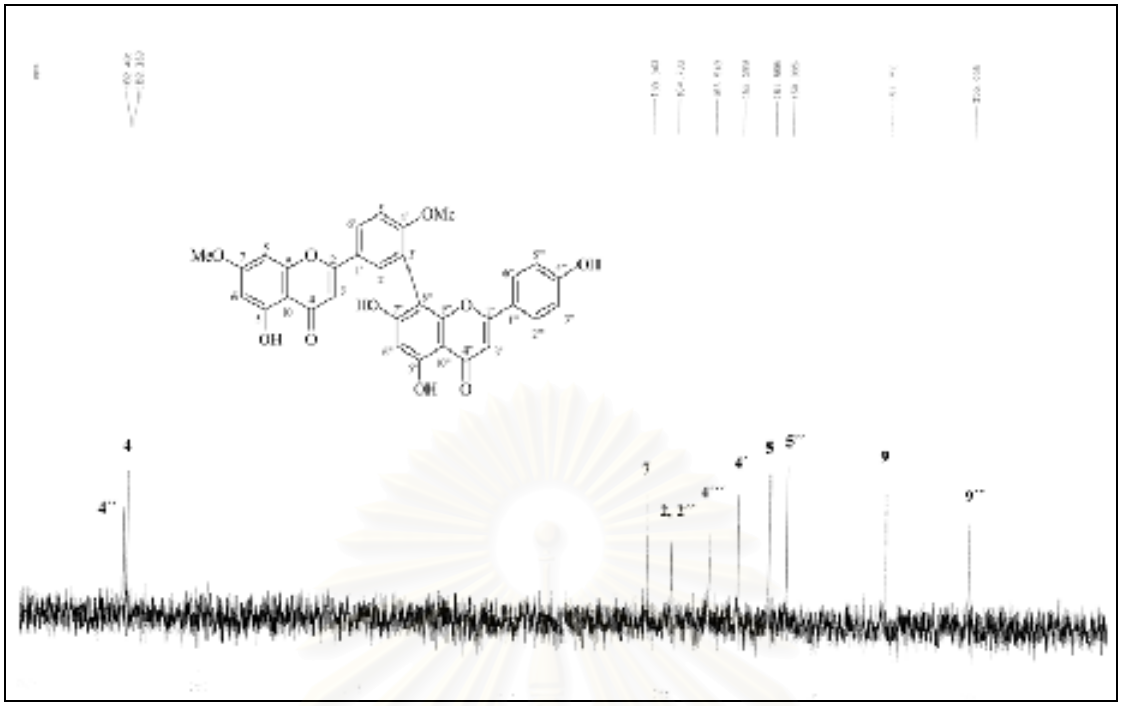

Figure 194c. ^{13}C NMR (125 MHz) Spectrum of compound ET-LC13 (δ_C 150-185 ppm)

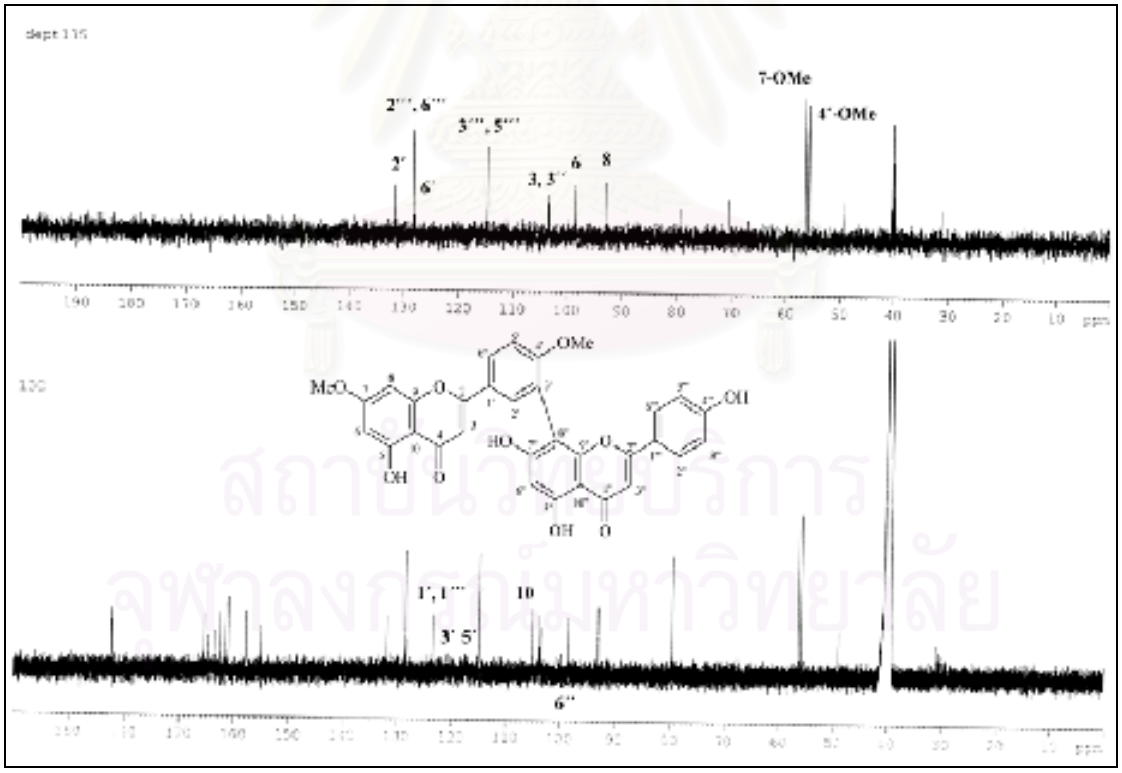

Figure 195. DEPT 135 and ^{13}C NMR Spectrum of compound ET-LC13

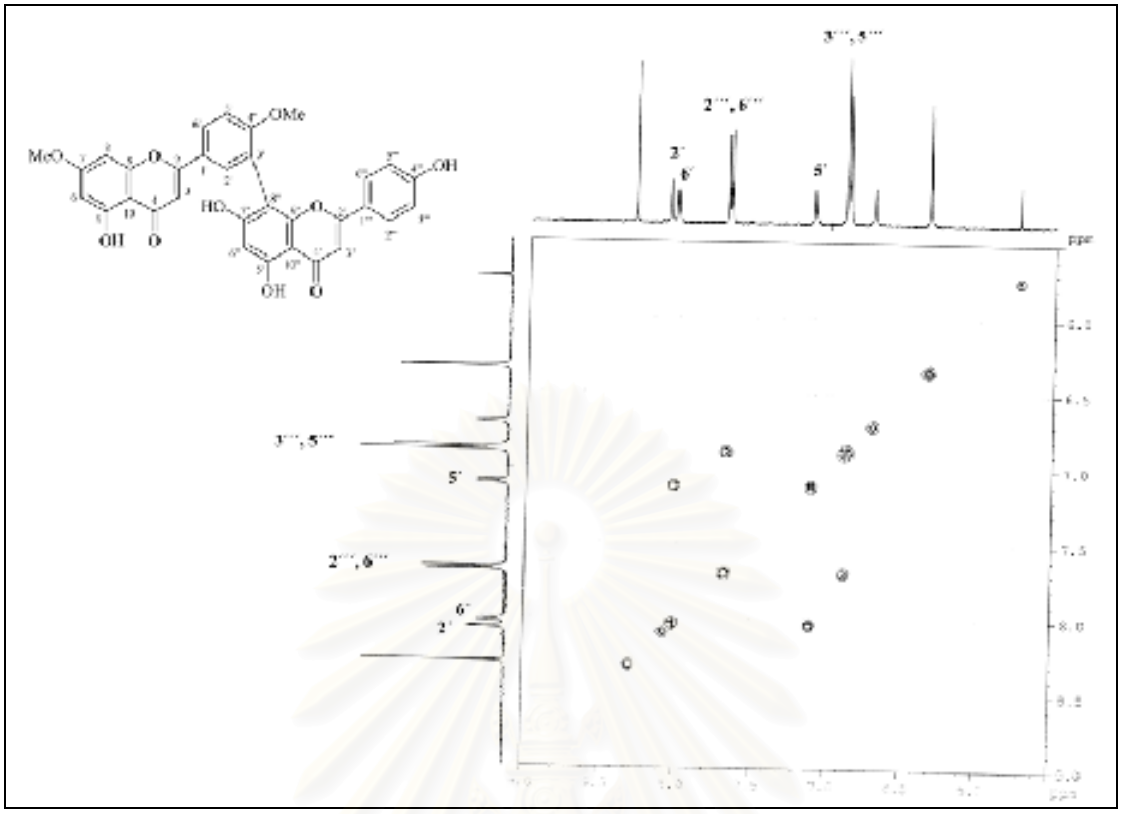

Figure 196. ^{1}H-^{1}H COSY Spectrum of compound ET-LC13 (δ_H 5.5-9.0 ppm)

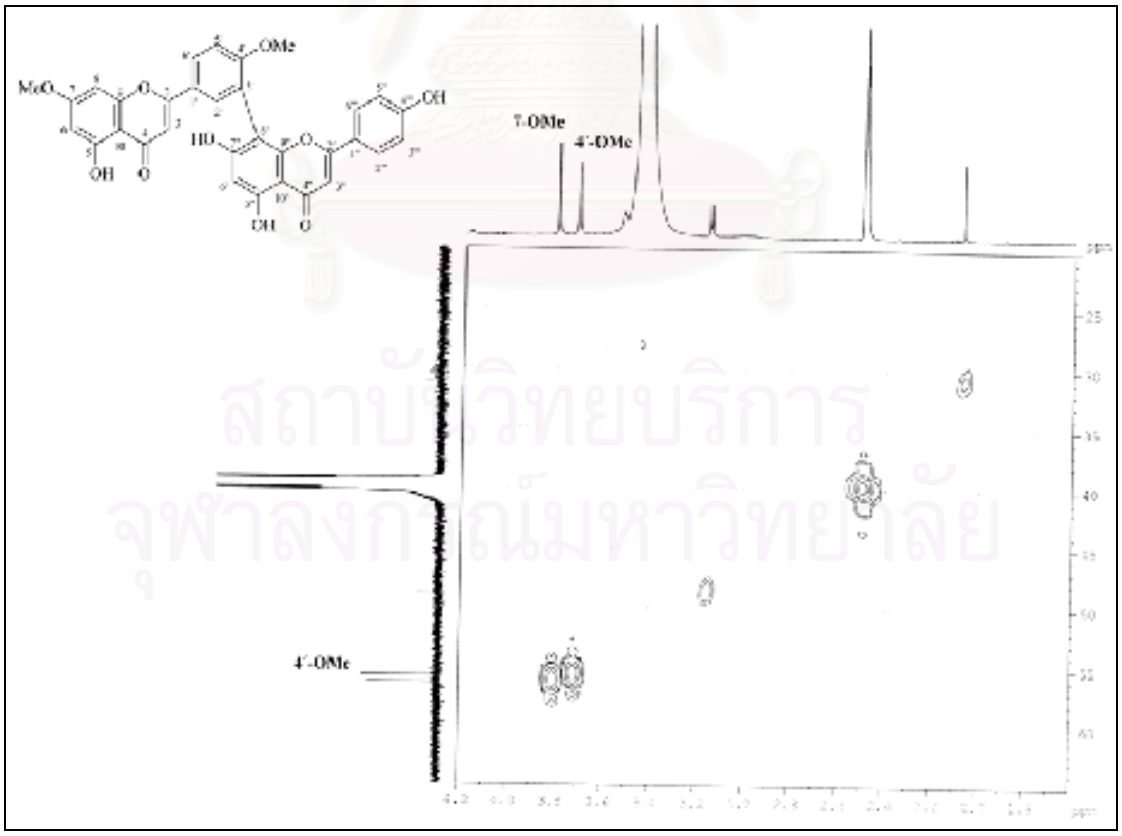

Figure 197a. HMQC Spectrum of compound ET-LC13
(δ_H 1.6-4.2 ppm, δ_C 20-65 ppm)

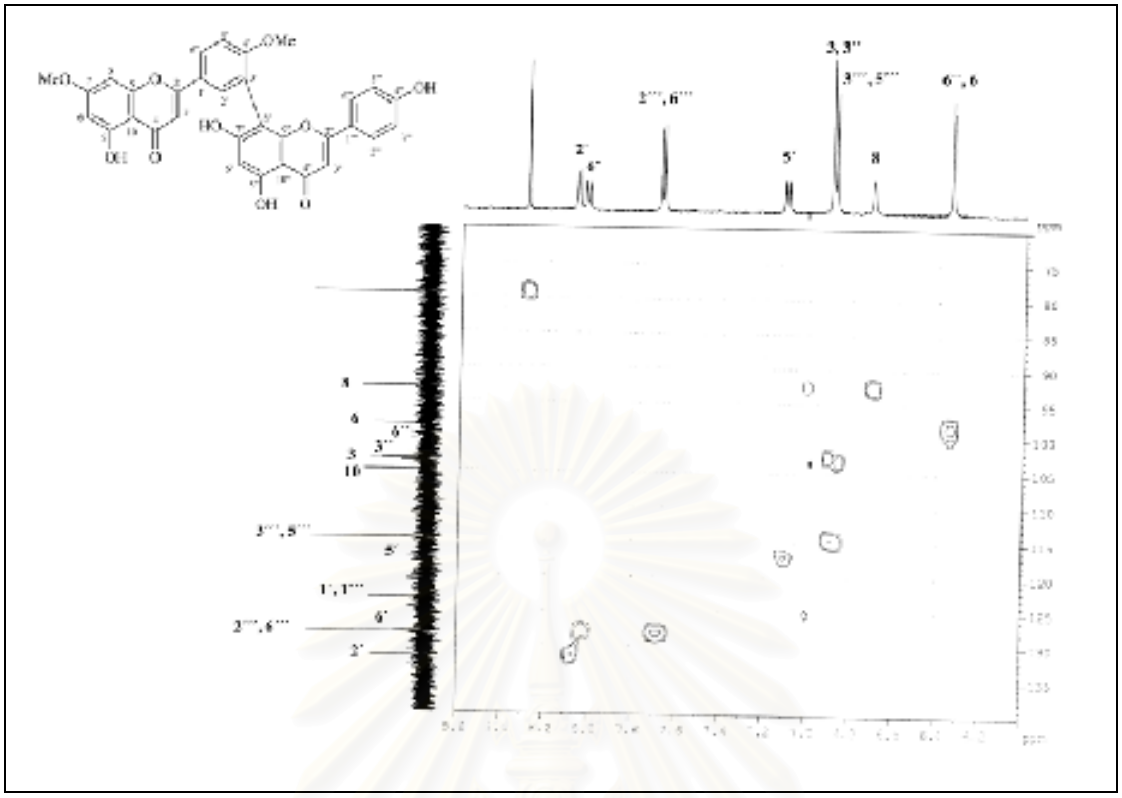

Figure 197b. HMQC Spectrum of compound ET-LC13
(δ_H 4.0-9.6 ppm, δ_C 70-140 ppm)

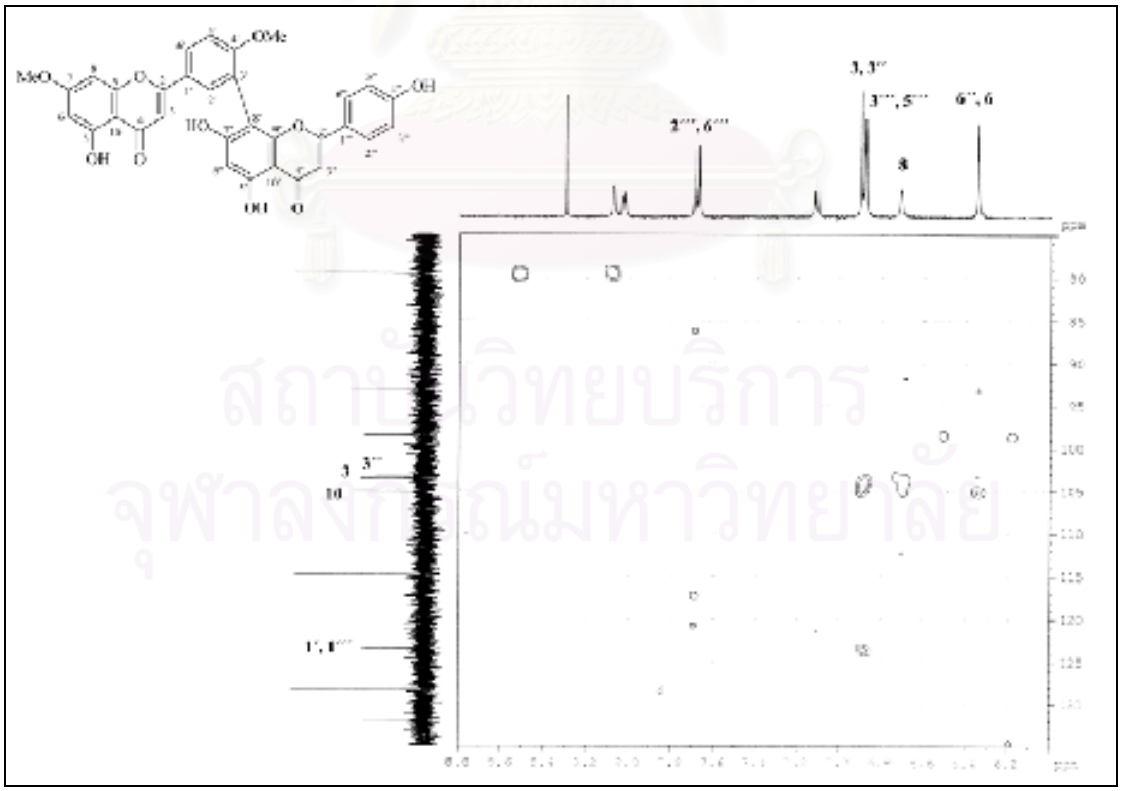

Figure 198a. HMBC Spectrum of compound ET-LC13
(δ_H 6.0-8.8 ppm, δ_C 75-135 ppm)

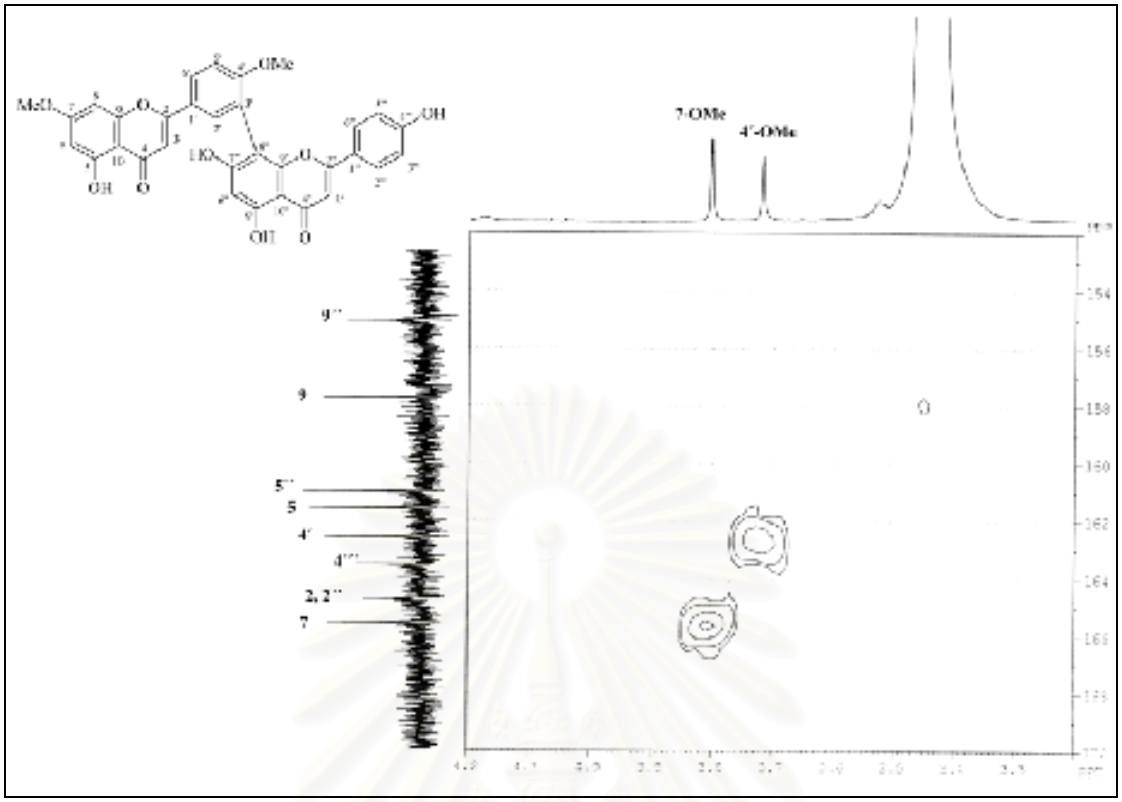

Figure 198b. HMBC Spectrum of compound ET-LC13
(δ_H 3.2-4.2 ppm, δ_C 152-170 ppm)

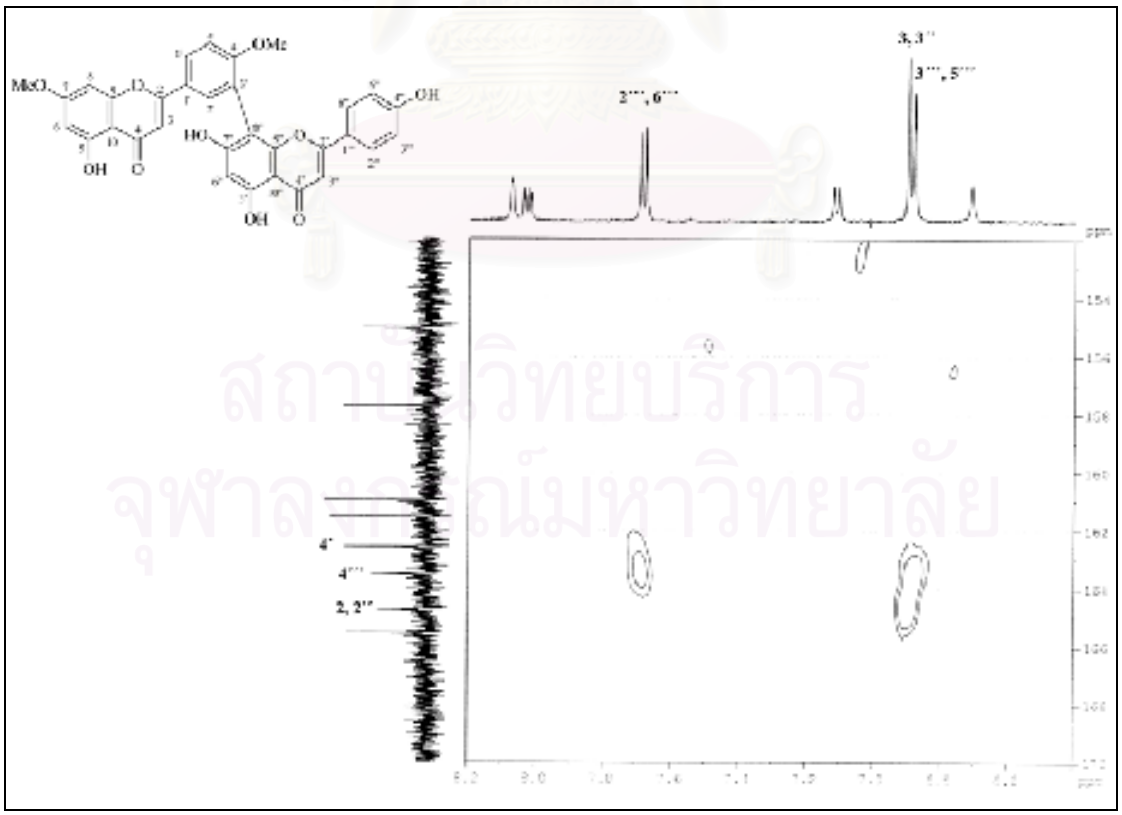

Figure 198c. HMBC Spectrum of compound ET-LC13
(δ_H 6.4-8.2 ppm, δ_C 152-170 ppm)

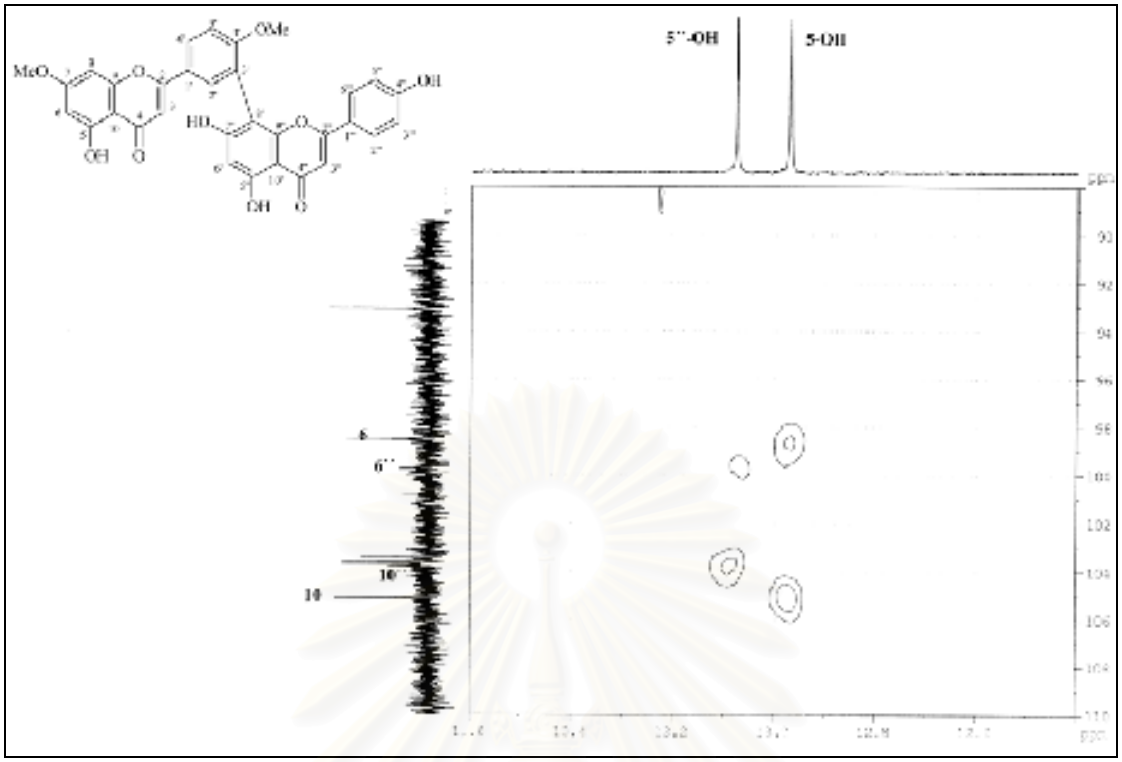

Figure 198d. HMBC Spectrum of compound ET-LC13
(δ_H 12.4-13.6 ppm, δ_C 88-110 ppm)

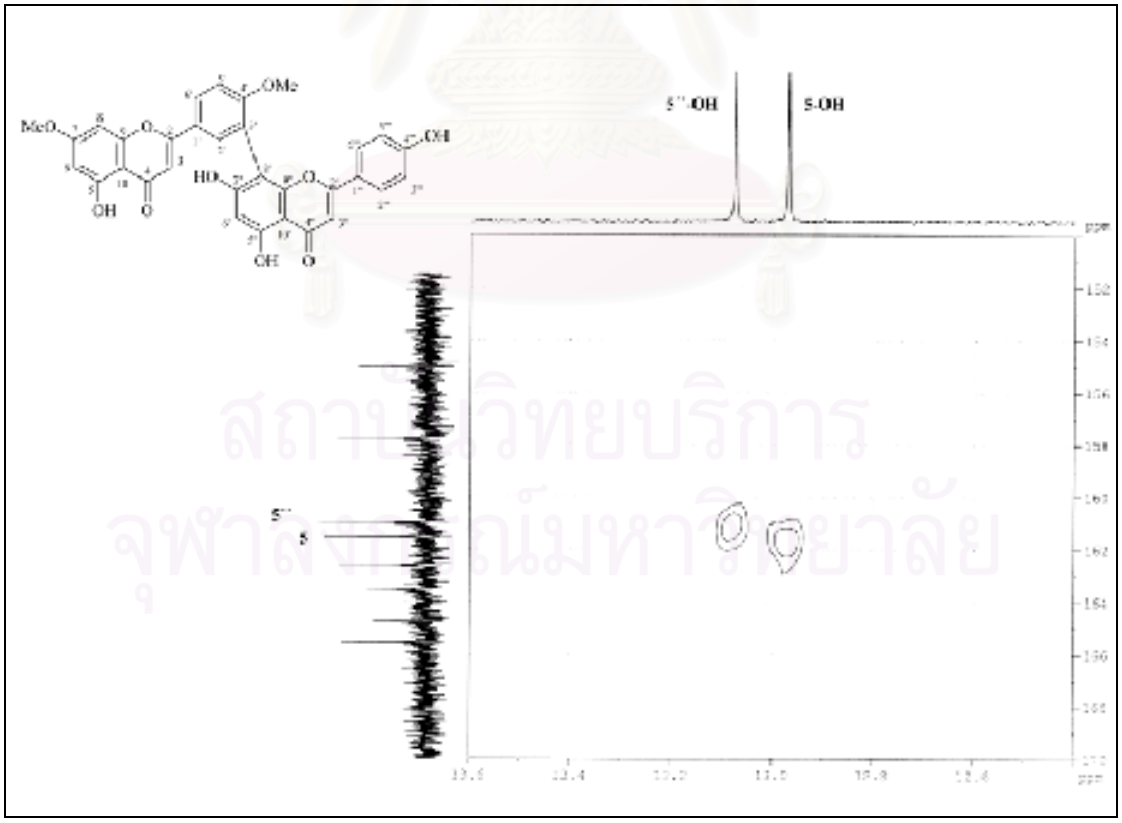

Figure 198e. HMBC Spectrum of compound ET-LC13
(δ_H 12.4-13.6 ppm, δ_C 150-170 ppm)

VITA

Miss Duangpen Pattamadilok was born in Bangkok on July 28, 1972. She received her B.Sc. in Pharmacy in 1995 and M.S. (Pharmacognosy) in 1998 from Faculty of Pharmaceutical Sciences, Chulalongkorn University. Currently, she is working at the Medicinal Plant Research Institute, Department of Medical Science, Ministry of Public Health, Thailand.

Publication

Pattamadilok, D and Suttisri, R. 2008. *Seco*-Terpenoids and Other Constituents from *Elateriospermum tapos*. J. Nat. Prod. 71: 292-294.

Wongsinkongman, P., Pattamadilok, D., Bansiddhi, J., Boonruad, T., Techadamrongsin, Y., and Chavalittumrong, P. 2006. Chemical specification of *Hyptis suaveolens* (L.) Poit. aerial parts. J. Thai Trad. Alt. Med. 4: 27-43.

Jirawattanapong, W., Bansiddhi, J., Techadamrongsin, Y., and Pattamadilok, D. 2005. Chemical specification of *Gynostemma pentaphyllum* (Thunb) Makino. Bull. Dept. Med. Sci. 47: 168-179.

Pattamadilok, D., Techadamrongsin, Y., and Bansiddhi, J. 2002. Chemical specification of *Orthosiphon aristatus* (Blume) Miq. Bull. Dept. Med. Sci. 44: 189-200.

Roengsumran, S., Jaiboon, N., Chaichit, N., Sommit, D., Pattamadilok, D., Chaichantipyuth, C., and Petsom, A. 2002. Hydrogen bonding in labdane diterpenoids, labda-7,12(*E*),14-triene-17-oic acid and labda-12(*Z*),14,17-triene-18-oic acid. J. Chem. Crystal. 32: 495-497.